DECLASSIFIED [redacted]

NASA TECHNICAL MEMORANDUM

UB
NASA TM X-1545

UB
NASA TM X-1545

UNCLASSIFIED

NASA TO 70-608 10/23/70

N70-78415
(ACCESSION NUMBER) (THRU)
313 1
(PAGES) (CODE)
(NASA CR OR TMX OR AD NUMBER) (CATEGORY)
FACILITY FORM 602

[redacted]

PREDICTED CHARACTERISTICS OF M2-F2 LIFTING BODY LAUNCHED FROM B-52 AIRPLANE WITH COMPARISON OF FLIGHT RESULTS

by Linwood W. McKinney and Richmond P. Boyden

Langley Research Center
Langley Station, Hampton, Va.

NATIONAL AERONAUTICS AND SPACE ADMINISTRATION • WASHINGTON, D. C. • APRIL 1968

[redacted]

Declassified by authority of NASA
Classification Change Notices No. 210
Dated **12-15-70

[redacted] NASA TM X-1545

PREDICTED CHARACTERISTICS OF M2-F2 LIFTING BODY LAUNCHED FROM B-52 AIRPLANE WITH COMPARISON OF FLIGHT RESULTS

By Linwood W. McKinney and Richmond P. Boyden

Langley Research Center
Langley Station, Hampton, Va.

[redacted]

[redacted]

[redacted]

[redacted]

NATIONAL AERONAUTICS AND SPACE ADMINISTRATION

[redacted]

[redacted]

PREDICTED CHARACTERISTICS OF M2-F2 LIFTING BODY LAUNCHED FROM B-52 AIRPLANE WITH COMPARISON OF FLIGHT RESULTS*

By Linwood W. McKinney and Richmond P. Boyden
Langley Research Center

SUMMARY

A high-speed wind-tunnel investigation has been made to determine the effects of the asymmetrical flow field beneath the right wing of the B-52 airplane on the static aerodynamic characteristics of the M2-F2 lifting body. Six-degree-of-freedom motion calculations were made to predict the effect of the asymmetrical flow field on the launch characteristics of the M2-F2 lifting body using the static wind-tunnel data as inputs.

The results of the computed motions indicate launches without contact between the M2-F2 fins and attachment pylon should be expected at altitudes above approximately 25 000 feet (7.6 km) at a Mach number of 0.60, 32 000 feet (9.8 km) at a Mach number of 0.70, and 43 000 feet (13.1 km) at a Mach number of 0.80 for stability augmentation off and stability augmentation on at a B-52 gross weight of 250 000 pounds (1112 kN). The minimum altitude for launches without contact at a B-52 airplane gross weight of 190 000 pounds (845 kN) was not defined by the range of the investigation. However, it is expected to be nearly the same as that predicted for a B-52 gross weight of 250 000 pounds (1112 kN) since a previous investigation has indicated launch contact to be influenced more by changes in dynamic pressure than changes in interference forces and moments resulting from changes in the B-52 angle of attack.

A comparison of the launch predictions with full-scale launch characteristics showed satisfactory agreement over the critical first second of the launch, with the exception of normal acceleration at the instant of launch. This discrepancy arises from the fact that the computed values of normal acceleration do not account for the pylon hook loads, and the flight values were taken from an accelerometer.

INTRODUCTION

The Flight Research Center of the National Aeronautics and Space Administration is currently engaged in a flight research program to investigate the subsonic handling

[redacted]

[redacted]

qualities and landing characteristics of several lifting-body reentry vehicles, one of which is the M2-F2 lifting body. It is proposed that these vehicles be carried to altitudes of 40 000 feet (12.2 km) to 50 000 feet (15.2 km) and launched through the asymmetrical flow field beneath the right wing of a B-52 airplane in the same manner as the X-15 research airplane (refs. 1 to 3). The X-15 pylon is retained on the B-52 and the lifting body is carried on a pylon adapter which is attached to the X-15 pylon.

An investigation of the launch characteristics of the M2-F2 lifting body from a preliminary location on the B-52 airplane is reported in reference 4. The investigation of reference 4 consisted of high-speed static wind-tunnel tests and six-degree-of-freedom motion studies, the results of which indicated that the safe launch envelope as a function of altitude and Mach number was not satisfactory to accomplish the desired flight research program. Therefore, the M2-F2 vehicle was relocated beneath the B-52 wing to provide more clearance between the M2-F2 fins and the attachment pylon.

The purpose of this paper is to present the results of an investigation of the computed launch characteristics of the M2-F2 vehicle launched from the final location beneath the B-52 wing. Static wind-tunnel data are presented for Mach numbers from 0.60 to 0.85 for a range of angles of attack of the M2-F2/B-52 combination and for angles of attack and sideslip of the M2-F2 vehicle in the presence of the B-52 model at several separation distances. Calculated drop motions are presented to show the effects of M2-F2 trim setting at launch, stability augmentation, M2-F2 launch weight, and B-52 angle of attack on the launch characteristics. A comparison of the predictions with the full-scale launch characteristics is also included.

SYMBOLS

The longitudinal force and moment coefficients are referred to the stability axes and the lateral data are referred to the body axes, as shown in figure 1(a). The reference dimensions used in reducing the data are model projected area ($S = 0.0998$ ft^2 (0.00927 m^2)), model length ($l = 6.65$ in. (0.1689 m)), and maximum body width ($b = 2.89$ in. (0.0734 m)). The angles and normal acceleration presented in the form of time histories are with reference to the principal-axis system, as indicated in figure 1(b).

Measurements for this investigation were taken in the U.S. Customary System of Units. Equivalent values are indicated herein parenthetically in the International System (SI) in the interest of promoting use of this system in future NASA reports. Details concerning the use of SI, together with physical constants and conversion factors, are given in reference 5.

a speed of sound, feet/second (meters/second)

b reference span, 2.89 inches (0.0734 meter)

C_D drag coefficient, $\frac{\text{Drag}}{\bar{q}S}$

C_L lift coefficient, $\frac{\text{Lift}}{\bar{q}S}$

C_l rolling-moment coefficient, $\frac{\text{Rolling moment}}{\bar{q}Sb}$

C_{l_p} rolling-moment coefficient due to rolling velocity, $\frac{\partial C_l}{\partial\left(\frac{pb}{2V}\right)}$, per radian

C_{l_r} rolling-moment coefficient due to yawing velocity, $\frac{\partial C_l}{\partial\left(\frac{rb}{2V}\right)}$, per radian

C_{l_β} effective-dihedral parameter (measured between $\beta = 5^\circ$ and $\beta = -5^\circ$), per degree

C_m pitching-moment coefficient, $\frac{\text{Pitching moment}}{\bar{q}S\mathscr{l}}$

C_{m_q} pitching-moment coefficient due to pitching velocity, $\frac{\partial C_m}{\partial\left(\frac{q\mathscr{l}}{2V}\right)}$, per radian

C_n yawing-moment coefficient, $\frac{\text{Yawing moment}}{\bar{q}Sb}$

C_{n_p} yawing-moment coefficient due to rolling velocity, $\frac{\partial C_n}{\partial\left(\frac{pb}{2V}\right)}$, per radian

C_{n_r} yawing-moment coefficient due to yawing velocity, $\frac{\partial C_n}{\partial\left(\frac{rb}{2V}\right)}$, per radian

C_{n_β} directional-stability parameter (measured between $\beta = 5^\circ$ and $\beta = -5^\circ$), per degree

C_Y side-force coefficient, $\frac{\text{Side force}}{\bar{q}S}$

C_{Y_β} side-force coefficient per degree of sideslip angle (measured between $\beta = 5^\circ$ and $\beta = -5^\circ$)

g acceleration due to gravity

h	altitude, feet (meters)
I_X, I_Y, I_Z	moments of inertia about X_{ref}, Y_{ref}, and Z_{ref}, slug-feet^2 (kilogram-meters^2)
I_{XZ}	product of inertia, slug-feet^2 (kilogram-meters^2)
K_I	rudder interconnect gain, δ_r/δ_a
K_p	roll damper gain, δ_a/p, seconds
K_q	pitch damper gain, δ_p/q, seconds
K_r	yaw damper gain, δ_r/r, seconds
L_β	dimensional effective dihedral parameter, $C_{l_\beta}\bar{q}Sb$, foot-pounds/degree (meter-newtons/degree)
l	model length, 6.65 inches (0.169 meter)
M	Mach number, V/a
M_X, M_Z	moments about X- and Z-axes, foot-pounds (meter-newtons)
N_β	dimensional directional stability parameter, $C_{n_\beta}\bar{q}Sb$, foot-pounds/degree (meter-newtons/degree)
N_β'	effective directional stability parameter
$\bar{n}$	normal acceleration along principal axes of M2-F2, g units
p	rolling velocity, radians/second or degrees/second
q	pitching velocity, radians/second or degrees/second
$\bar{q}$	free-stream dynamic pressure, $\frac{1}{2}\rho V^2$, pounds/foot^2 (newtons/meter^2)
R	radius

r	yawing velocity, radians/second or degrees/second
S	reference area, 0.0998 foot^2 (0.00927 meter^2)
t	time, seconds
V	free-stream velocity, feet/second (meters/second)
W_{B-52}	weight of B-52 airplane, pounds (newtons)
W_{M2-F2}	weight of M2-F2 vehicle, pounds (newtons)
X,Y,Z	Euler axes
X_p,Z_p	M2-F2 principal axes
X_{ref},Y_{ref},Z_{ref}	M2-F2 reference axes
x_b,y_b,z_b	coordinates of M2-F2 lifting body, feet (meters)
Z'	vertical axis normal to B-52 reference line
x,y,z	distances along X-, Y-, and Z-axes, feet (meters)
z'	distance along Z'-axis, feet (meters)
α	angle of attack of M2-F2 reference line, degrees
α_{B-52}	angle of attack of B-52 reference line, degrees
$\Delta\alpha$	incidence angle of M2-F2 reference line relative to B-52 reference line, degrees
β	angle of sideslip of M2-F2 reference line, degrees
β_{B-52}	angle of sideslip of M2-F2/B-52 combination, degrees
$\Delta\beta$	angle of sideslip of M2-F2 reference line relative to B-52 reference line, degrees

δ_a differential deflection of upper-surface flaps when used as ailerons, $\delta_{f,right} - \delta_{f,left}$, degrees

δ_p lower-surface-flap deflection measured from local body surface, positive when trailing edge is down, degrees

δ_r rudder deflection, positive when trailing edge is deflected to left, degrees

δ_f upper-surface-flap deflection measured from local body surface, positive when trailing edge is down, degrees

ϵ inclination of M2-F2 principal axes from angle-of-attack reference axes, positive when principal axes are inclined nose down with respect to reference axes, degrees

θ Euler pitch angle, degrees

ρ mass density of air, slugs/foot^3 (kilograms/meter^3)

ϕ Euler roll angle, degrees

ψ Euler yaw angle, degrees

Subscripts:

B-52 B-52 airplane

d effect of dampers

M2-F2 M2-F2 lifting body

max maximum

ref reference axes

s stability axes

A dot over a symbol indicates the first derivative with respect to time.

MODELS AND APPARATUS

The models used for the wind-tunnel investigation were 0.025-scale representations of the B-52 airplane and the M2-F2 lifting-body configuration. The location of the M2-F2 vehicle on the B-52 airplane is shown in figure 2. Geometric characteristics of the M2-F2 model are given in figure 3. The M2-F2 vehicle was sting supported beneath the B-52 wing as shown by the photographs of figure 4. The support system was designed to allow the M2-F2 vehicle to be rotated about the center of gravity in both the pitch and yaw planes at several separation distances beneath the B-52 wing.

TESTS AND CORRECTIONS

The force tests were made in the Langley high-speed 7- by 10-foot tunnel at Mach numbers of 0.60, 0.70, 0.80, and 0.85, corresponding to Reynolds numbers from approximately 1.8×10^6 to 2.3×10^6 based on M2-F2 model length. The test parameters were angles of attack of the B-52/M2-F2 combination and angles of attack and sideslip of the M2-F2 vehicle in the presence of the B-52 model at separation distances corresponding to 0, 2.0, 4.0, 8.0, and 12.0 feet (0, 0.60, 1.2, 2.4, and 3.6 m) full scale. The basic M2-F2 control surface settings for all tests except the control effectiveness test were $\delta_p = 25^\circ$, $\delta_f = -10^\circ$, and $\delta_r = \pm 10^\circ$.

During the test of the M2-F2 vehicle in the carry location, sufficient clearance between the pylon fairing and the M2-F2 vehicle was allowed to insure that fouling was not encountered as a result of sting and balance deflections under load. Corrections to the angles of attack and sideslip due to bending of the main support system and the M2-F2 sting and balance system have been applied to the data. Blockage corrections were obtained by the method of reference 6 considering the drag of both models and have been applied to the data.

The jet-boundary corrections to angles of attack obtained by the method of reference 7 for the B-52 model have been applied. The drag data are presented uncorrected for base pressure.

PRESENTATION OF RESULTS

The results of the study are presented in the following figures:

	Figure
Wind-tunnel data:	
M2-F2 alone	5 and 6
M2-F2 in B-52 flow field	7 to 10
Effect of B-52 angle of attack	11
B-52 buffet boundary	12

Figure

Motion-study calculations:
M2-F2 reference section used in motion studies 13
Effect of δ_f on fin-tip loci 14
Effect of B-52 angle of attack on fin-tip loci 15
Effect of separation distance on M2-F2 rolling and yawing accelerations 16
Effect of B-52 angle of attack on fin-tip loci when W_{B-52} = 190 000 pounds (845 kN) 17
Effect of B-52 angle of attack on fin-tip loci with M2-F2 dampers on 18
Effect of M2-F2 launch weight on fin-tip loci 19
Effect of δ_f on M2-F2 motions . . . . . 20 and 21
Variation of $N_{\beta'}$ with M2-F2 angle of attack 22
Effect of δ_f on M2-F2 motions with dampers on . . . . . 23 and 24
Effect of δ_f on M2-F2 motions when W_{B-52} = 190 000 pounds (845 kN) . . . . . 25 to 28
Effect of B-52 angle of attack on M2-F2 motions . . . . . 29 and 30
Effect of B-52 angle of attack on M2-F2 motions when W_{B-52} = 190 000 pounds (845 kN) 31
Effect of B-52 angle of attack on M2-F2 launch motions for W_{M2-F2} = 9030 pounds (40.2 kN) 32
Launch envelope 33
Comparison of flight and predicted motions 34

RESULTS AND DISCUSSION

Wind-Tunnel Data and Motion Calculations

The results of the wind-tunnel force tests are presented in figures 5 and 6. Figure 5 presents the basic interference-free data obtained on the 0.025-scale model of the M2-F2 launch vehicle. A comparison of the data presented in figure 5 with data obtained at the Ames Research Center on a larger model is presented in figure 6 for Mach numbers of 0.60 and 0.80. The agreement shown is considered acceptable for this study. Figures 7 to 10 show the longitudinal and lateral-directional data obtained on the M2-F2 model in the B-52 interference flow field as a function of B-52 angle of attack for several values of M2-F2 incidence angle $\Delta\alpha$, separation distance z', and sideslip angle $\Delta\beta$, at Mach numbers of 0.60, 0.70, 0.80, and 0.85. Physical and aerodynamic damping and control characteristics intended to be representative of the M2-F2 launch vehicle were compiled by the Flight Research Center and are given in tables I to III.

TABLE I.- PHYSICAL AND DAMPER CHARACTERISTICS OF THE M2-F2

Measurement	Values used in predictions		Values of M2-F2 flight vehicle
	Lightweight M2-F2	Heavyweight M2-F2	
Weight of M2-F2, W_{M2-F2}, lb (kN)	5029 (22.4)	9244 (41.2)	5930 (26.4)
Moment of inertia about X_{ref}-axis, I_X, slug-ft^2 (kg-m^2)	952.3 (1291)	1113.8 (1510)	956.3 (1297)
Moment of inertia about Y_{ref}-axis, I_Y, slug-ft^2 (kg-m^2)	4388.5 (5951)	7001.2 (9494)	5583.0 (7571)
Moment of inertia about Z_{ref}-axis, I_Z, slug-ft^2 (kg-m^2)	4833.4 (6554)	7466.0 (10 124)	6005.0 (8143)
Product of inertia, I_{XZ}, slug-ft^2 (kg-m^2)	-334.6 (-454)	-673.3 (-913)	-417.0 (-565)
Inclination, ϵ, deg	-4.9	-6.0	-4.69
Pitch damper gain, K_q, sec	0.5	0.5	0.60
Roll damper gain, K_p, sec	-0.25	-0.25	-0.60
Yaw damper gain, K_r, sec	0.25	0.25	0.60
Rudder interconnect gain, K_I	-0.30	-0.30	-0.60

TABLE II.- DAMPER LIMITS FOR THE M2-F2

	Values used in predictions	Values of M2-F2 flight vehicle
Damper authority limits:		
$\delta_{a,d}$, deg	±20	±5
$\delta_{p,d}$, deg	±5	±5
$\delta_{r,d}$, deg	±5	±4.2
Damper rate limits:		
$\dot{\delta}_{a,d}$, deg/sec	±30	±30
$\dot{\delta}_{p,d}$, deg/sec	±25	±25
$\dot{\delta}_{r,d}$, deg/sec	±30	±22.5

TABLE III.- AERODYNAMIC DAMPING DERIVATIVES OF THE M2-F2

Measurement	Value at –			
	M = 0.60	M = 0.70	M = 0.80	M = 0.85
C_{m_q}, per rad	-0.145	-0.315	-0.490	-0.490
C_{l_p}, per rad	-.205	-.220	-.235	-.235
C_{n_p}, per rad	.122	.147	.1715	.1715
C_{l_r}, per rad	.348	.385	.4320	.4320
C_{n_r}, per rad	-1.395	-1.505	-1.630	-1.630

In order to assess the launch characteristics of the M2-F2/B-52 combination, M2-F2 interference data as a function of incidence angles, separation distance, and sideslip angle are required at a constant B-52 angle of attack and Mach number. As an example of the gross effects of the interference flow field on the M2-F2 forces and moments, figure 11 is included. In this figure, C_L, C_m, C_l, C_n, and C_Y at $\Delta\alpha = -5^{\circ}$ for several B-52 angles of attack are shown as functions of separation distance z', with free-stream values of the coefficients appearing on the plots at z' = 40 feet (12.2 m).

Time histories of the M2-F2 motions were computed by solving a system of six-degree-of-freedom rigid body equations of motion programed to allow nonlinear variations of the aerodynamic coefficients as a function of α_{M2-F2}, β_{M2-F2}, and z. The equations were solved by performing a Kutta-Runge variable-step-size integration procedure. The cross-plotted wind-tunnel static interference data were stored in the computer as a function of α_{M2-F2}, β_{M2-F2}, and separation distance for a constant B-52 angle of attack and Mach number. Appropriate values of the aerodynamic coefficients as functions of α_{M2-F2}, β_{M2-F2}, and z were determined from tabular values by using linear interpolation. The computer program is designated D-1085 and is available from the Analytical Computing Division of the Langley Research Center.

The area in the B-52 flight envelope where calculated launches were made corresponds to that of the investigation of reference 4 and is shown in figure 12. Plotted in figure 12 are the B-52 buffet boundary as a function of Mach number and the variation of altitude with Mach number for trimmed flight at various B-52 angles of attack for gross weights of 250 000 pounds (1112 kN) and 190 000 pounds (845 kN), which are taken as maximum and minimum weight conditions, respectively. The area between the buffet boundary and the line for $\alpha_{B-52} = -2^{\circ}$ represents the region where computed launches have been studied in the present investigation. The variables in the launch studies were B-52 altitude and angle of attack, gross weight of the M2-F2 vehicle, Mach number, stability augmentation, and pitch trim setting.

The results of the study are presented in the form of locus plots (paths) of the trailing edge of the M2-F2 fin tips, the center of gravity in the YZ reference plane at discrete values of time, and time histories of the quantities z, $\bar{n}$, α, θ, ϕ, β, and ψ as in reference 4. In figure 13 a sketch of the vehicle shows the points for which loci were computed. A cross section showing the initial relationship between the M2-F2 fins and the X-15 pylon (as seen by looking through the M2-F2 center of gravity in the direction of flight) is included on each of the locus plots for reference purposes. For the launch conditions where contact is indicated by the locus plots, the subsequent effect of the contact is not included in the time-history calculations. To assess the effects of artificial damping on the drop motions, a rate damper system about all axes was included

in the system of motion equations as in reference 4. Limits for damper-imposed control deflection rate and magnitude are given in table II.

Fin-Tip Loci

Effect of δ_f.- Primary pitch control of the M2-F2 vehicle is achieved by deflecting the upper flap. The effect of pitch-control setting δ_f at launch on the fin-tip loci is shown in figure 14 for Mach numbers of 0.60 and 0.80 at a B-52 weight of 250 000 pounds (1112 kN). When the M2-F2 vehicle is in the captive flight location, the pylon adapter shields the M2-F2 upper surface controls and renders them essentially ineffective; therefore, the initial loci of the fin tips are unaffected by changes in upper surface pitch-control setting. There is, however, a definite effect of δ_f on the fin-tip loci at times greater than three-tenths of a second. Since the purpose of the locus plots is to aid in analyzing the contact problem associated with the launches, the remaining analysis presented in this section of the paper will be made with $\delta_f = -15^{\circ}$, which is the value required to trim at reasonable angles of attack consistent with an acceptable launch motion.

Effect of B-52 angle of attack.- Figure 15 shows the effect of increasing the B-52 angle of attack for Mach numbers of 0.60, 0.70, 0.80, and 0.85 at a B-52 weight of 250 000 pounds (1112 kN). As the B-52 angle of attack is increased, the flight altitude is also increased, as shown in figure 12. Therefore, the effects seen in figure 15 result both from variations in interference forces and moments with B-52 angle of attack and changes in dynamic pressure. The trends of the launch characteristics with changes in B-52 angle of attack agree with the investigation of reference 4, in that as the B-52 angle of attack is increased, the paths of the M2-F2 fin tips become more nearly vertical for all Mach numbers and as a result the launch characteristics are improved at the higher B-52 angles of attack. Actual contact between the M2-F2 fin tips and the X-15 pylon is shown in figure 15(c) for a B-52 angle of attack of -2°.

The effect of Mach number on the paths of the fin tips as seen in figure 15 essentially results from the effect of Mach number on the interference forces and moments, since, if compressibility effects on the B-52 lift curves are neglected, the dynamic pressure is constant through the Mach number range for a constant B-52 angle of attack. As an example of the Mach number effect on the interference forces and moments, figure 16 is included. Figure 16 shows the effect of Mach number on the interference rolling and yawing accelerations as a function of separation distance z for a B-52 angle of attack of 0°. The negative rolling acceleration over the range from $z = 0$ to $z = 1$ foot (0.3048 m) is increased by approximately 100 percent at $M = 0.80$ and is responsible for the contact of M2-F2 fin and X-15 pylon shown in figure 15(c).

The loci of the M2-F2 fin tips calculated for launches with the B-52 weight reduced to 190 000 pounds (845 kN) are shown in figure 17. The reduction in dynamic pressure at the lower B-52 wing loading results in improved launch characteristics.

Effect of dampers.- Calculated loci of the fin tips for launches at $M = 0.60$, 0.70, and 0.80 with stability augmentation about all axes are shown in figure 18 for a B-52 weight of 250 000 pounds (1112 kN) and M2-F2 weight of 5029 pounds (22.4 kN). The effect of stability augmentation on the fin-tip loci is negligible over the time period in which contact between the fin tips and X-15 pylon is possible. (See ref. 4.)

Effect of launch weight.- Loci of the M2-F2 fin tips for calculated launches with the M2-F2 weight increased to 9030 pounds (40.2 kN) are shown in figure 19 for Mach numbers of 0.60, 0.70, and 0.80. Increasing the M2-F2 weight and changing the inertial characteristics as shown in table I retarded rotation of the fins somewhat but did not eliminate the contact between the M2-F2 fin and the X-15 pylon at $\alpha_{B-52} = -2^{\circ}$ and $M = 0.80$.

Motion After Launch

Effect of δ_f.- Figures 20 and 21 show the effect of initial pitch-control setting on the computed M2-F2 motions after launch for $\alpha_{B-52} = -1^{\circ}$, 0°, 2°, and 4° at $M = 0.60$ and $\alpha_{B-52} = 0^{\circ}$ at $M = 0.80$. The altitudes simulated correspond to level flight of the B-52 at a gross weight of 250 000 pounds (1112 kN). The normal acceleration at launch is independent of the δ_f setting since, as pointed out in the previous section, the upper surface controls are shielded by the pylon adapter and are therefore ineffective. An increase in negative pitching moment is obtained as the M2-F2 vehicle separates from the pylon and control effectiveness is regained. This results in large negative angles of attack during the initial 1.2 to 2.0 seconds of the computed launches for $\delta_f = -10^{\circ}$ to -15°. Increases in B-52 angle of attack with the accompanying decrease in dynamic pressure reduced the maximum negative angles of attack obtained at $M = 0.60$ (fig. 20). An apparent effect of δ_f setting is noted in the lateral motions in that divergent β and ϕ angles generally occur when large negative α excursions are obtained. Large α-excursions may follow as a result of inertia coupling. As an aid in understanding the effects of δ_a on the lateral motion transients in the interference flow field, a limited examination of the lateral-directional characteristics of the M2-F2 vehicle in free air has been made. Values of N_{β}' $\left(\text{where } N_{\beta}' = \left(\dfrac{N_{\beta} + \dfrac{I_{XZ}}{I_Z} L_{\beta}}{1 - \dfrac{I_{XZ}^2}{I_X I_Z}}\right)_s\right)$, which approximates the frequency squared on the Dutch roll oscillation, are shown in figure 22 as a function of angle of attack for Mach numbers from 0.60 to 0.85. As the angle of attack decreases,

the effective directional stability as measured by N_{β}' deteriorates rapidly. This effect of angle of attack on the directional stability characteristics is evident in the computed time histories of β as shown in figures 20 to 21. It should also be pointed out that the high roll angles shown in the computed launch motion transients are primarily the result of roll due to sideslip rather than rolling moment induced by the interference flow field.

The computed launch motions of the M2-F2 vehicle with a rate damper system simulated about all axes are shown in figure 23 at $M = 0.60$ and in figure 24 at $M = 0.80$. Significant improvements are noted in the launch characteristics with the rate damper system simulated. The improvements noted in the lateral-directional motions result from the effects of both the lateral dampers and the longitudinal dampers, since the lateral-directional characteristics are a function of angle of attack.

The effect of reducing the B-52 gross weight to 190 000 pounds (845 kN) which results in a reduced dynamic pressure for a given B-52 angle of attack and Mach number is shown in figures 25 to 28 for dampers off and dampers on. This reduction in dynamic pressure results in improved launch motion transients as would be expected.

Effect of B-52 angle of attack.- Figures 29 to 31 show the effect of changes in B-52 angle of attack on the computed motion transients for a B-52 gross weight of 250 000 pounds (1112 kN) with dampers off and dampers on and a B-52 gross weight of 190 000 pounds (845 kN) with dampers on at Mach numbers of 0.70, 0.80, and 0.85. The effects of B-52 angle of attack shown result from changes in both the interference forces and moments due to angle of attack and changes in dynamic pressure required to simulate level flight of the B-52 airplane at the different angles of attack. In general, as the B-52 angle of attack is increased (dynamic pressure reduced), the severity of the motion transients is reduced for all Mach numbers shown.

Effect of M2-F2 launch weight.- Computed motion transients for the heavyweight M2-F2 $\left(W_{M2-F2} = 9030 \text{ pounds } (40.2 \text{ kN})\right)$ are shown in figure 32 for $M = 0.60$, 0.70, and 0.80 and a B-52 gross weight of 250 000 pounds (1112 kN). A comparison of figure 32 with figures 20(a), 20(d), and 29 indicates the heavyweight M2-F2 generally has longitudinal motions comparable to the lightweight M2-F2 but has more extreme lateral-directional motions. The exception to this is the $M = 0.60$, $\alpha_{B-52} = 4^{\circ}$ case. The difference in the motions after launch for $\alpha_{B-52} < 4^{\circ}$ for the two weight conditions is believed to be a result of the heavyweight M2-F2 separating from the B-52 at a slower rate and thus, because of the reduced negative normal acceleration, staying in the interference flow field for a larger time. This condition provides more time for the lateral-directional motions to build up, particularly in roll.

Safe launch envelope.- Figure 33 shows the predicted safe launch envelope as a function of altitude and Mach number as determined by contact between the M2-F2 fin tips and pylon adapter. The upper boundary was determined by the B-52 airplane buffet

boundary and therefore varies for the two weight conditions (figs. 33(a) and 33(b)). The lower boundary was determined by computed points of contact at a B-52 gross weight of 250 000 pounds (1112 kN) at $M = 0.70$ and 0.80. Inasmuch as actual cases of contact were not computed for a B-52 gross weight of 190 000 pounds (845 kN), the contact boundary for a B-52 gross weight of 250 000 pounds (1112 kN) is shown in figure 33(b) for reference. The contact boundaries indicate launches without contact should be expected at altitudes above approximately 32 000 feet (9.8 km) at $M = 0.70$ and 43 000 feet (13.1 km) at $M = 0.80$ for dampers off and dampers on at a B-52 gross weight of 250 000 pounds (1112 kN). The minimum altitude investigated at $M = 0.60$ was 25 000 feet (7.6 km) and the results indicate launches without contact should be expected at and above this altitude. The minimum altitude for launches without contact was not defined by the range of the investigation for a B-52 gross weight of 190 000 pounds (845 kN); however, it would be expected to be nearly the same as that predicted for a B-52 gross weight of 250 000 pounds (1112 kN) since in reference 4 the boundary appeared to be influenced more by changes in dynamic pressure than by changes in interference forces and moments resulting from variations in B-52 angle of attack. The maximum roll angles computed during the 2-second duration of the launch calculations are also summarized in figure 33. The various cross-hatched areas in the Mach number altitude plane were obtained from cross plots of the maximum roll angle and indicate regions where ϕ_{max} was equal to or less than 20°, 40°, 60°, and 80°. Since the purpose of this investigation was to assess the probability of contact at launch, no attempt is made to discuss the maximum roll angles shown with respect to vehicle controllability problems.

Comparison of flight and predicted motions.- Launch motion calculations using initial conditions and time histories of control surface position measured in flight have been made and are compared with the motion time histories measured in flight in figure 34. The M2-F2 weight and inertias used in the calculation corresponded to the actual vehicle and are listed in the figure. The agreement between the flight and predicted motions is satisfactory over the critical first second of the launch, with the exception of $\bar{n}$ at $t = 0$. This discrepancy arises from the fact that the computed values of $\bar{n}$ do not account for the pylon hook loads, and the flight values were taken from an accelerometer. Differences in trim angle of attack between the model and flight vehicle are indicated by the difference in pitch attitude. This trim difference may contribute significantly to the poor agreement shown in the roll angle comparison at times greater than 1 second.

CONCLUDING REMARKS

A high-speed wind-tunnel investigation has been made to determine the effects of the asymmetrical flow field beneath the right wing of the B-52 airplane on the static

aerodynamic characteristics of the M2-F2 lifting body. Six-degree-of-freedom motion calculations were made to predict the effect of the asymmetrical flow field on the launch characteristics of the M2-F2 vehicle using the static wind-tunnel data as inputs.

The results of the computed motions indicate launches without contact between the M2-F2 fins and attachment pylon should be expected at altitudes above approximately 25 000 feet (7.6 km) at M = 0.60, 32 000 feet (9.8 km) at M = 0.70, and 43 000 feet (13.1 km) at M = 0.80 for stability augmentation off and stability augmentation on at a B-52 gross weight of 250 000 pounds (1112 kN). The minimum altitude for launches without contact at a B-52 gross weight of 190 000 pounds (845 kN) was not defined by the range of the investigation. However, it is expected to be nearly the same as that predicted for a B-52 gross weight of 250 000 pounds (1112 kN) since a previous investigation has indicated launch contact to be influenced more by changes in dynamic pressure than changes in interference forces and moments resulting from changes in the B-52 angle of attack.

A comparison of the launch predictions with full-scale launch characteristics showed satisfactory agreement over the critical first second of the launch, with the exception of normal acceleration at the instant of launch. This discrepancy arises from the fact that the computed values of normal acceleration do not account for the pylon hook loads, and the flight values were taken from an accelerometer.

Langley Research Center,
National Aeronautics and Space Administration,
Langley Station, Hampton, Va., October 24, 1967,
124-07-02-71-23.

REFERENCES

1. Alford, William J., Jr.; and Taylor, Robert T.: Aerodynamic Characteristics of the X-15/B-52 Combination. NASA MEMO 6-8-59L, 1959.

2. Taylor, Robert T.; and Alford, William J., Jr.: A Wind-Tunnel Investigation of the Carry Loads and Mutual Interference Effects of 1/40-Scale Models of the X-15 and B-52 Airplanes in Combination. NASA TM X-184, 1959.

3. Matranga, Gene J.: Launch Characteristics of the X-15 Research Airplane as Determined in Flight. NASA TN D-723, 1961.

4. McKinney, Linwood W.; Boyden, Richmond P.; and Taylor, Robert T.: Static Wind-Tunnel Investigation and Motion Studies of the M2-F2 Vehicle Launched From a Preliminary Location on the B-52 Airplane. NASA TM X-1225, 1966.

5. Mechtly, E. A.: The International System of Units – Physical Constants and Conversion Factors. NASA SP-7012, 1964.

6. Herriot, John G.: Blockage Corrections for Three-Dimensional-Flow Closed-Throat Wind Tunnels, With Consideration of the Effect of Compressibility. NACA Rept. 995, 1950. (Supersedes NACA RM A7B28.)

7. Gillis, Clarence L.; Polhamus, Edward C.; and Gray, Joseph L., Jr.: Charts for Determining Jet-Boundary Corrections for Complete Models in 7- by 10-Foot Closed Rectangular Wind Tunnels. NACA WR L-123, 1945. (Formerly NACA ARR L5G31.)

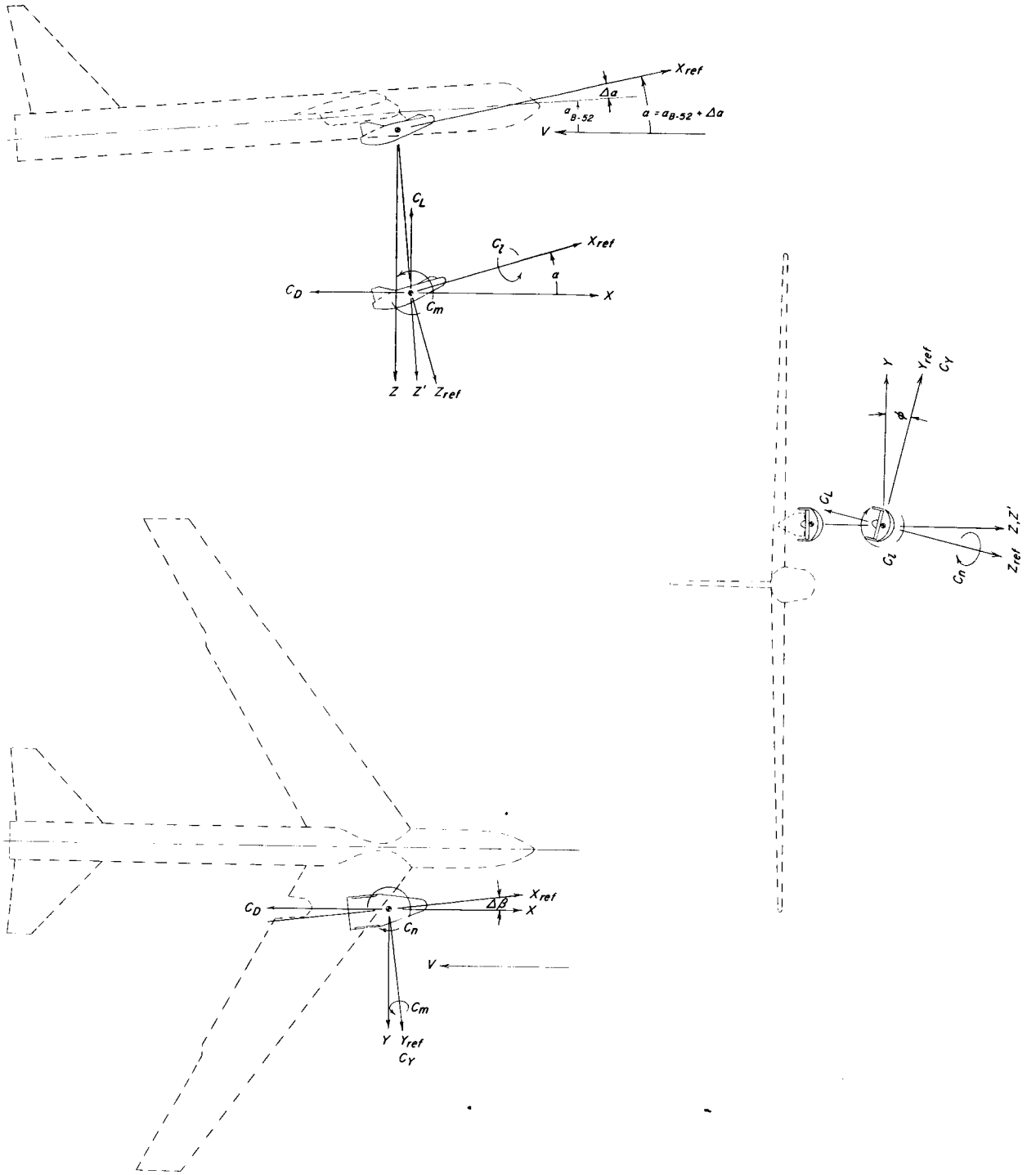

(a) Axes system used in wind-tunnel tests.

Figure 1.- System of axes used in the investigation.

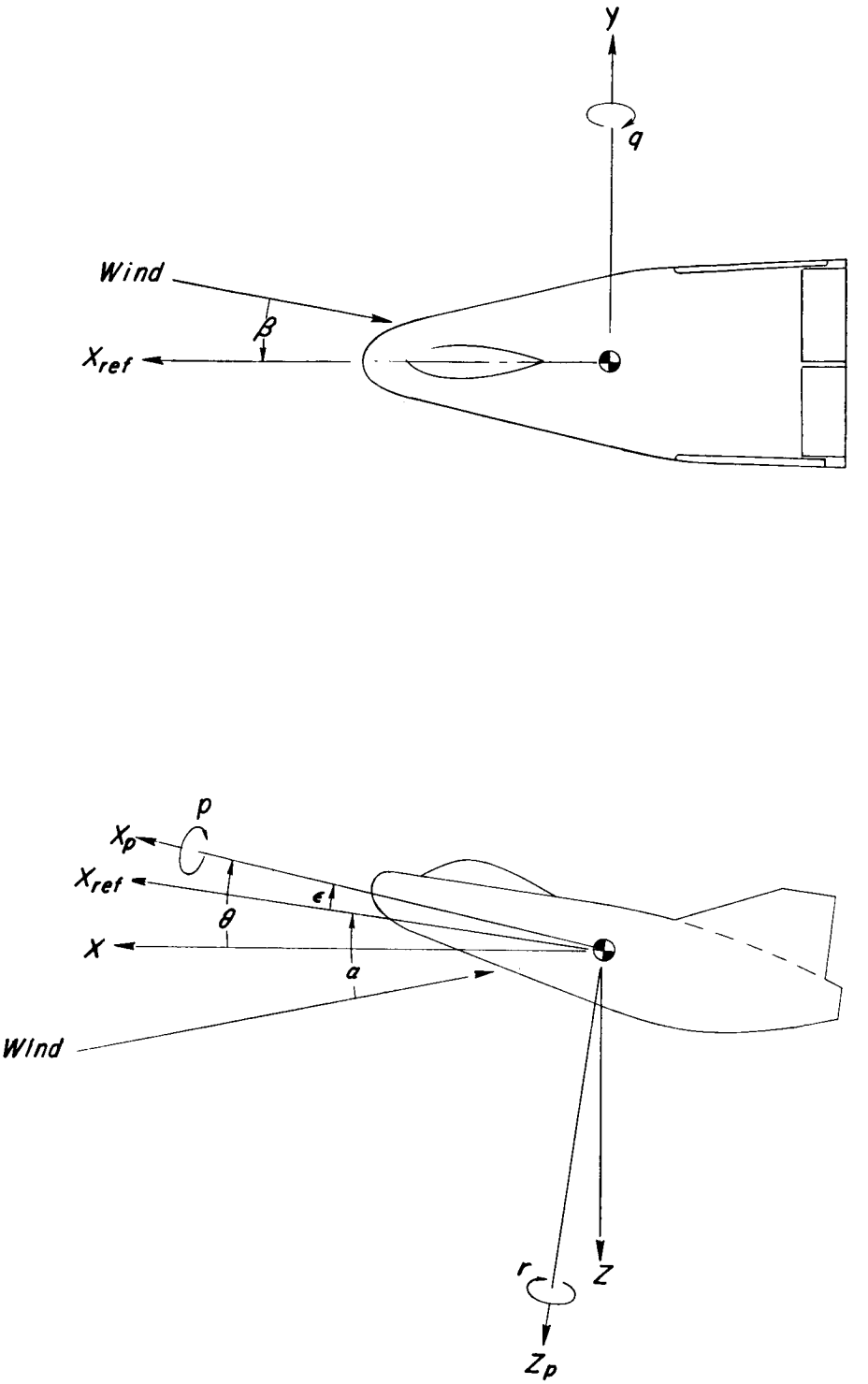

(b) Axes system used in motion calculations.

Figure 1.- Concluded.

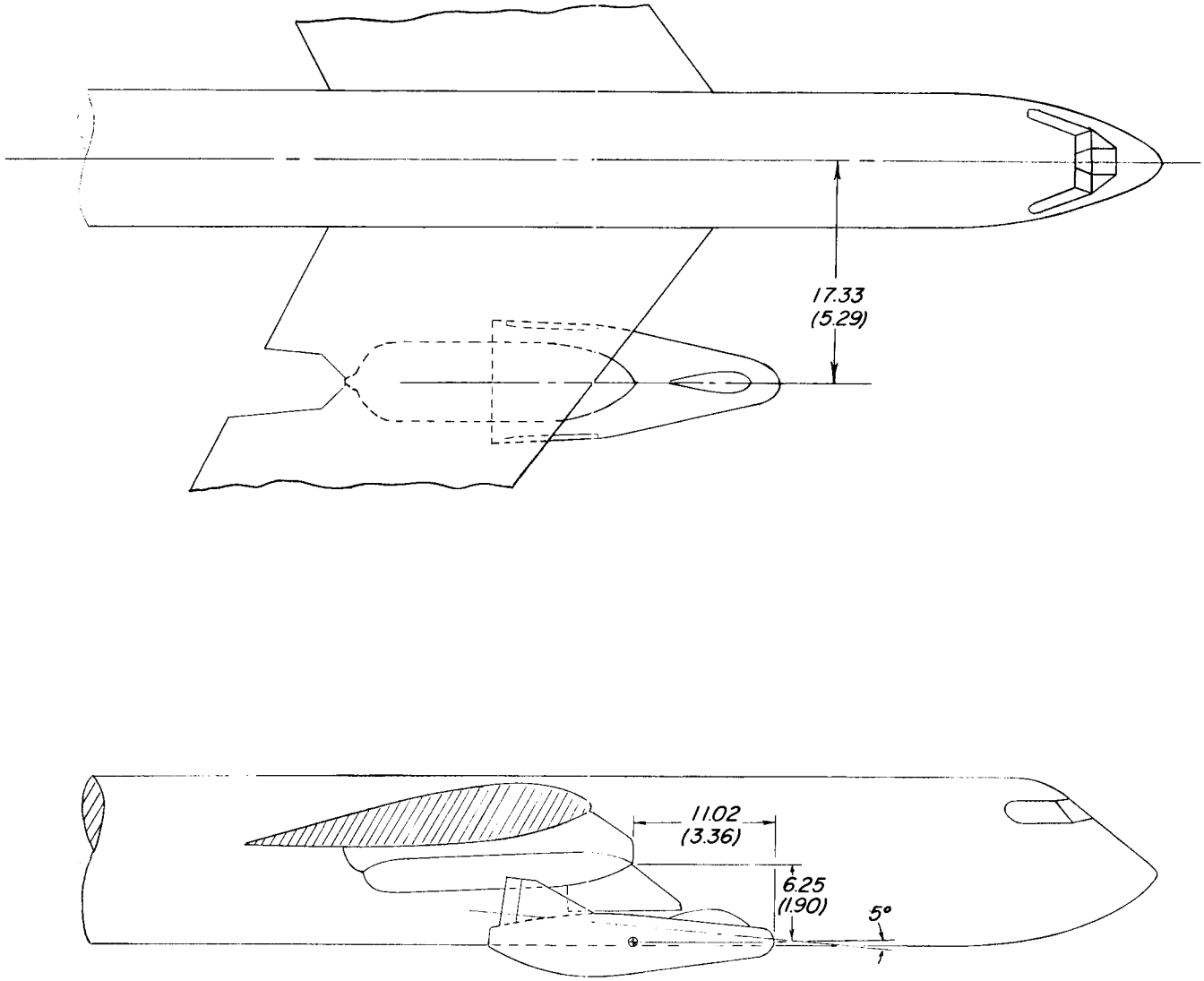

Figure 2.- Location of M2-F2 vehicle on B-52 airplane. All dimensions shown in feet and parenthetically in meters.

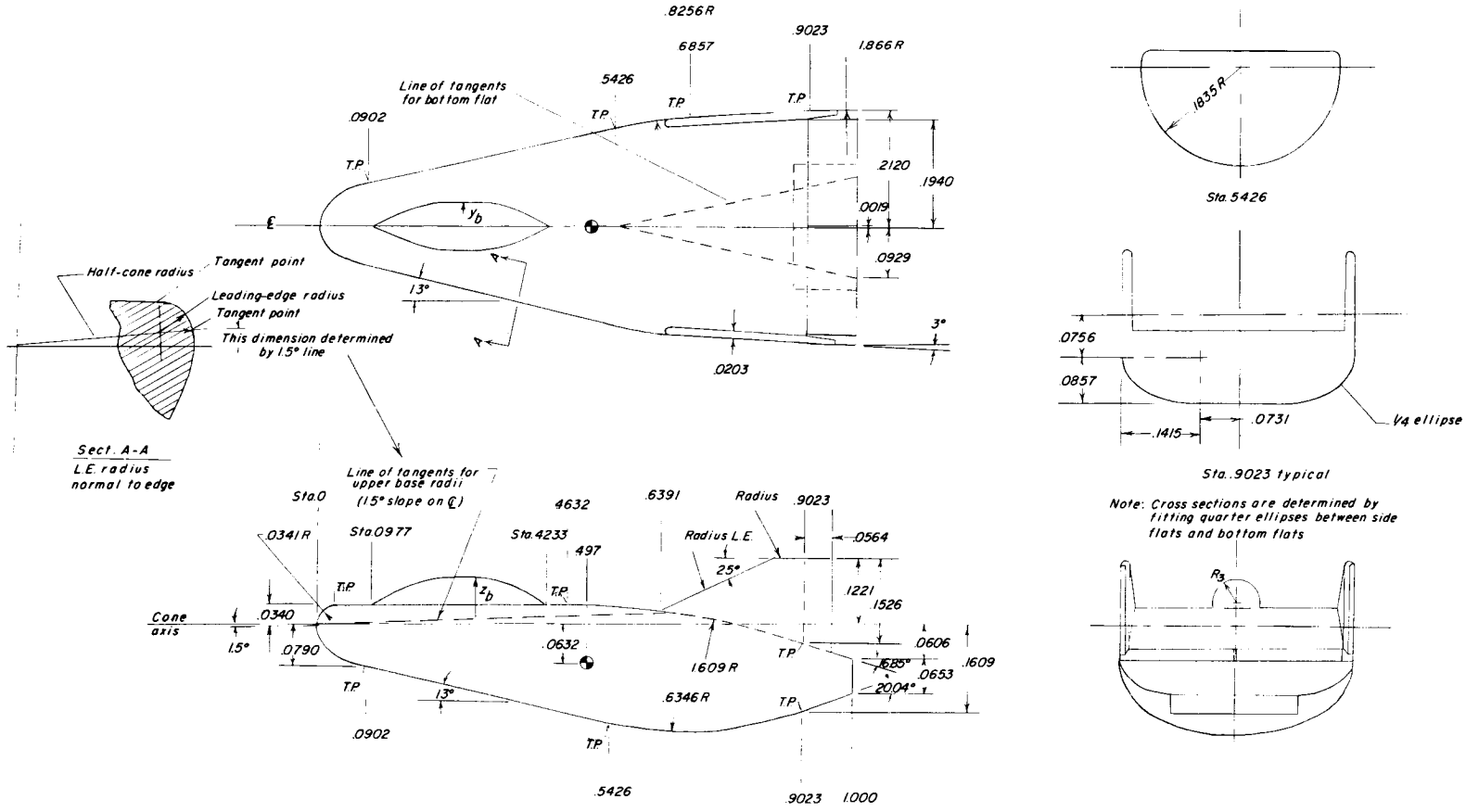

Equation for nose shapes

$$\frac{y_b}{l} = .038618\sqrt{\frac{x_b}{l}} - .012390\left(\frac{x_b}{l}\right) - .408407\left(\frac{x_b}{l}\right)^2 + 18.70215\left(\frac{x_b}{l}\right)^3$$

Figure 3.- Geometric characteristics of M2-F2 model. All dimensions shown in percent body length l, where l = 0.554 foot (0.1689 m). T.P. designates tangent point.

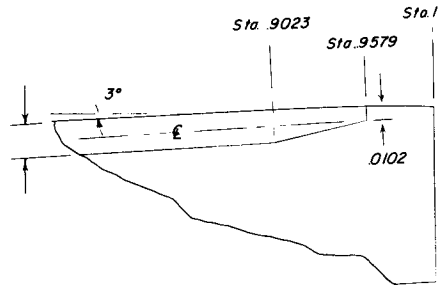

Rudder detail

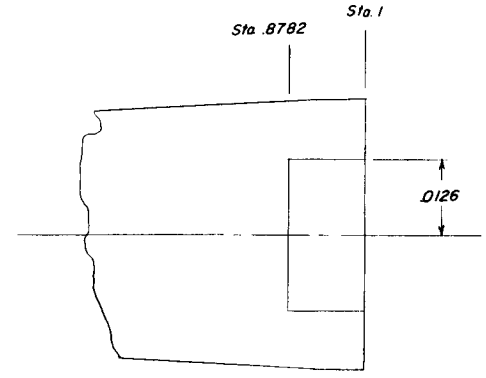

Bottom flap
(projected)

The true flap chord = 0.0130

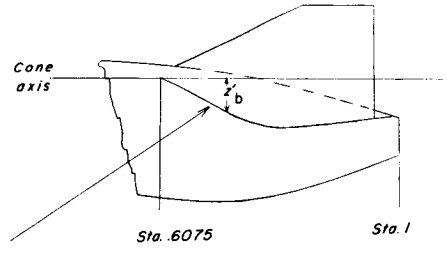

Line of tangents between
side flat and elliptical surfaces

Fus. sta.	z'_b/l
0.6075	0
.7323	.0624
.7564	.0731
.7789	.0794
.8060	.0830
.8300	.0833
.8541	.0821
.8767	.0794
1.0000	.0605

Canopy Coordinates

Fus. sta.	y_b/l
0.0977	0
.1015	.0126
.1053	.0174
.1090	.0211
.1128	.0240
.1504	.0388
.1880	.0427
.2298	.0445
Straight line	
.2707	.0445
.3008	.0435
.3383	.0382
.3759	.0259
.4135	.0067
.4233	0

Fus. sta.	z_b/l	R_3
0.0940	0.0269	0.0085
.0132	.0660	.0340
.1692	.0791	.0415
.2068	.0848	.0442
.2298	.0854	.0451
Constant section		
.3008	.0838	.0439
.3383	.0762	.0406
.3759	.0626	.0260
.4135	.0408	.0064
.4286	.0029	0

Figure 3.- Concluded.

[redacted]

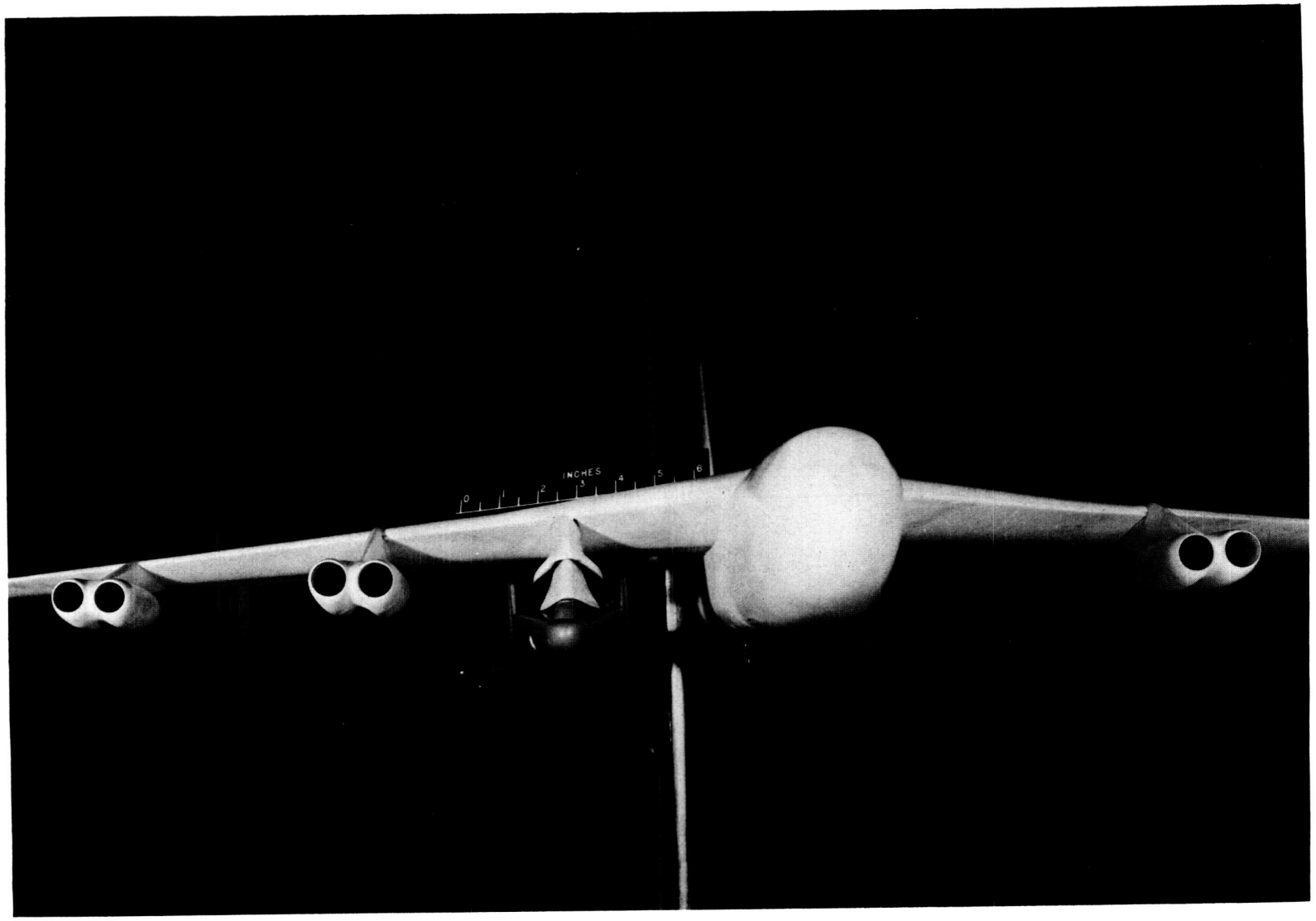

(a) Front view.

L-65-4664

Figure 4.- Photograph of models in wind tunnel.

[redacted]

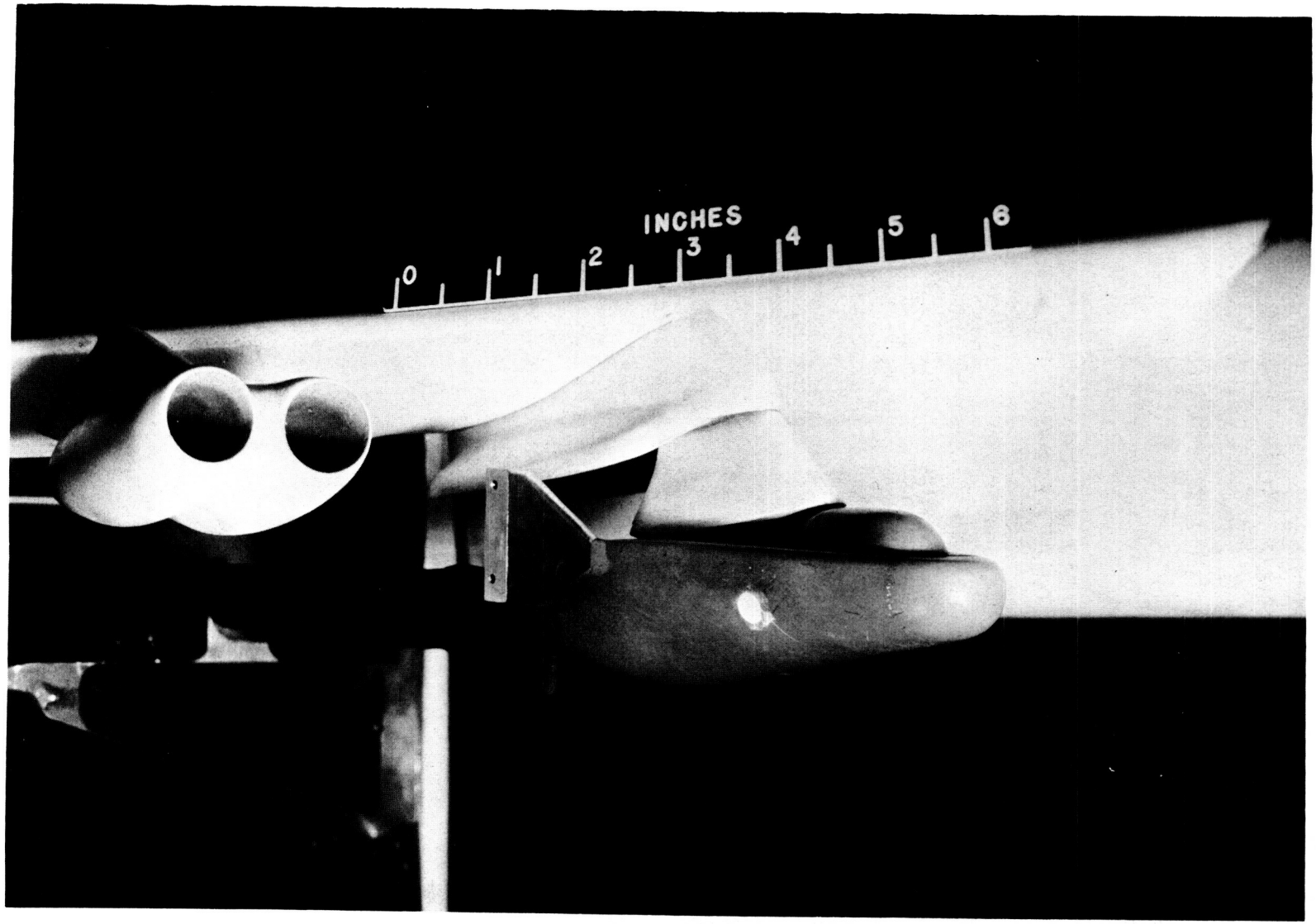

(b) Three-quarter front view.

L-65-4661

Figure 4.- Continued.

[redacted]

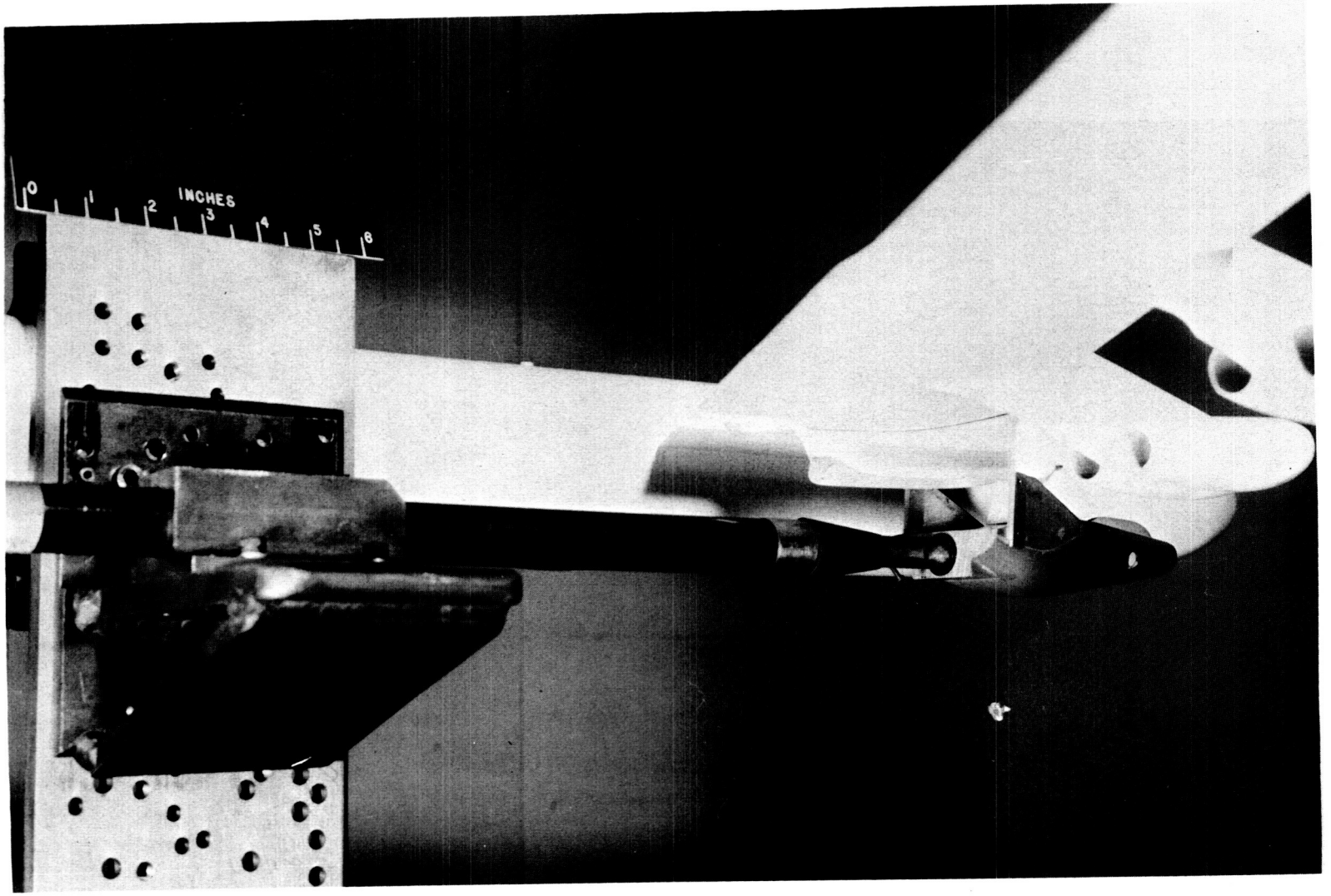

(c) Three-quarter rear view.

L-65-4662

Figure 4.- Continued.

[redacted]

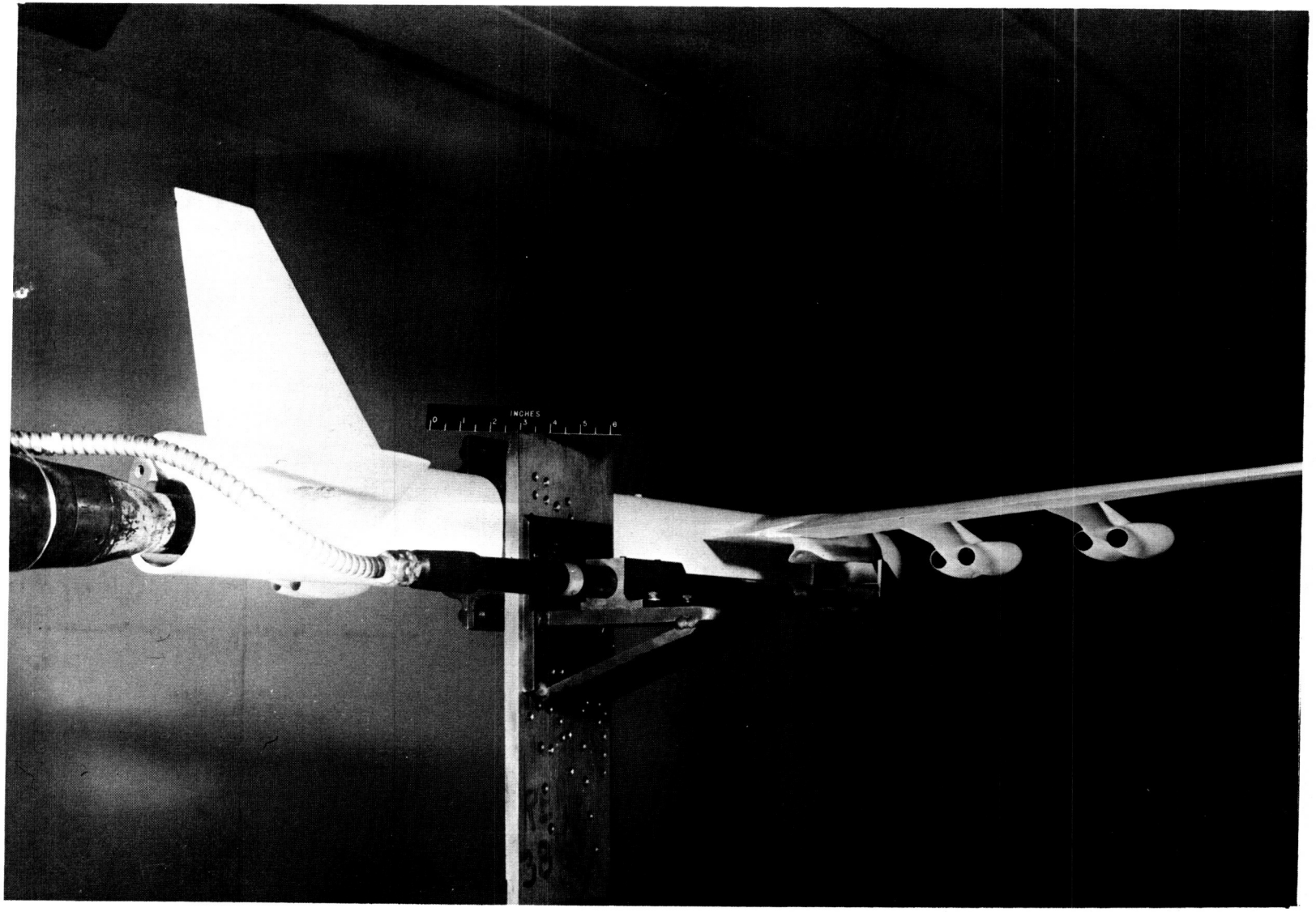

(d) One-quarter rear view.

L-65-4665

Figure 4.- Concluded.

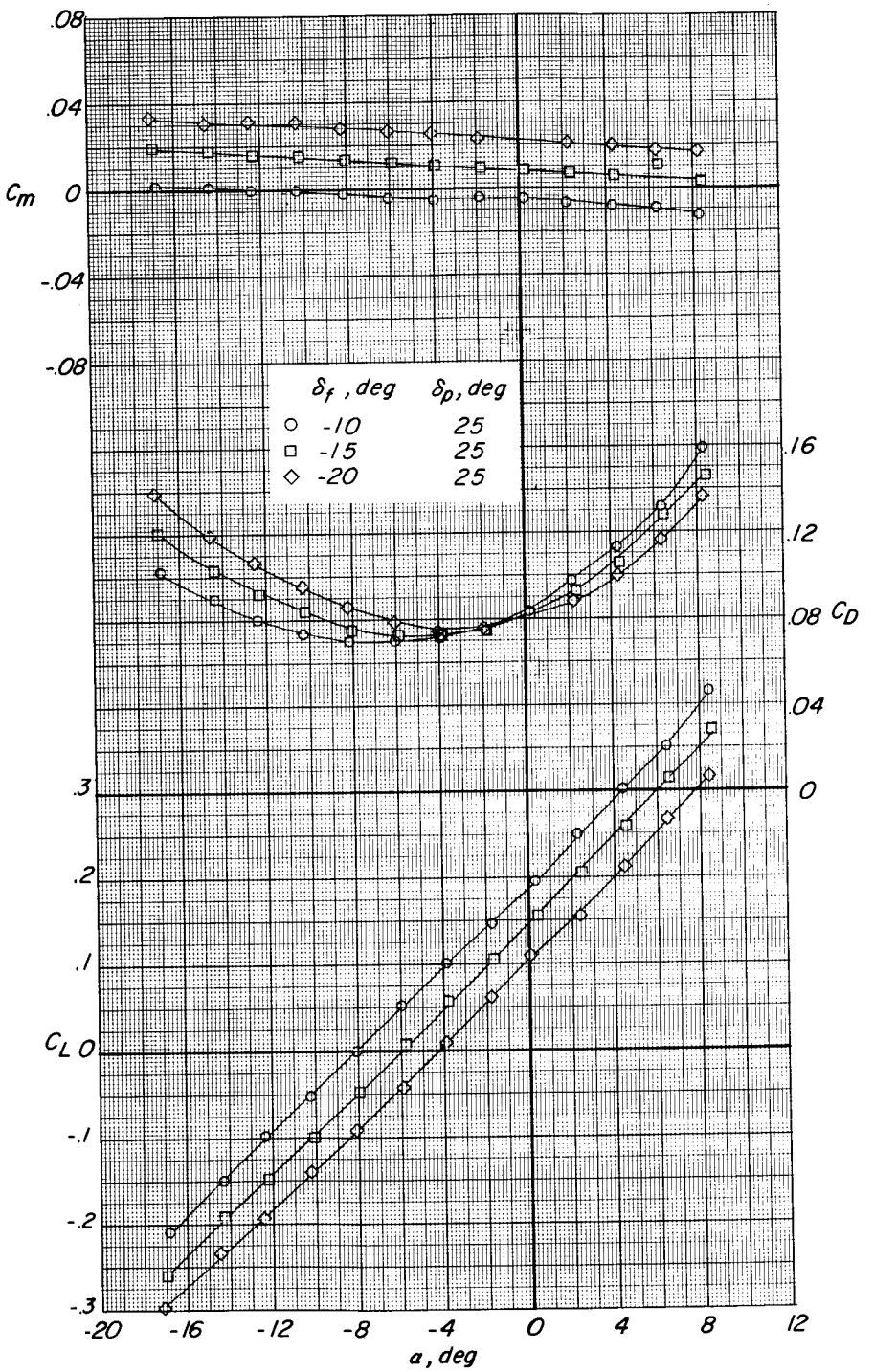

(a) M = 0.60.

Figure 5.- Aerodynamic characteristics of M2-F2 vehicle alone. Nominal control settings are $\delta_p = 25^0$, $\delta_f = -10^0$, and 10^0 rudder flare.

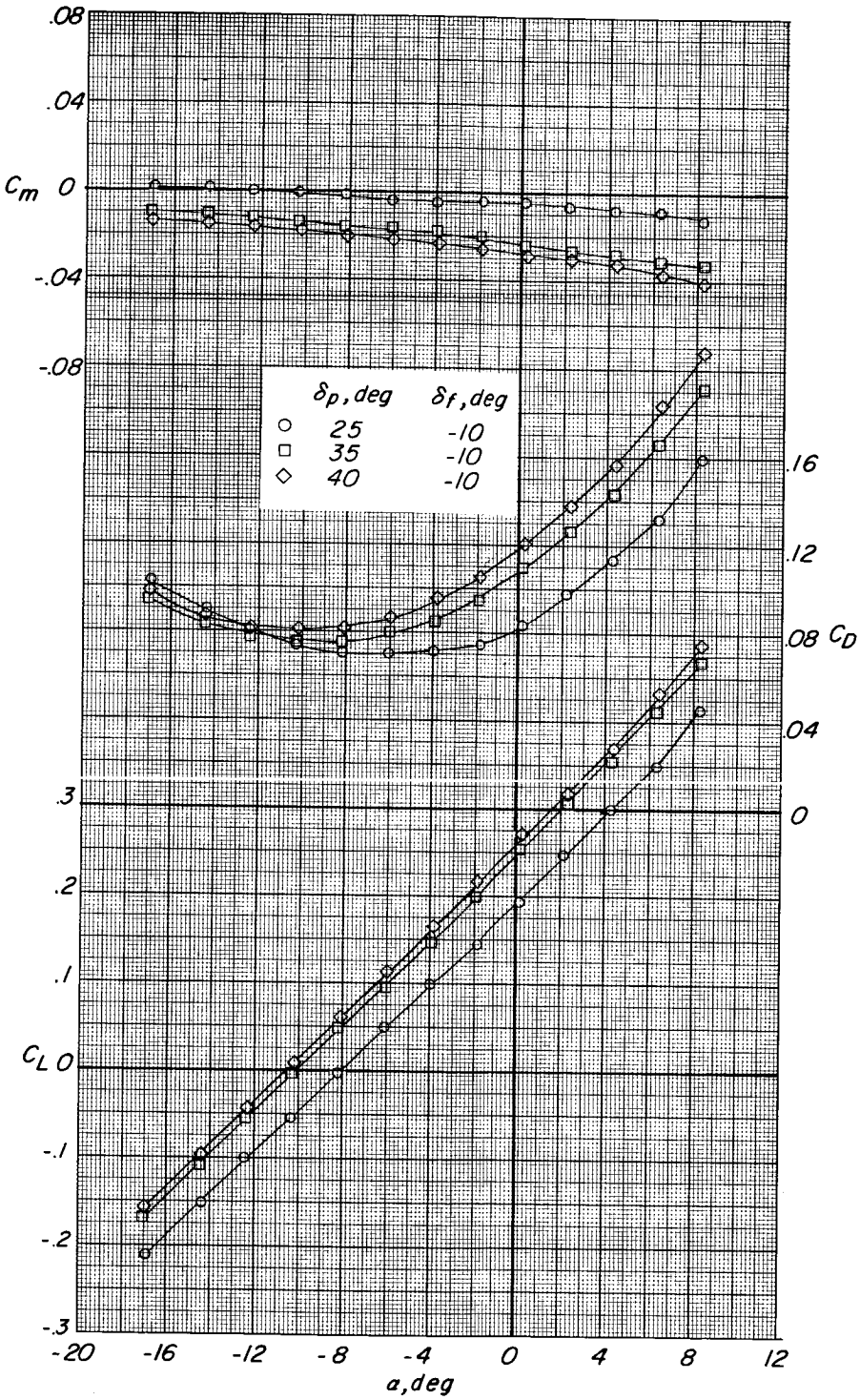

(a) Continued.

Figure 5.- Continued.

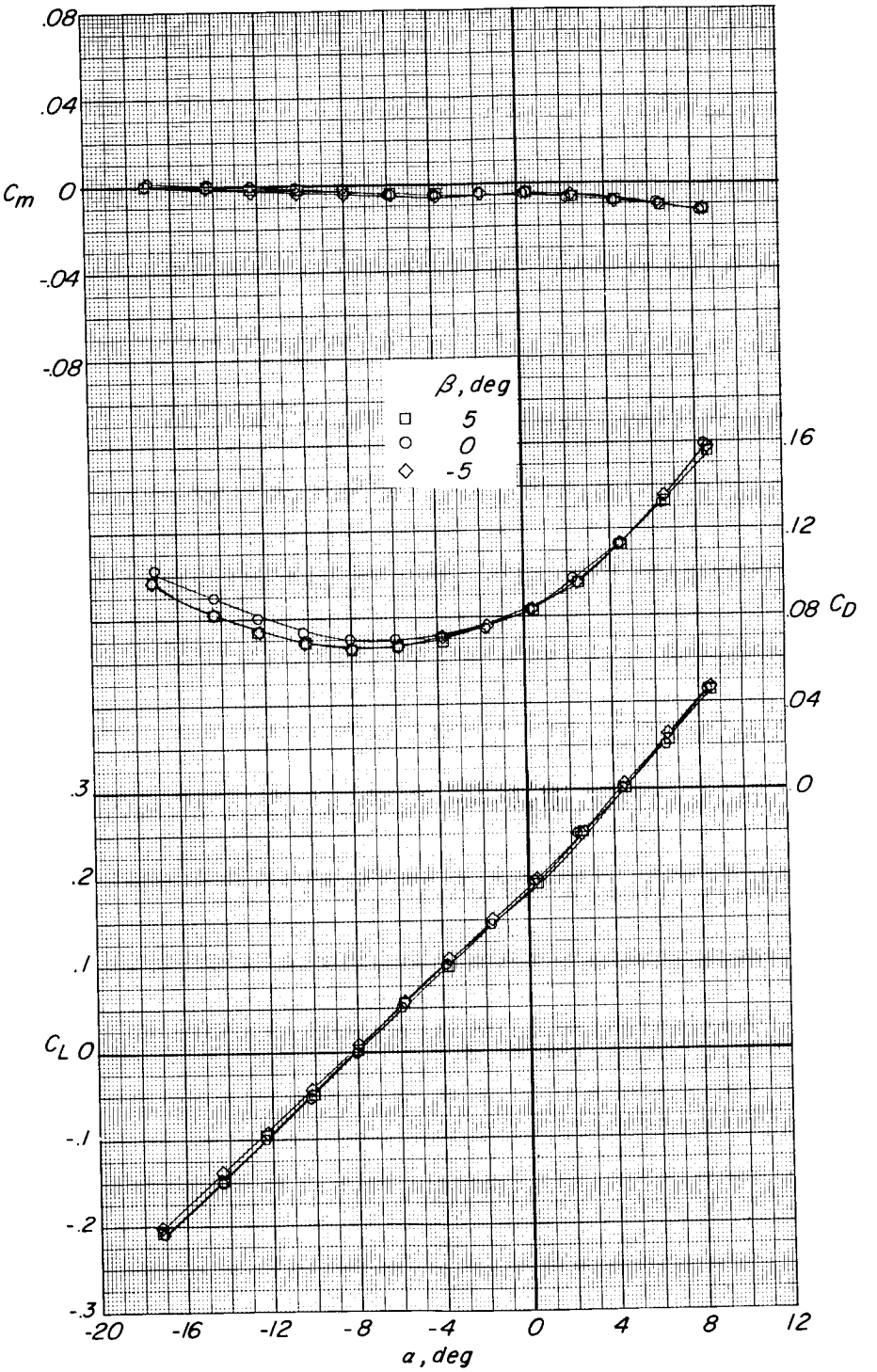

(a) Continued.

Figure 5.- Continued.

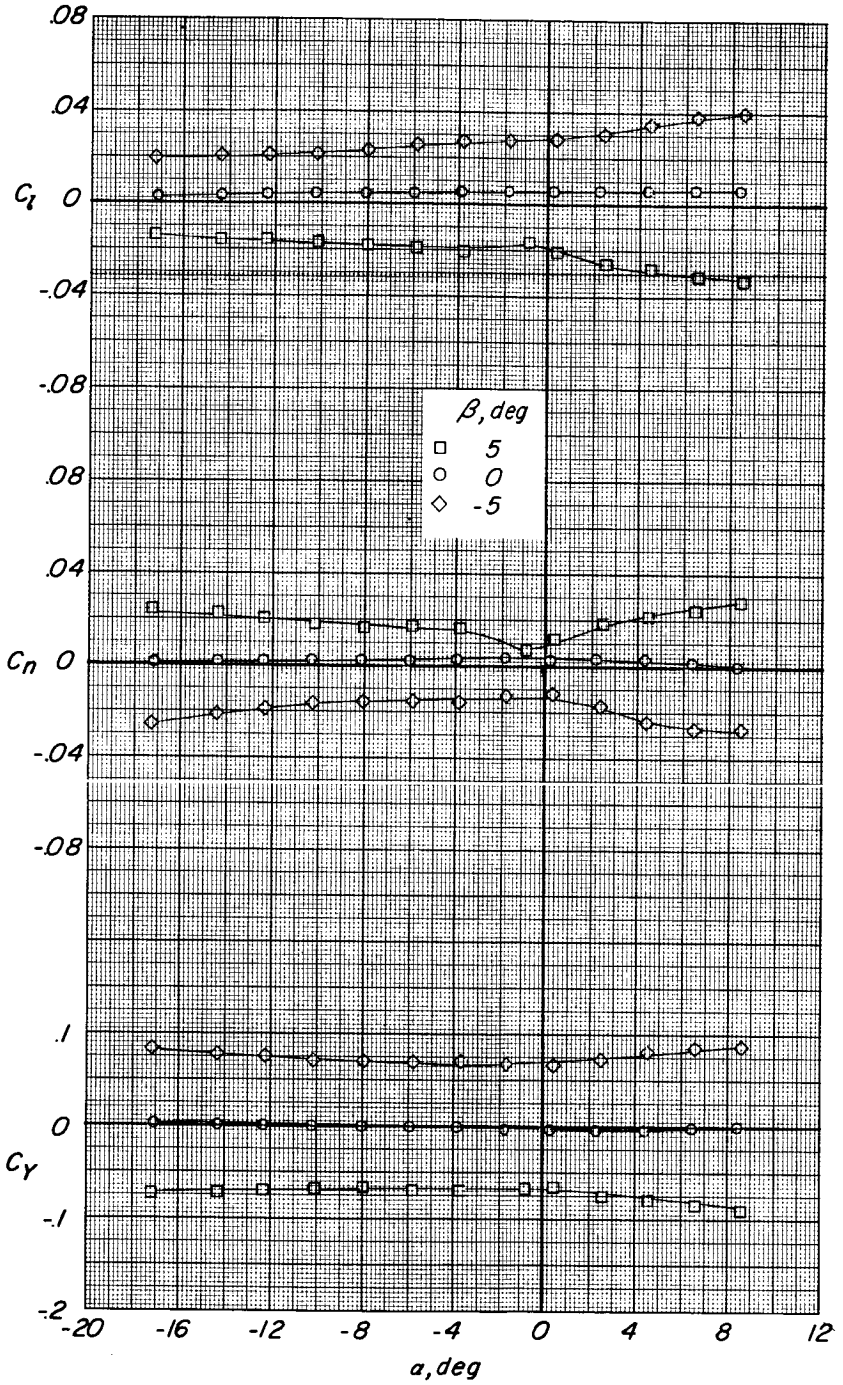

(a) Continued.

Figure 5.- Continued.

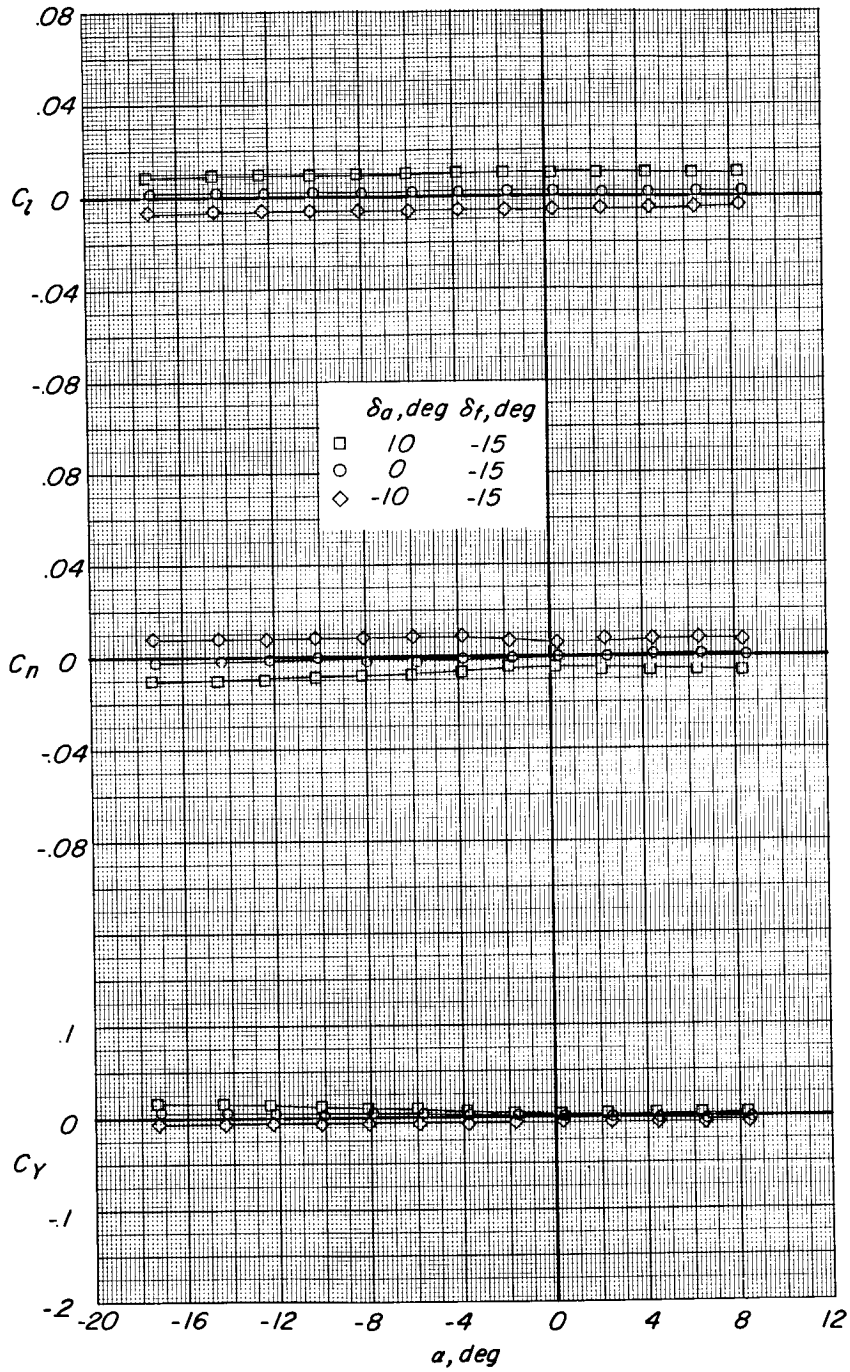

(a) Continued.

Figure 5.- Continued.

[redacted] DECLASSIFIED

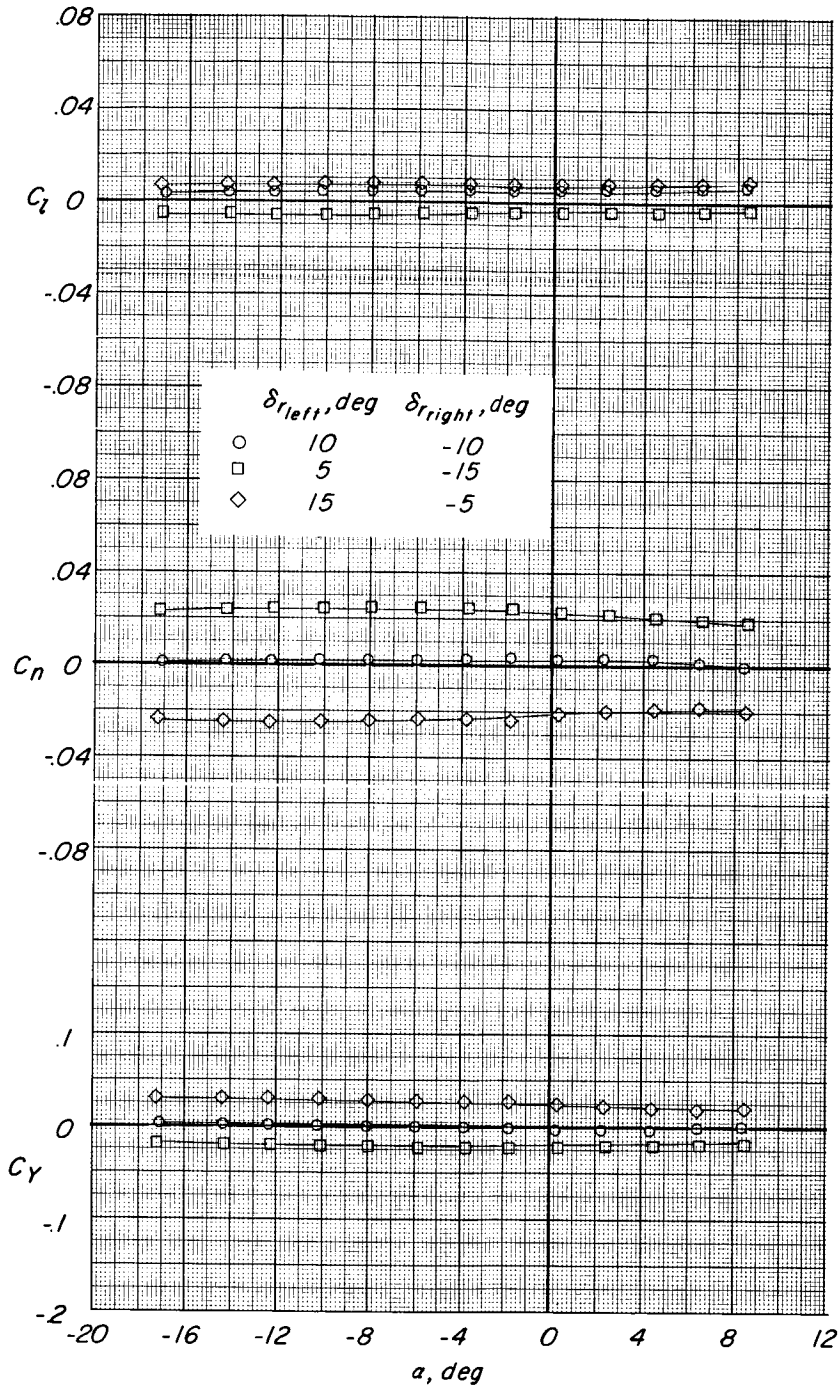

(a) Continued.

Figure 5.- Continued.

[redacted]

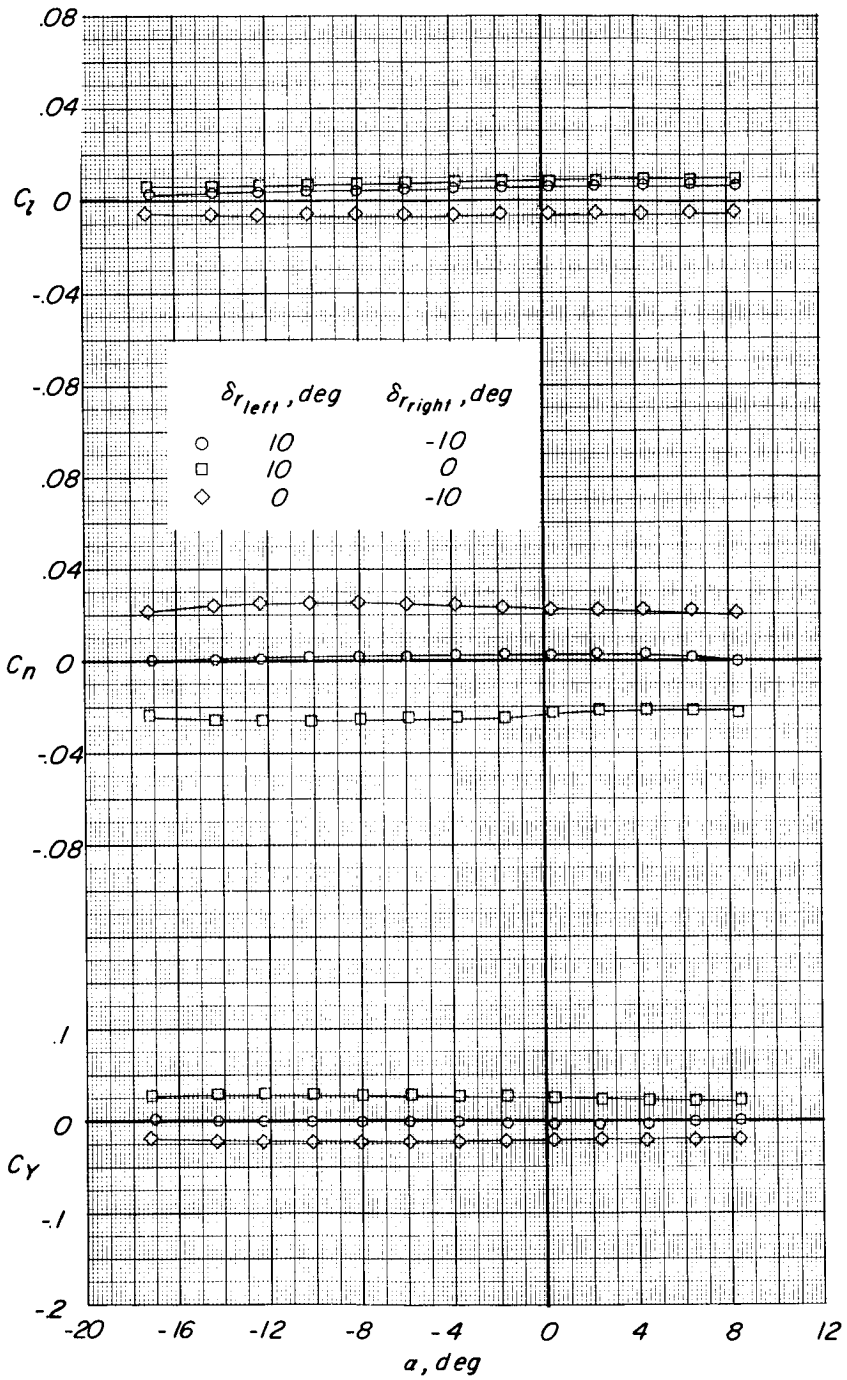

(a) Concluded.

Figure 5.- Continued.

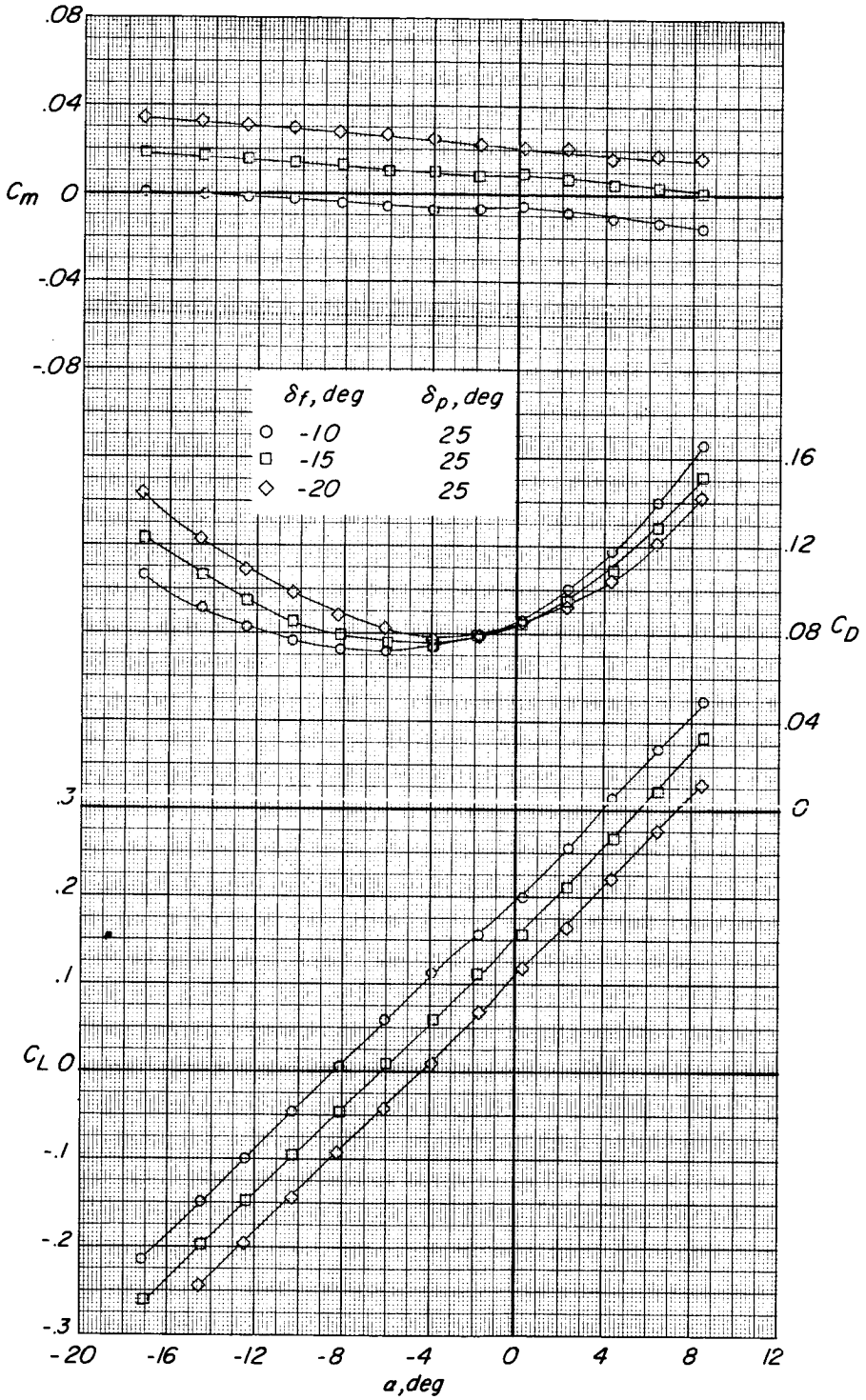

(b) M = 0.70.

Figure 5.- Continued.

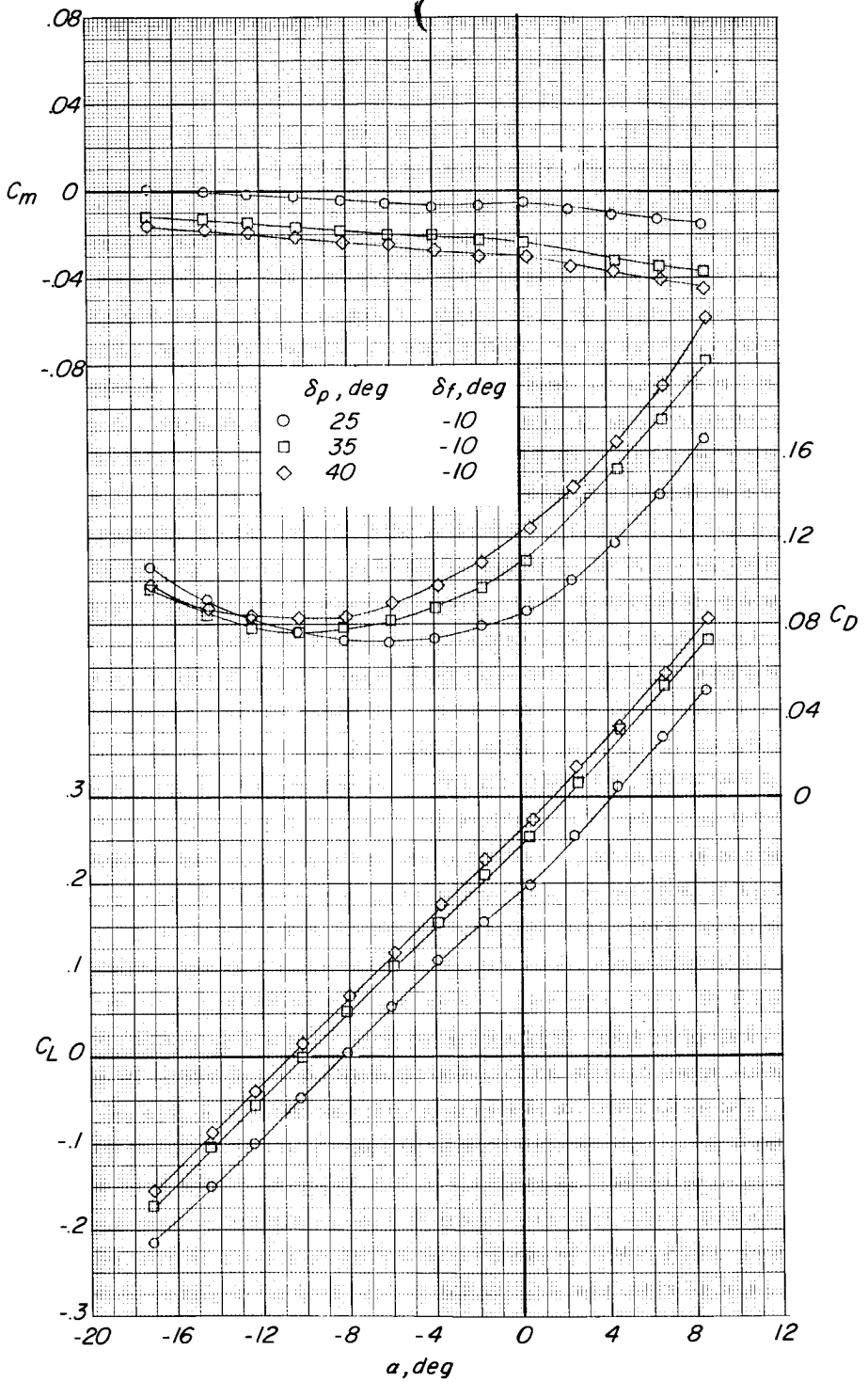

(b) Continued.

Figure 5.- Continued.

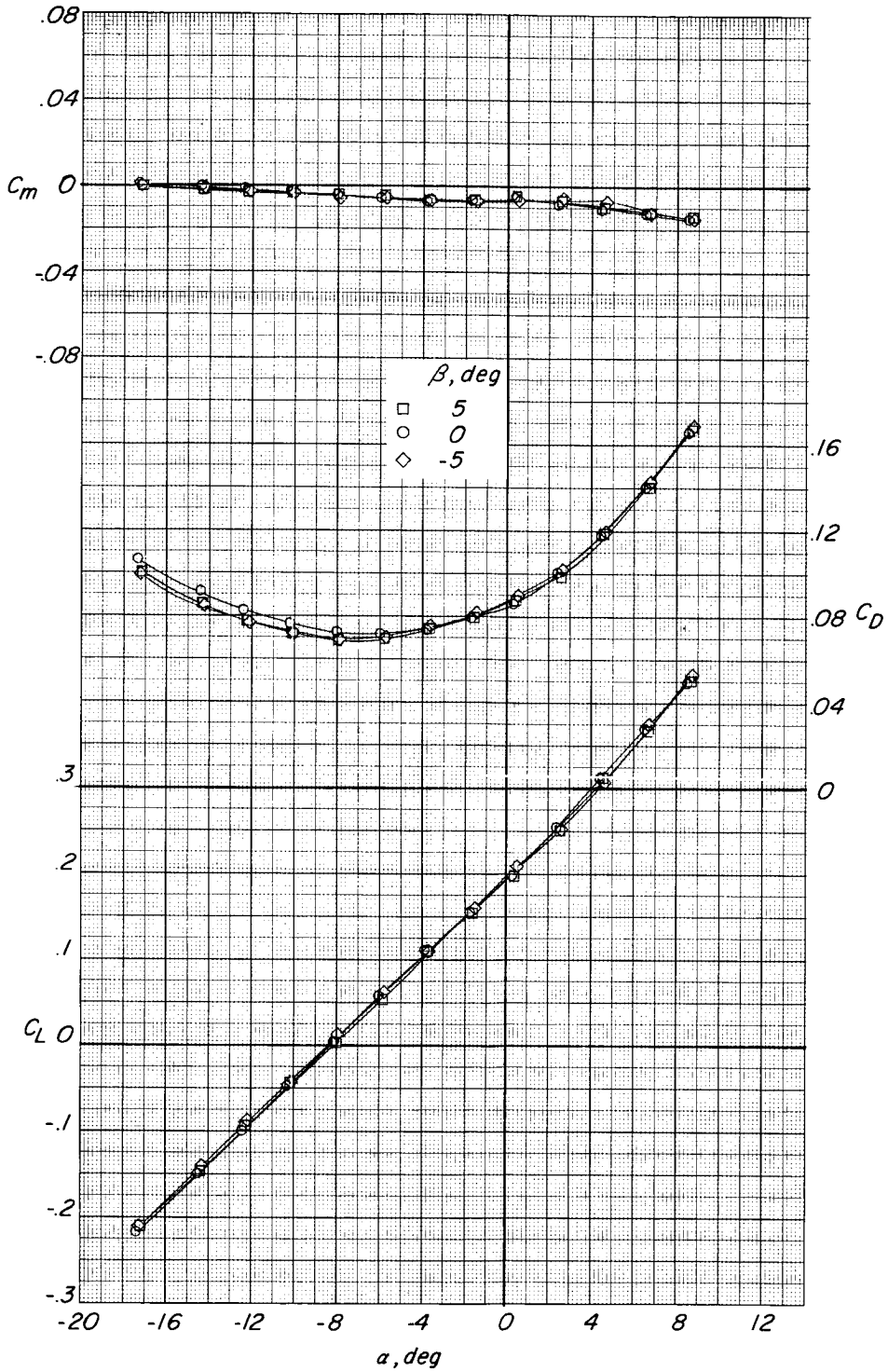

(b) Continued.

Figure 5.- Continued.

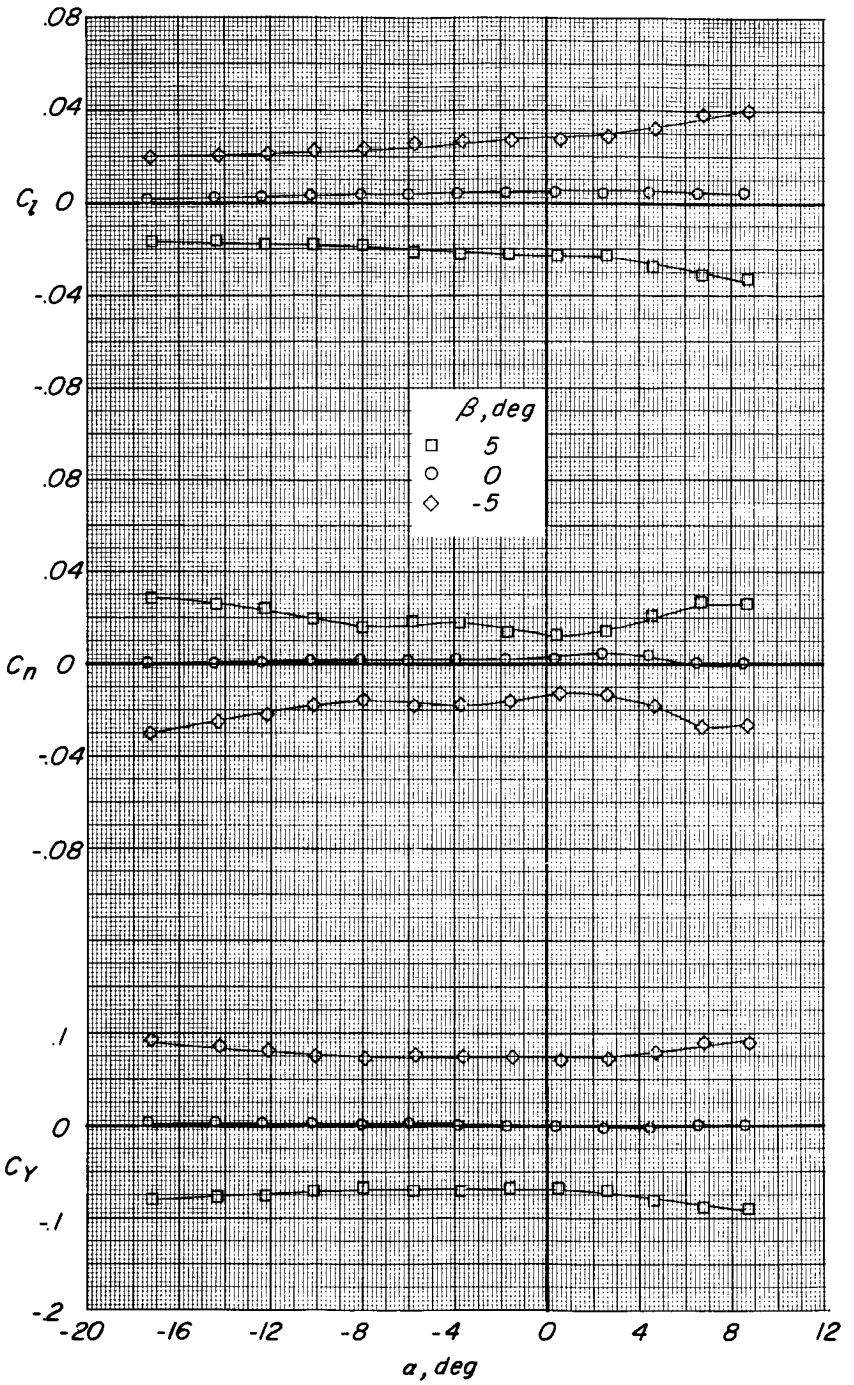

(b) Continued.

Figure 5.- Continued.

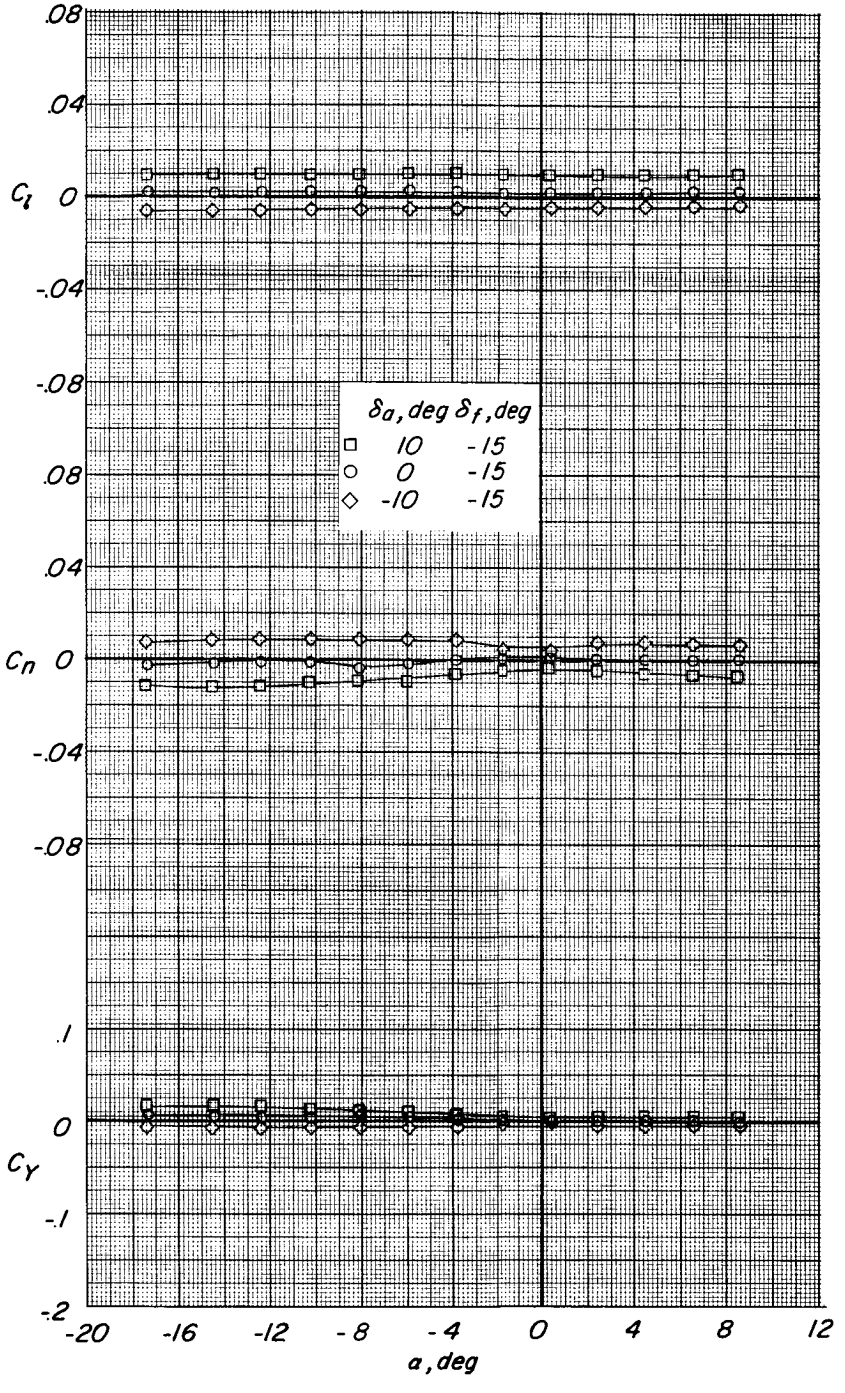

(b) Continued.

Figure 5.- Continued.

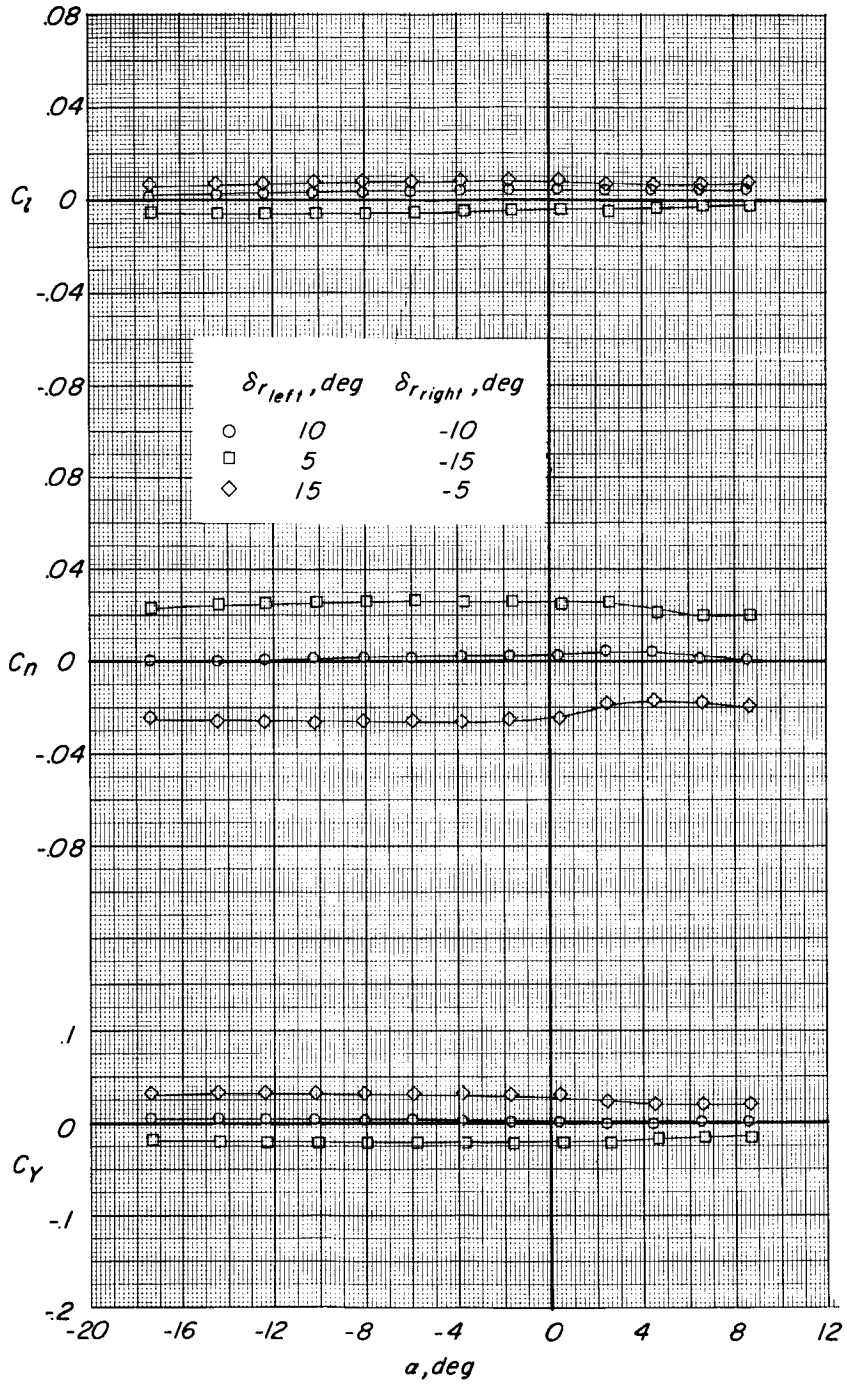

(b) Continued.

Figure 5.- Continued.

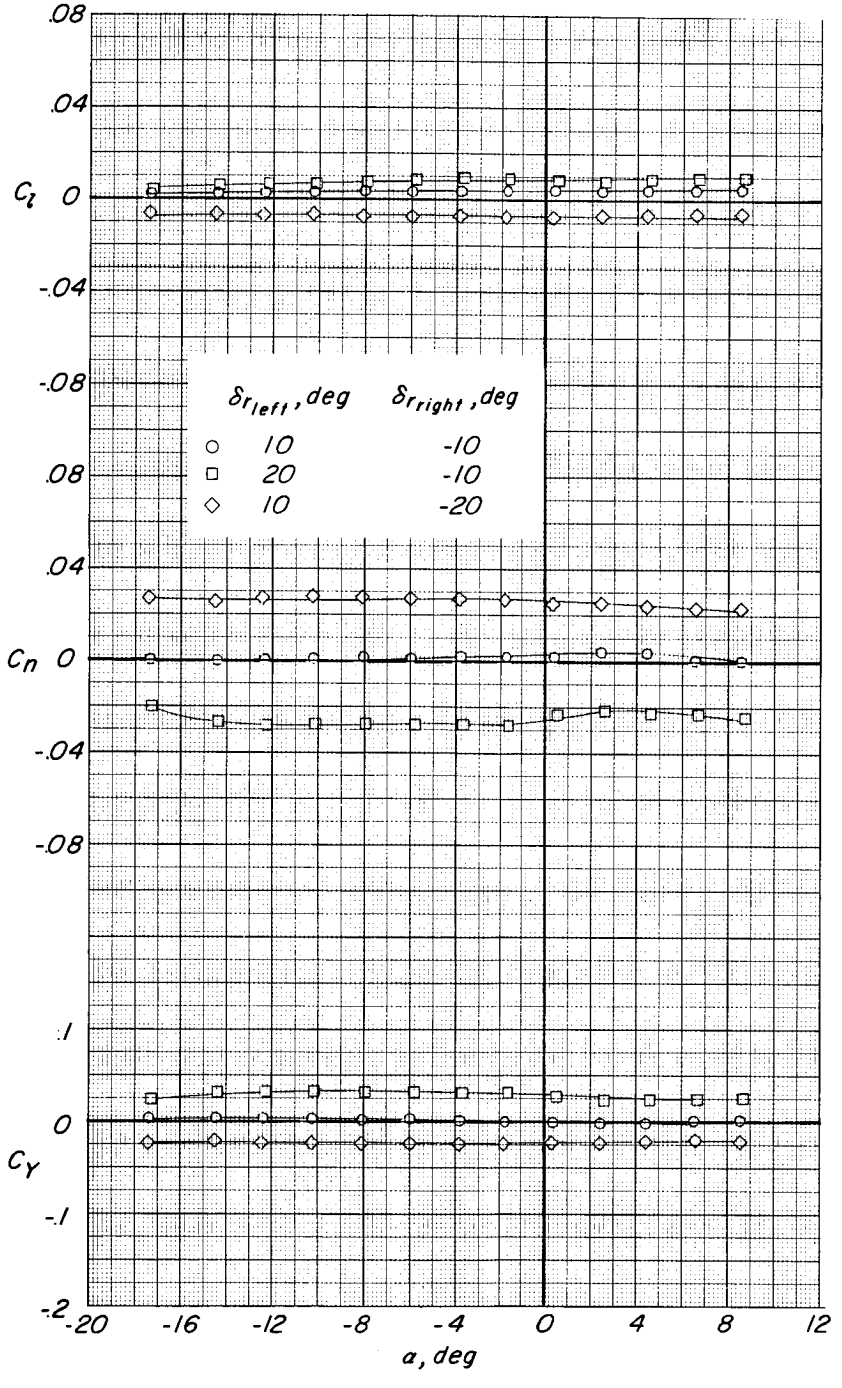

(b) Concluded.

Figure 5.- Continued.

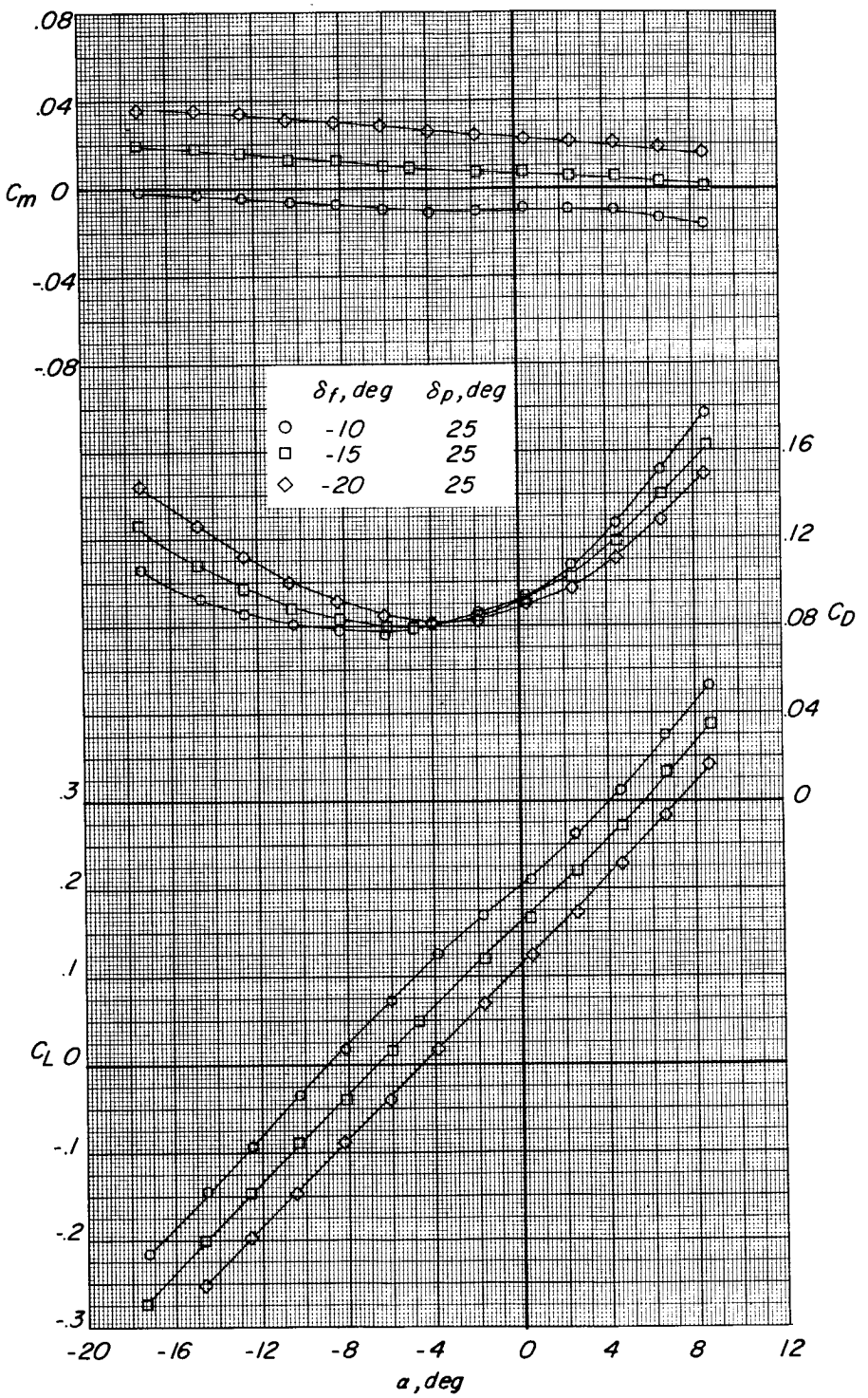

(c) M = 0.80.

Figure 5.- Continued.

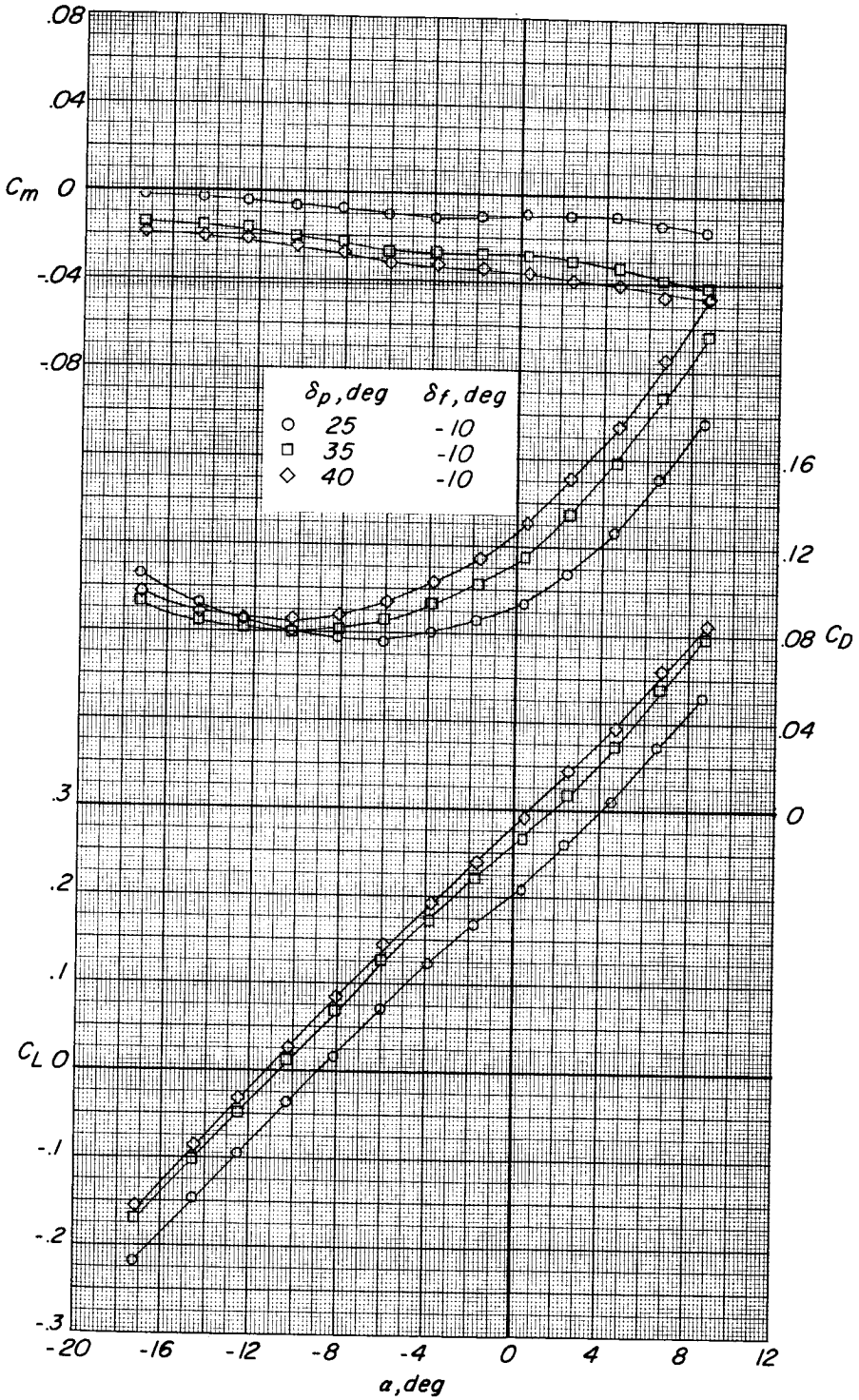

(c) Continued.

Figure 5.- Continued.

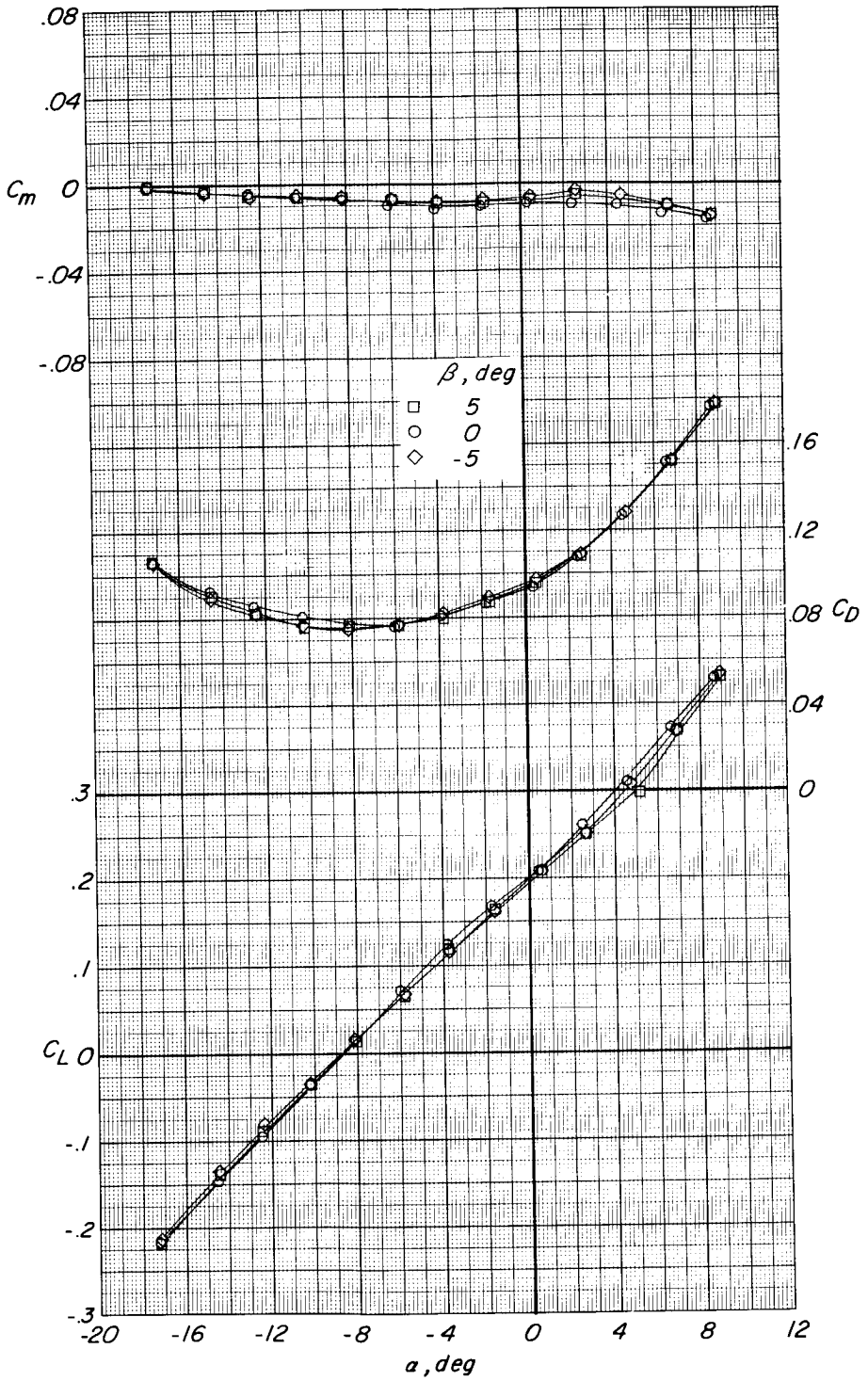

(c) Continued.

Figure 5.- Continued.

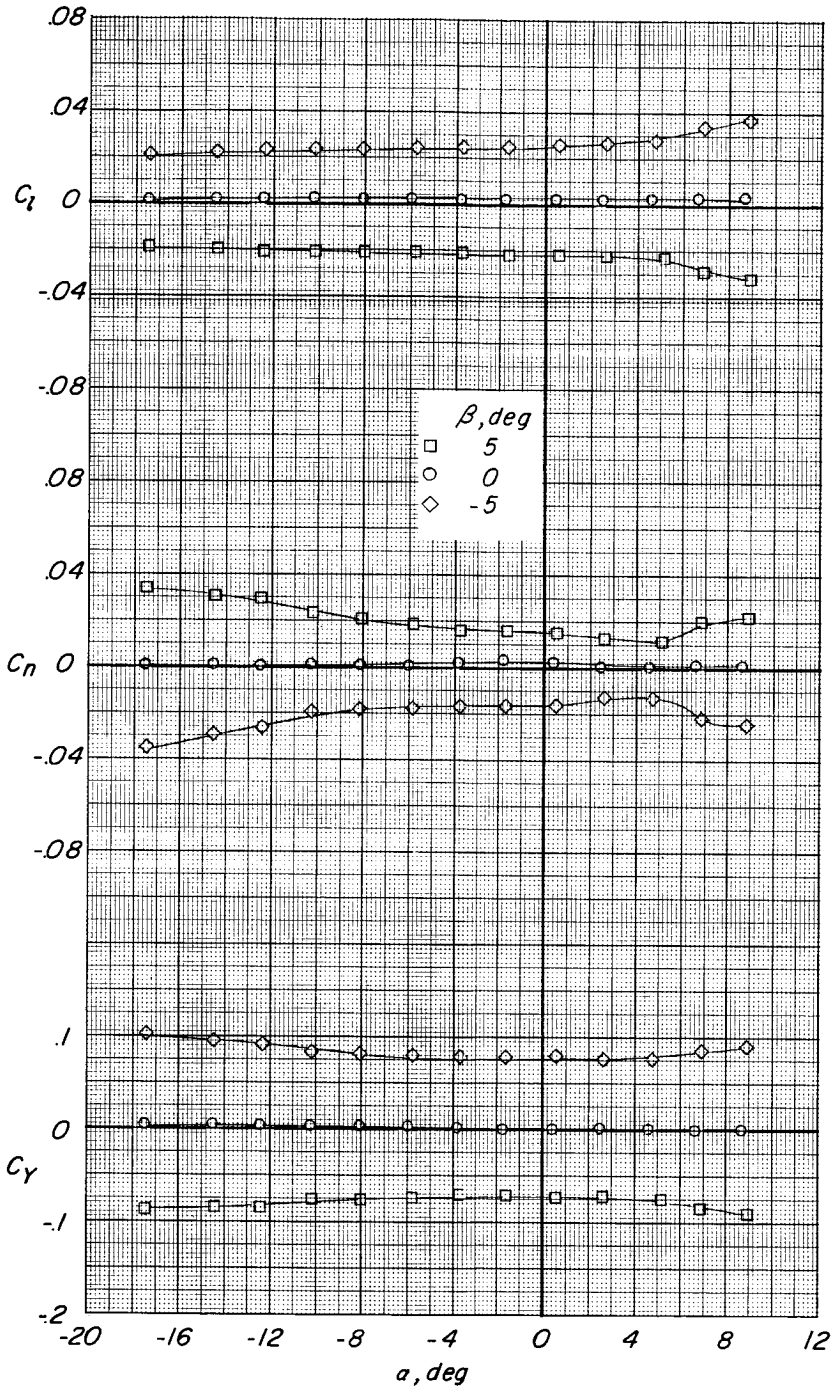

(c) Continued.

Figure 5.- Continued.

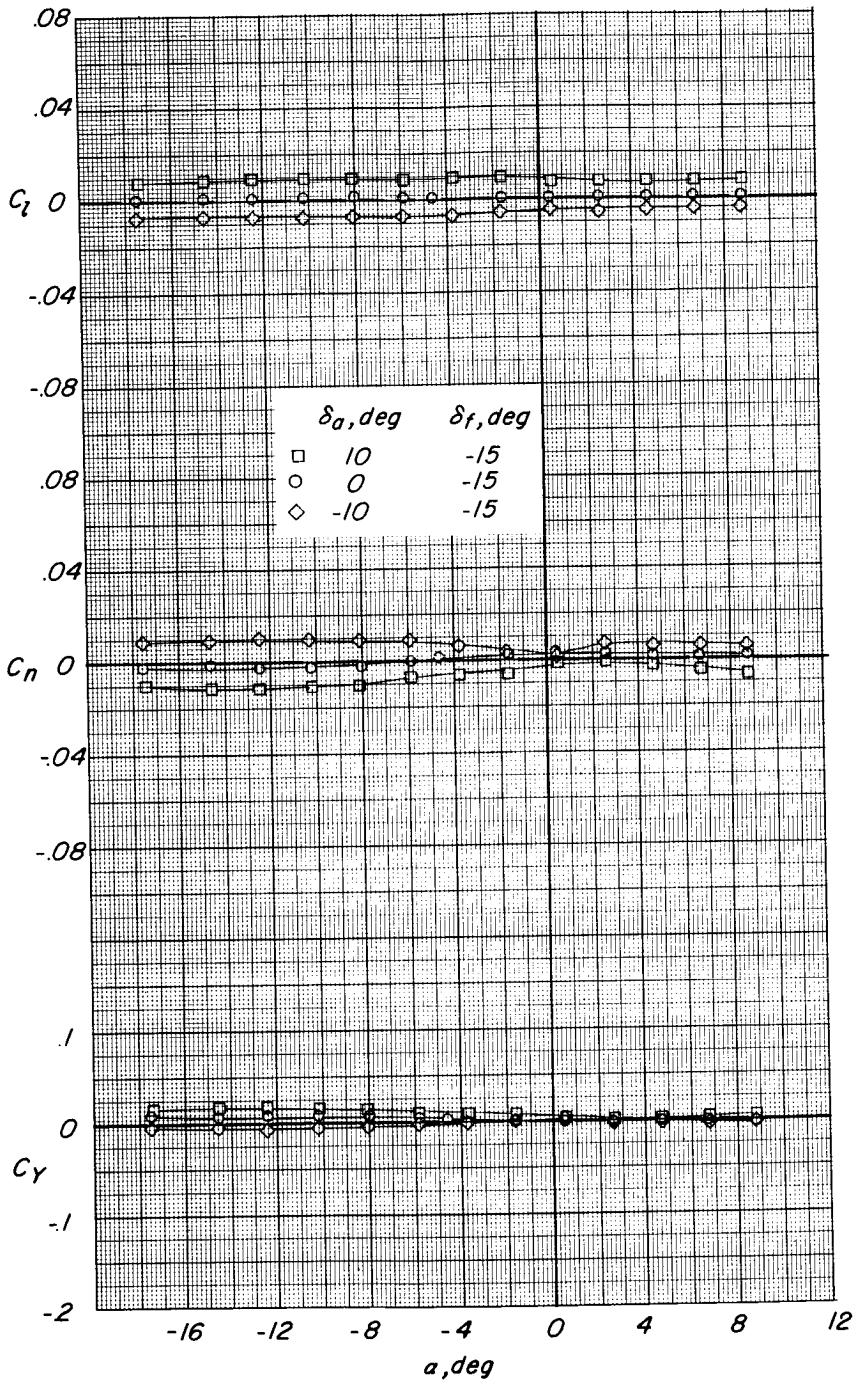

(c) Continued.

Figure 5.- Continued.

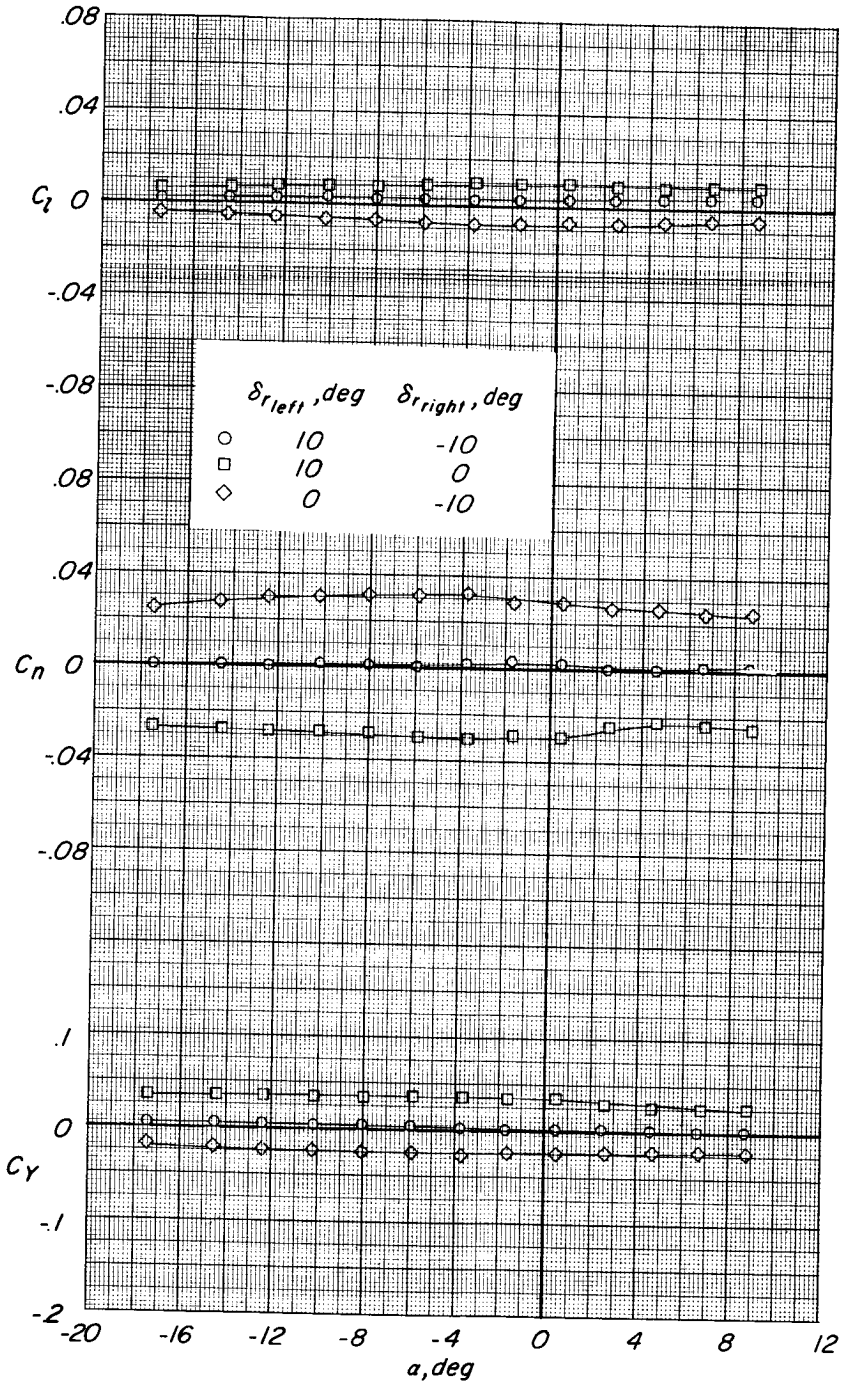

(c) Continued.

Figure 5.- Continued.

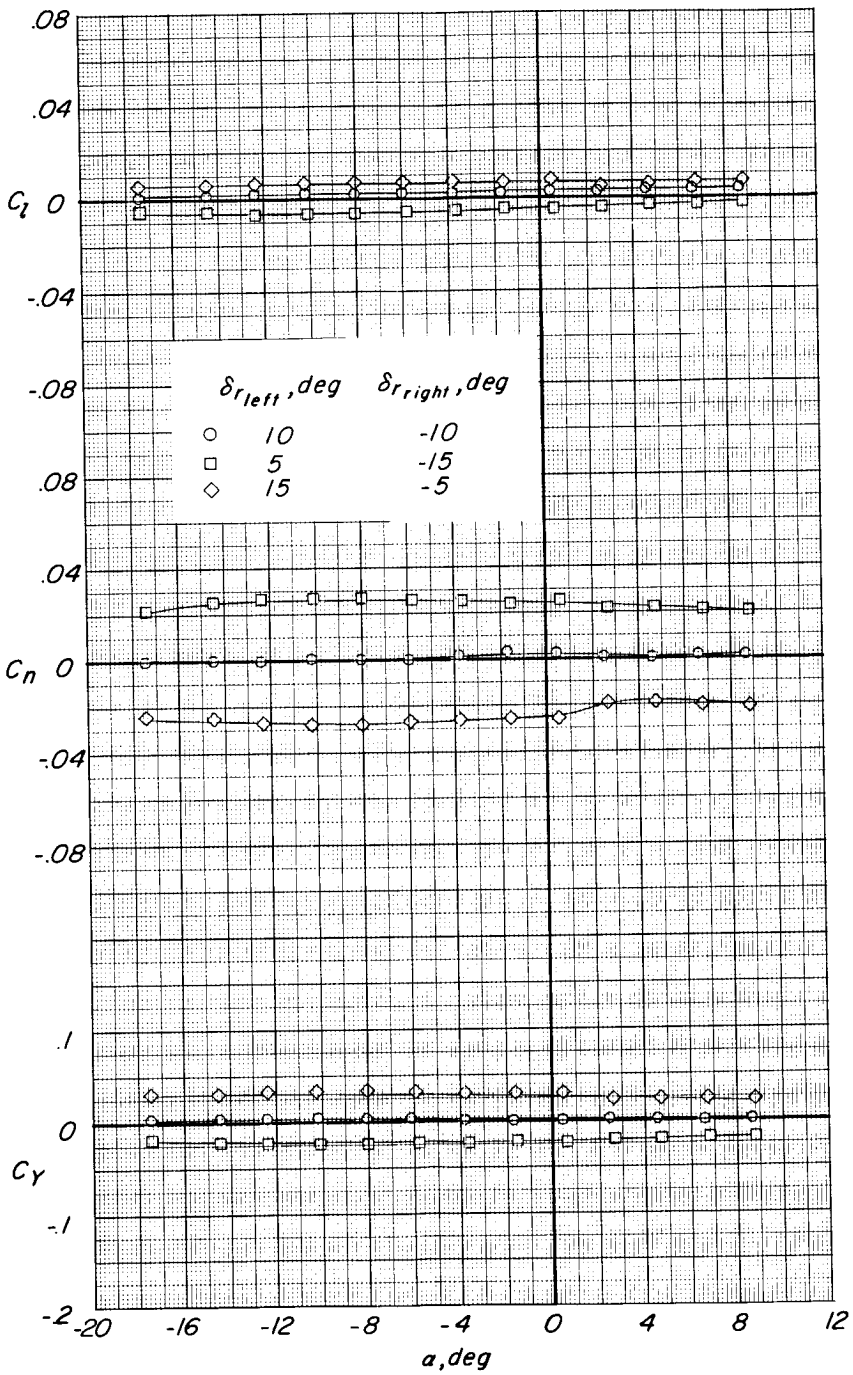

(c) Concluded.

Figure 5.- Continued.

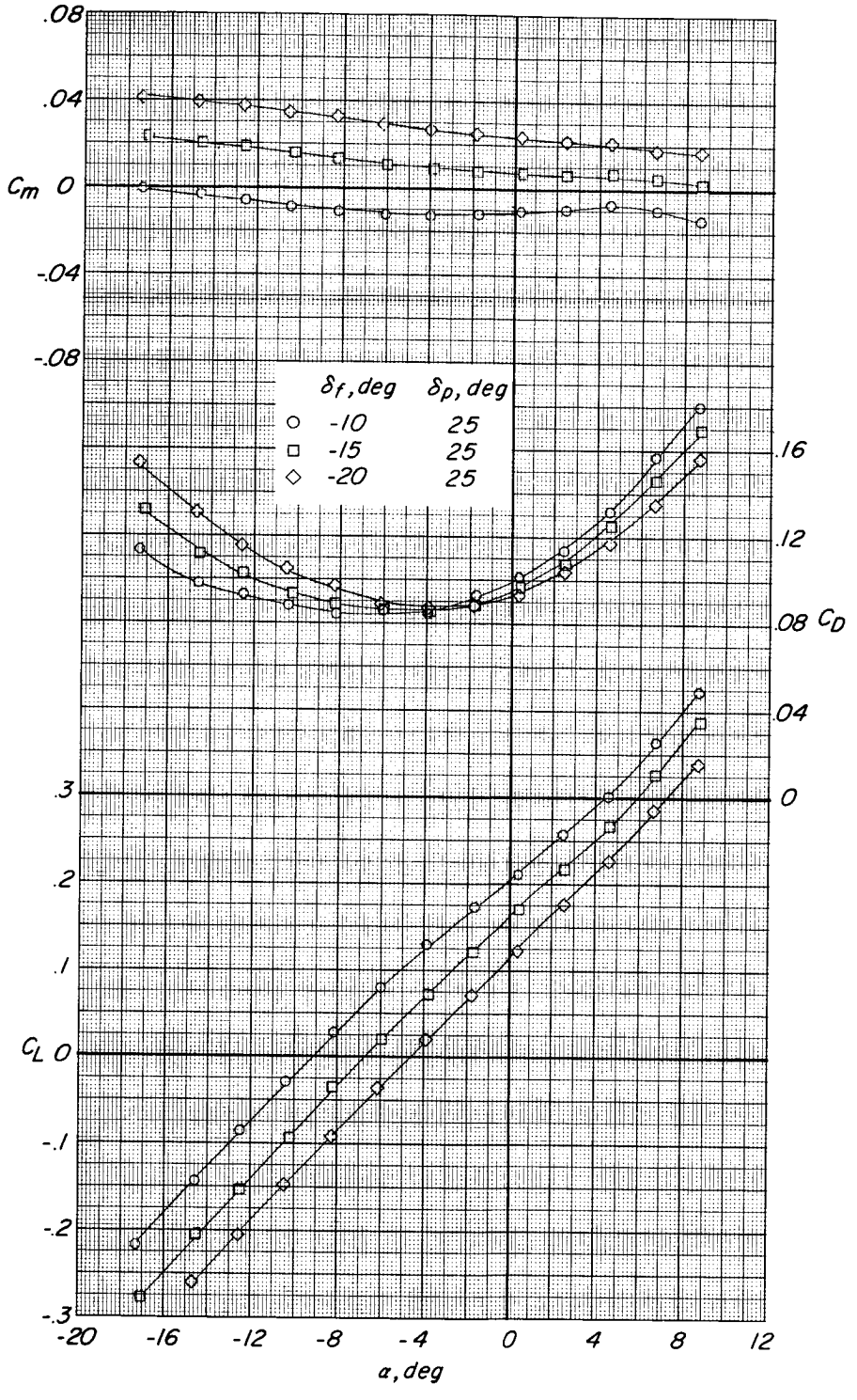

(d) M = 0.85.

Figure 5.- Continued.

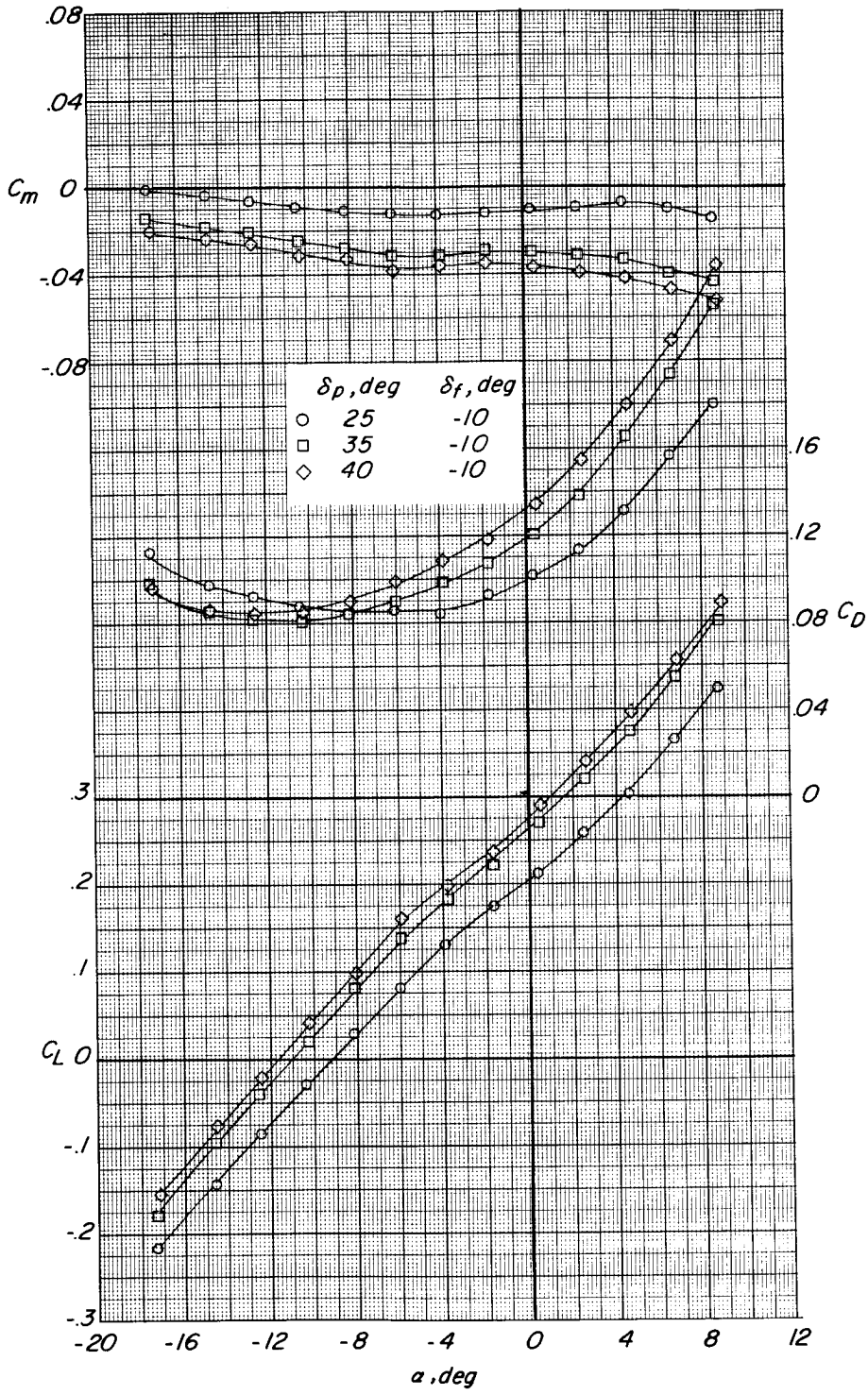

(d) Continued.

Figure 5.- Continued.

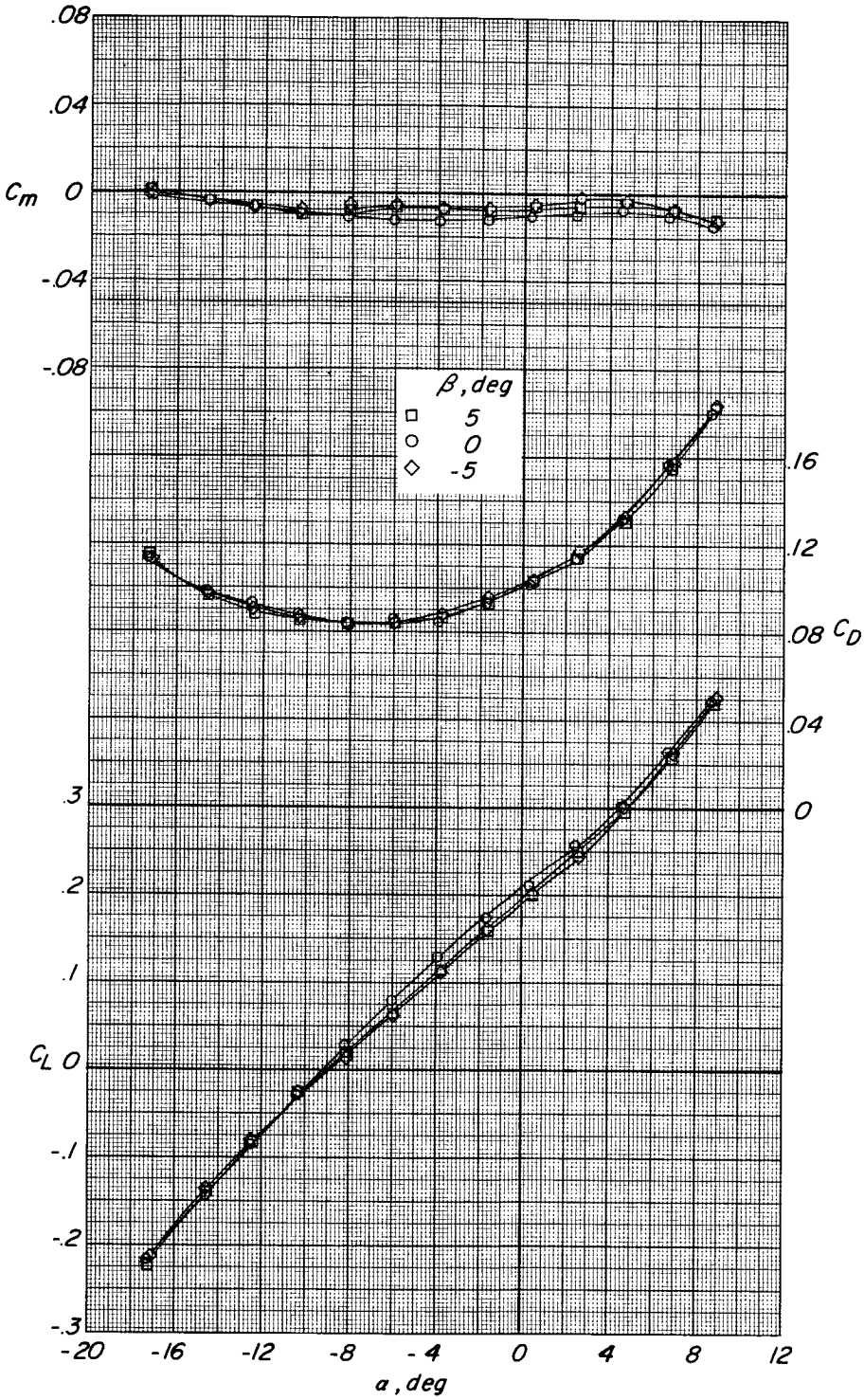

(d) Continued.

Figure 5.- Continued.

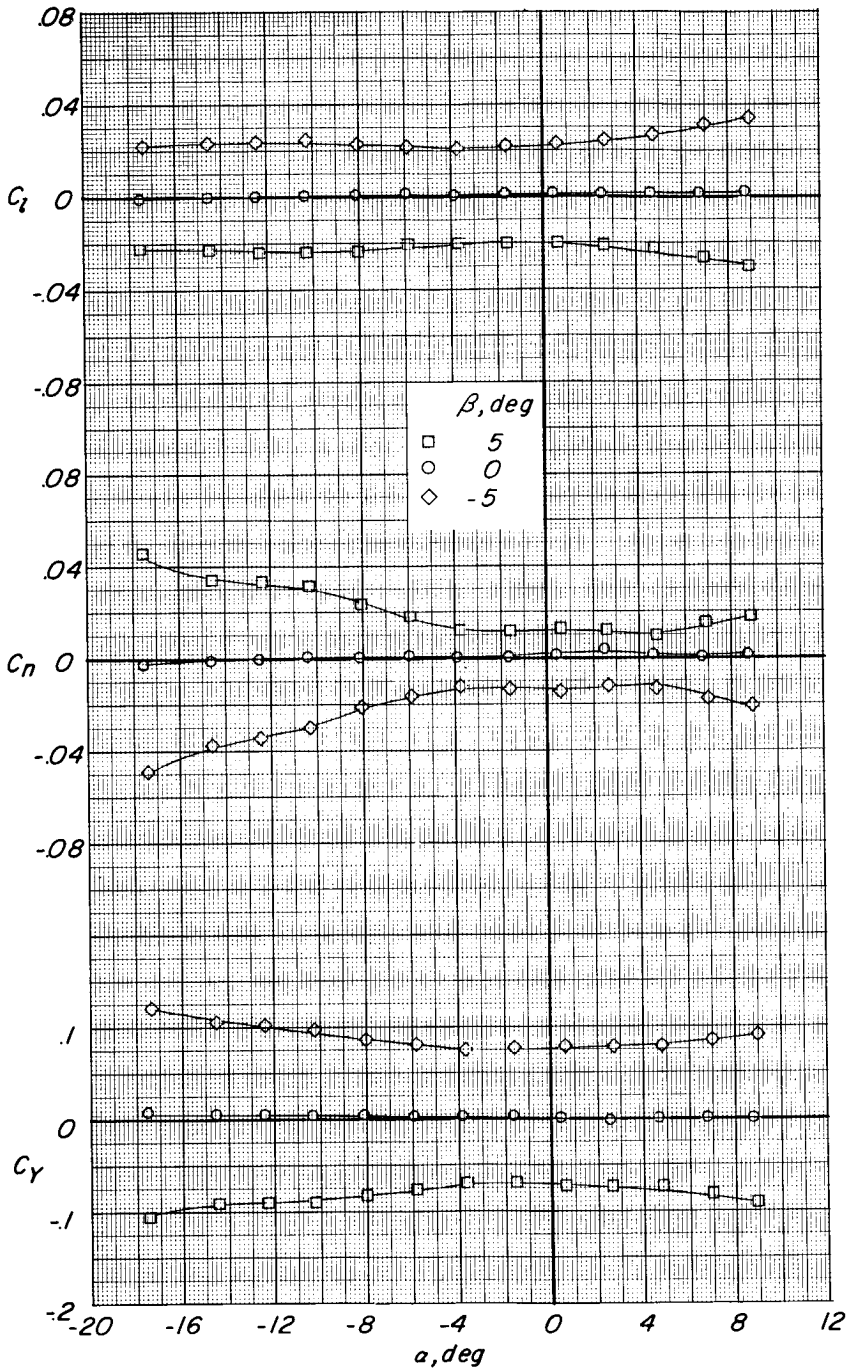

(d) Continued.

Figure 5.- Continued.

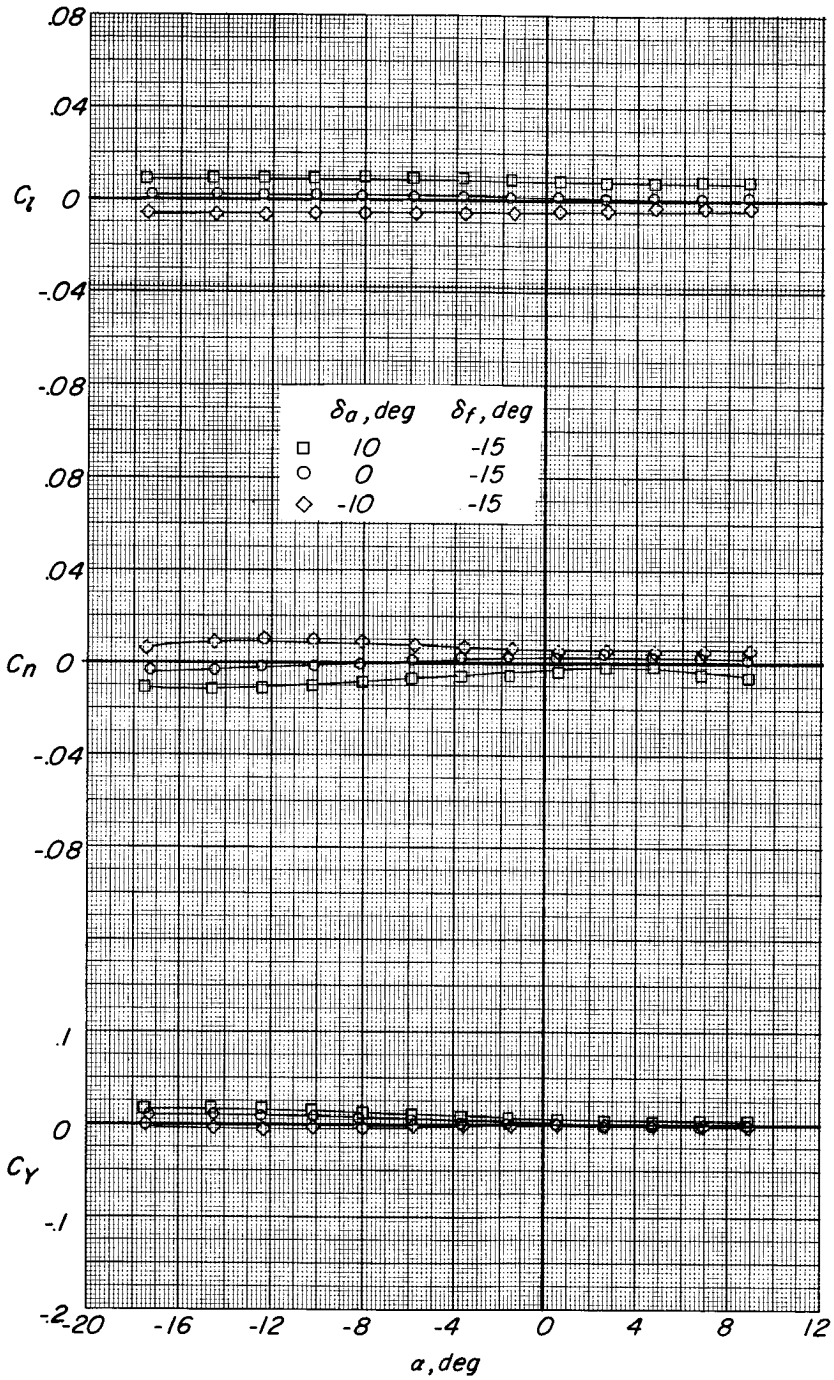

(d) Continued.

Figure 5.- Continued.

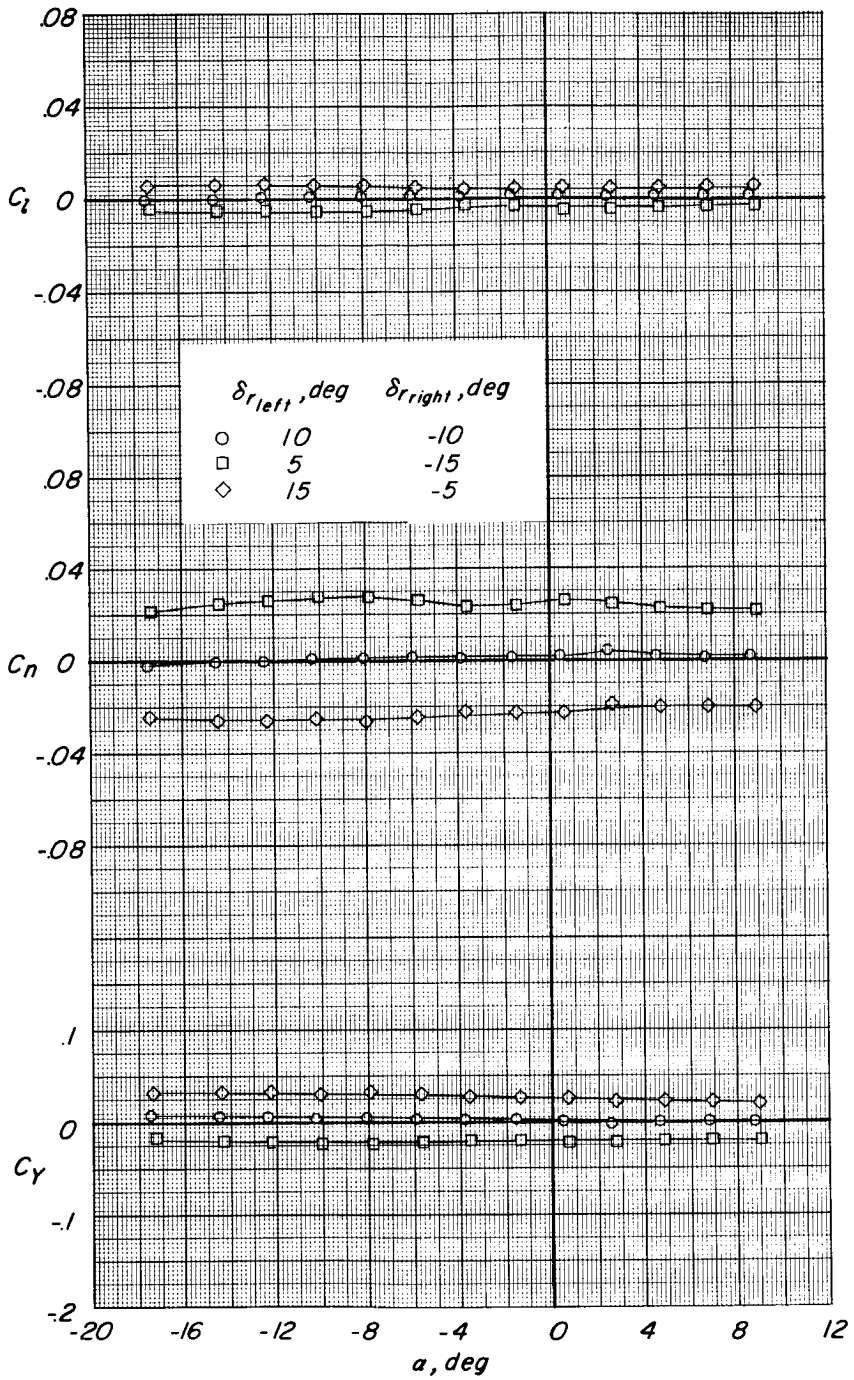

(d) Continued.

Figure 5.- Continued.

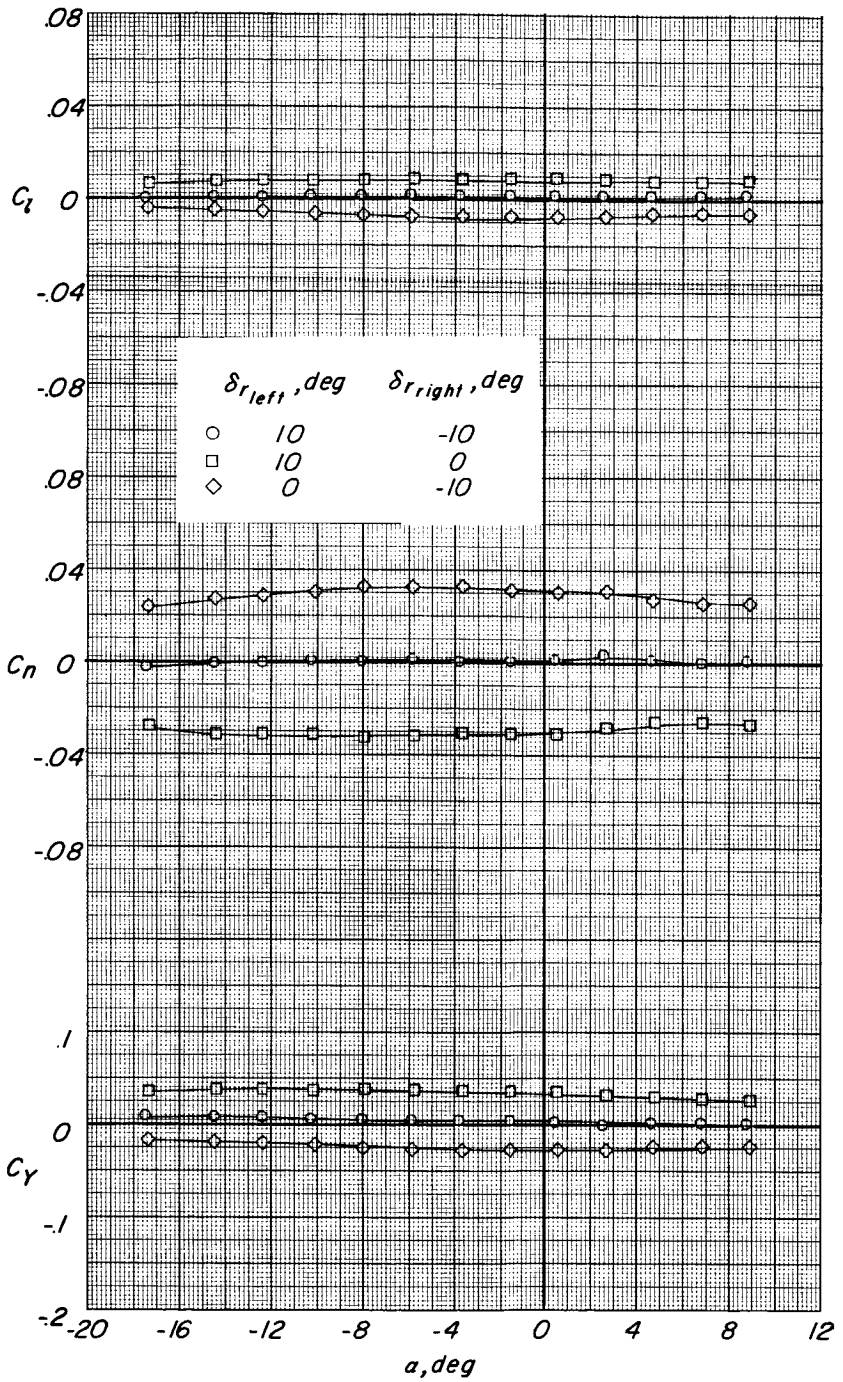

(d) Concluded.

Figure 5.- Concluded.

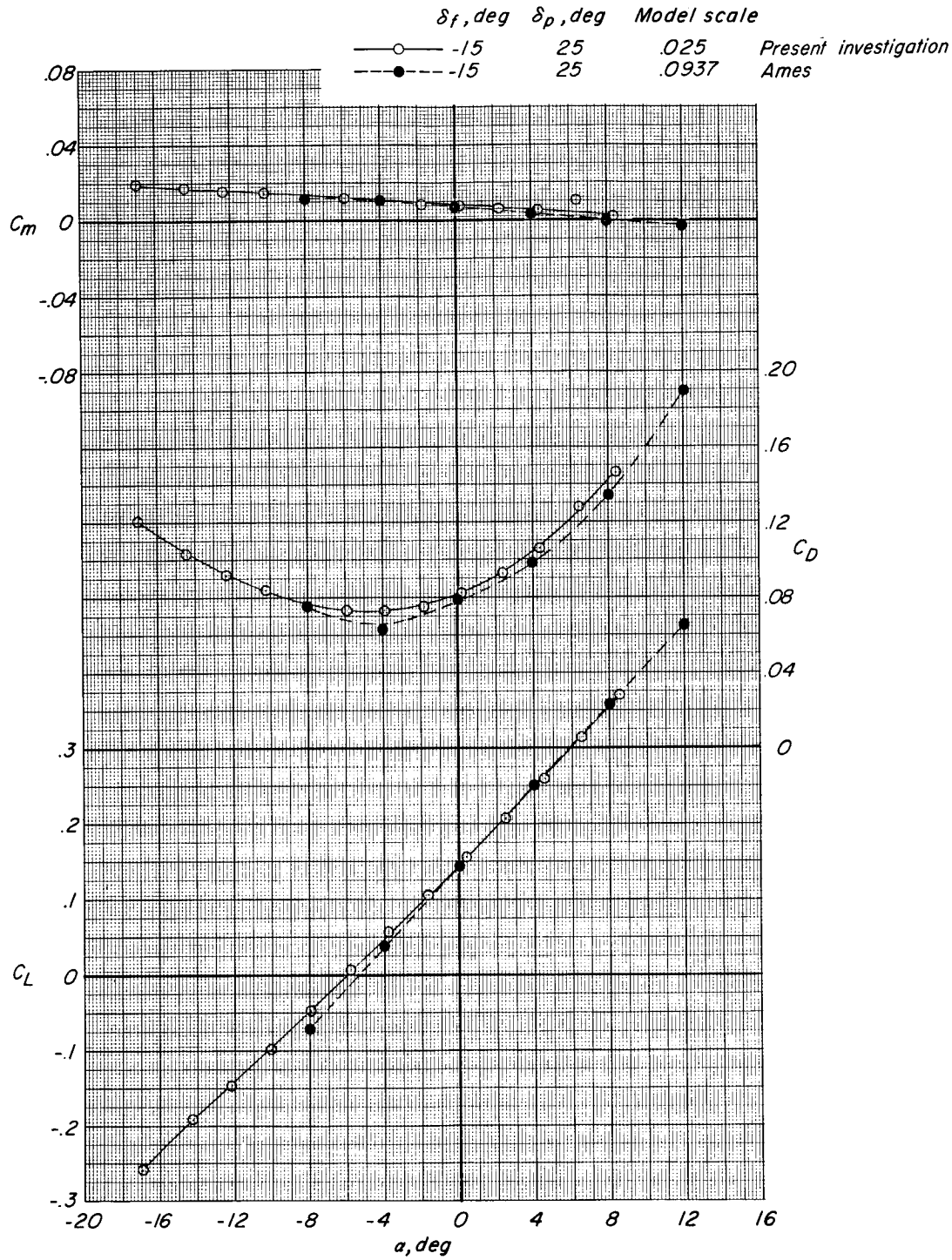

(a) M = 0.60.

Figure 6.- Comparison of M2-F2 free-stream characteristics obtained in present investigation with unpublished data obtained on 0.0937-scale model of the M2-F2. 10° rudder flare.

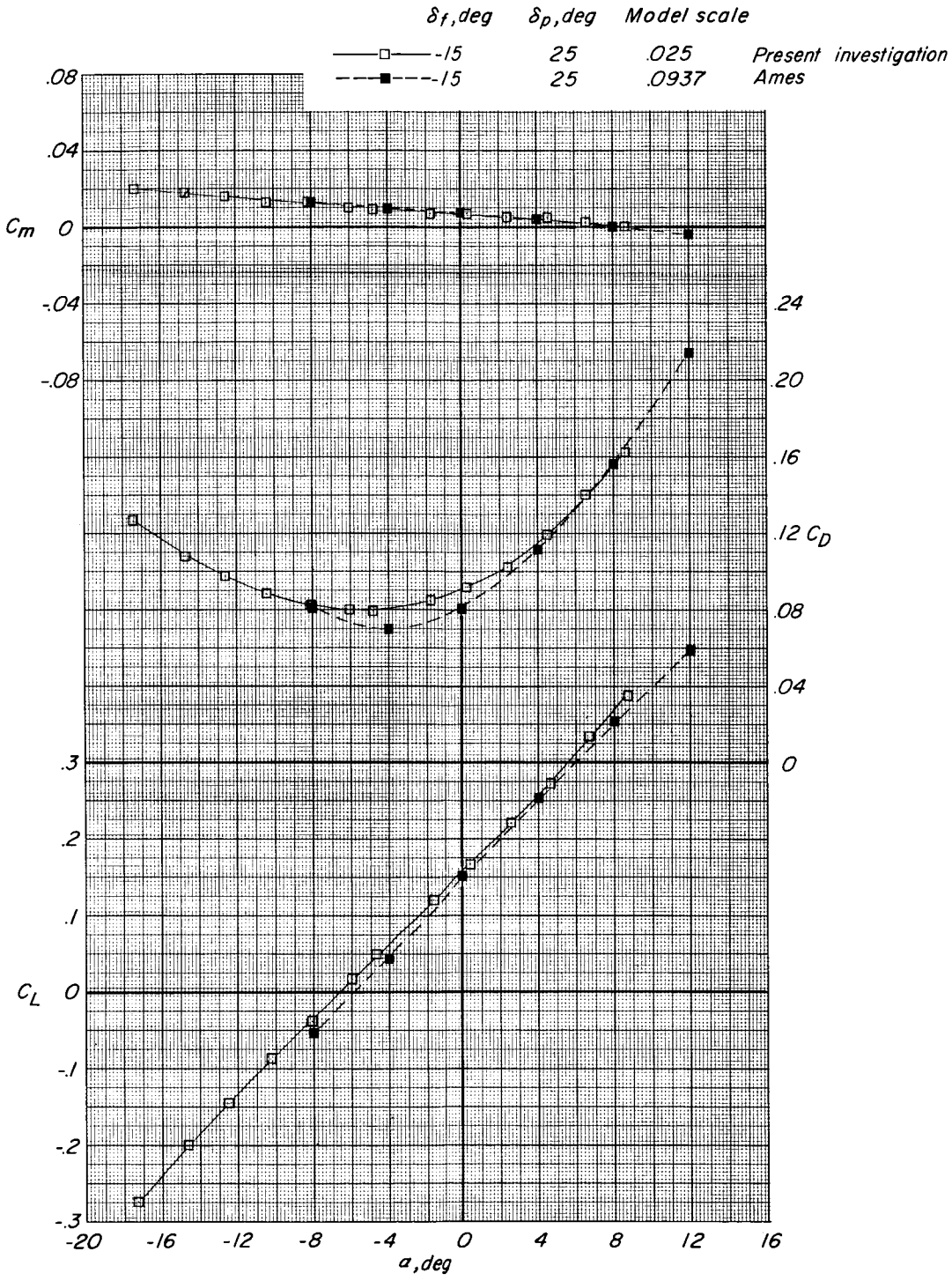

(b) M = 0.80.

Figure 6.- Continued.

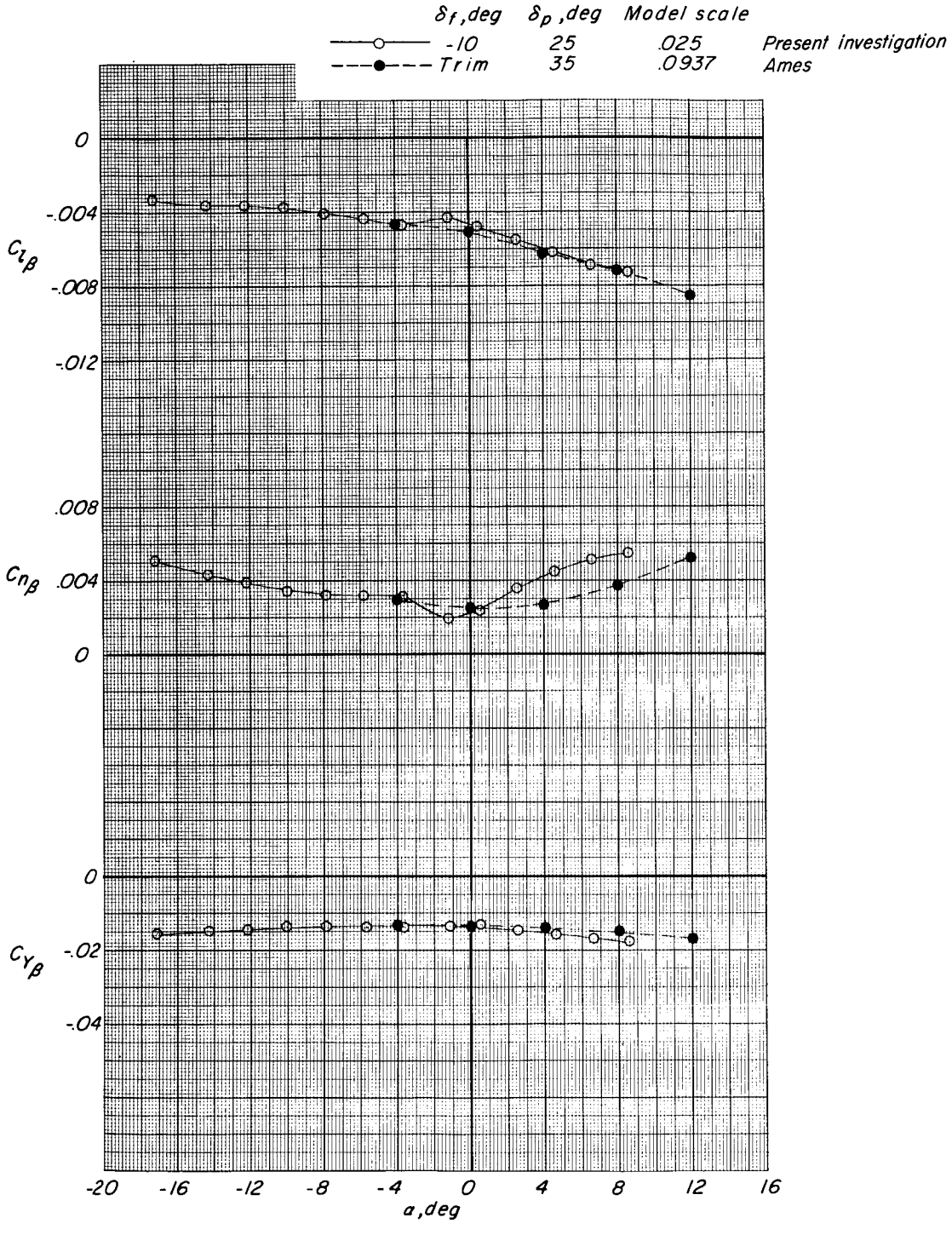

(a) Concluded.

Figure 6.- Continued.

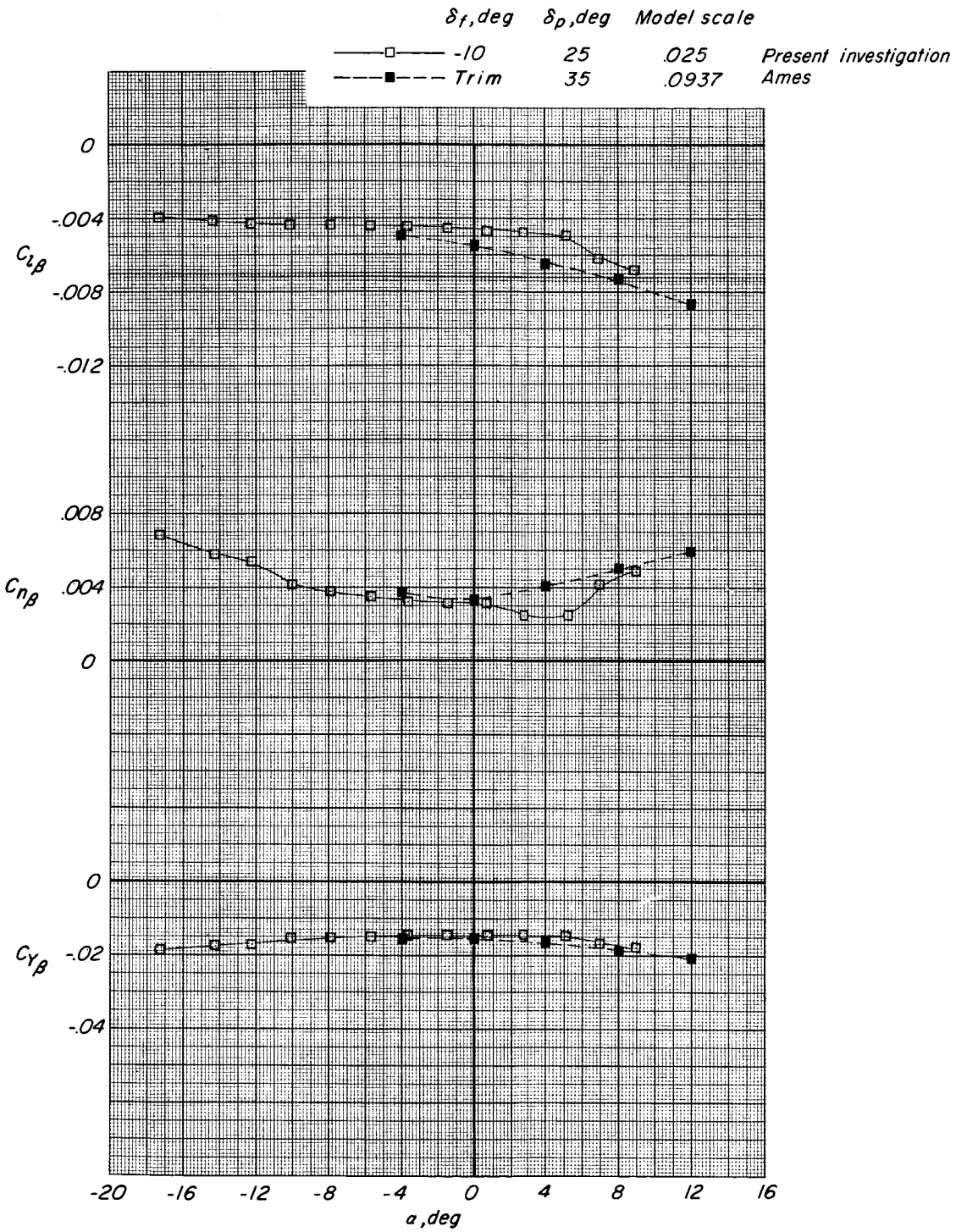

(b) Concluded.

Figure 6.- Concluded.

[redacted]

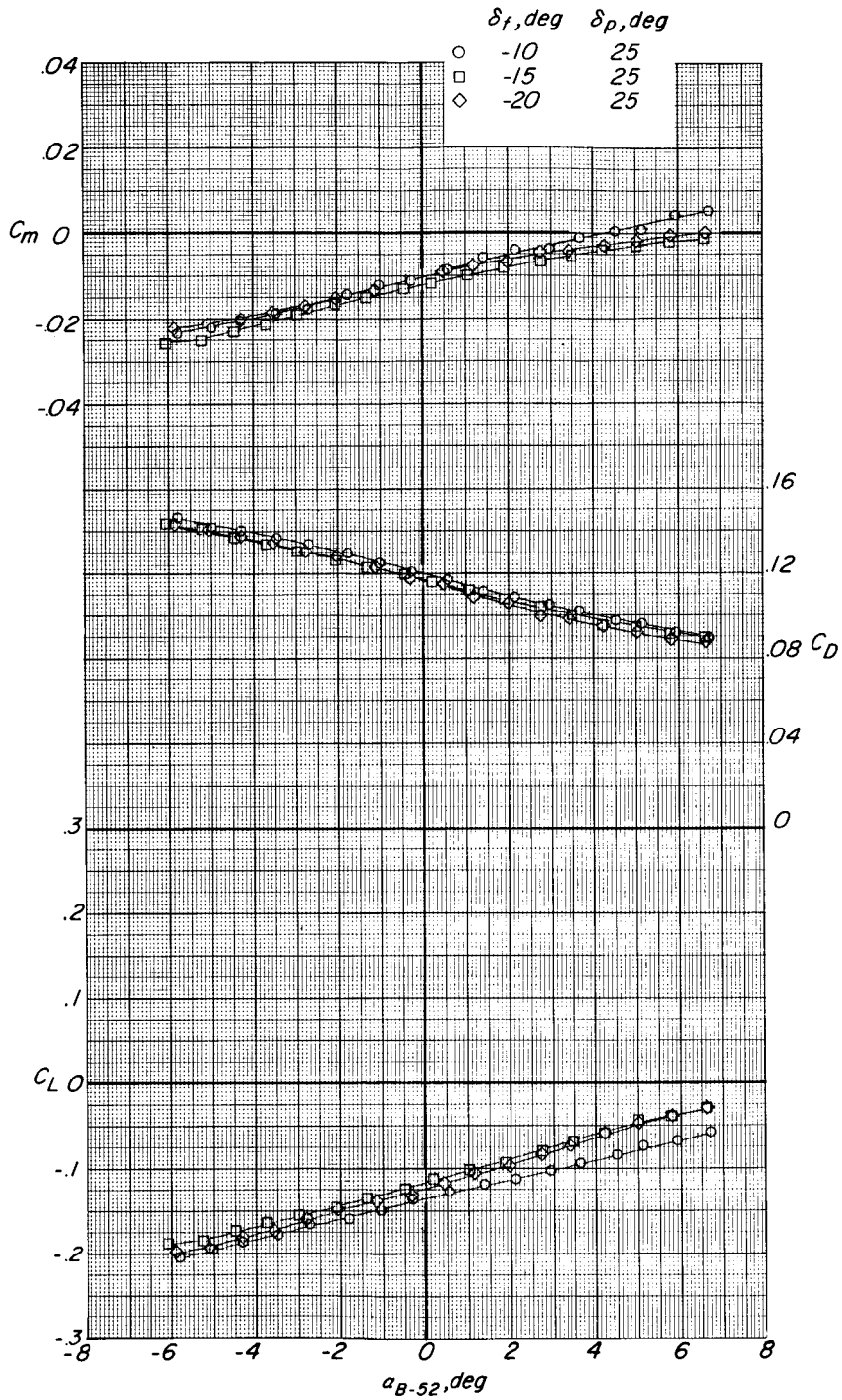

(a) z' = 0.

Figure 7.- Aerodynamic characteristics of M2-F2 model in presence of B-52 model. M = 0.60; nominal control settings are $\delta_p = 25^0$, $\delta_f = -10^0$, and 10^0 rudder flare.

[redacted]

DECLASSIFIED

[redacted]

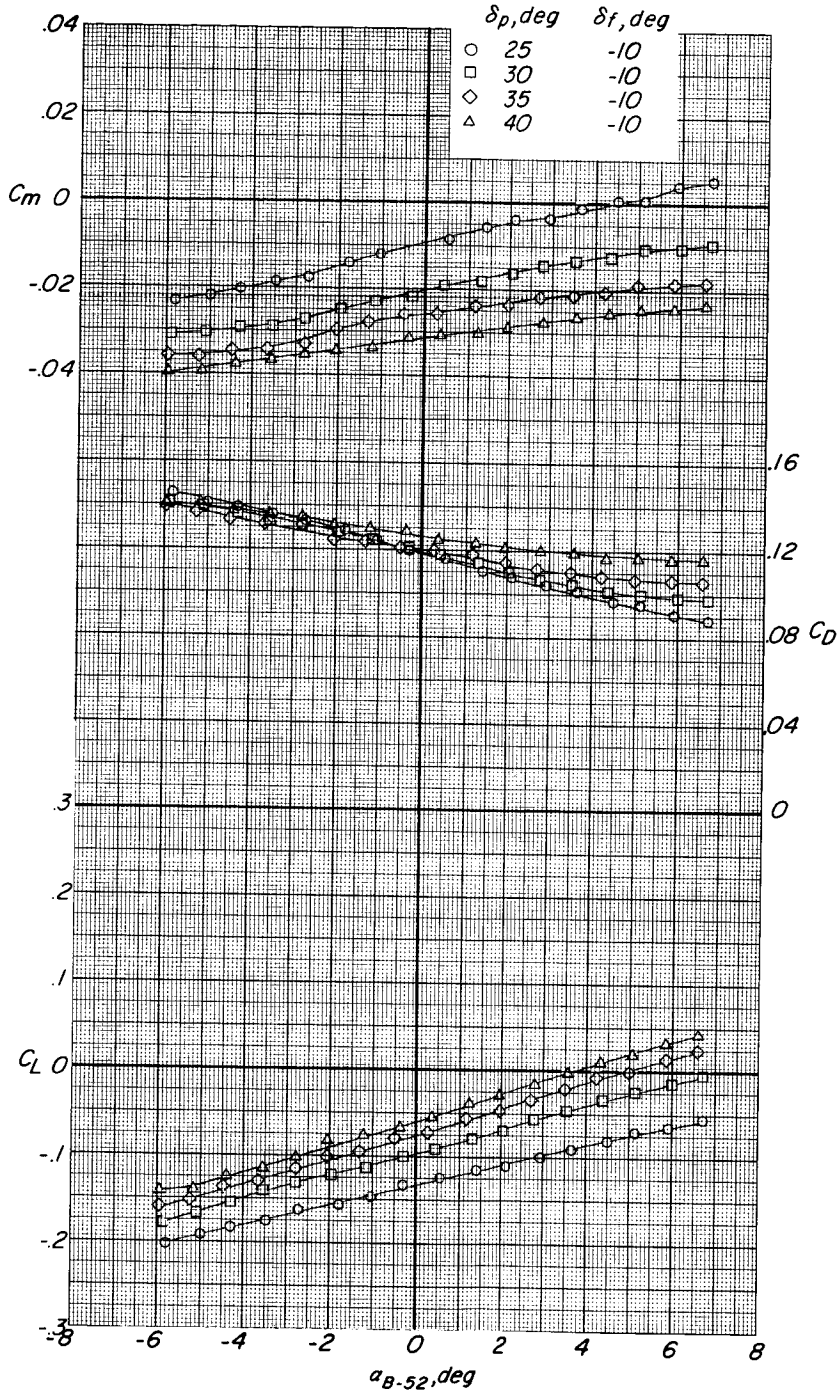

(a) Continued.

Figure 7.- Continued.

[redacted]

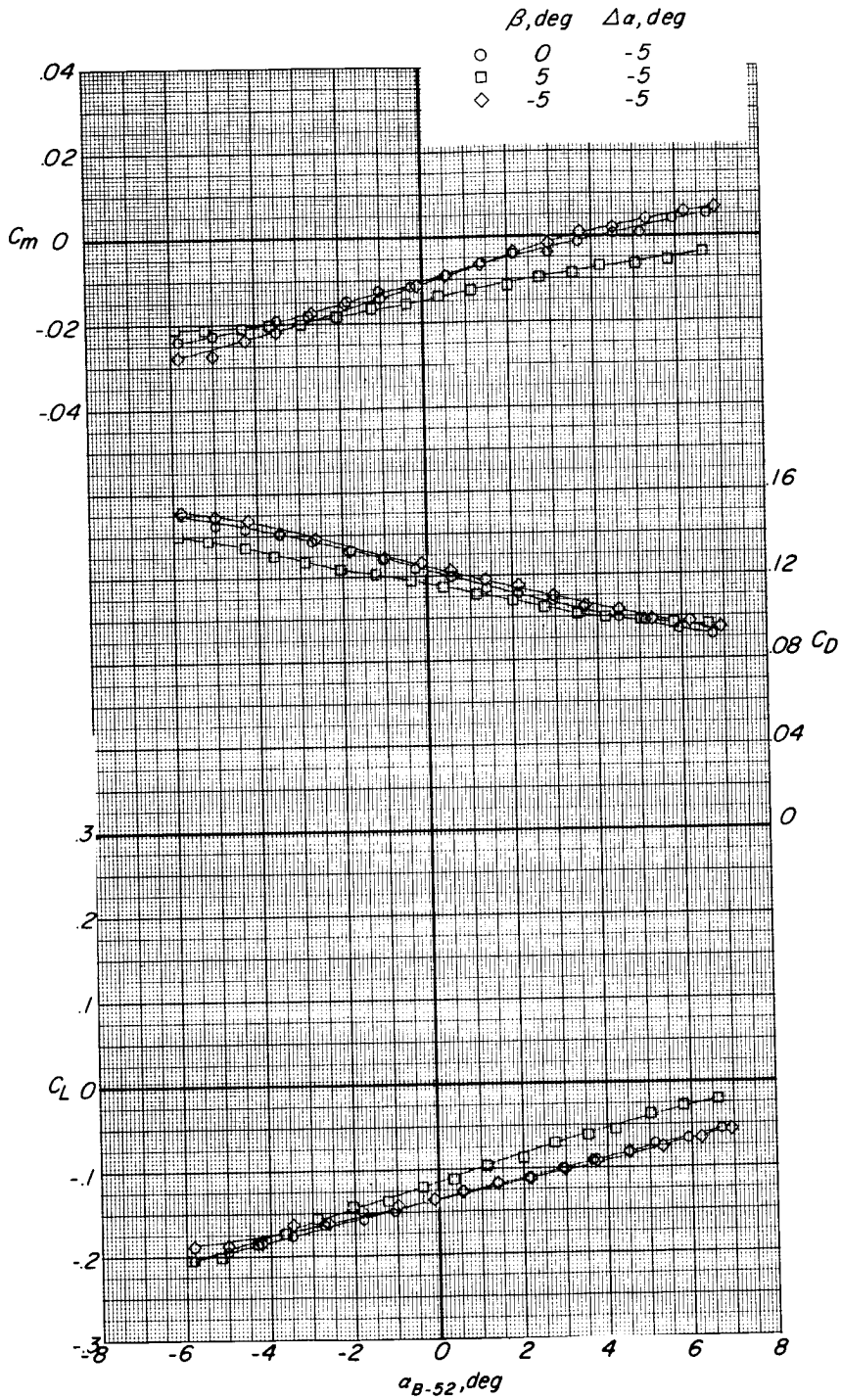

(a) Continued.

Figure 7.- Continued.

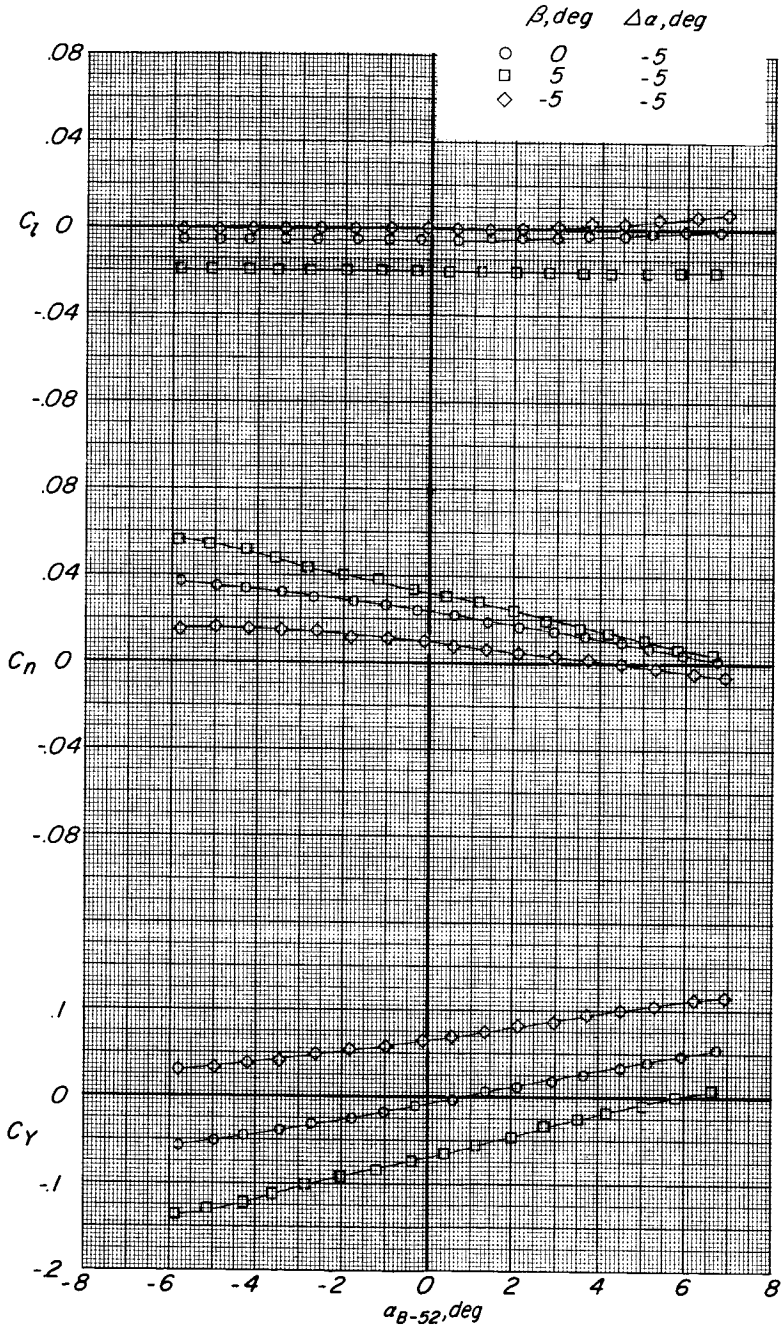

(a) Continued.

Figure 7.- Continued.

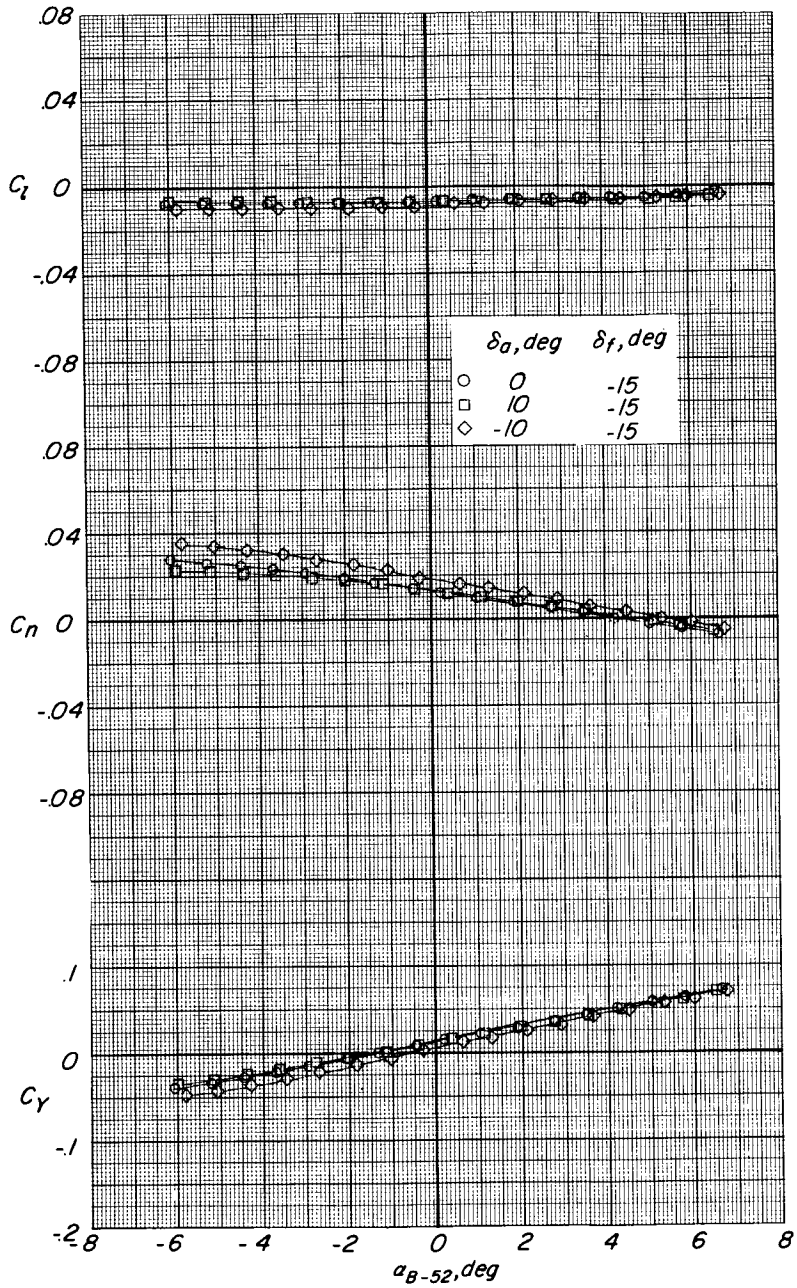

(a) Continued.

Figure 7.- Continued.

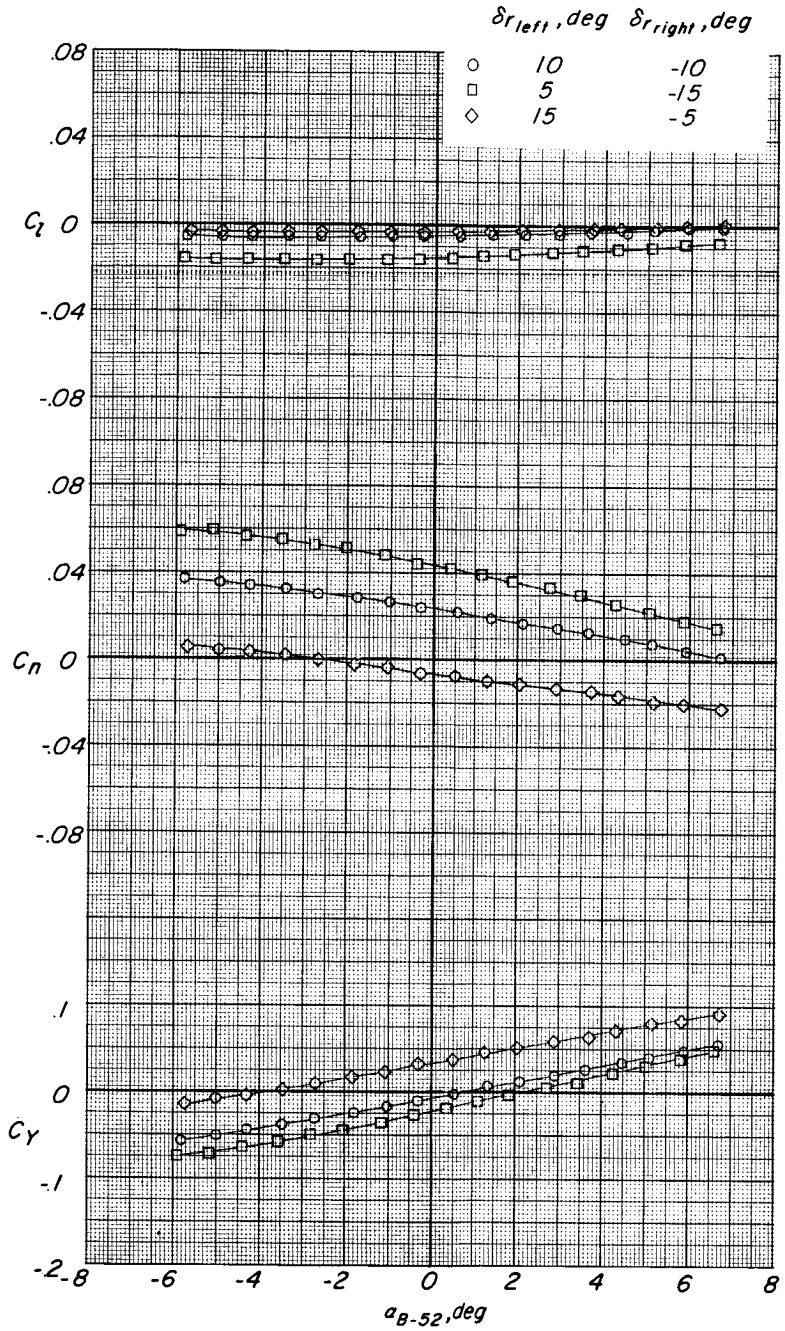

(a) Concluded.

Figure 7.- Continued.

[redacted]

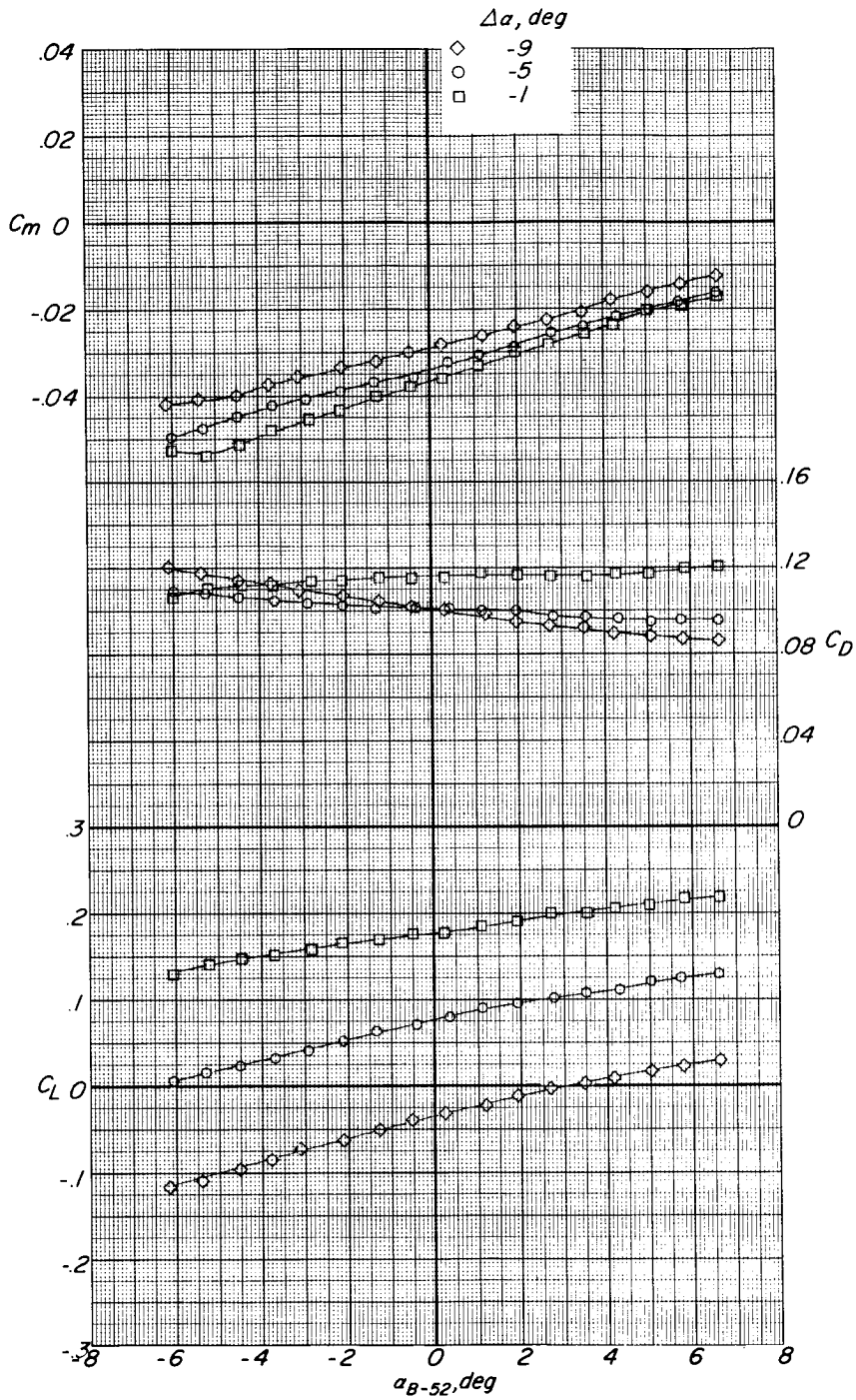

(b) z' = 2.0 feet (0.61 m).

Figure 7.- Continued.

[redacted]

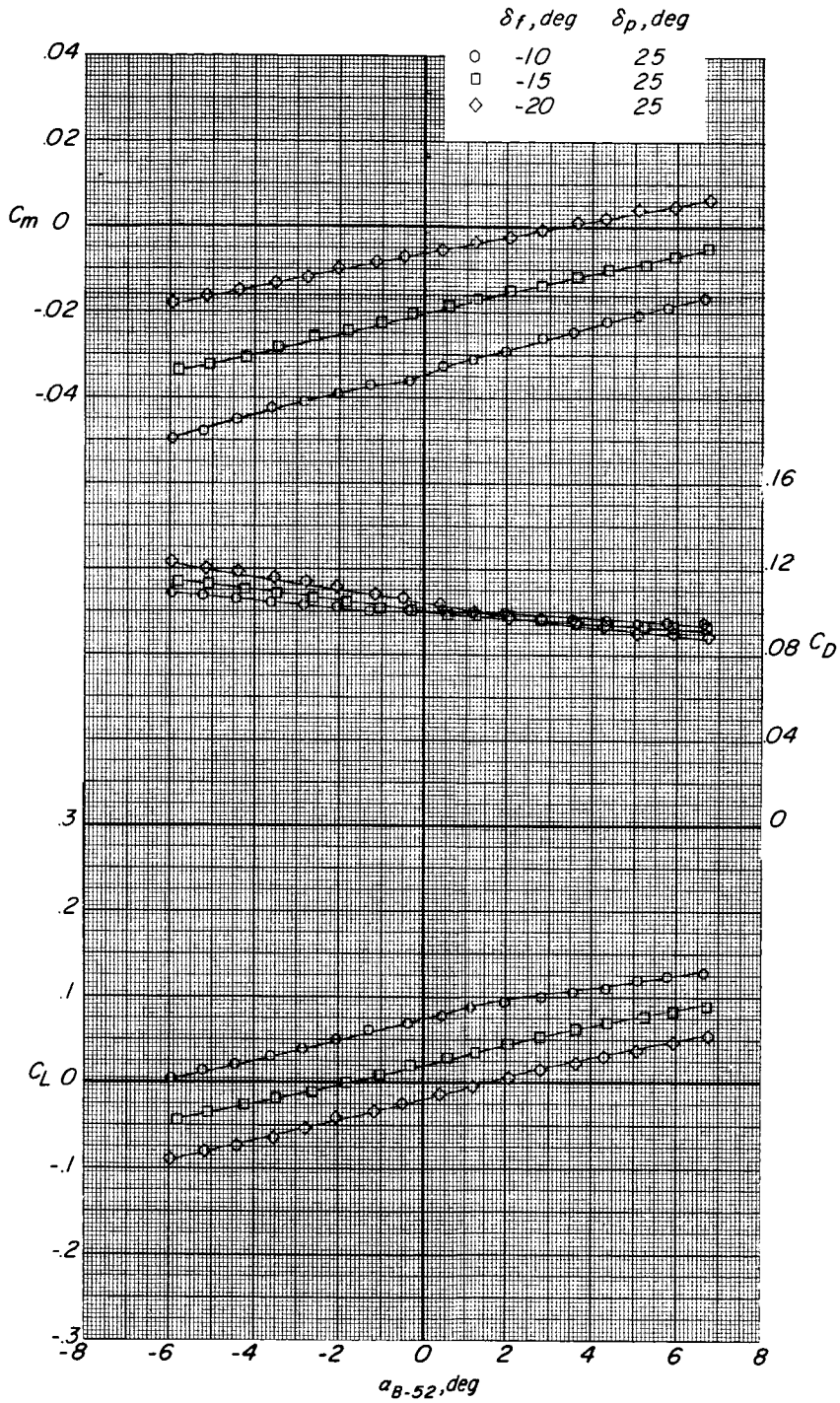

(b) Continued.

Figure 7.- Continued.

[redacted]

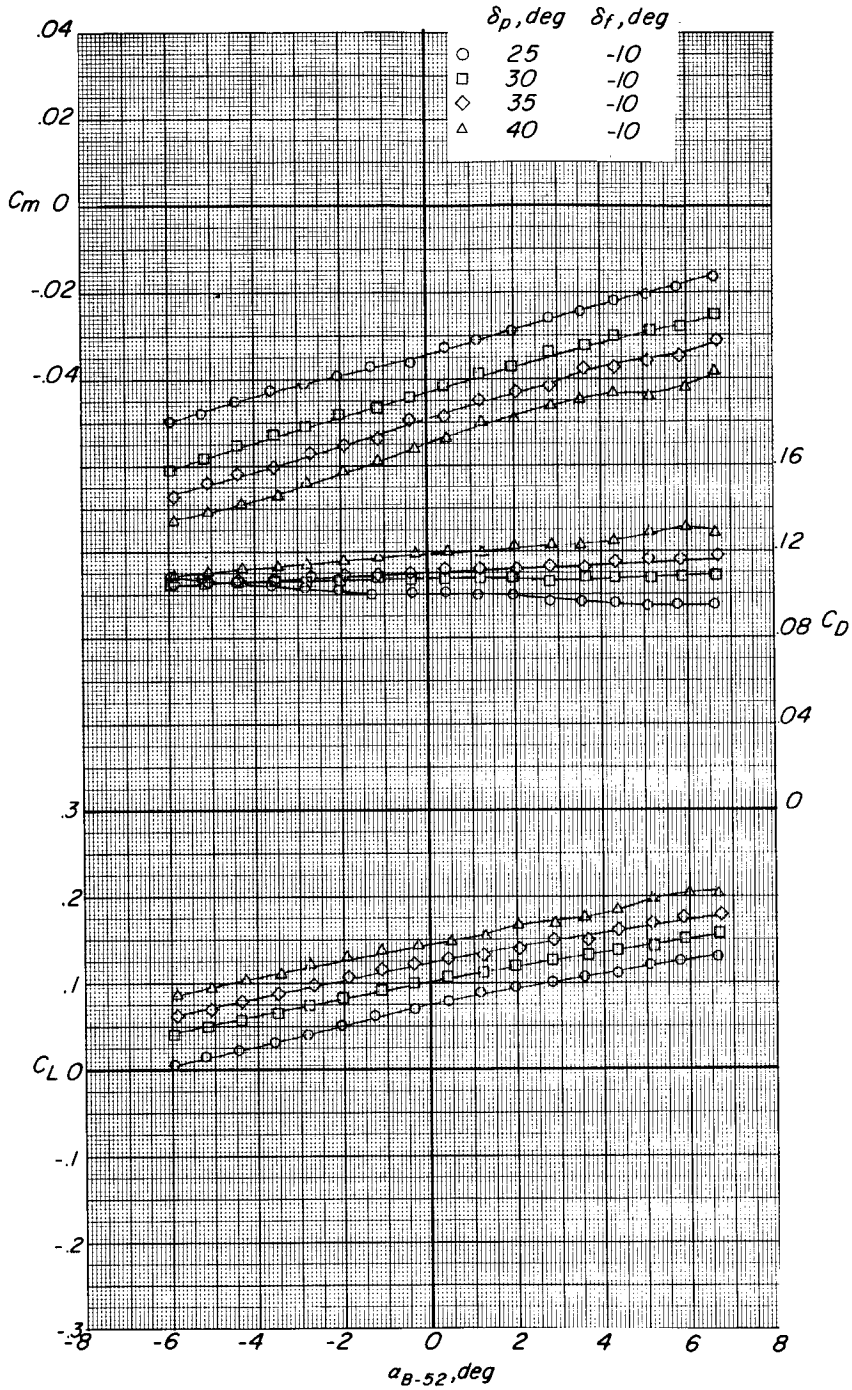

(b) Continued.

Figure 7.- Continued.

[redacted]

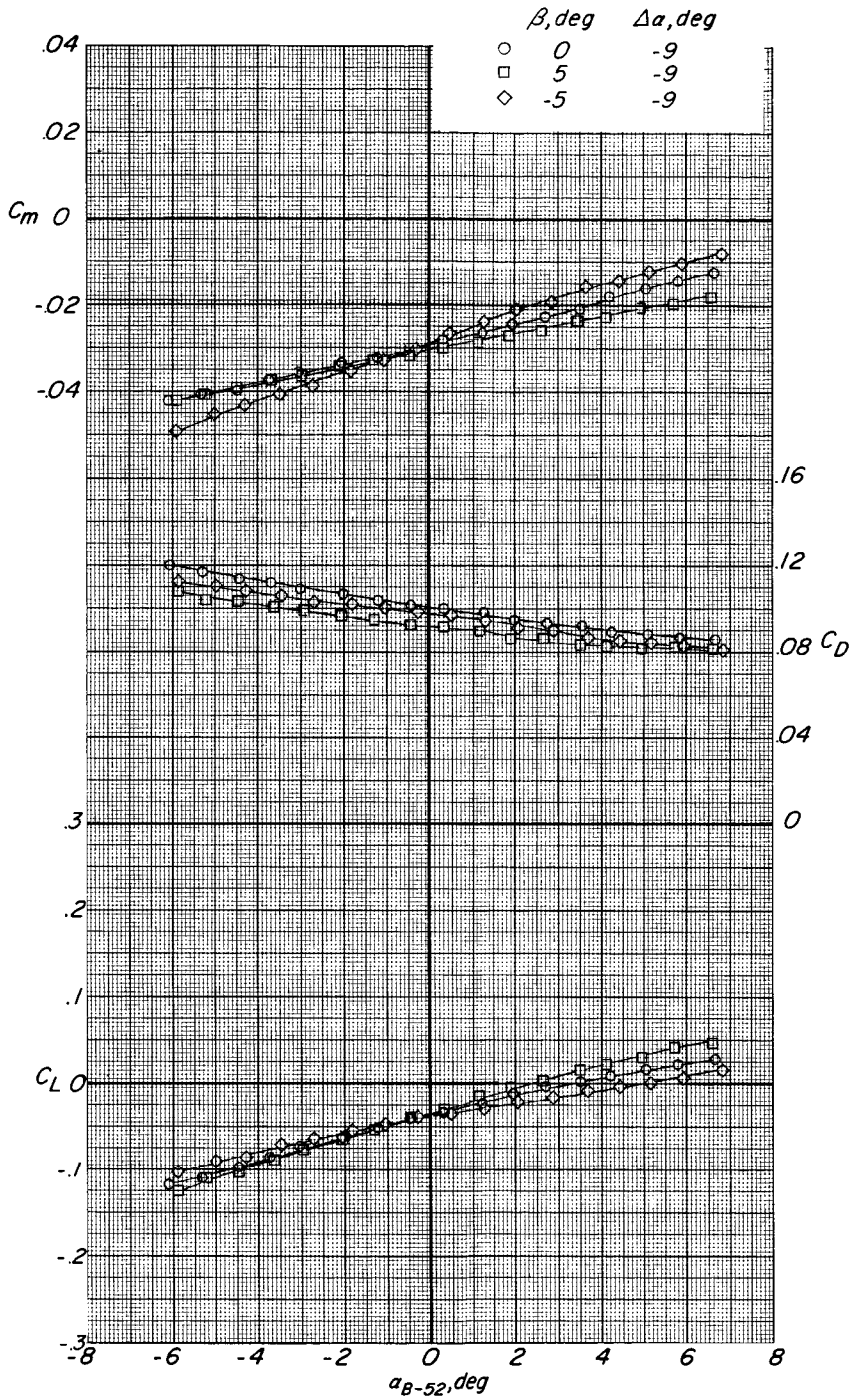

(b) Continued.

Figure 7.- Continued.

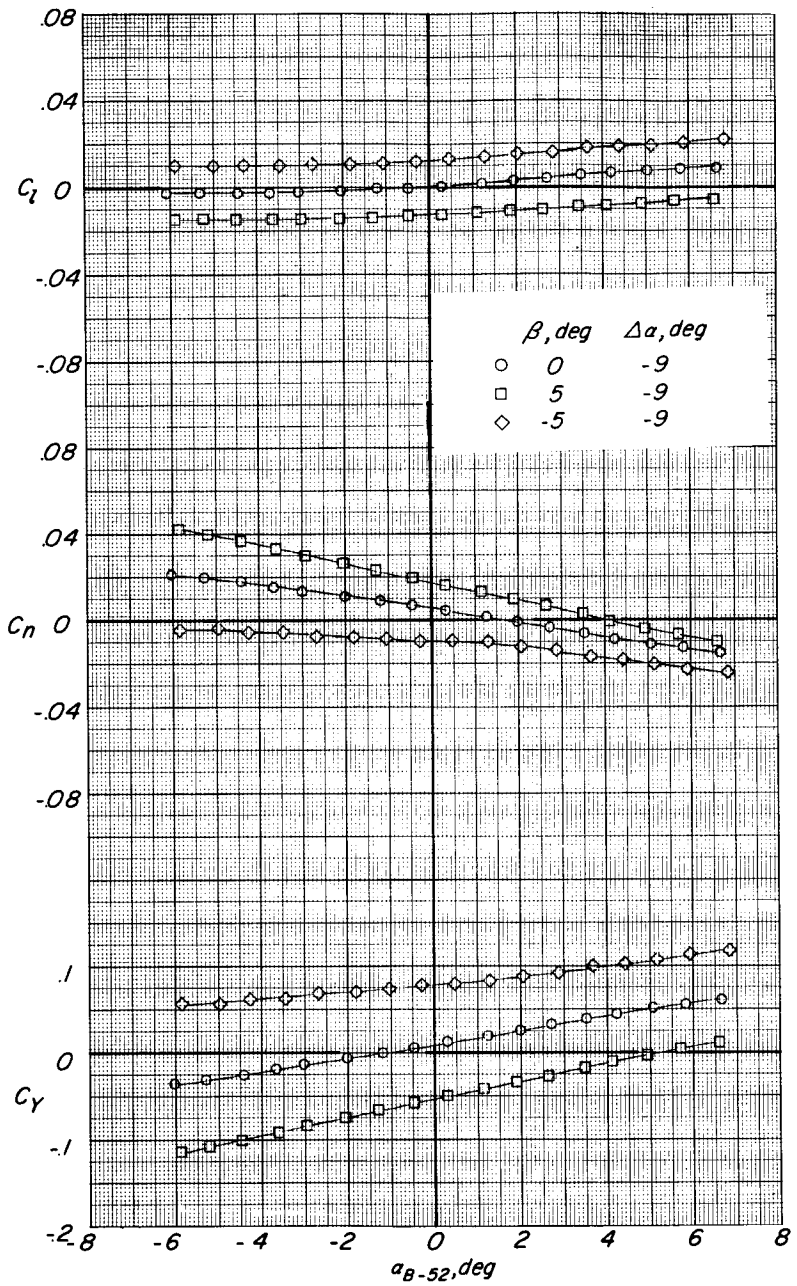

(b) Continued.

Figure 7.- Continued.

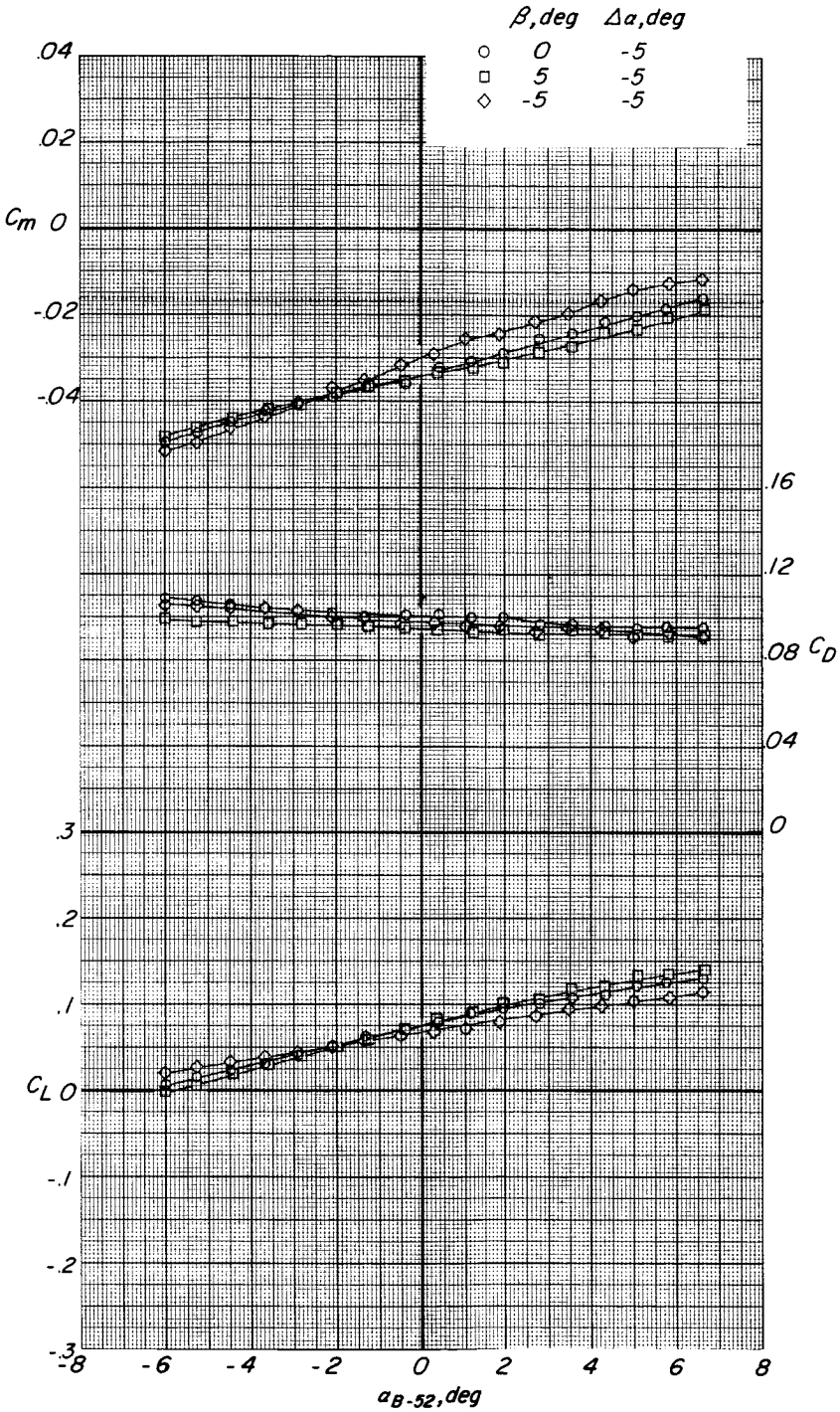

(b) Continued.

Figure 7.- Continued.

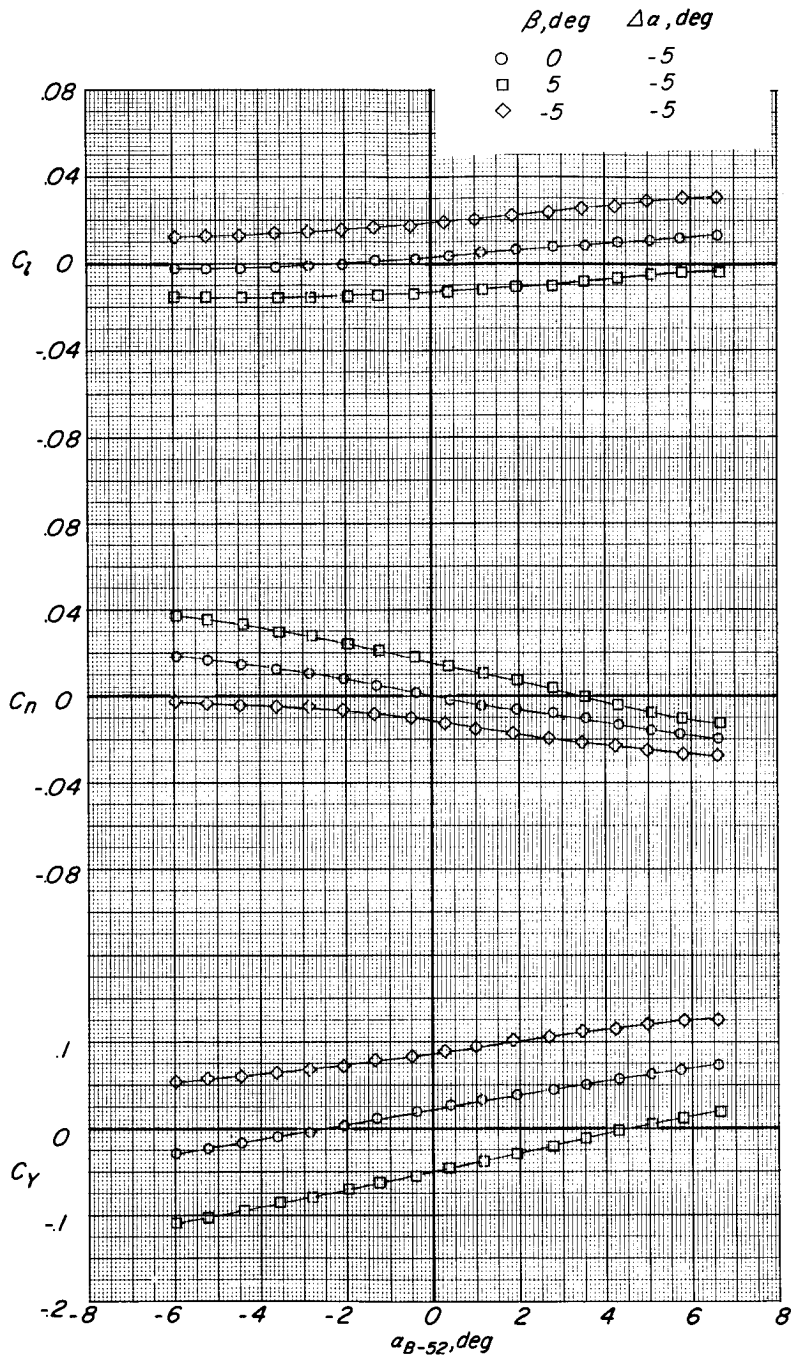

(b) Continued.

Figure 7.- Continued.

DECLASSIFIED

[redacted]

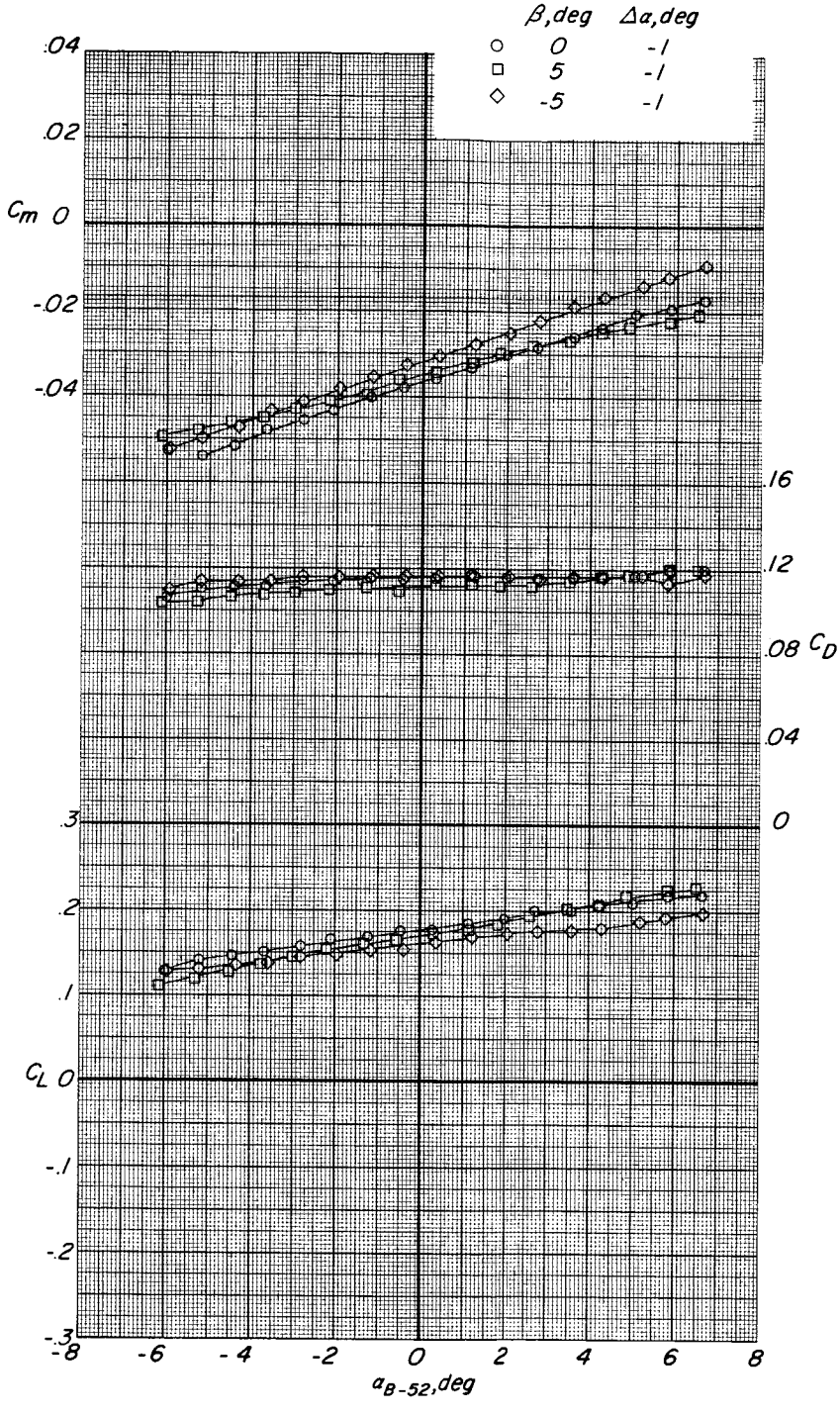

(b) Continued.

Figure 7.- Continued.

[redacted]

[redacted]

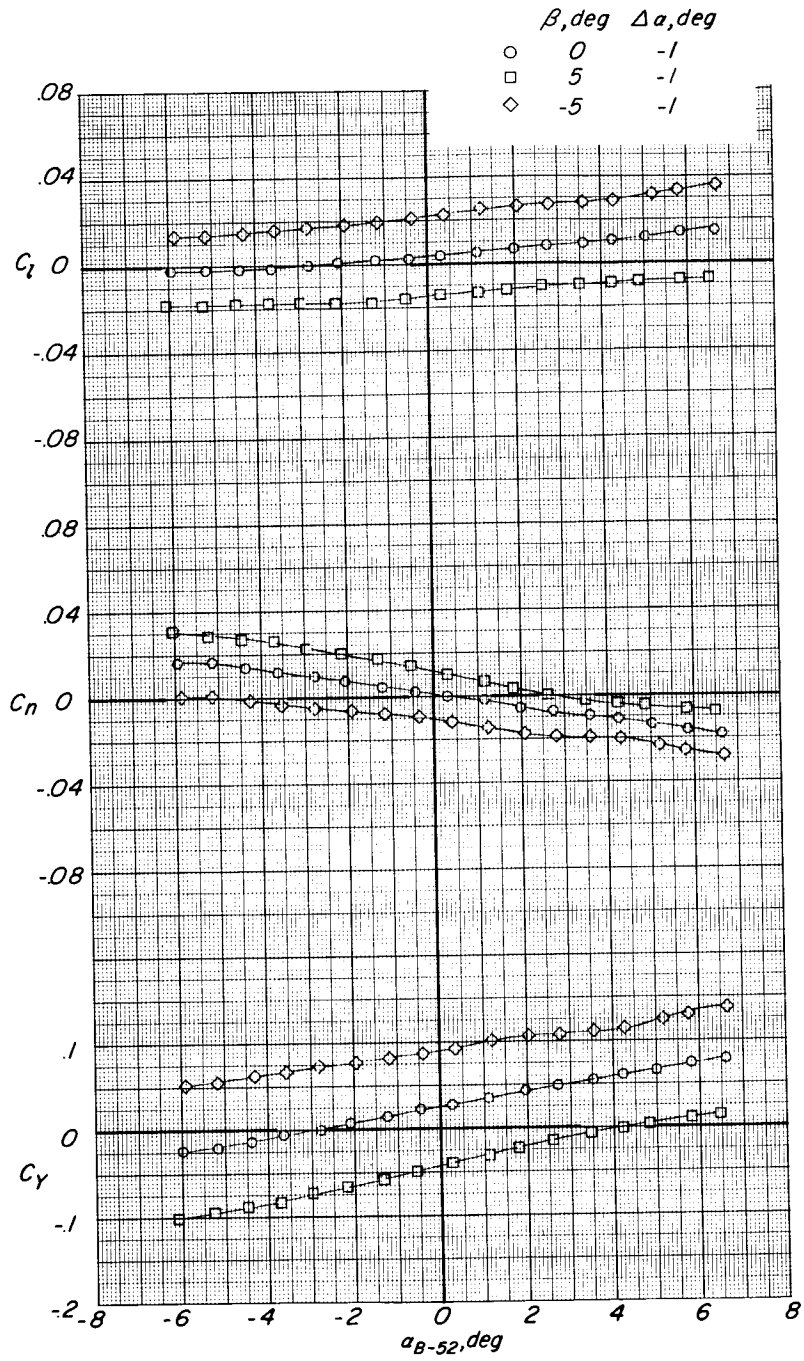

(b) Continued.

Figure 7.- Continued.

[redacted]

DECLASSIFIED

[redacted]

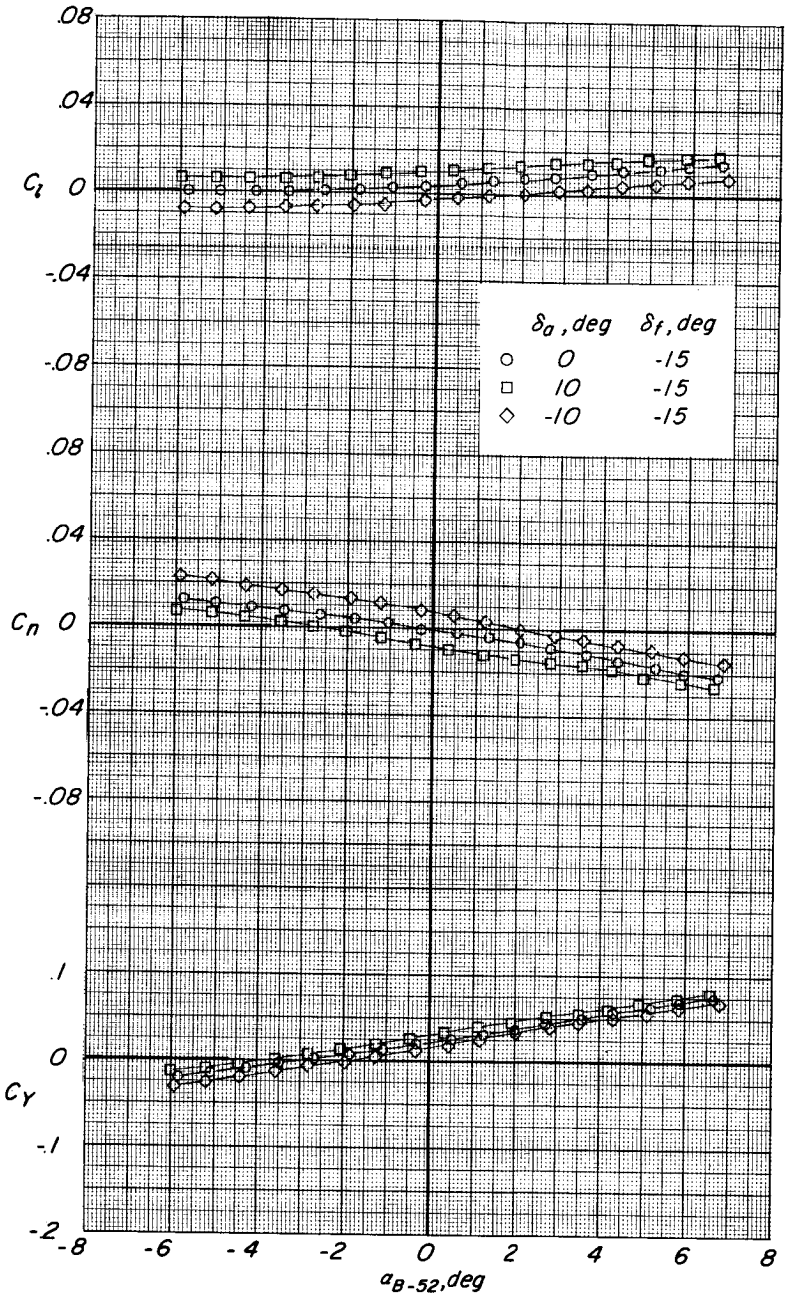

(b) Continued.

Figure 7.- Continued.

[redacted]

[redacted]

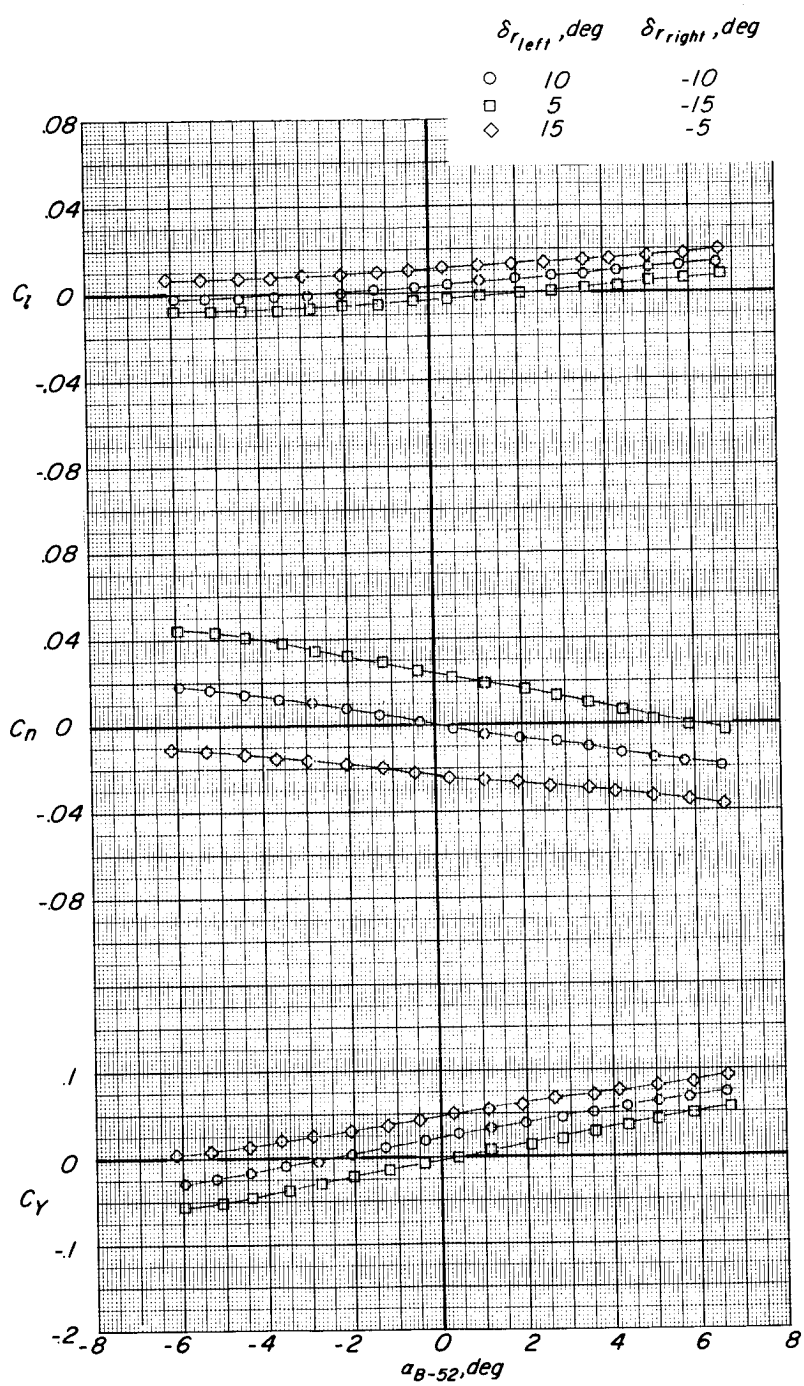

(b) Concluded.

Figure 7.- Continued.

[redacted]

DECLASSIFIED

[redacted]

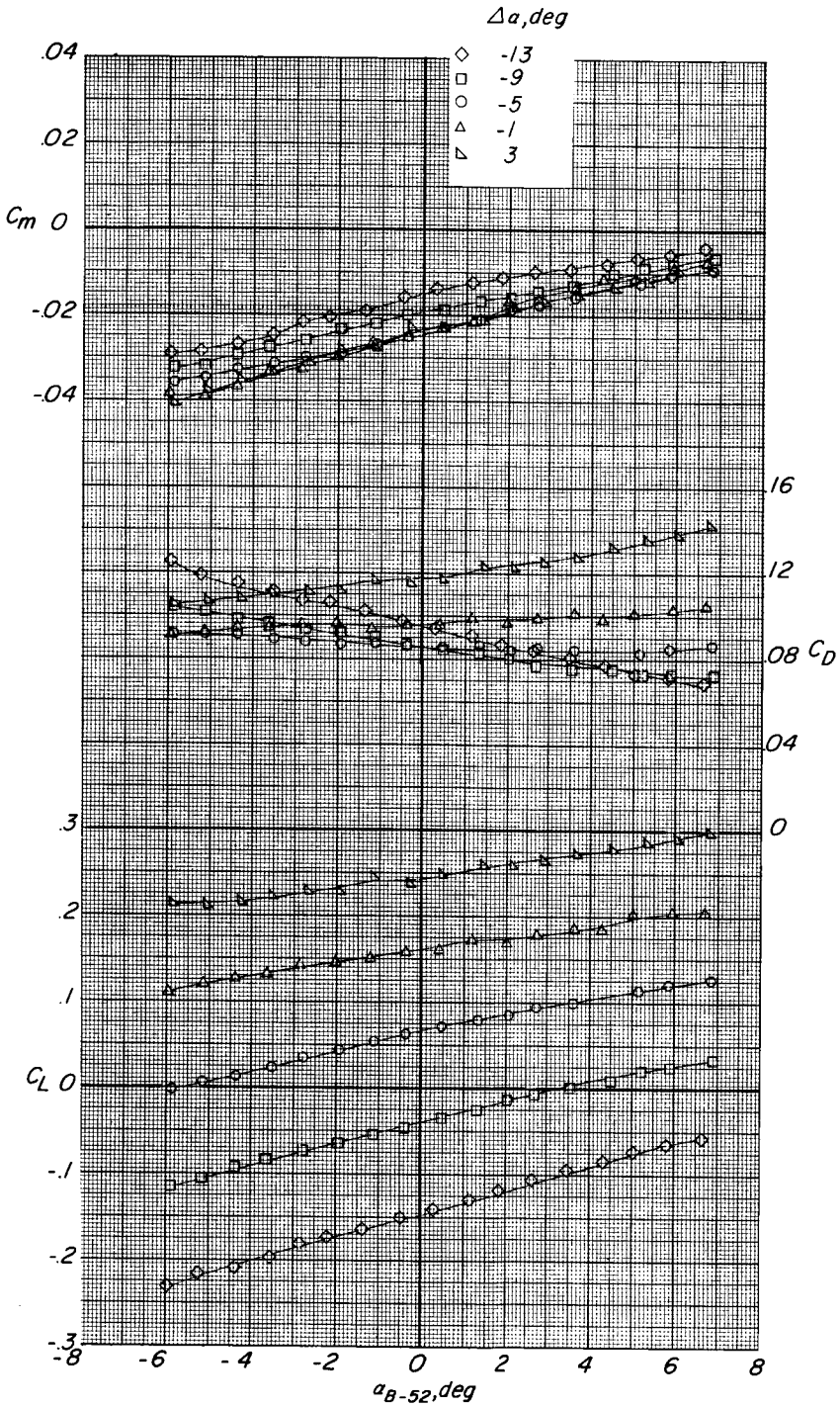

(c) z' = 4.0 feet (1.22 m).

Figure 7.- Continued.

[redacted]

[redacted]

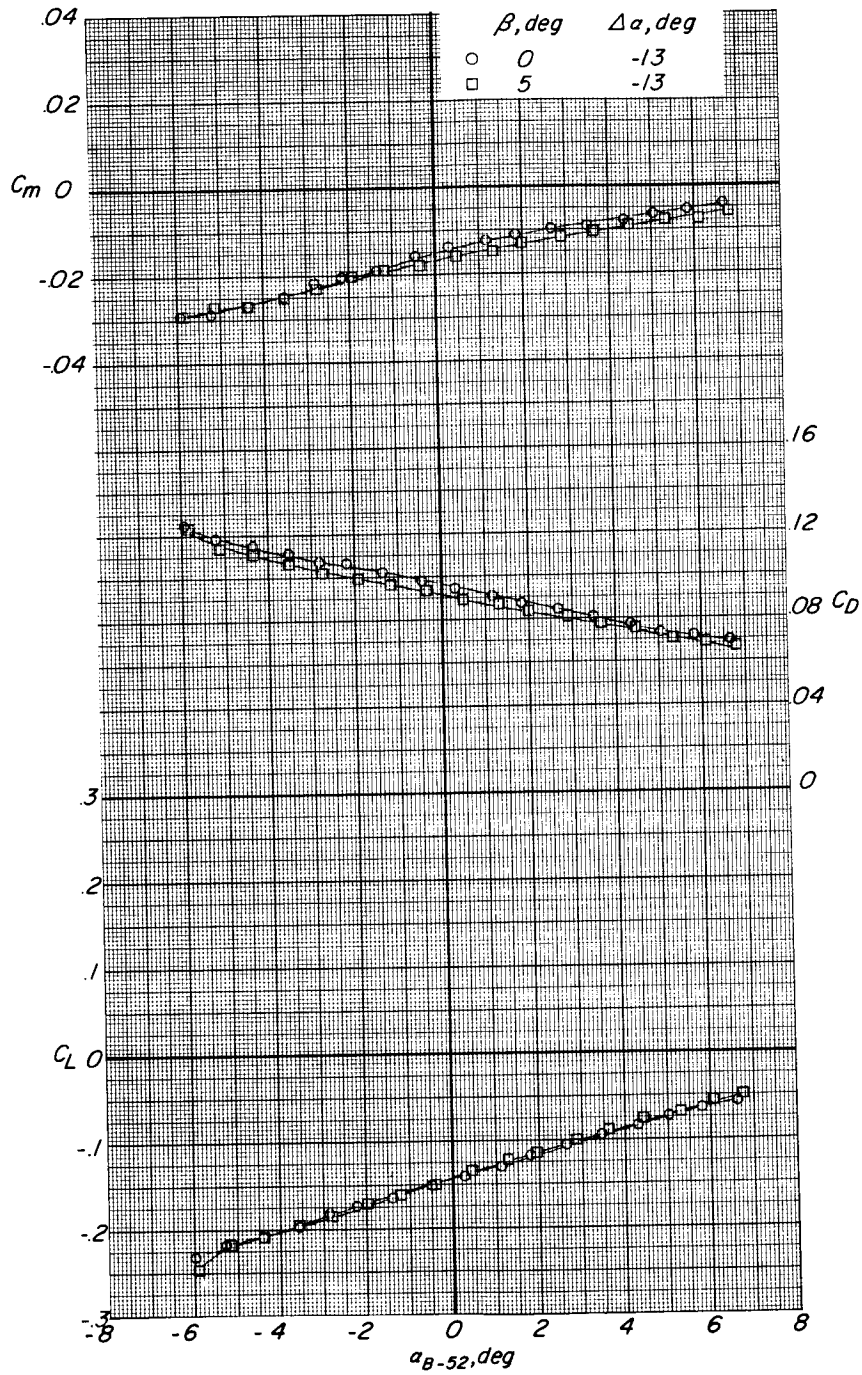

(c) Continued.

Figure 7.- Continued.

[redacted]

DECLASSIFIED

[redacted]

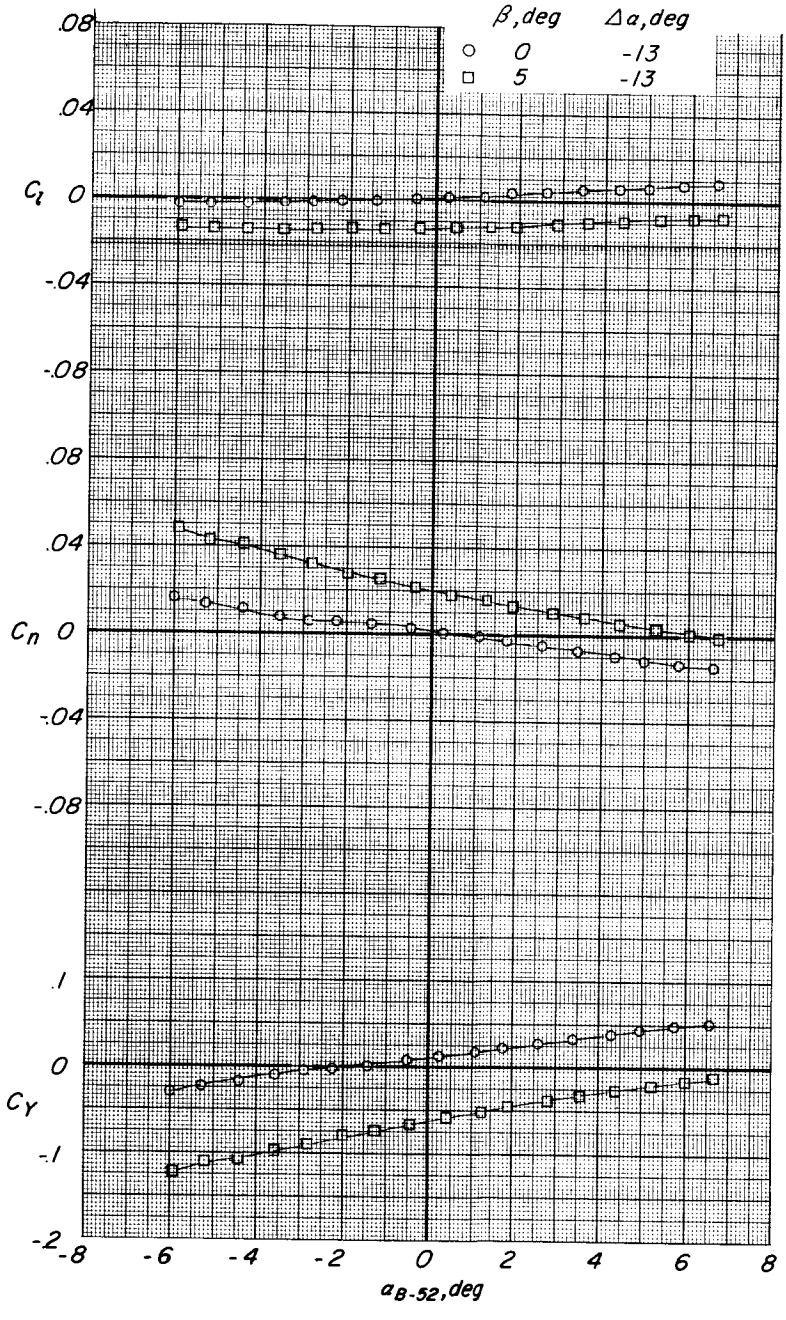

(c) Continued.

Figure 7.- Continued.

[redacted]

[redacted]

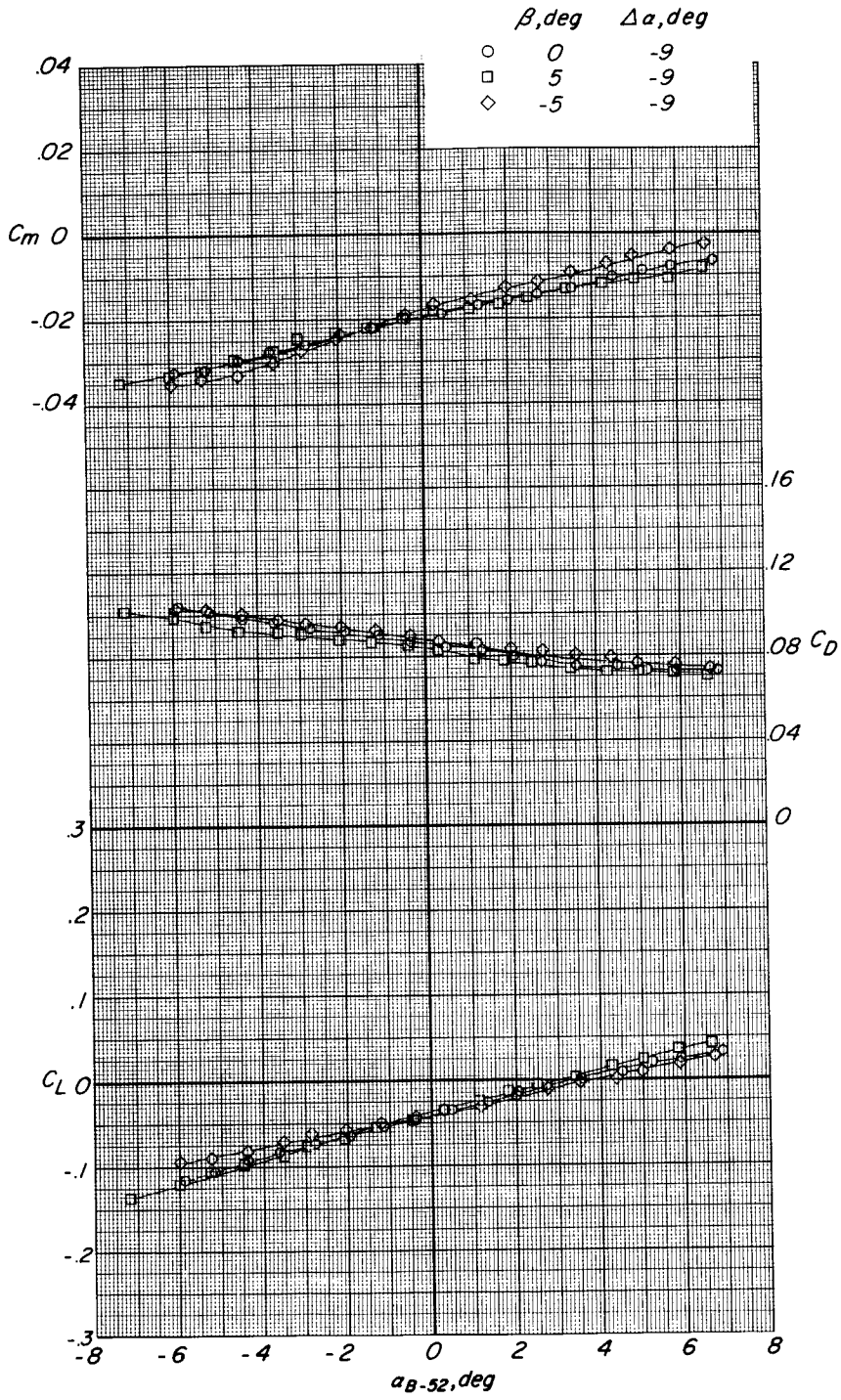

(c) Continued.

Figure 7.- Continued.

[redacted]

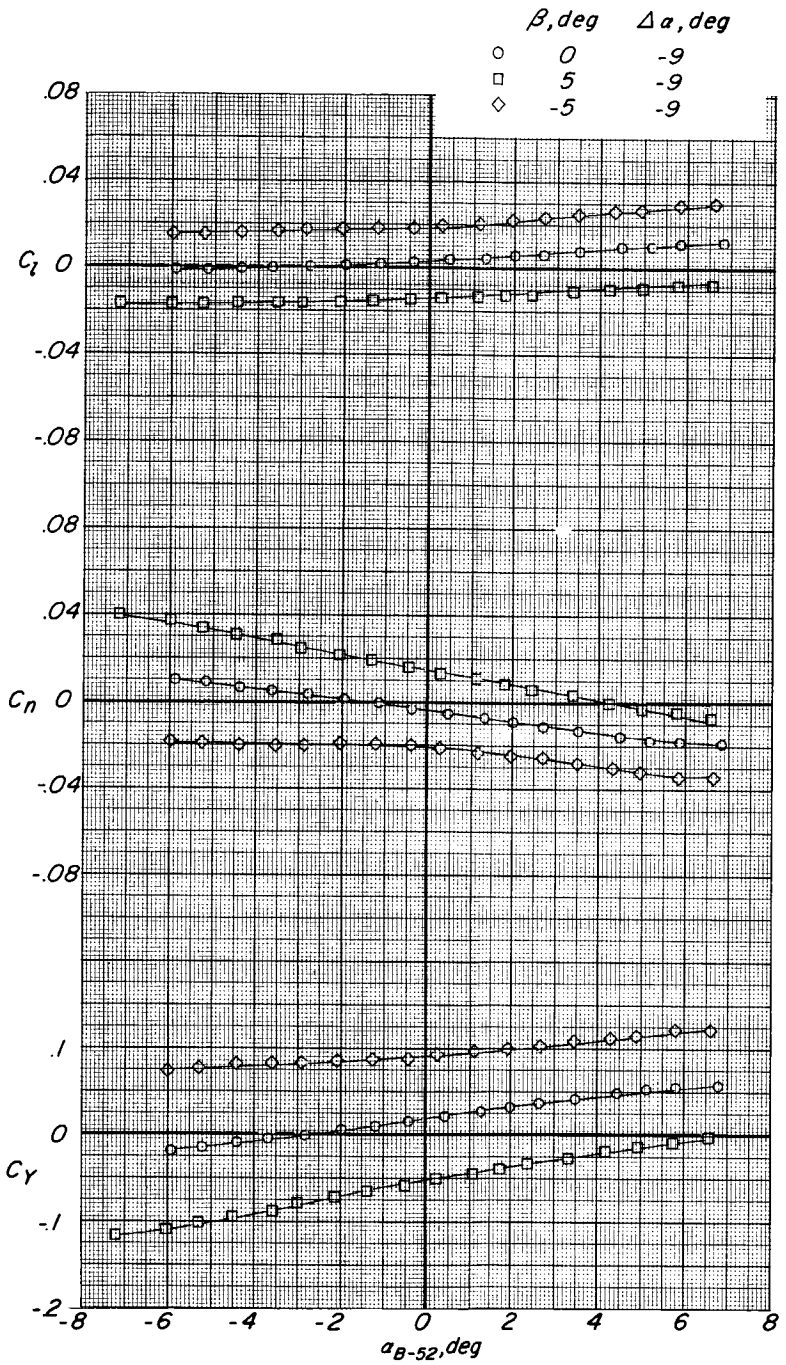

(c) Continued.

Figure 7.- Continued.

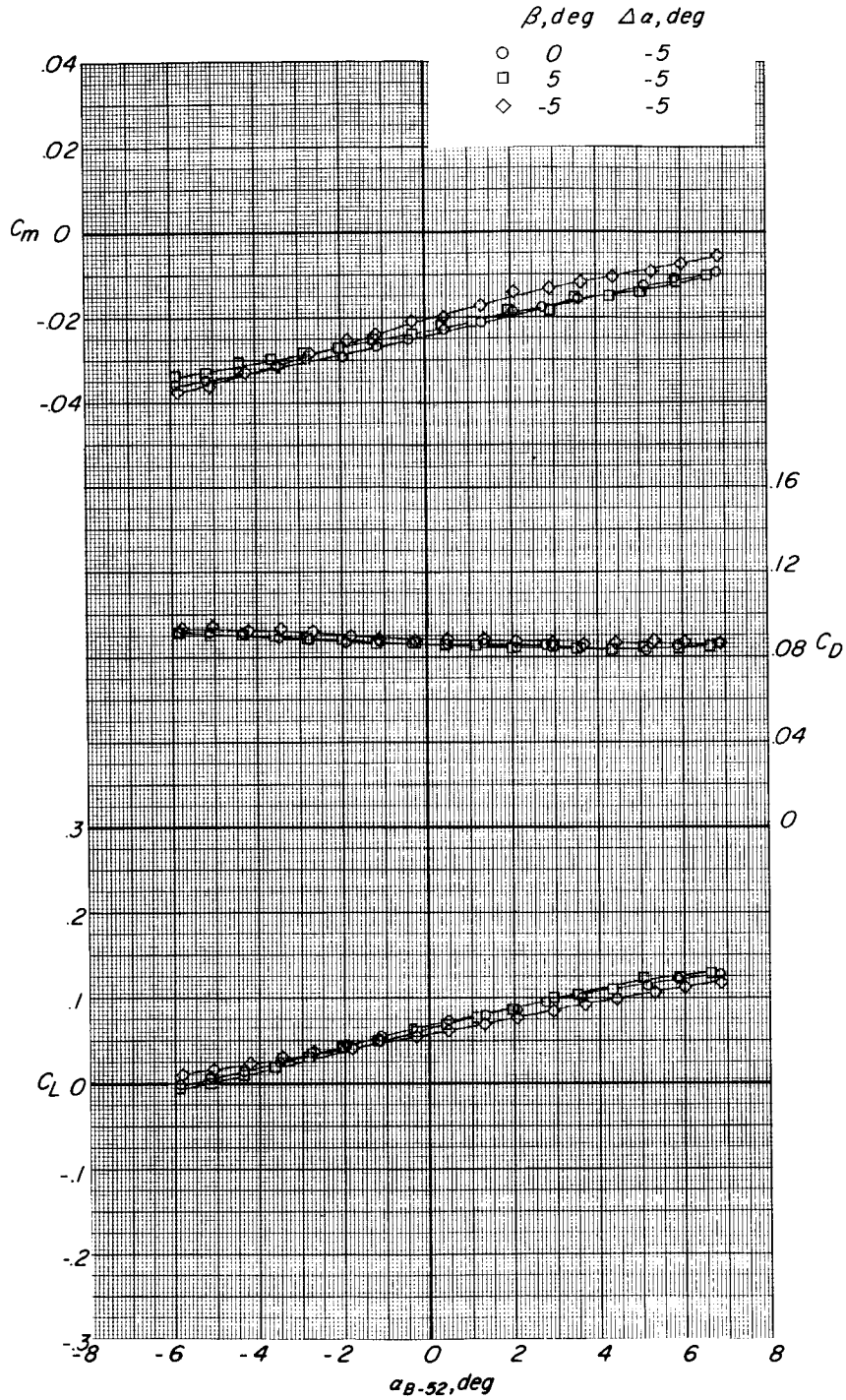

(c) Continued.

Figure 7.- Continued.

DECLASSIFIED

[redacted]

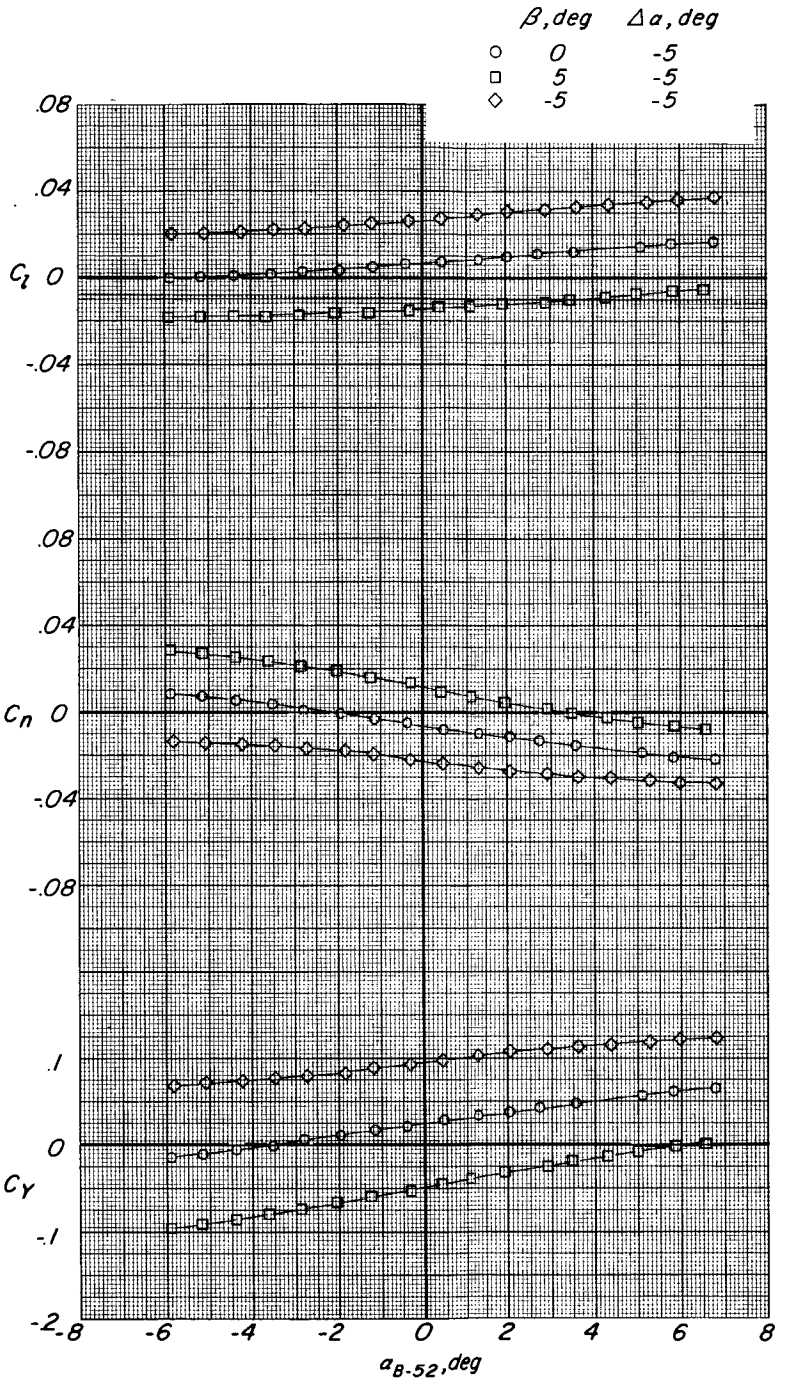

(c) Continued.

Figure 7.- Continued.

[redacted]

[redacted]

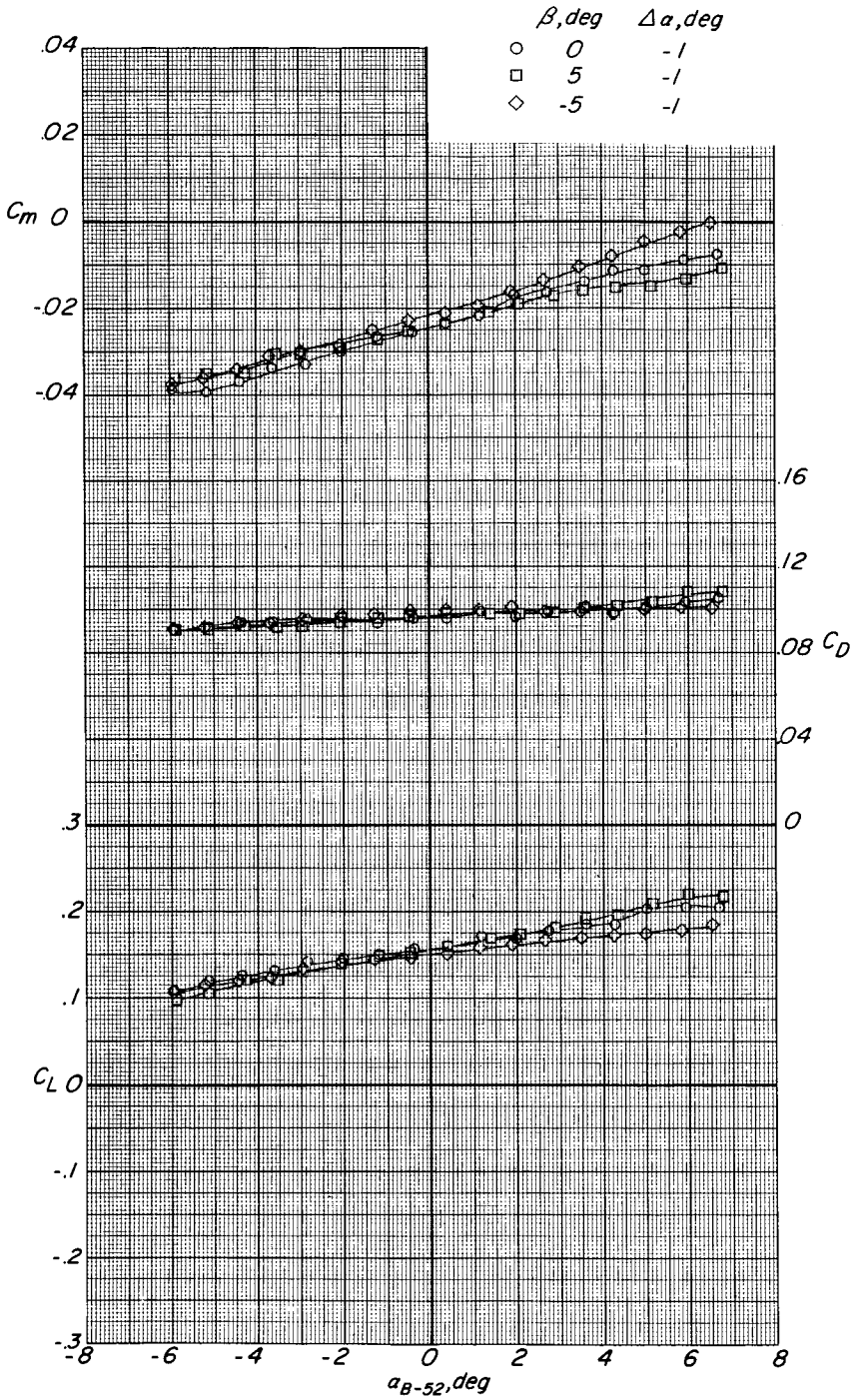

(c) Continued.

Figure 7.- Continued.

[redacted]

DECLASSIFIED

[redacted]

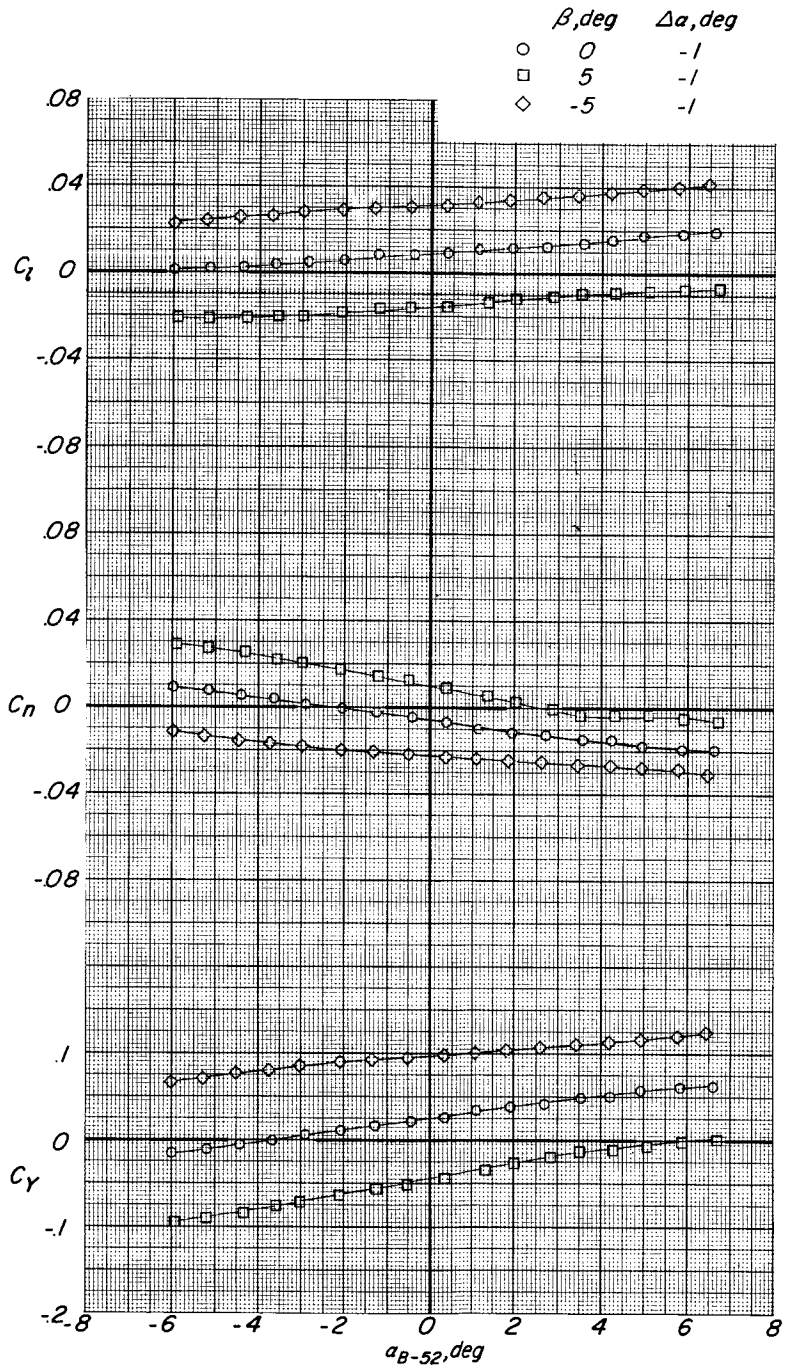

(c) Continued.

Figure 7.- Continued.

[redacted]

[redacted]

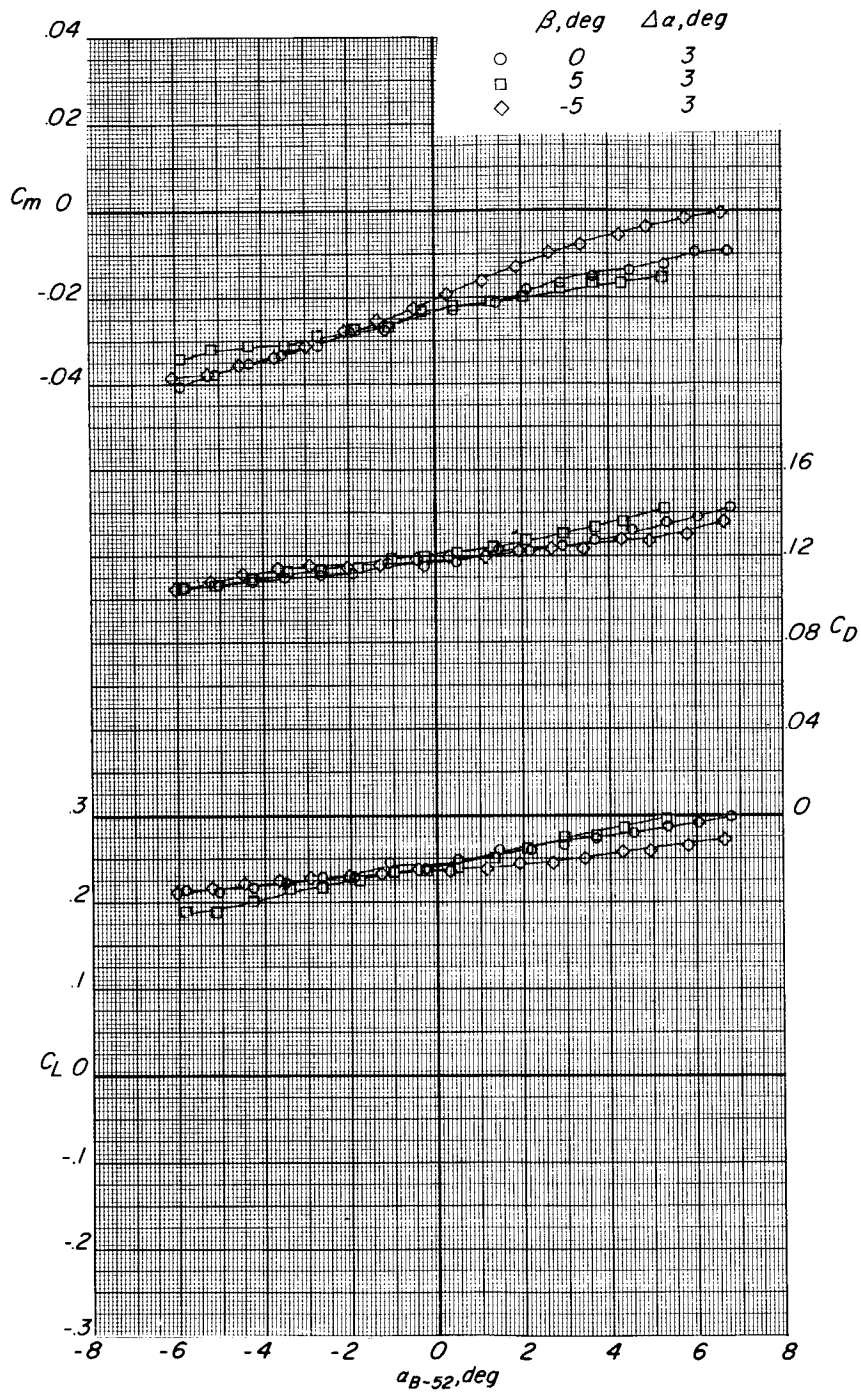

(c) Continued.

Figure 7.- Continued.

[redacted]

DECLASSIFIED

[redacted]

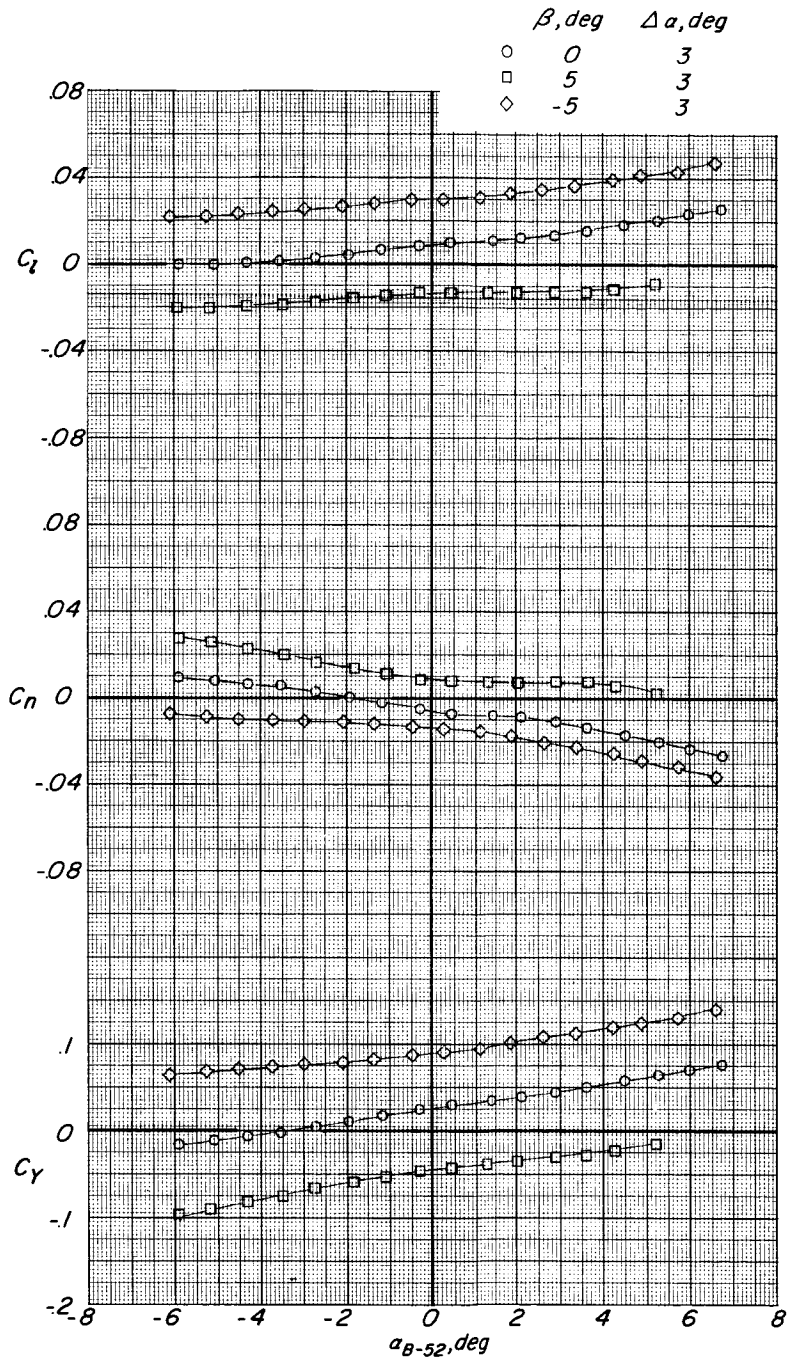

(c) Concluded.

Figure 7.- Continued.

[redacted]

[redacted]

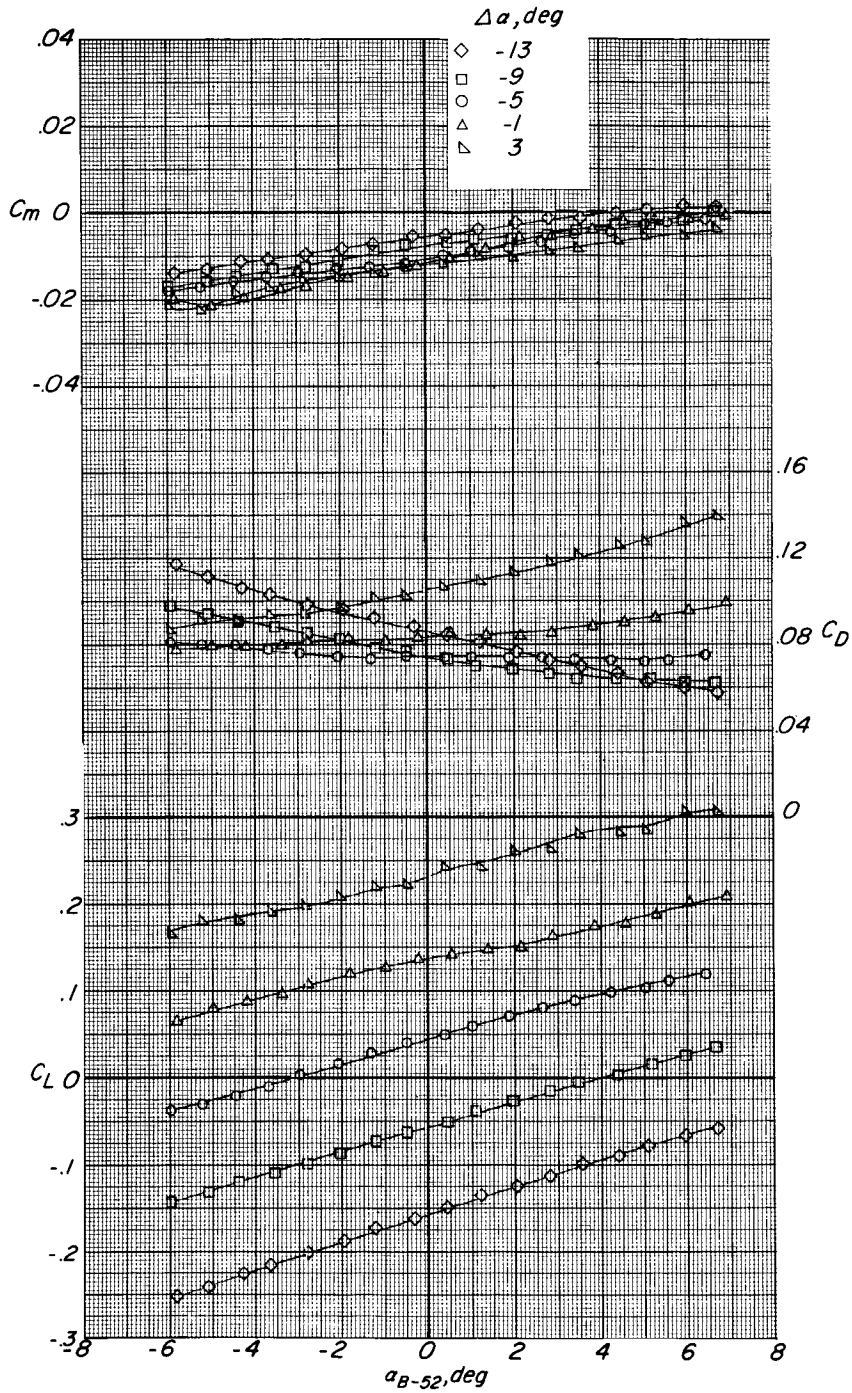

(d) z' = 8.0 feet (2.44 m).

Figure 7.- Continued.

[redacted]

DECLASSIFIED

[redacted]

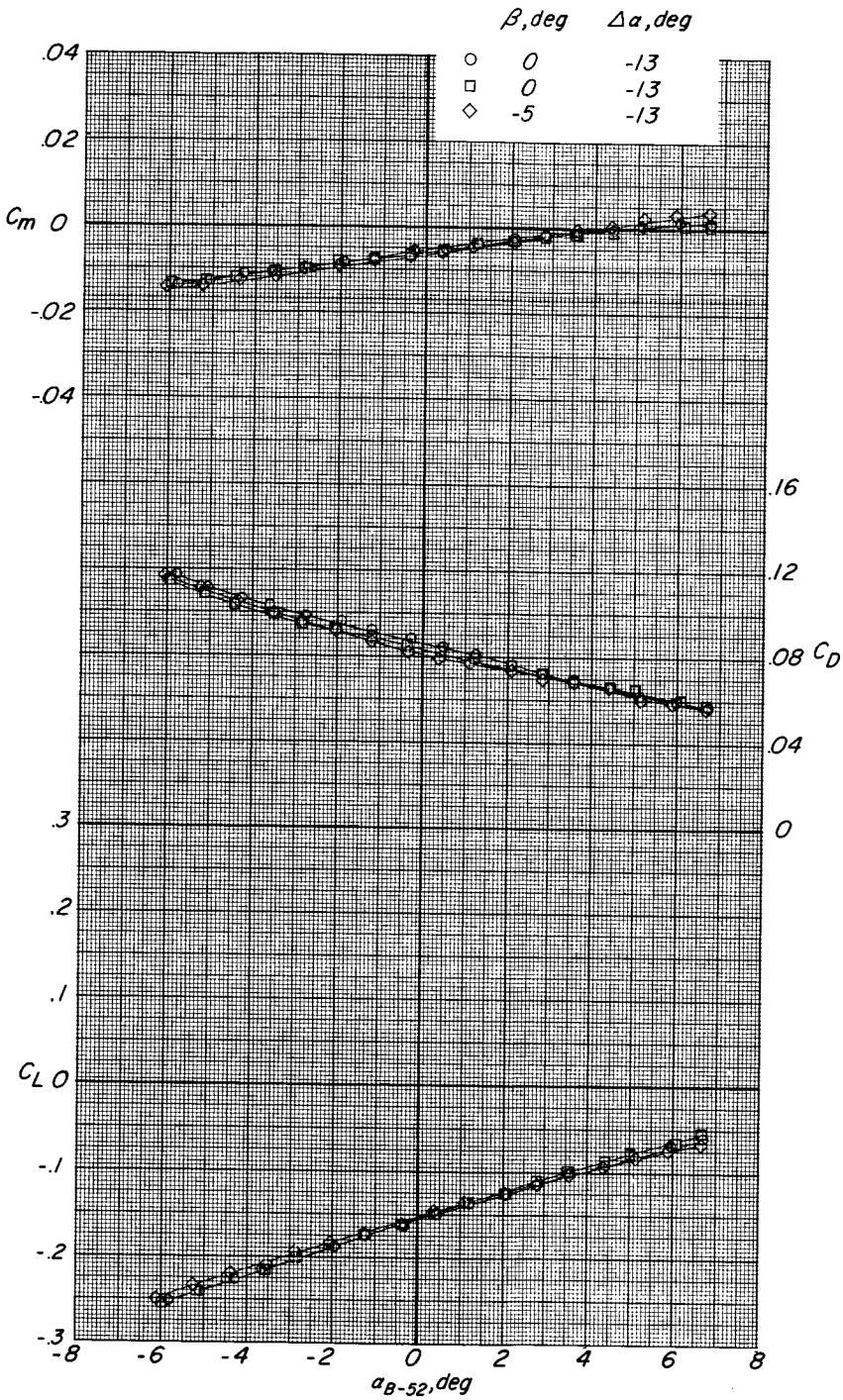

(d) Continued.

Figure 7.- Continued.

[redacted]

[redacted]

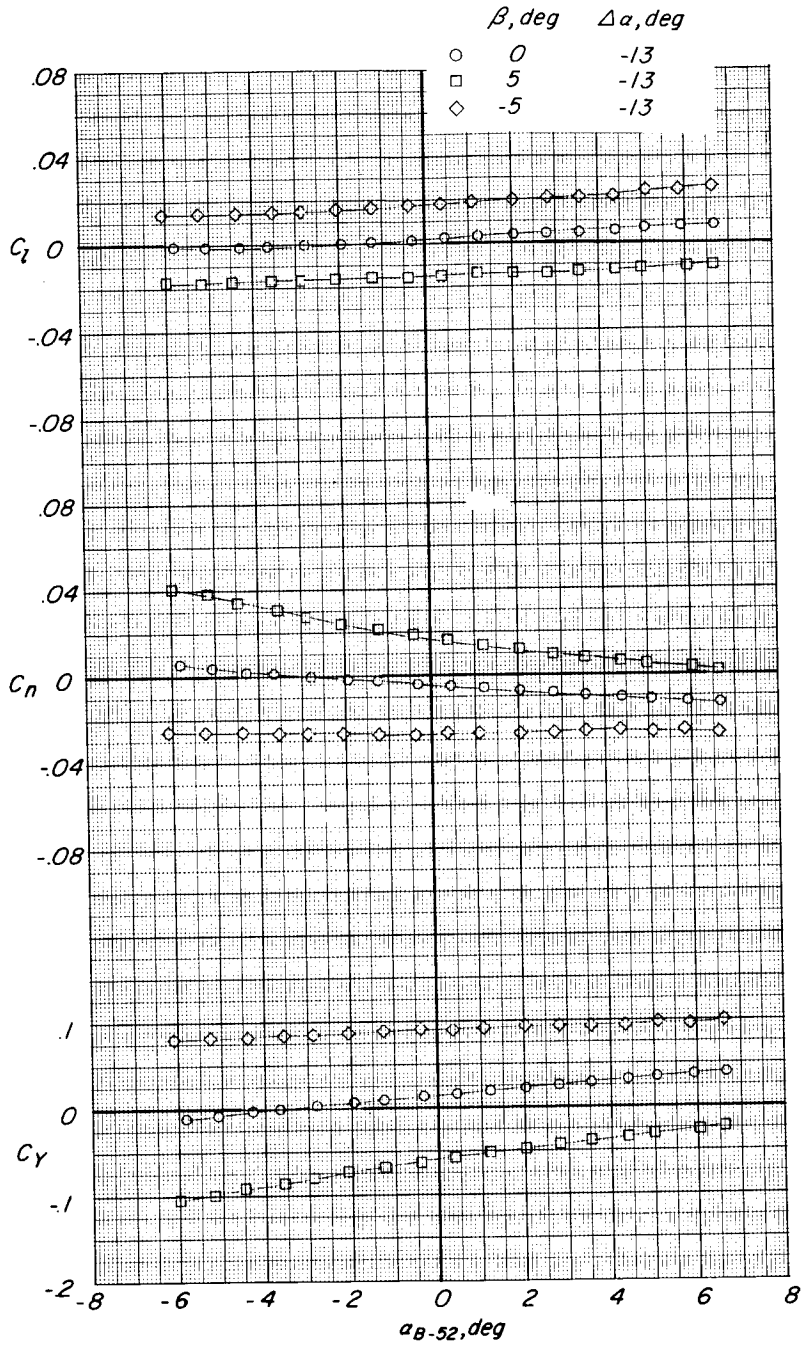

(d) Continued.

Figure 7.- Continued.

[redacted]

DECLASSIFIED

[redacted]

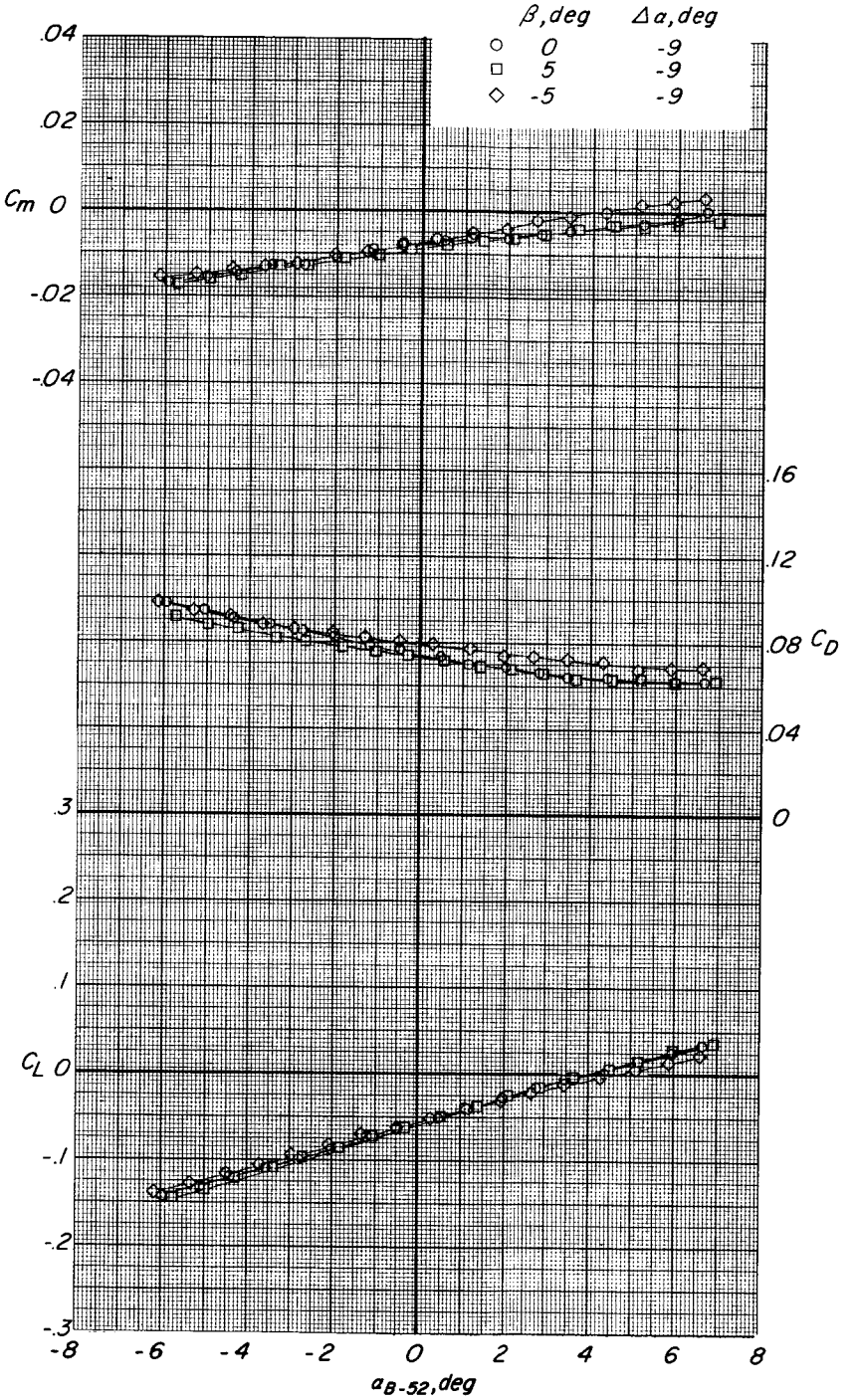

(d) Continued.

Figure 7.- Continued.

[redacted]

[redacted]

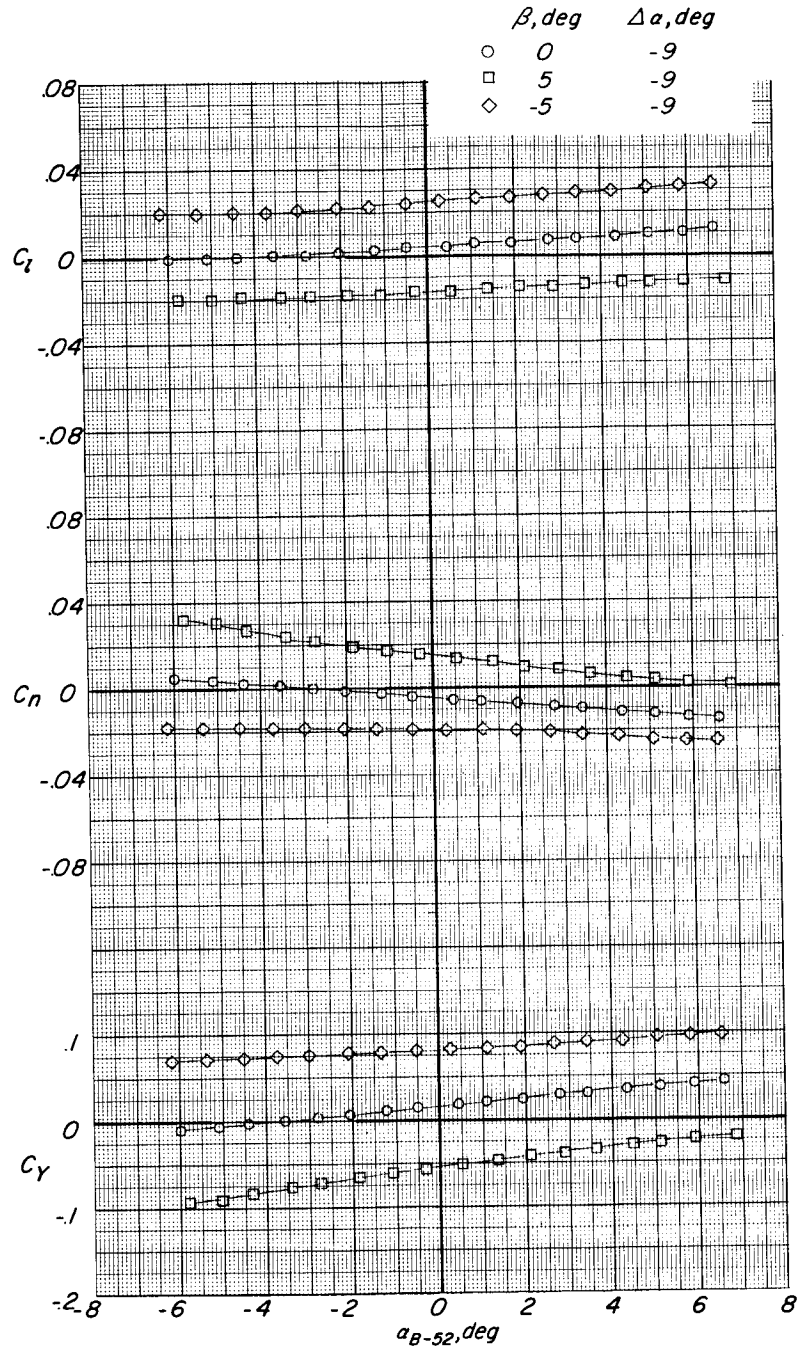

(d) Continued.

Figure 7.- Continued.

[redacted]

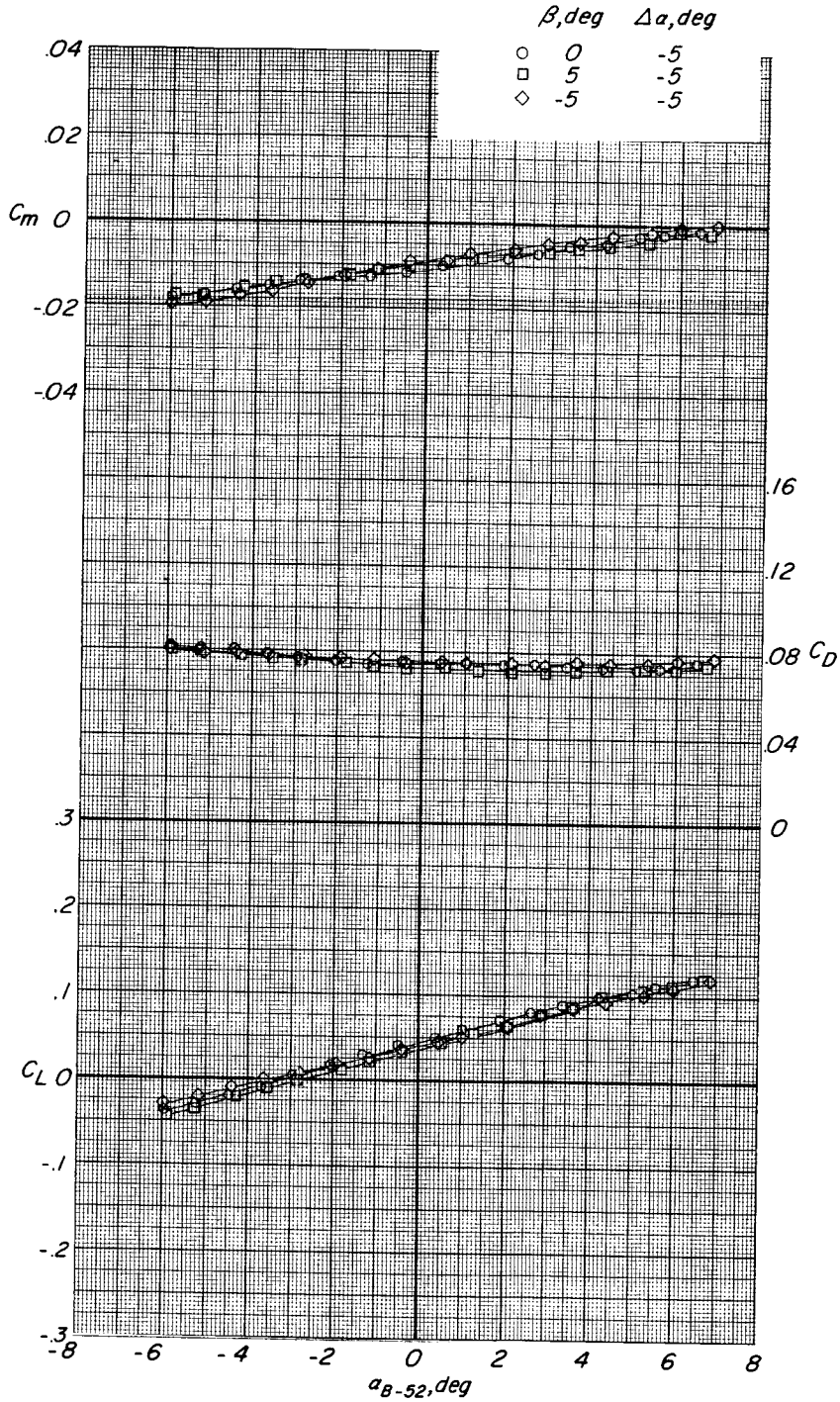

(d) Continued.

Figure 7.- Continued.

[redacted]

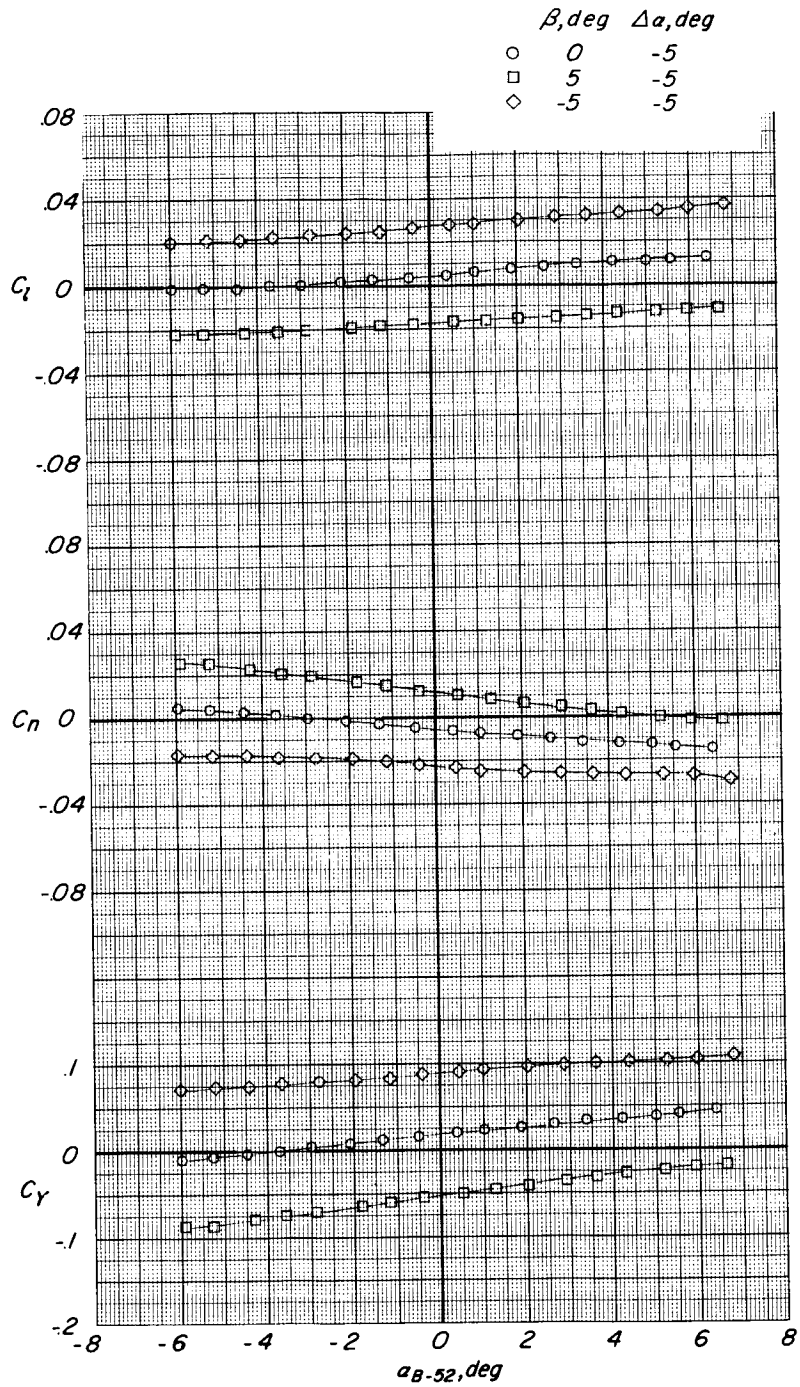

(d) Continued.

Figure 7.- Continued.

[redacted]

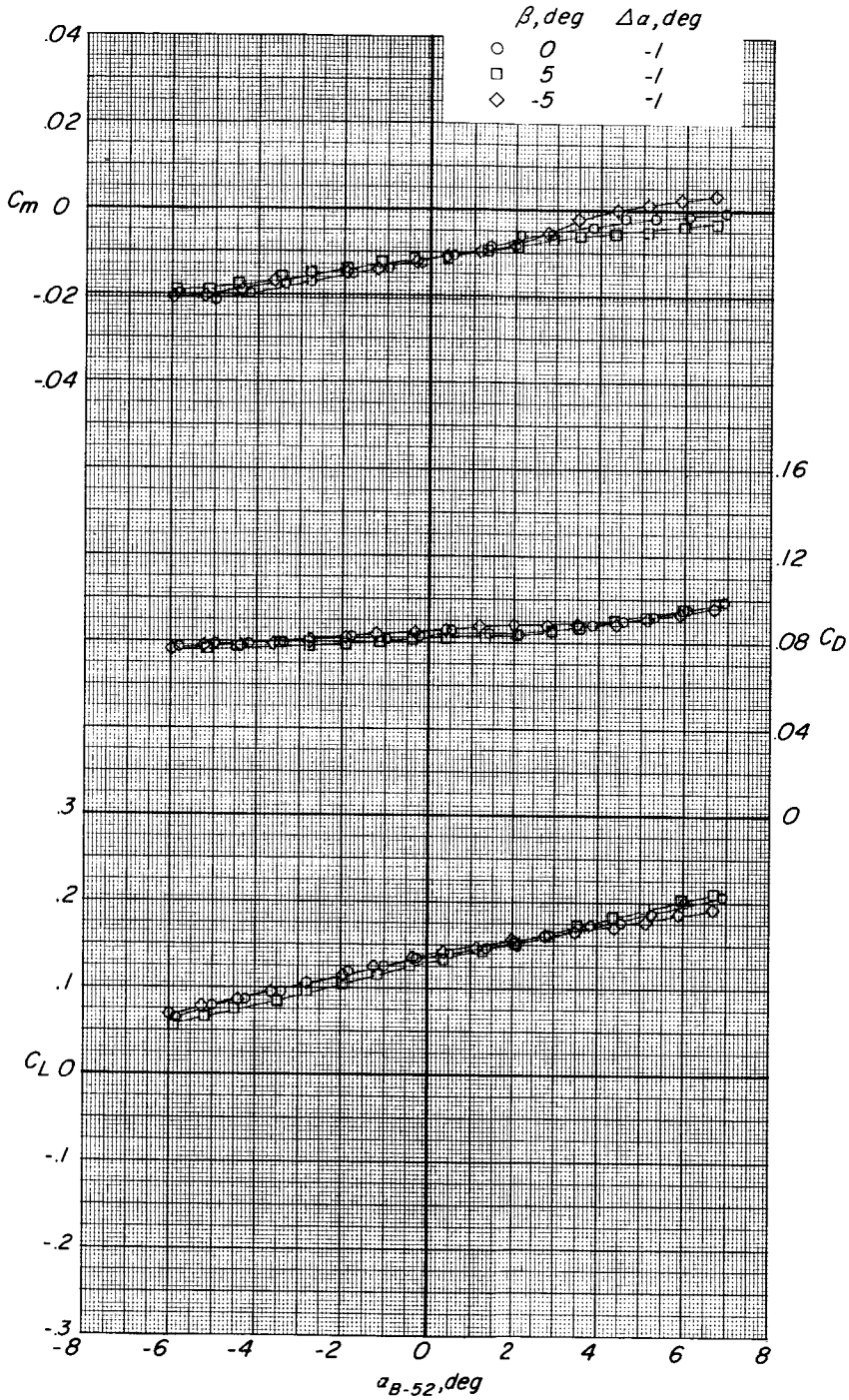

(d) Continued.

Figure 7.- Continued.

[redacted]

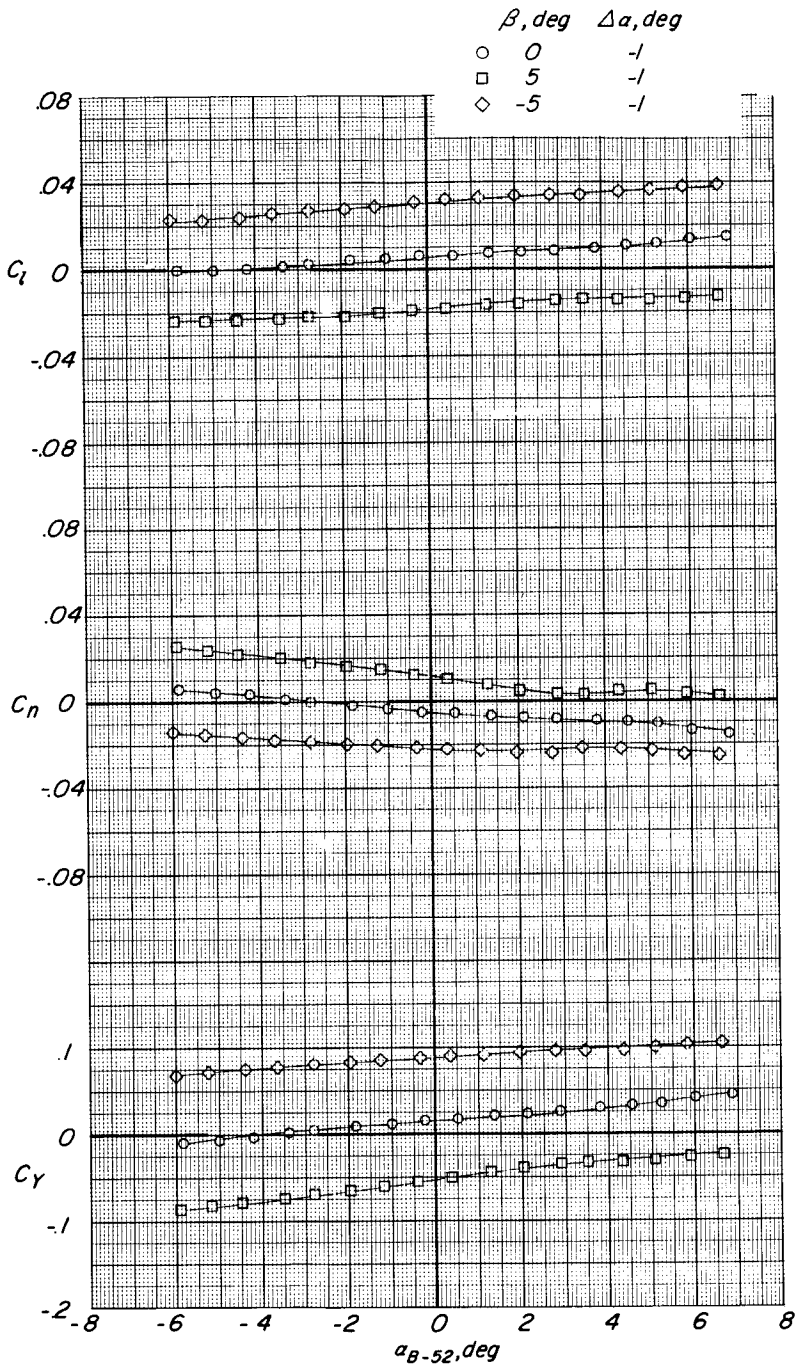

(d) Continued.

Figure 7.- Continued.

[redacted]

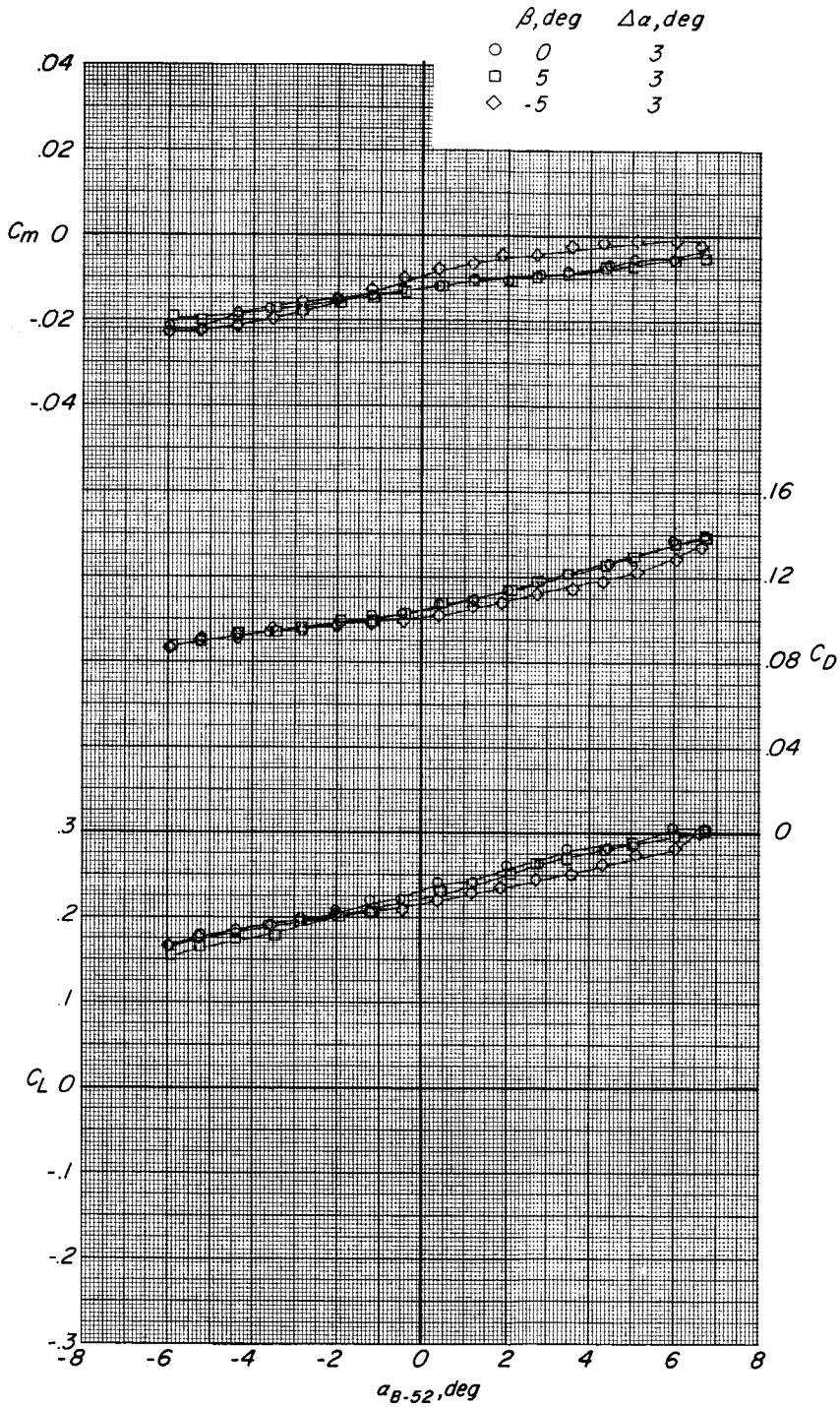

(d) Continued.

Figure 7.- Continued.

[redacted]

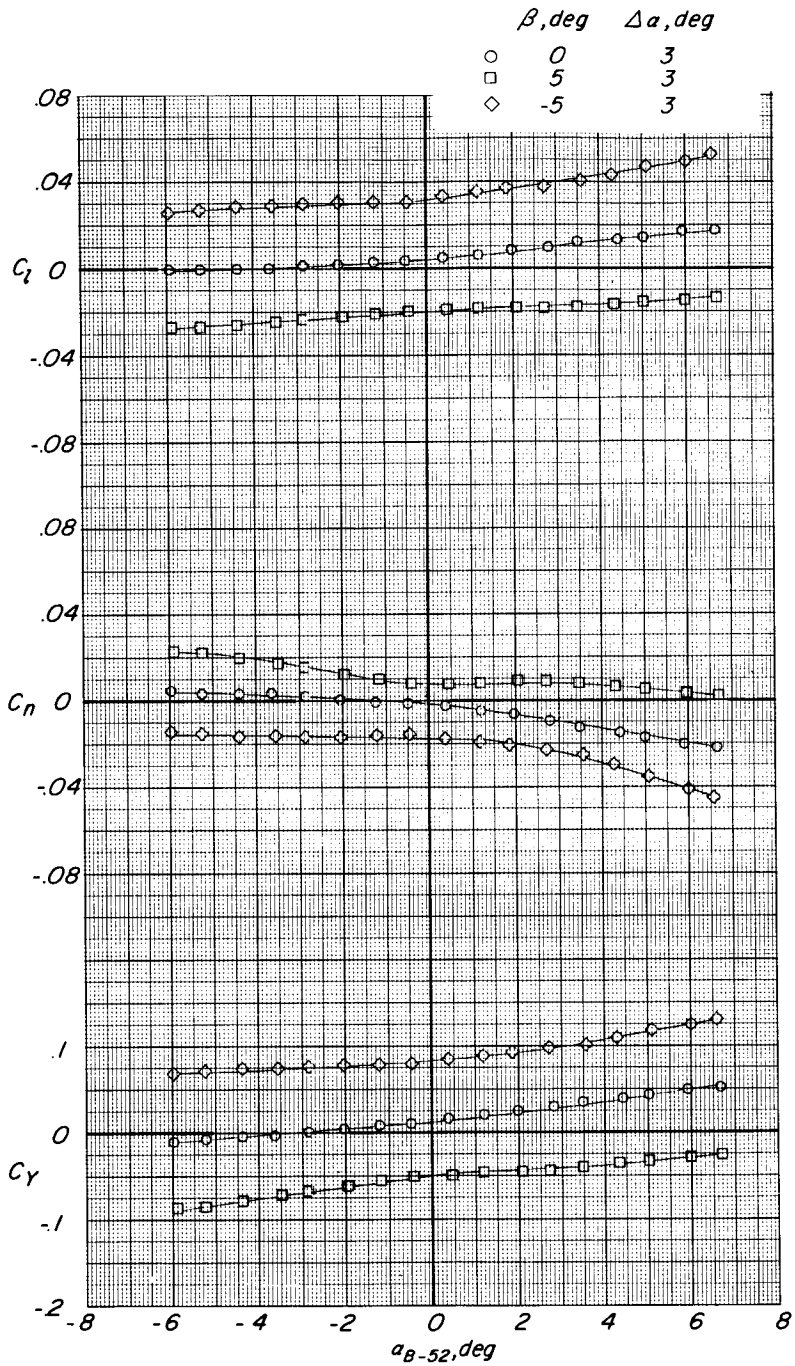

(d) Concluded.

Figure 7.- Continued.

[redacted]

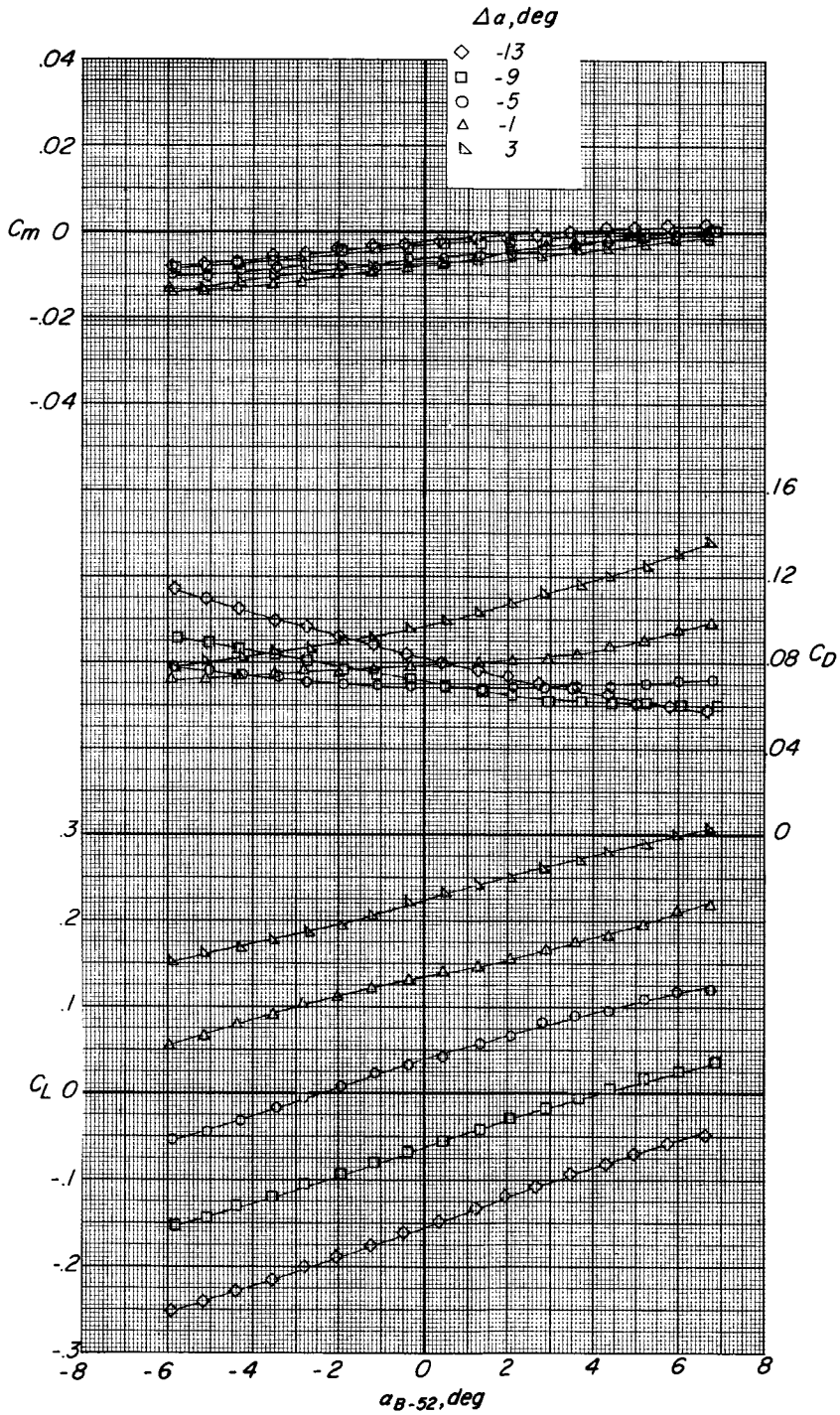

(e) z' = 12.0 feet (3.66 m).

Figure 7.- Continued.

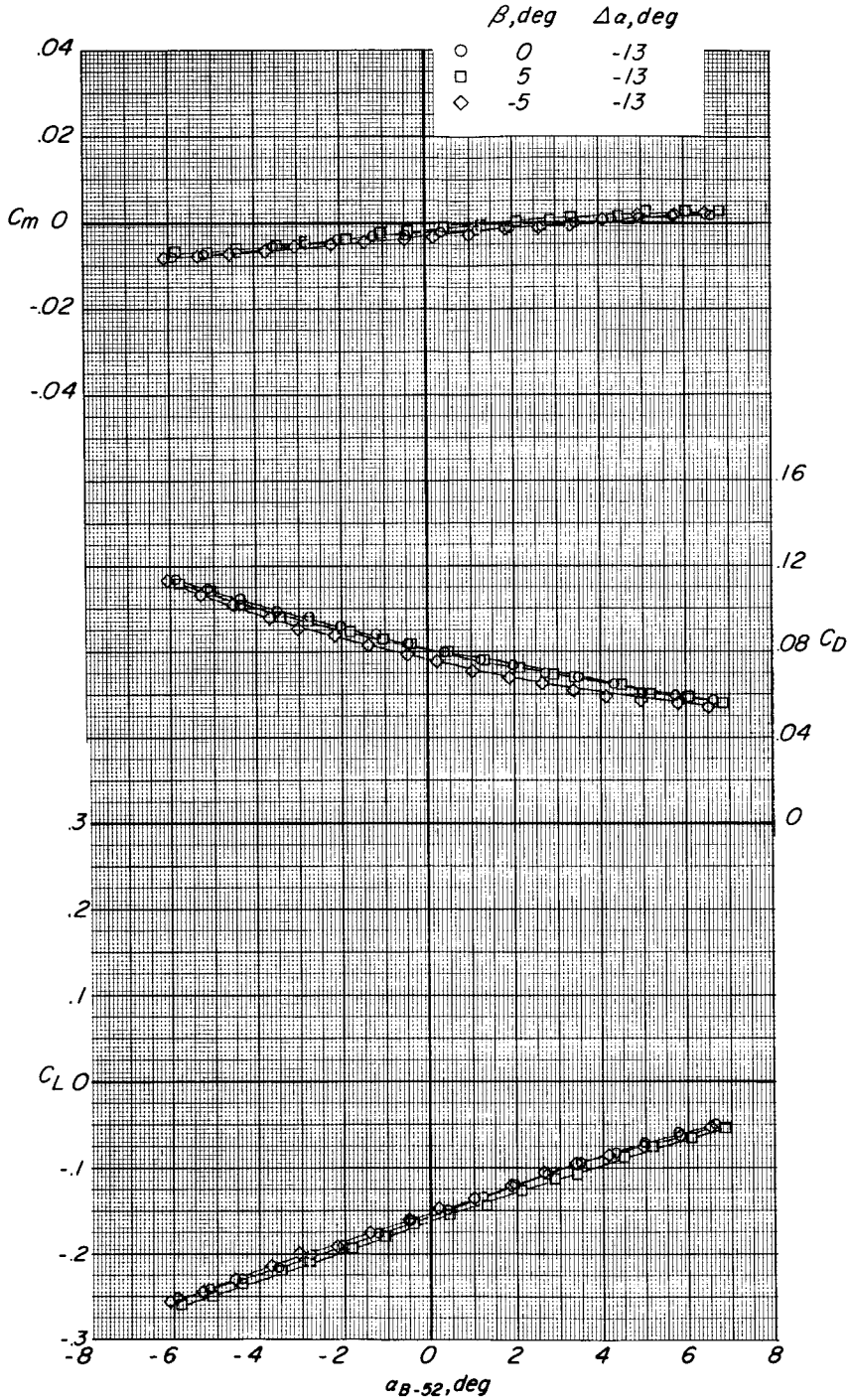

(e) Continued.

Figure 7.- Continued.

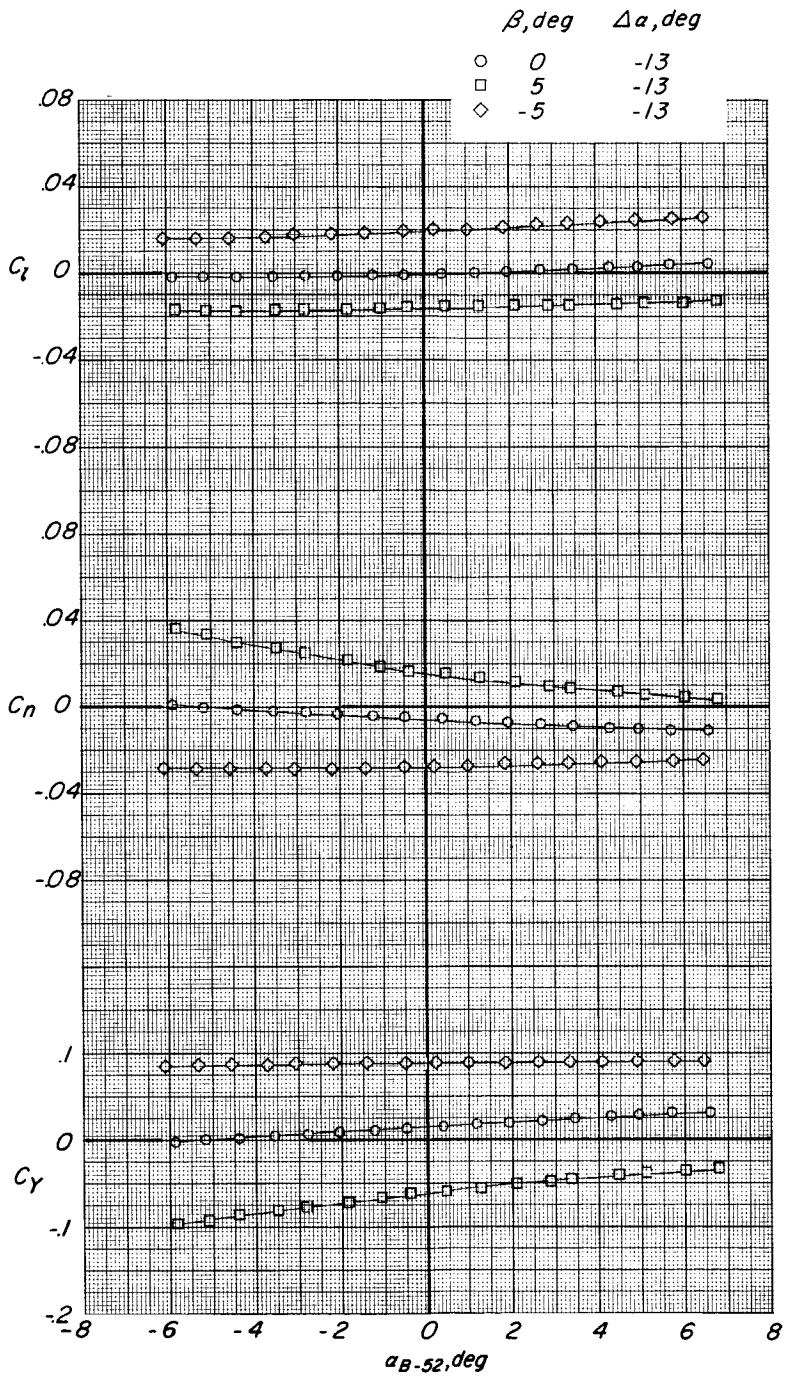

(e) Continued.

Figure 7.- Continued.

[redacted]

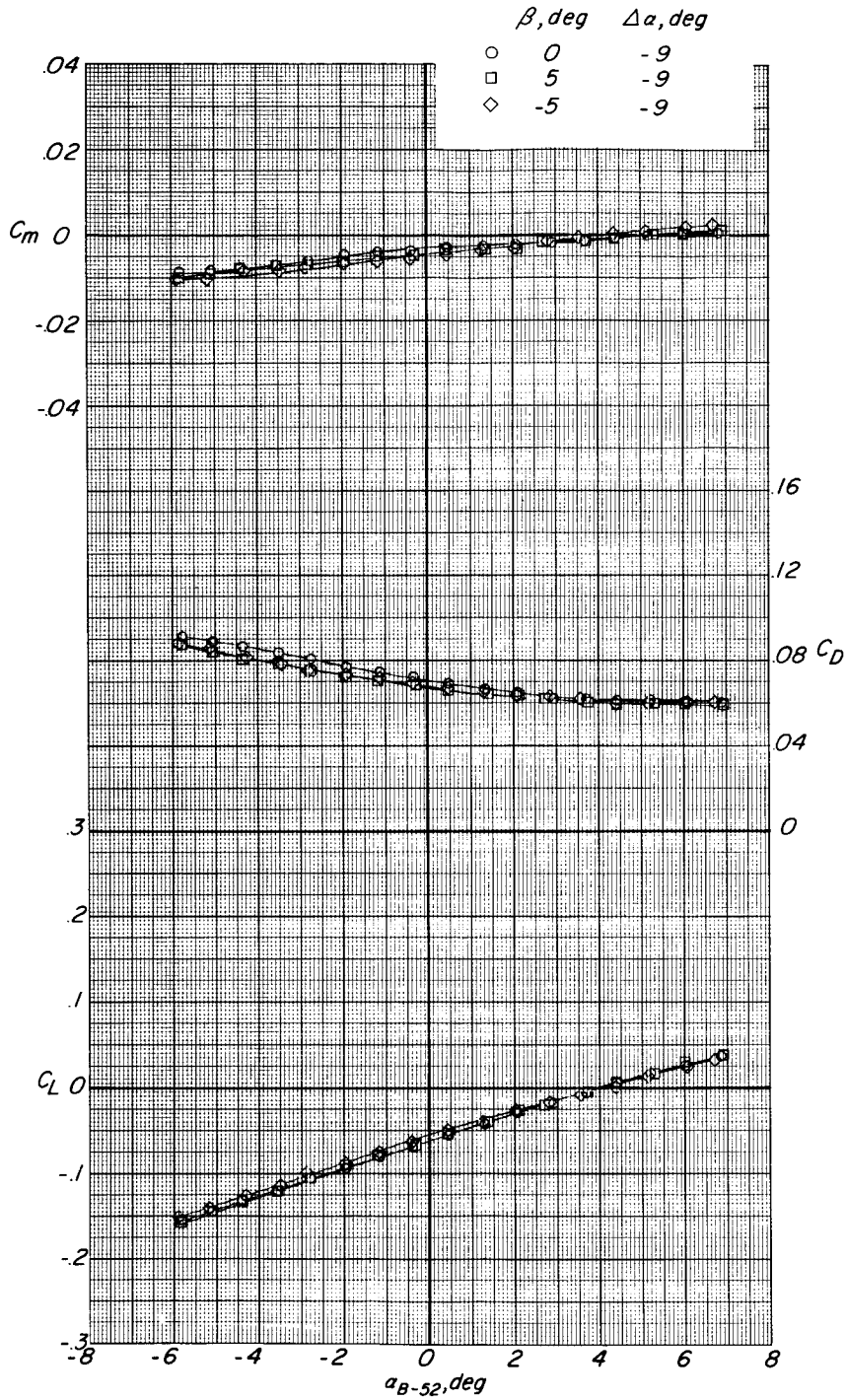

(e) Continued.

Figure 7.- Continued.

[redacted]

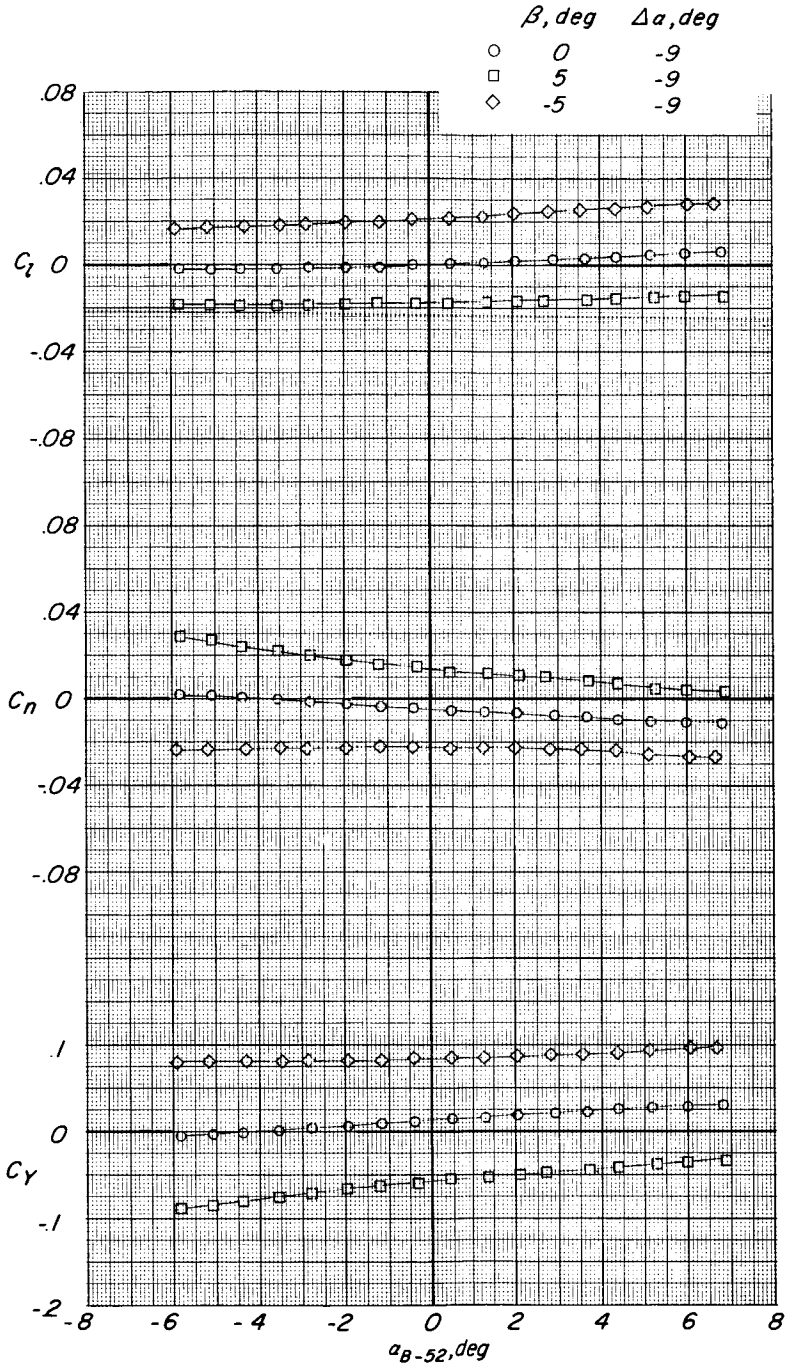

(e) Continued.

Figure 7.- Continued.

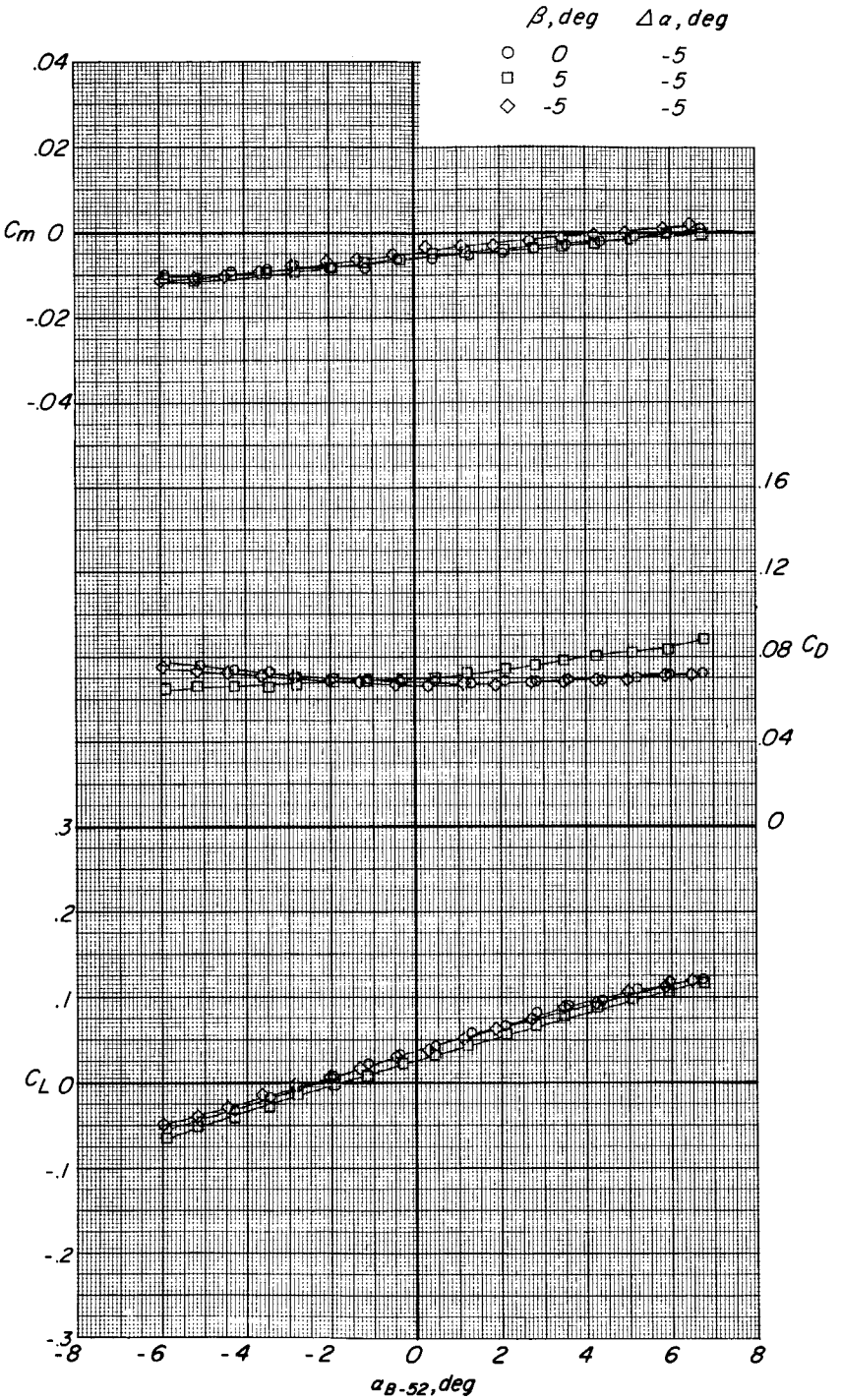

(e) Continued.

Figure 7.- Continued.

[redacted] DECLASSIFIED

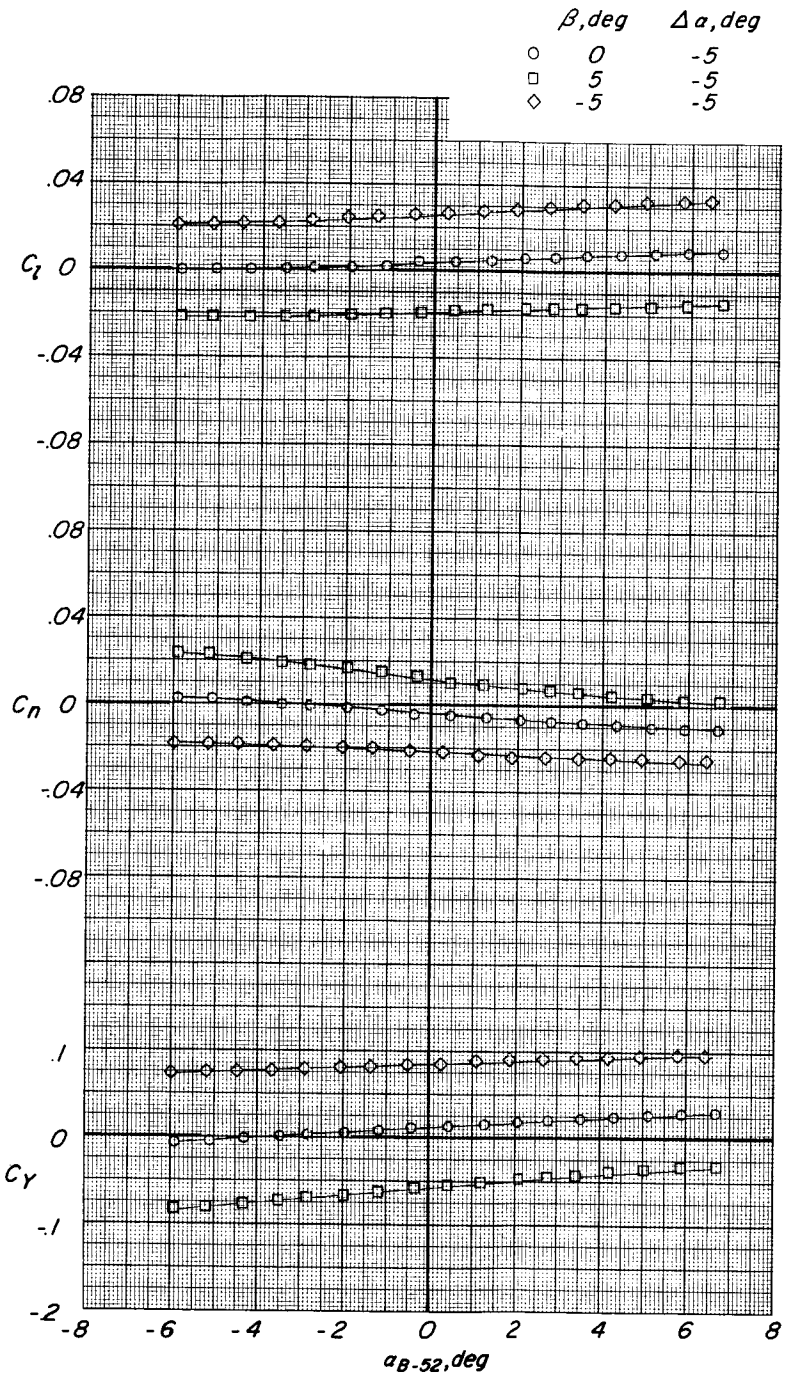

(e) Continued.

Figure 7.- Continued.

[redacted]

[redacted]

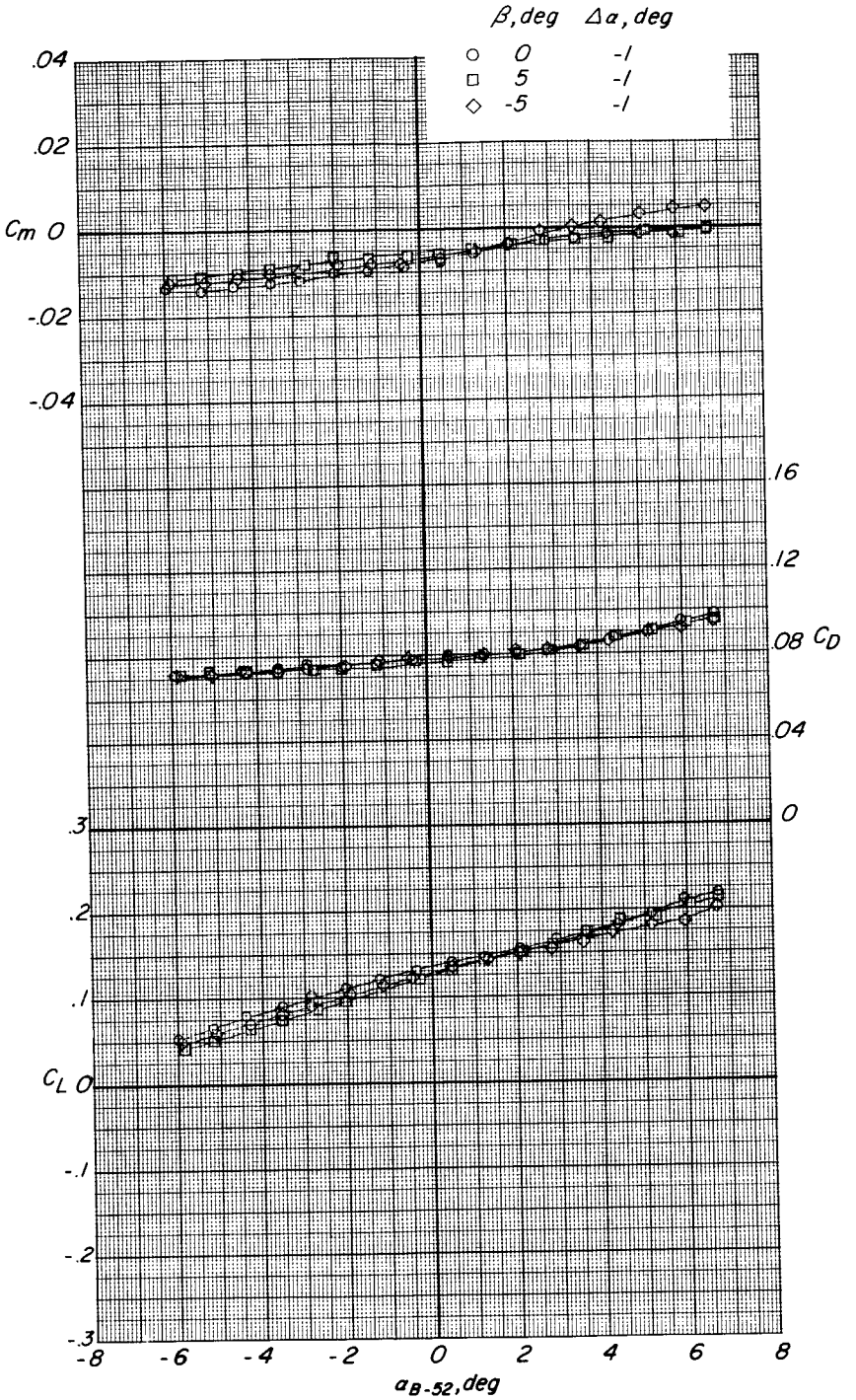

(e) Continued.

Figure 7.- Continued.

[redacted]

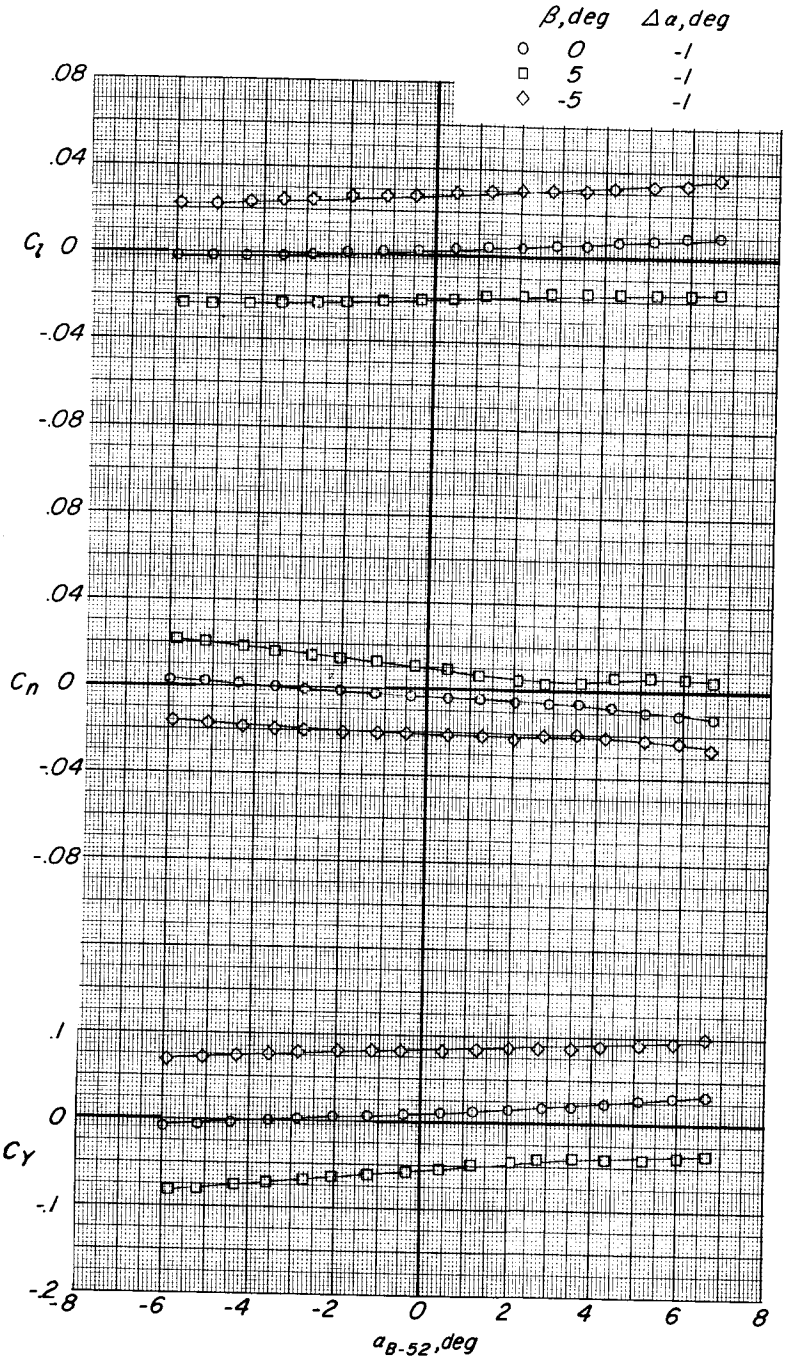

(e) Continued.

Figure 7.- Continued.

[redacted]

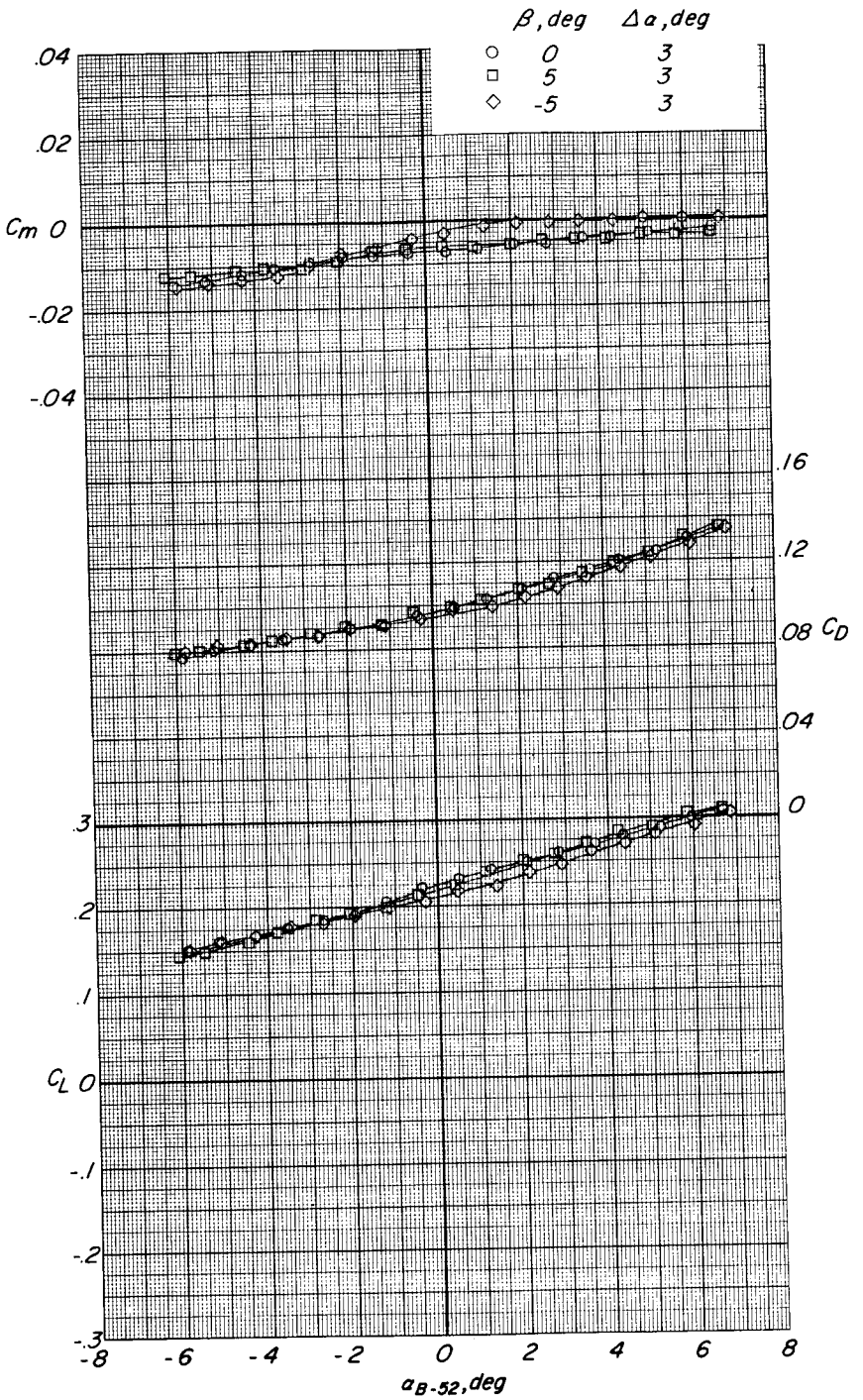

(e) Continued.

Figure 7.- Continued.

[redacted]

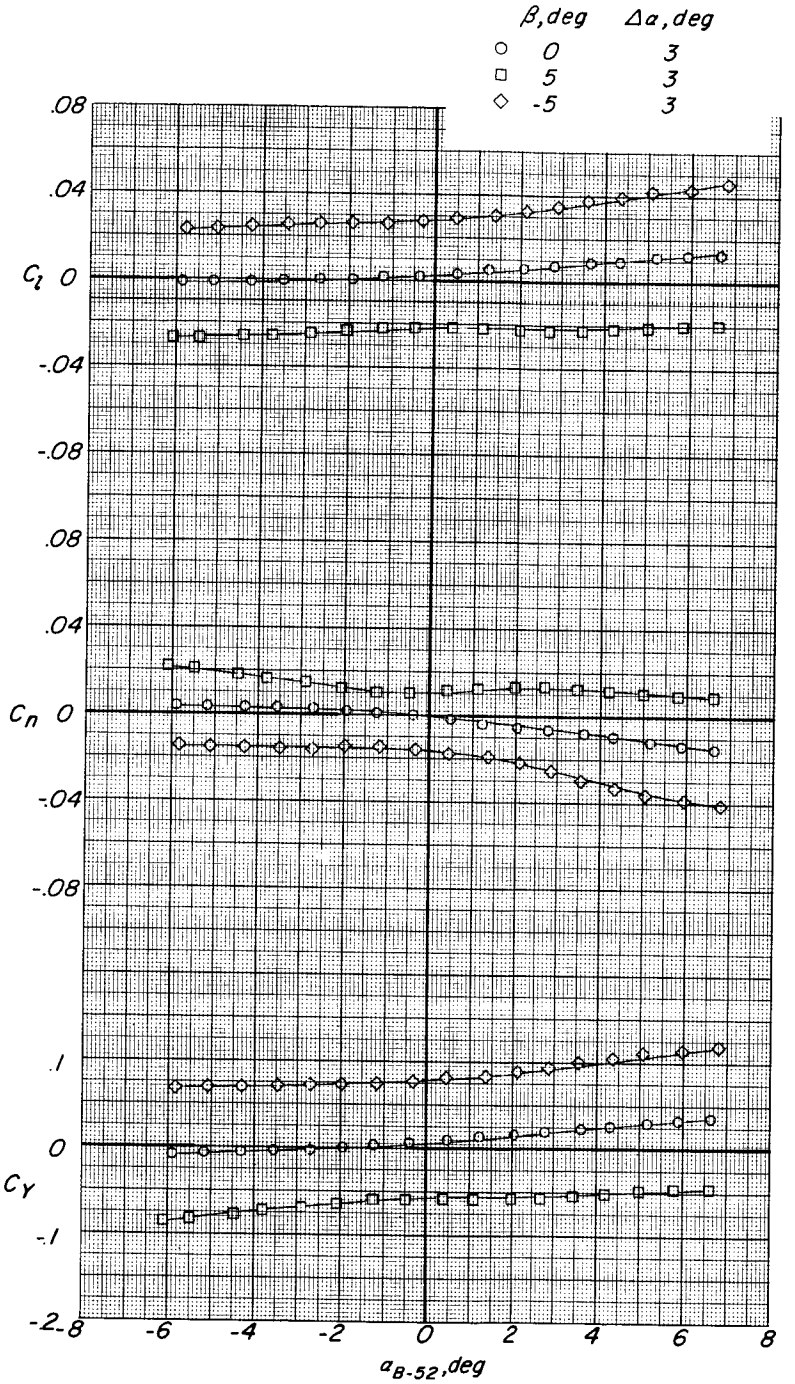

(e) Concluded.

Figure 7.- Concluded.

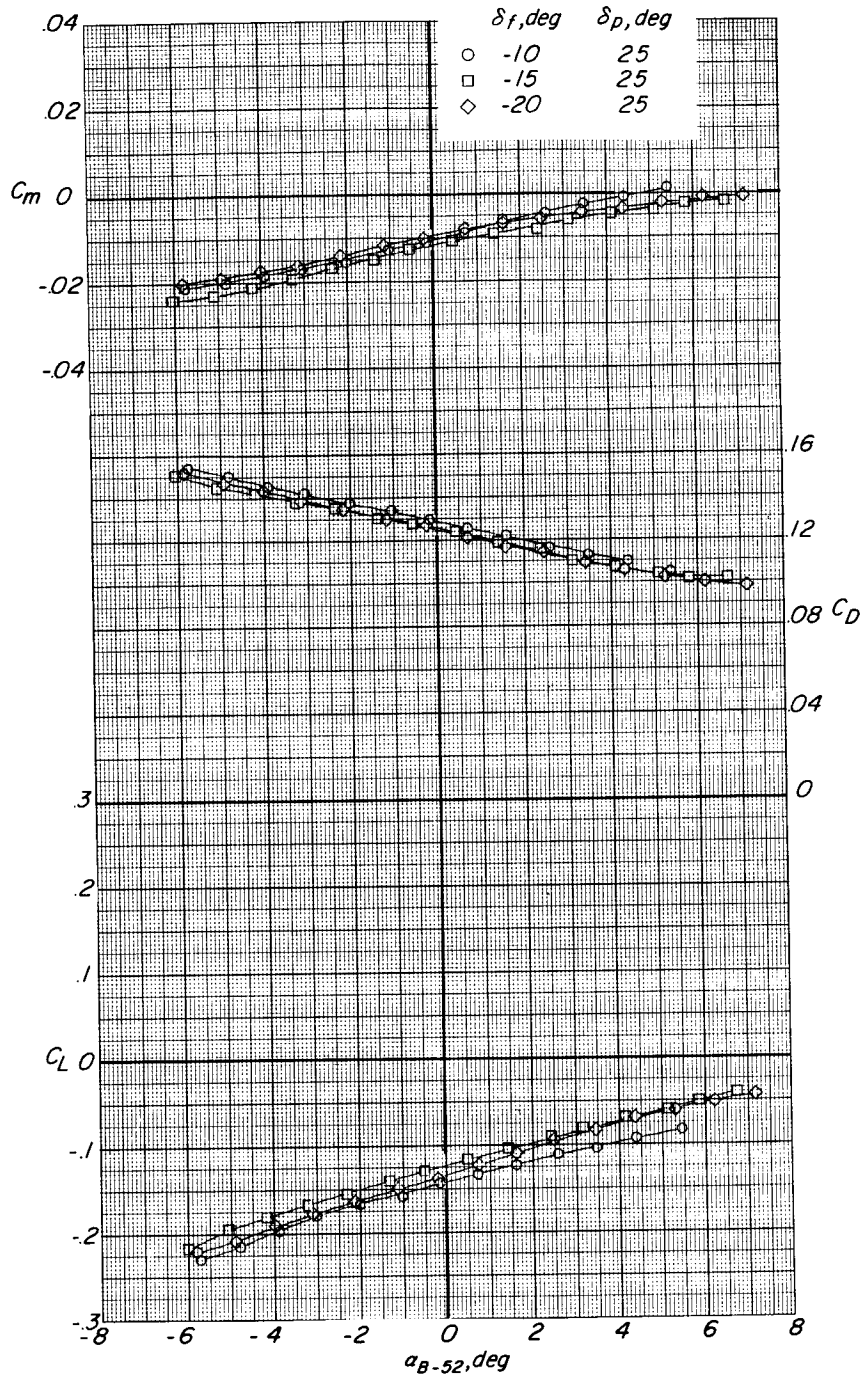

(a) z' = 0.

Figure 8.- Aerodynamic characteristics of M2-F2 model in presence of B-52 model. M = 0.70; nominal control settings are $\delta_p = 25^0$, $\delta_f = -10^0$, and 10^0 rudder flare.

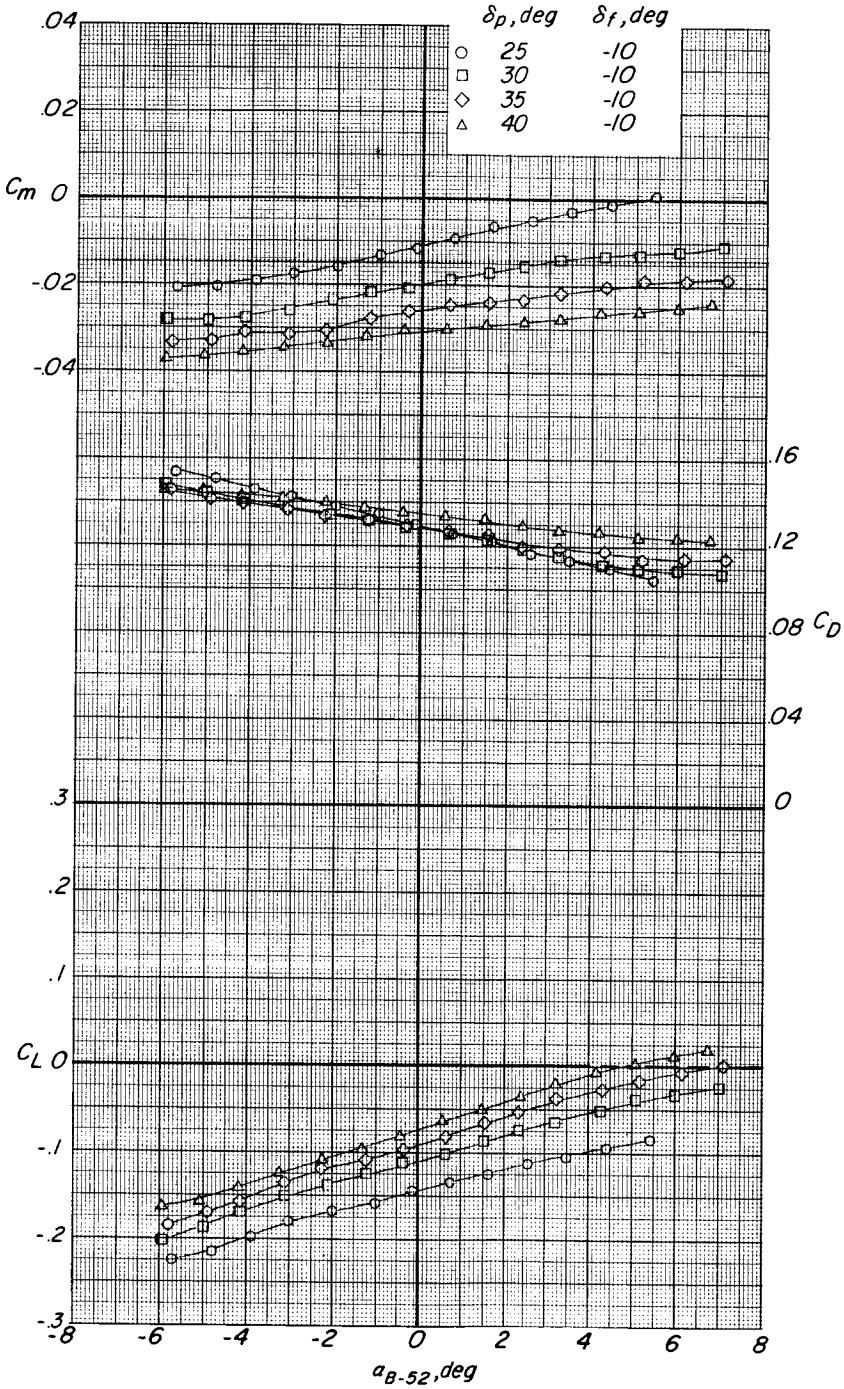

(a) Continued.

Figure 8.- Continued.

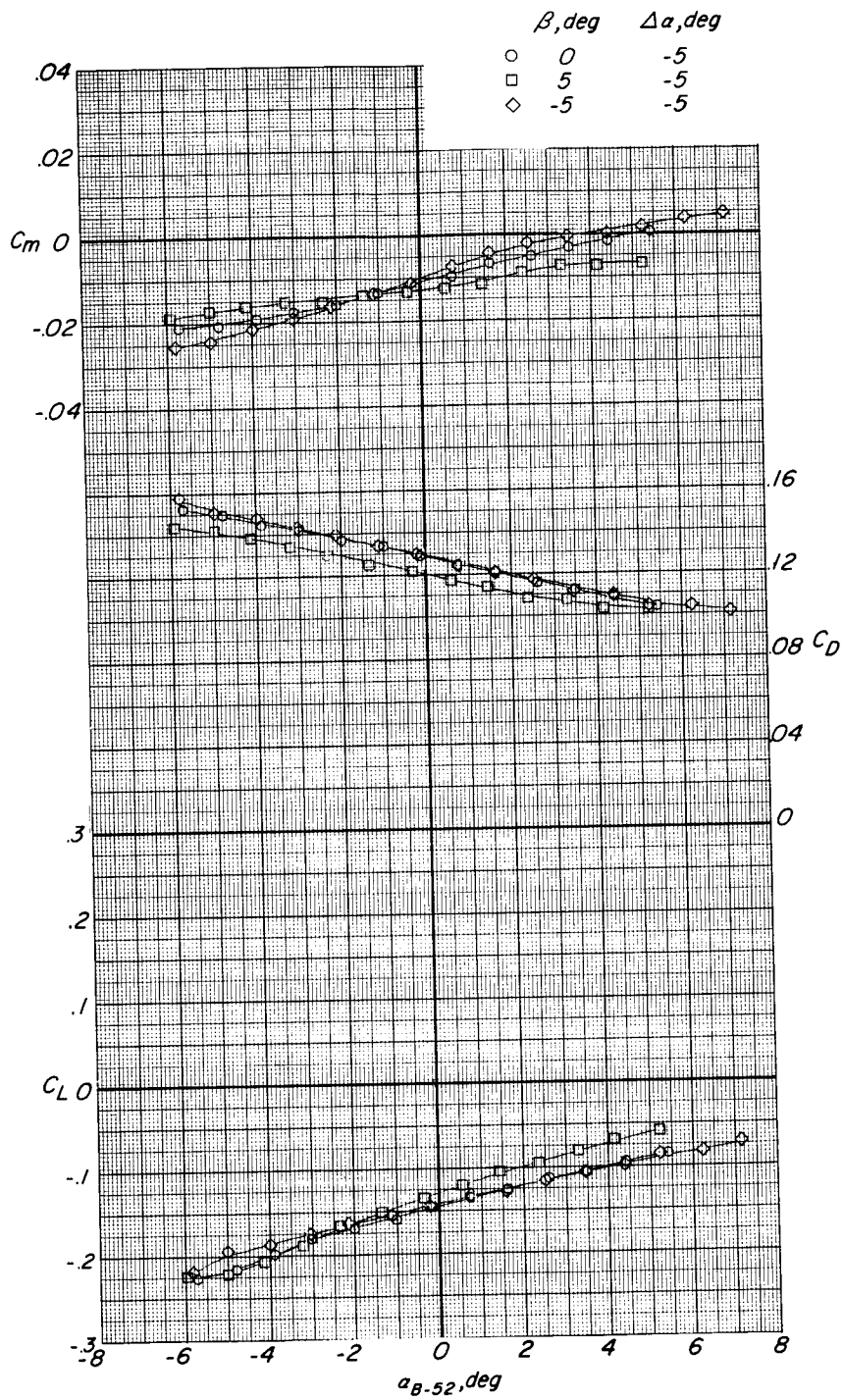

(a) Continued.

Figure 8.- Continued.

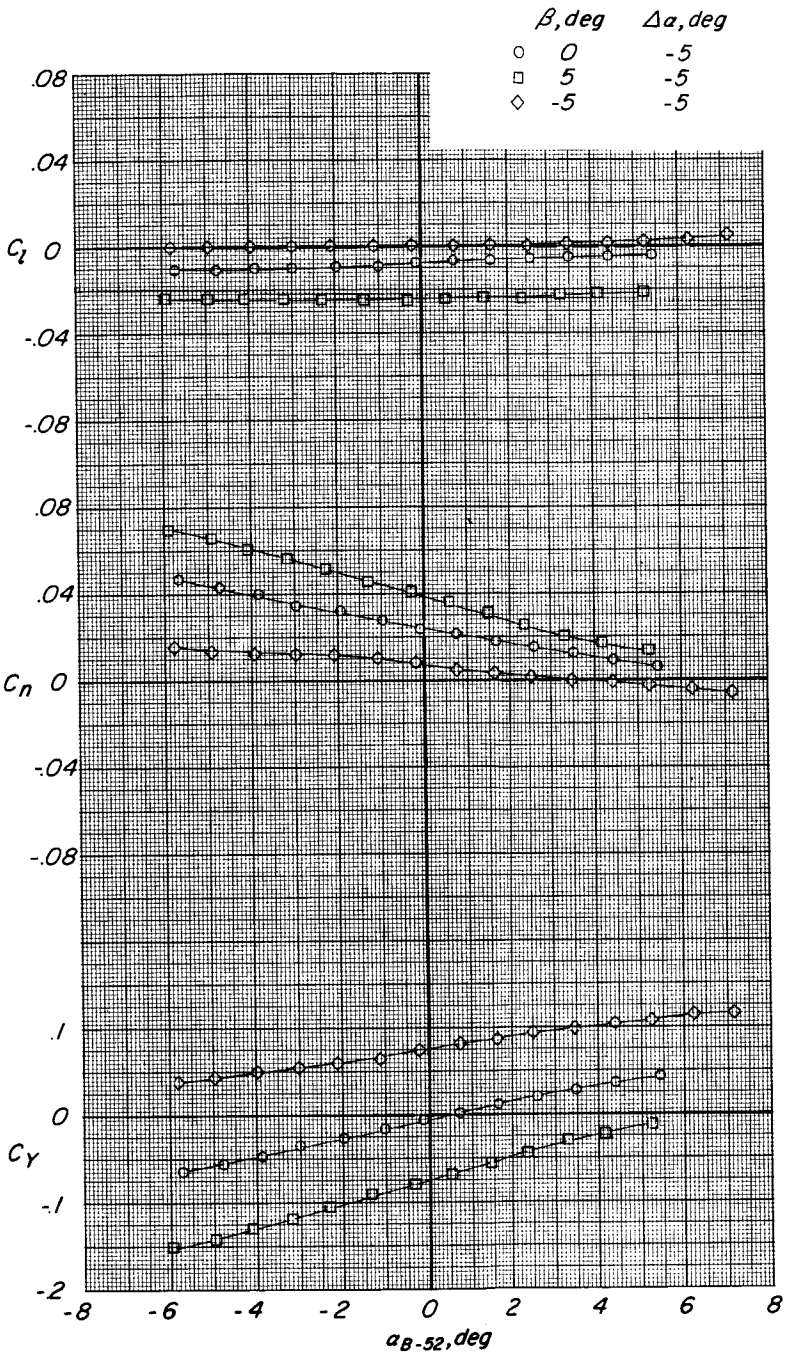

(a) Continued.

Figure 8.- Continued.

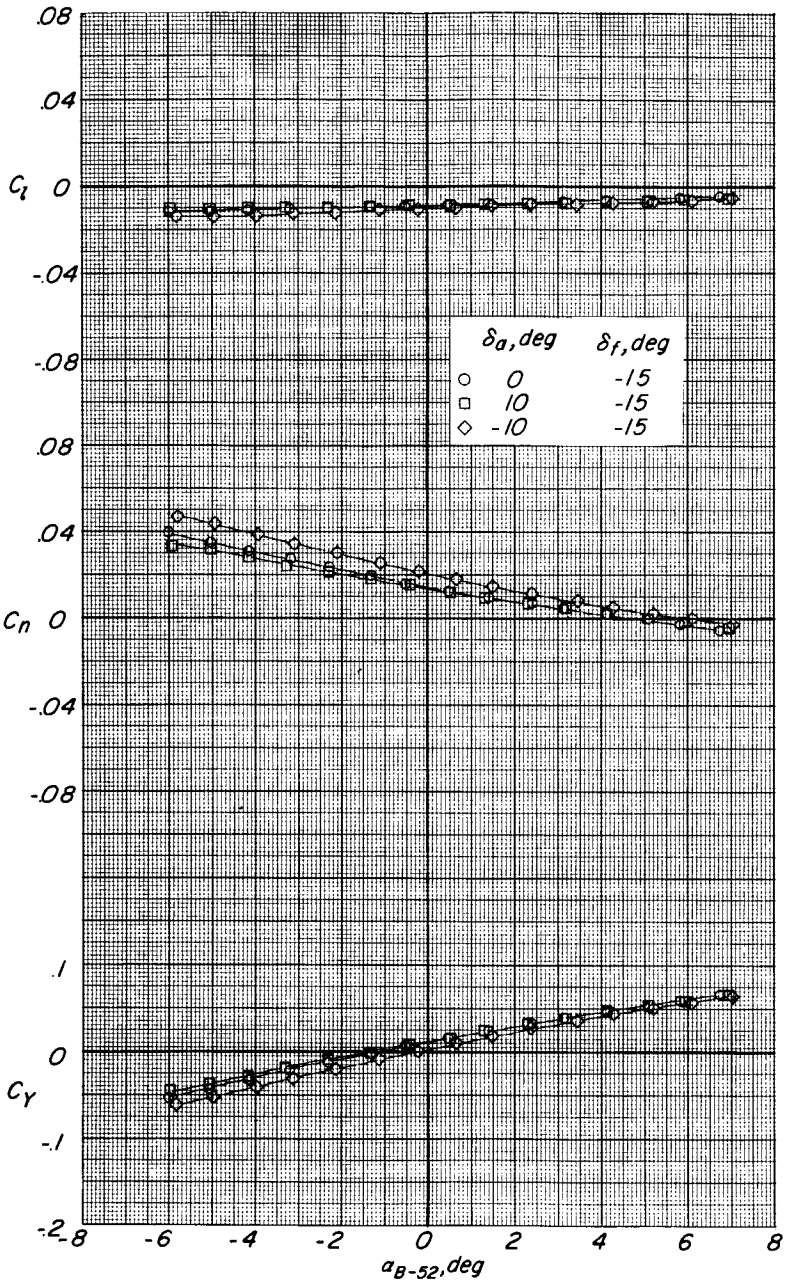

(a) Continued.

Figure 8.- Continued.

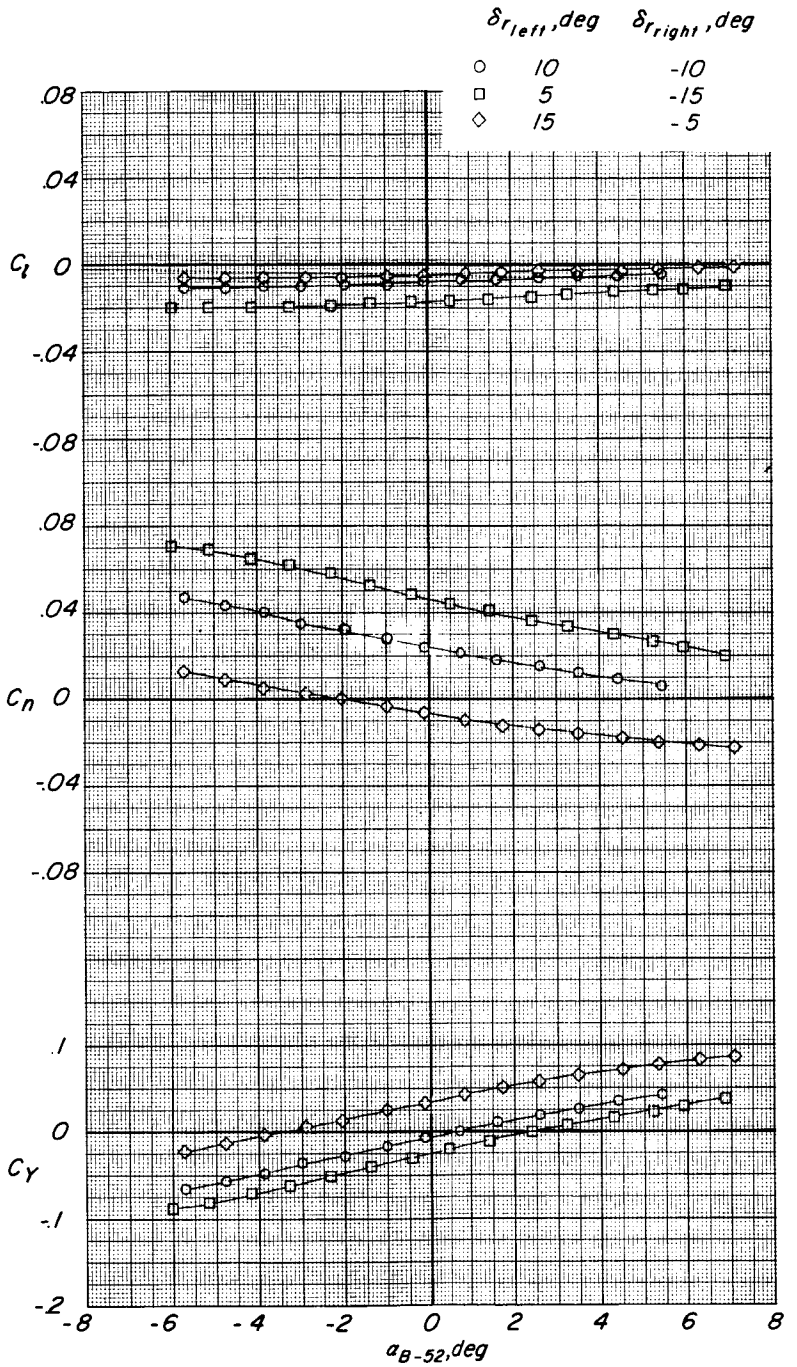

(a) Concluded.

Figure 8.- Continued.

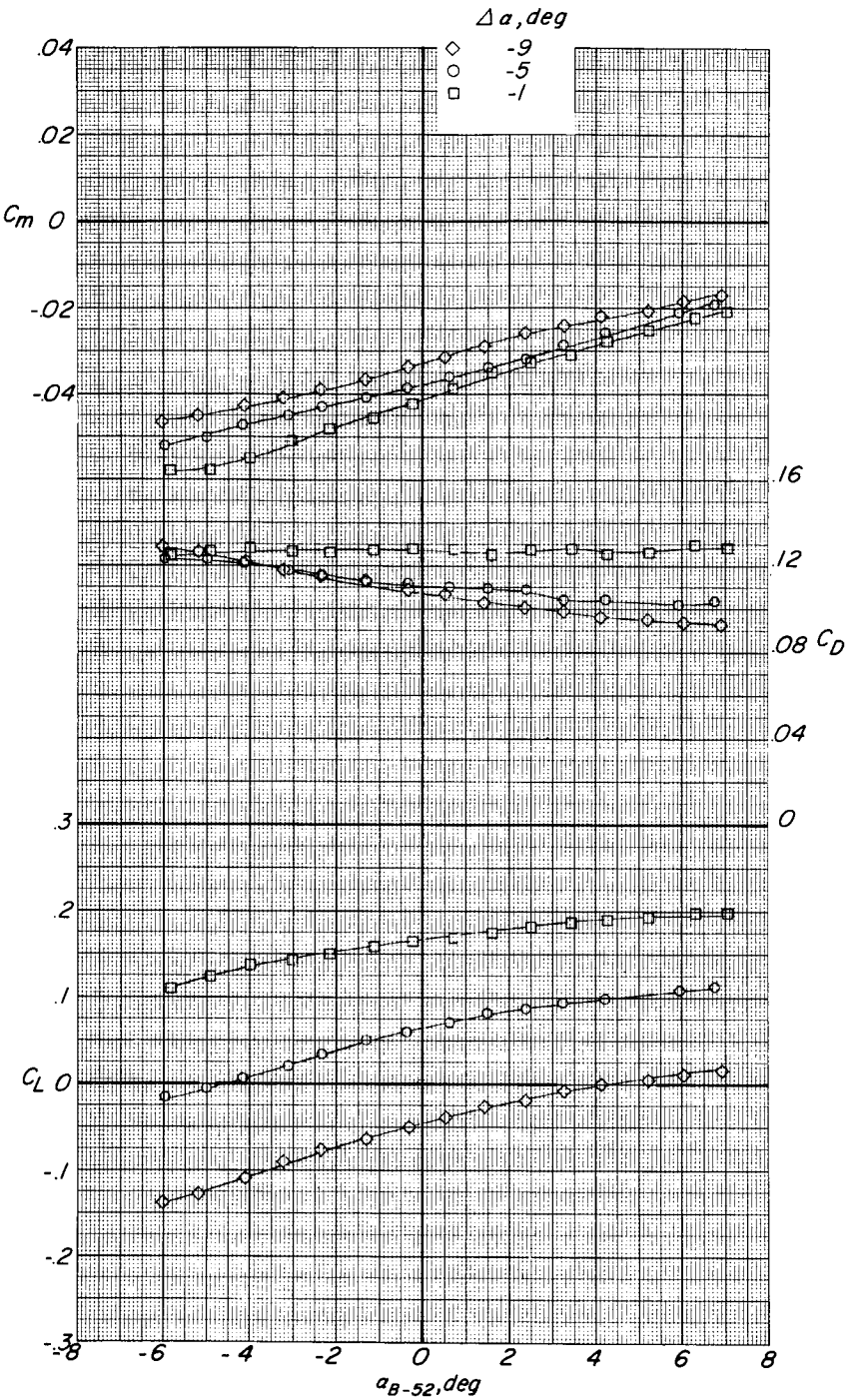

(b) z' = 2.0 feet (0.61 m).

Figure 8.- Continued.

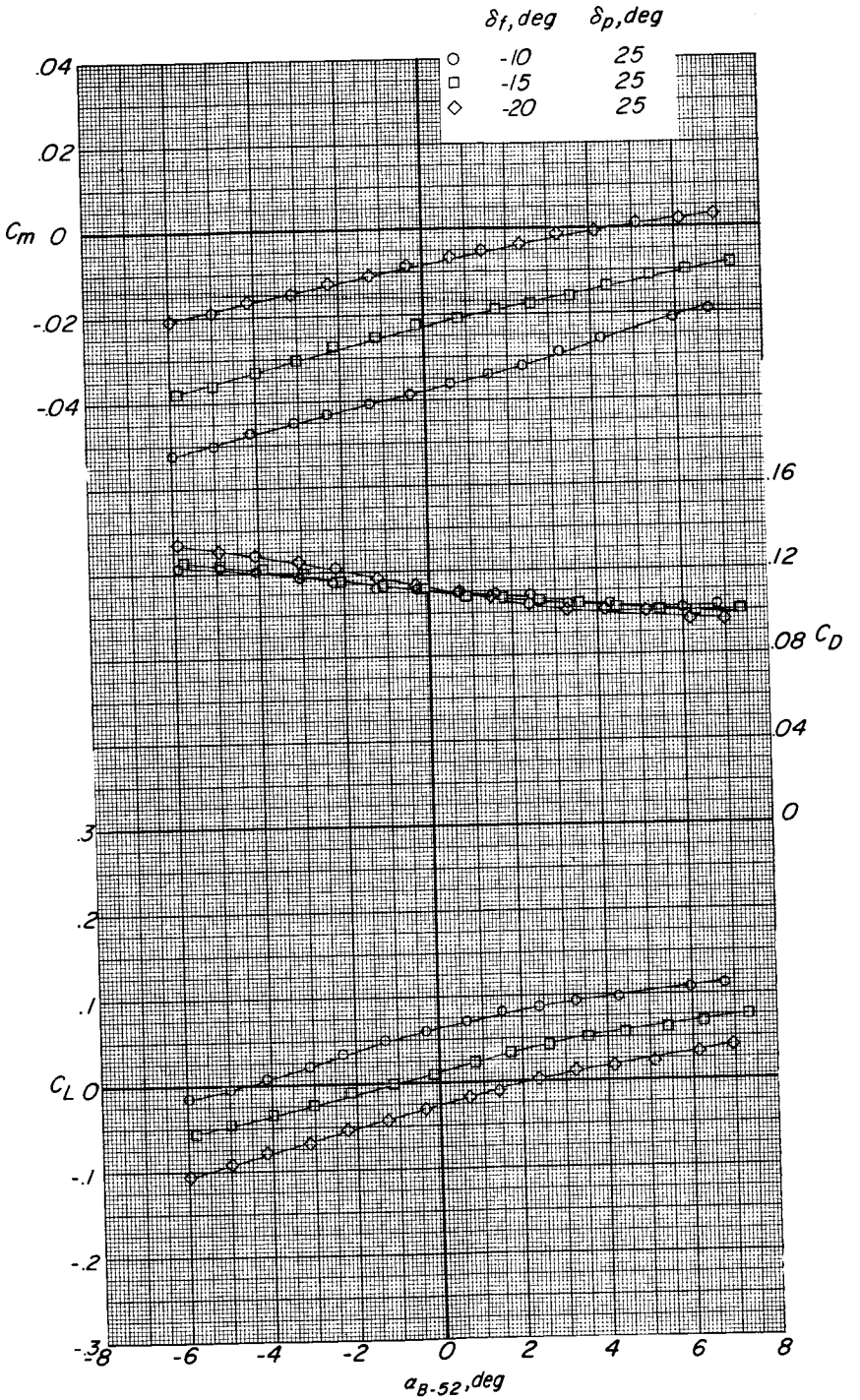

(b) Continued.

Figure 8.- Continued.

[redacted]

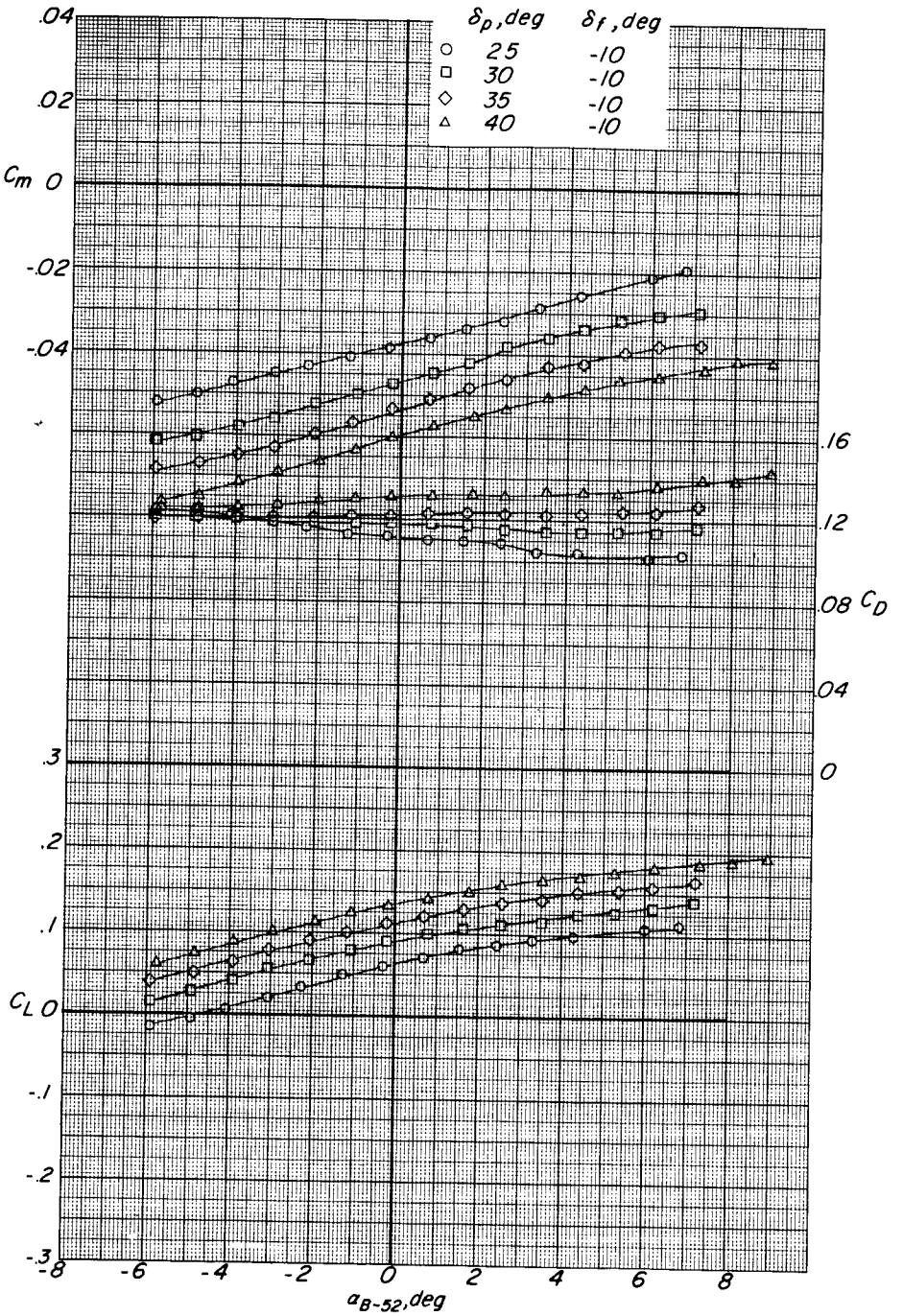

(b) Continued.

Figure 8.- Continued.

[redacted]

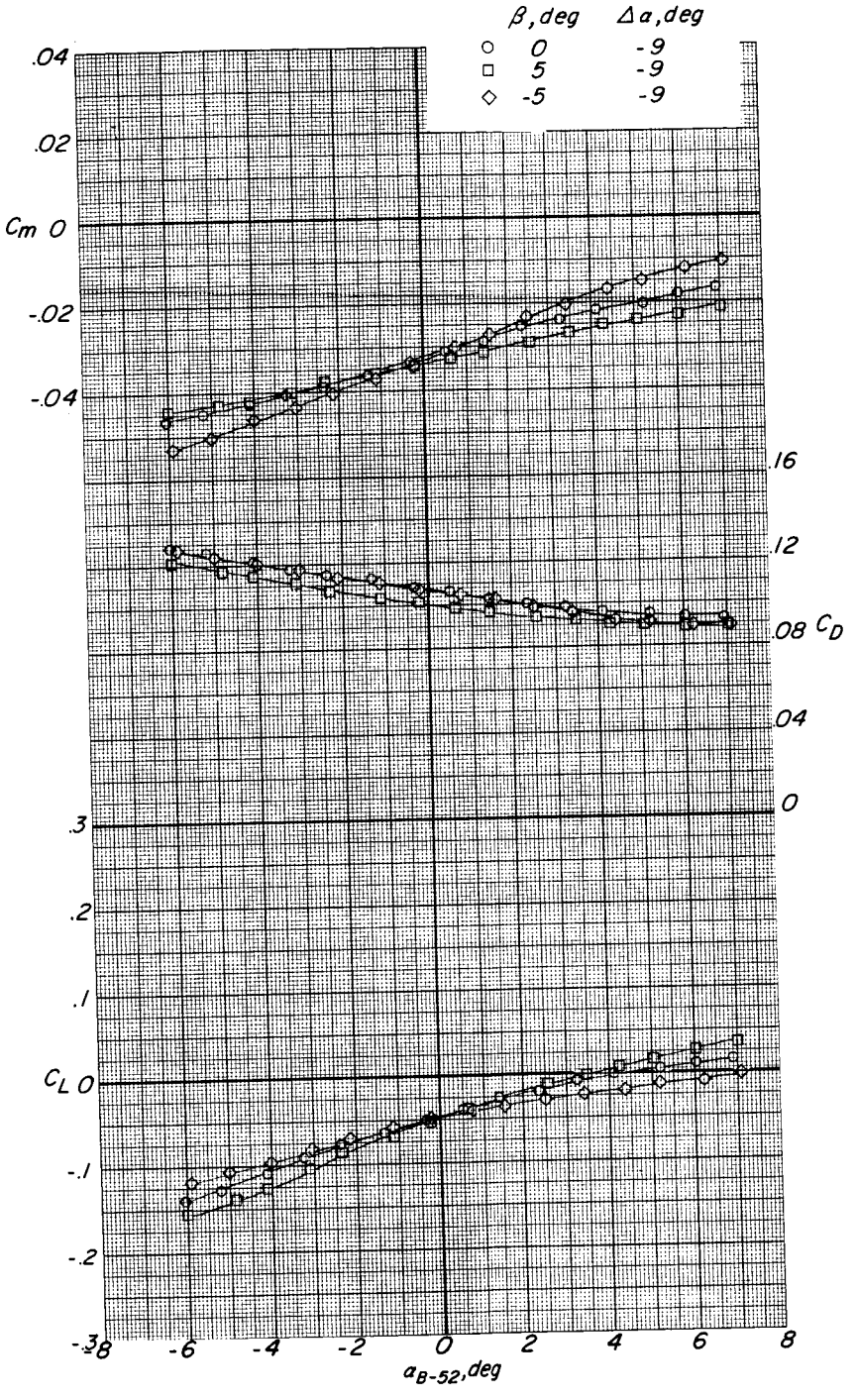

(b) Continued.

Figure 8.- Continued.

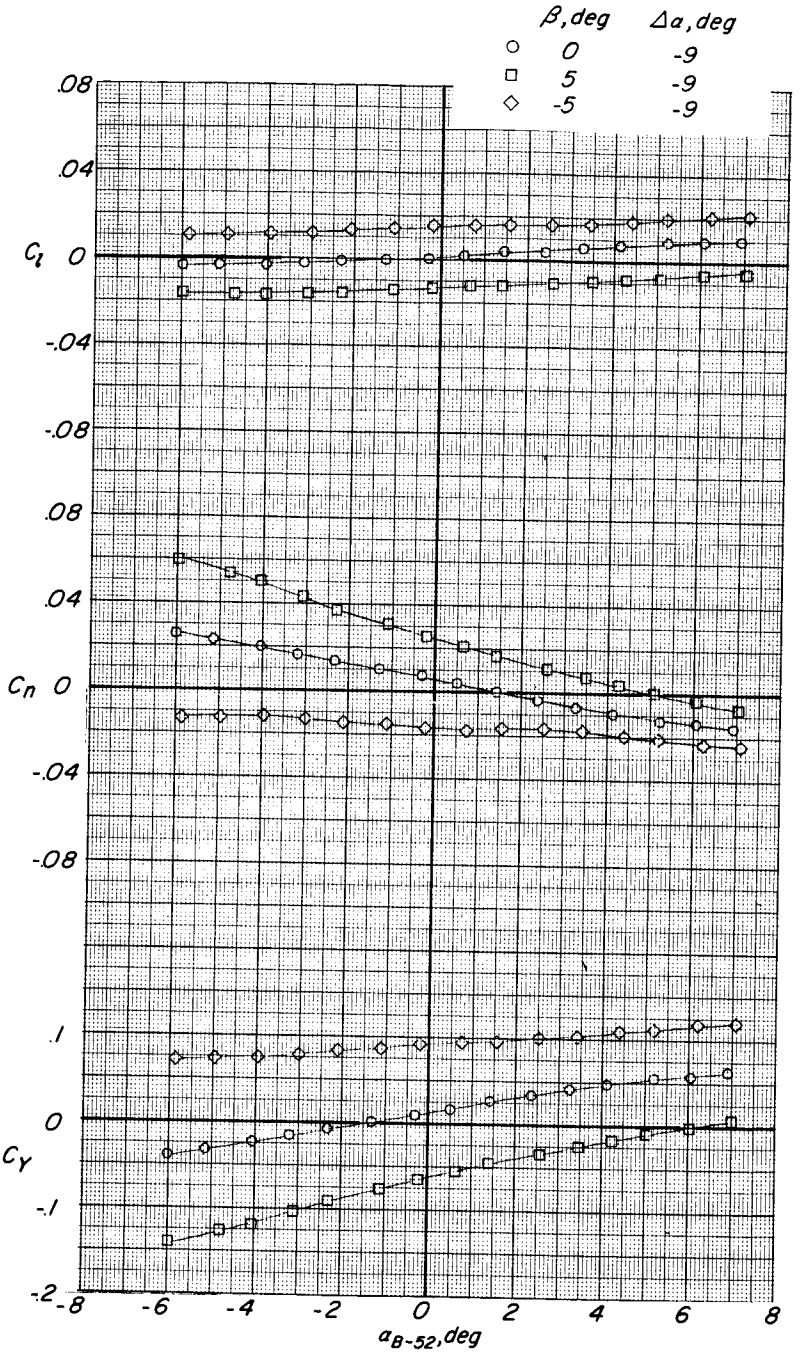

(b) Continued.

Figure 8.- Continued.

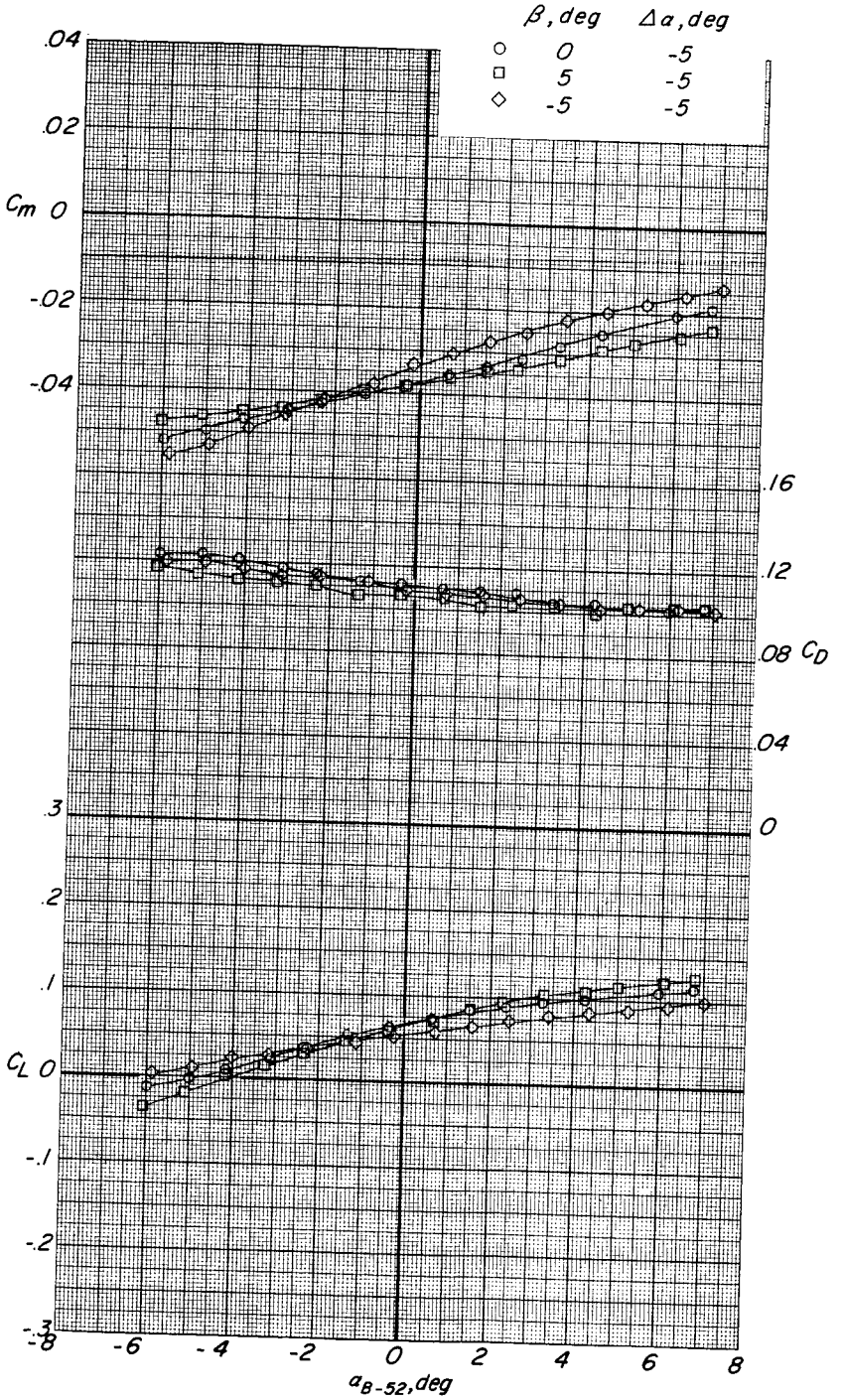

(b) Continued.

Figure 8.- Continued.

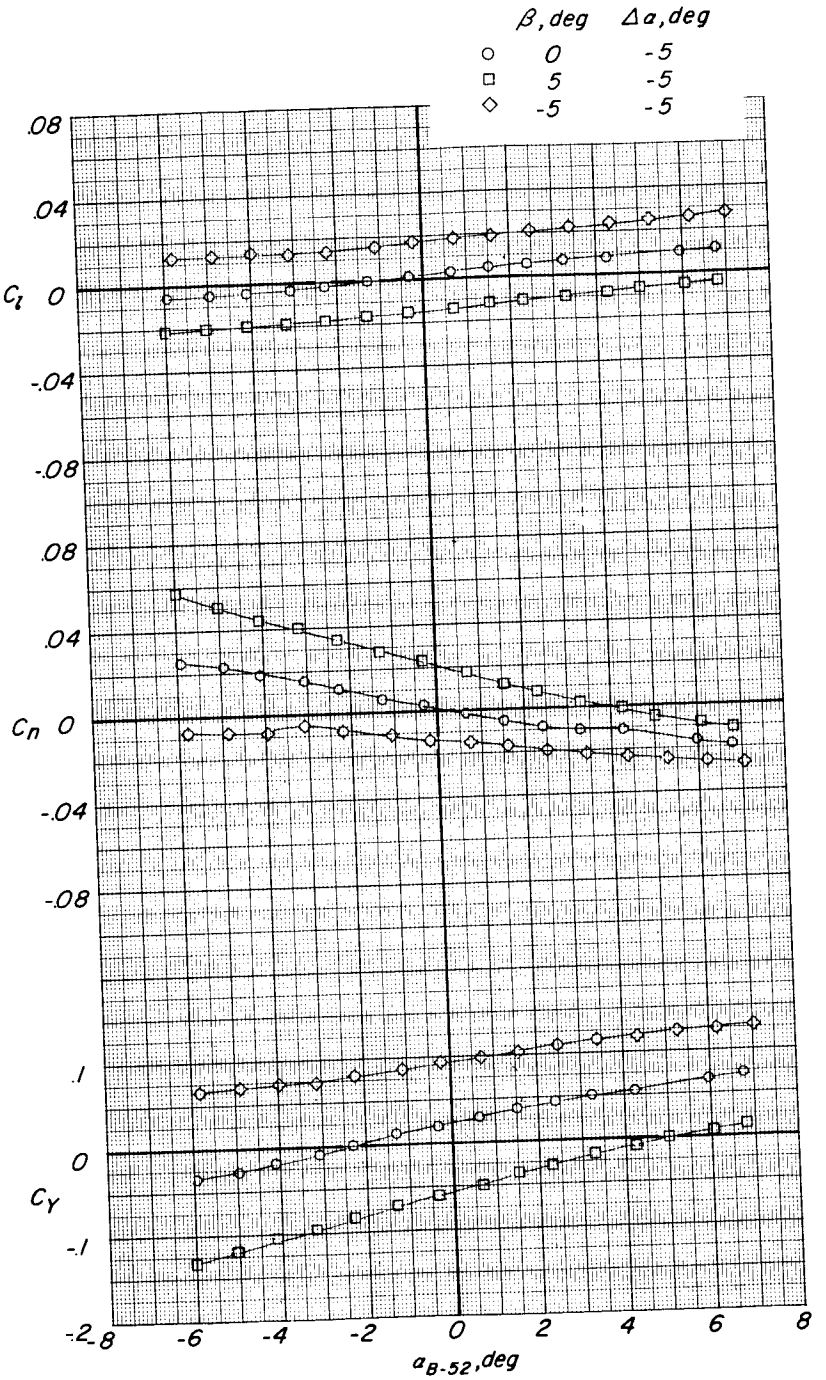

(b) Continued.

Figure 8.- Continued.

DECLASSIFIED

[redacted]

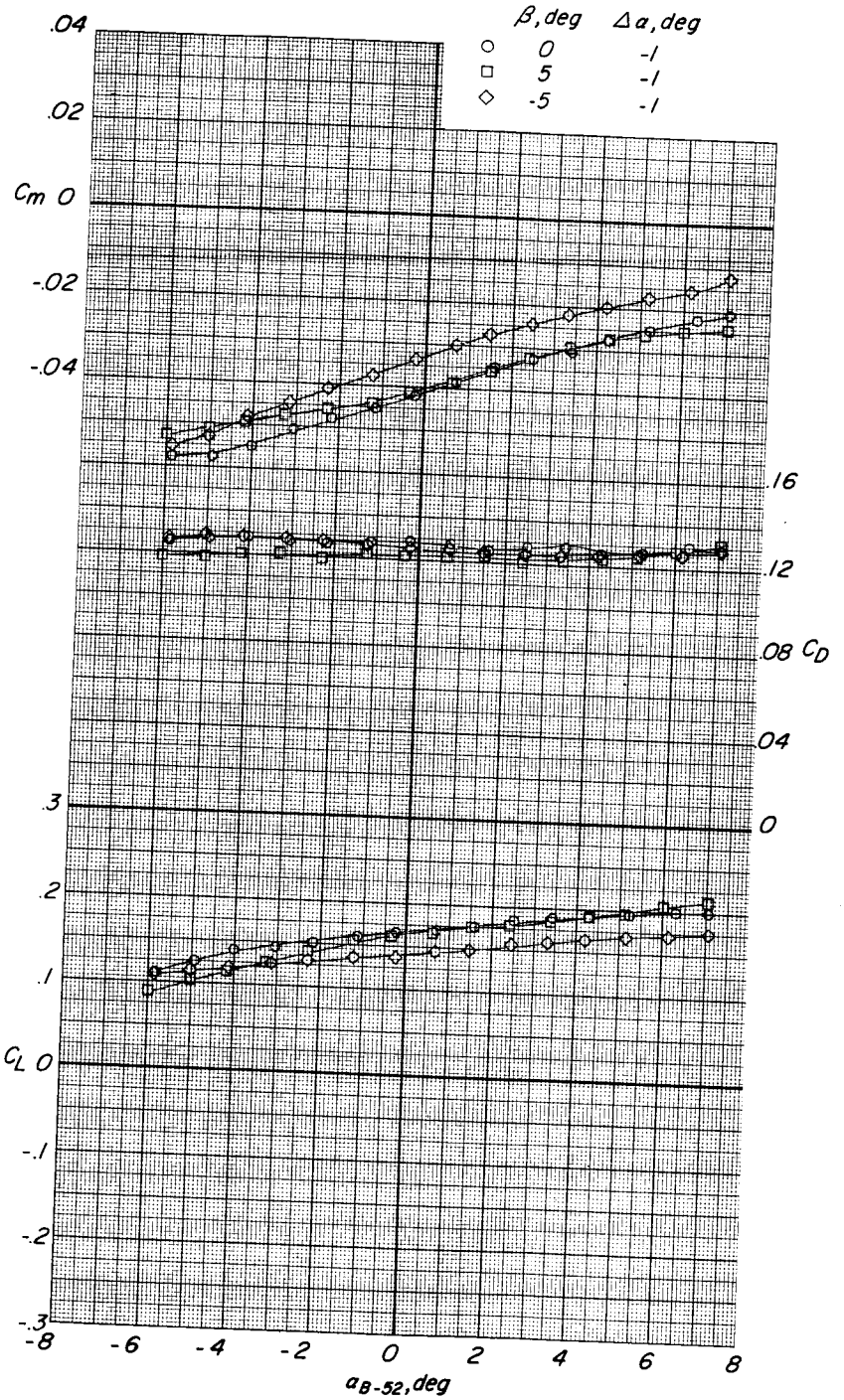

(b) Continued.

Figure 8.- Continued.

[redacted]

DECLASSIFIED

[redacted]

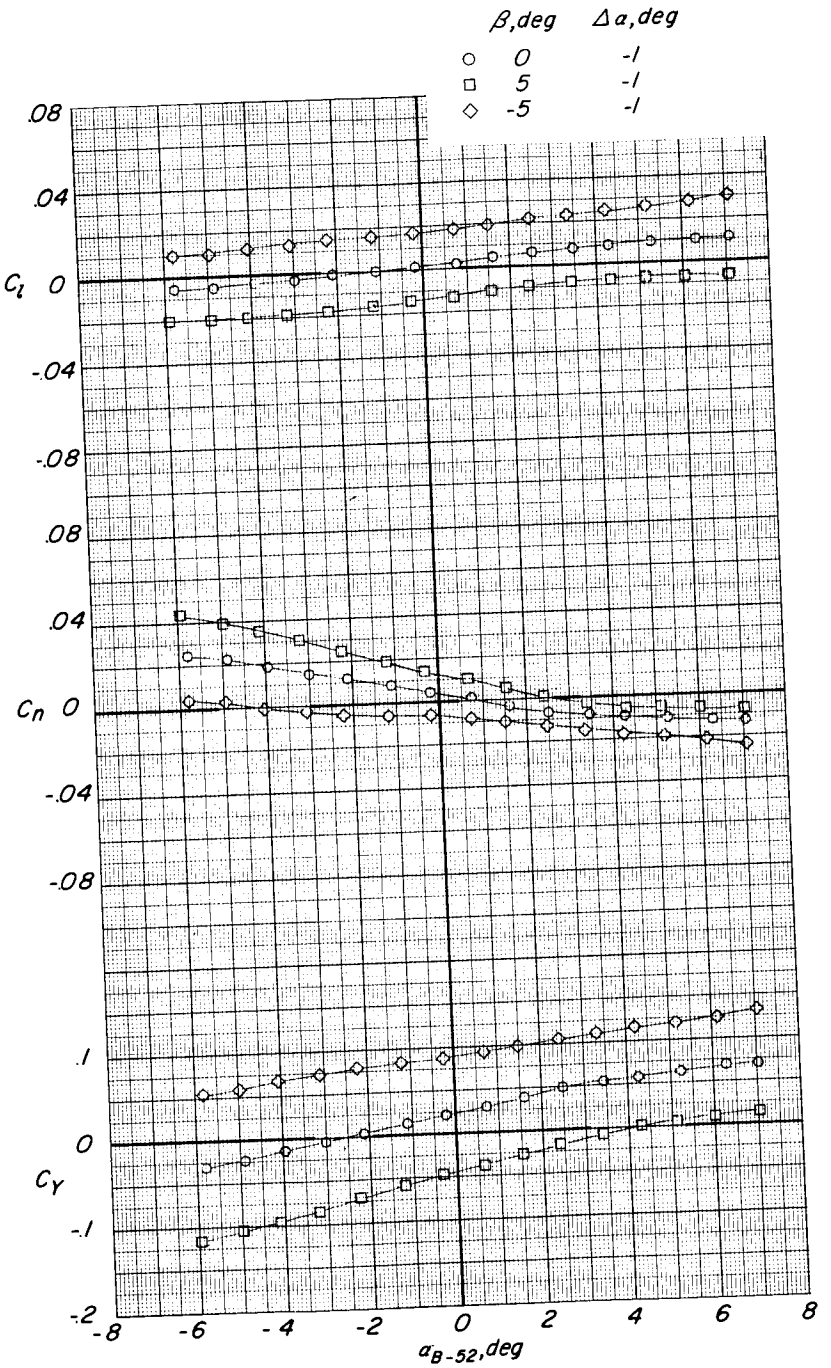

(b) Continued.

Figure 8.- Continued.

[redacted]

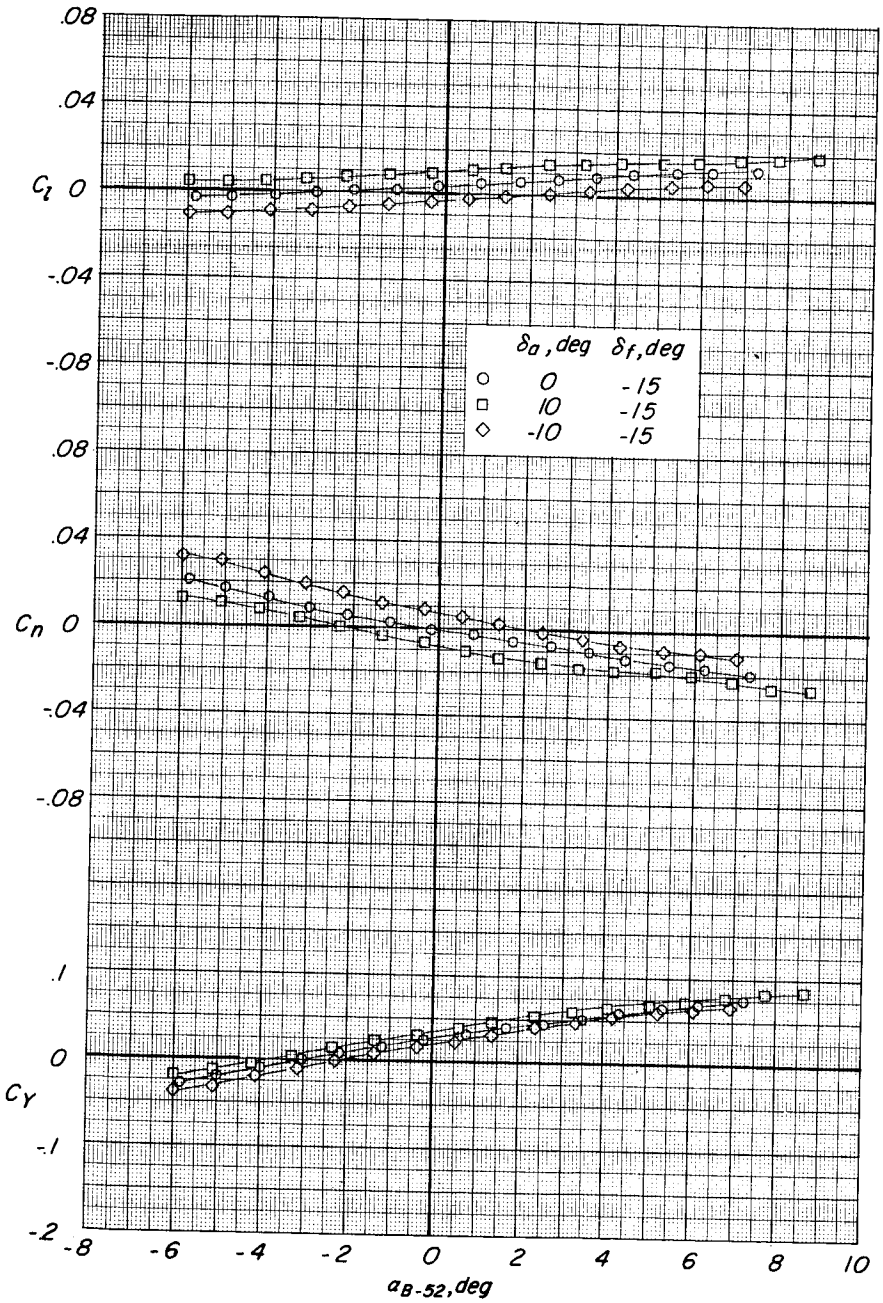

(b) Continued.

Figure 8.- Continued.

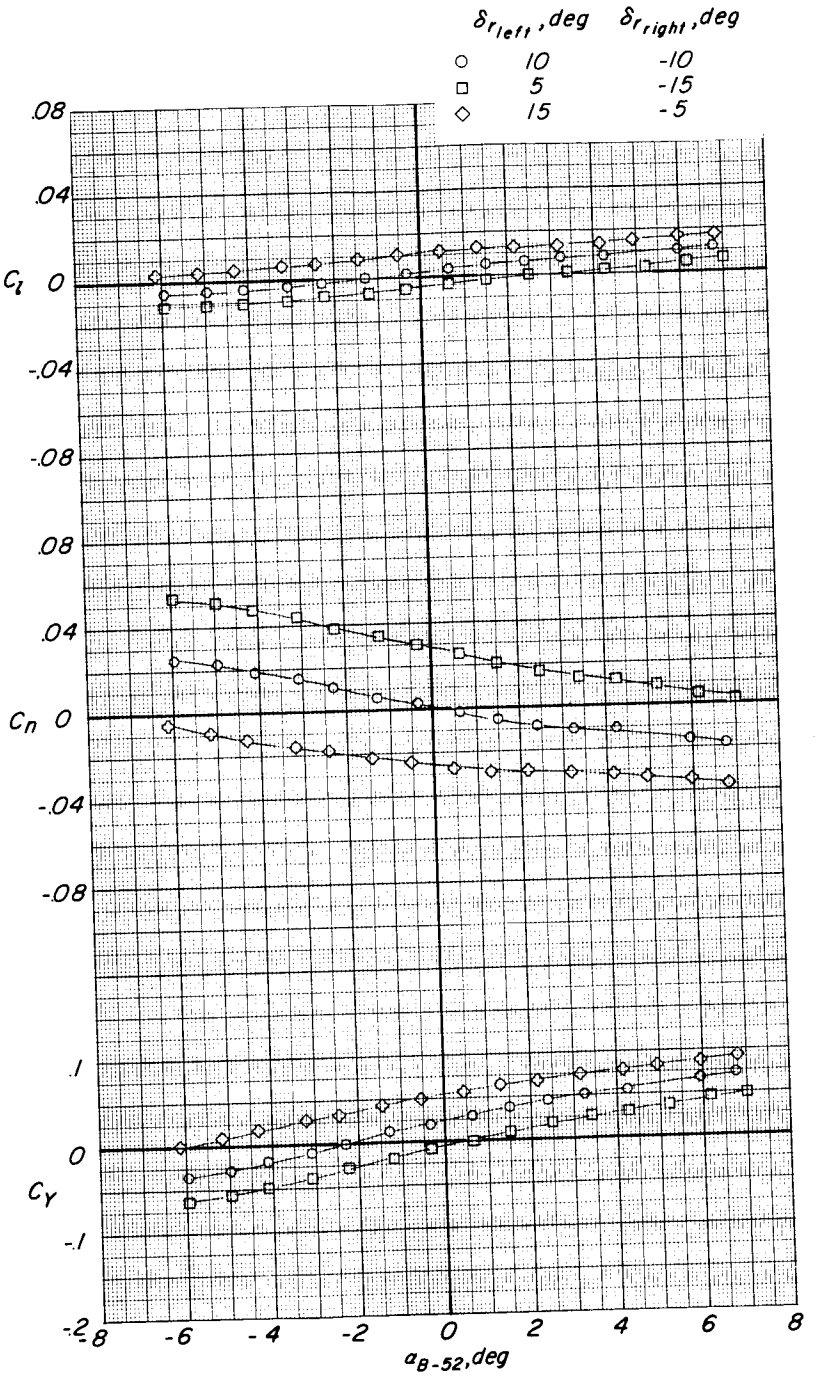

(b) Concluded.

Figure 8.- Continued.

[redacted] DECLASSIFIED

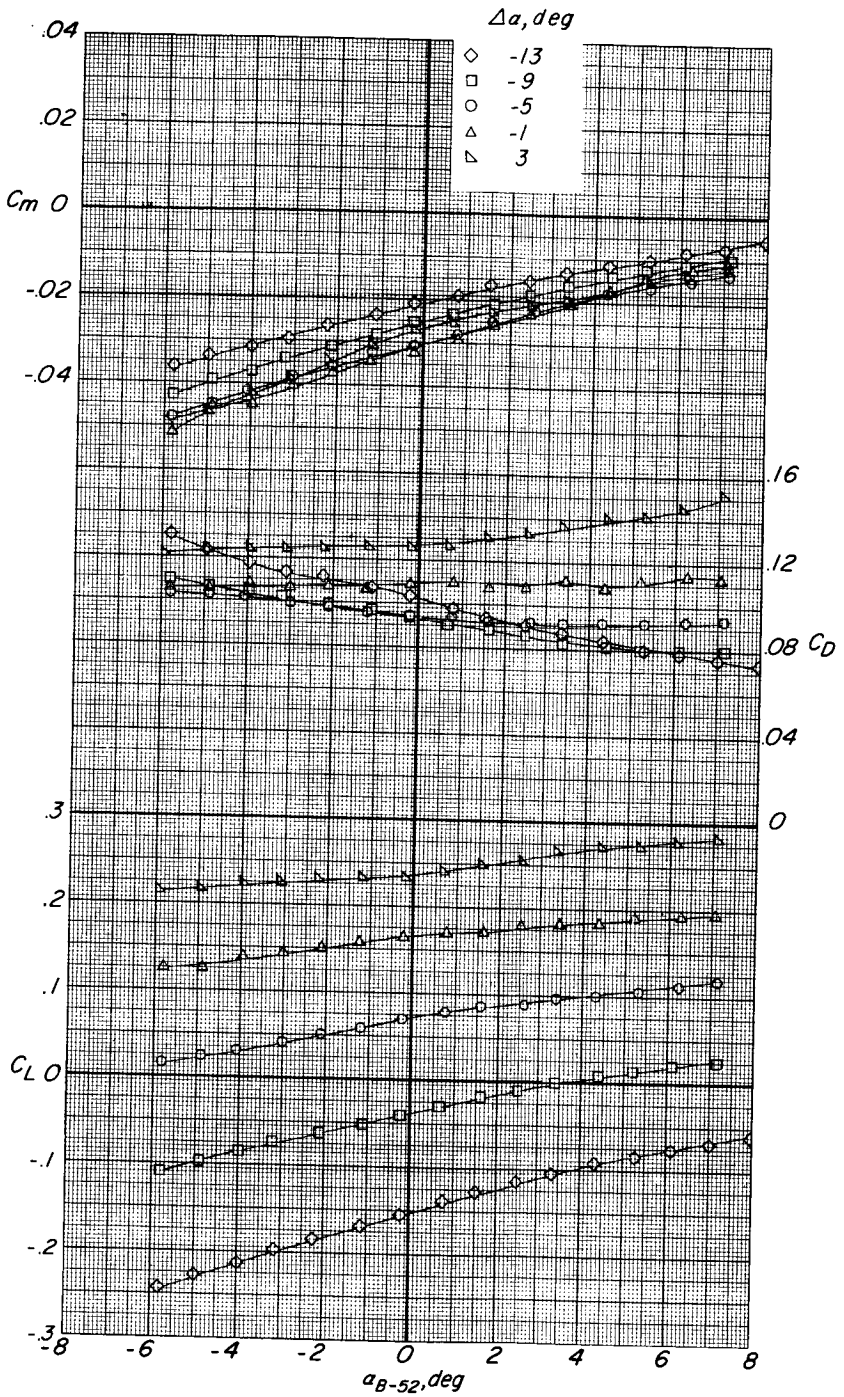

(c) z' = 4.0 feet (1.22 m).

Figure 8.- Continued.

[redacted]

[redacted]

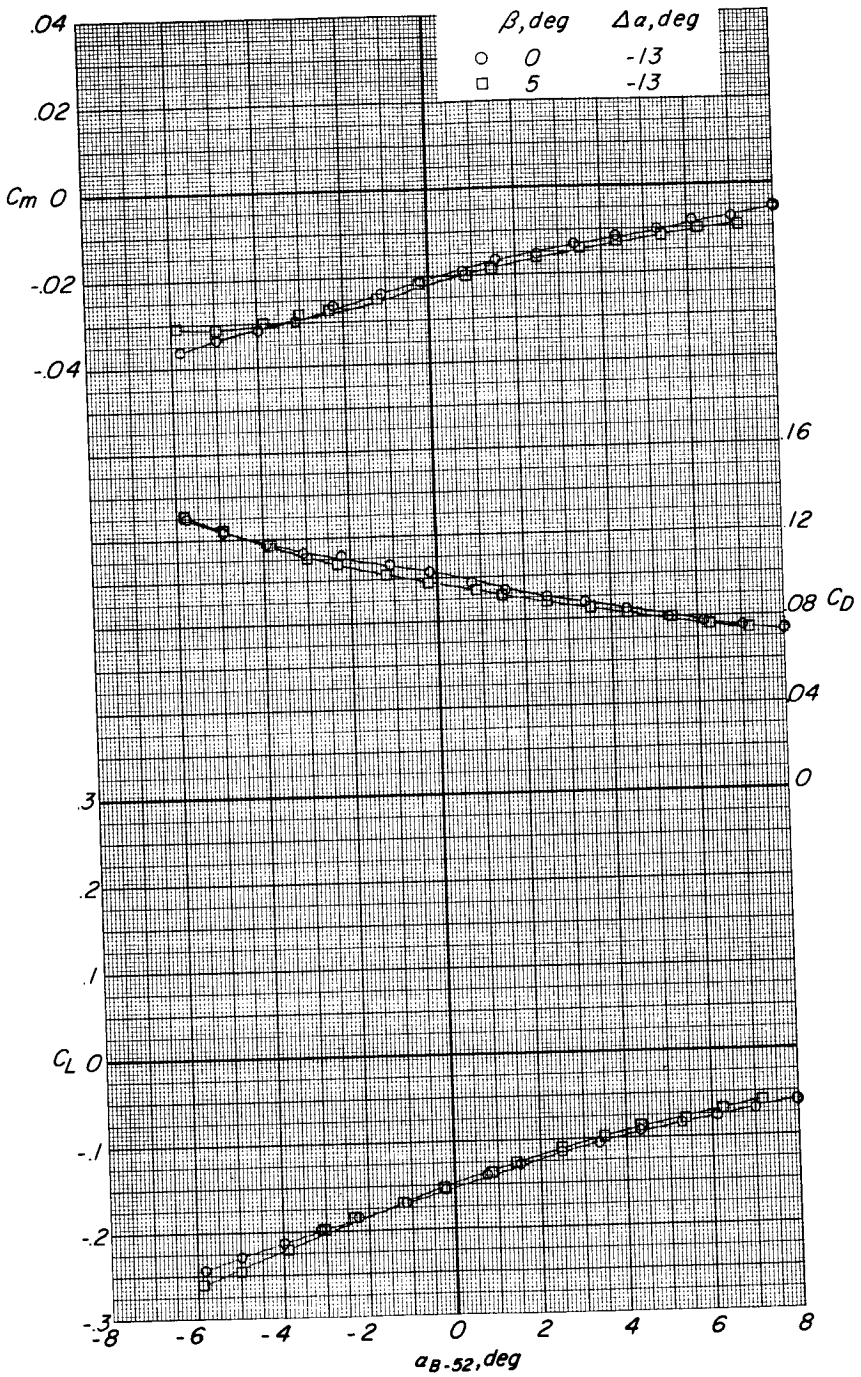

(c) Continued.

Figure 8.- Continued.

[redacted]

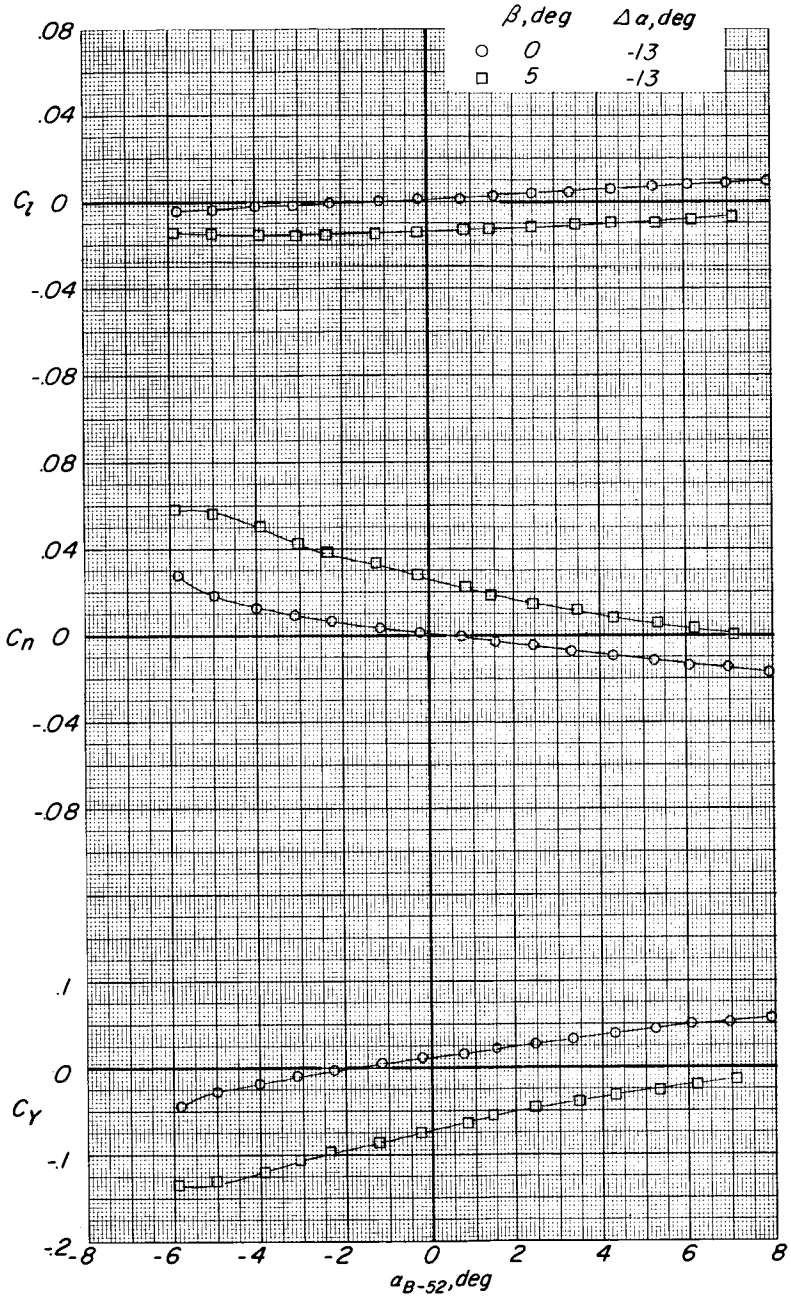

(c) Continued.

Figure 8.- Continued.

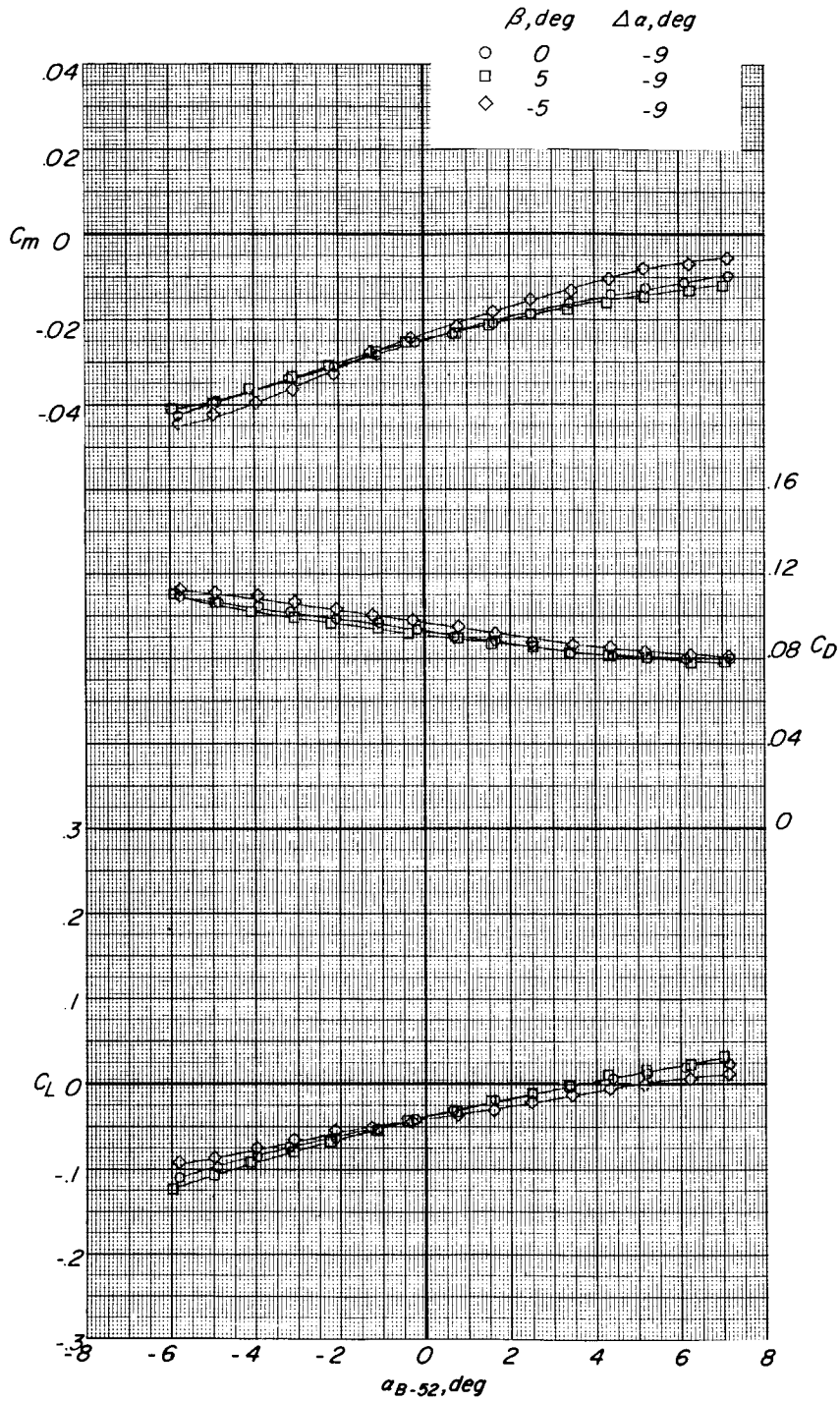

(c) Continued.

Figure 8.- Continued.

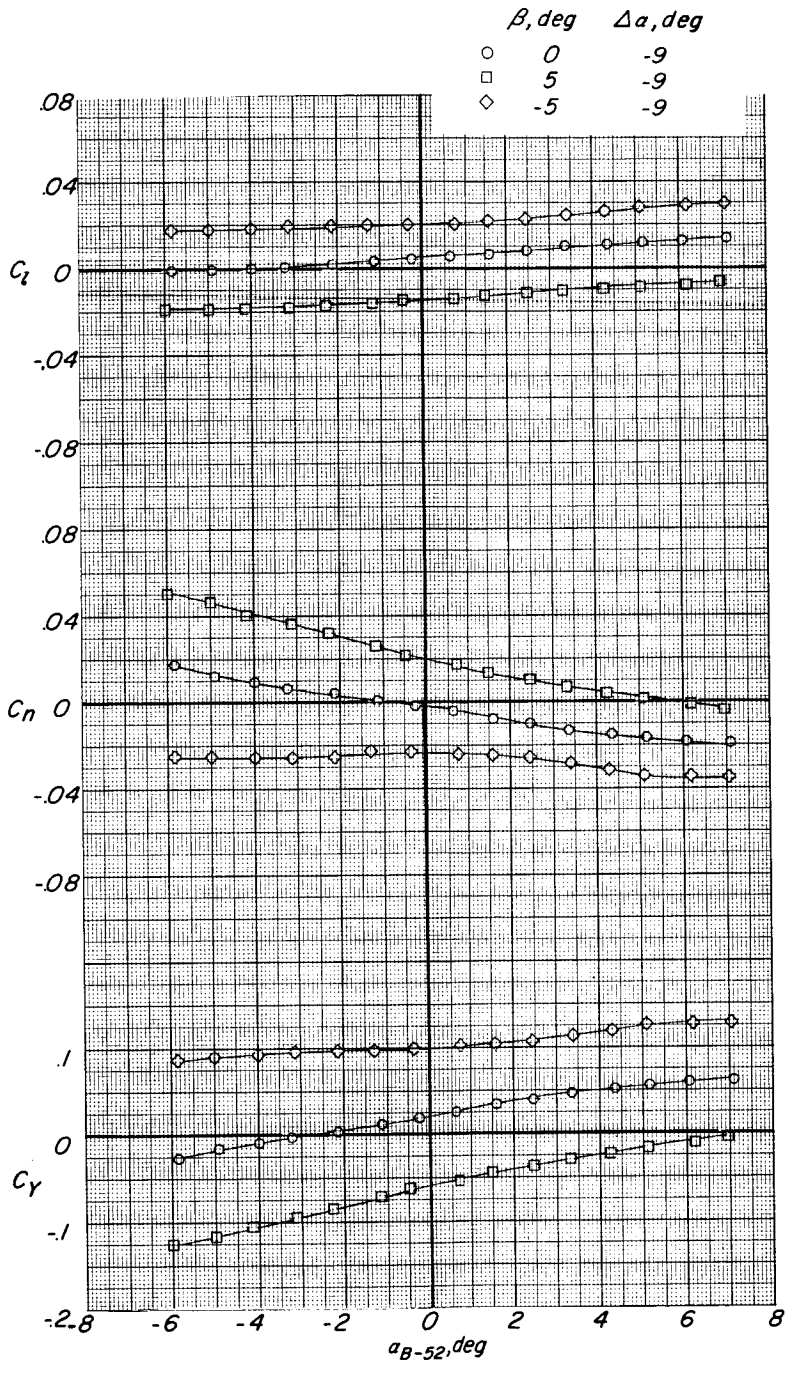

(c) Continued.

Figure 8.- Continued.

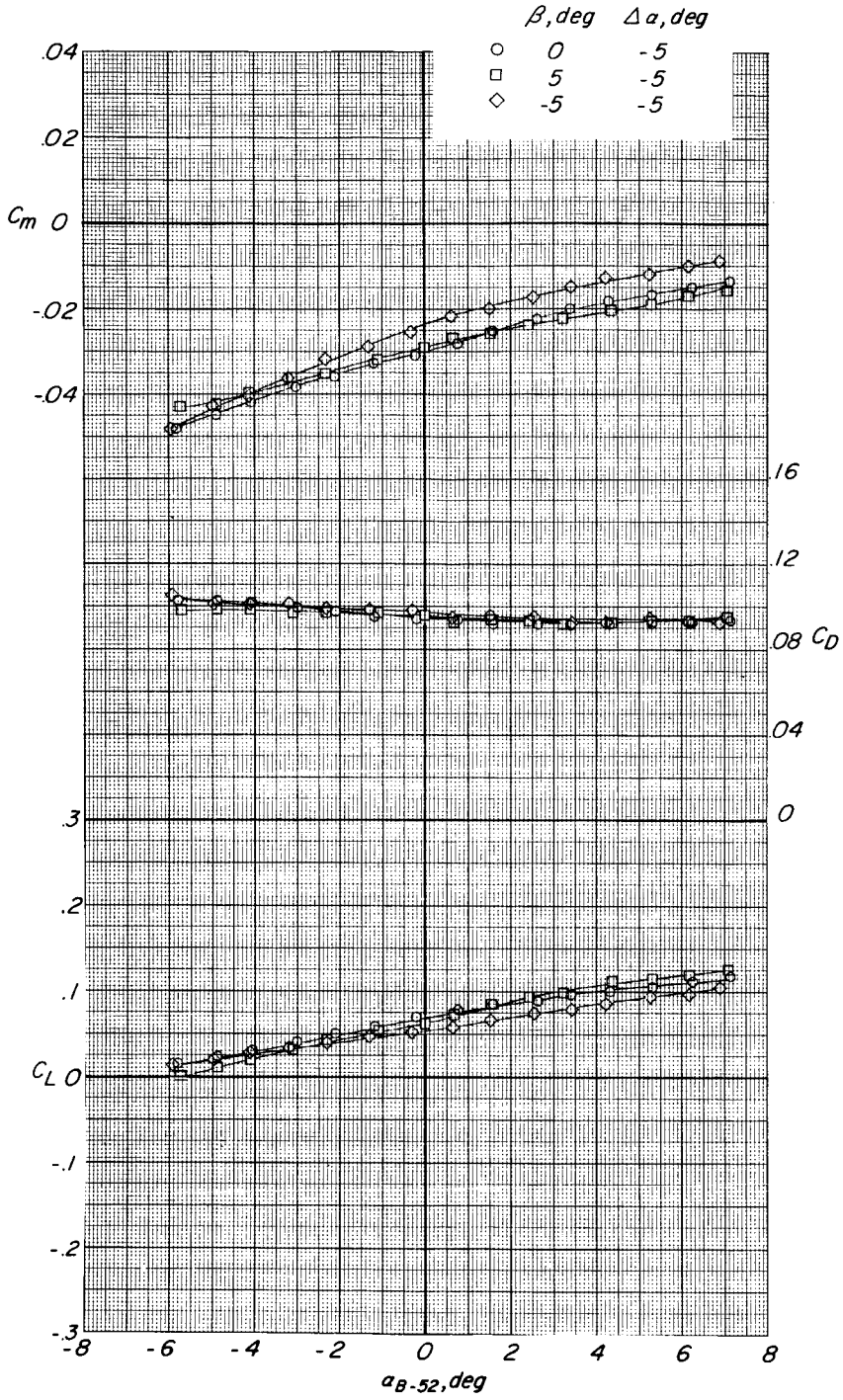

(c) Continued.

Figure 8.- Continued.

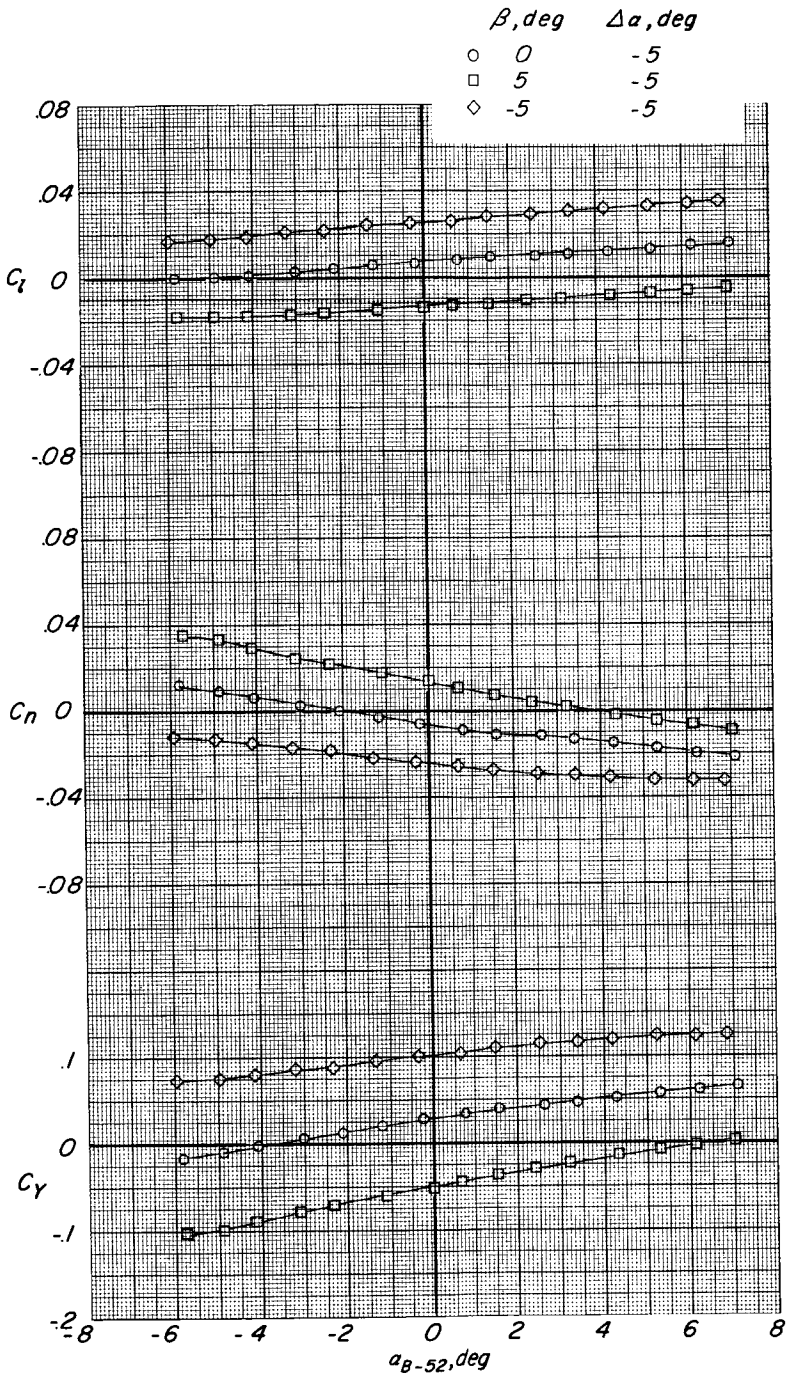

(c) Continued.

Figure 8.- Continued.

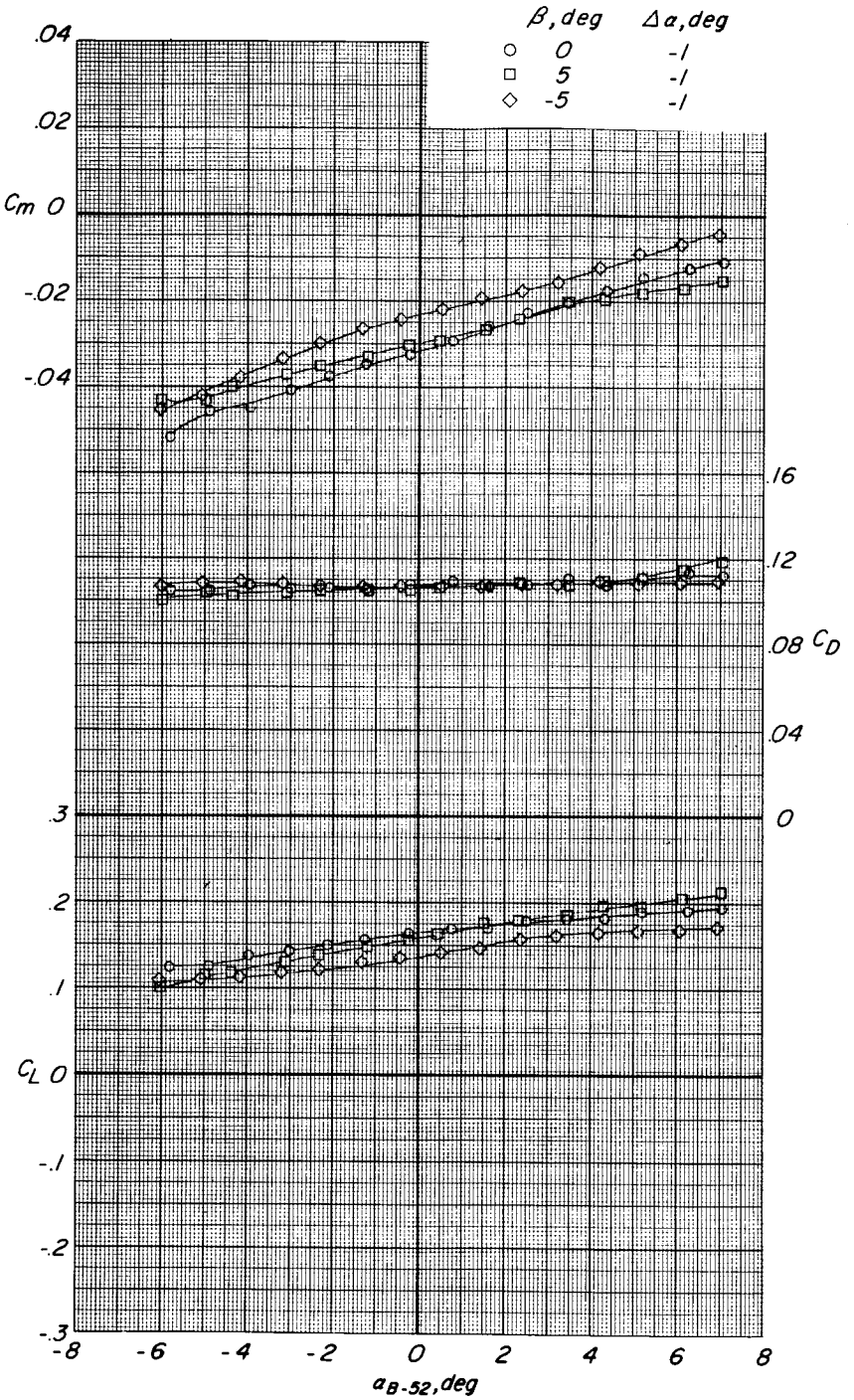

(c) Continued.

Figure 8.- Continued.

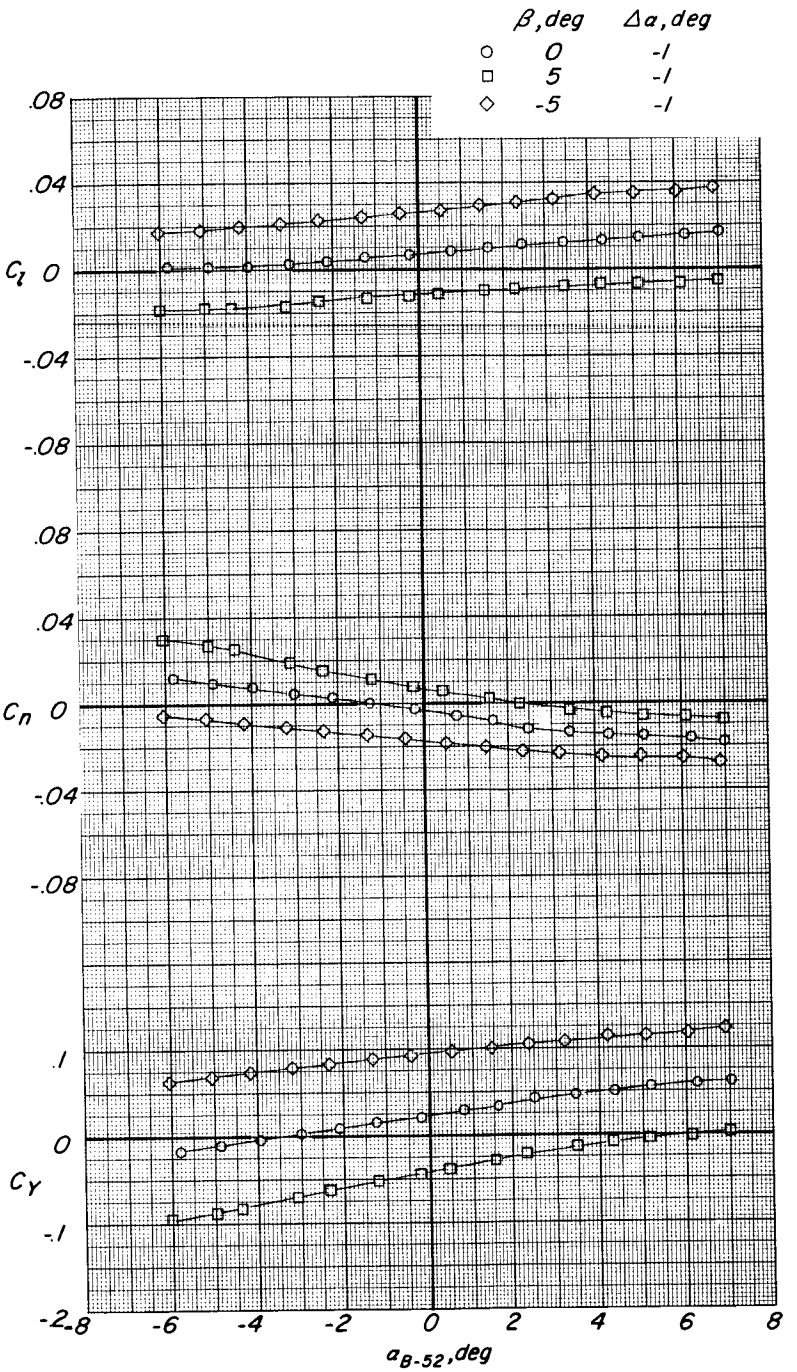

(c) Continued.

Figure 8.- Continued.

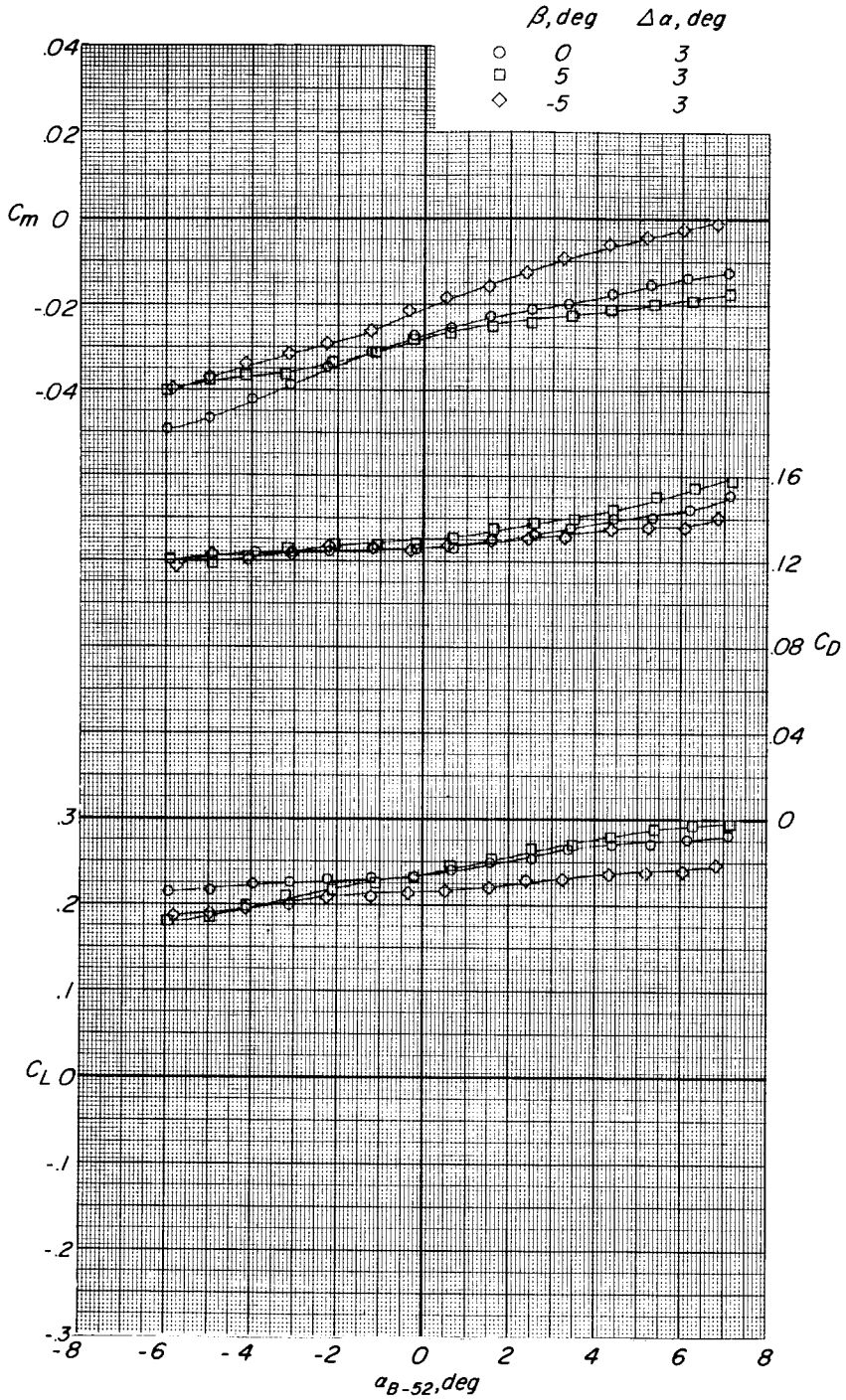

(c) Continued.

Figure 8.- Continued.

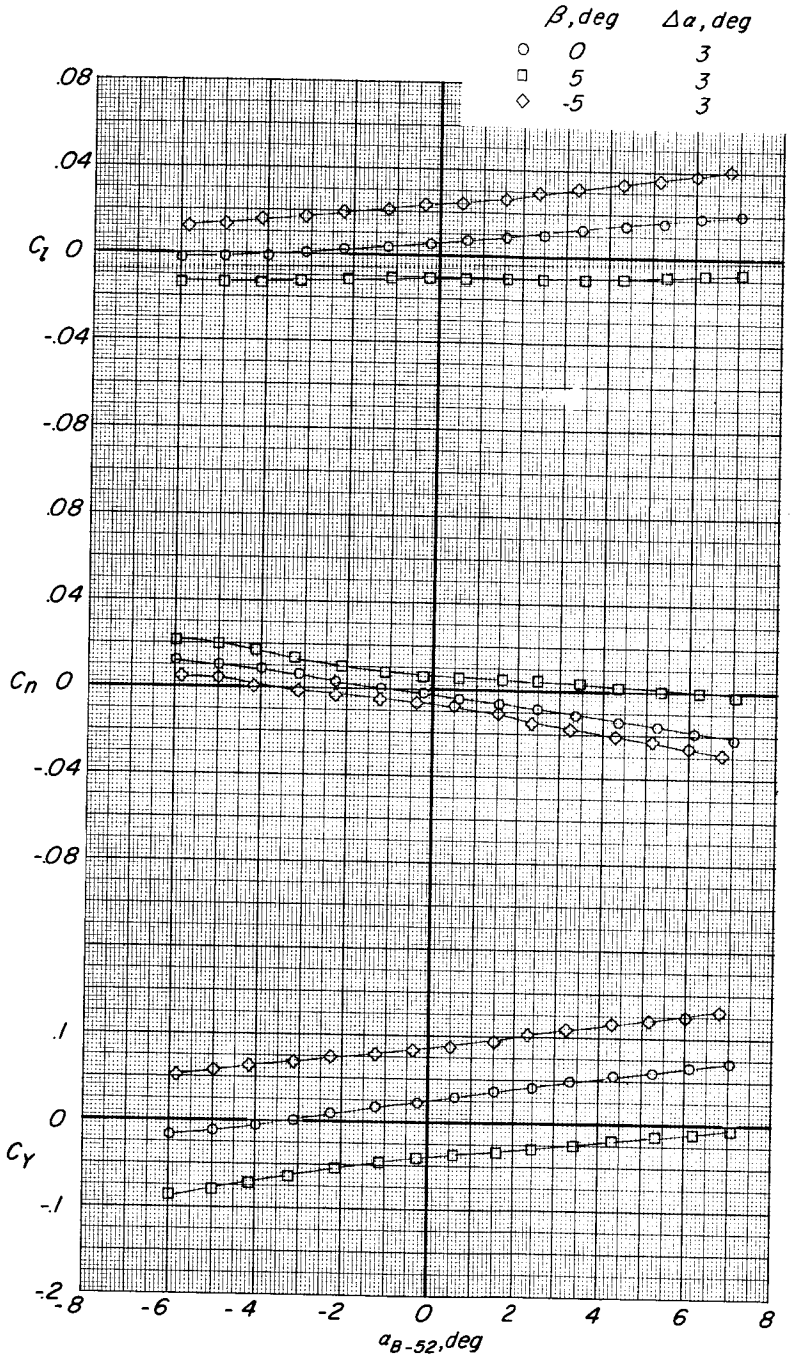

(c) Concluded.

Figure 8.- Continued.

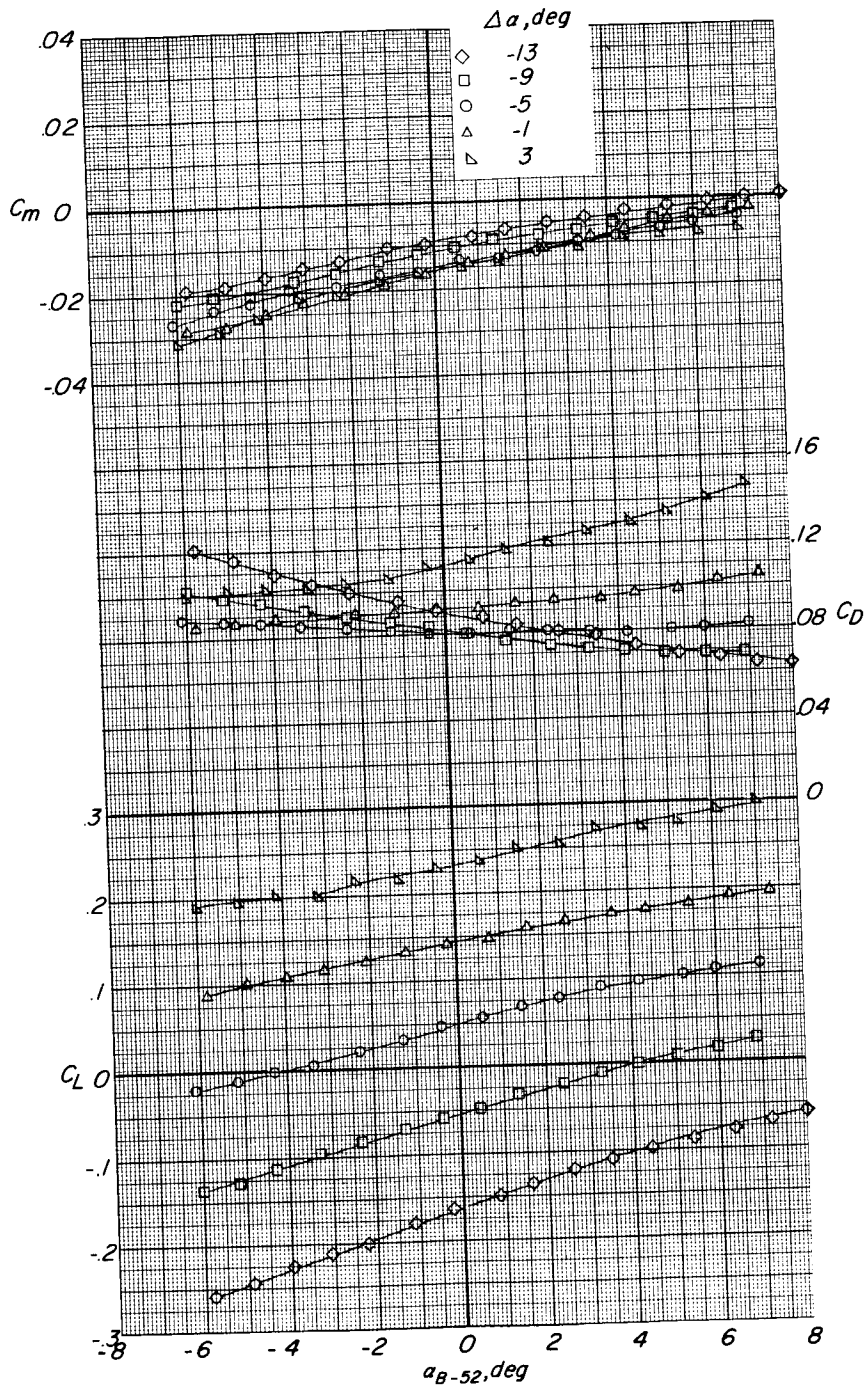

(d) z' = 8.0 feet (2.44 m).

Figure 8.- Continued.

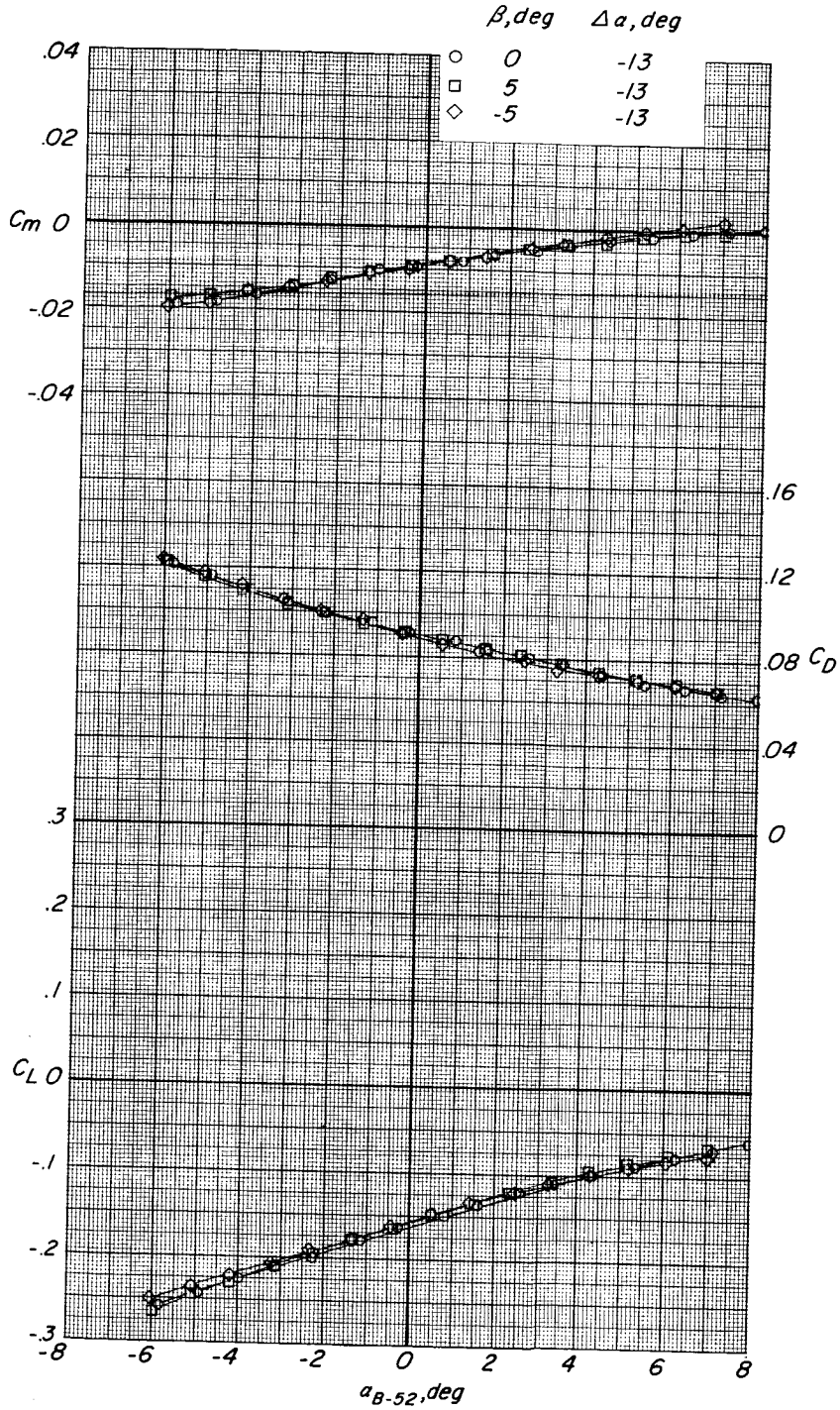

(d) Continued.

Figure 8.- Continued.

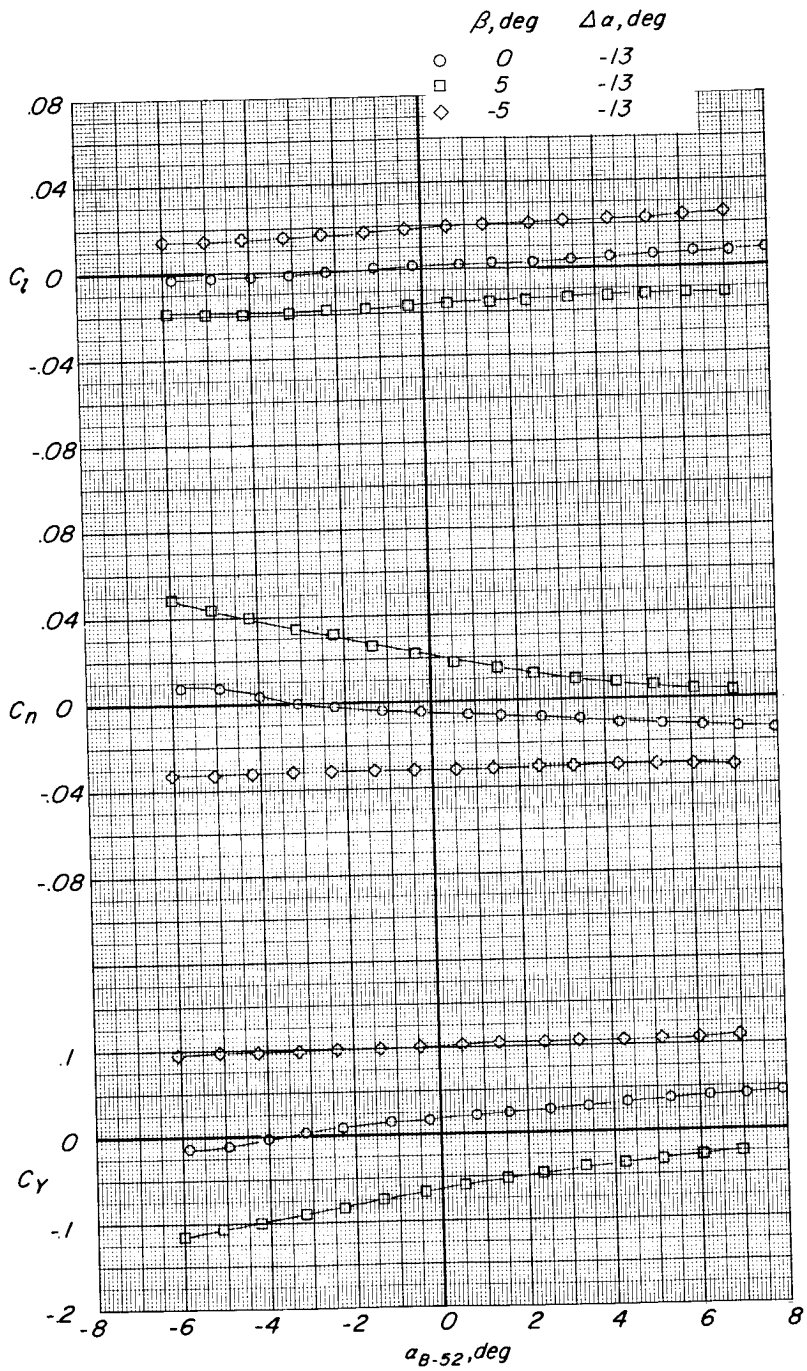

(d) Continued.

Figure 8.- Continued.

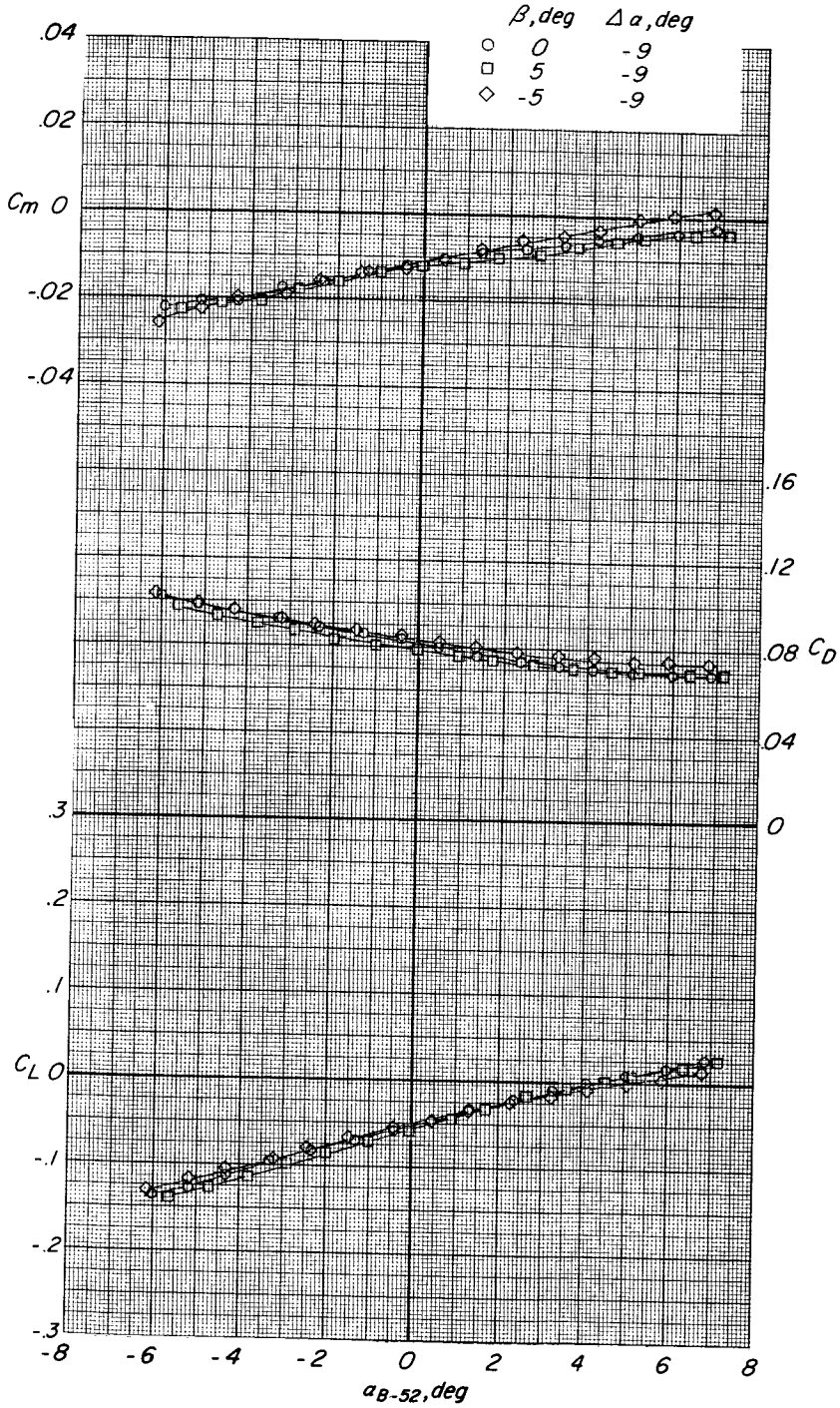

(d) Continued.

Figure 8.- Continued.

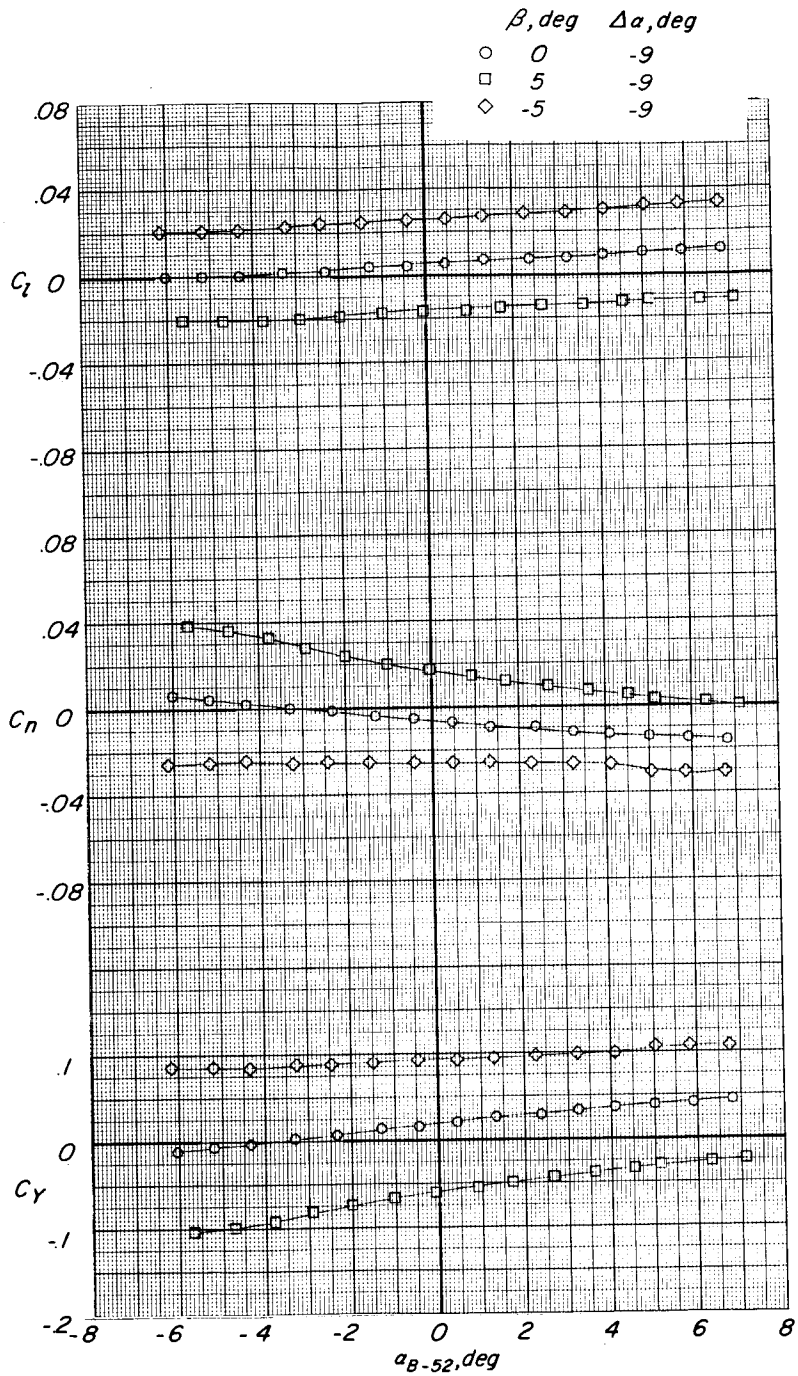

(d) Continued.

Figure 8.- Continued.

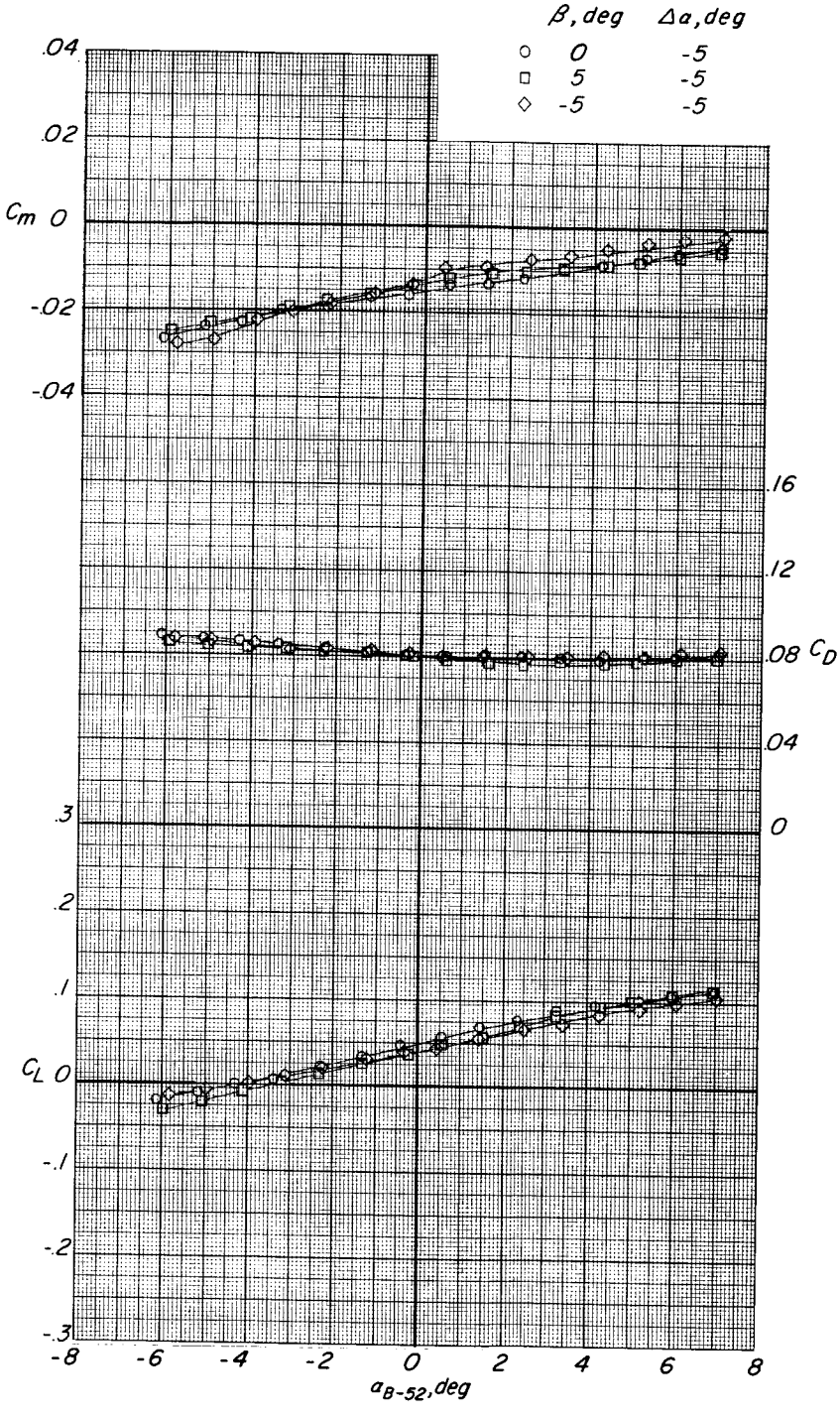

(d) Continued.

Figure 8.- Continued.

DECLASSIFIED

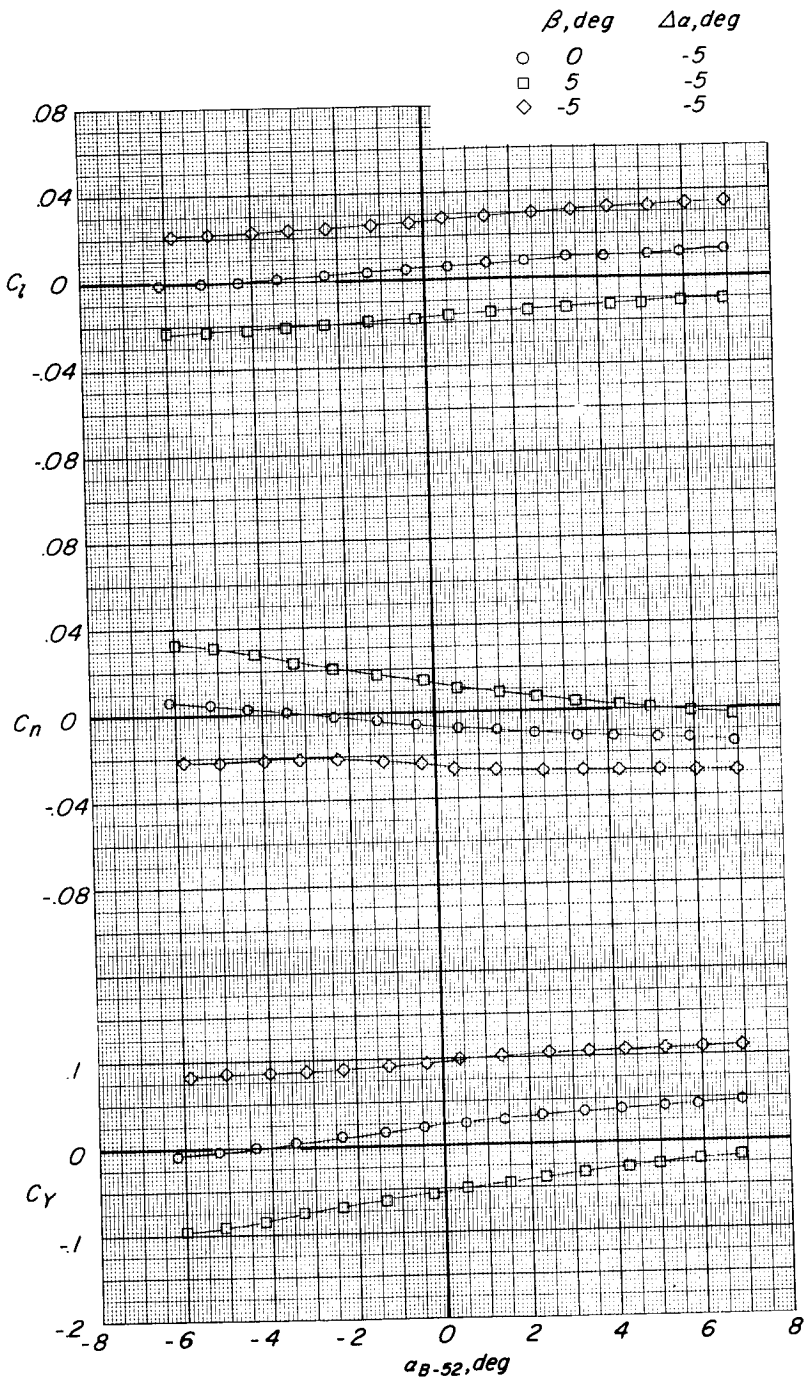

(d) Continued.

Figure 8.- Continued.

[redacted]

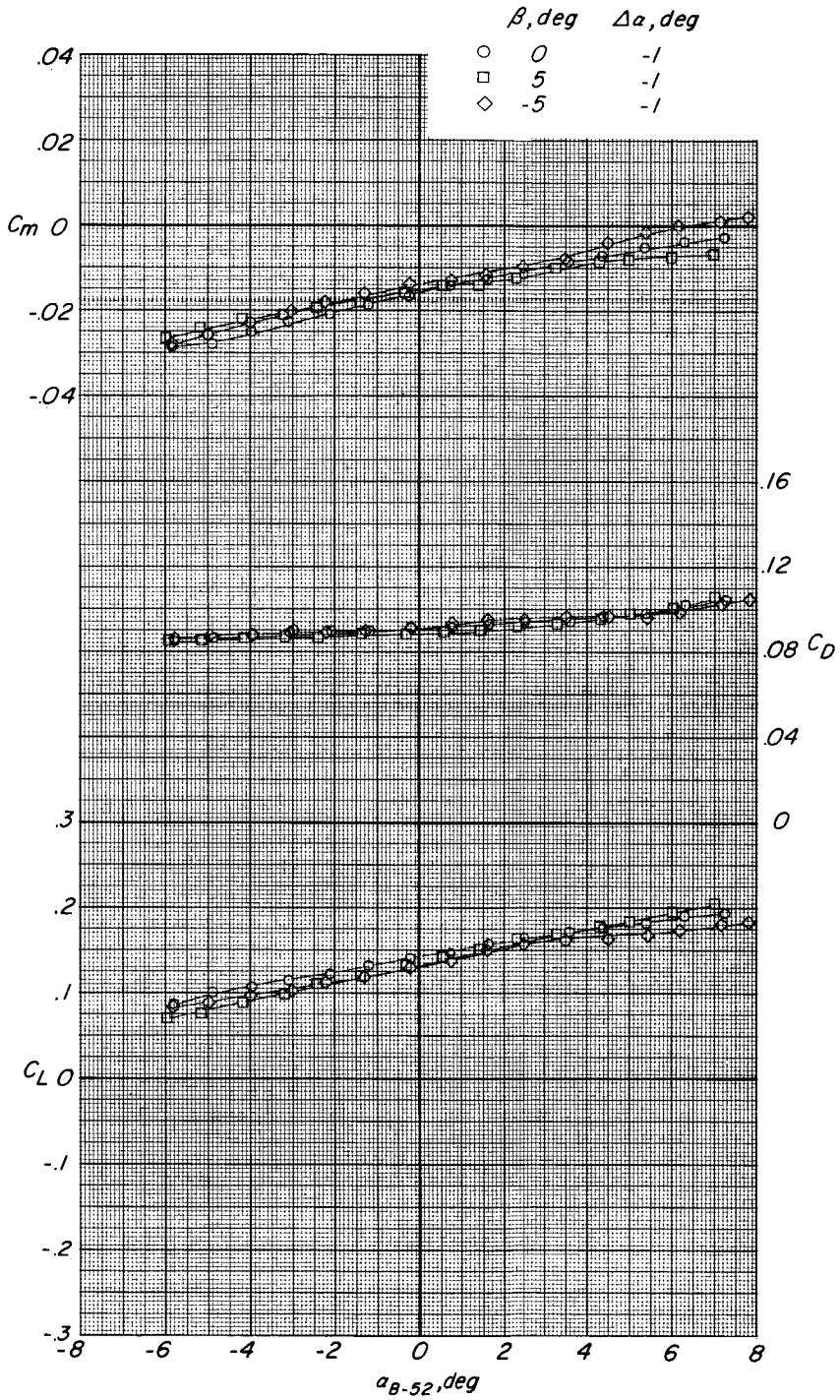

(d) Continued.

Figure 8.- Continued.

[redacted]

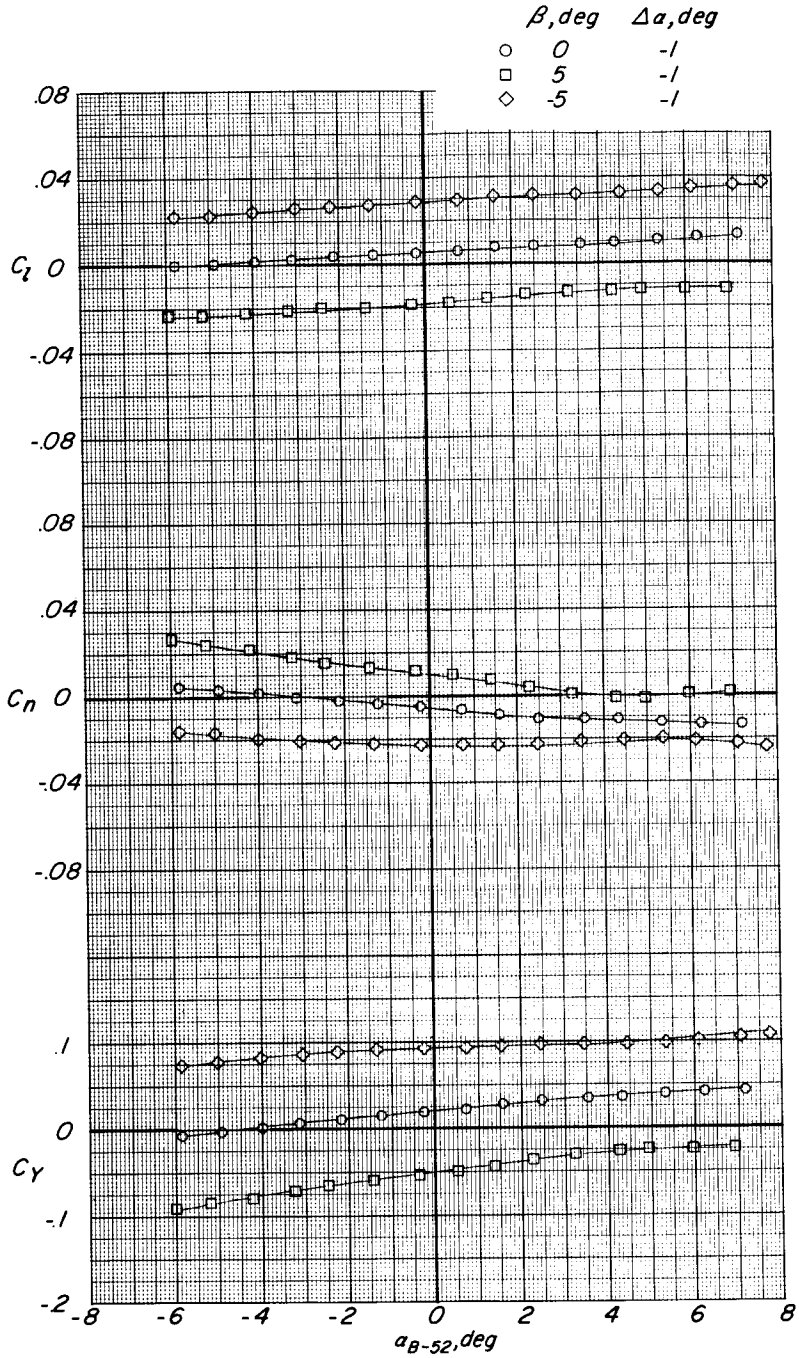

(d) Continued.

Figure 8.- Continued.

[redacted]

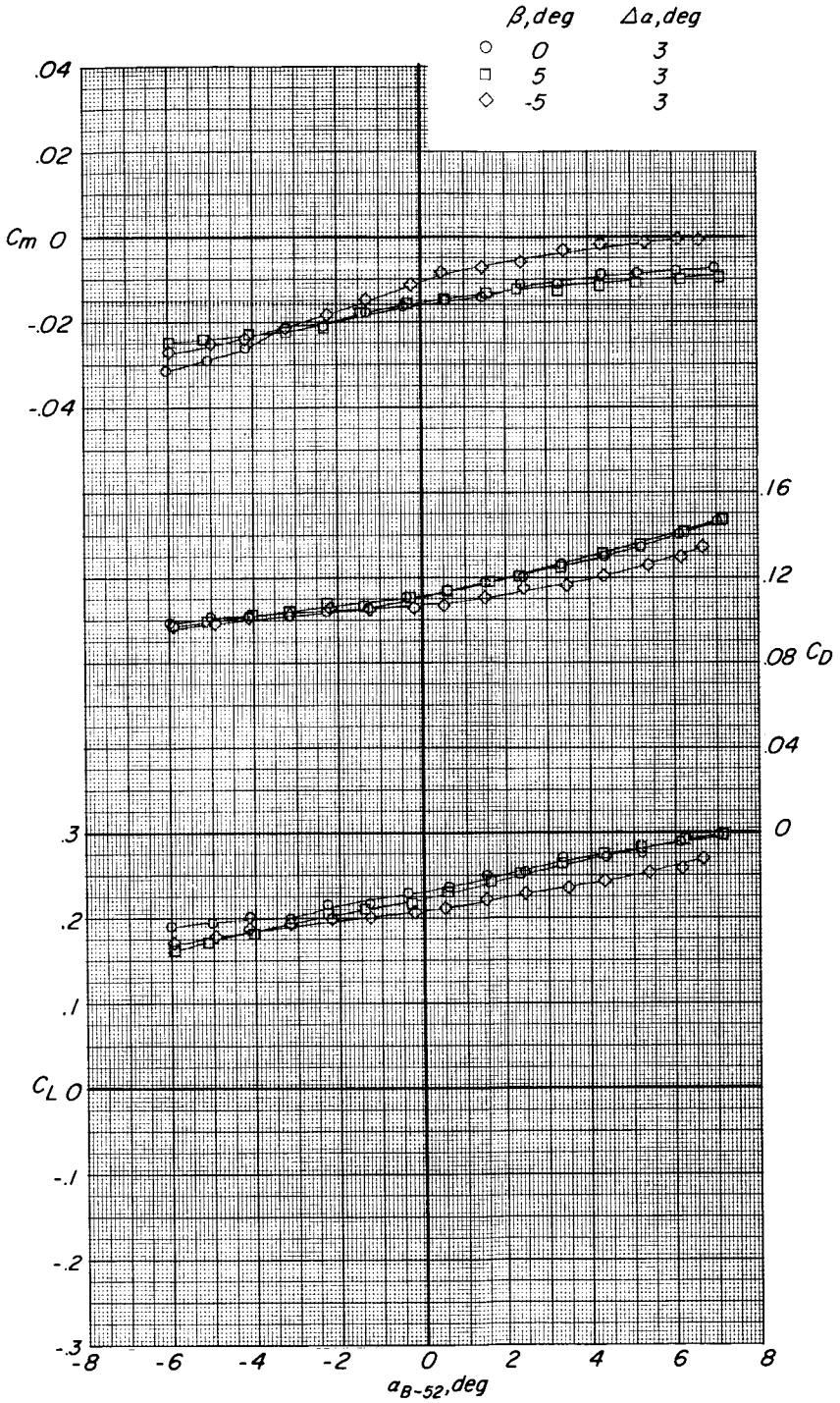

(d) Continued.

Figure 8.- Continued.

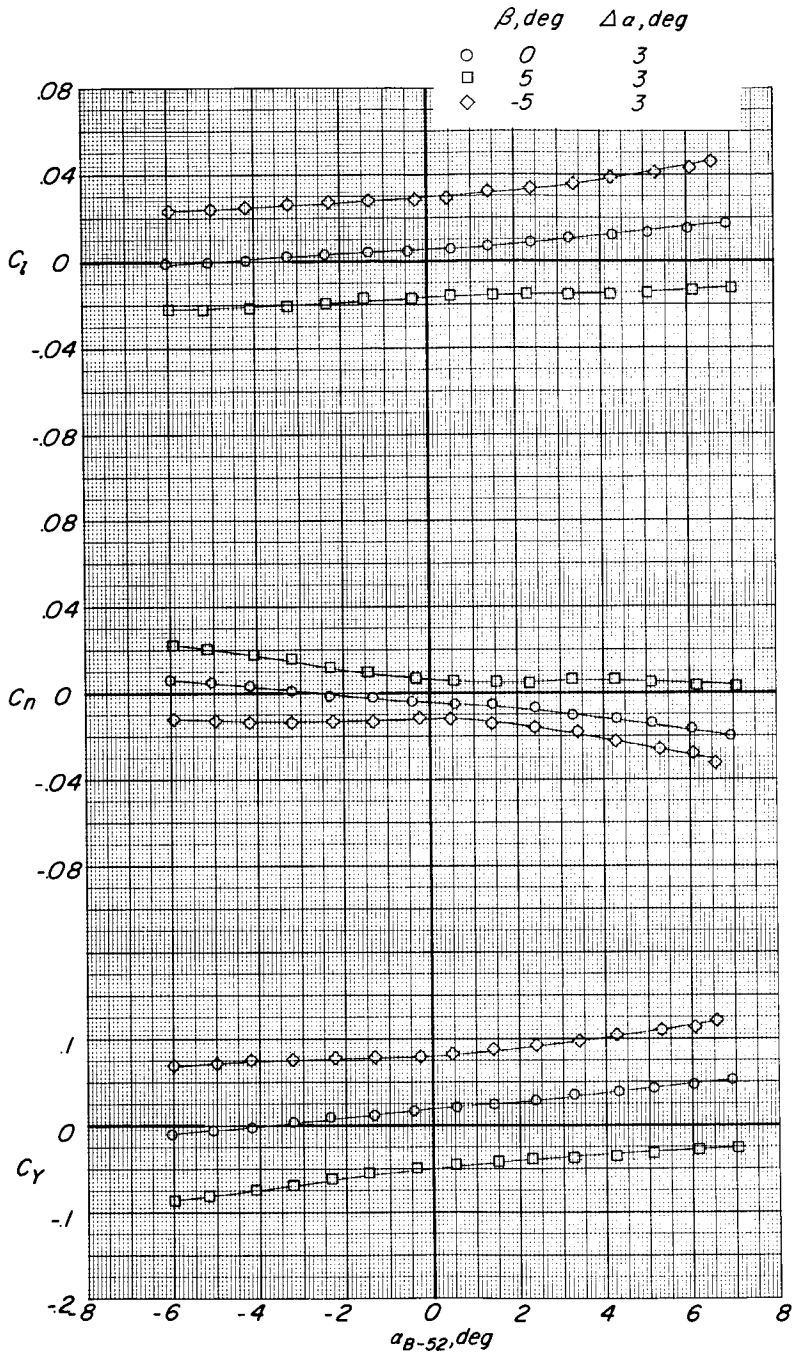

(d) Concluded.

Figure 8.- Continued.

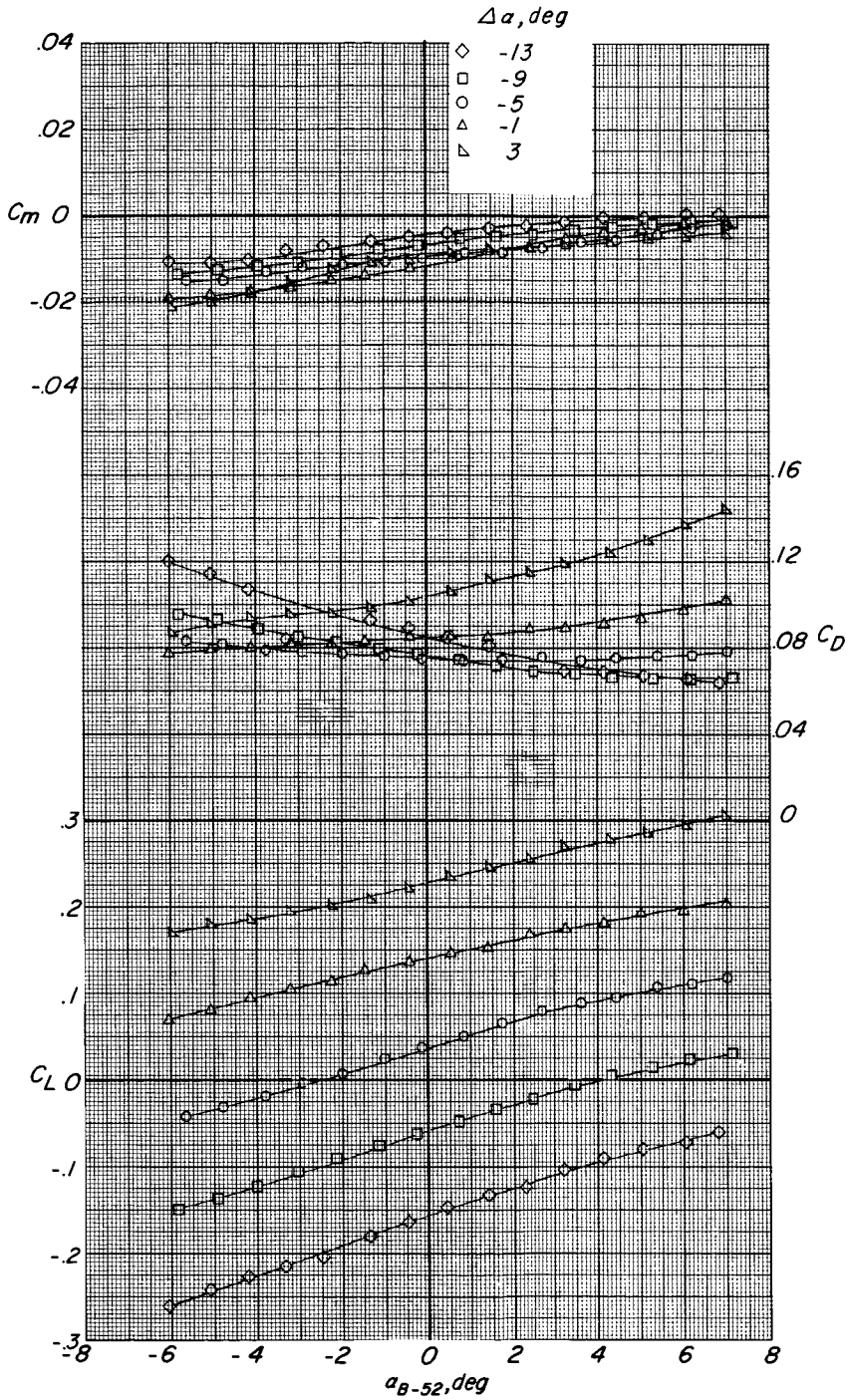

(e) z' = 12.0 feet (3.66 m).

Figure 8.- Continued.

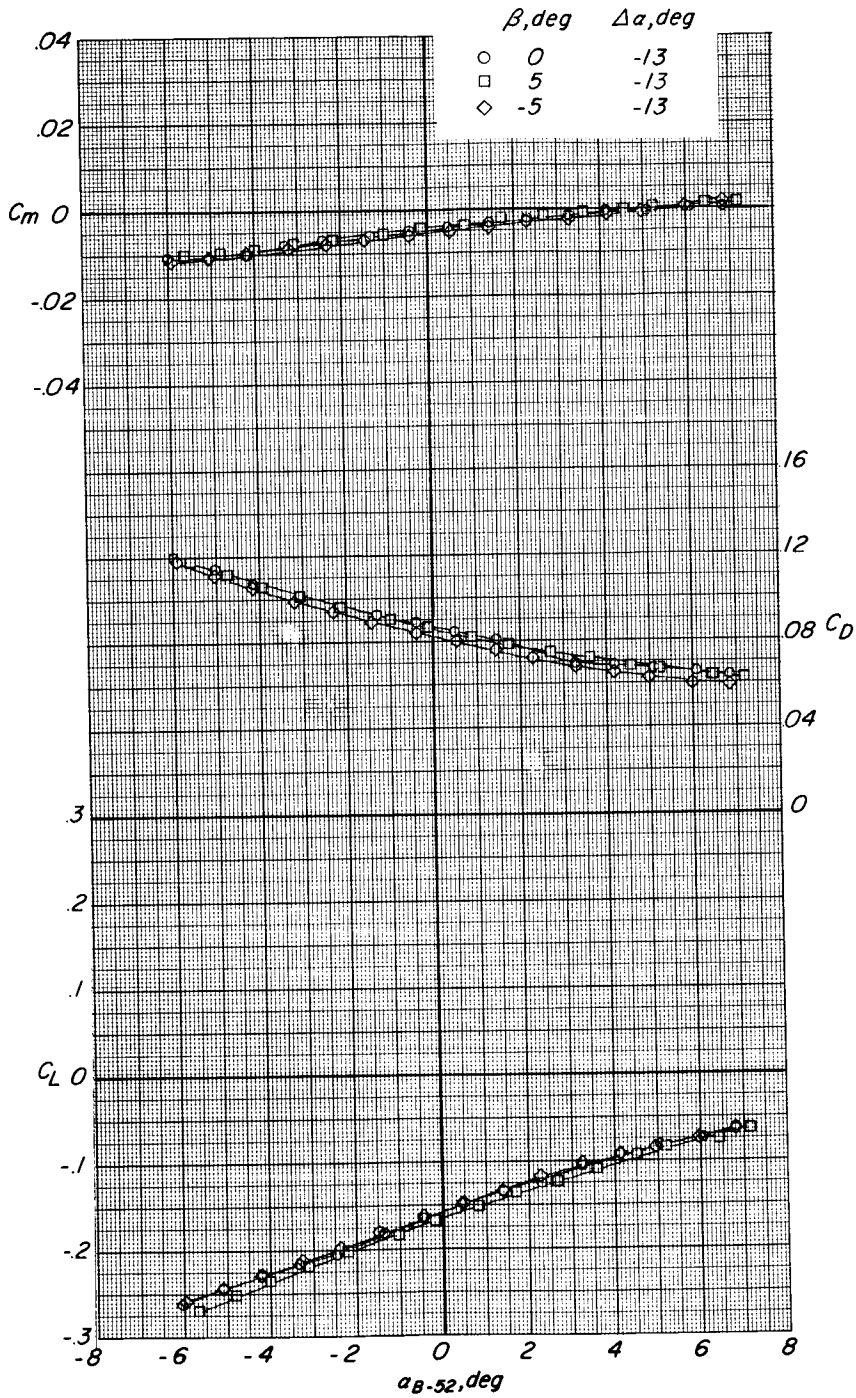

(e) Continued.

Figure 8.- Continued.

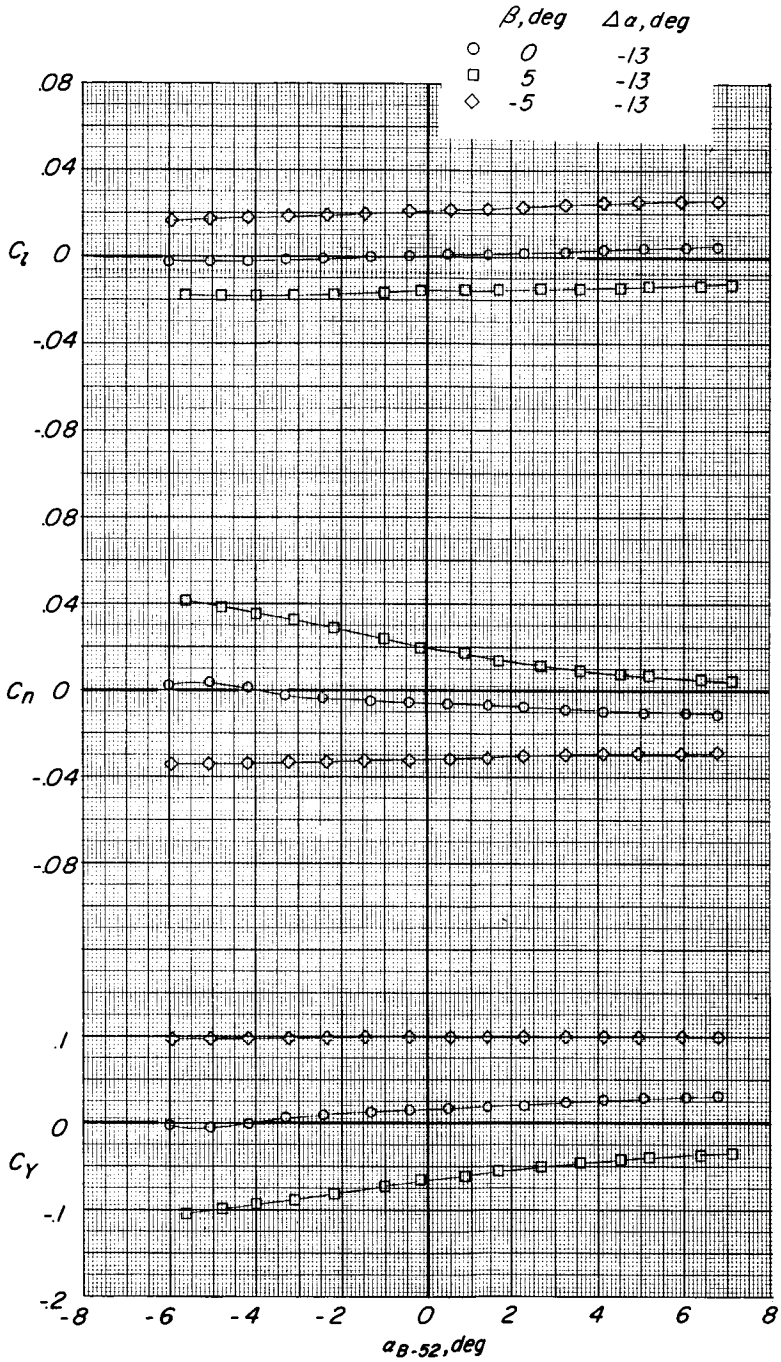

(e) Continued.

Figure 8.- Continued.

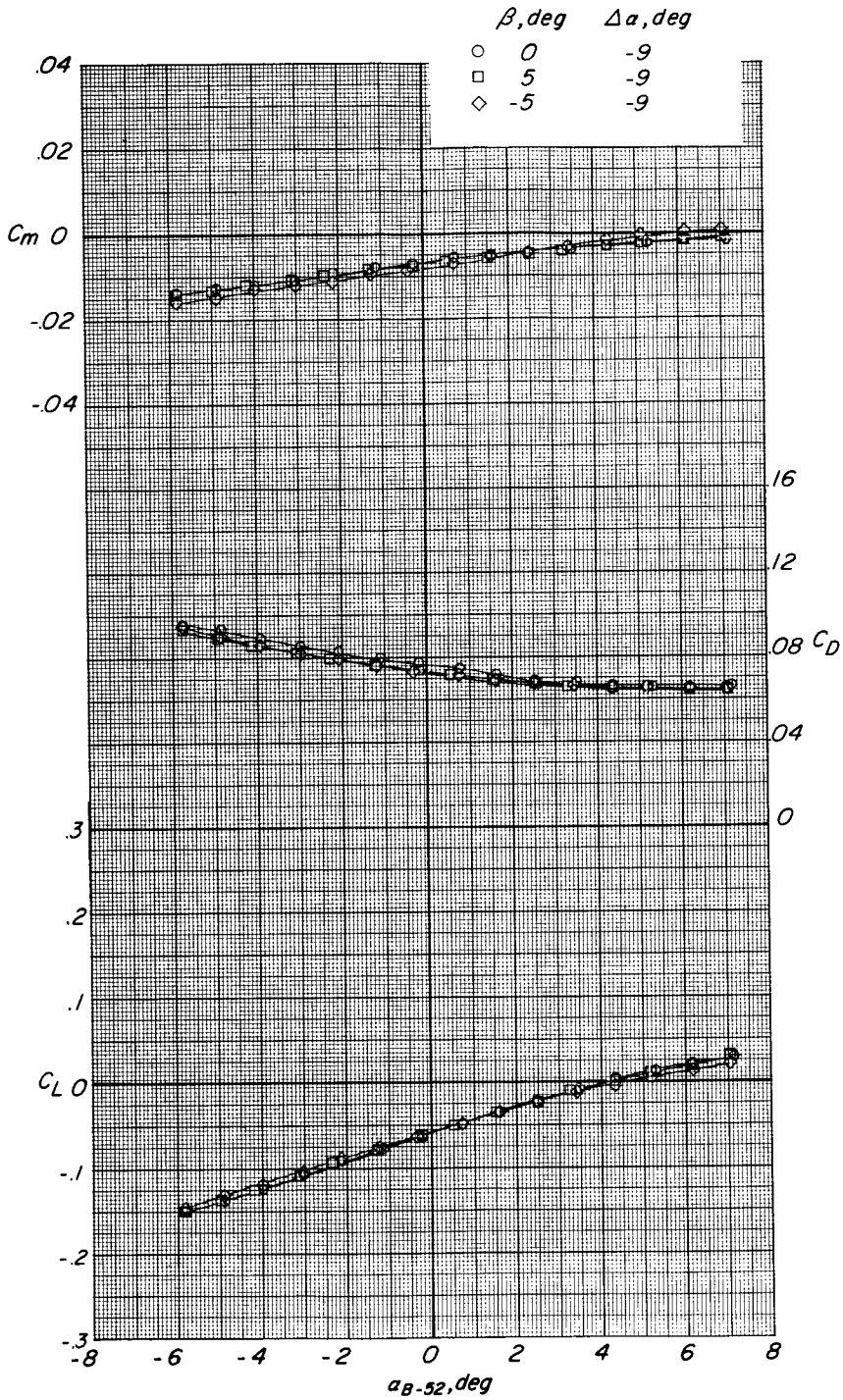

(e) Continued.

Figure 8.- Continued.

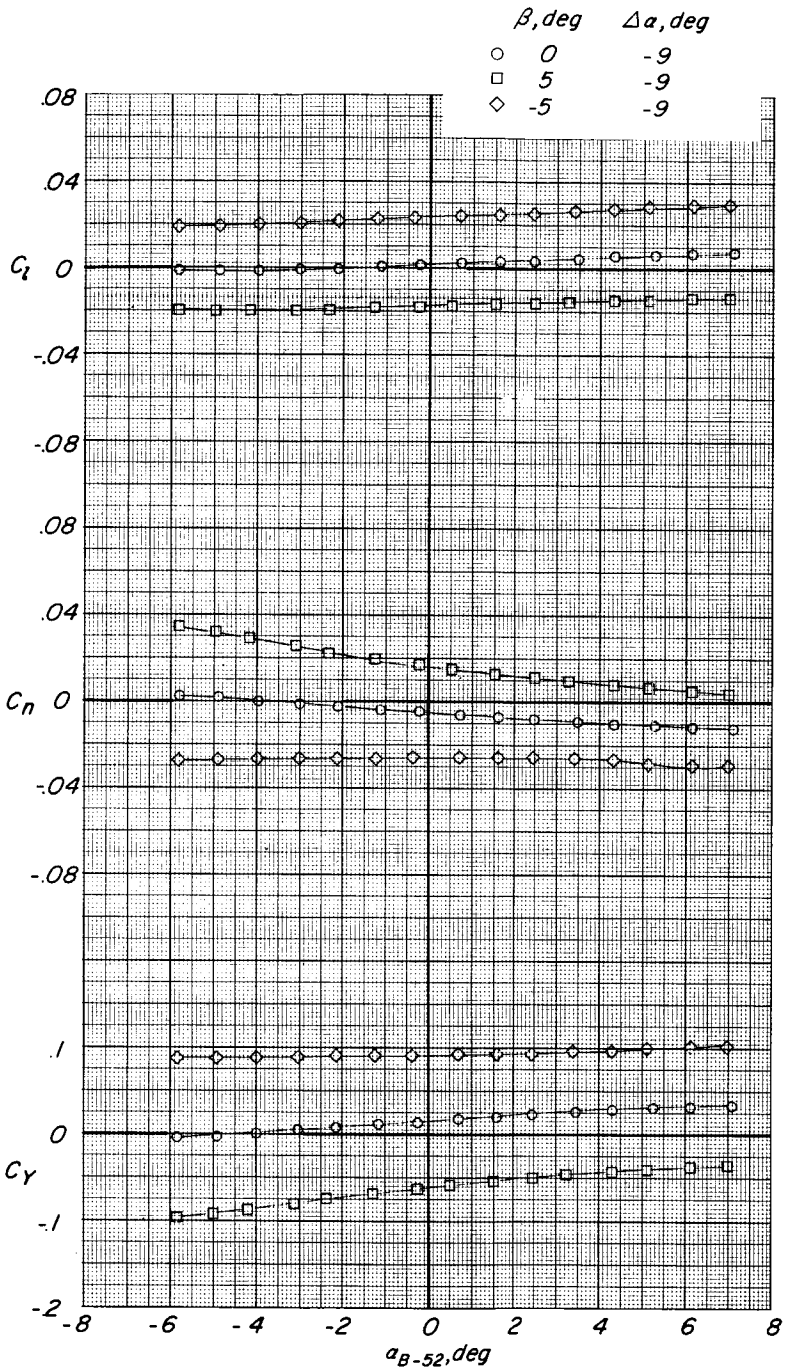

(e) Continued.

Figure 8.- Continued.

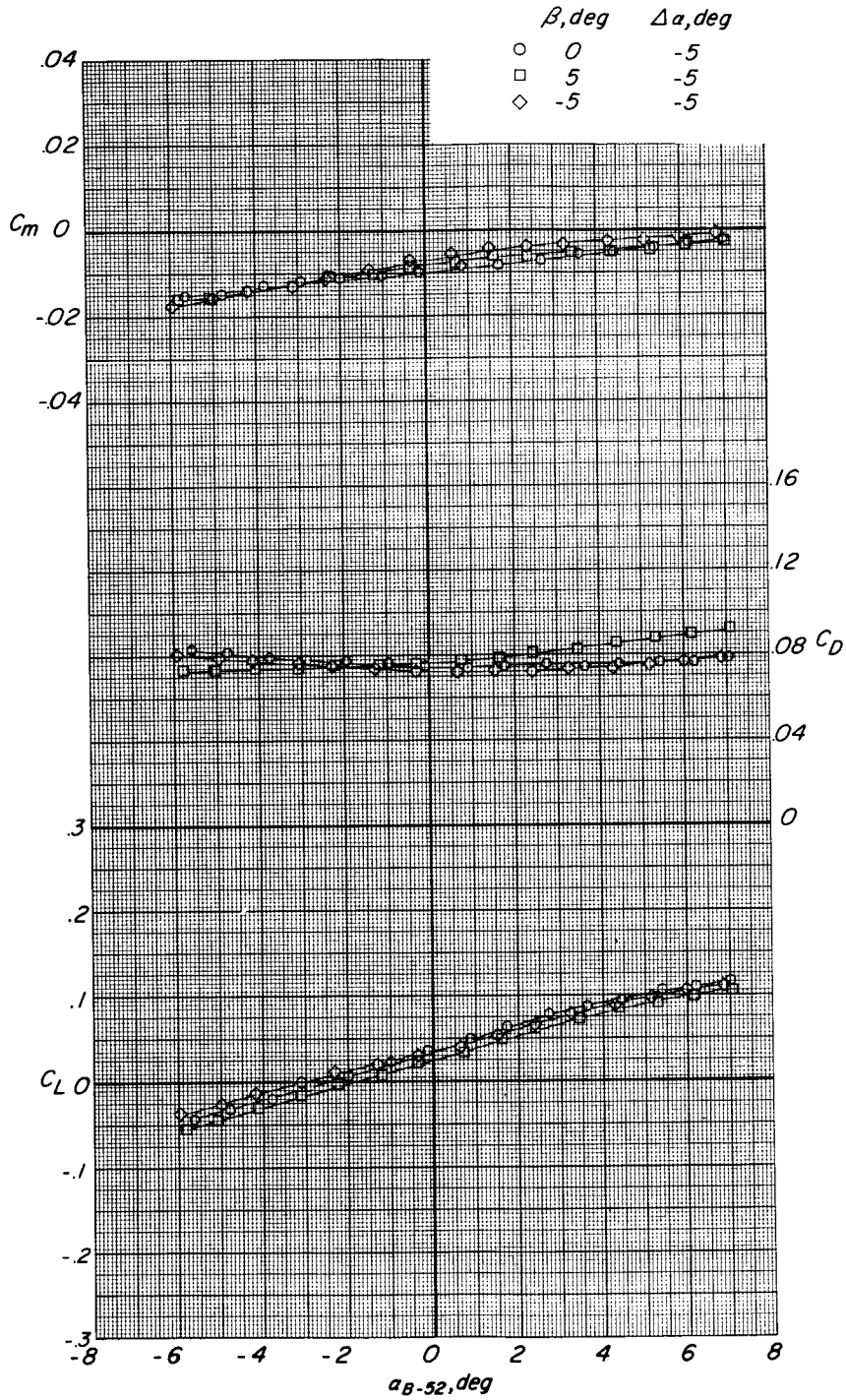

(e) Continued.

Figure 8.- Continued.

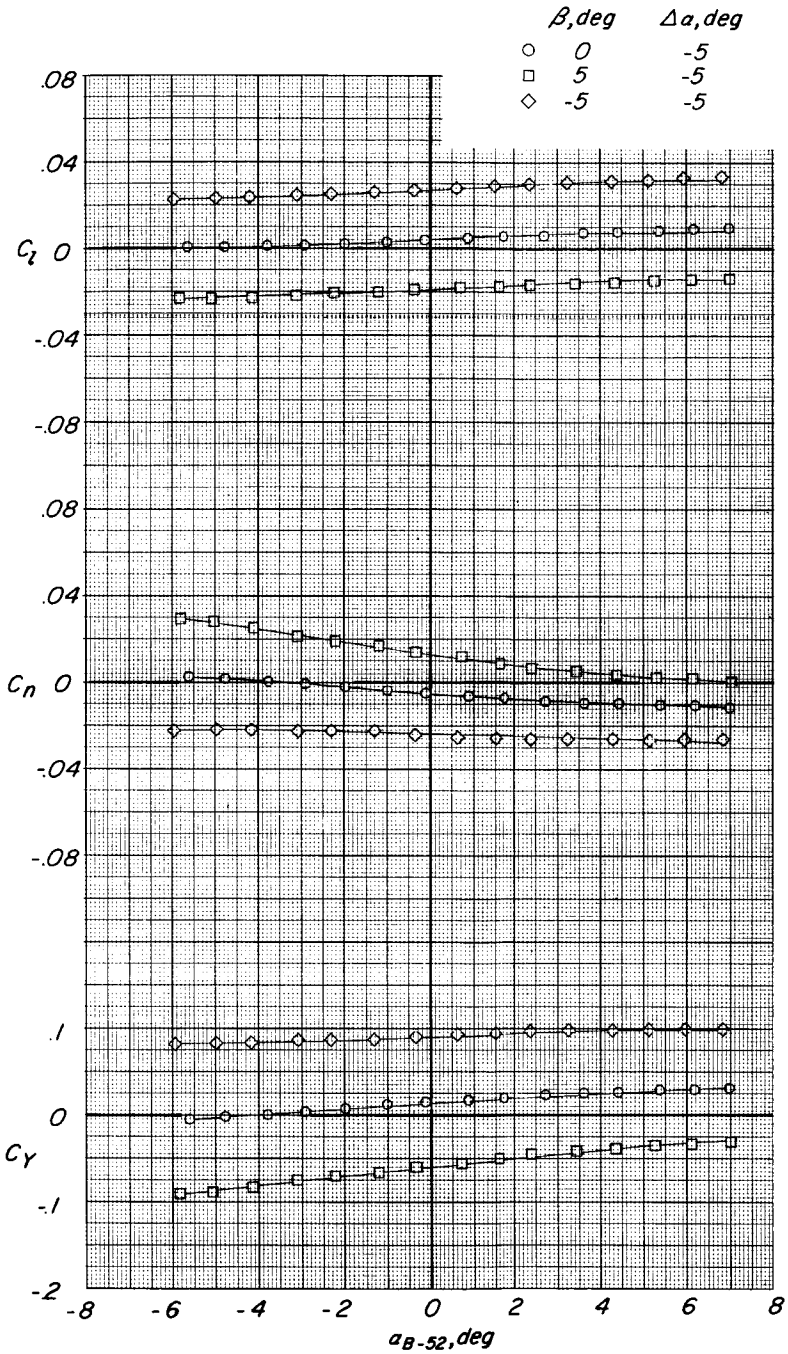

(e) Continued.

Figure 8.- Continued.

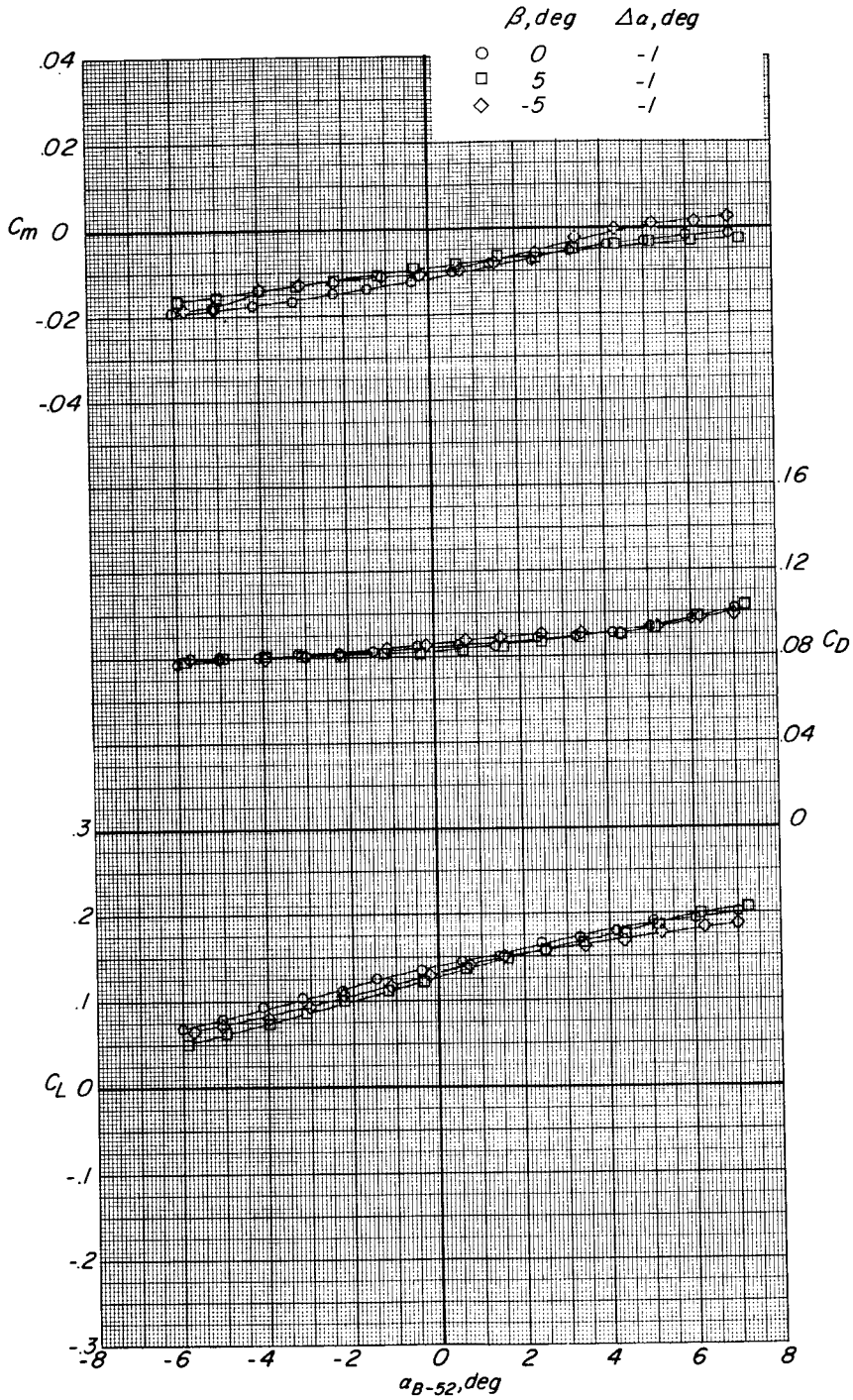

(e) Continued.

Figure 8.- Continued.

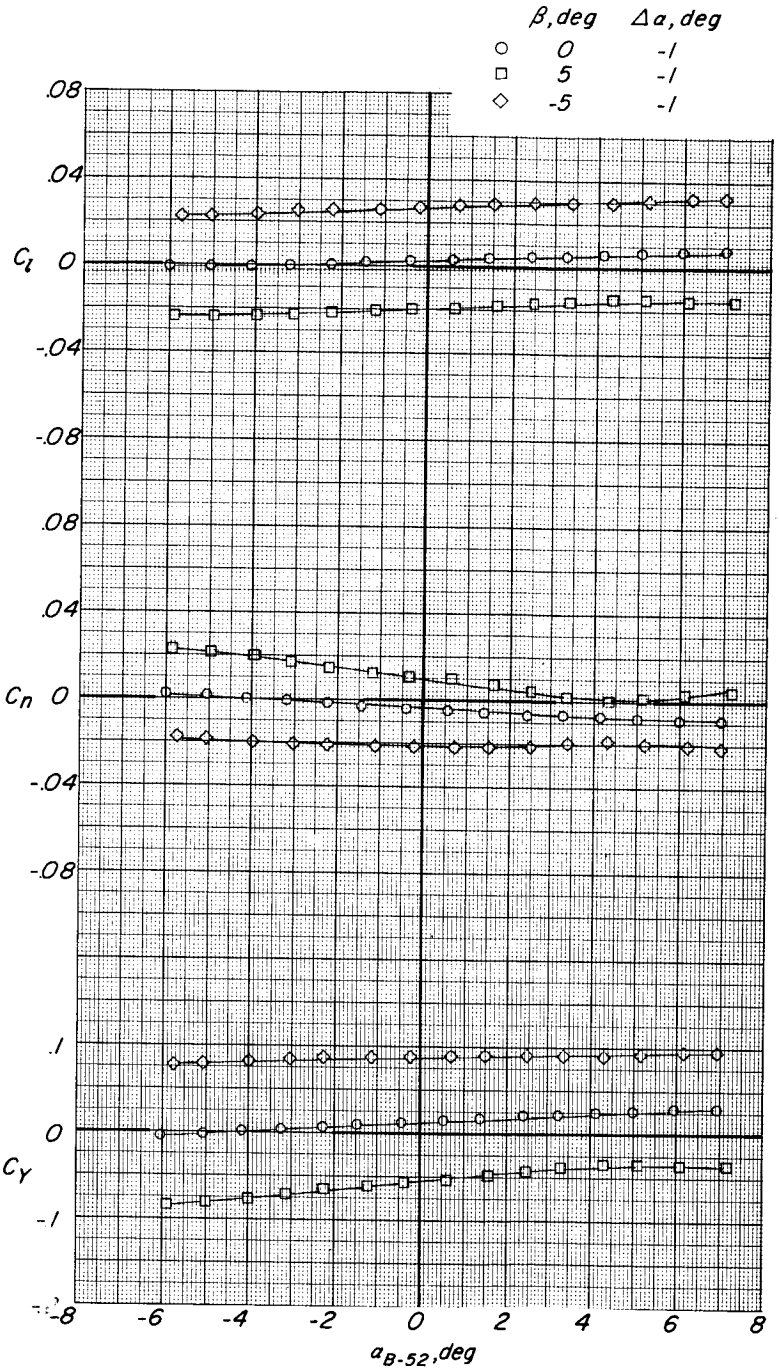

(e) Continued.

Figure 8.- Continued.

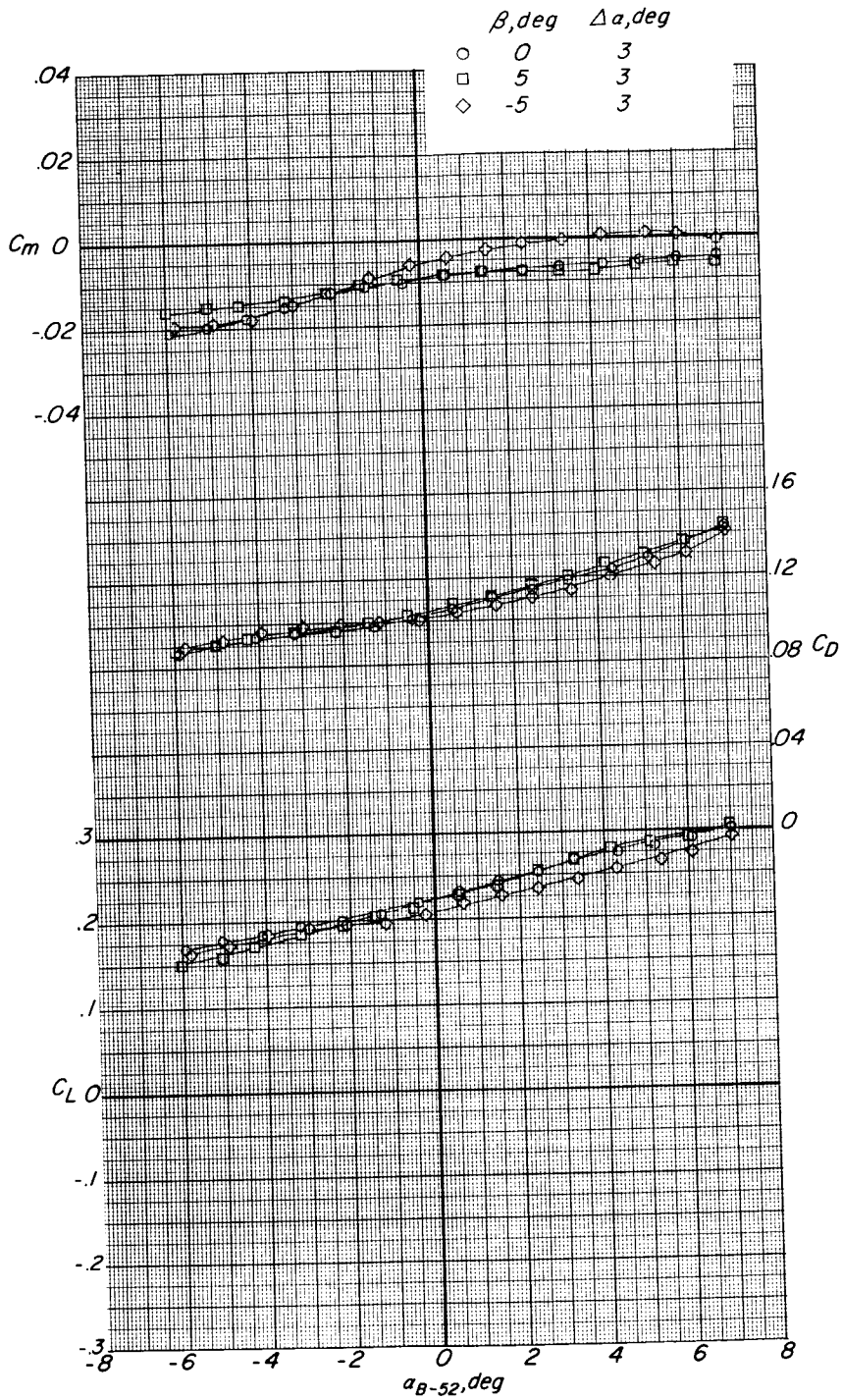

(e) Continued.

Figure 8.- Continued.

[redacted] DECLASSIFIED

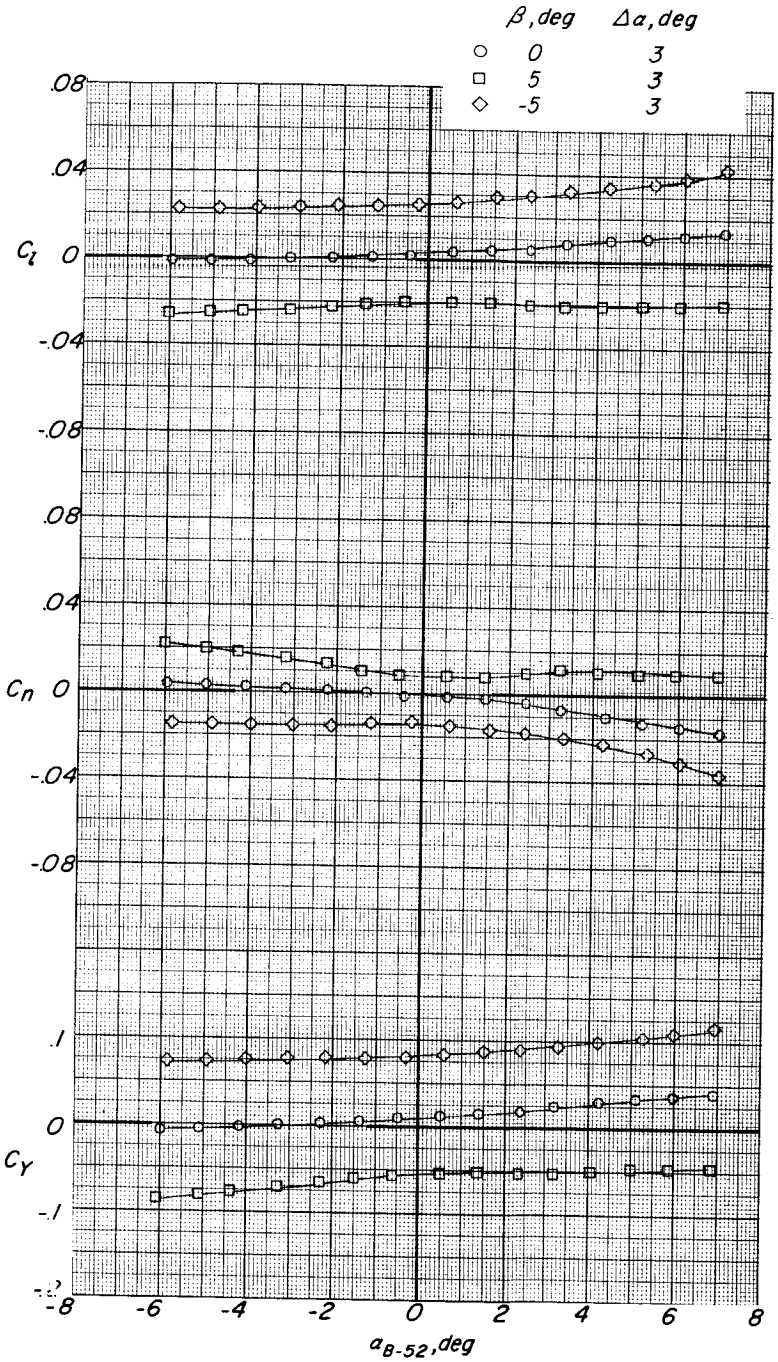

(e) Concluded.

Figure 8.- Concluded.

[redacted]

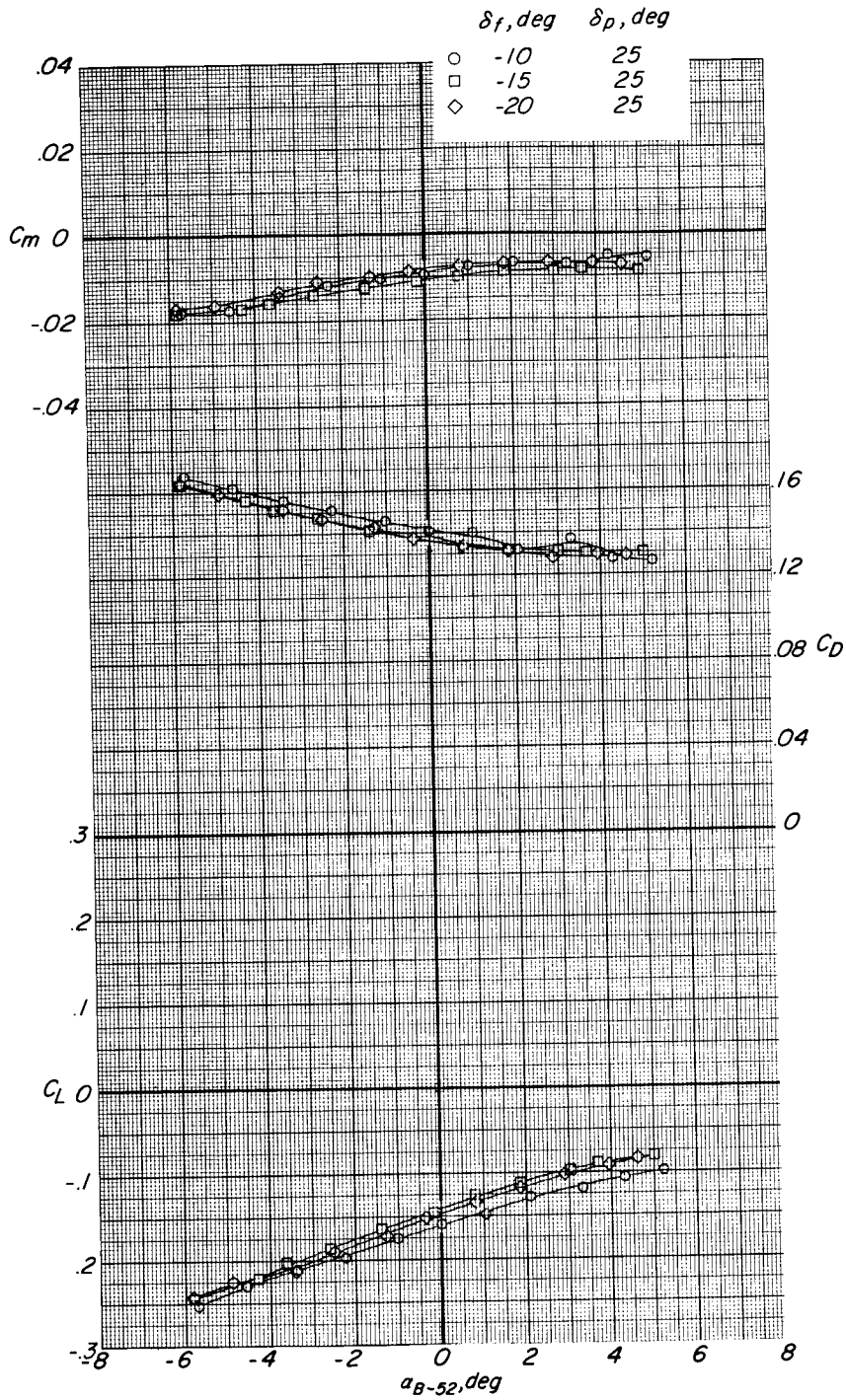

(a) z' = 0.

Figure 9.- Aerodynamic characteristics of M2-F2 model in presence of B-52 model. M = 0.80; nominal control settings are $\delta_p = 25^0$, $\delta_f = -10^0$, and 10^0 rudder flare.

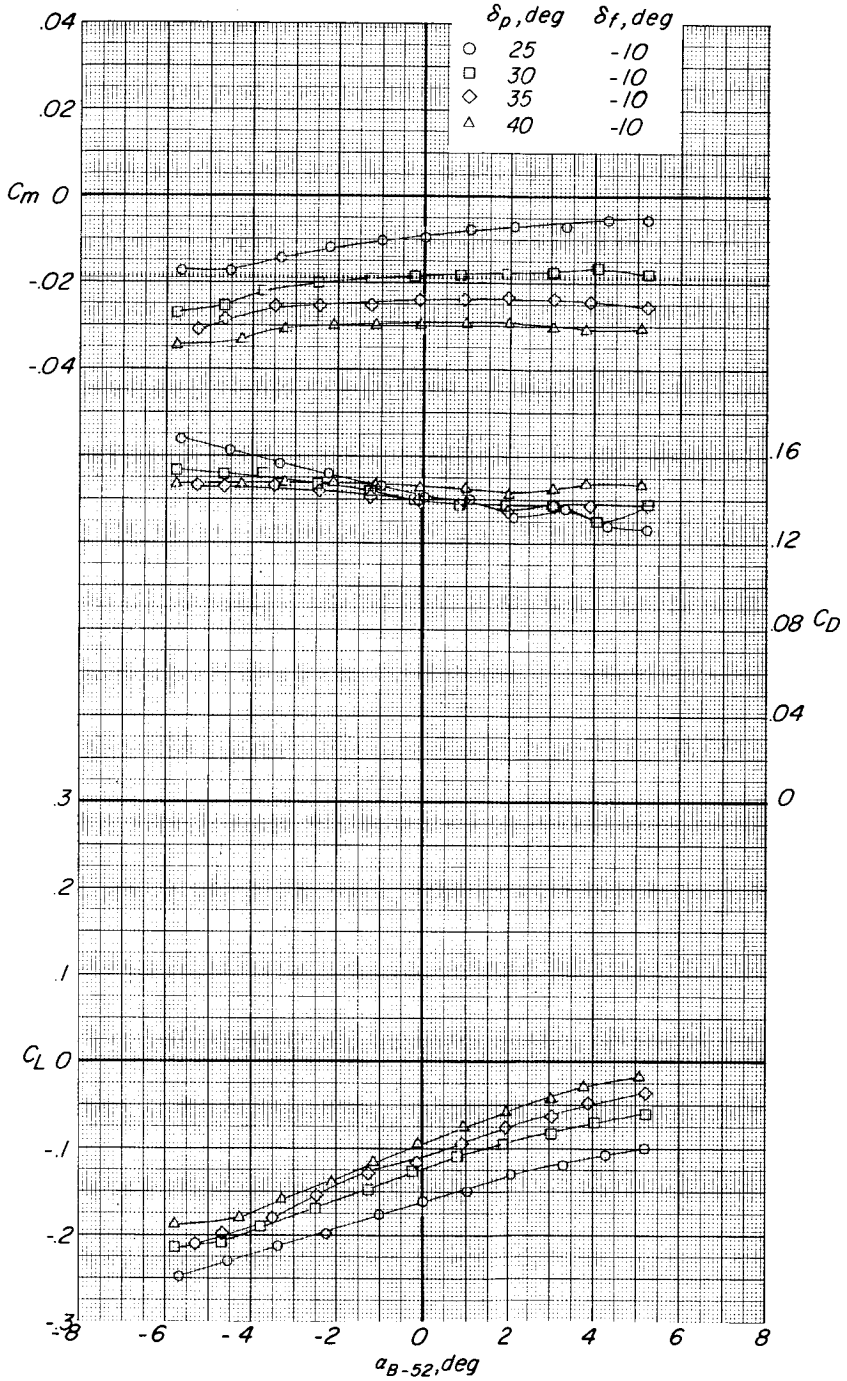

(a) Continued.

Figure 9.- Continued.

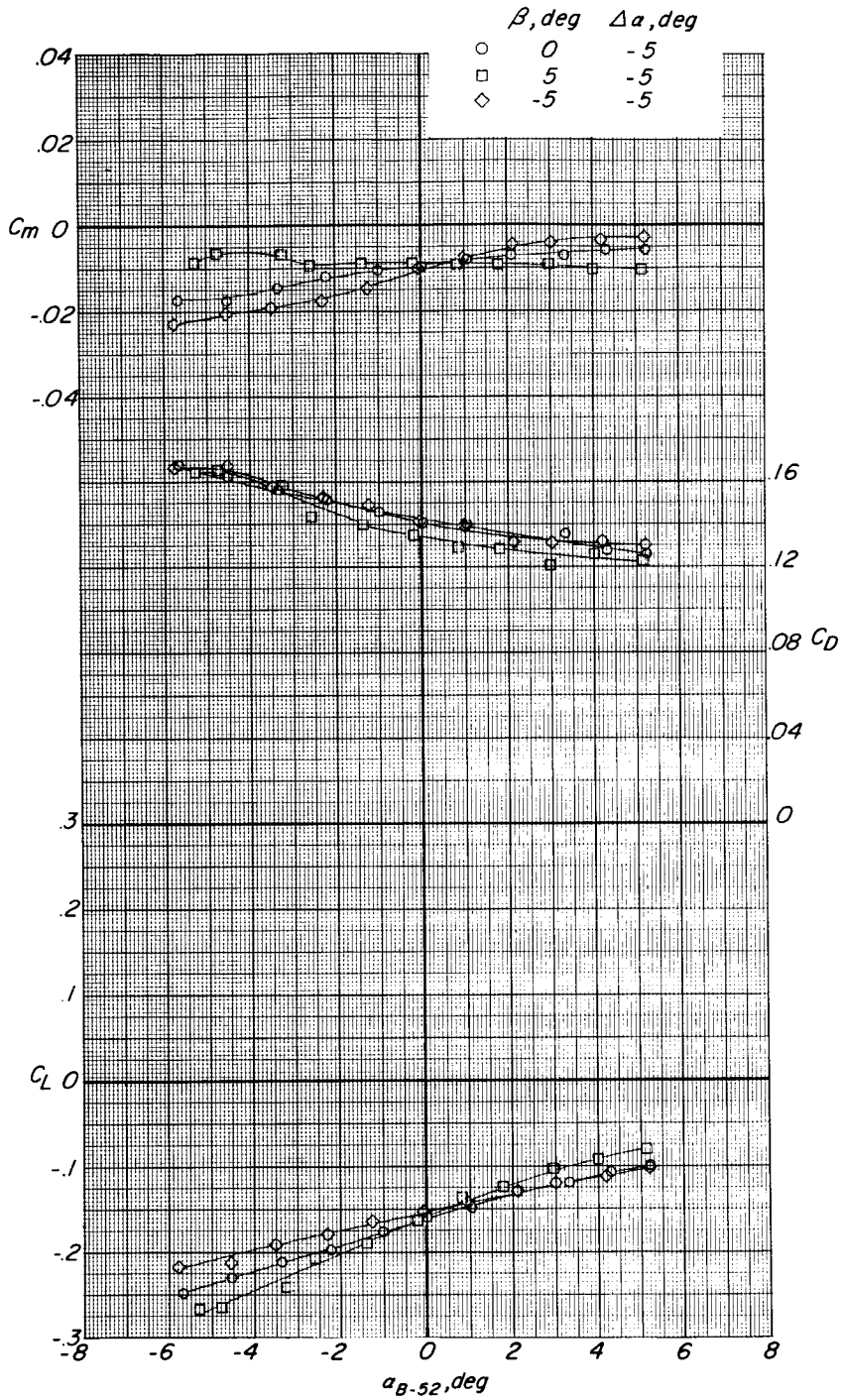

(a) Continued.

Figure 9.- Continued.

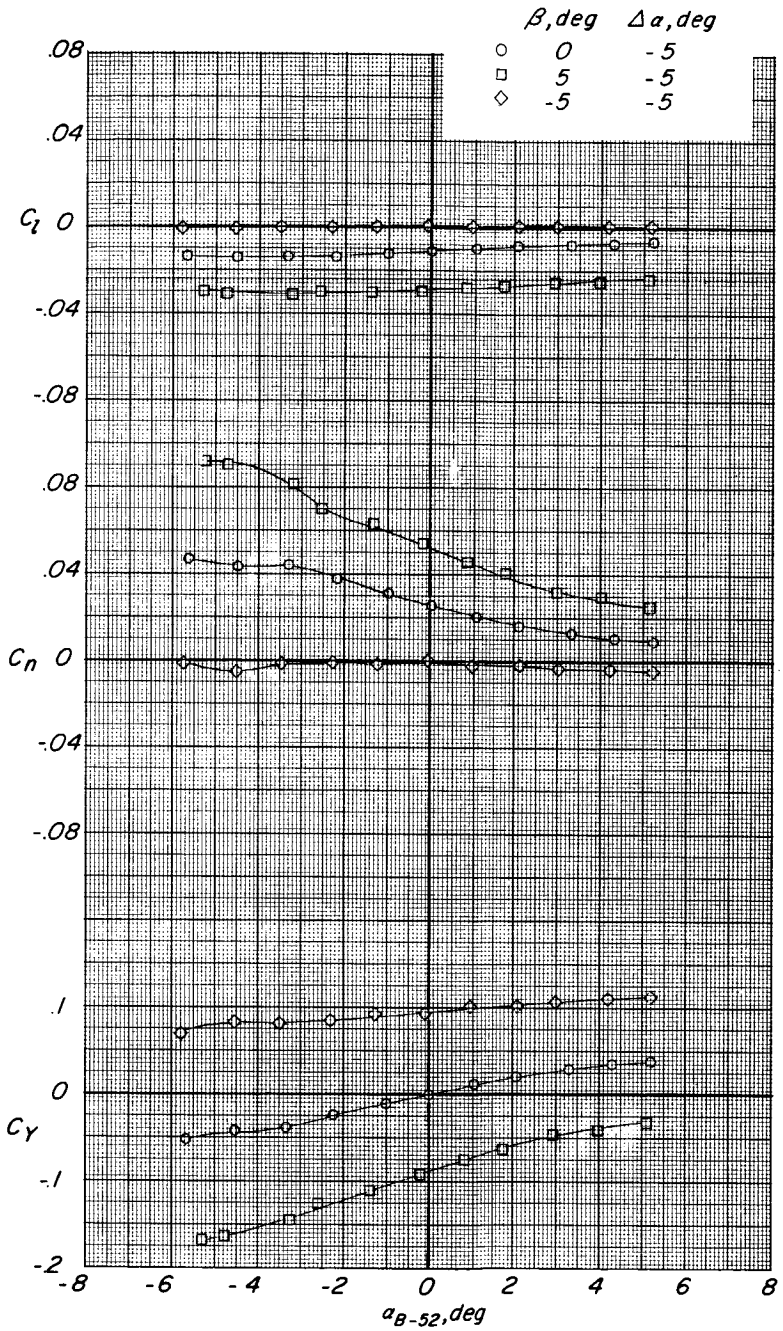

(a) Continued.

Figure 9.- Continued.

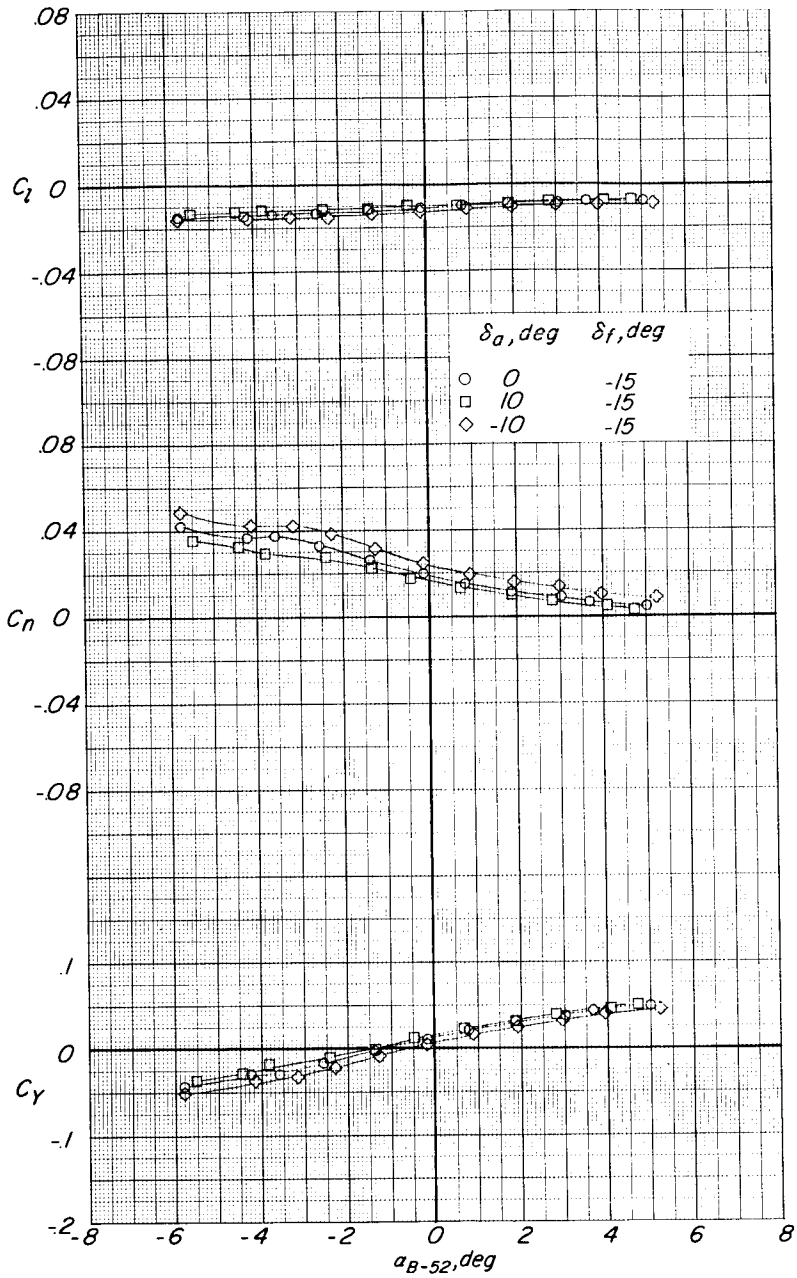

(a) Continued.

Figure 9.- Continued.

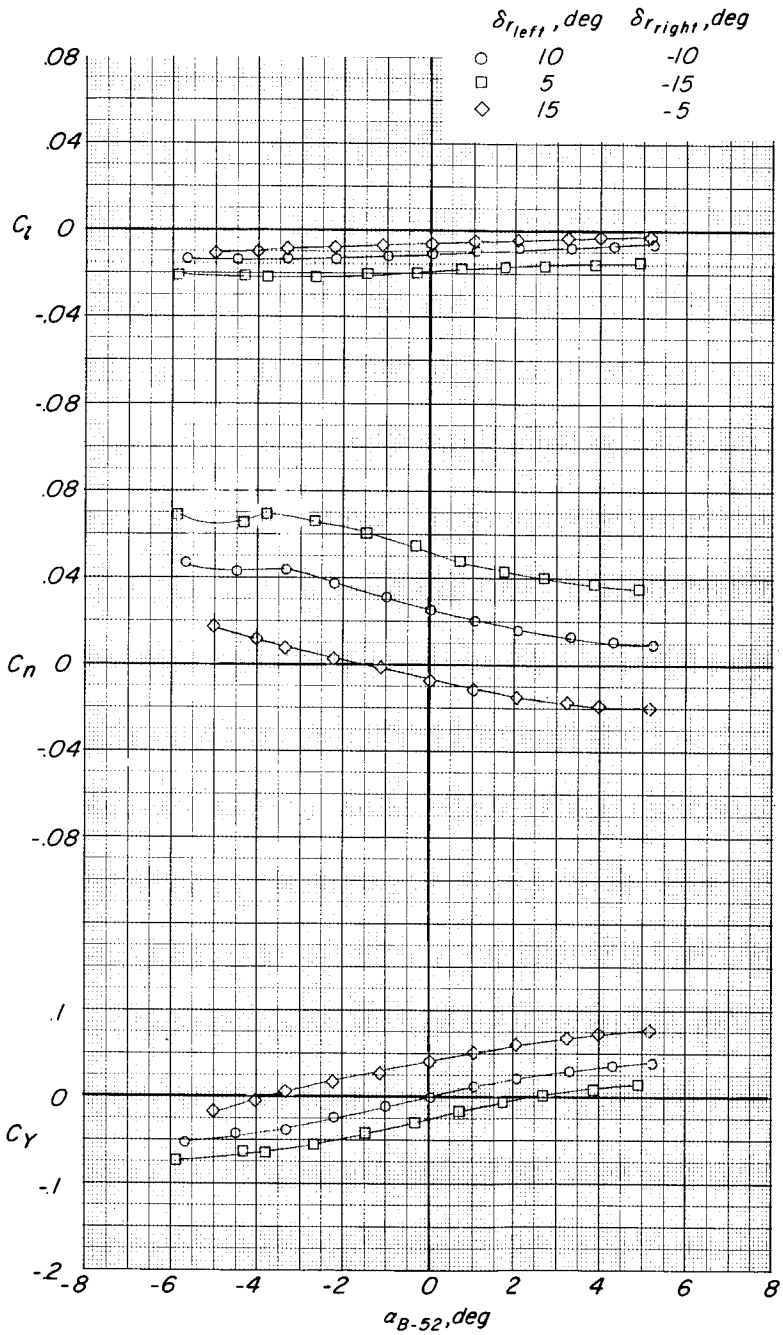

(a) Concluded.

Figure 9.- Continued.

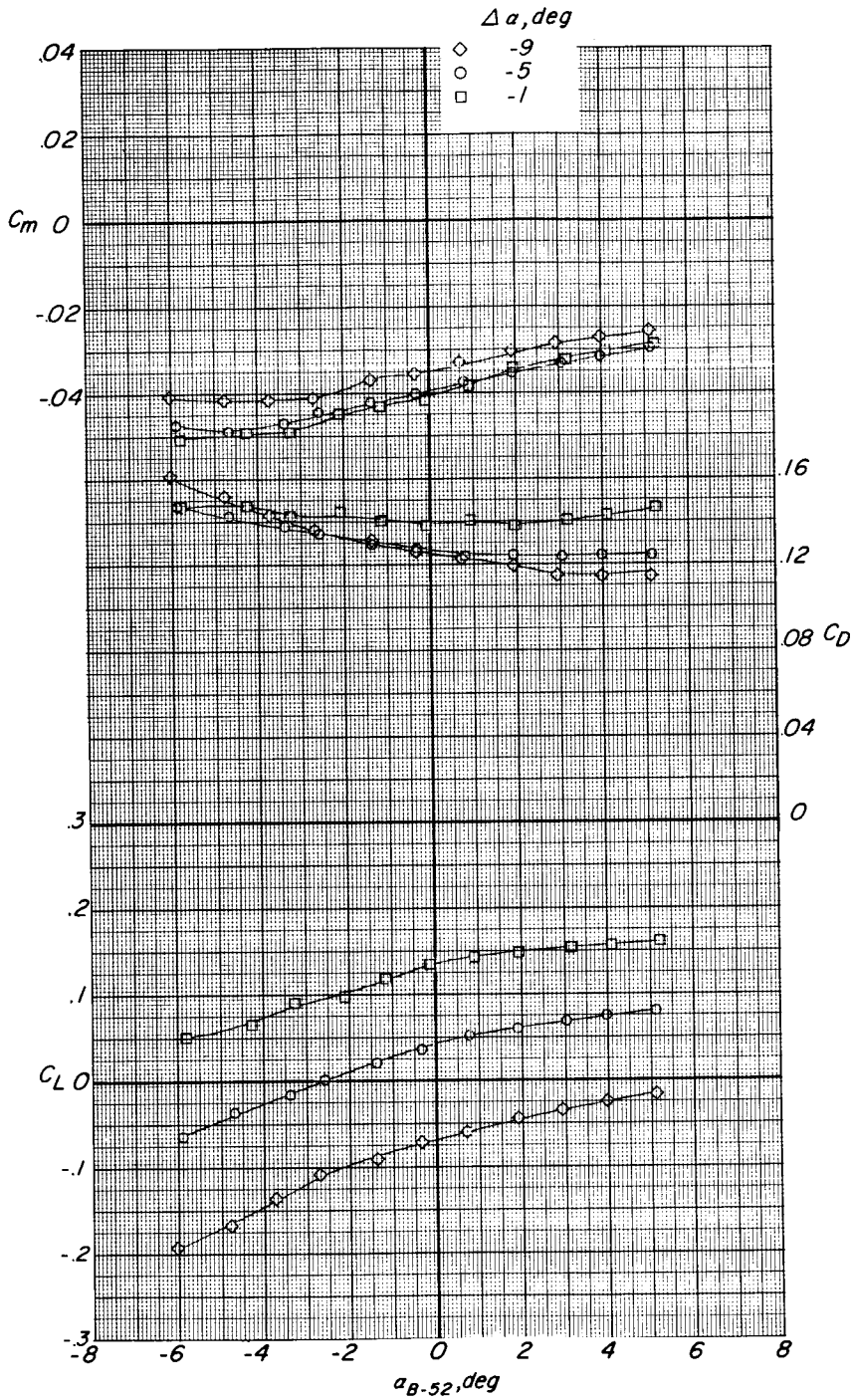

(b) z' = 2.0 feet (0.61 m).

Figure 9.- Continued.

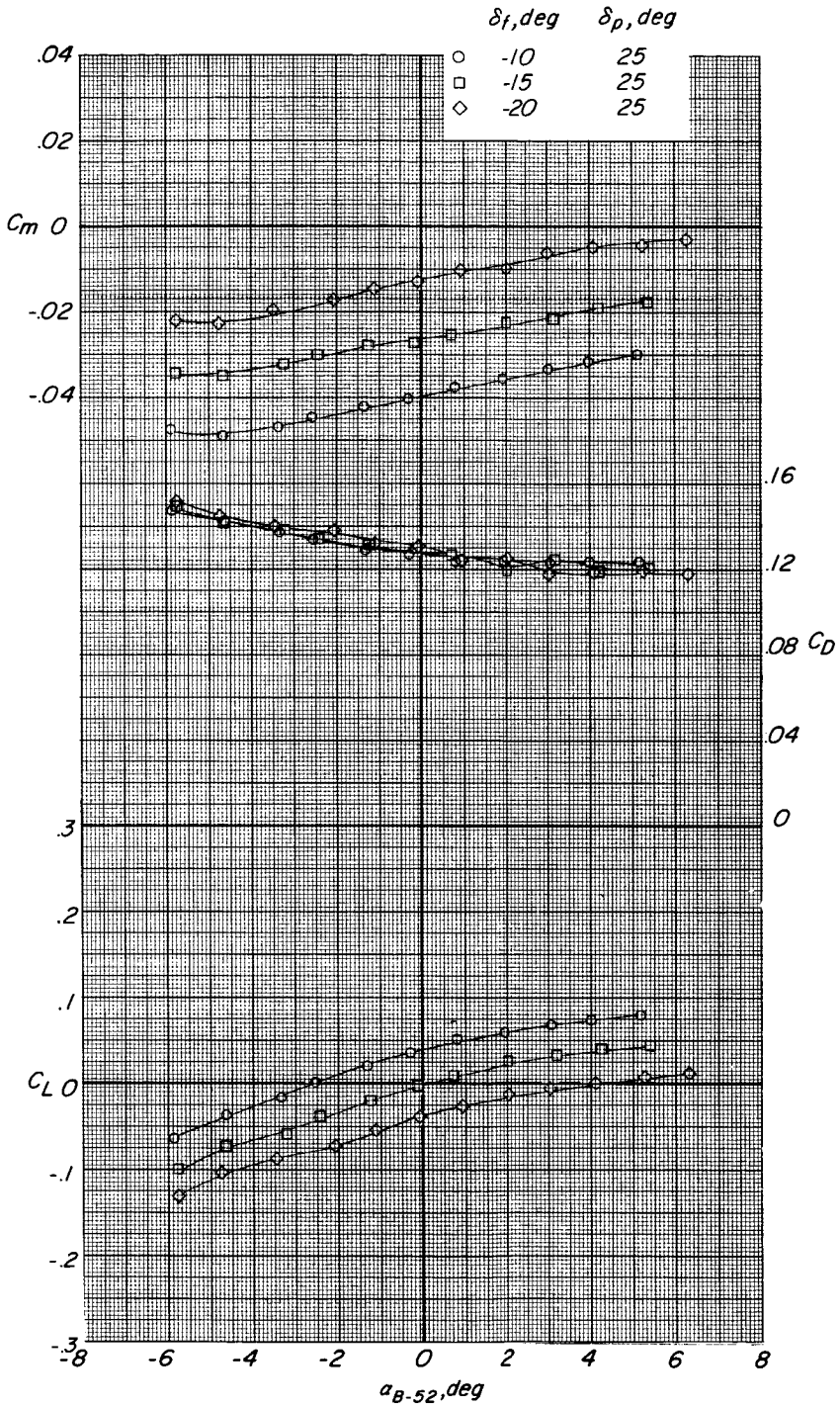

(b) Continued.

Figure 9.- Continued.

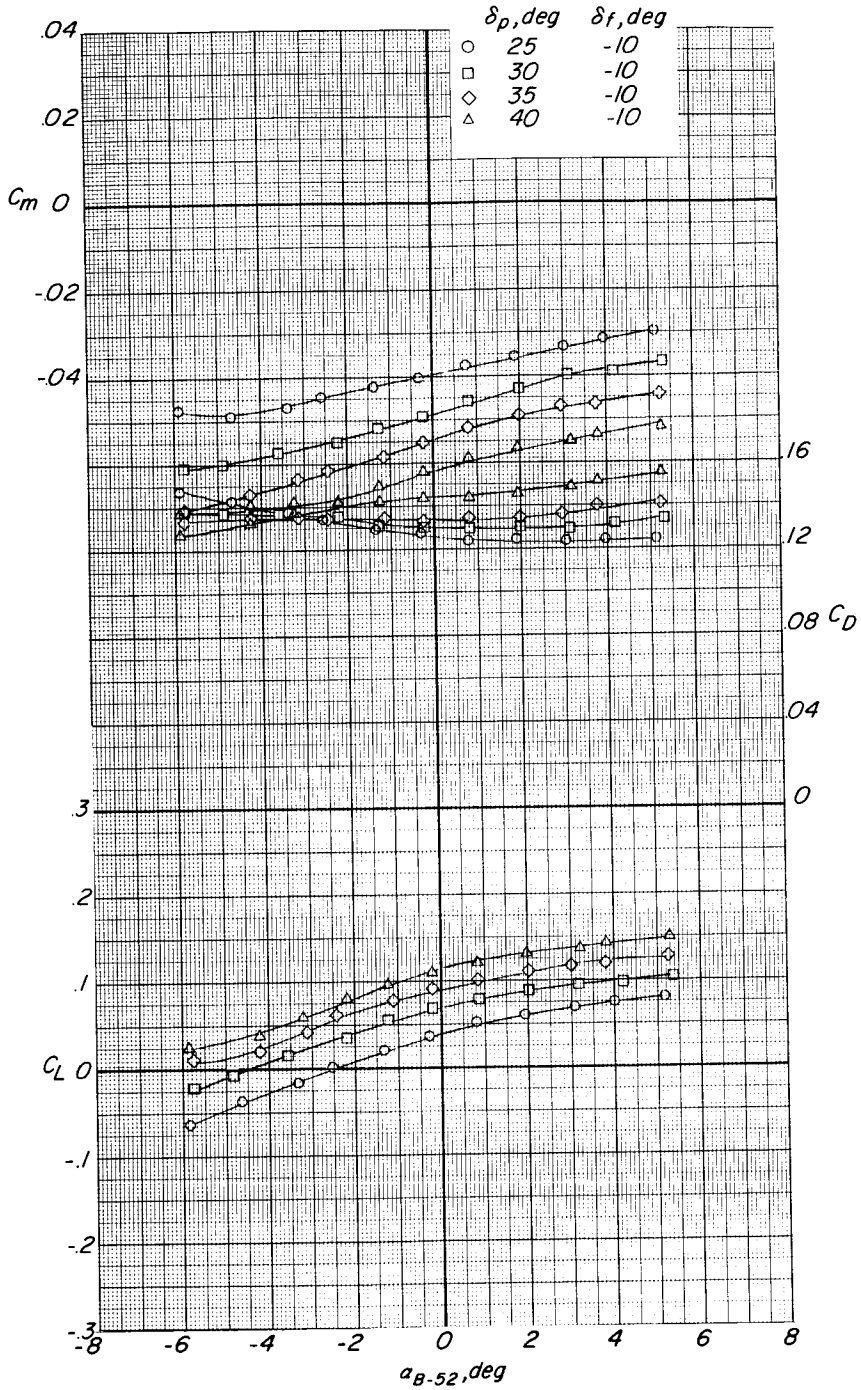

(b) Continued.

Figure 9.- Continued.

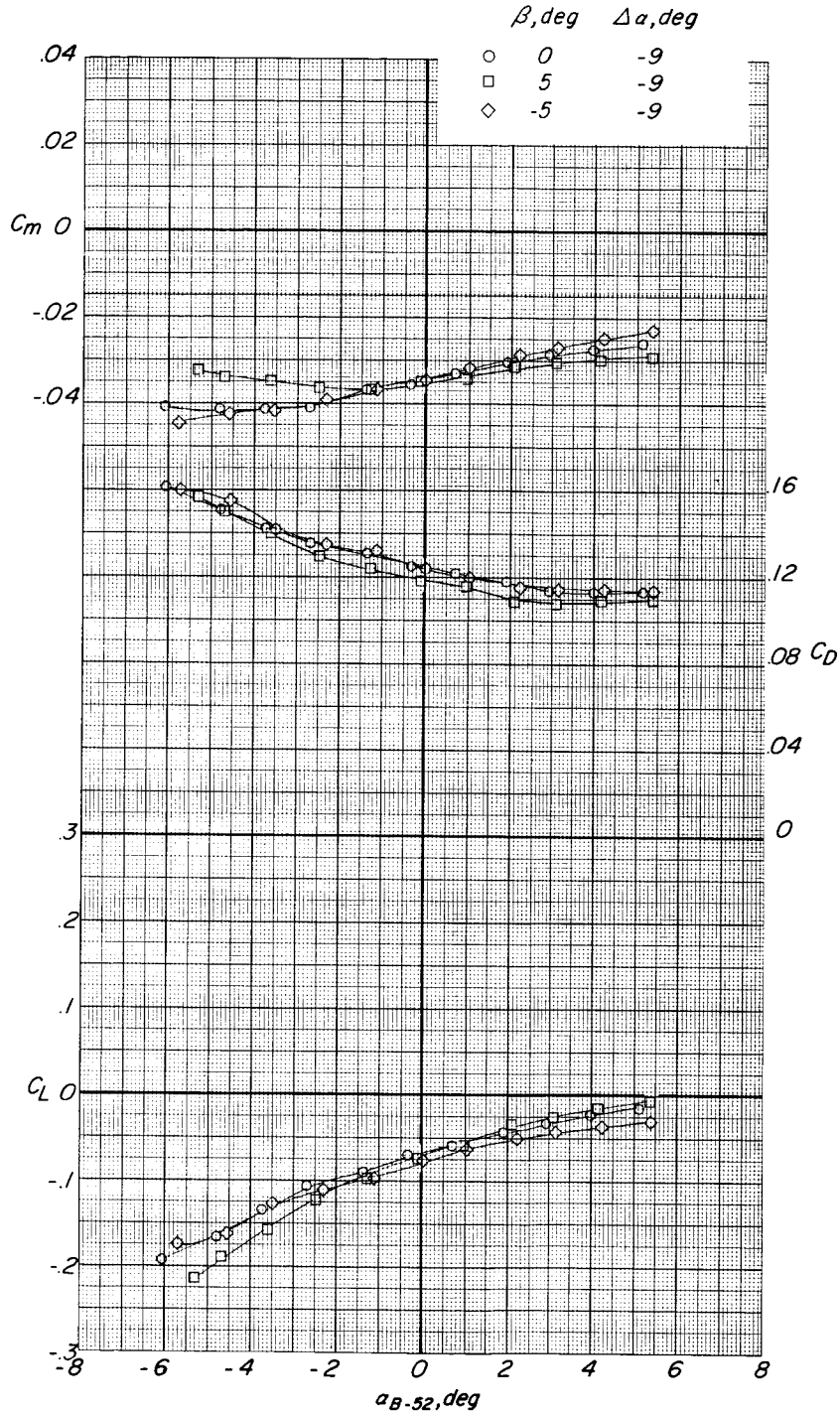

(b) Continued.

Figure 9.- Continued.

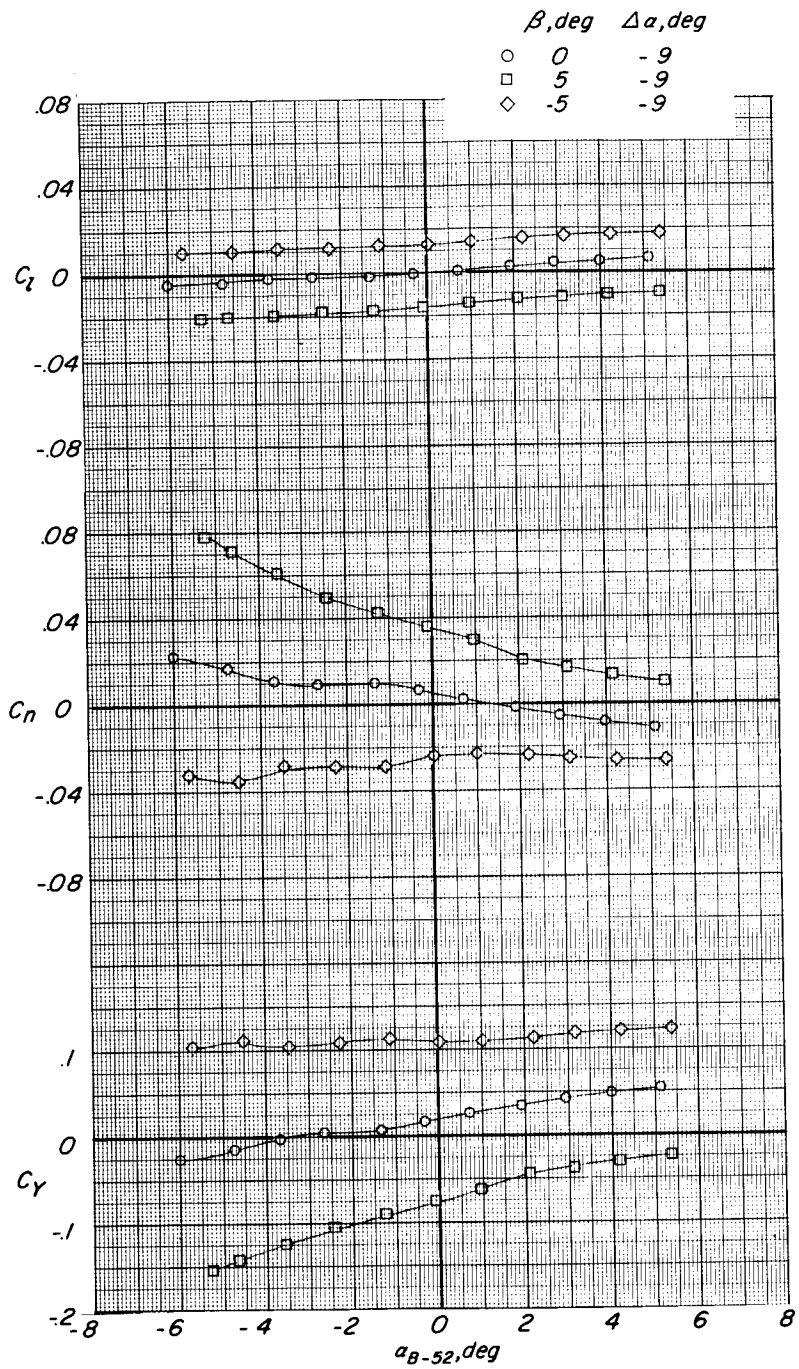

(b) Continued.

Figure 9.- Continued.

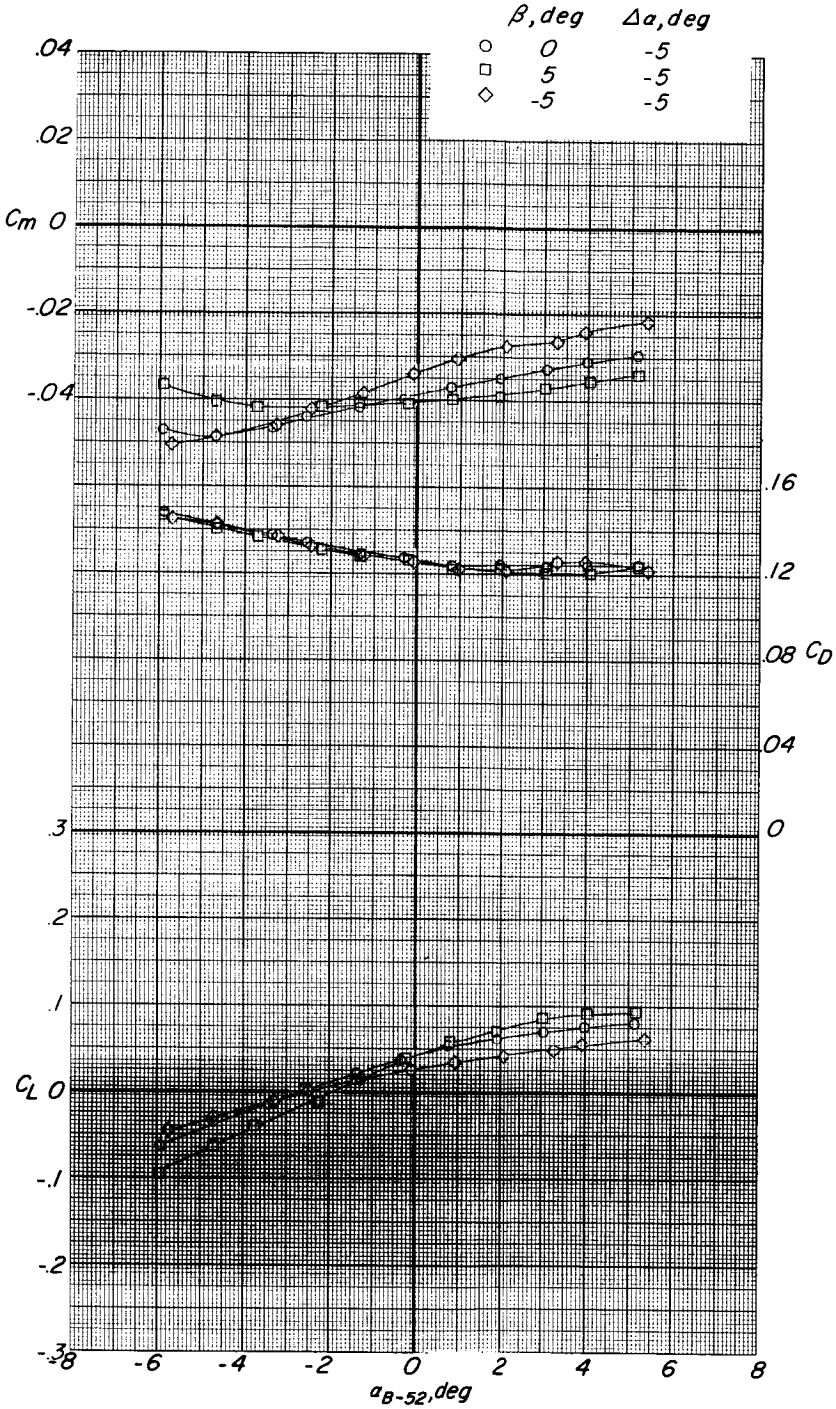

(b) Continued.

Figure 9.- Continued.

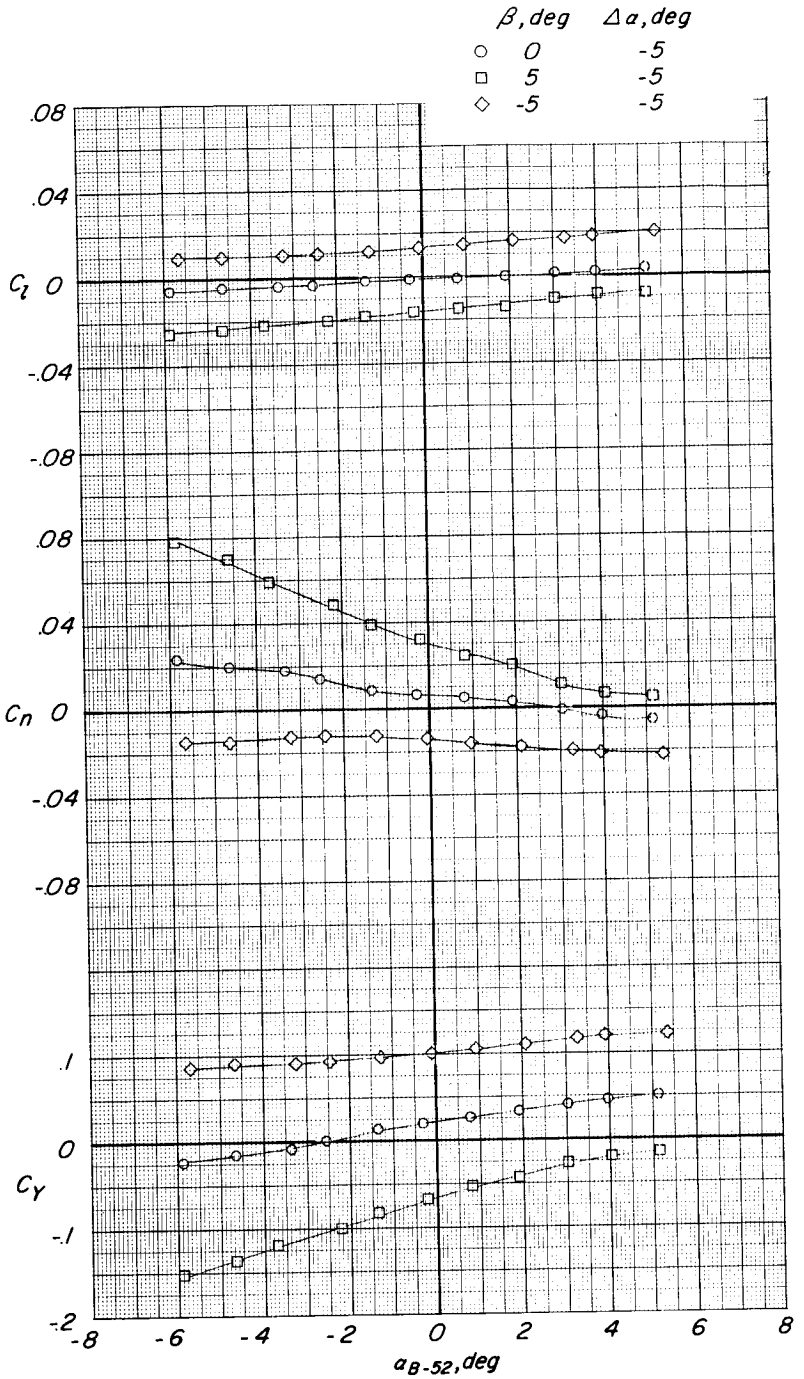

(b) Continued.

Figure 9.- Continued.

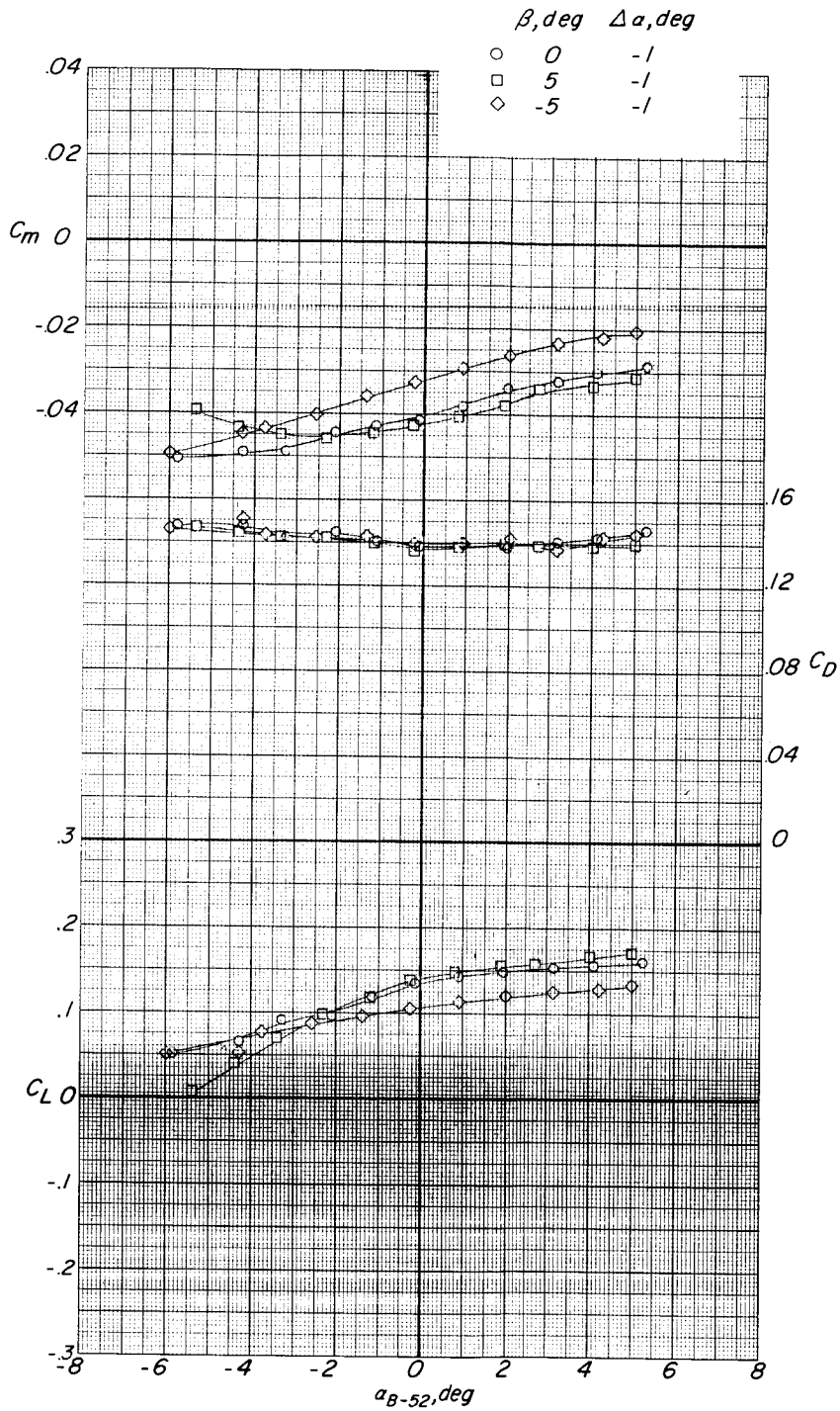

(b) Continued.

Figure 9.- Continued.

[redacted]

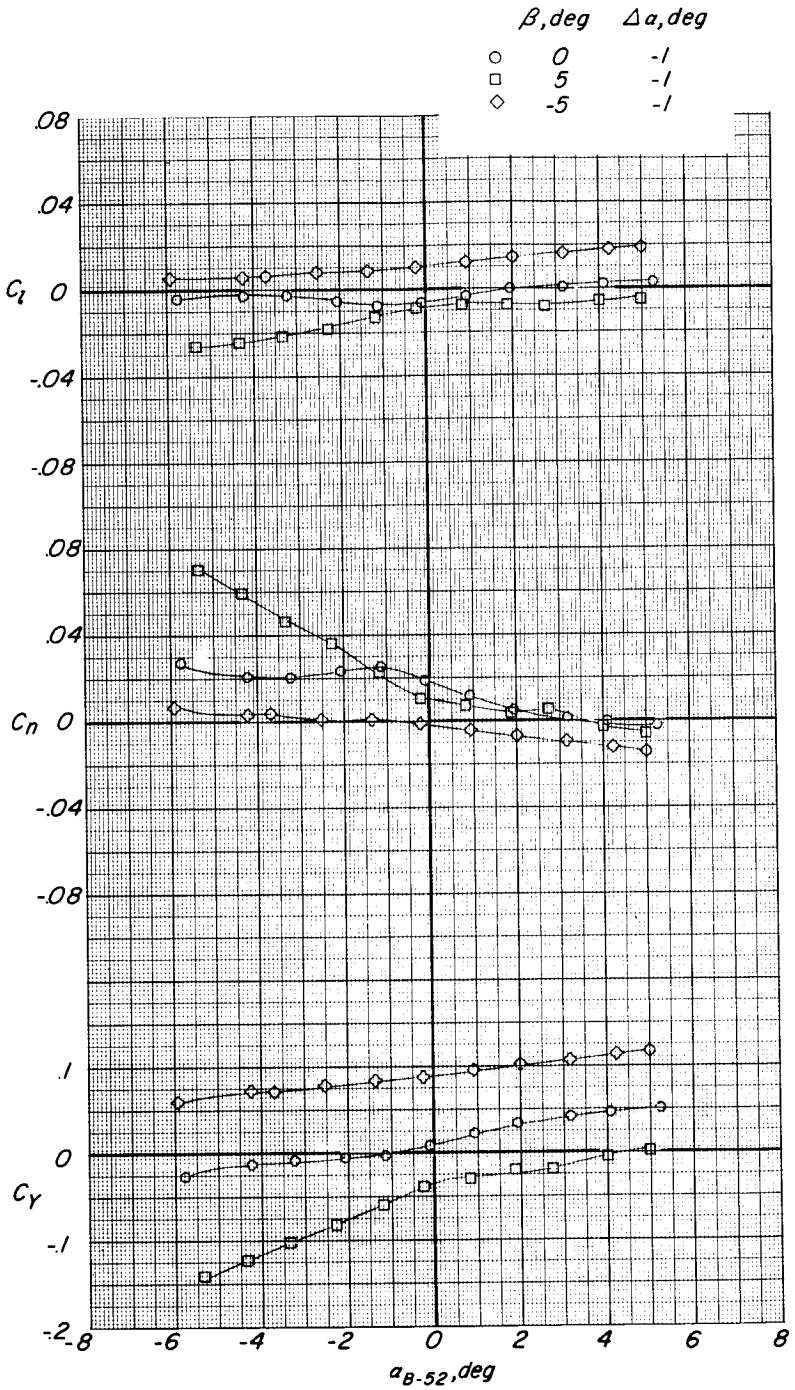

(b) Continued.

Figure 9.- Continued.

[redacted]

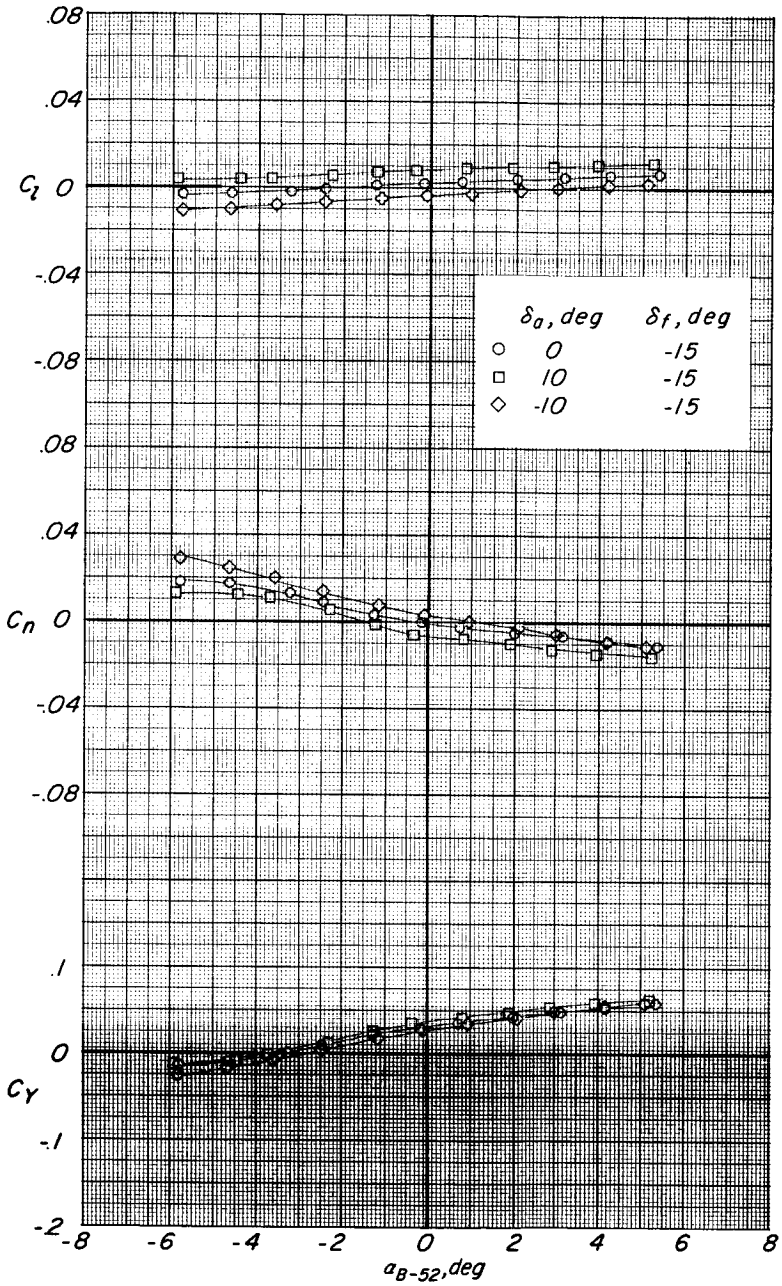

(b) Continued.

Figure 9.- Continued.

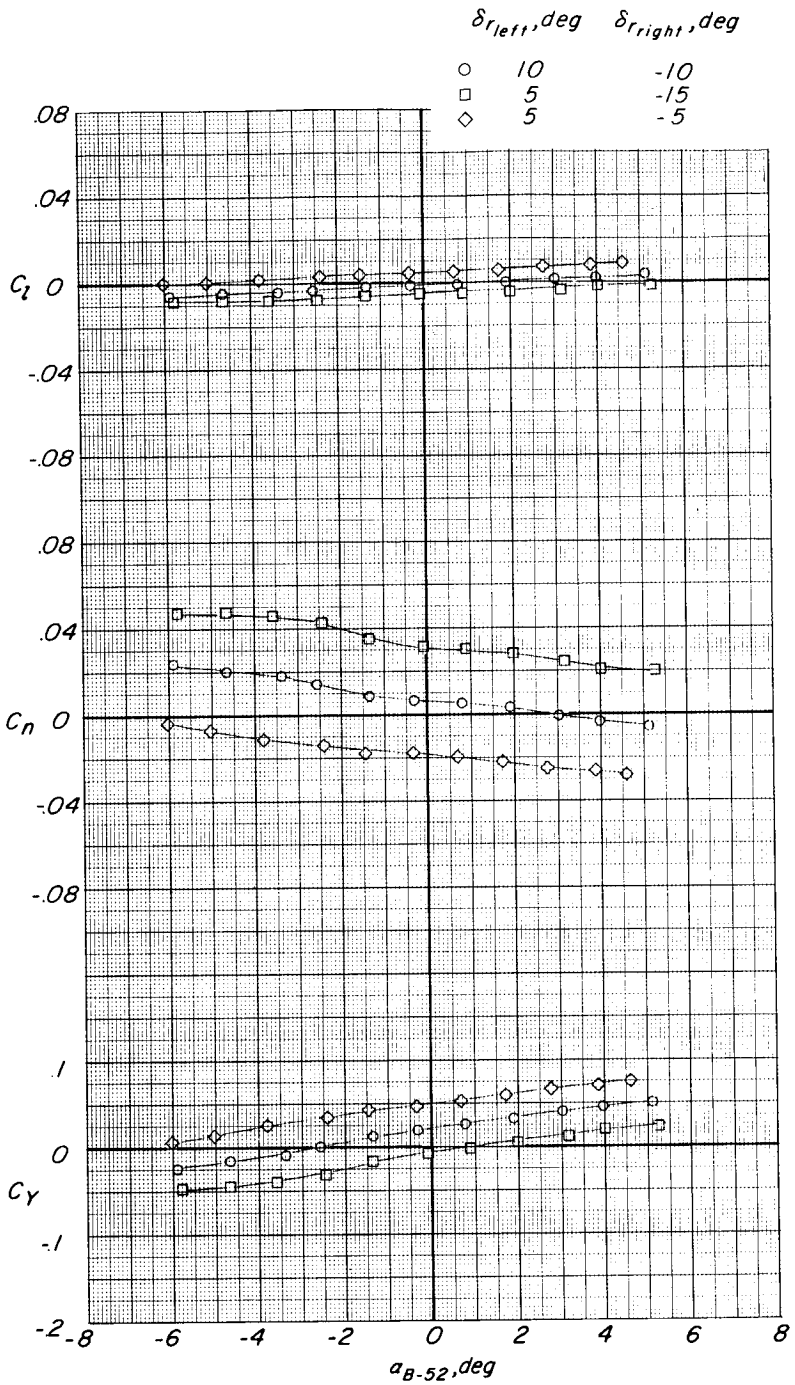

(b) Concluded.

Figure 9.- Continued.

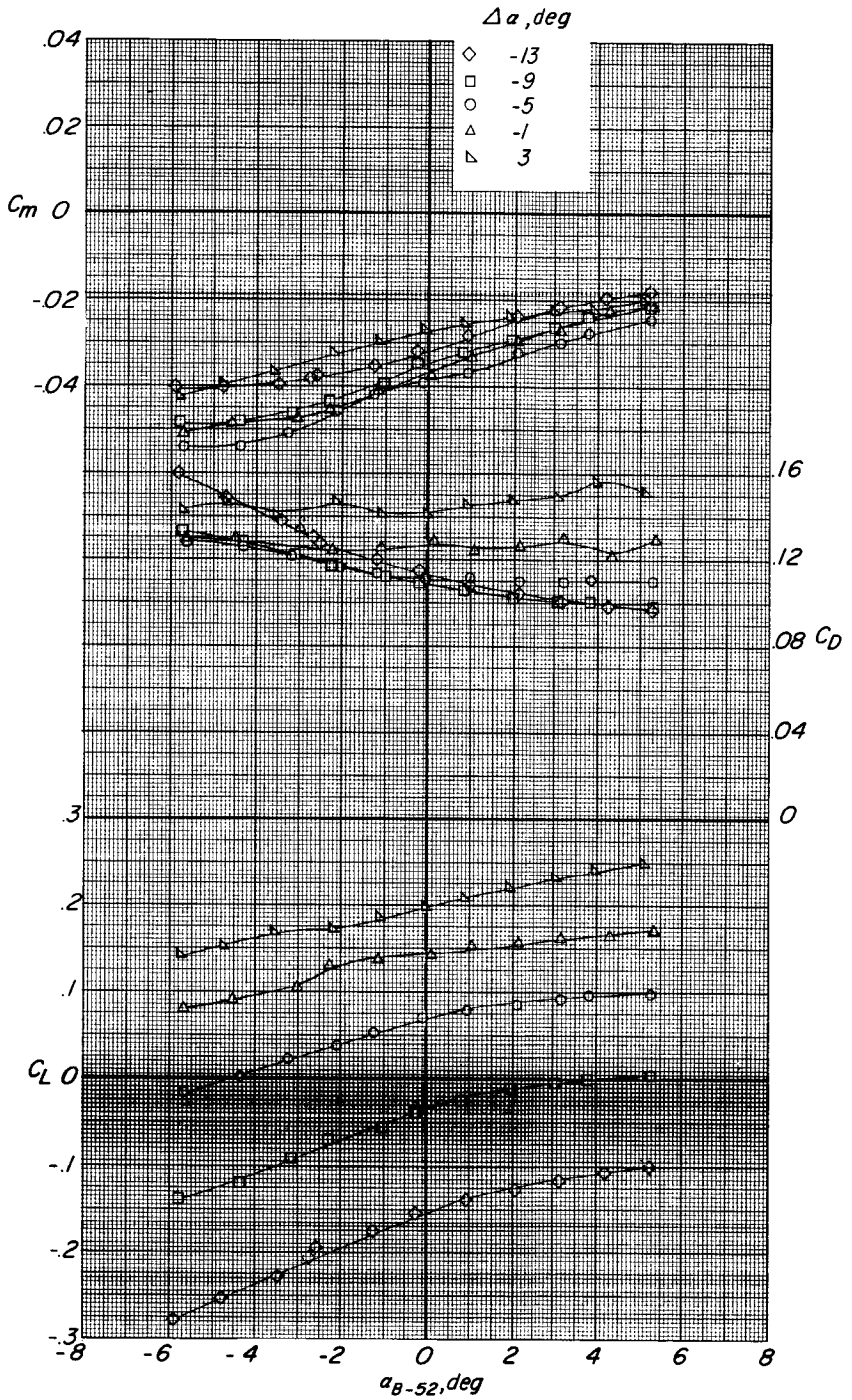

(c) z' = 4.0 feet (1.22 m).

Figure 9.- Continued.

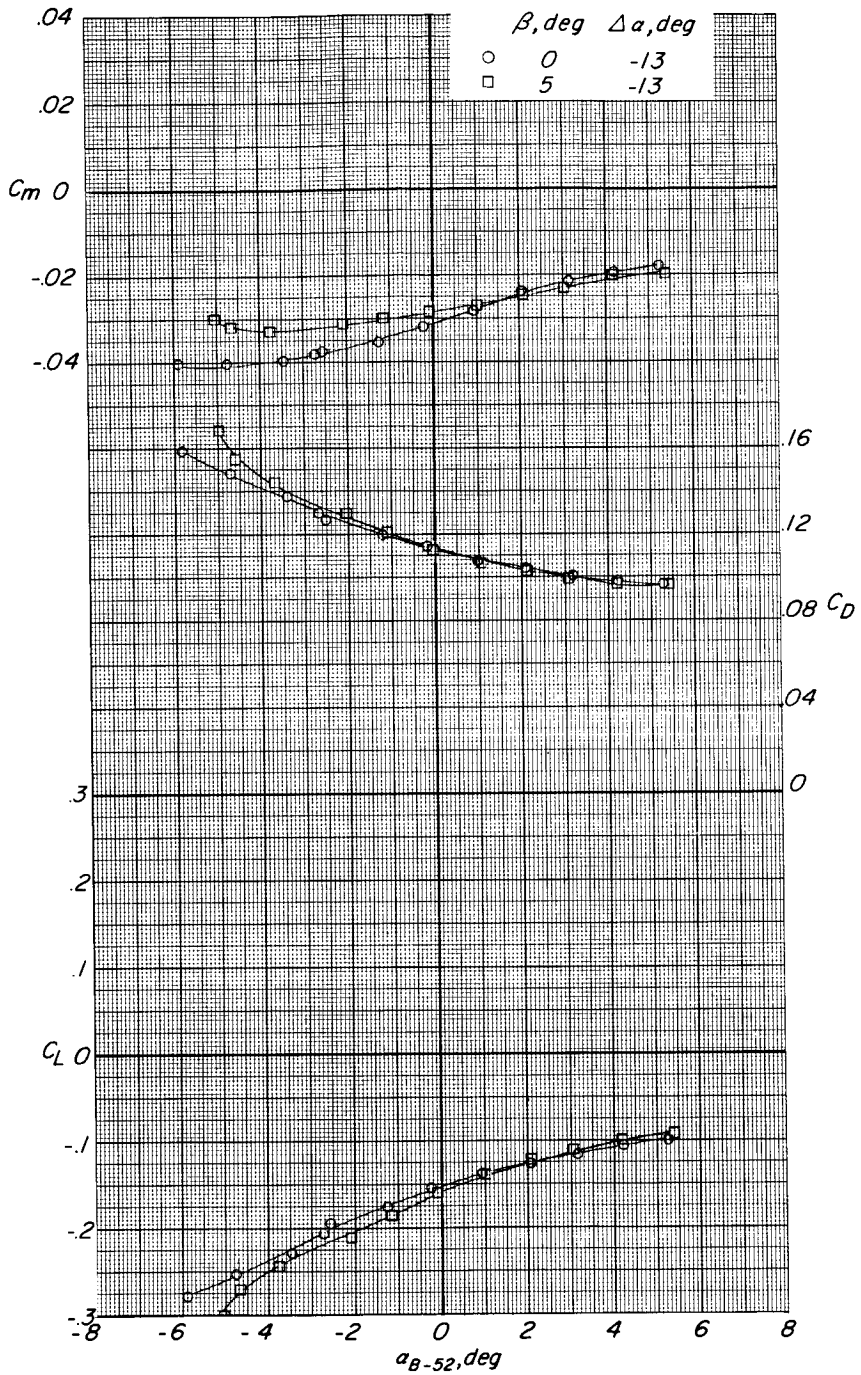

(c) Continued.

Figure 9.- Continued.

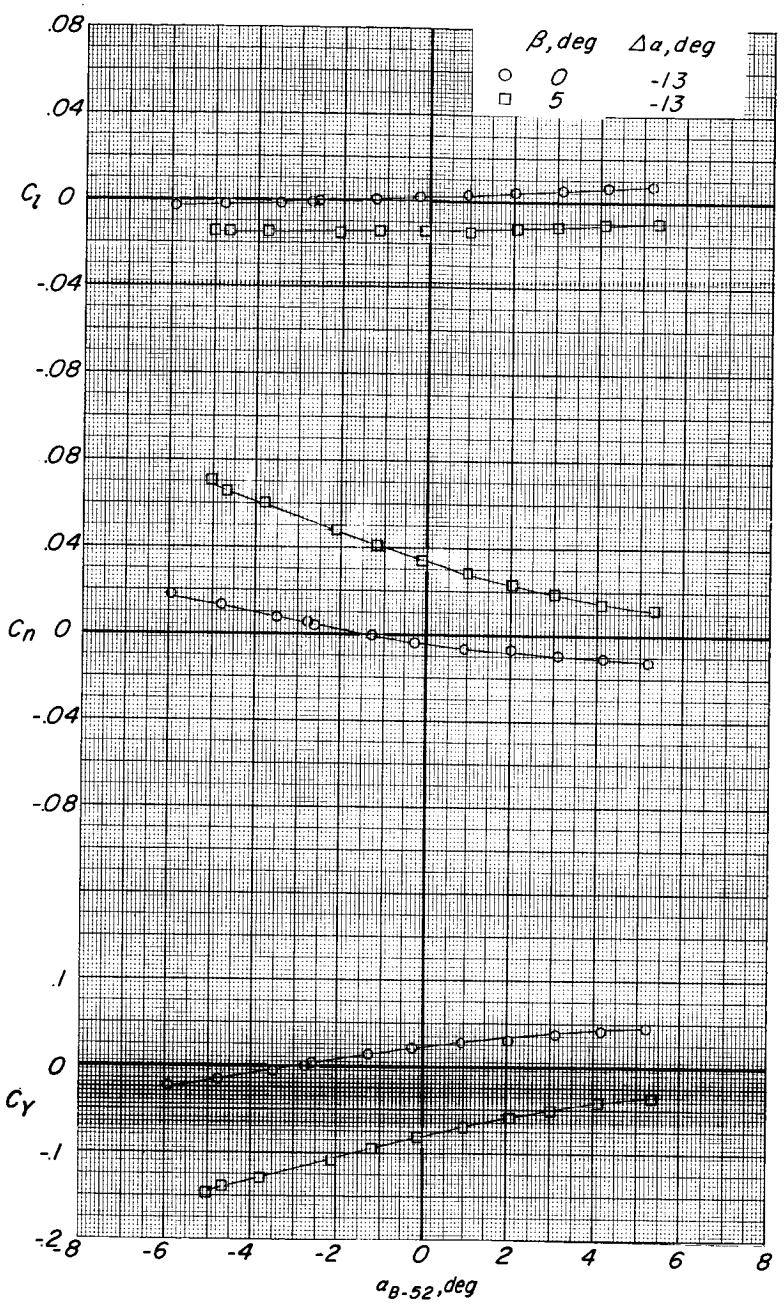

(c) Continued.

Figure 9.- Continued.

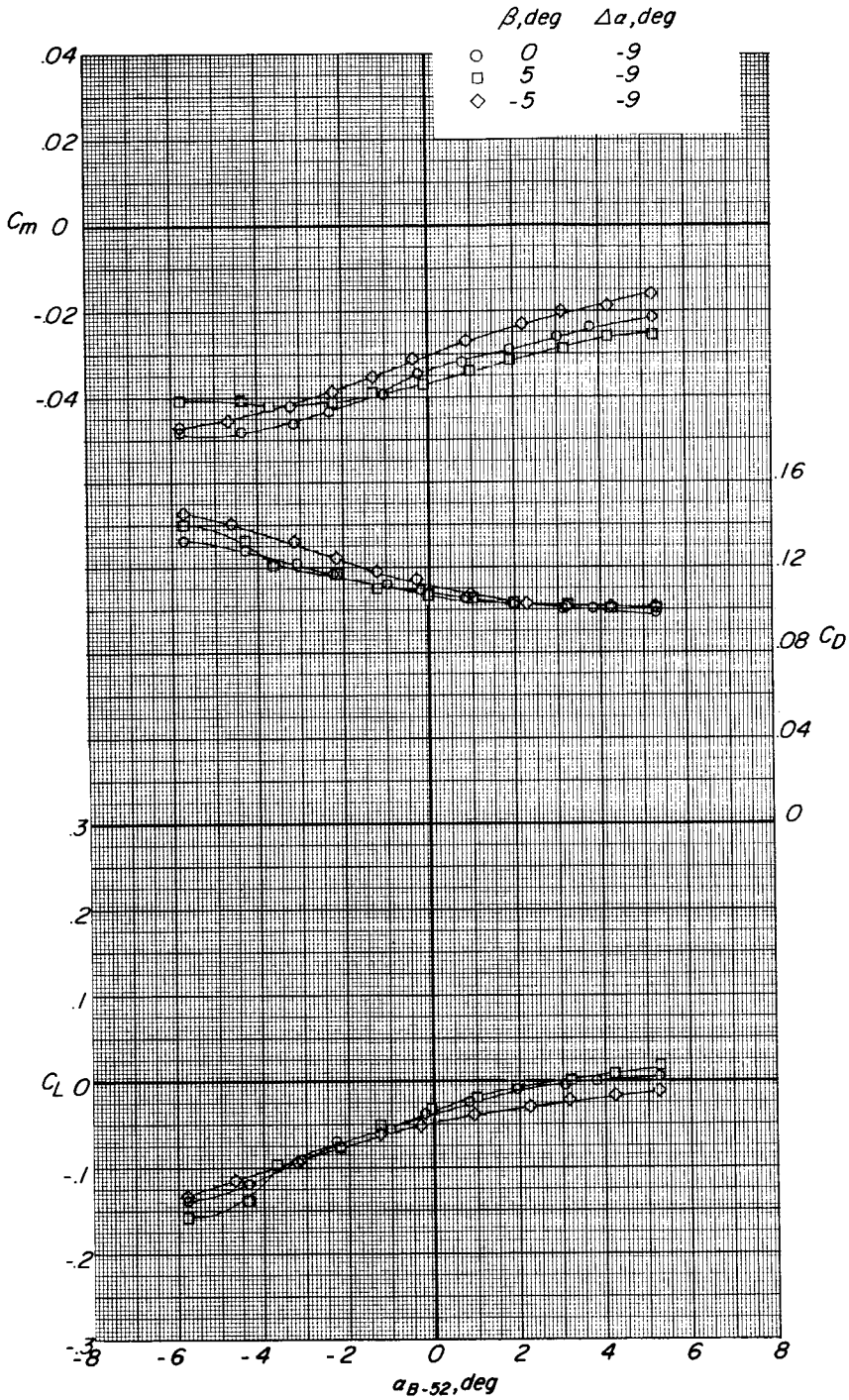

(c) Continued.

Figure 9.- Continued.

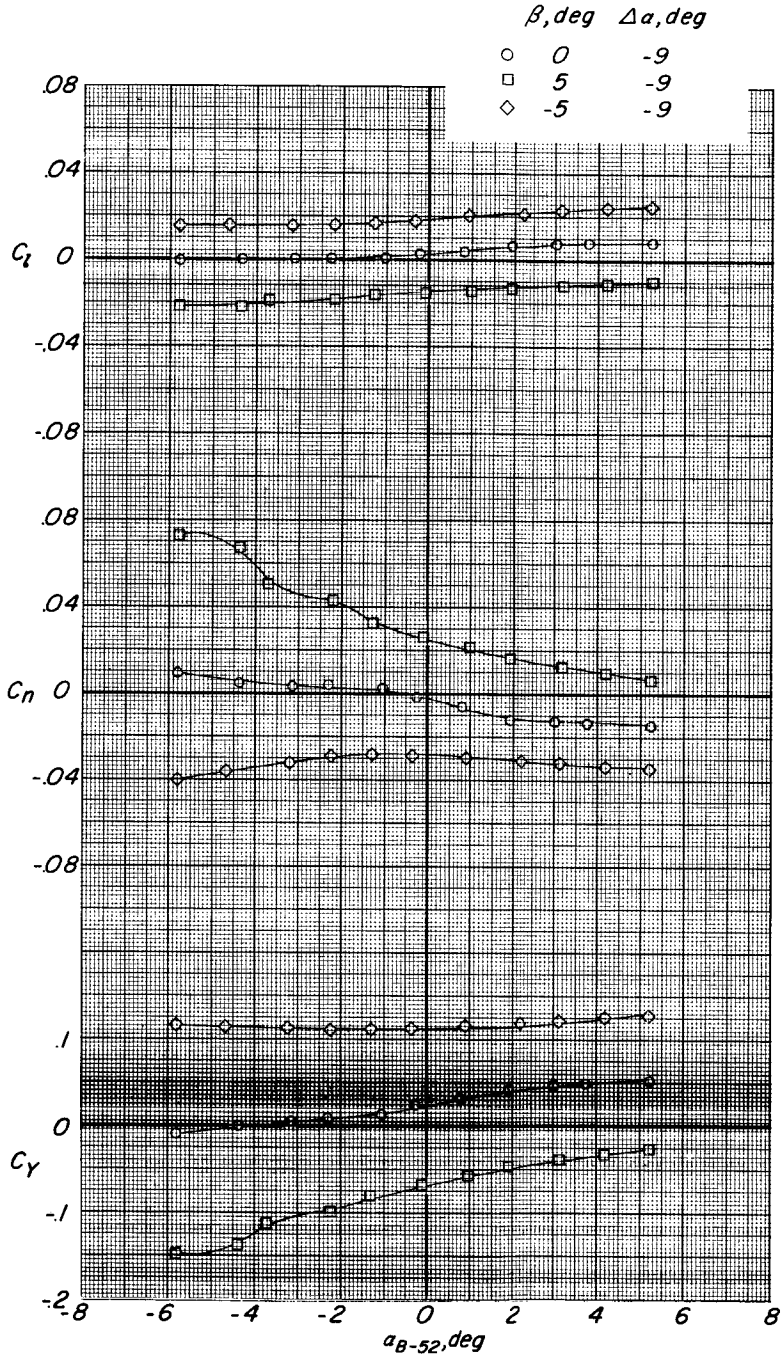

(c) Continued.

Figure 9.- Continued.

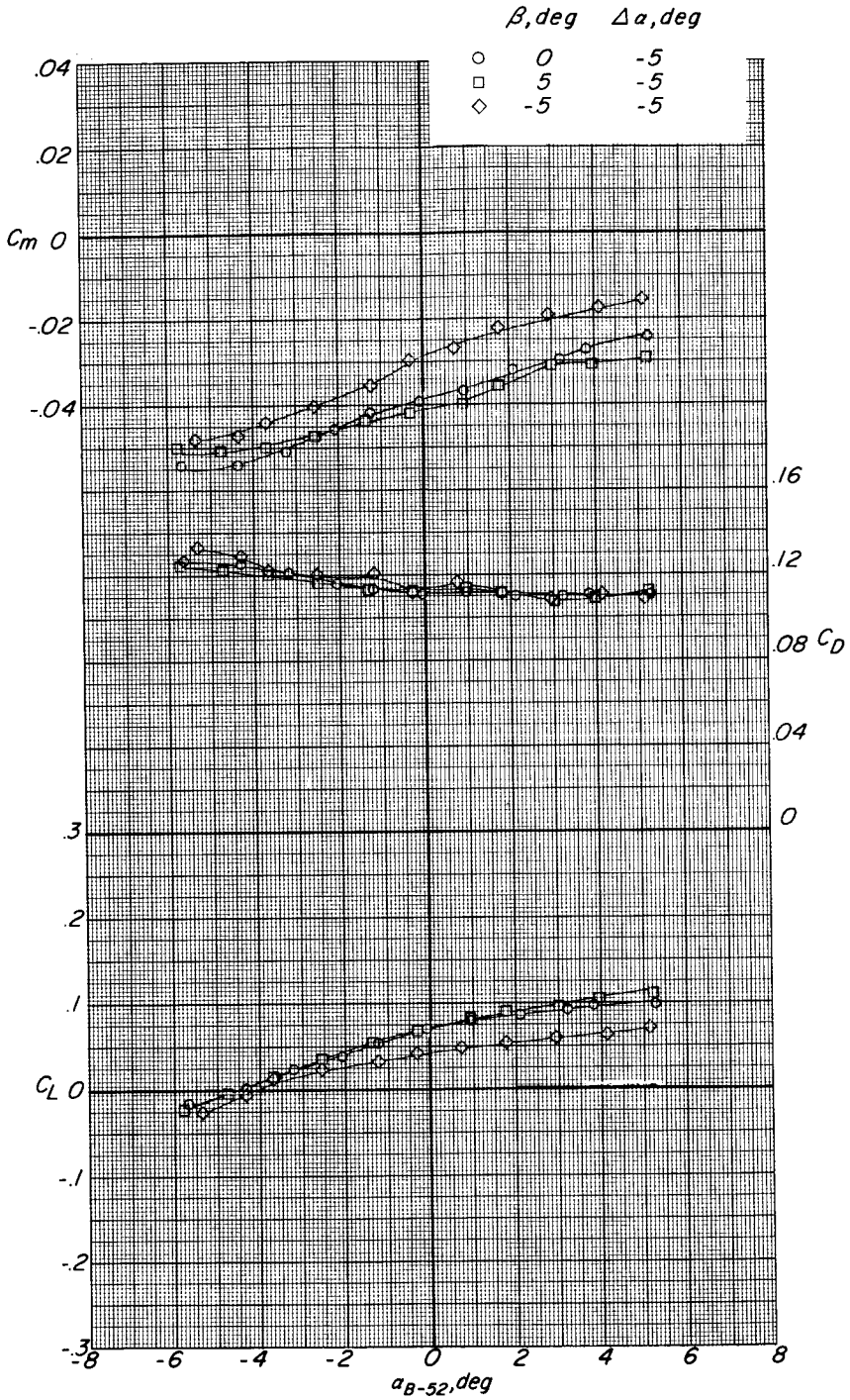

(c) Continued.

Figure 9.- Continued.

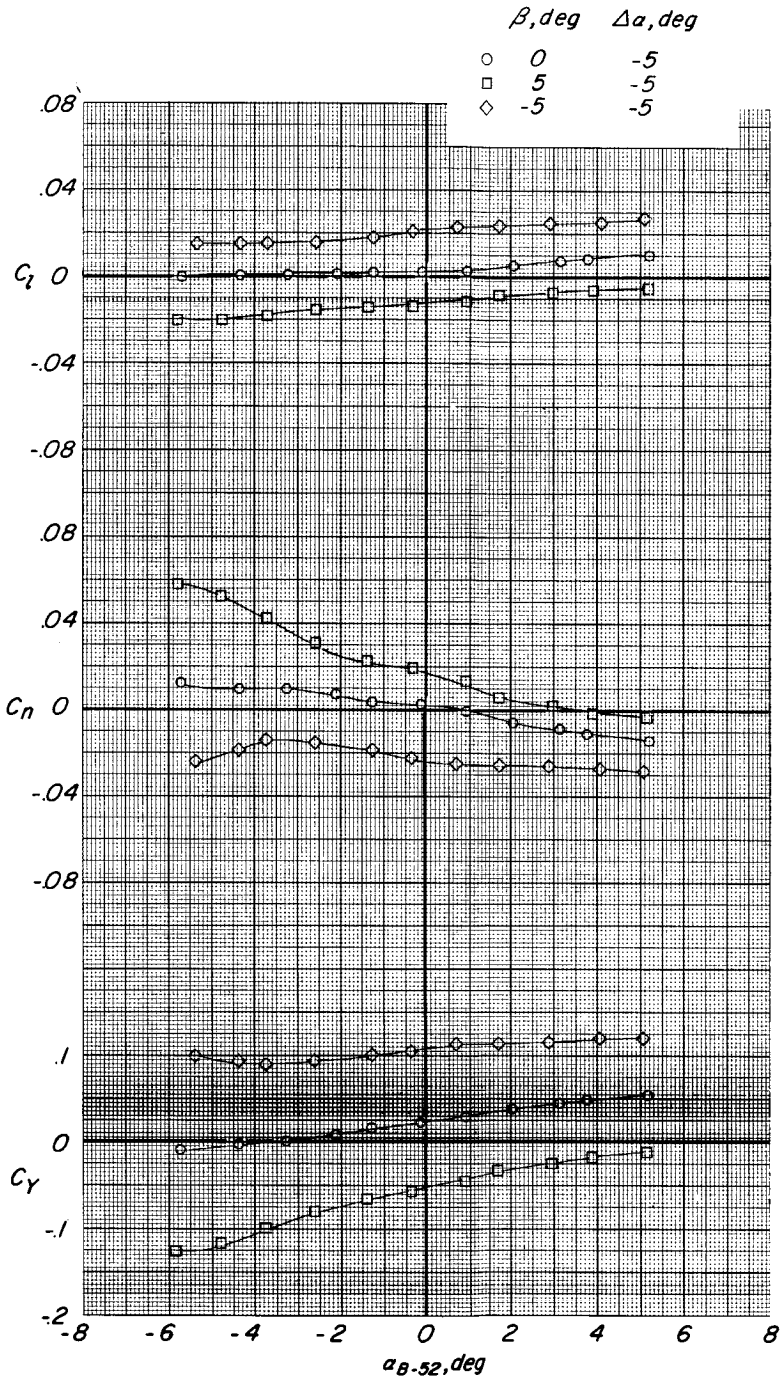

(c) Continued.

Figure 9.- Continued.

[redacted]

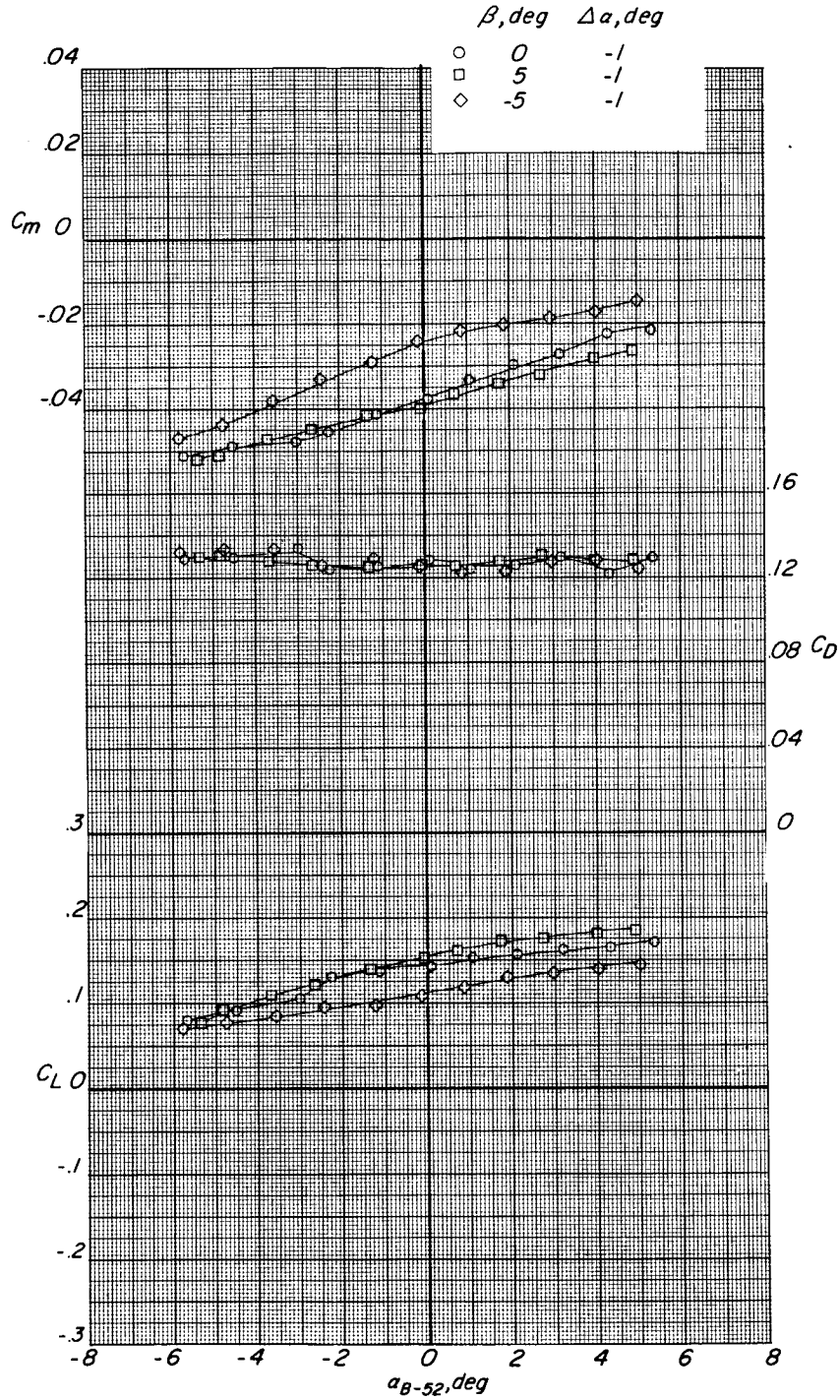

(c) Continued.

Figure 9.- Continued.

[redacted]

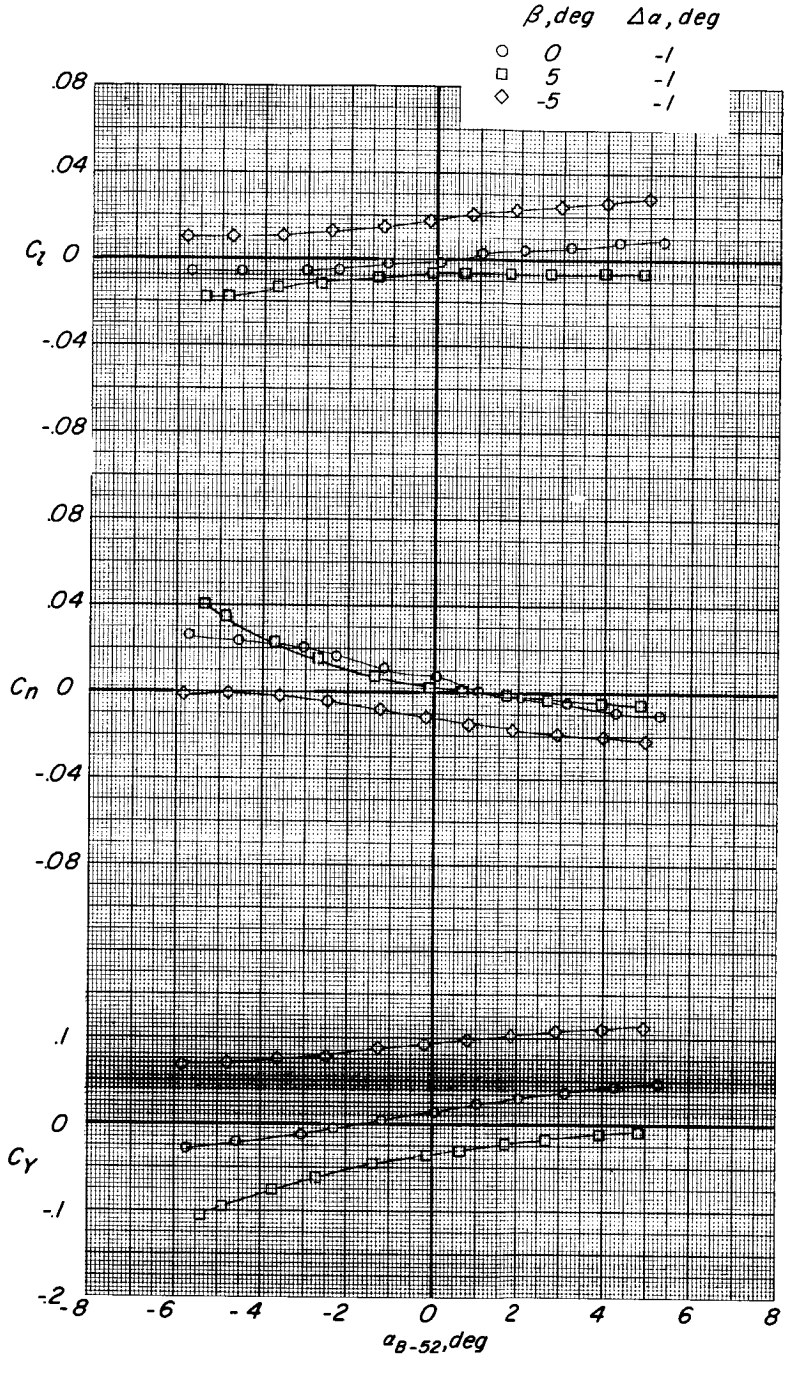

(c) Continued.

Figure 9.- Continued.

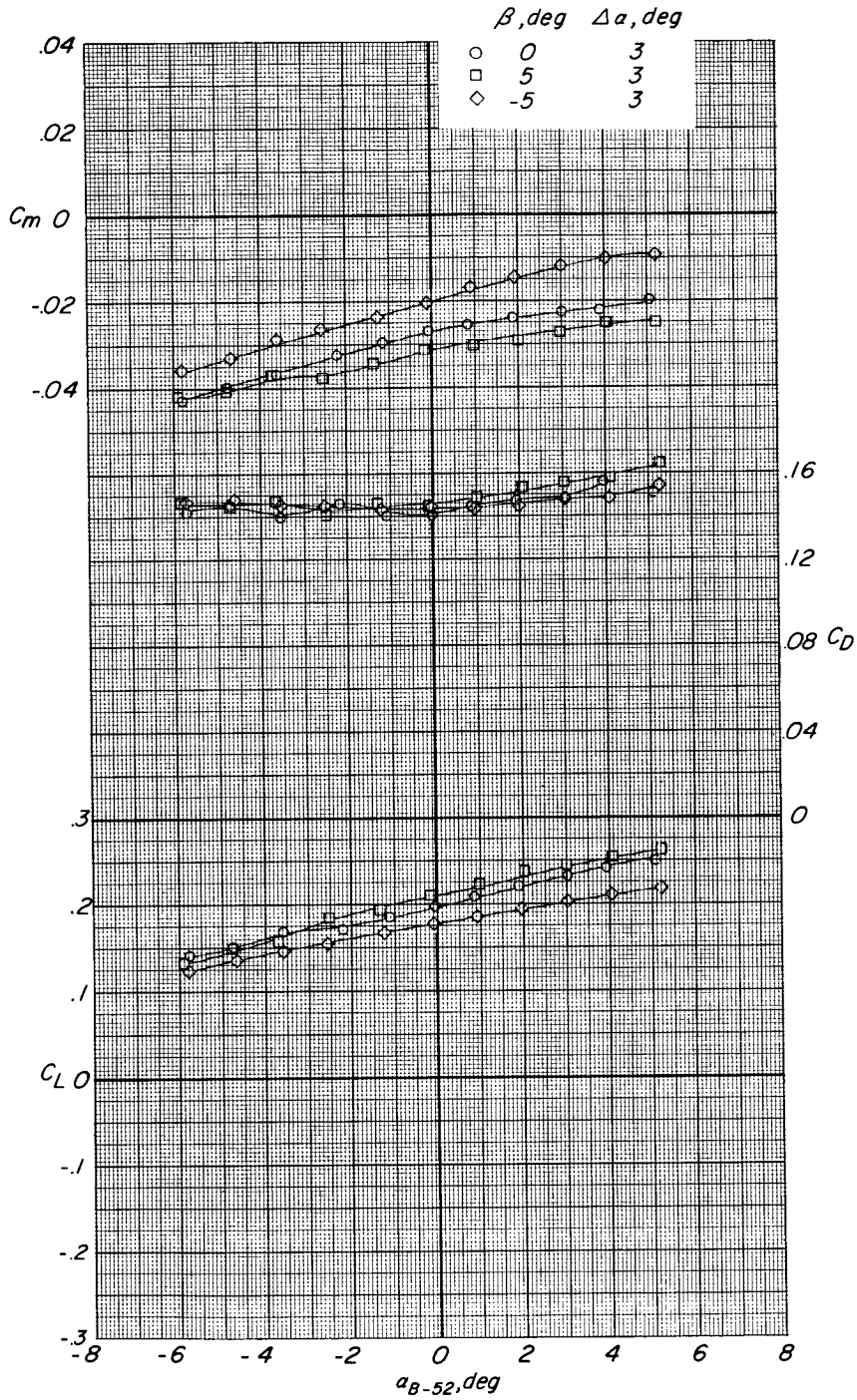

(c) Continued.

Figure 9.- Continued.

[redacted] UNCLASSIFIED

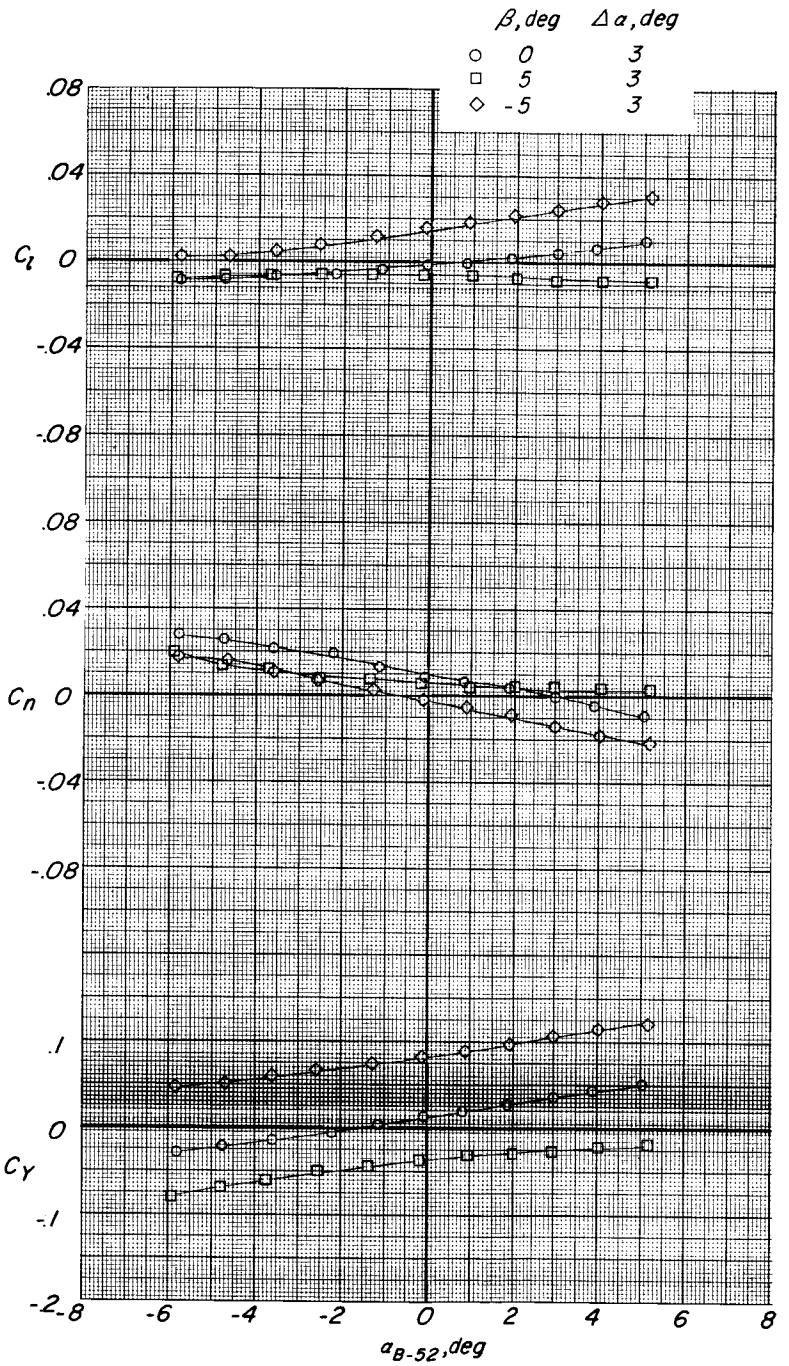

(c) Concluded.

Figure 9.- Continued.

[redacted]

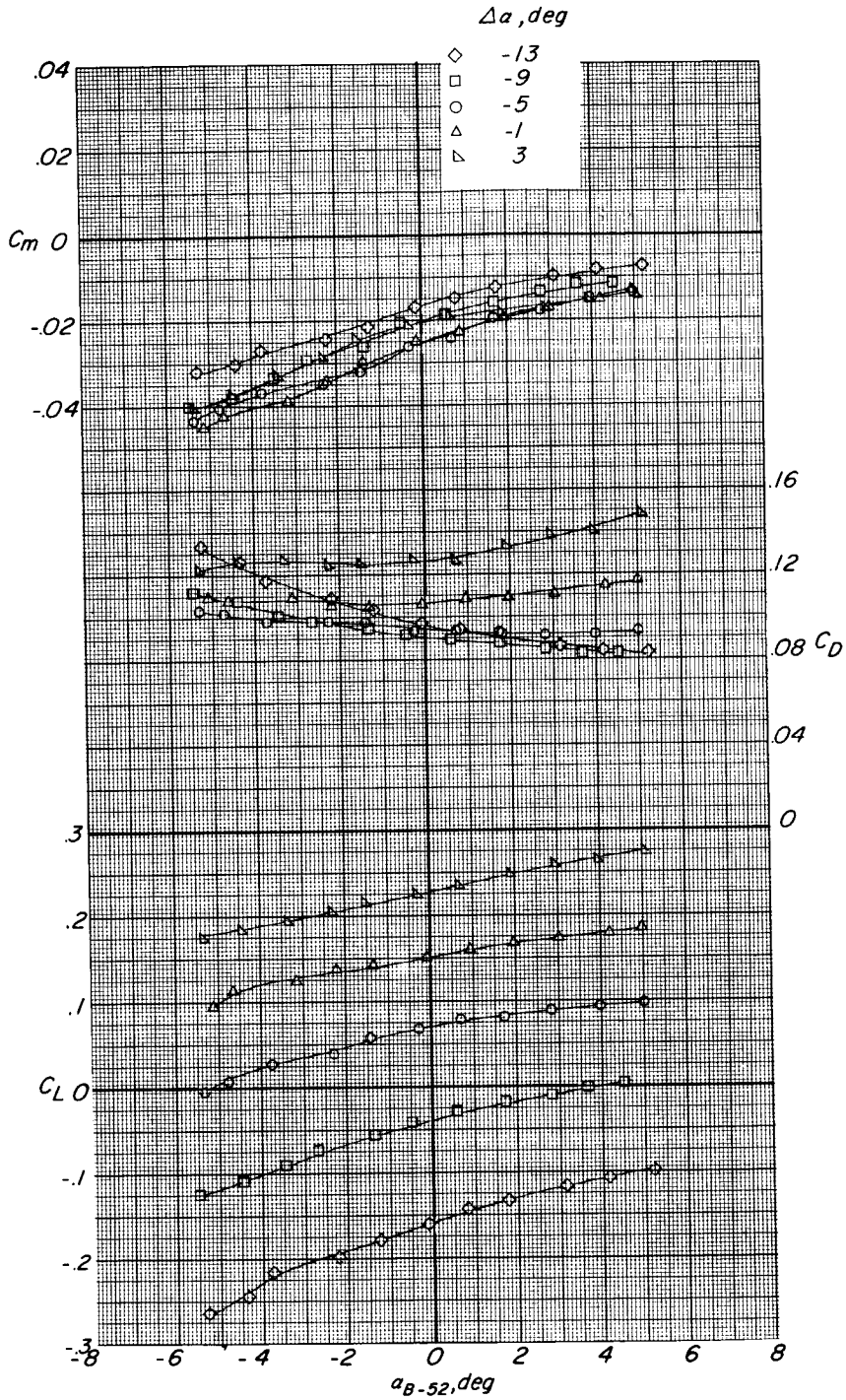

(d) z' = 8.0 feet (2.44 m).

Figure 9.- Continued.

[redacted] DECLASSIFIED

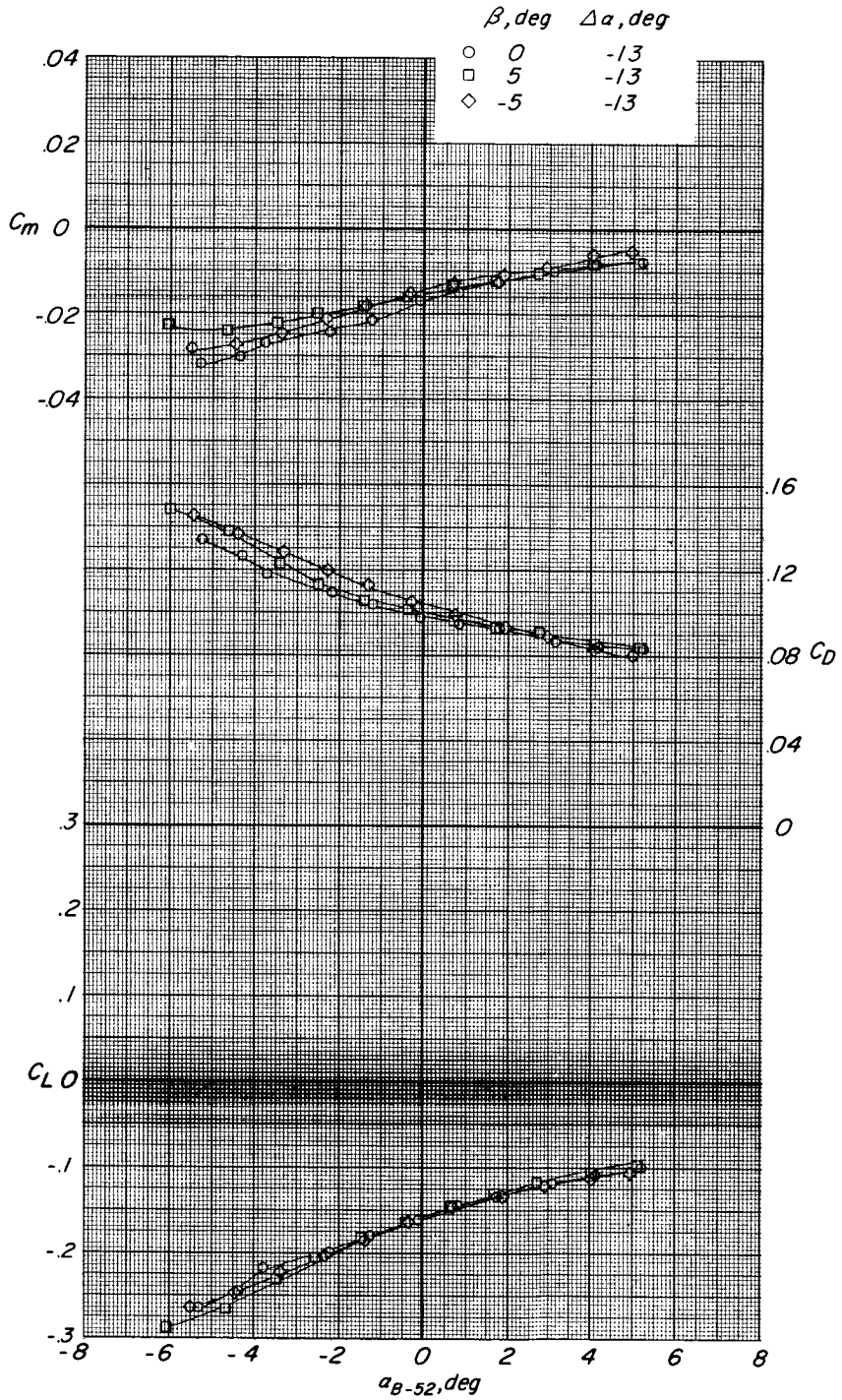

(d) Continued.

Figure 9.- Continued.

[redacted]

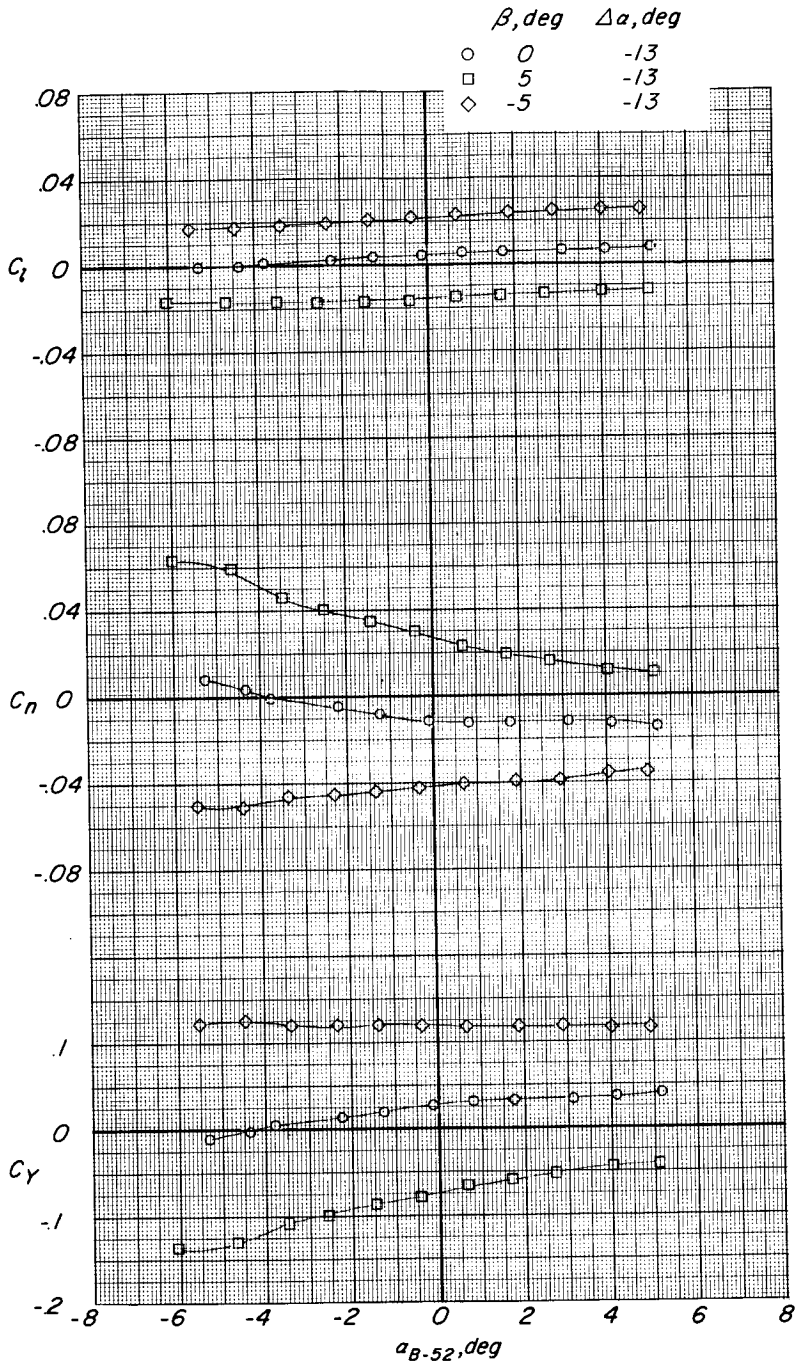

(d) Continued.

Figure 9.- Continued.

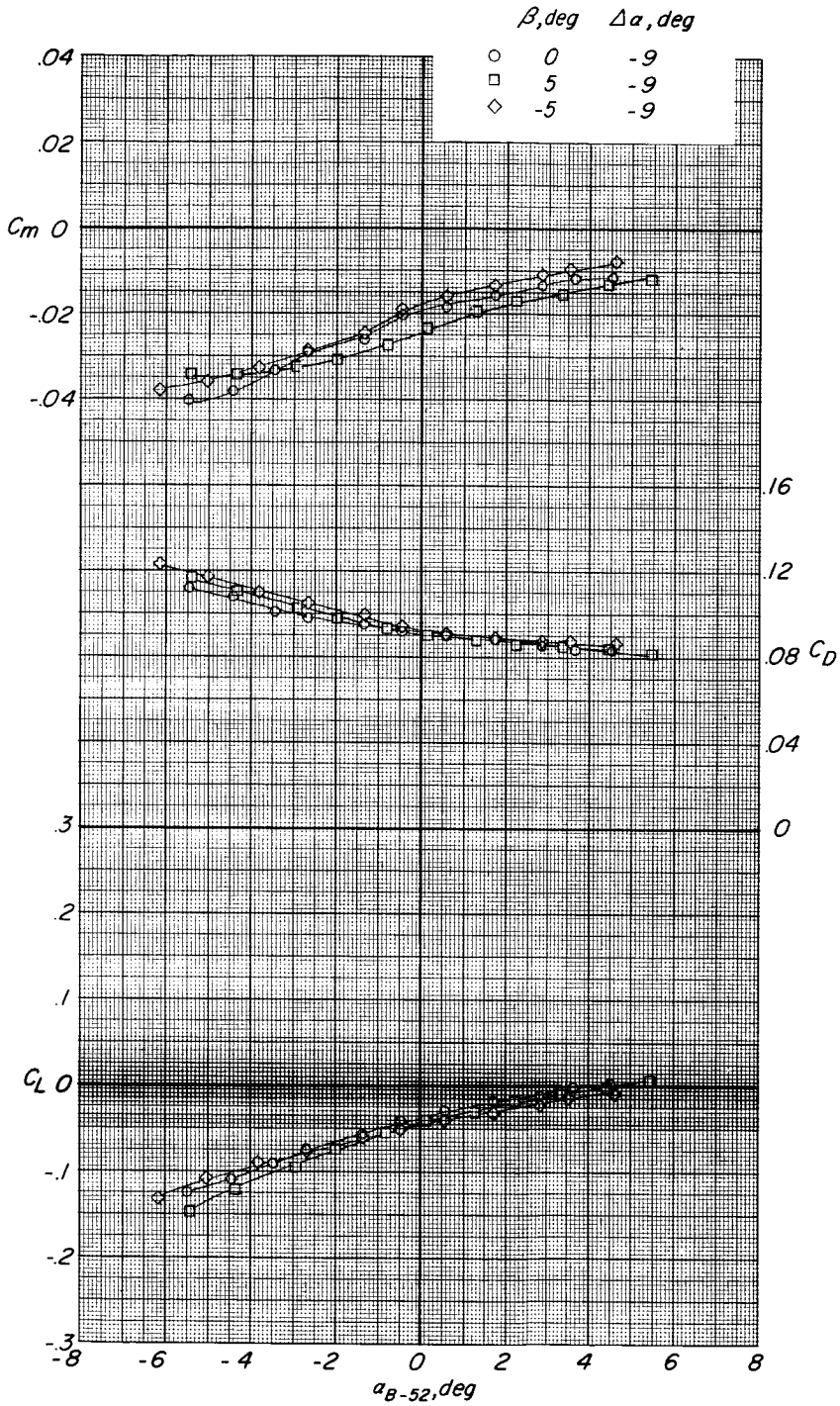

(d) Continued.

Figure 9.- Continued.

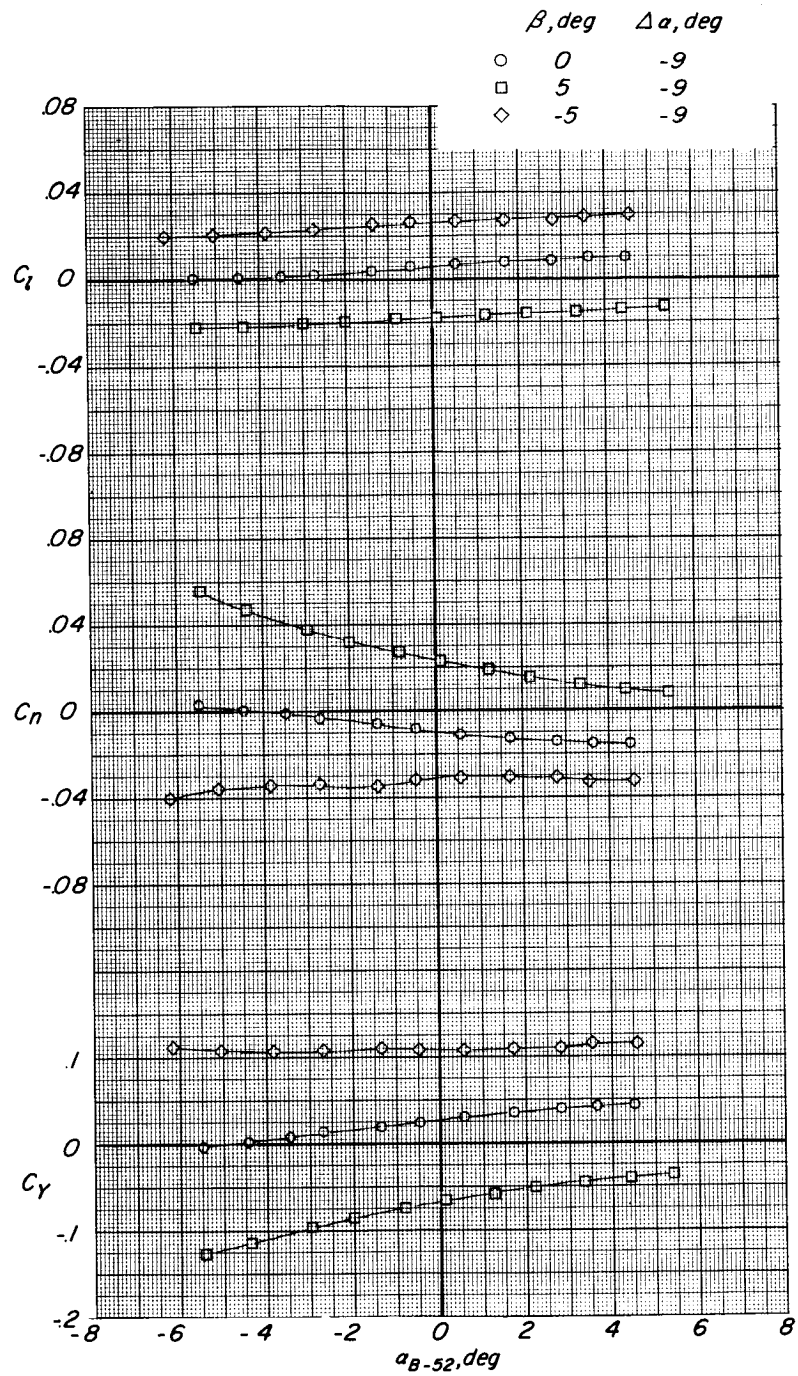

(d) Continued.

Figure 9.- Continued.

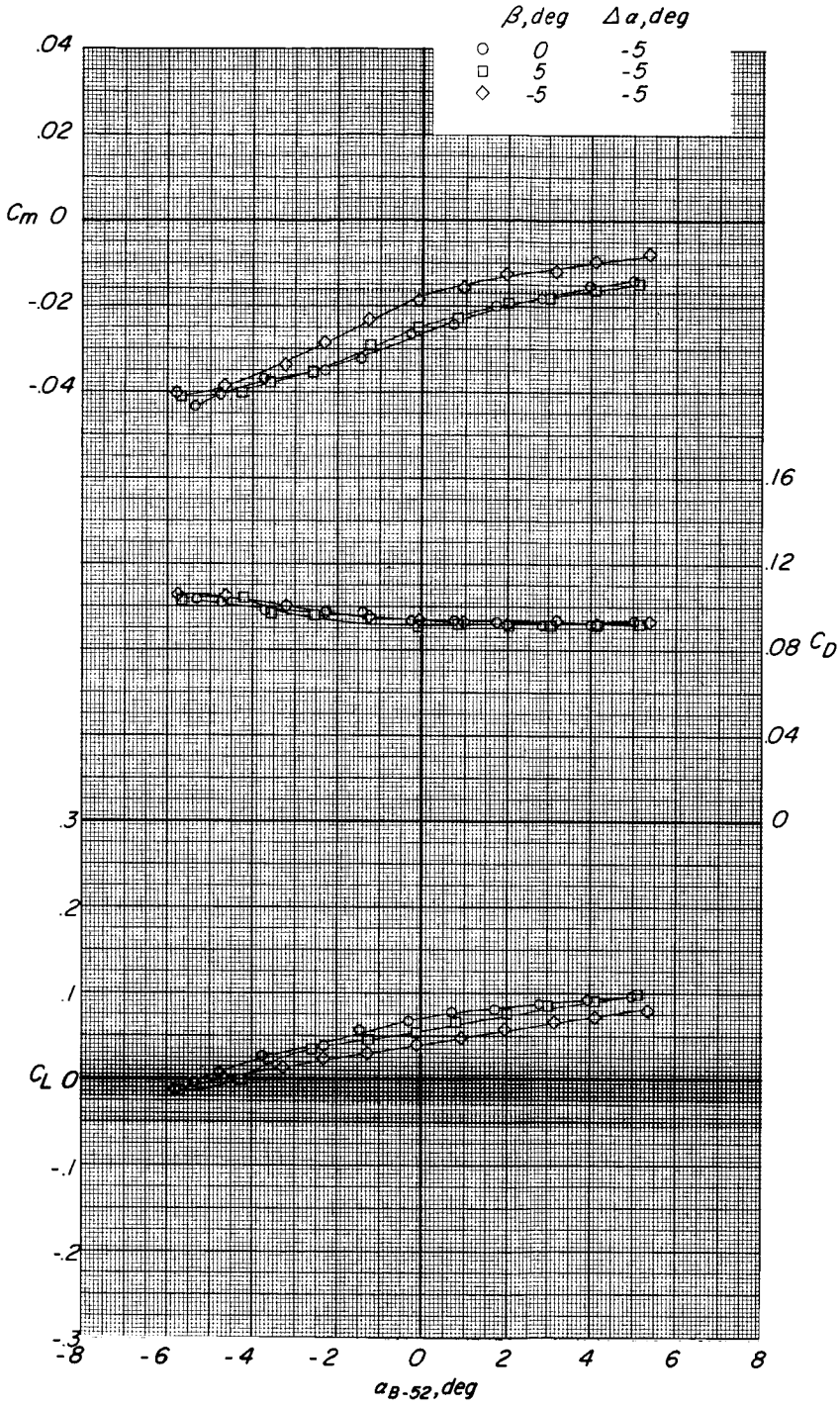

(d) Continued.

Figure 9.- Continued.

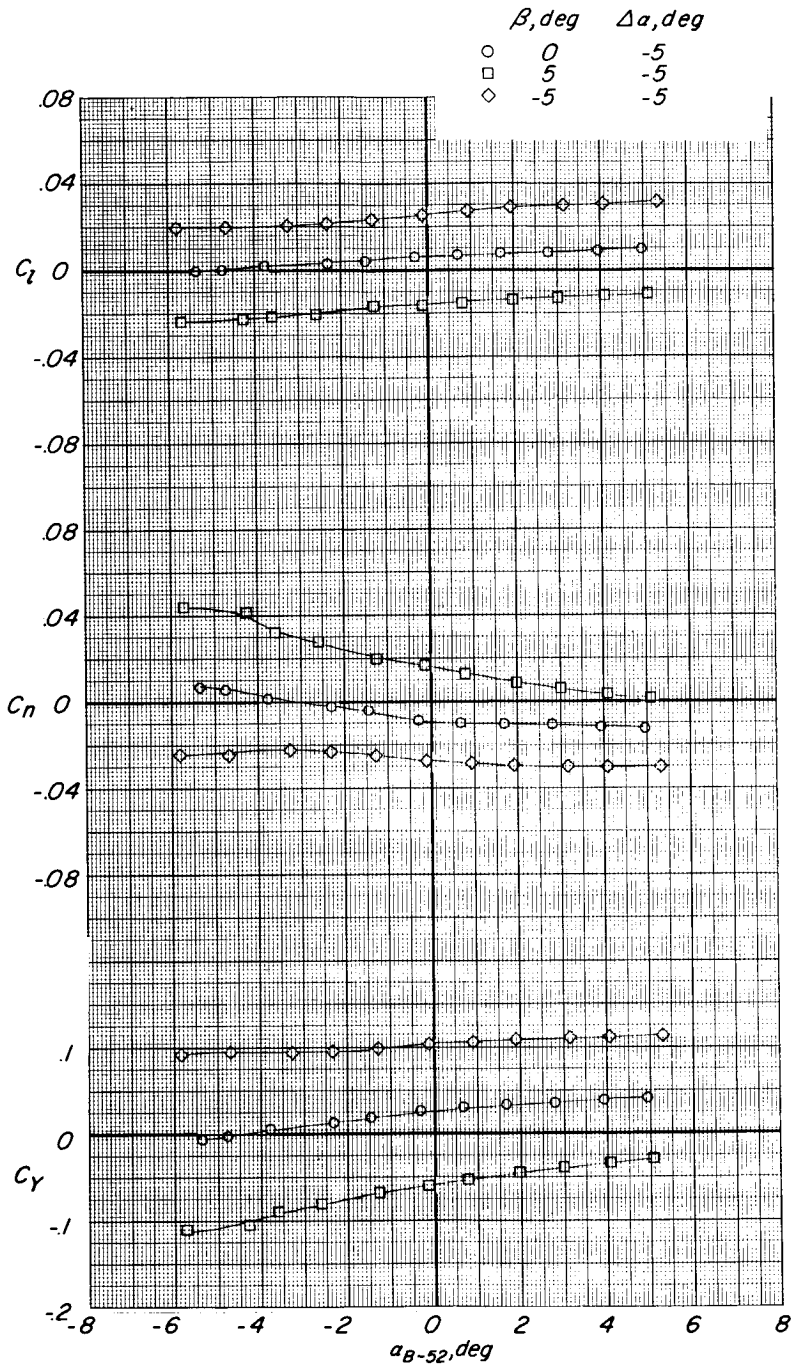

(d) Continued.

Figure 9.- Continued.

[redacted] DECLASSIFIED

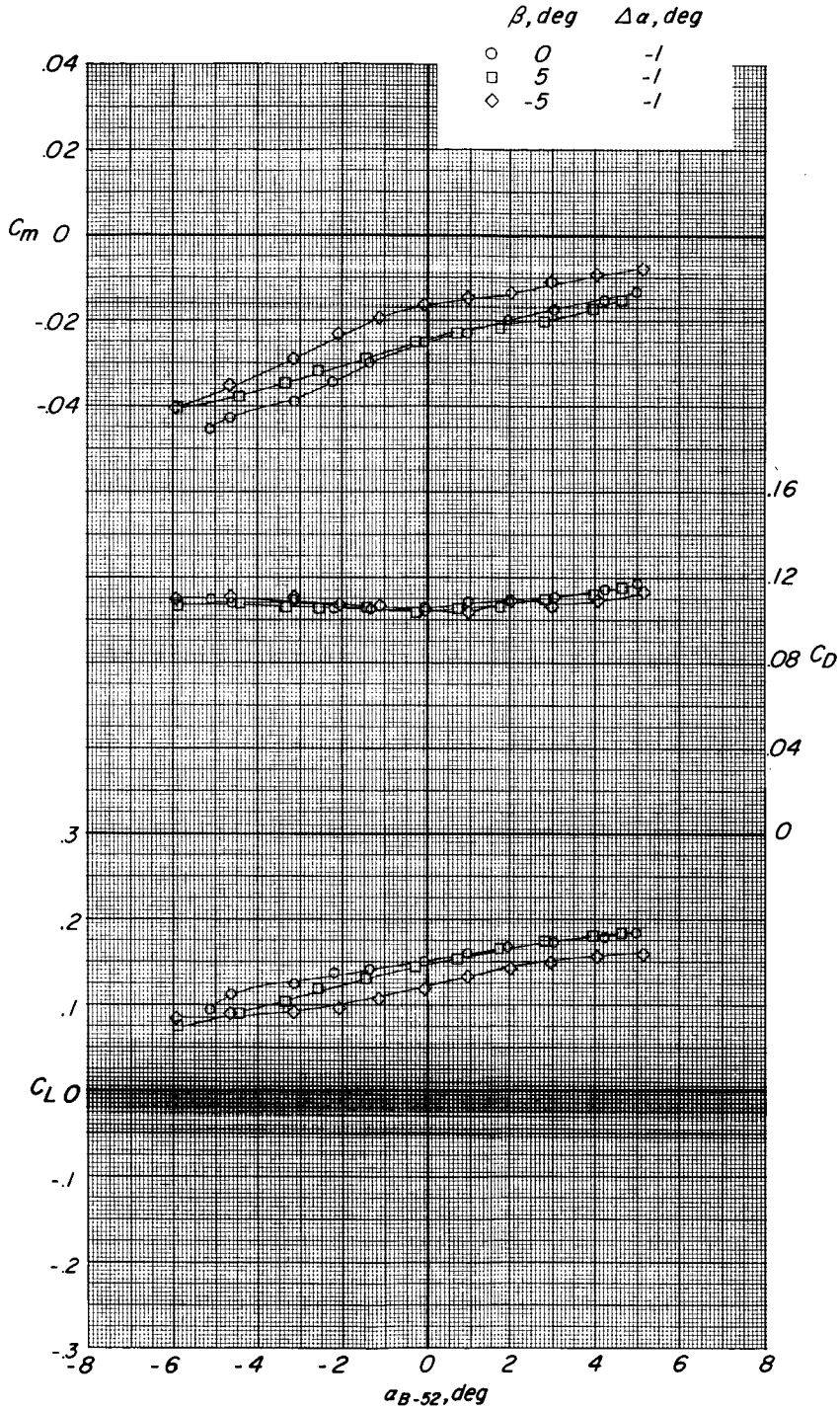

(d) Continued.

Figure 9.- Continued.

[redacted]

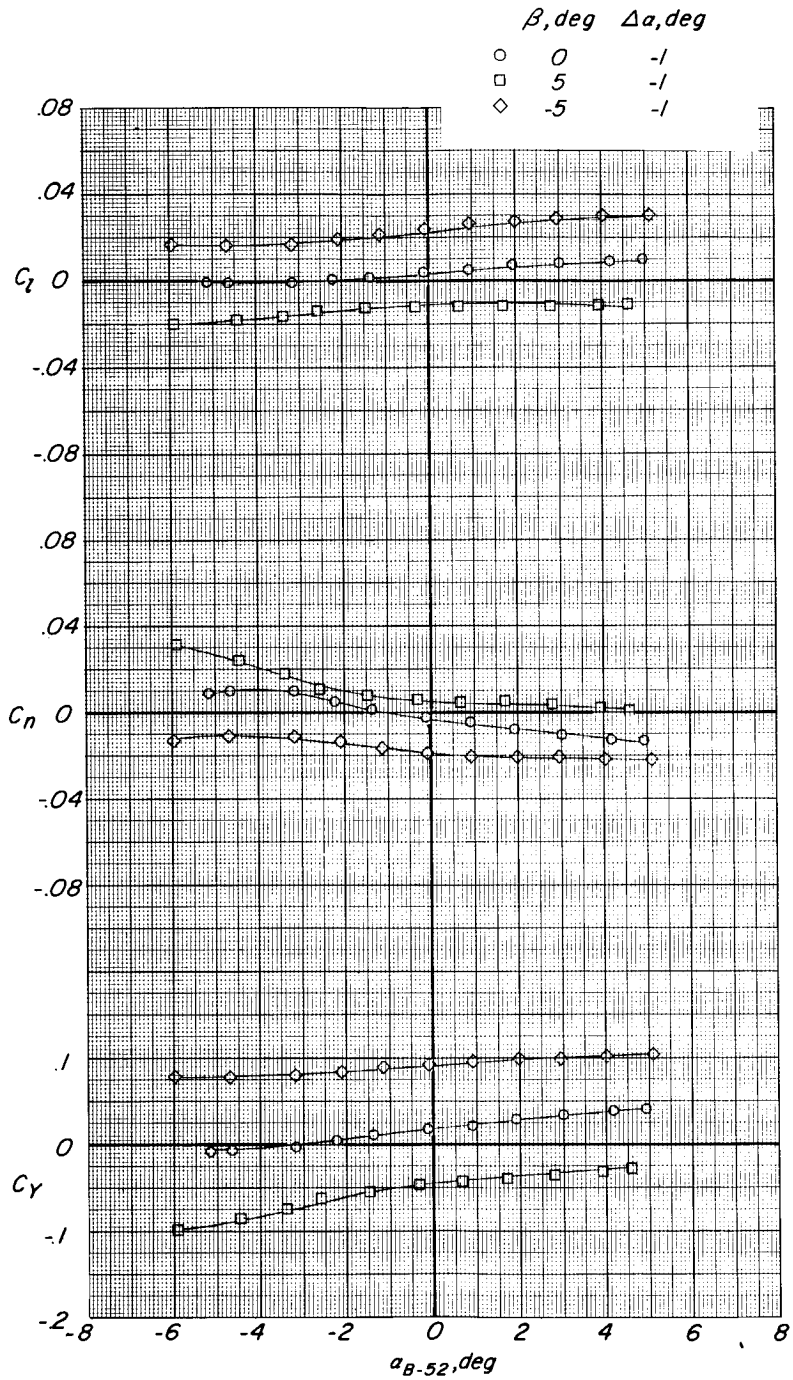

(d) Continued.

Figure 9.- Continued.

DECLASSIFIED

[redacted]

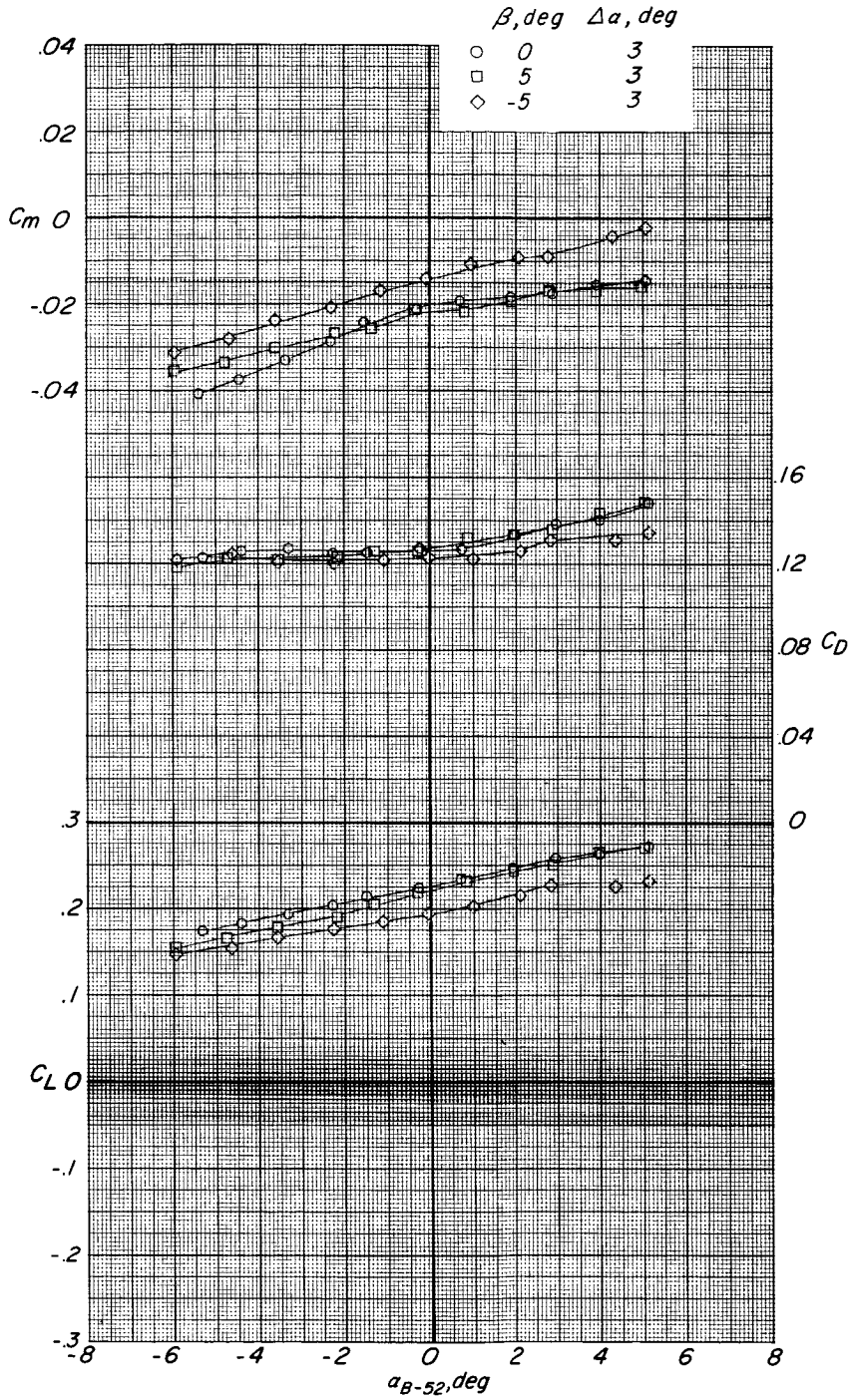

(d) Continued.

Figure 9.- Continued.

[redacted]

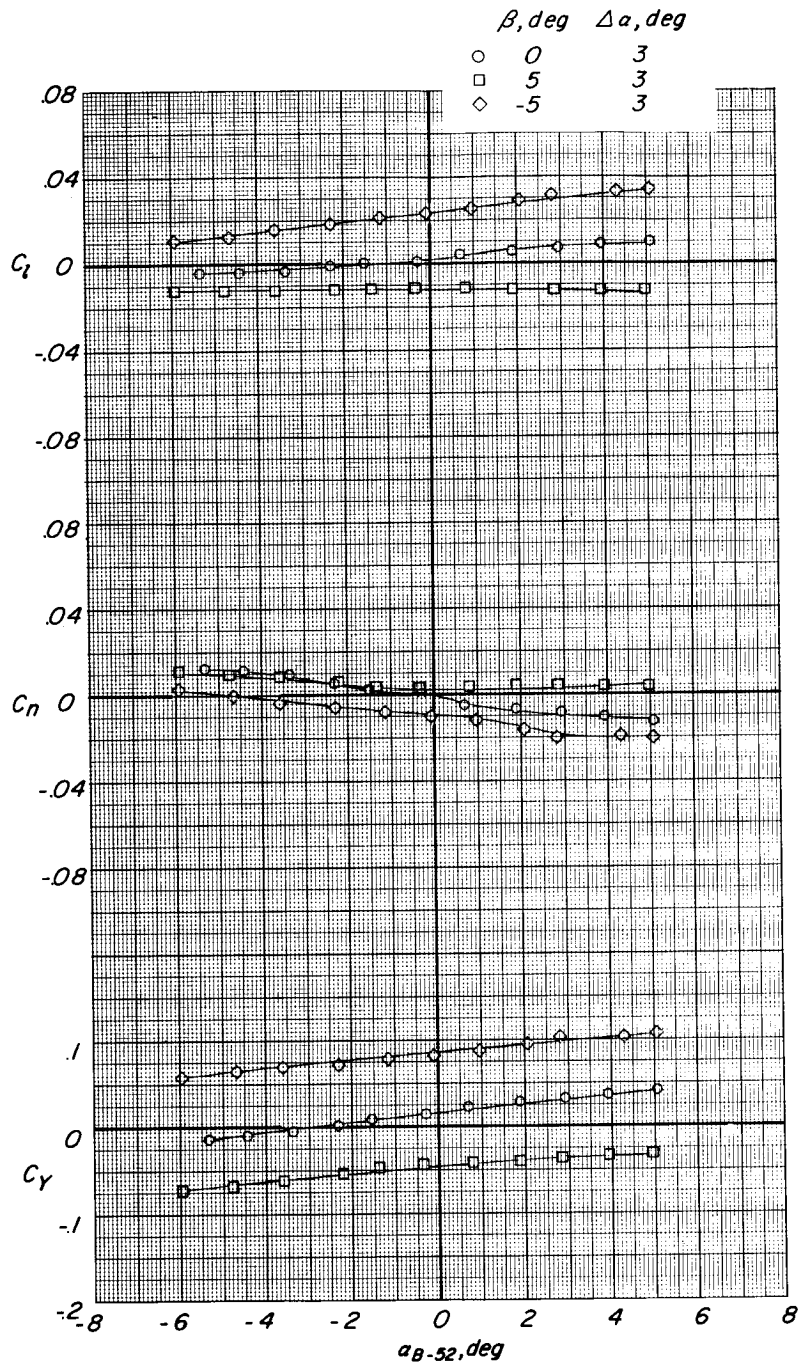

(d) Concluded.

Figure 9.- Continued.

DECLASSIFIED

[redacted]

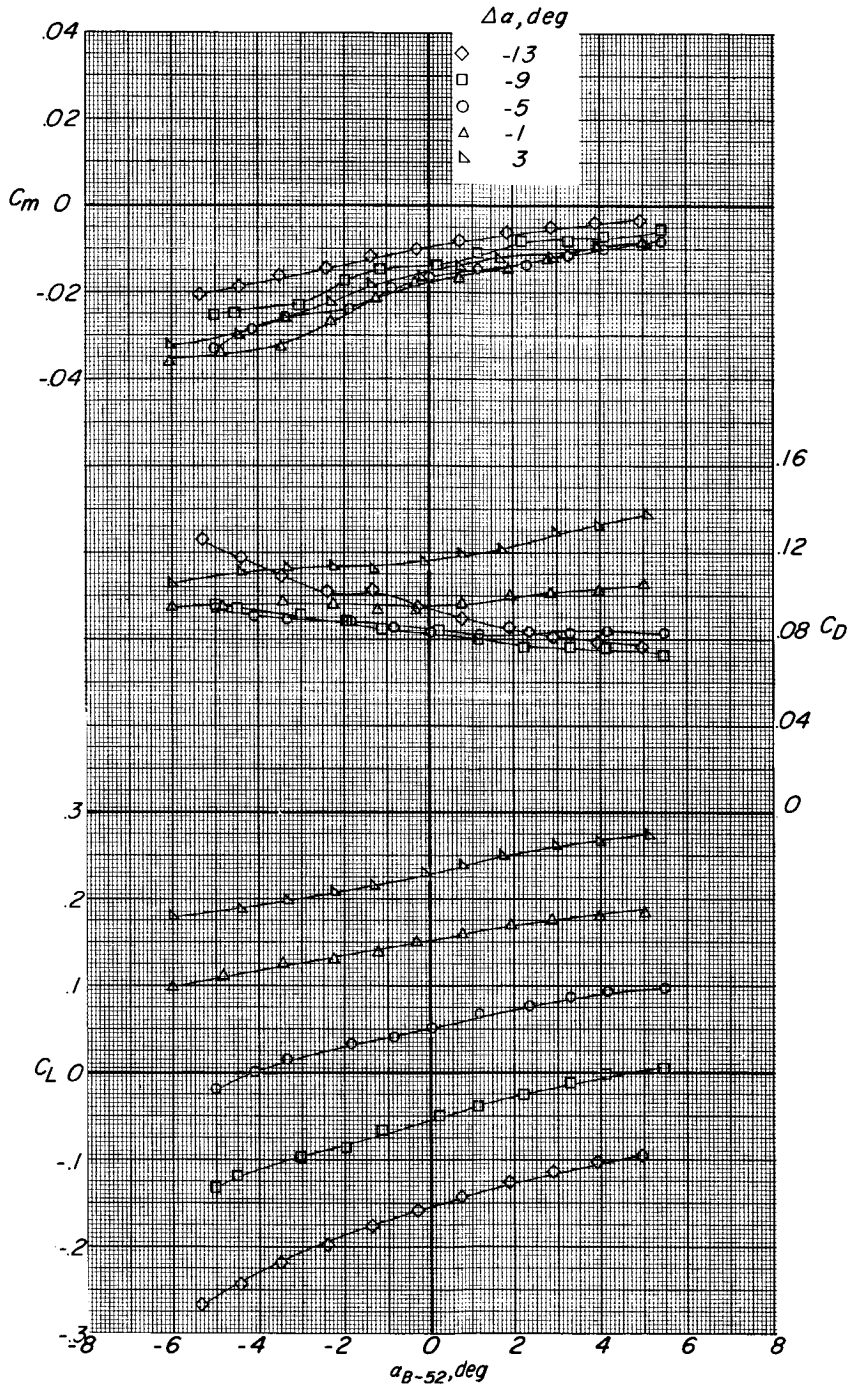

(e) z' = 12.0 feet (3.66 m).

Figure 9.- Continued.

[redacted]

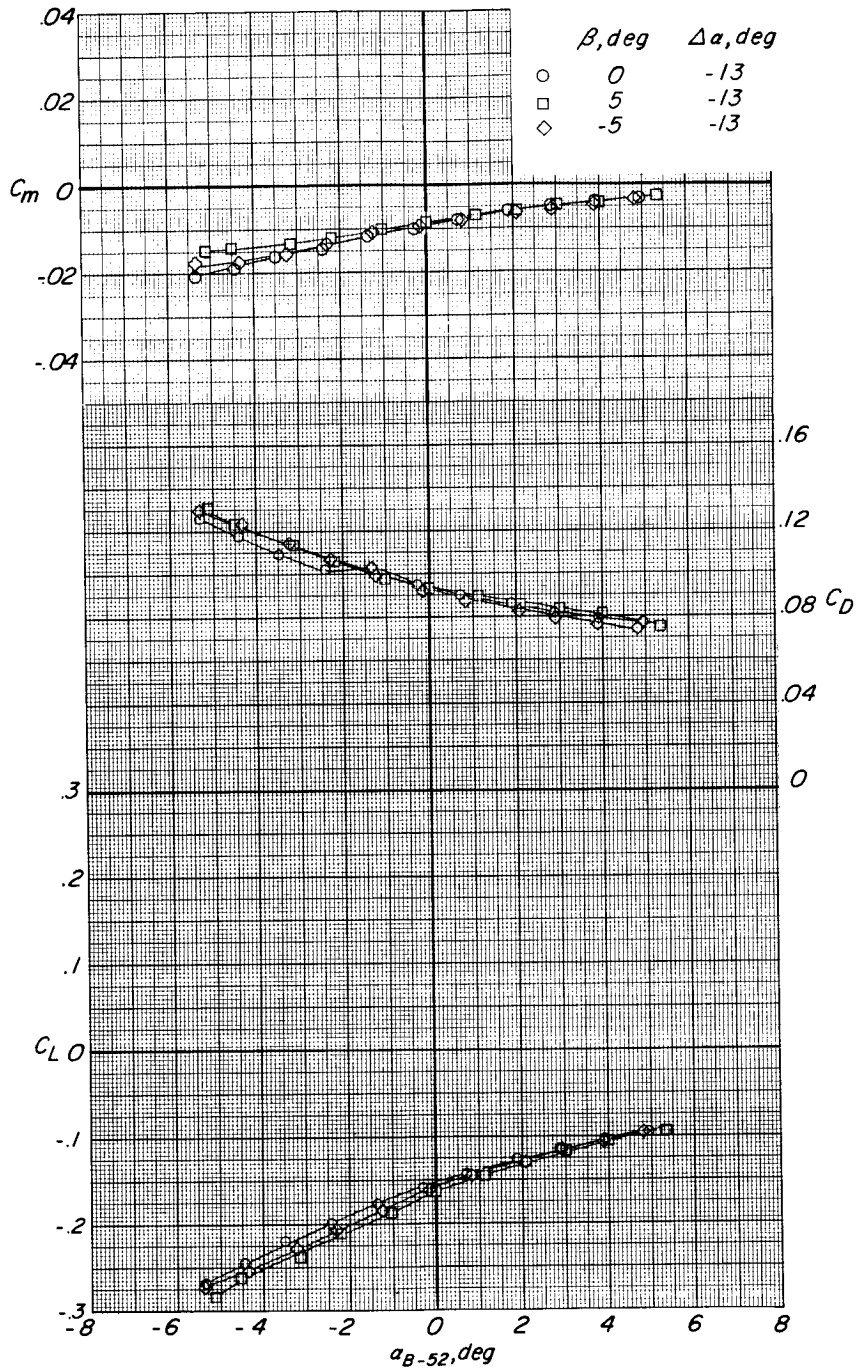

(e) Continued.

Figure 9.- Continued.

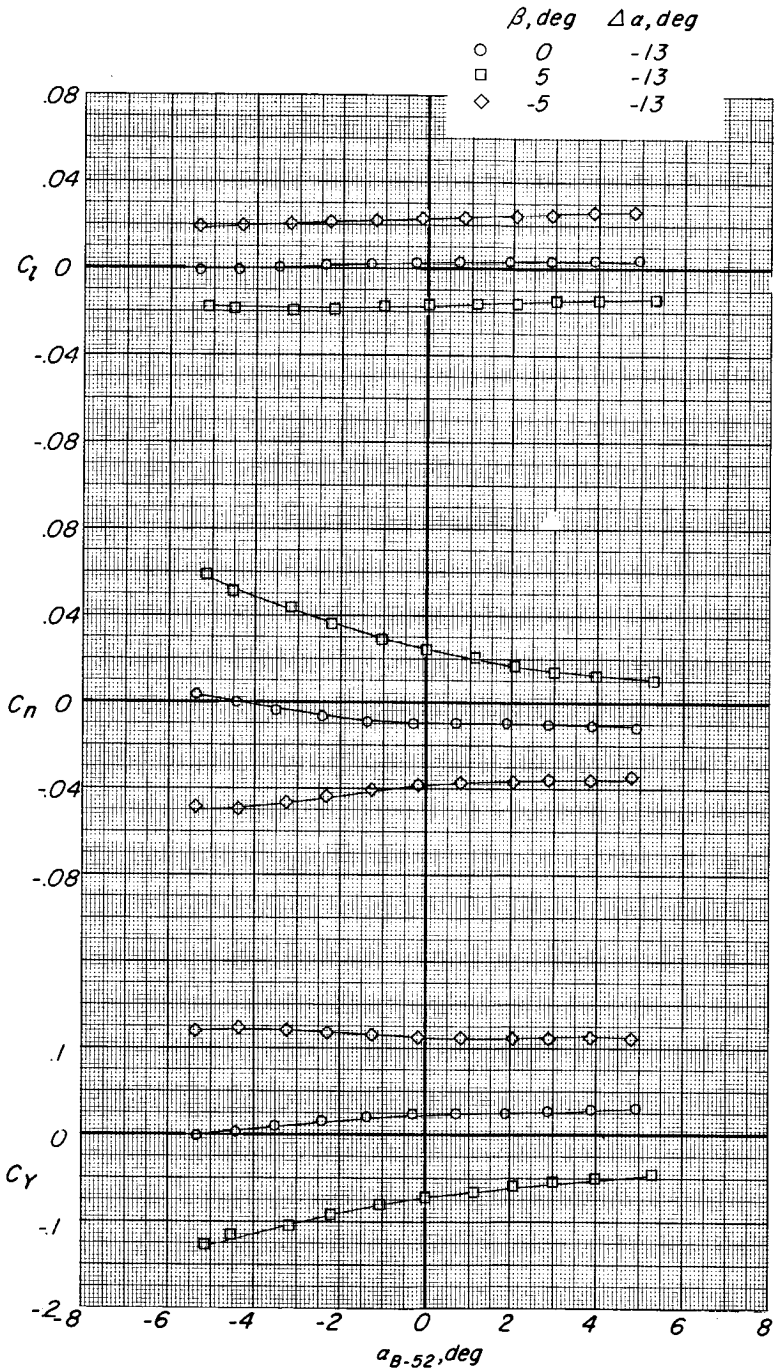

(e) Continued.

Figure 9.- Continued.

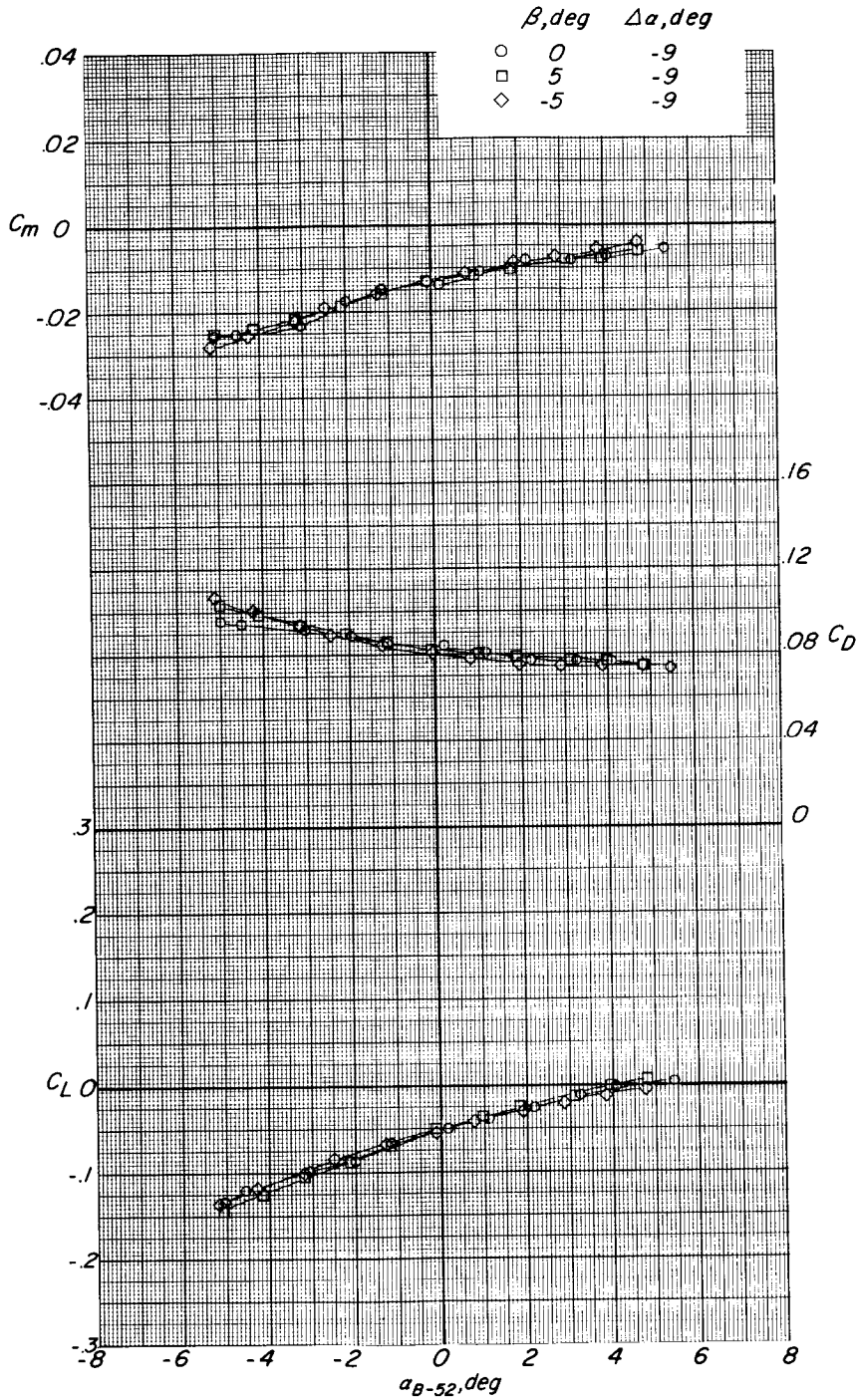

(e) Continued.

Figure 9.- Continued.

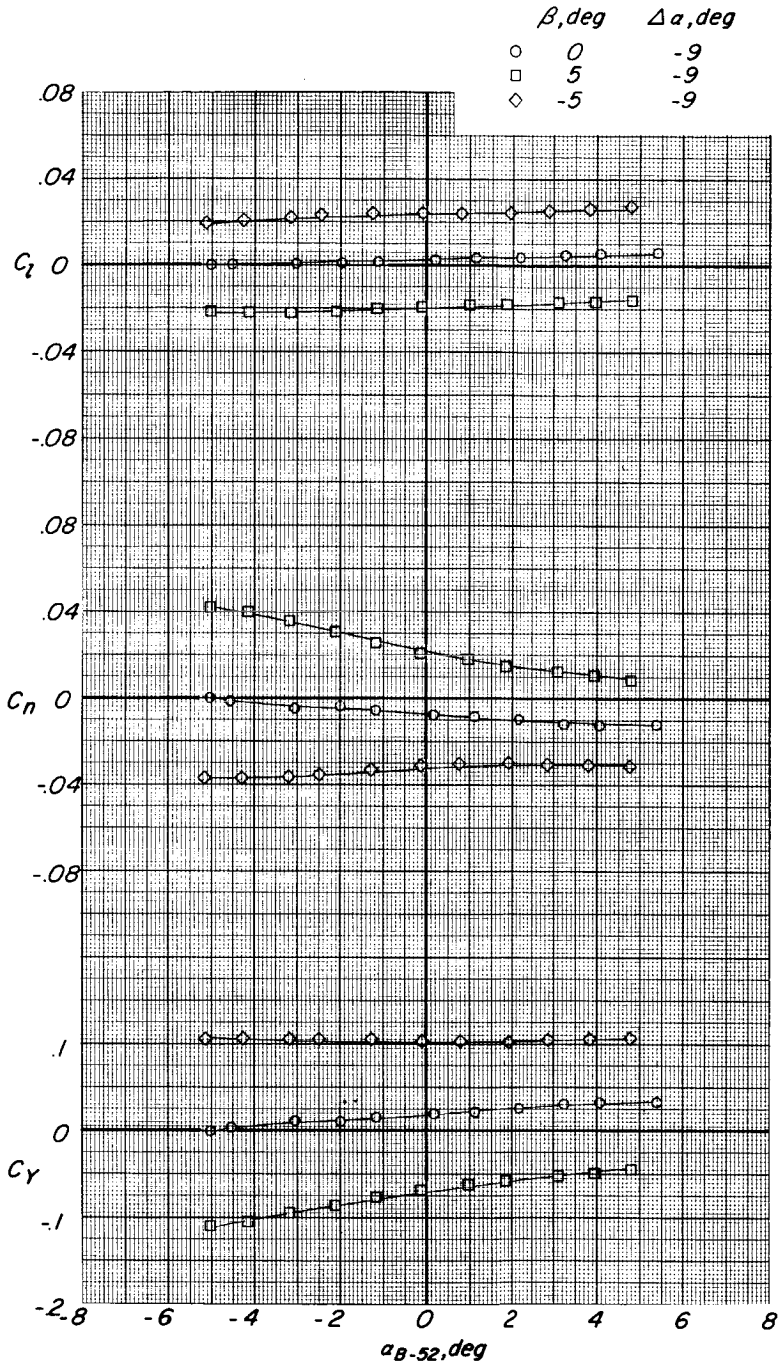

(e) Continued.

Figure 9.- Continued.

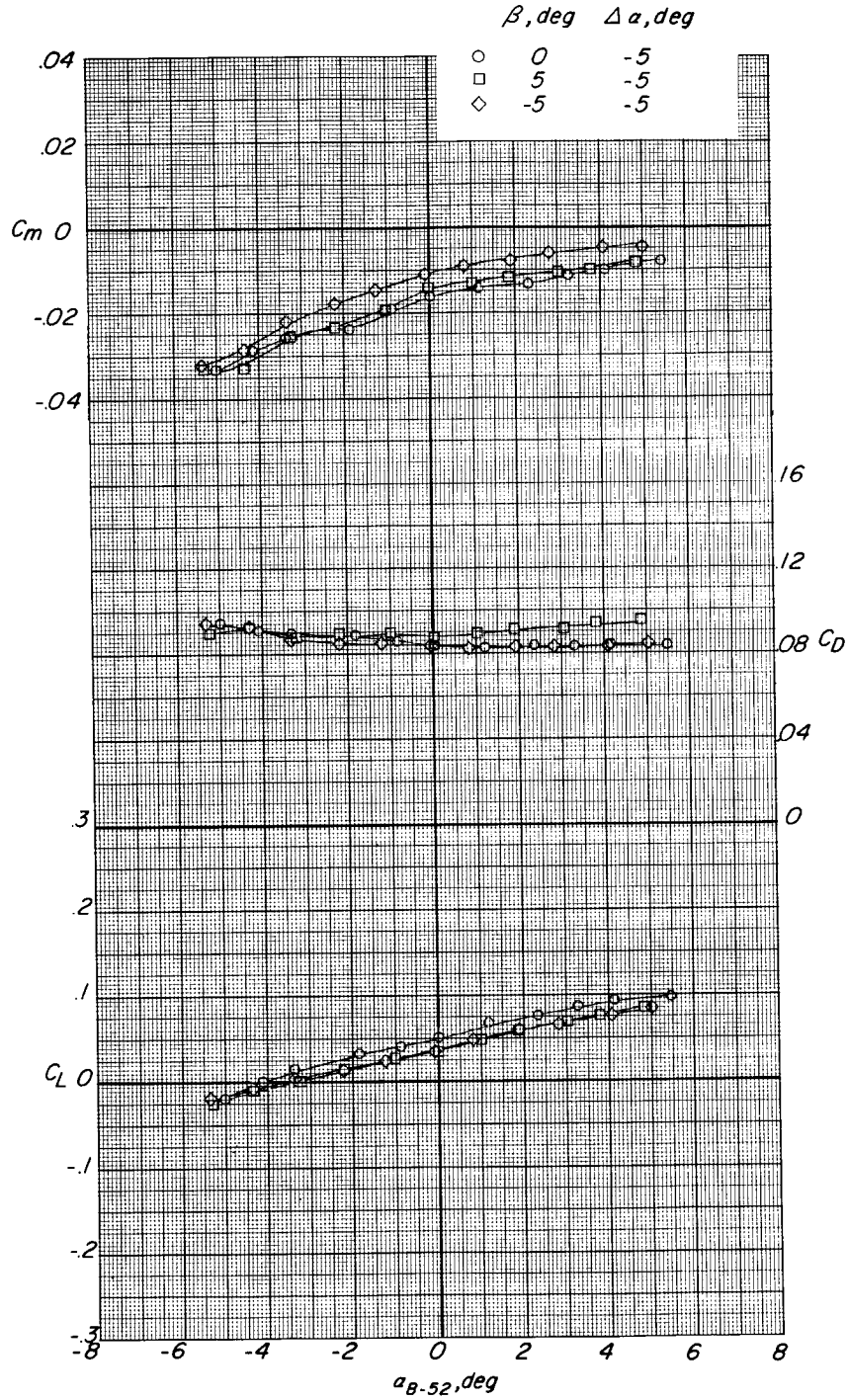

(e) Continued.

Figure 9.- Continued.

[redacted] DECLASSIFIED

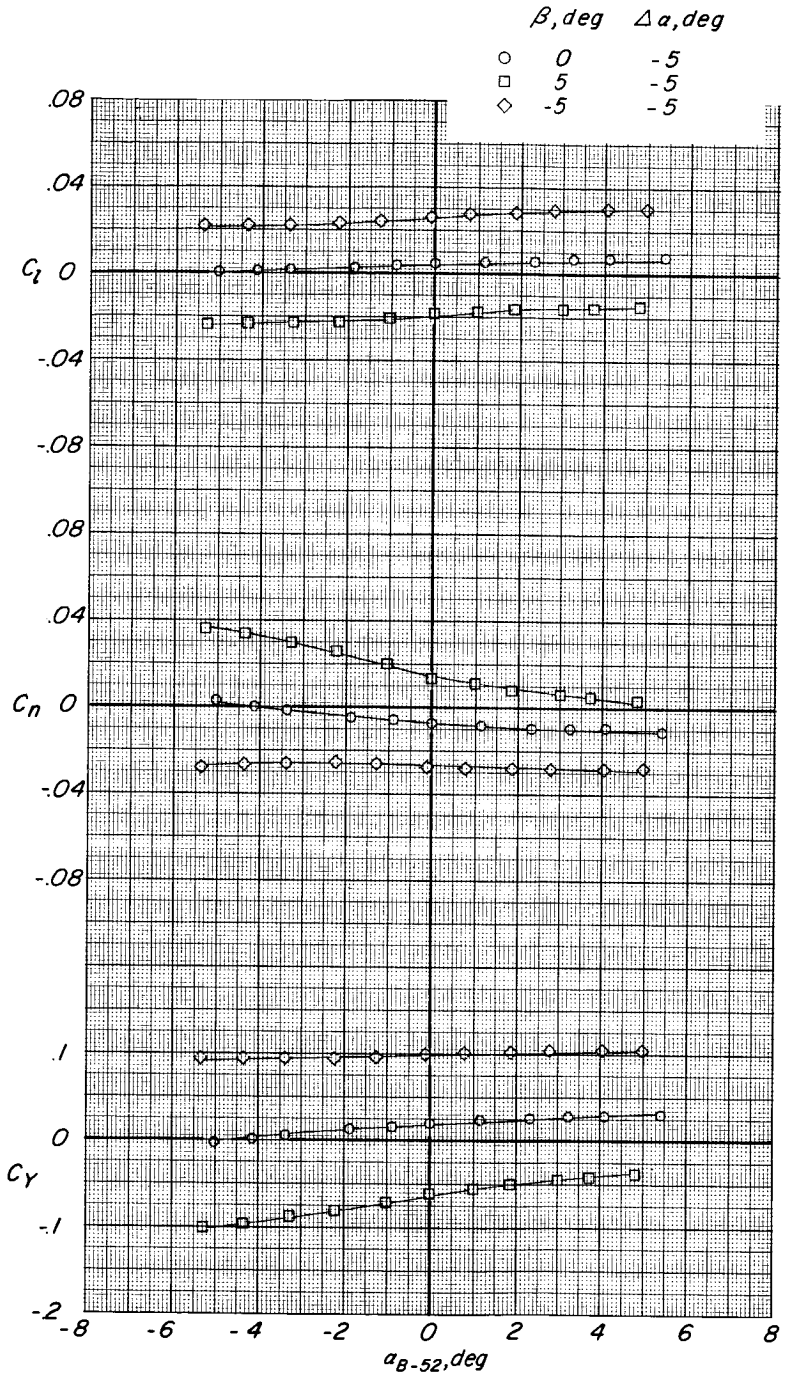

(e) Continued.

Figure 9.- Continued.

[redacted]

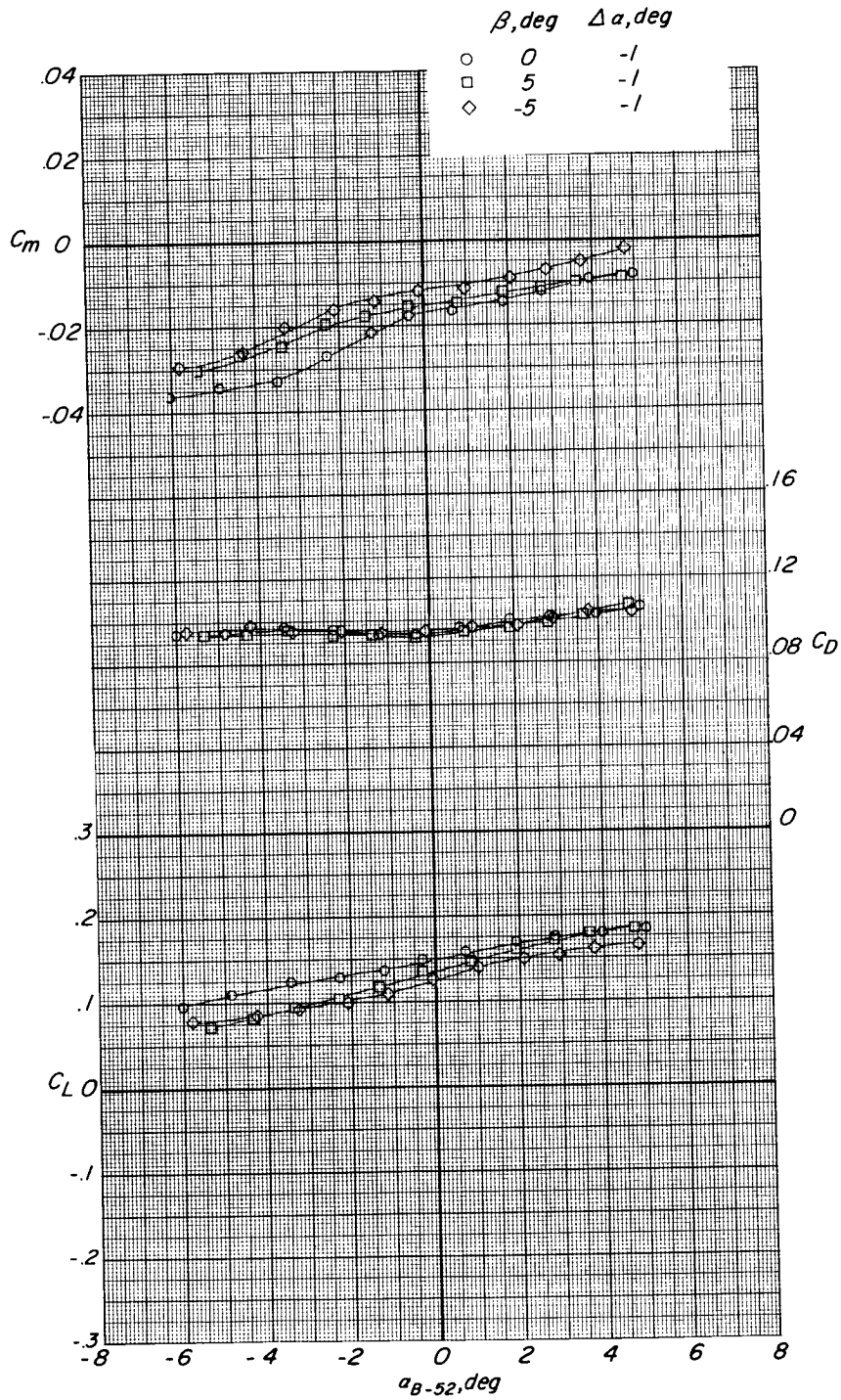

(e) Continued.

Figure 9.- Continued.

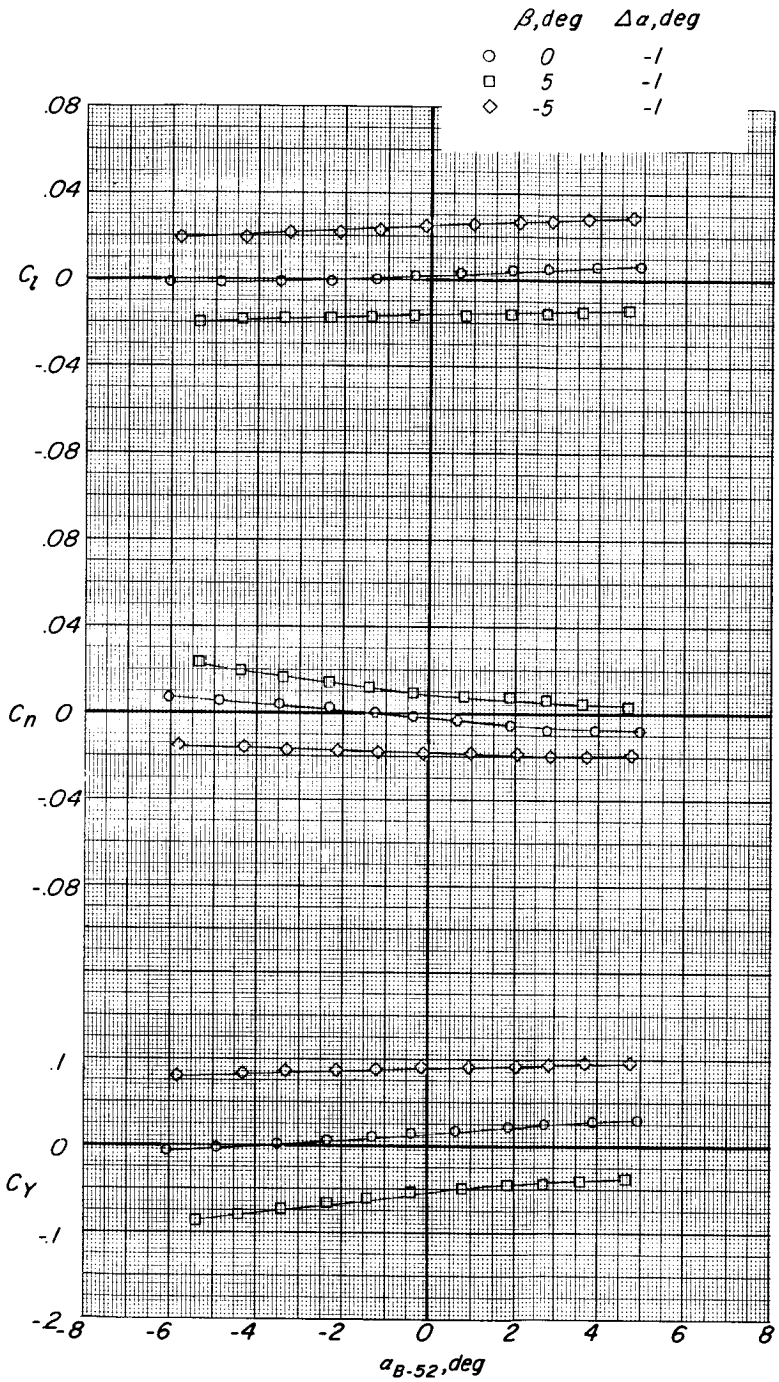

(e) Continued.

Figure 9.- Continued.

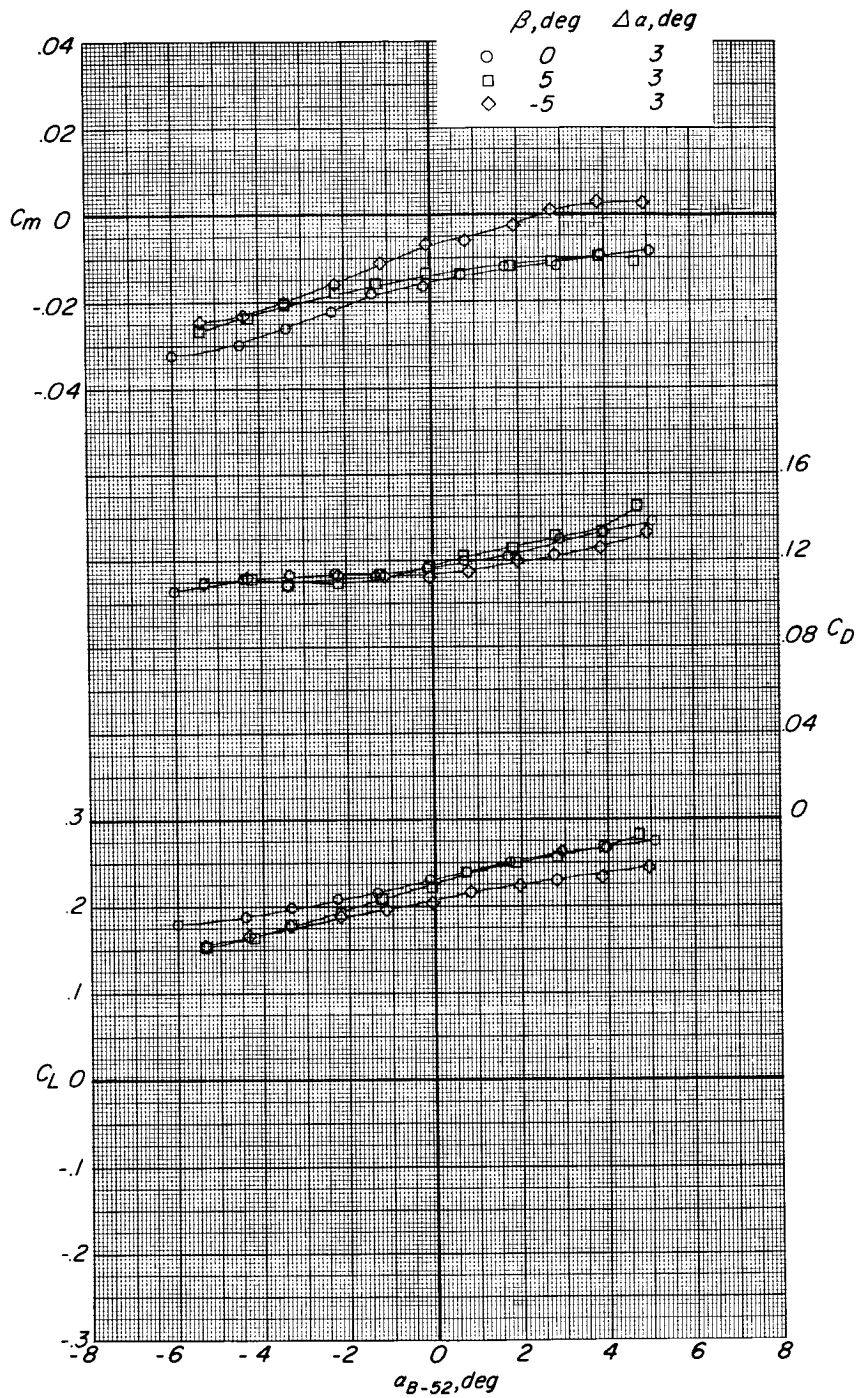

(e) Continued.

Figure 9.- Continued.

[redacted] CLASSIFIED

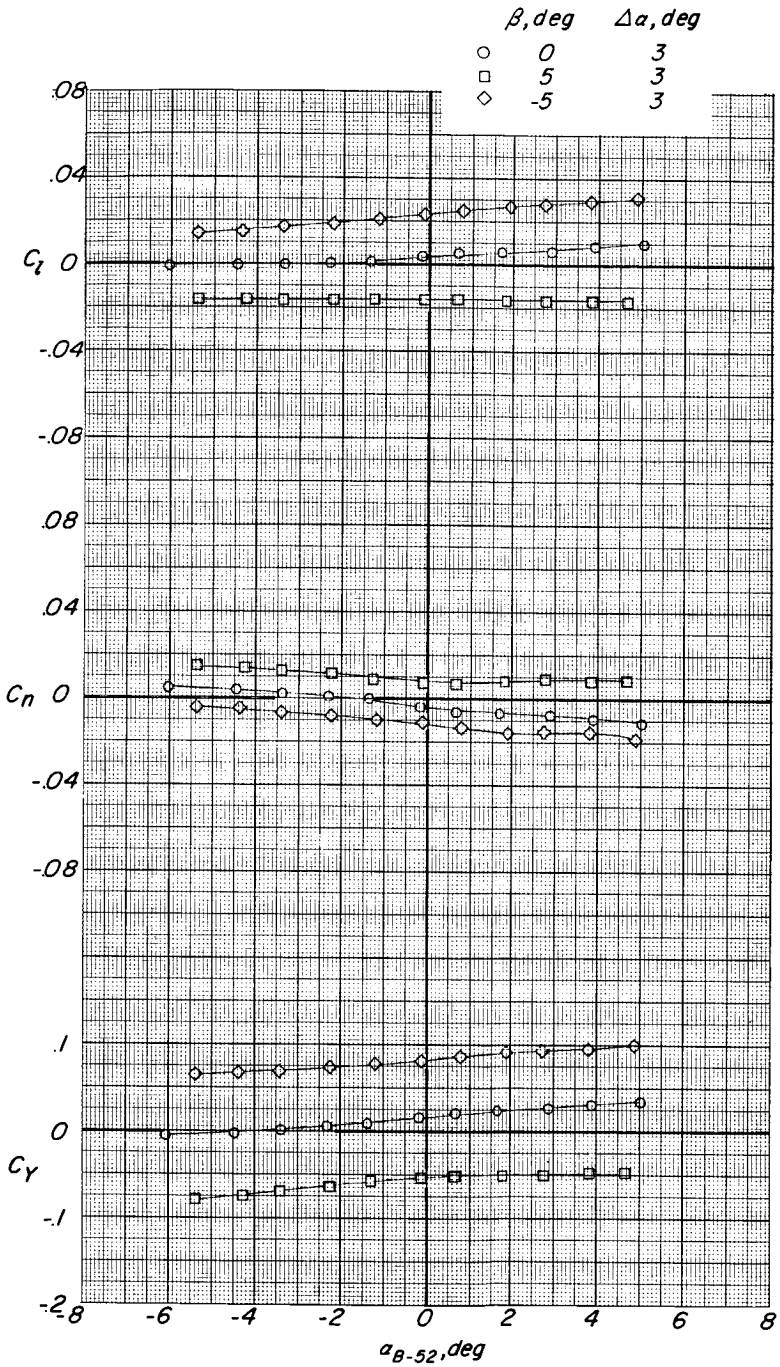

(e) Concluded.

Figure 9.- Concluded.

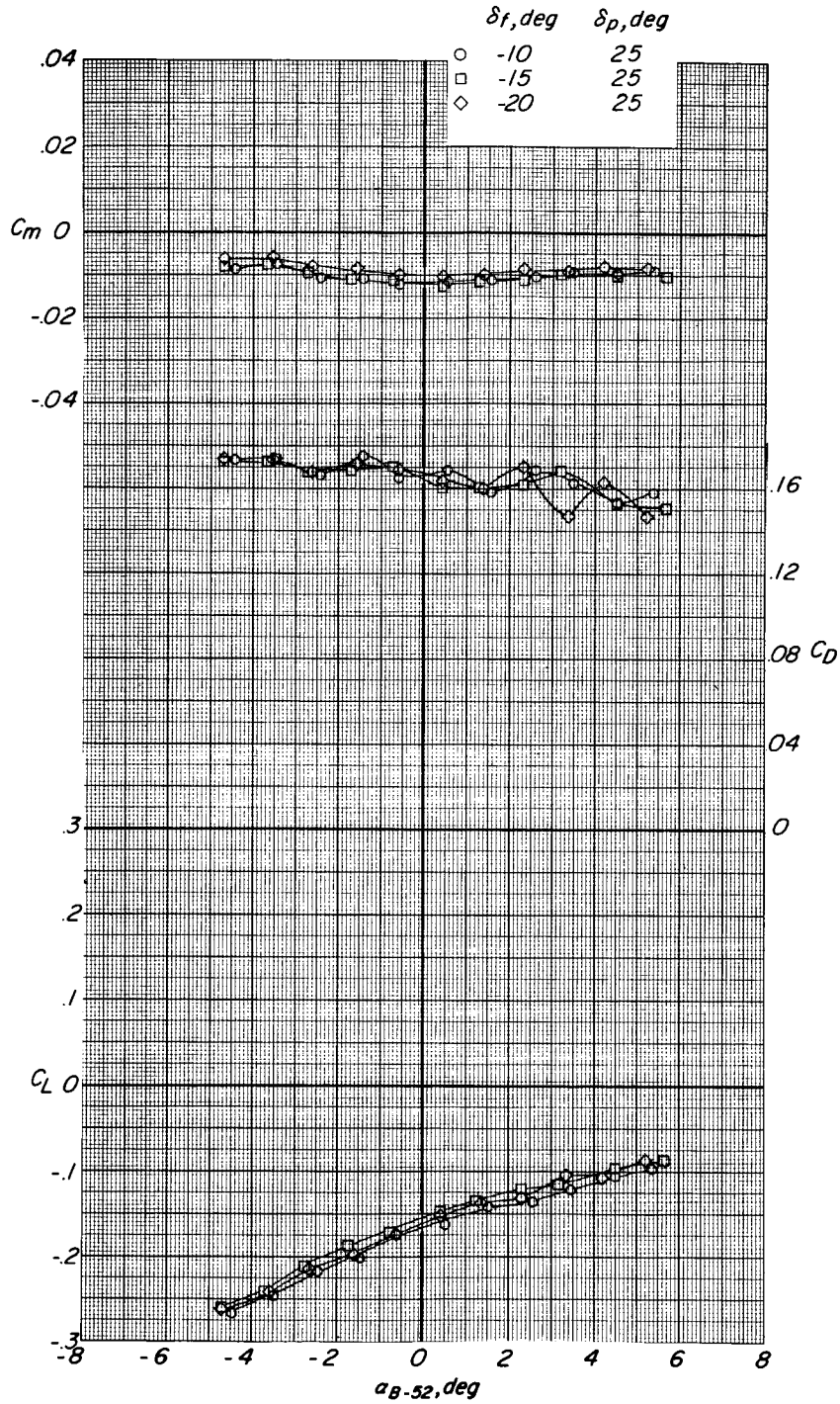

(a) z' = 0.

Figure 10.- Aerodynamic characteristics of M2-F2 model in presence of B-52 model. M = 0.85; nominal control settings are $\delta_p = 25^0$, $\delta_f = -10^0$, and 10^0 rudder flare.

[redacted] DECLASSIFIED

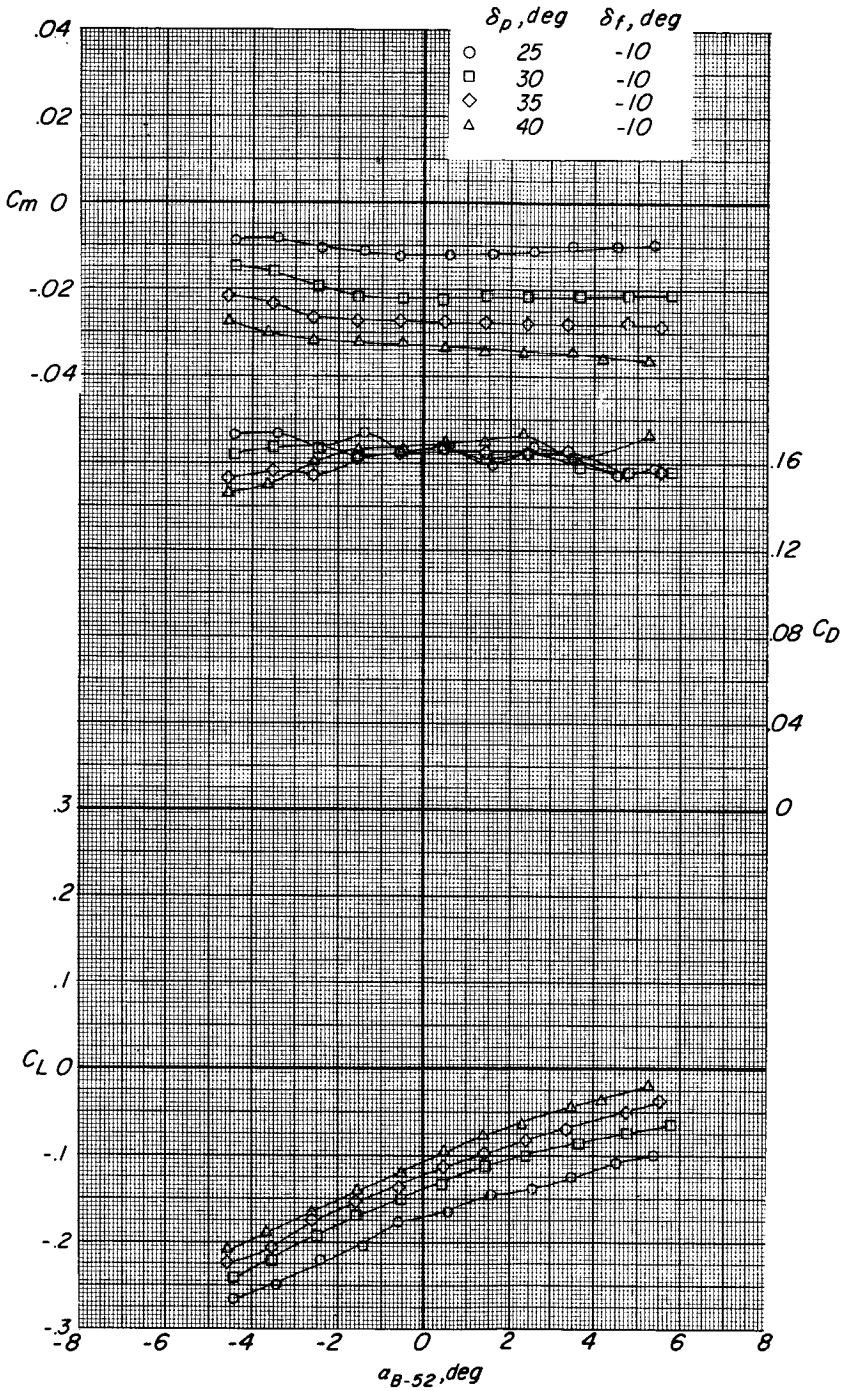

(a) Continued.

Figure 10.- Continued.

[redacted]

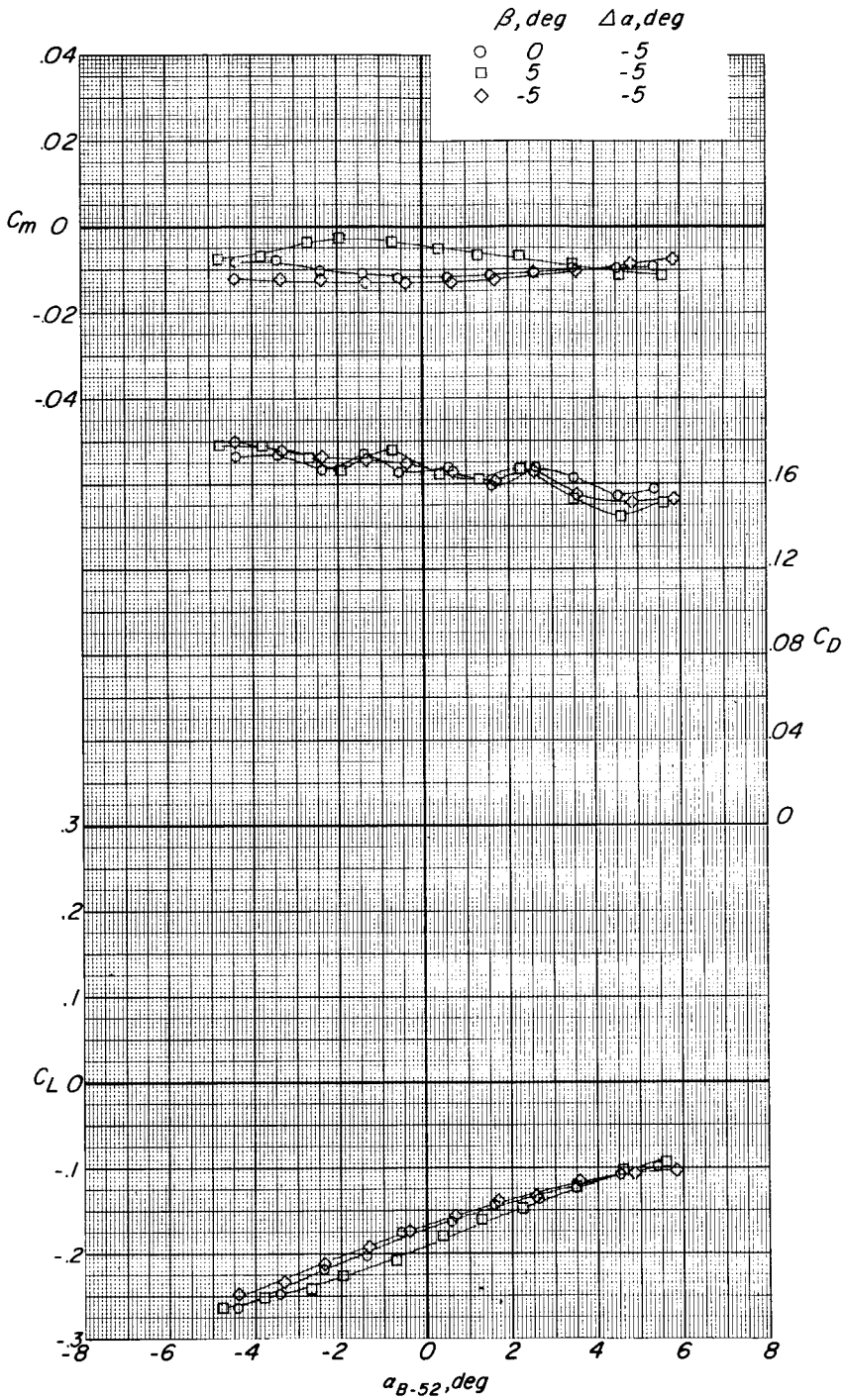

(a) Continued.

Figure 10.- Continued.

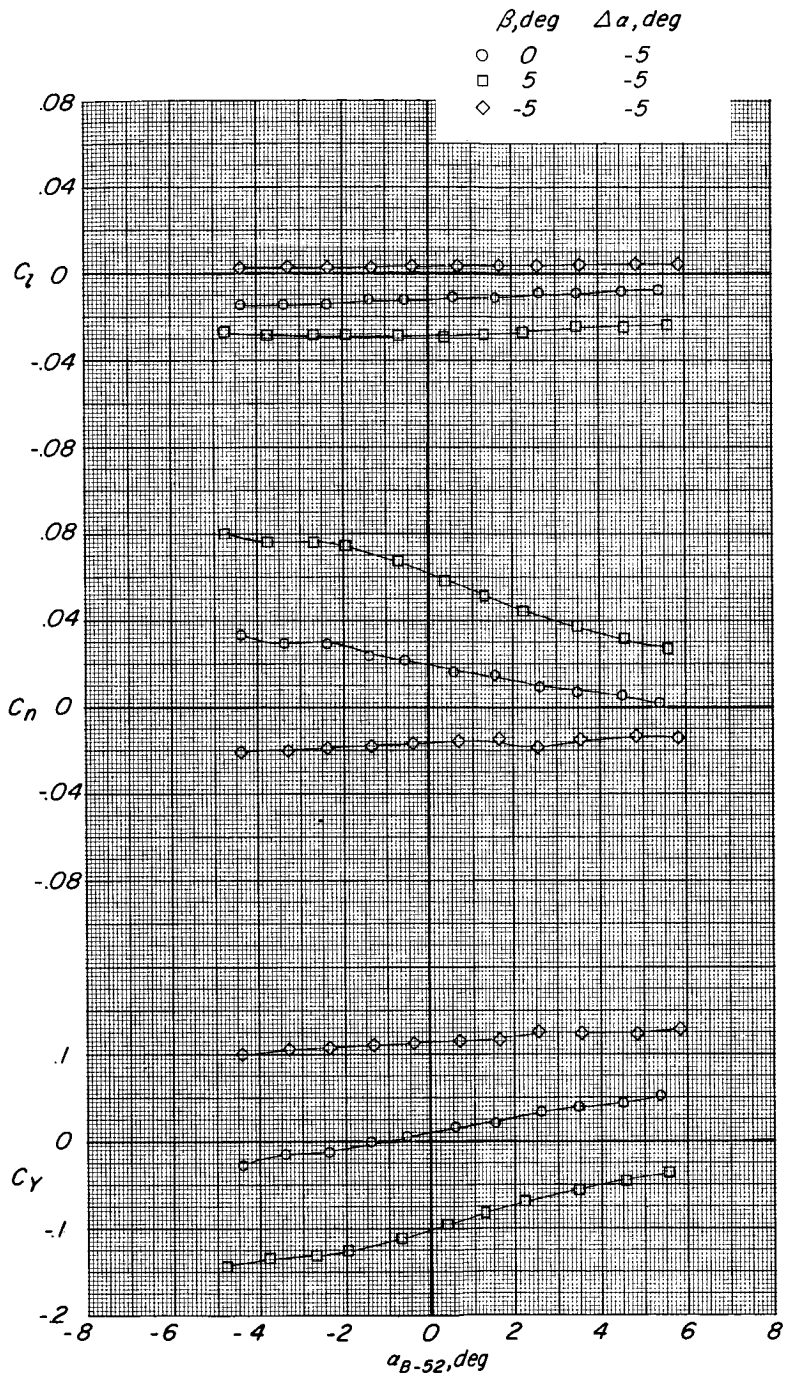

(a) Continued.

Figure 10.- Continued.

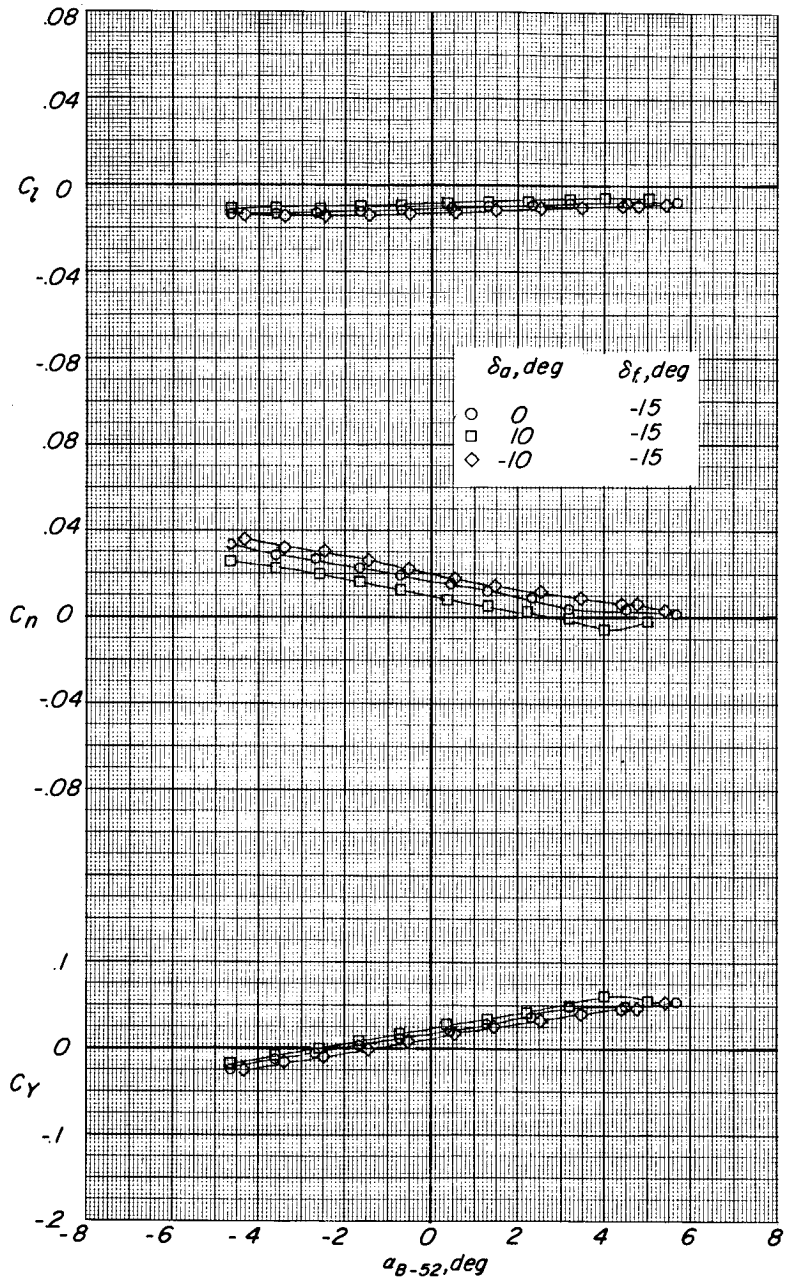

(a) Continued.

Figure 10.- Continued.

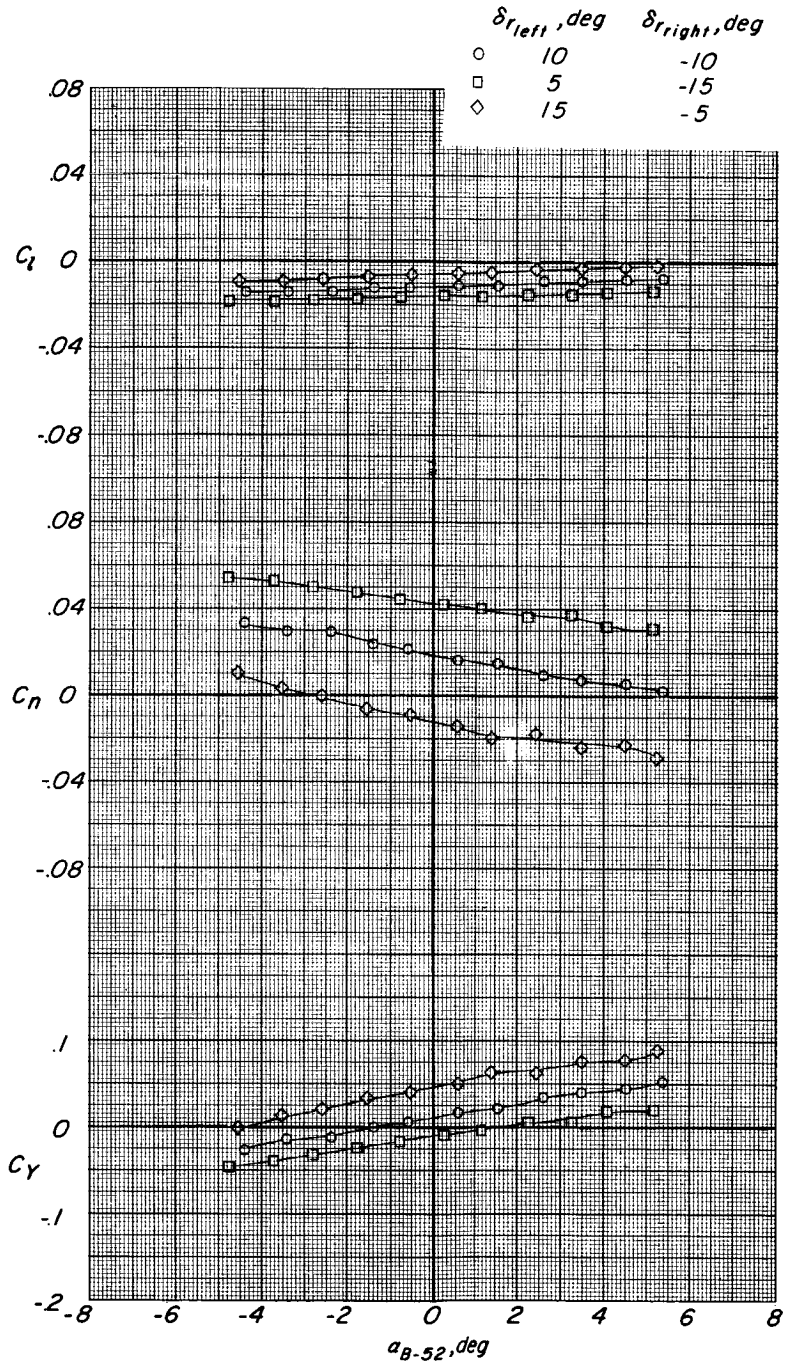

(a) Concluded.

Figure 10.- Continued.

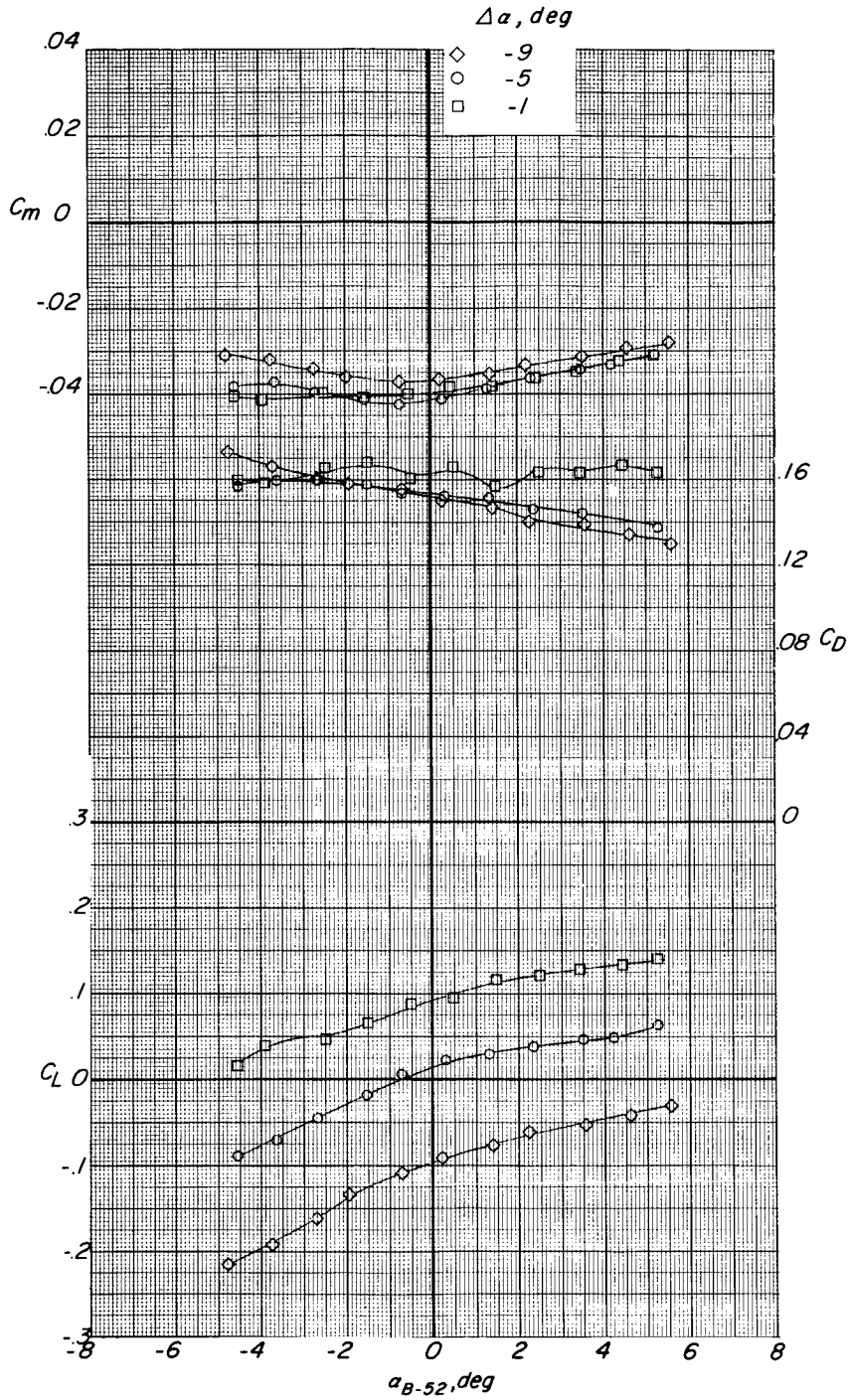

(b) z' = 2.0 feet (0.61 m).

Figure 10.- Continued.

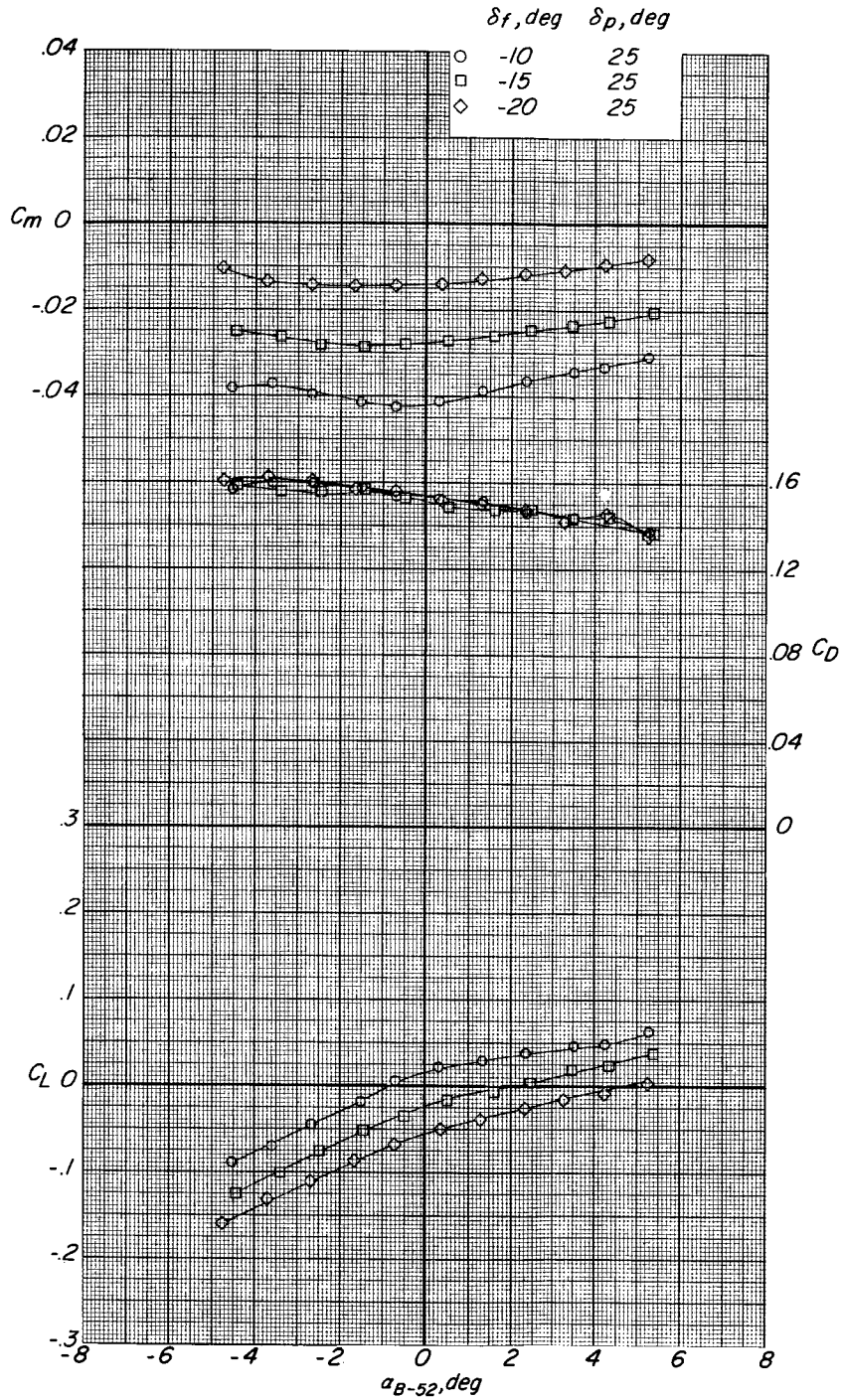

(b) Continued.

Figure 10.- Continued.

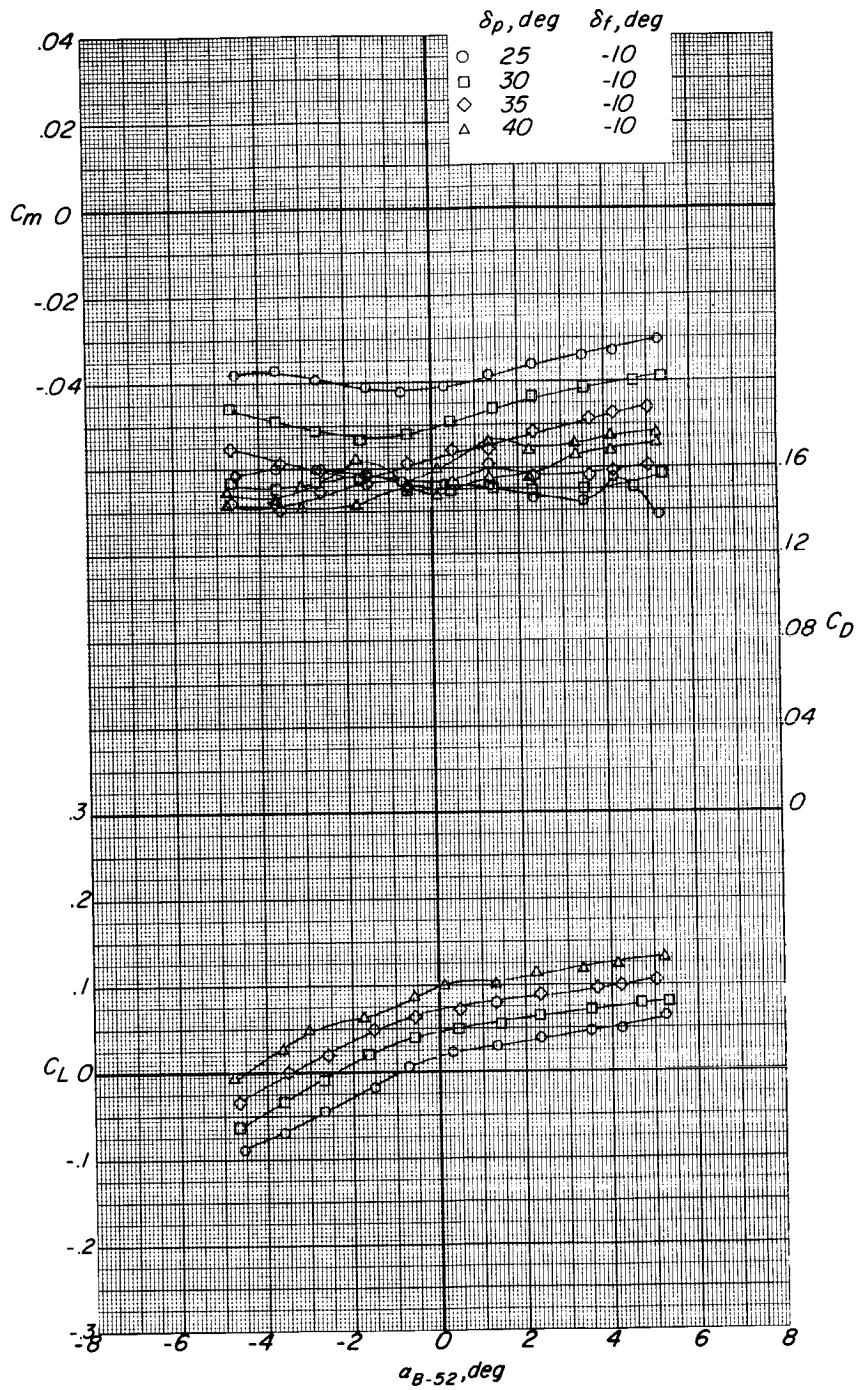

(b) Continued.

Figure 10.- Continued.

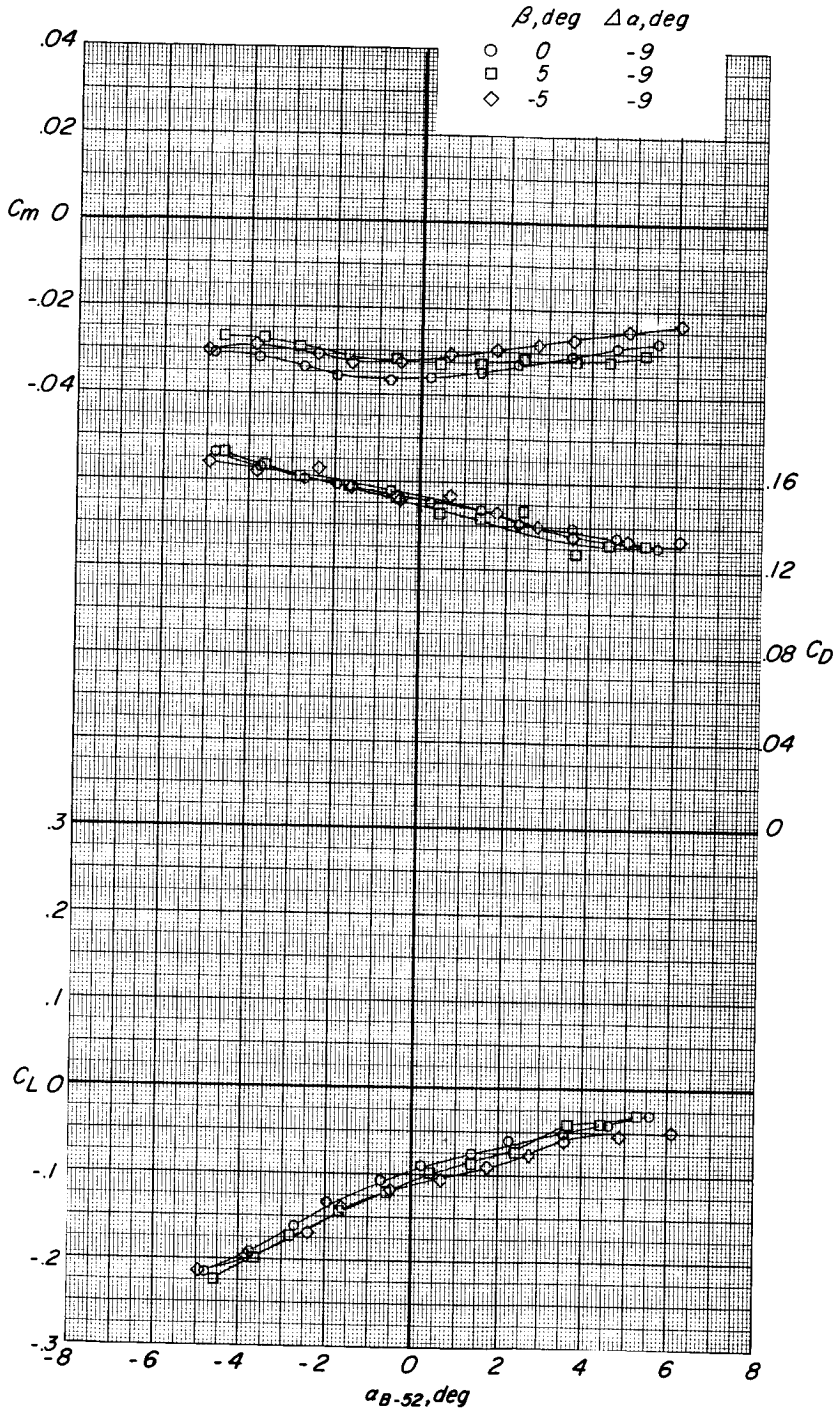

(b) Continued.

Figure 10.- Continued.

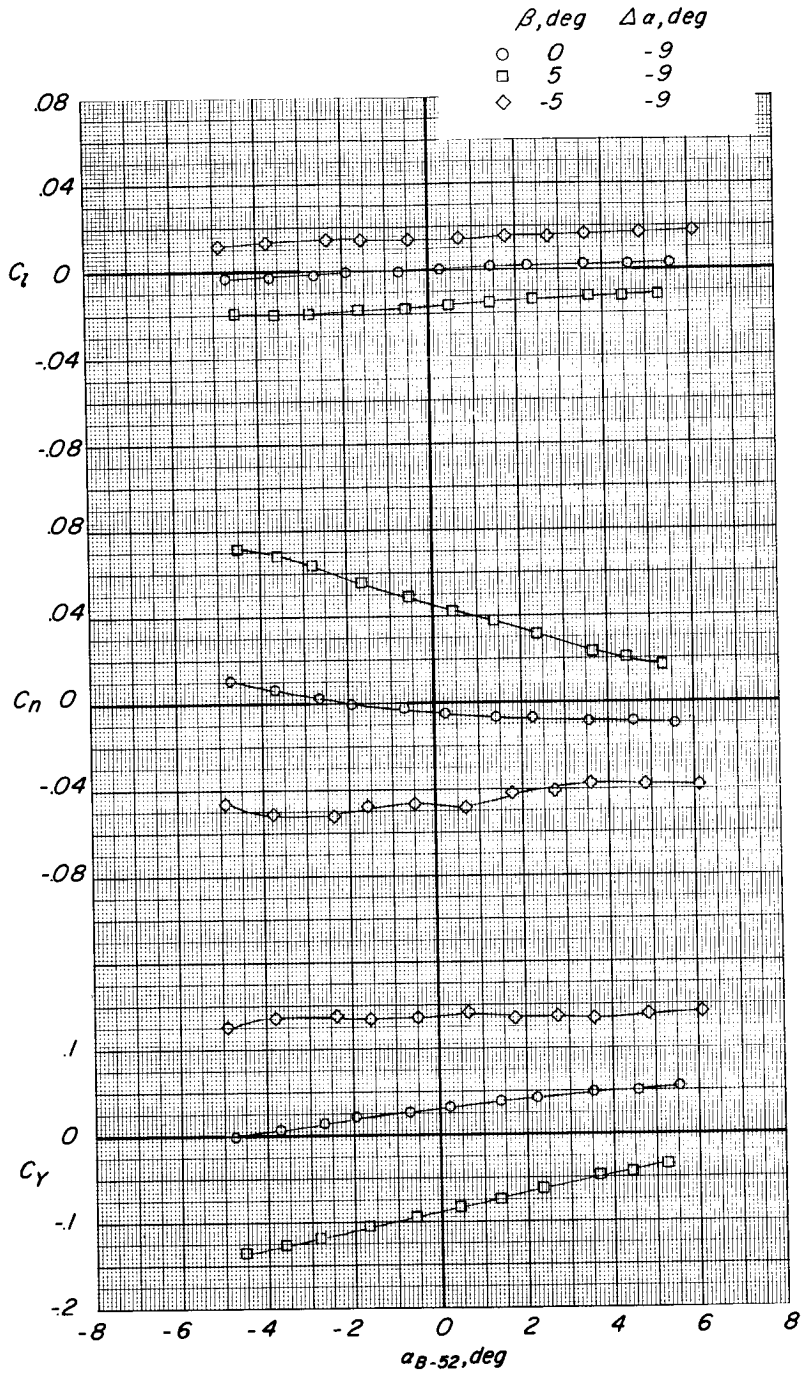

(b) Continued.

Figure 10.- Continued.

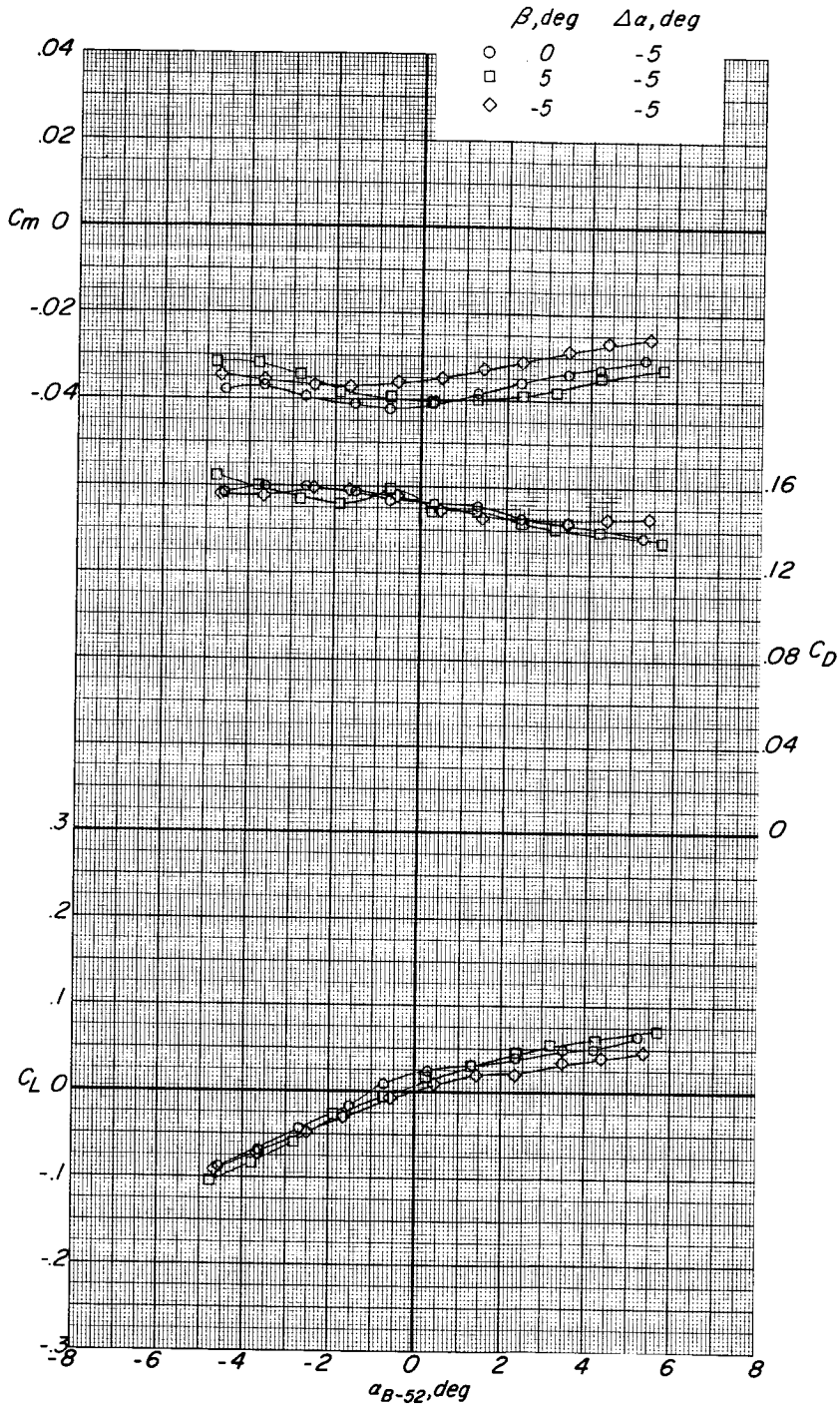

(b) Continued.

Figure 10.- Continued.

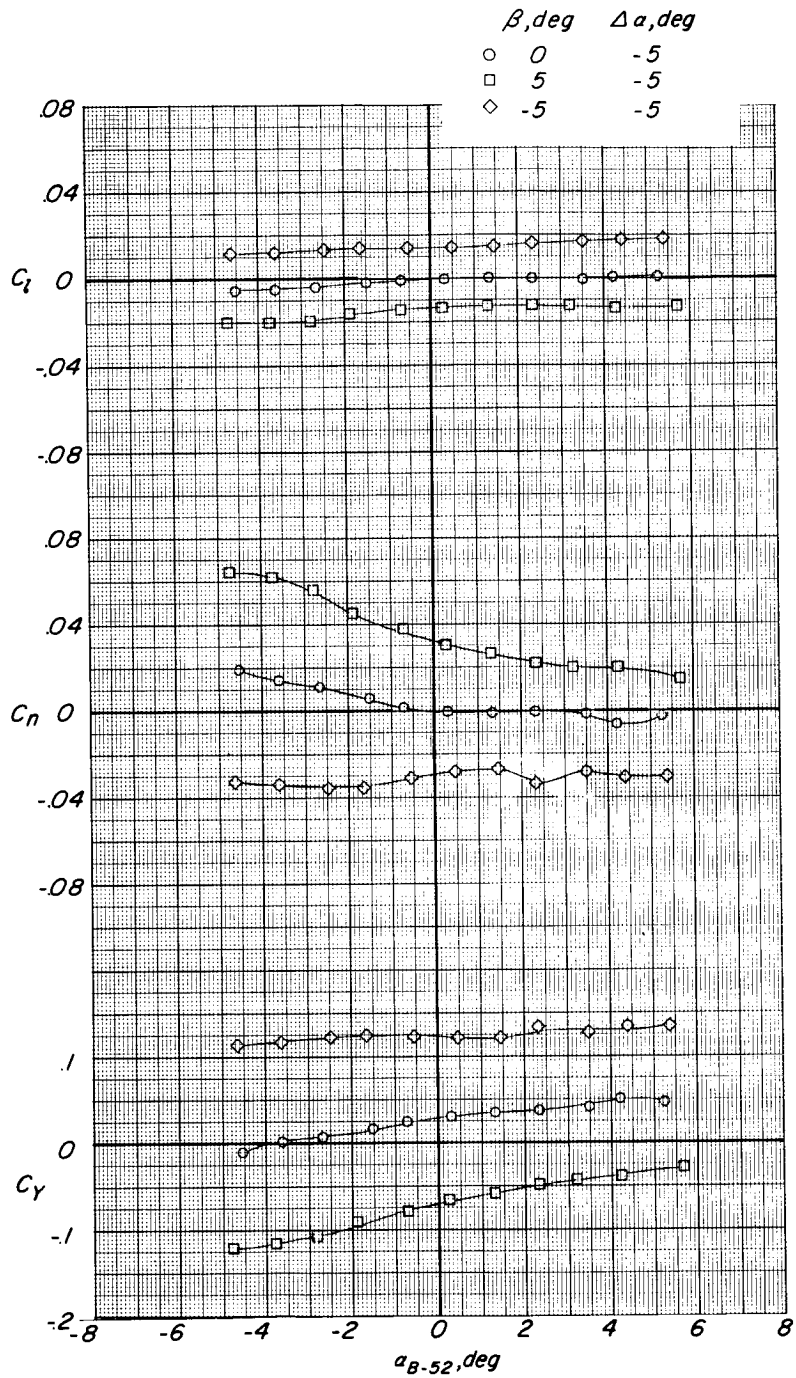

(b) Continued.

Figure 10.- Continued.

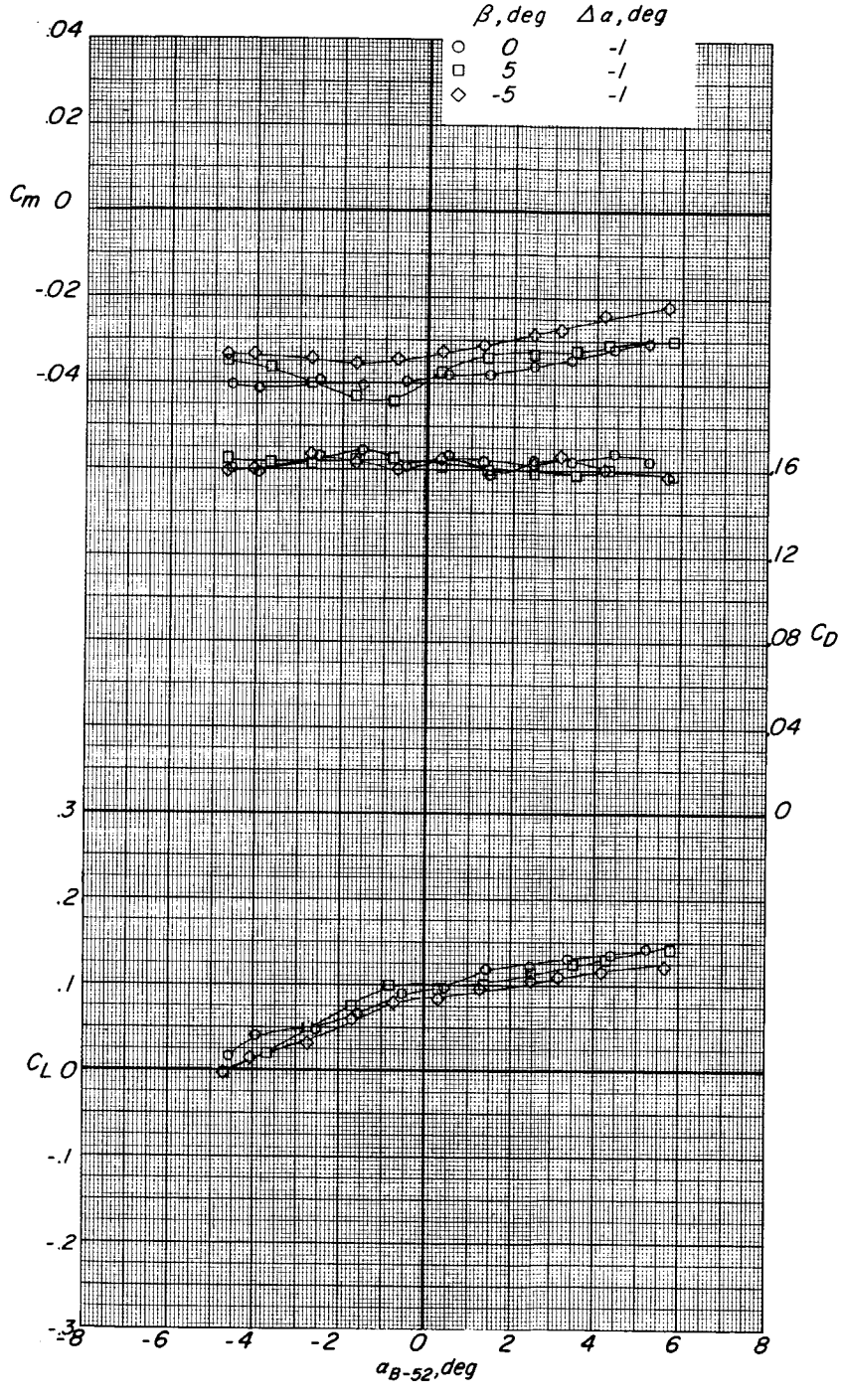

(b) Continued.

Figure 10.- Continued.

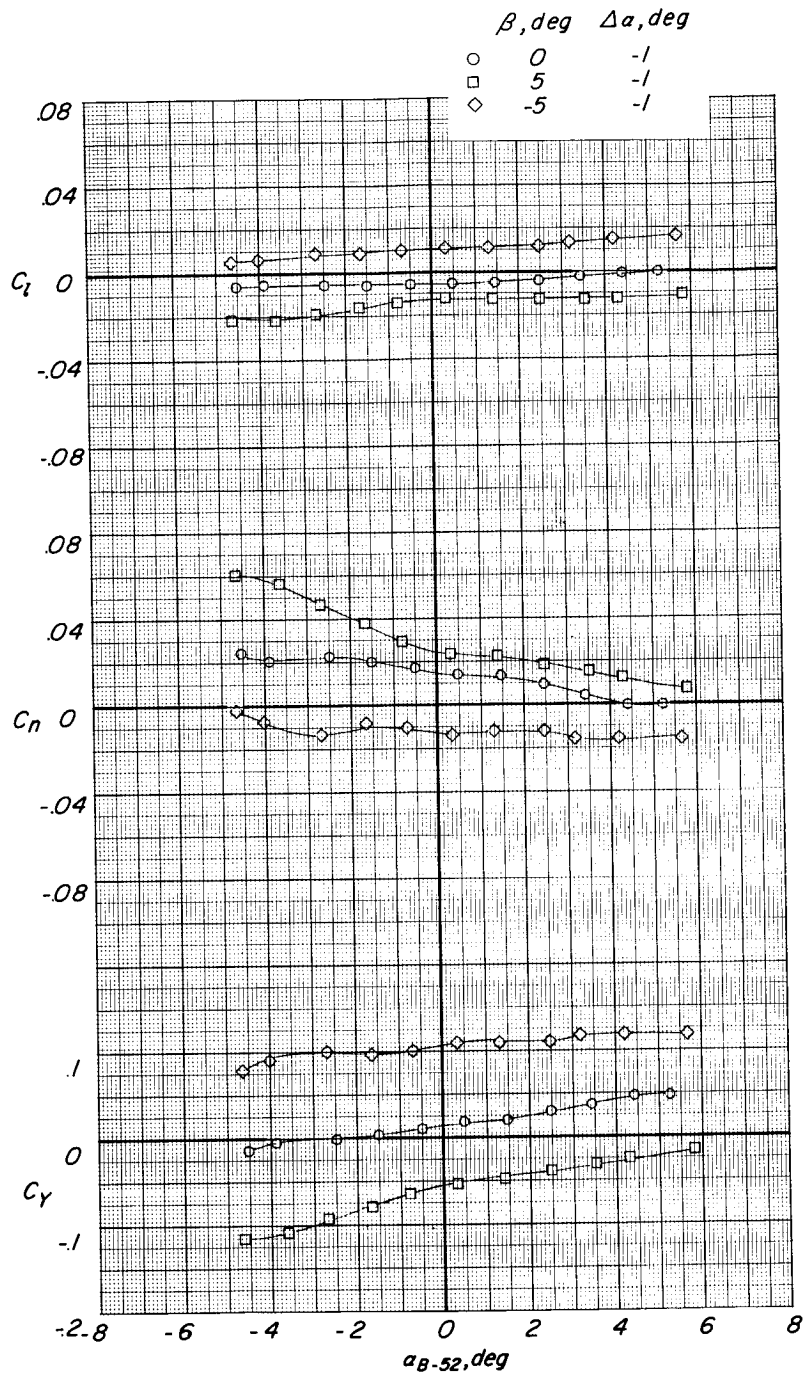

(b) Continued.

Figure 10.- Continued.

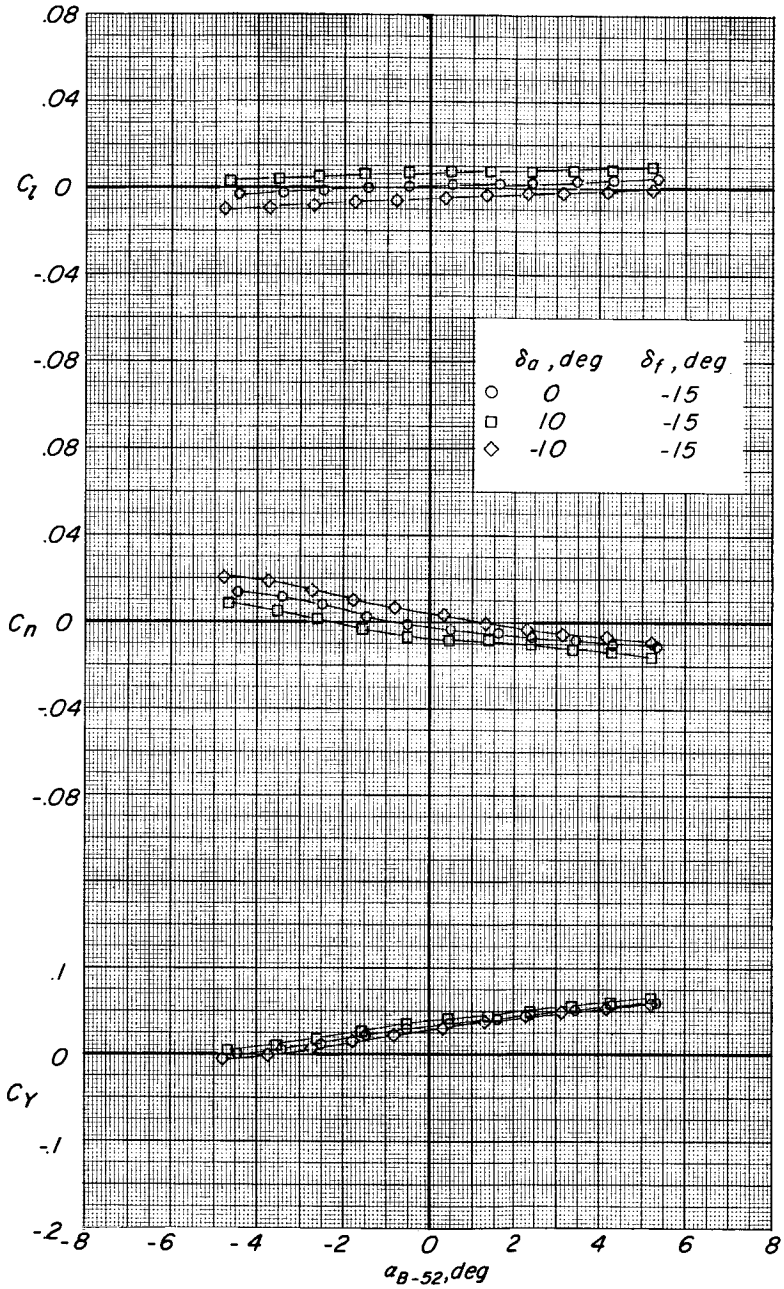

(b) Continued.

Figure 10.- Continued.

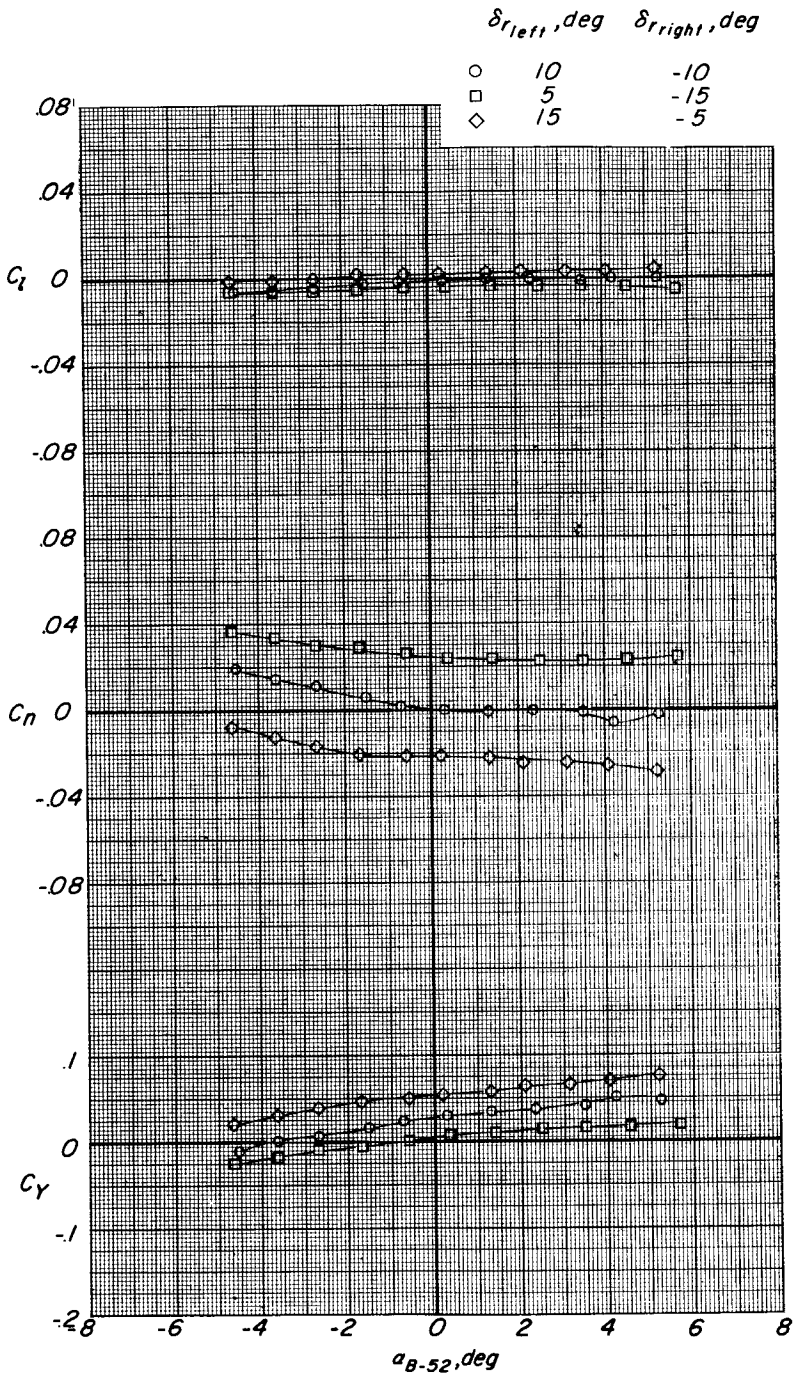

(b) Concluded.

Figure 10.- Continued.

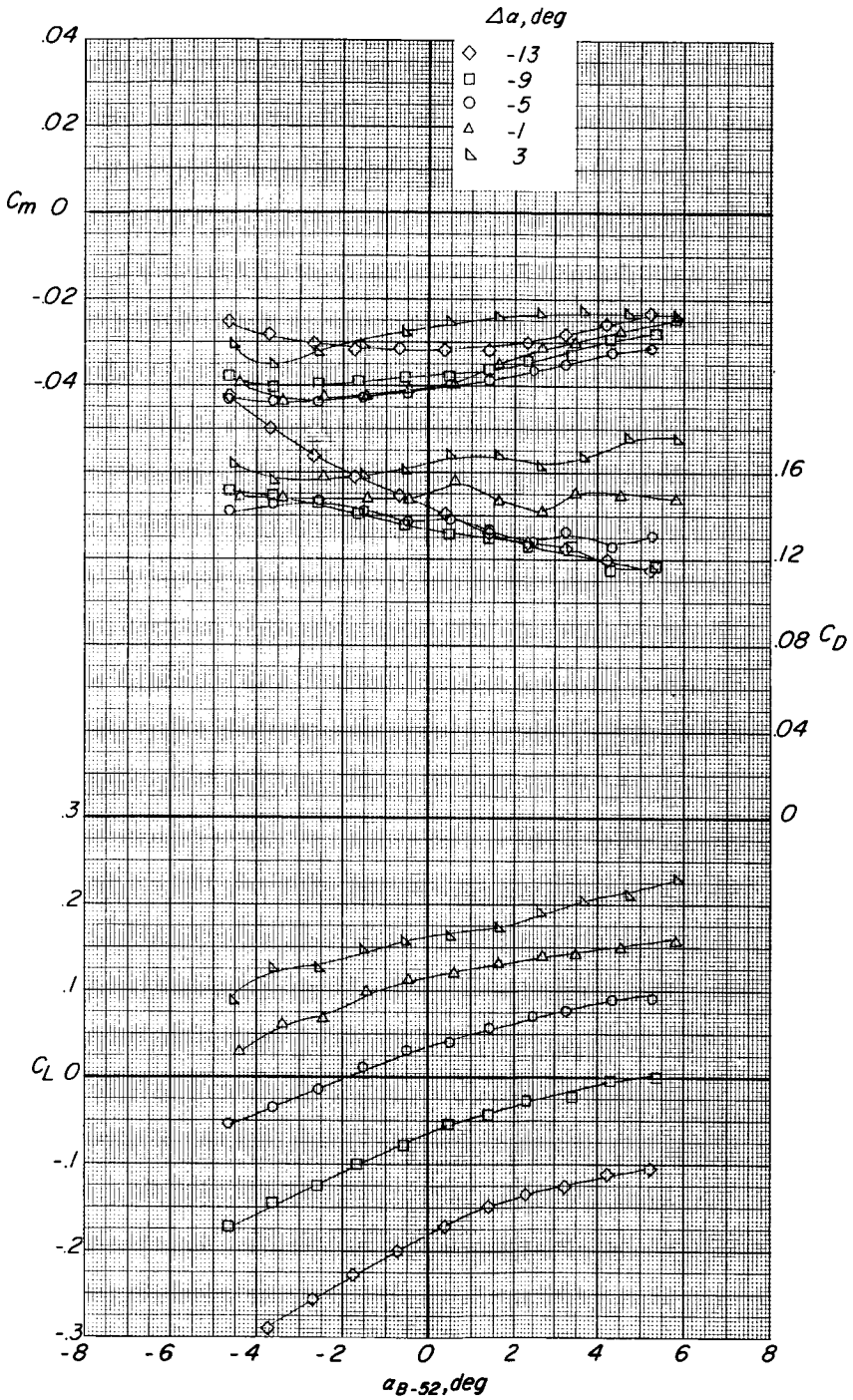

(c) z' = 4.0 feet (1.22 m).

Figure 10.- Continued.

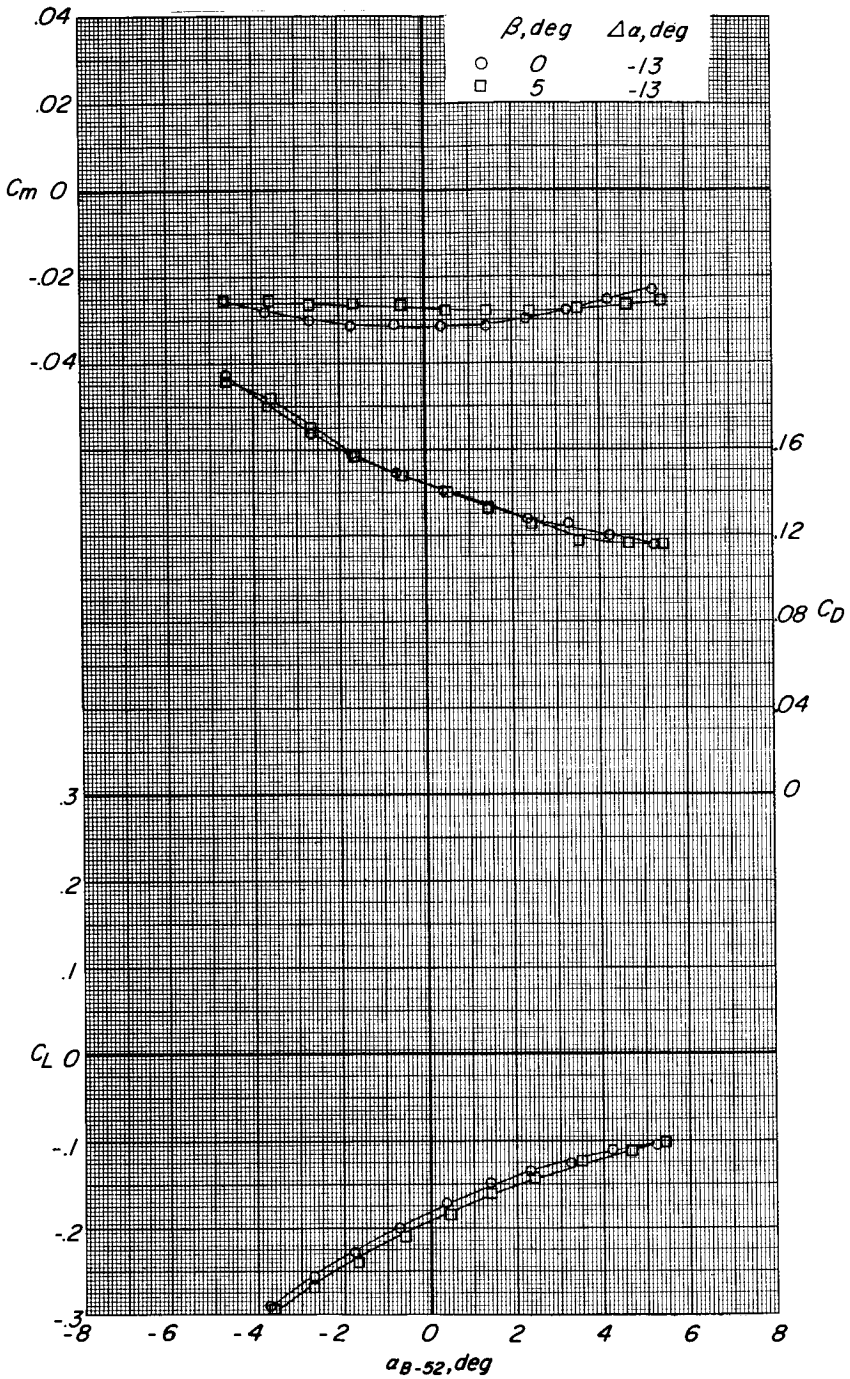

(c) Continued.

Figure 10.- Continued.

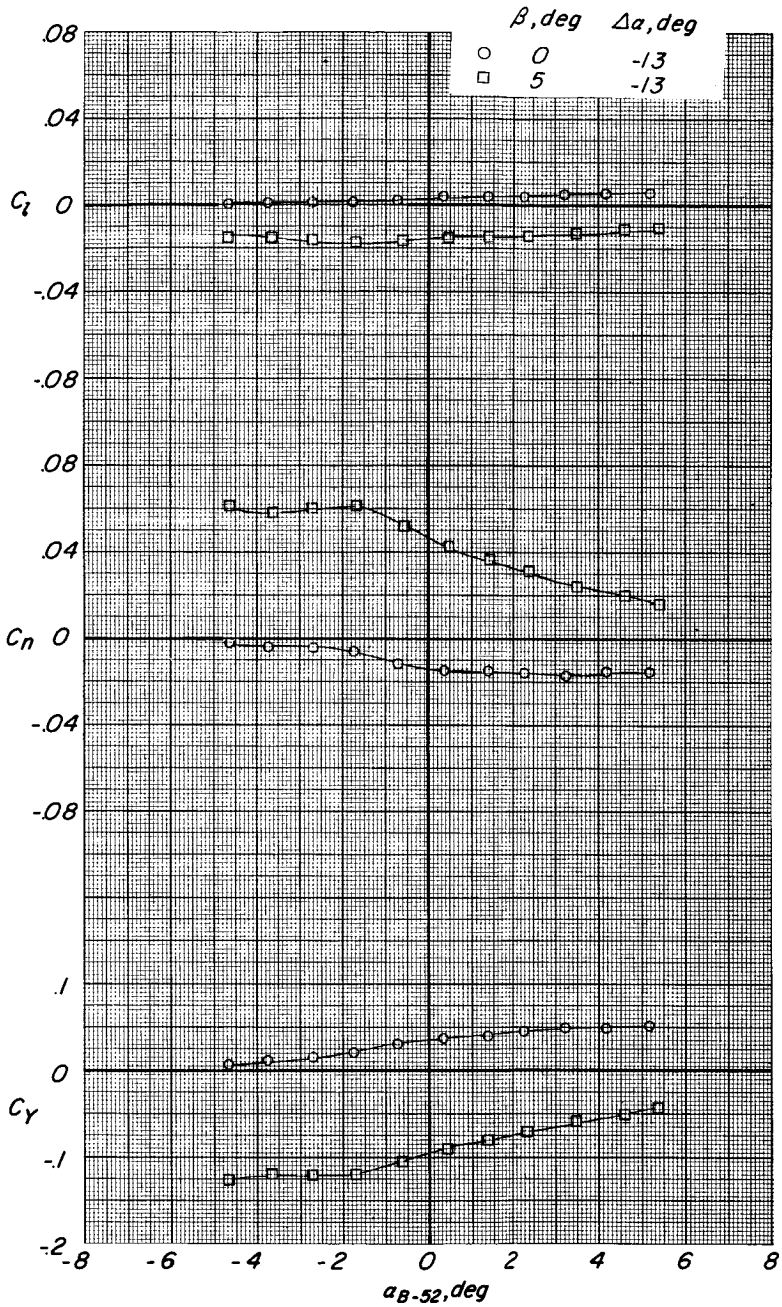

(c) Continued.

Figure 10.- Continued.

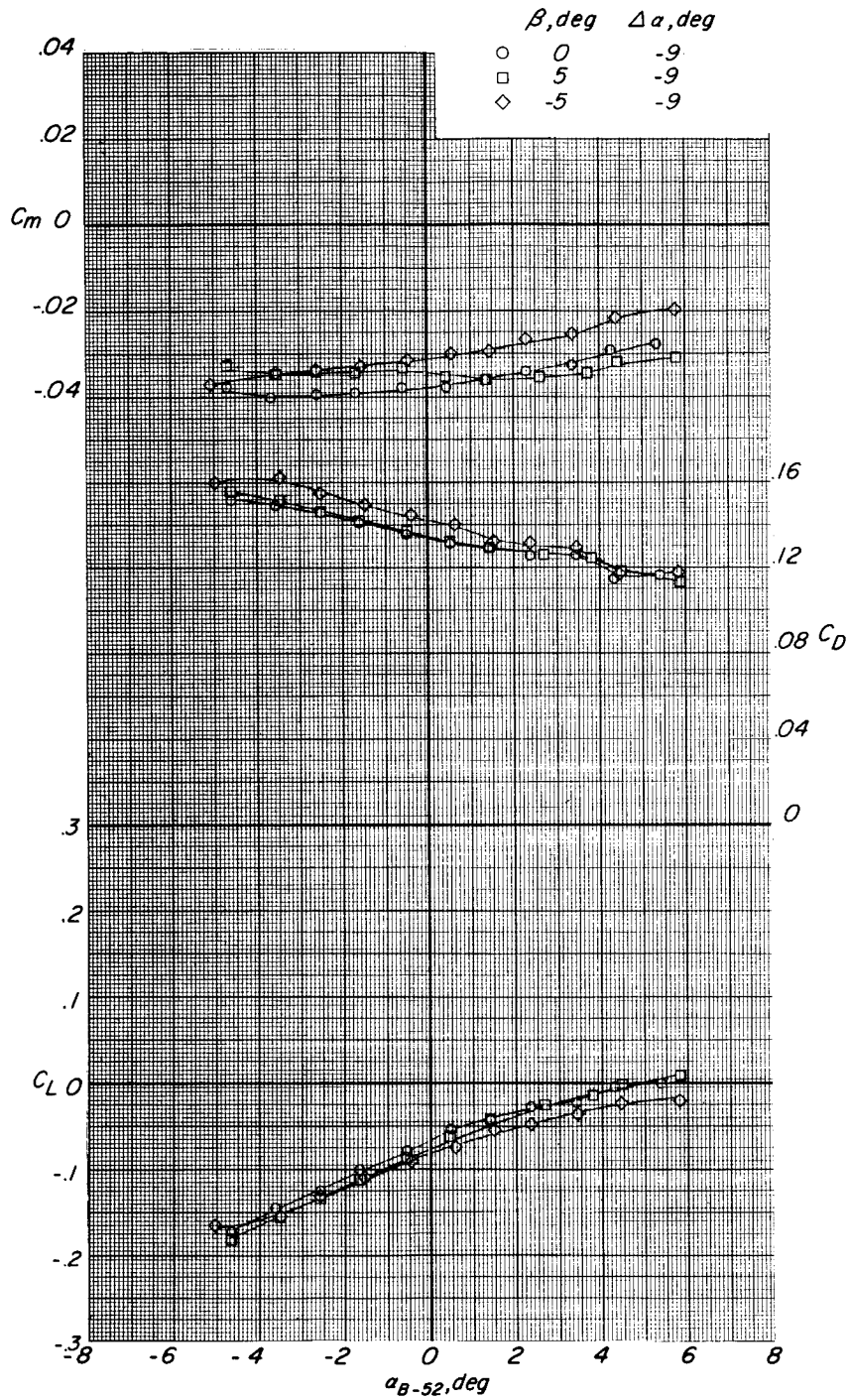

(c) Continued.

Figure 10.- Continued.

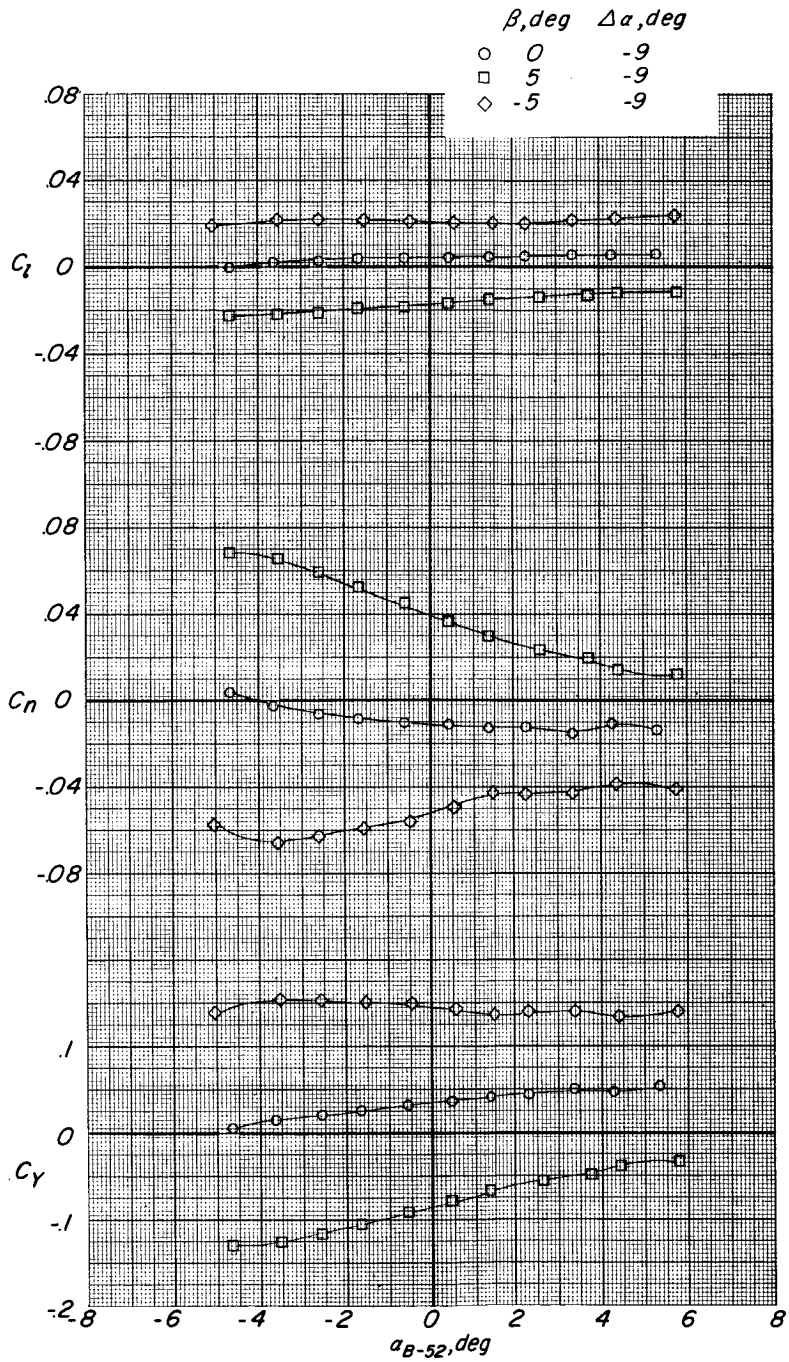

(c) Continued.

Figure 10.- Continued.

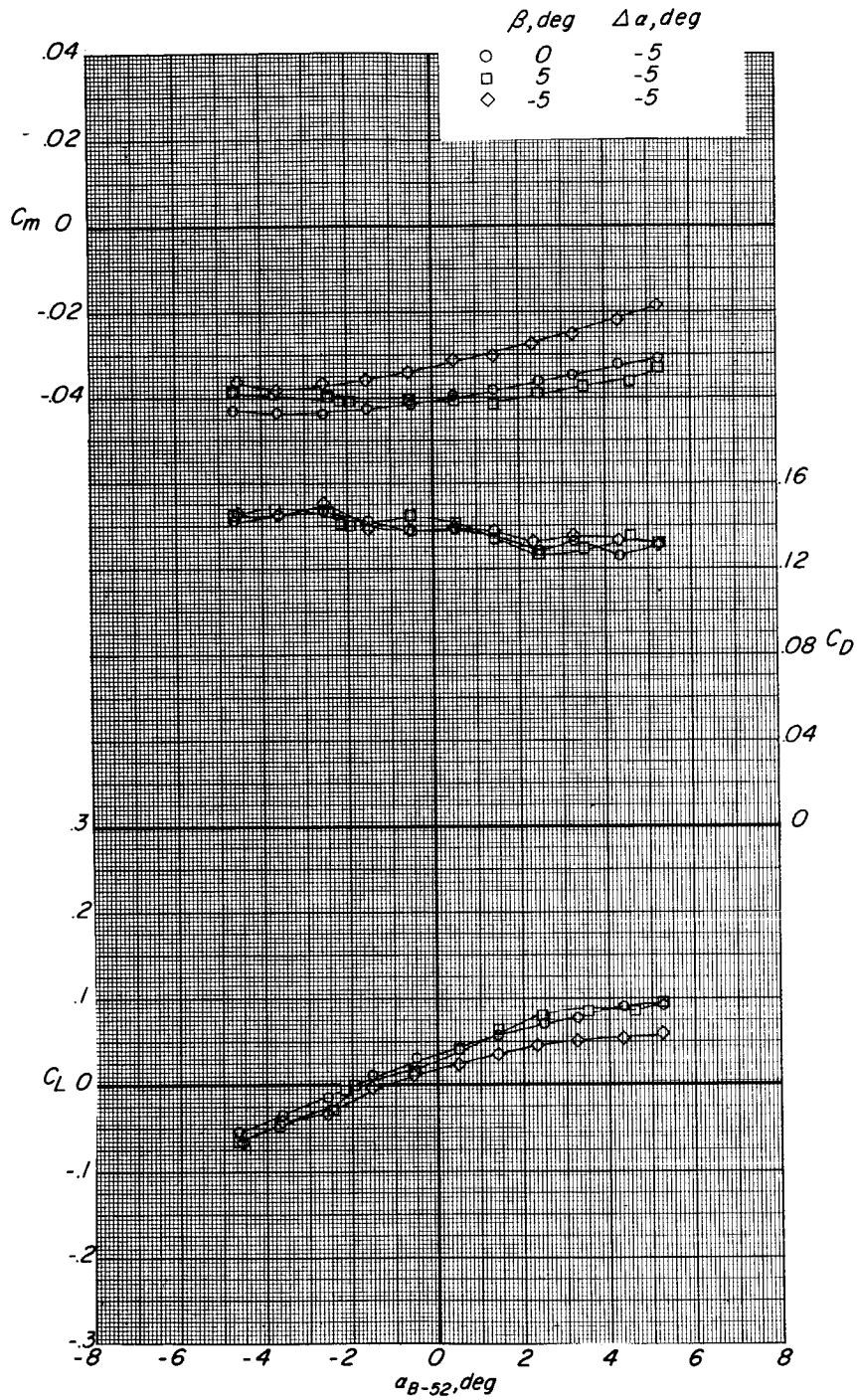

(c) Continued.

Figure 10.- Continued.

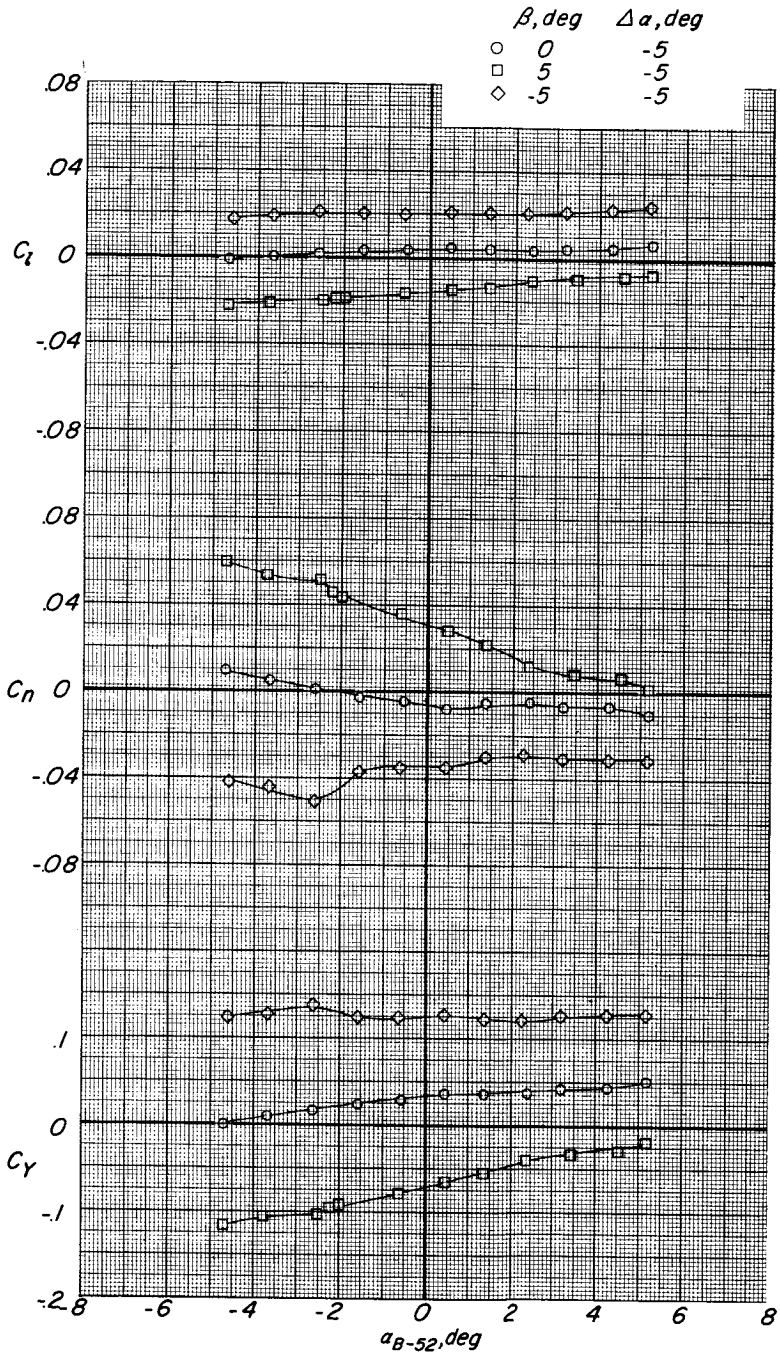

(c) Continued.

Figure 10.- Continued.

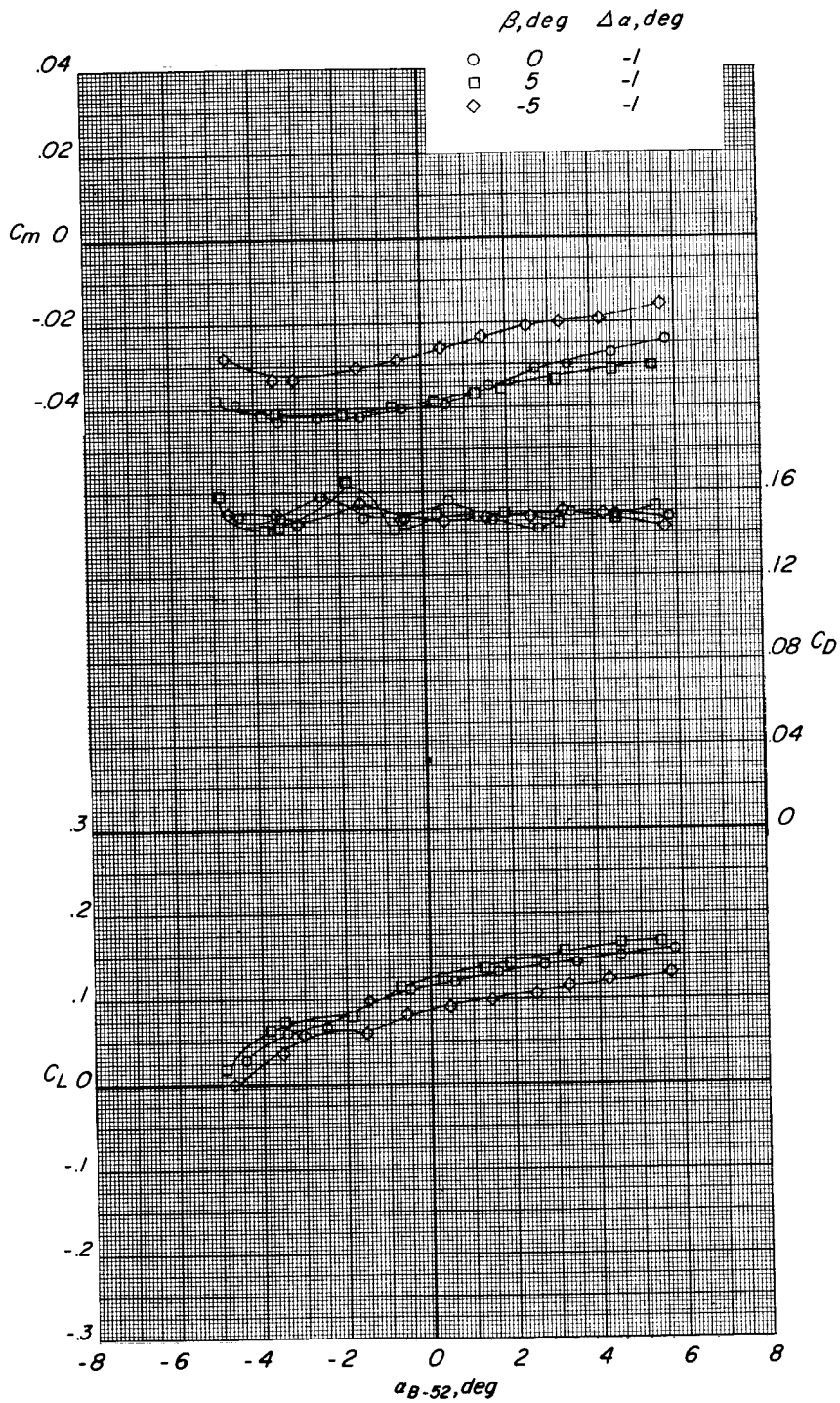

(c) Continued.

Figure 10.- Continued.

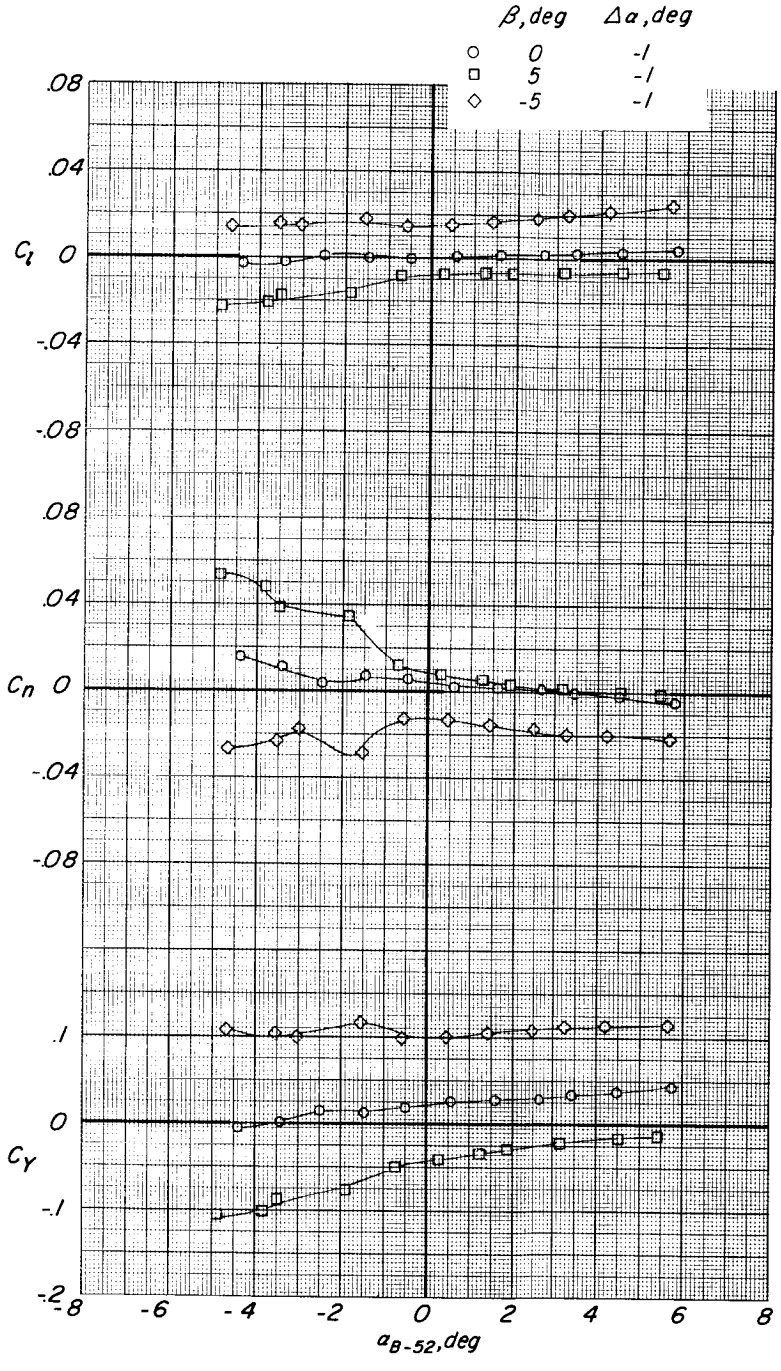

(c) Continued.

Figure 10.- Continued.

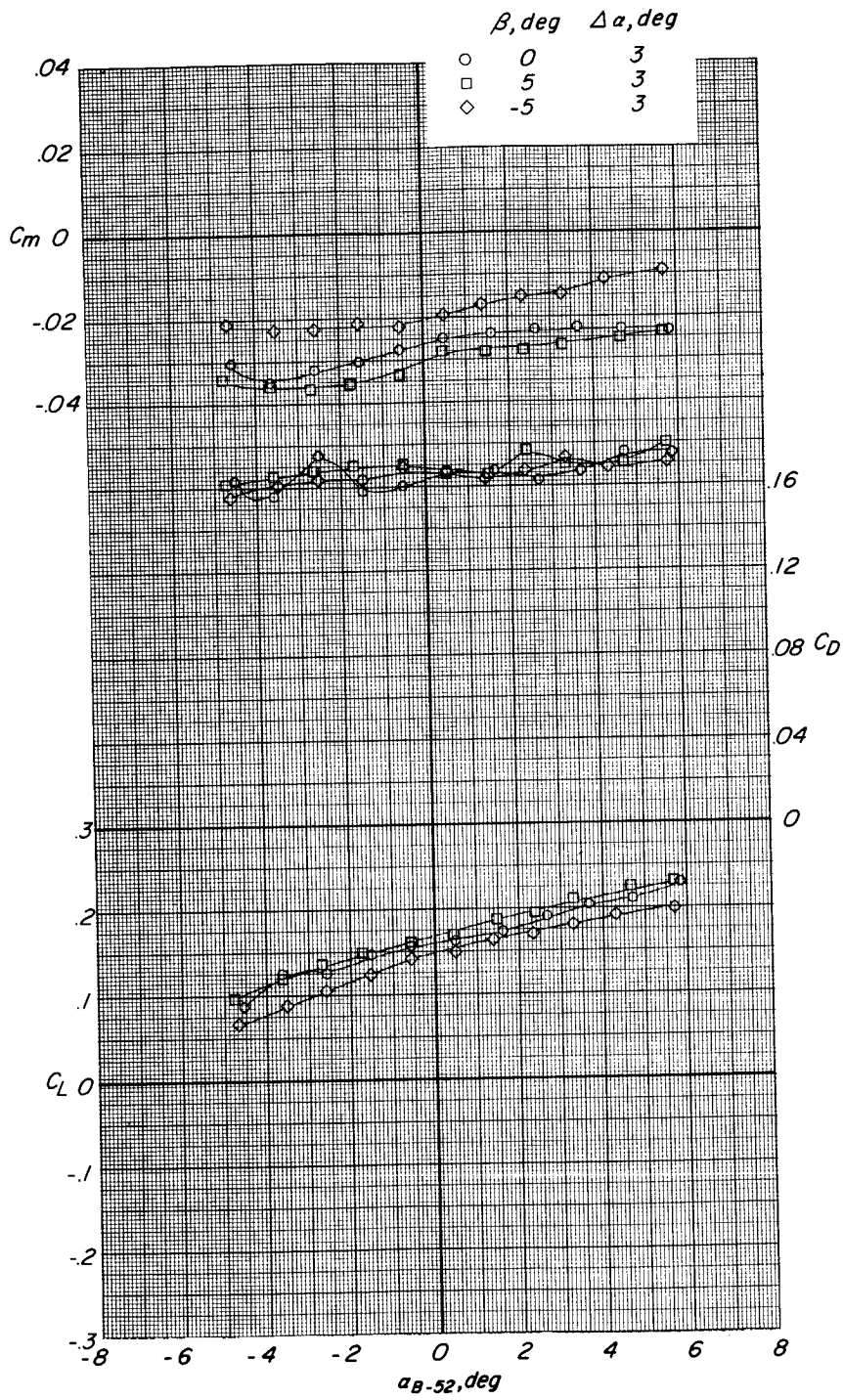

(c) Continued.

Figure 10.- Continued.

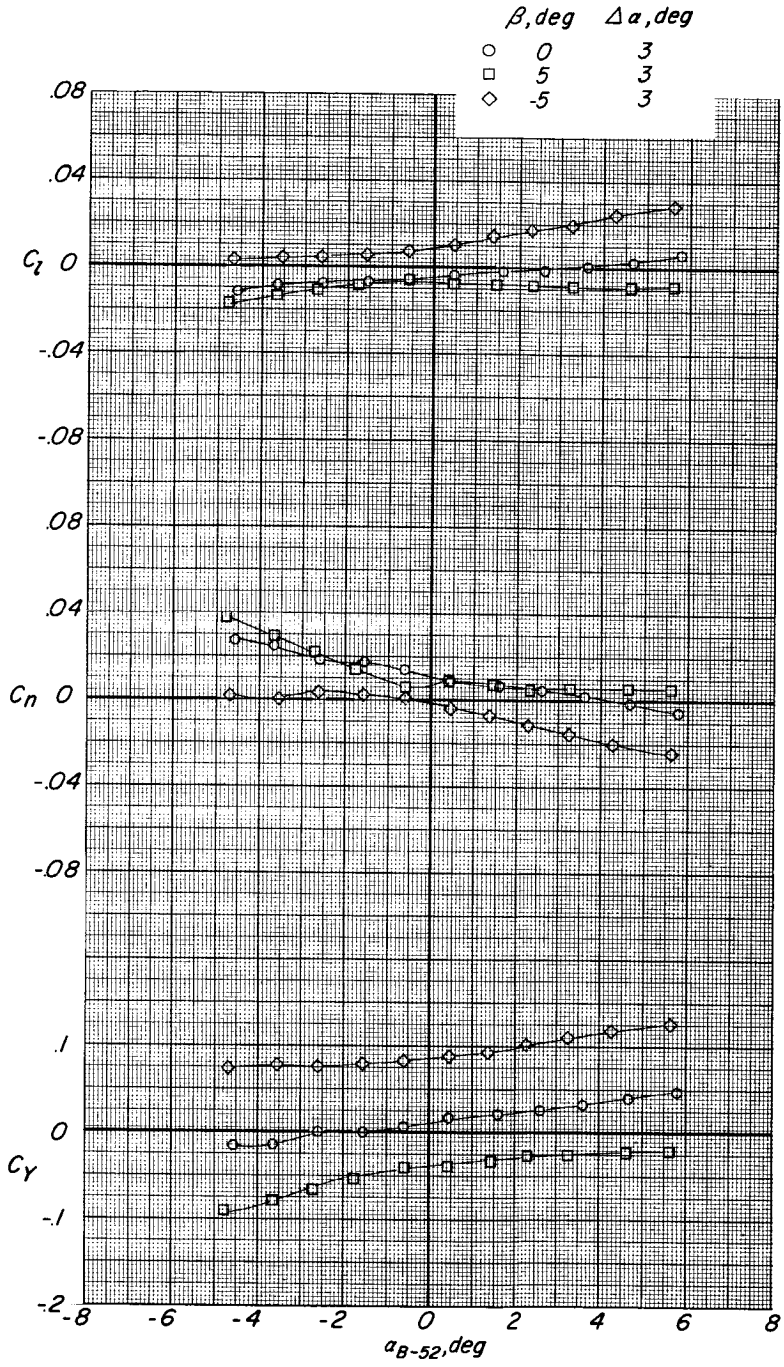

(c) Concluded.

Figure 10.- Continued.

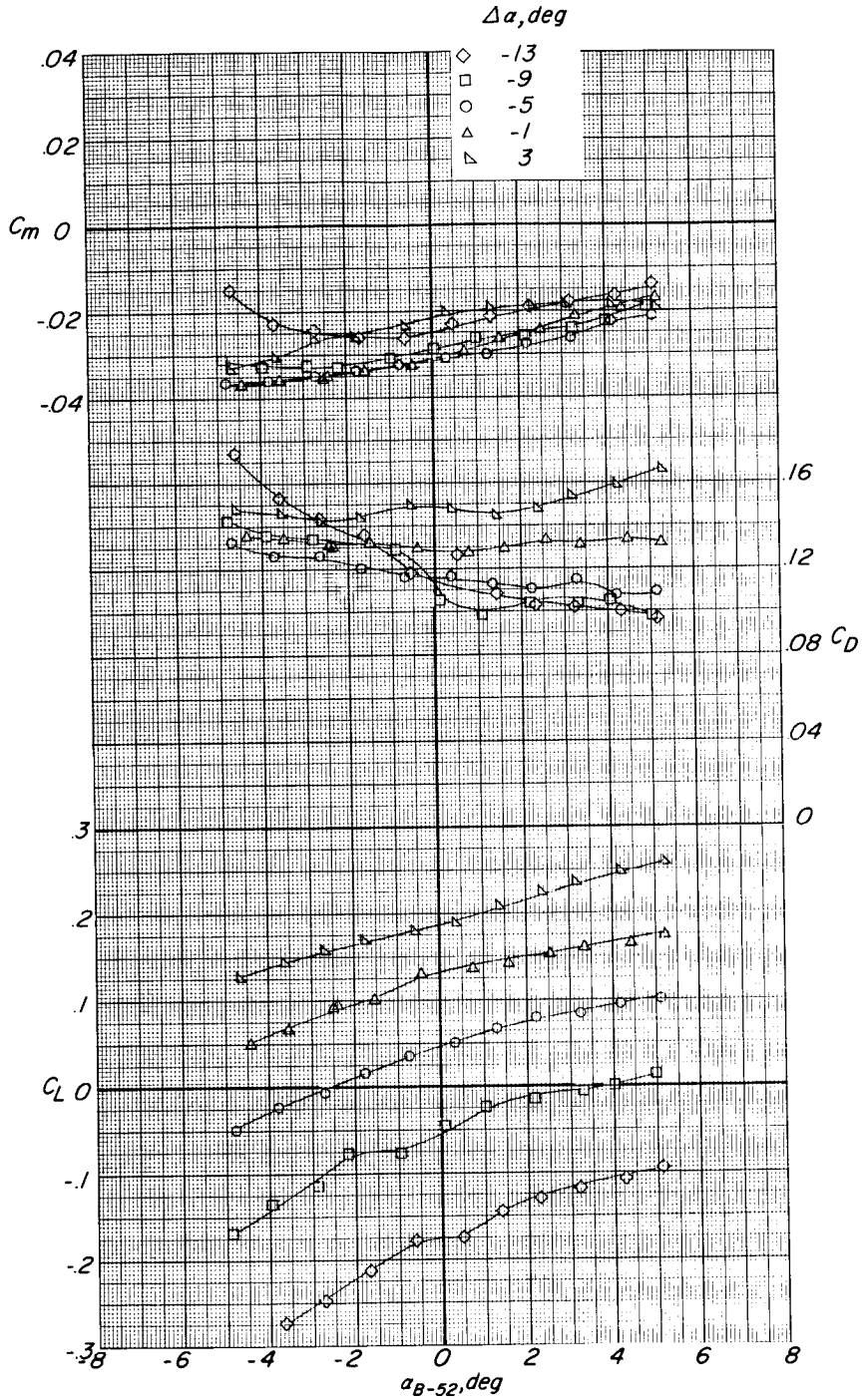

(d) z' = 8.0 feet (2.44 m).

Figure 10.- Continued.

[redacted] DECLASSIFIED

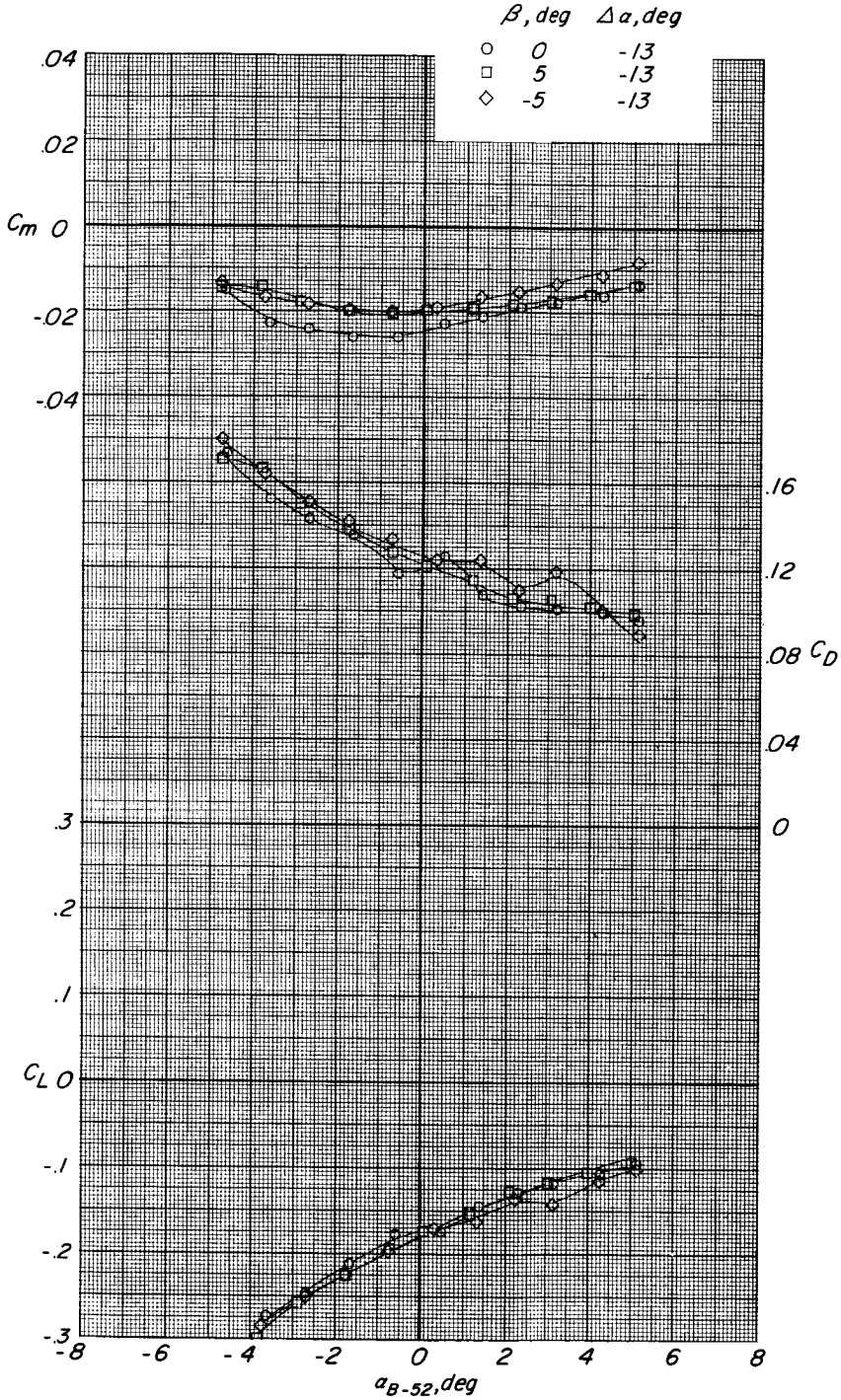

(d) Continued.

Figure 10.- Continued.

[redacted]

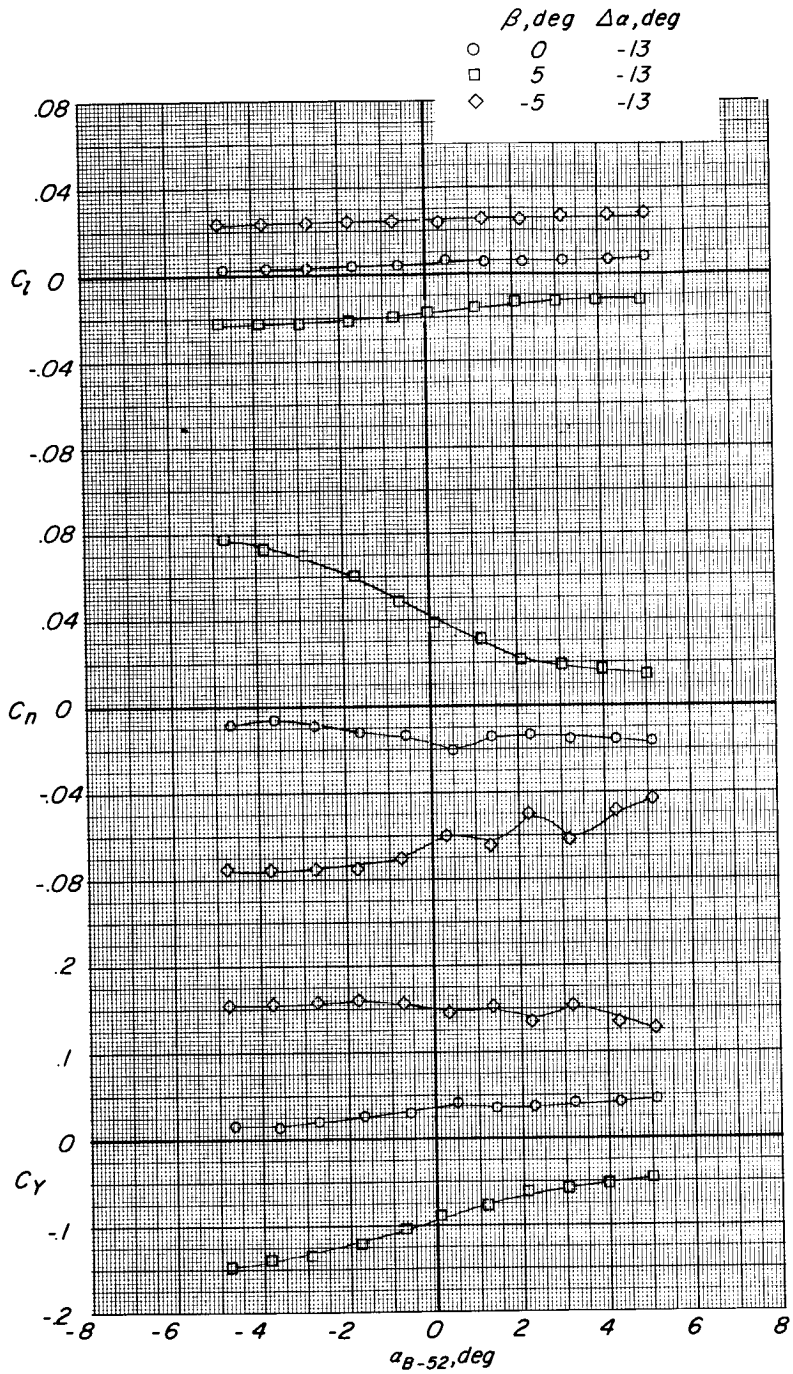

(d) Continued.

Figure 10.- Continued.

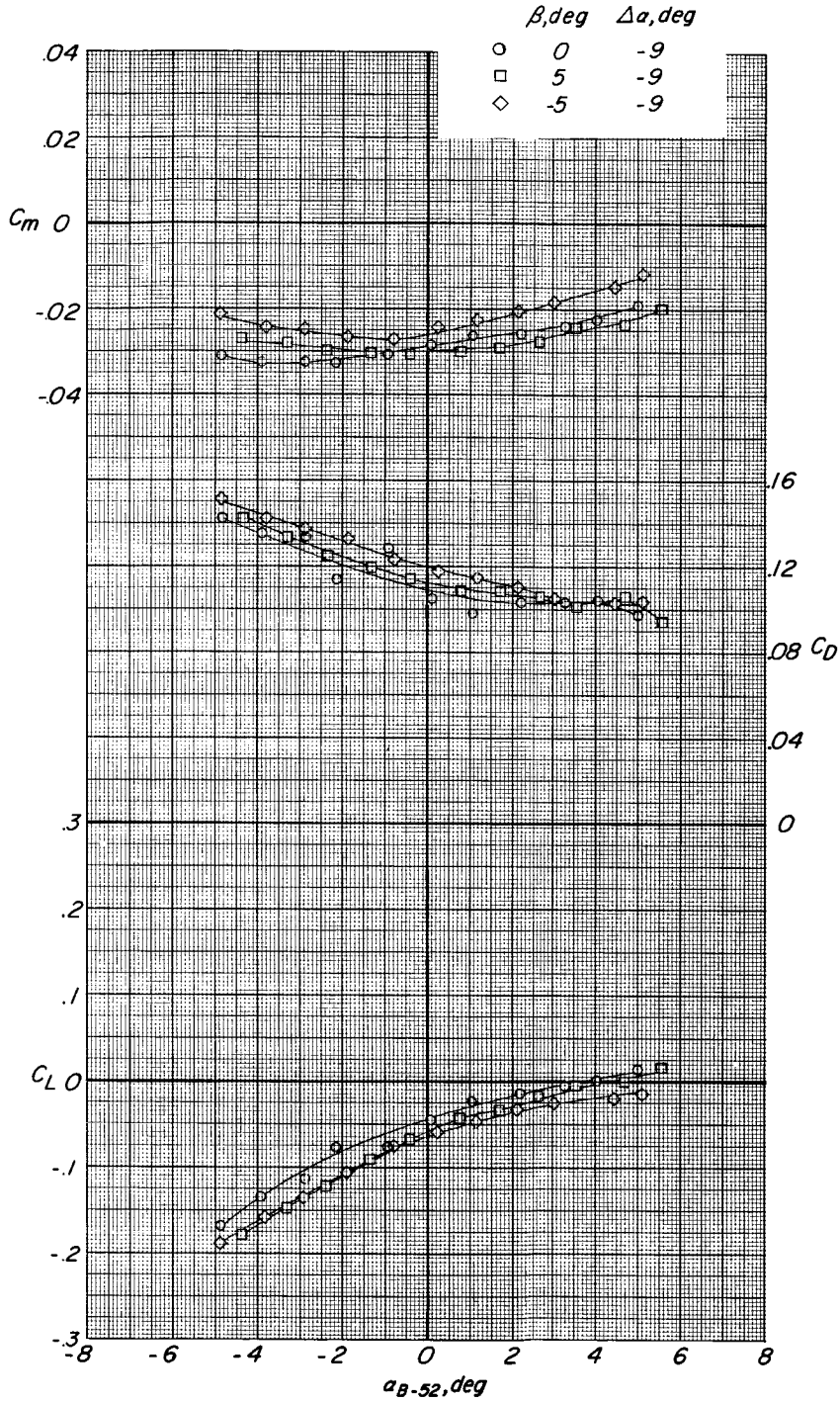

(d) Continued.

Figure 10.- Continued.

[redacted]

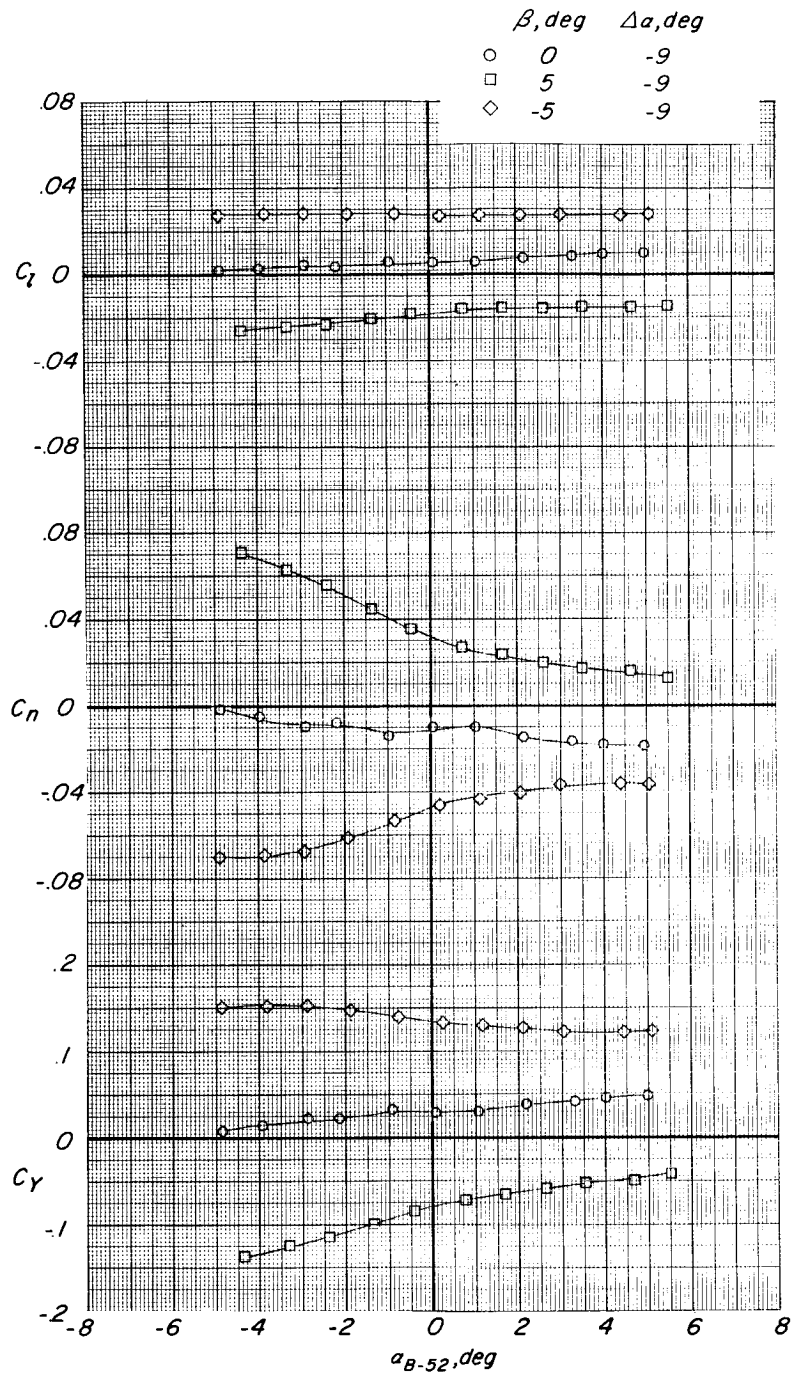

(d) Continued.

Figure 10.- Continued.

[redacted]

[redacted]ASSIFIED

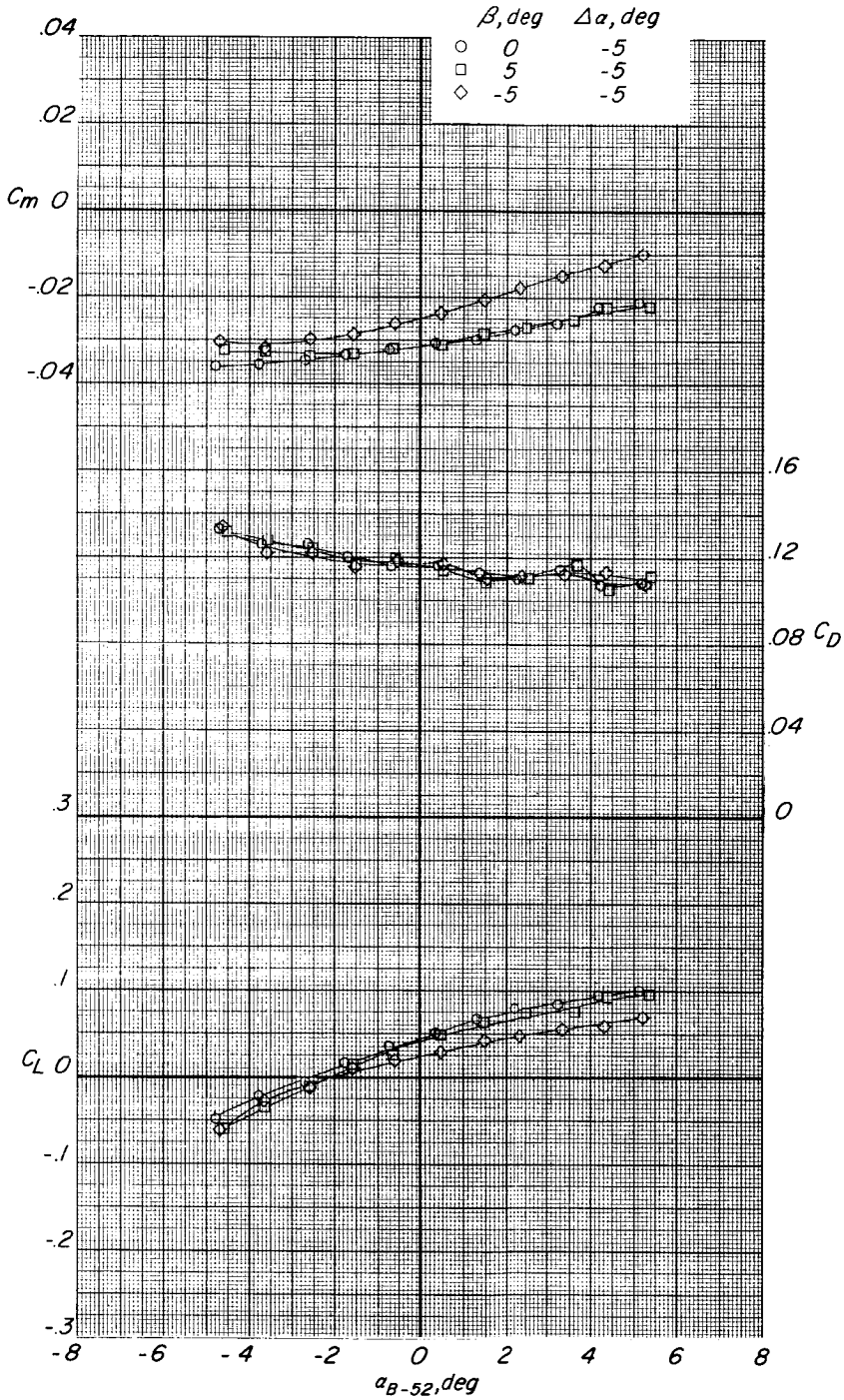

(d) Continued.

Figure 10.- Continued.

[redacted]

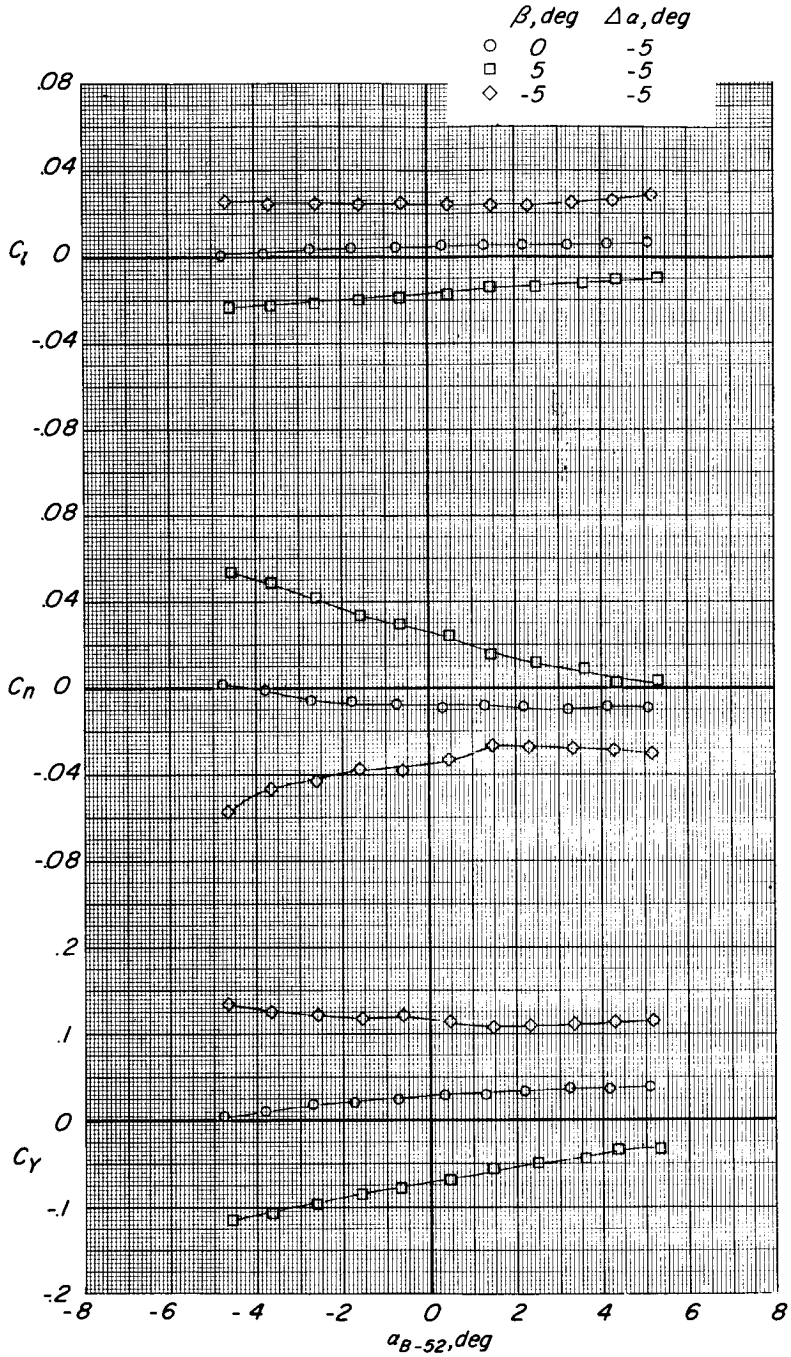

(d) Continued.

Figure 10.- Continued.

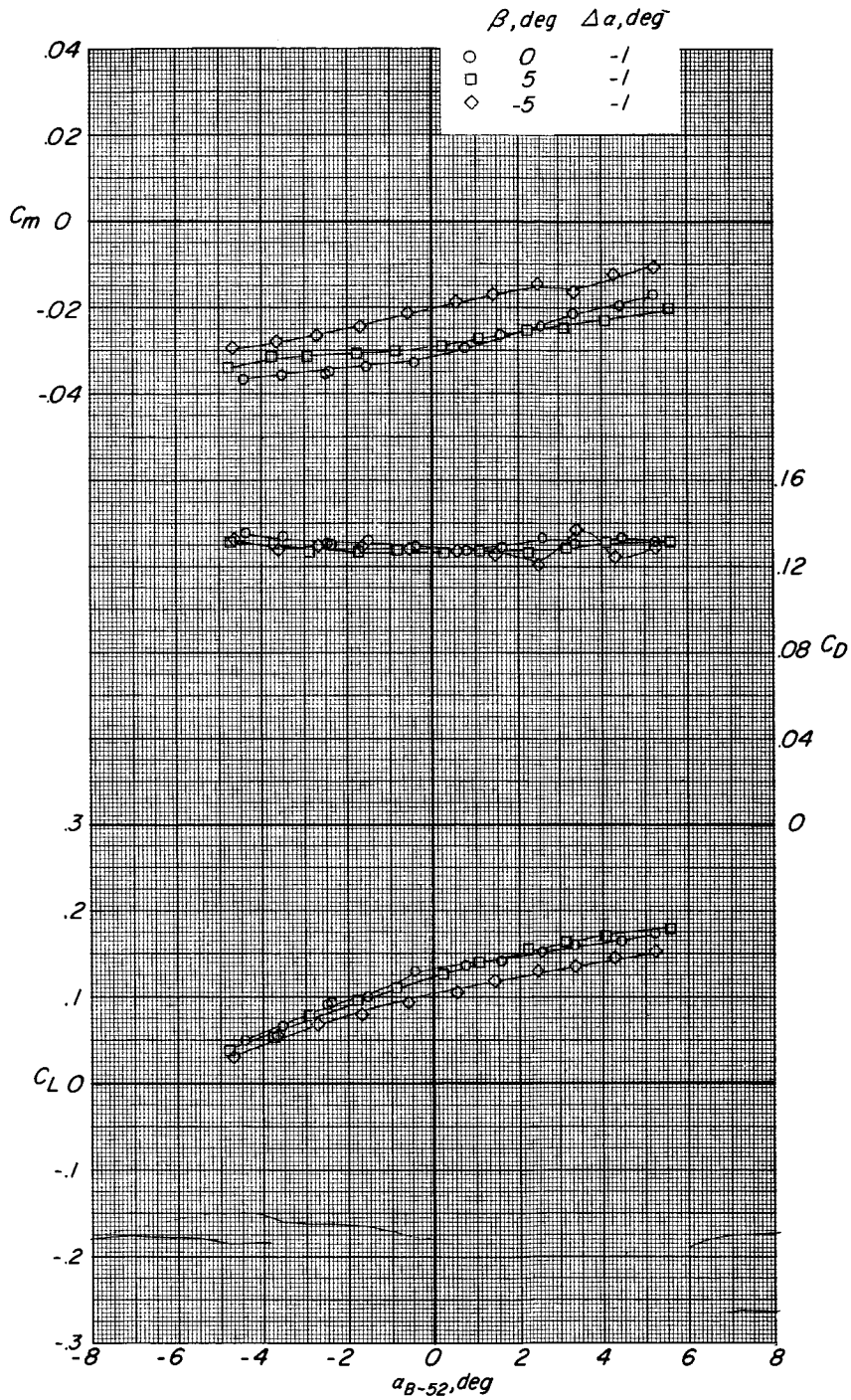

(d) Continued.

Figure 10.- Continued.

[redacted]

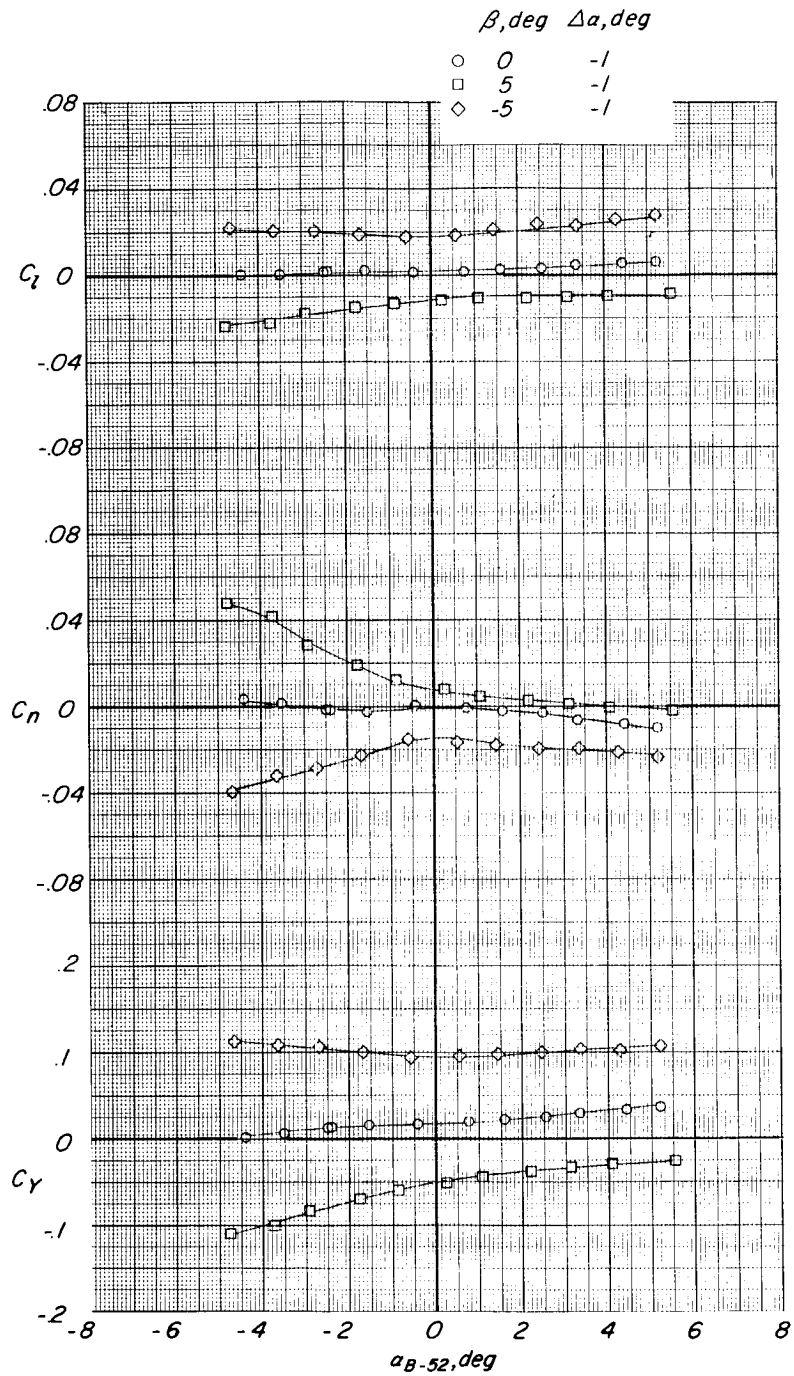

(d) Continued.

Figure 10.- Continued.

[redacted]

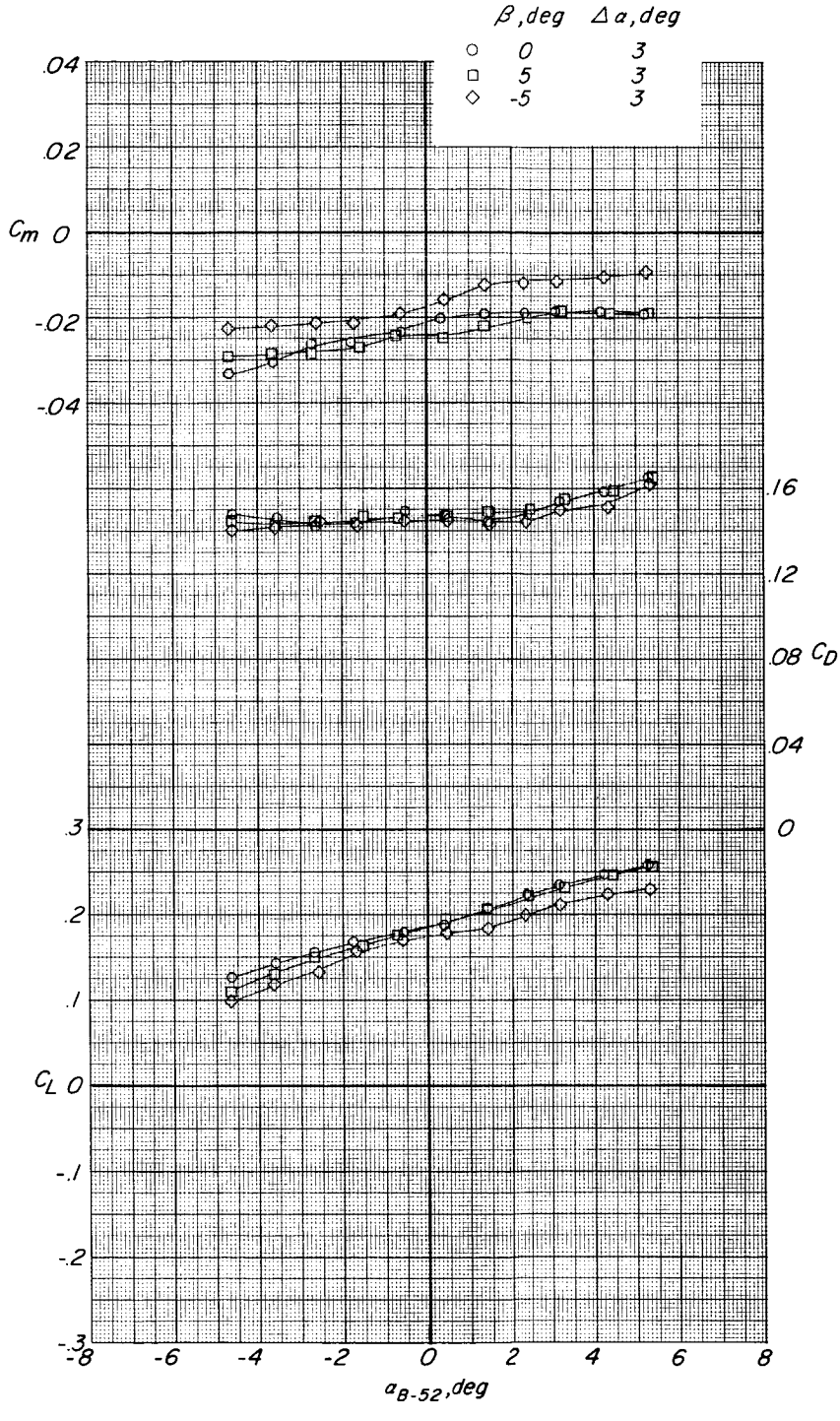

(d) Continued.

Figure 10.- Continued.

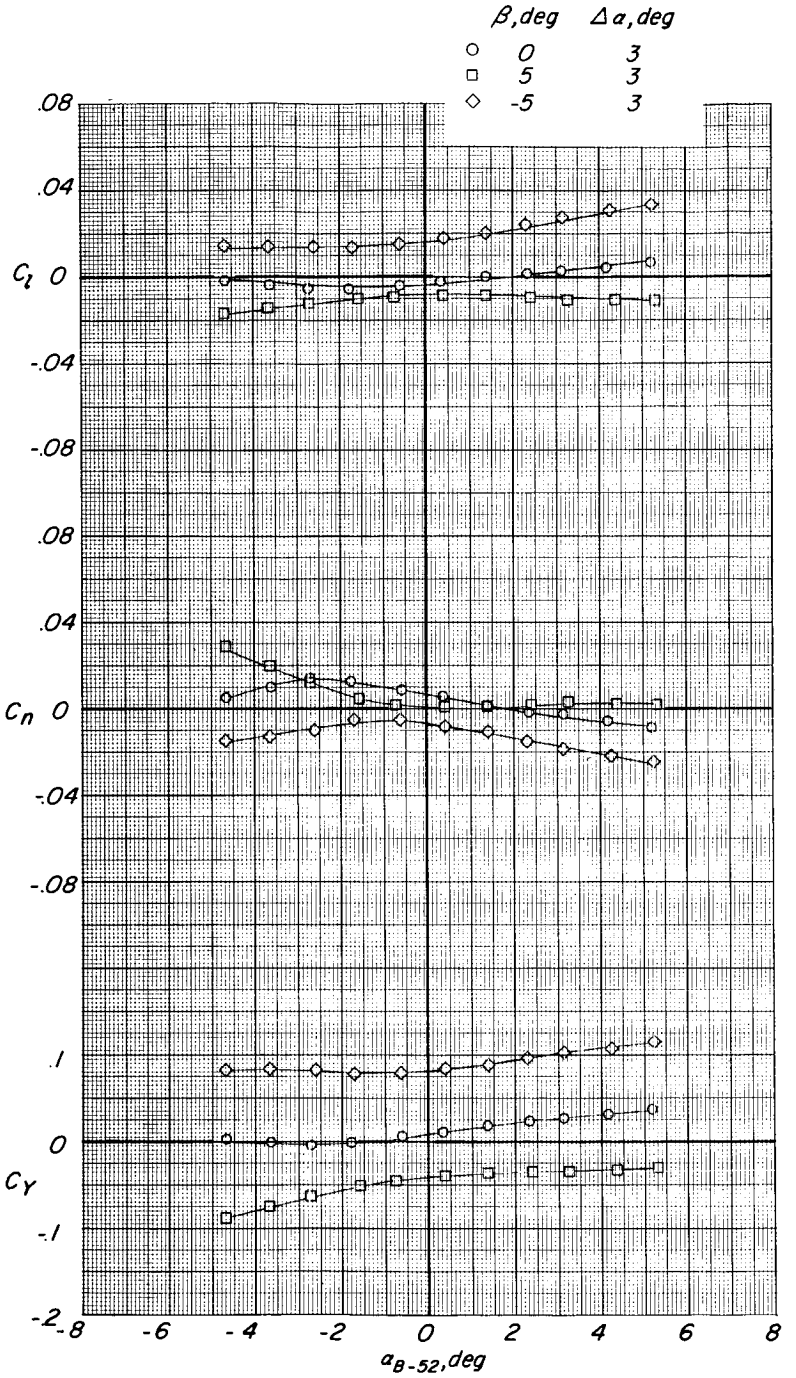

(d) Concluded.

Figure 10.- Continued.

DECLASSIFIED

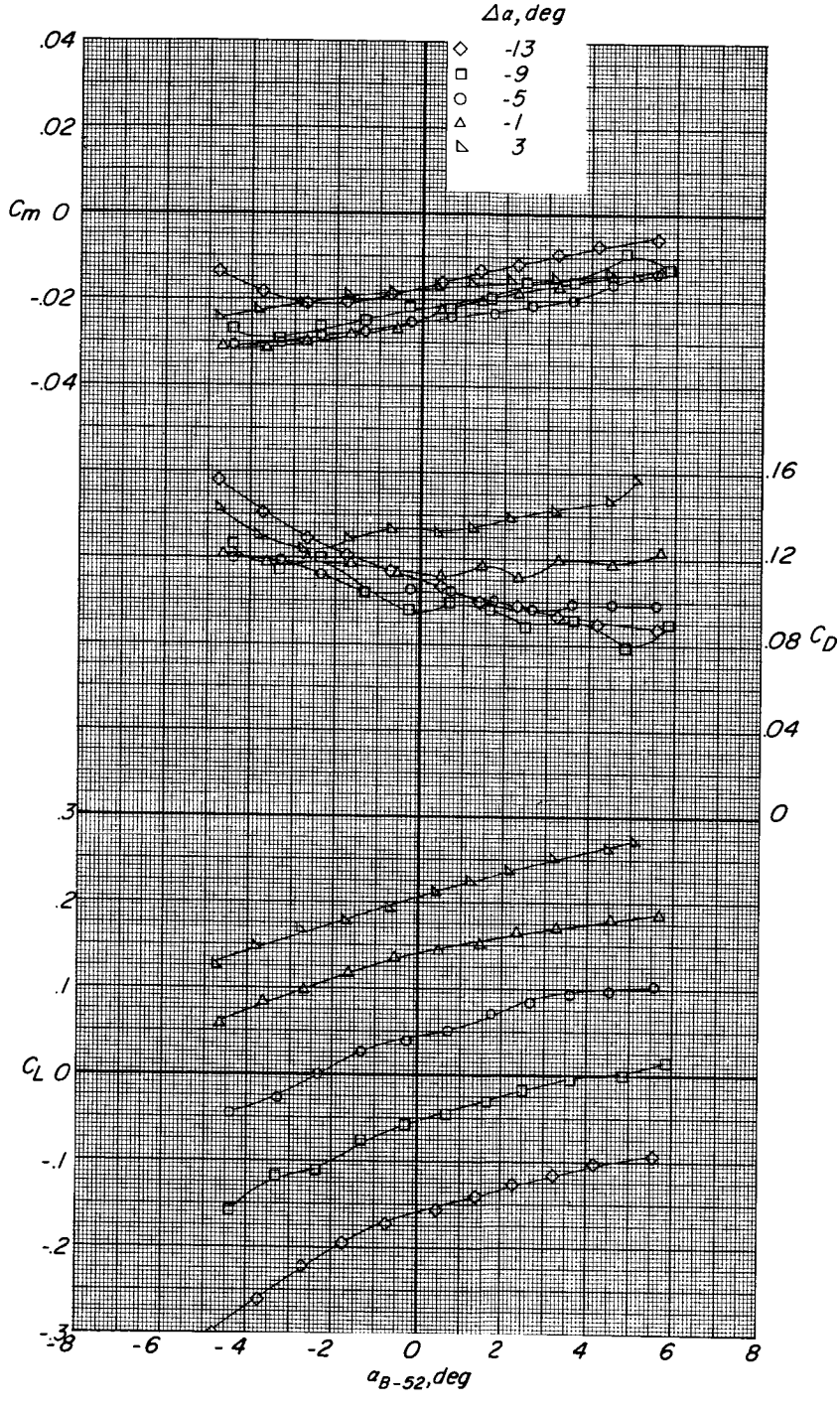

(e) z' = 12.0 feet (3.66 m).

Figure 10.- Continued.

[redacted]

[redacted]

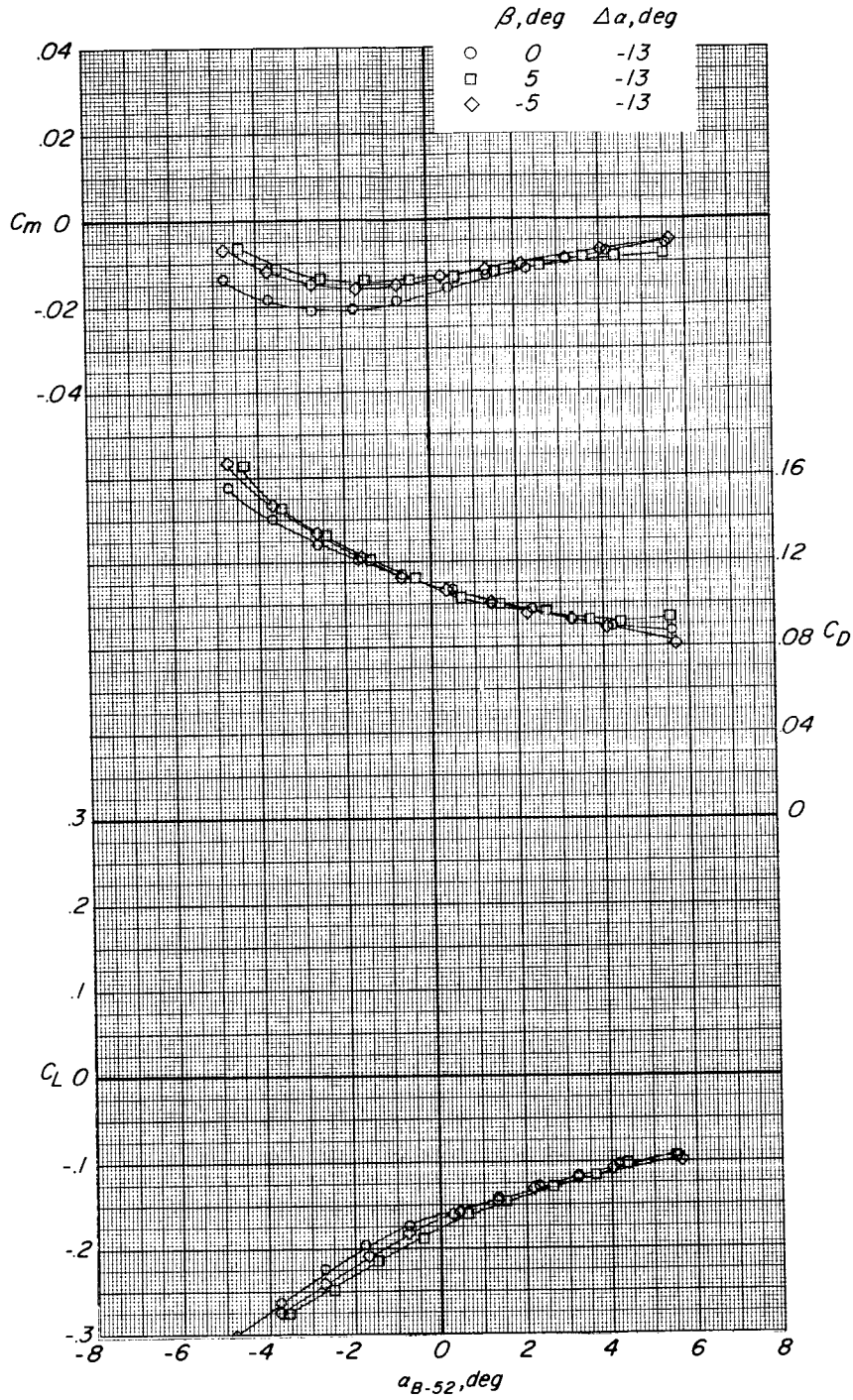

(e) Continued.

Figure 10.- Continued.

[redacted]

DECLASSIFIED

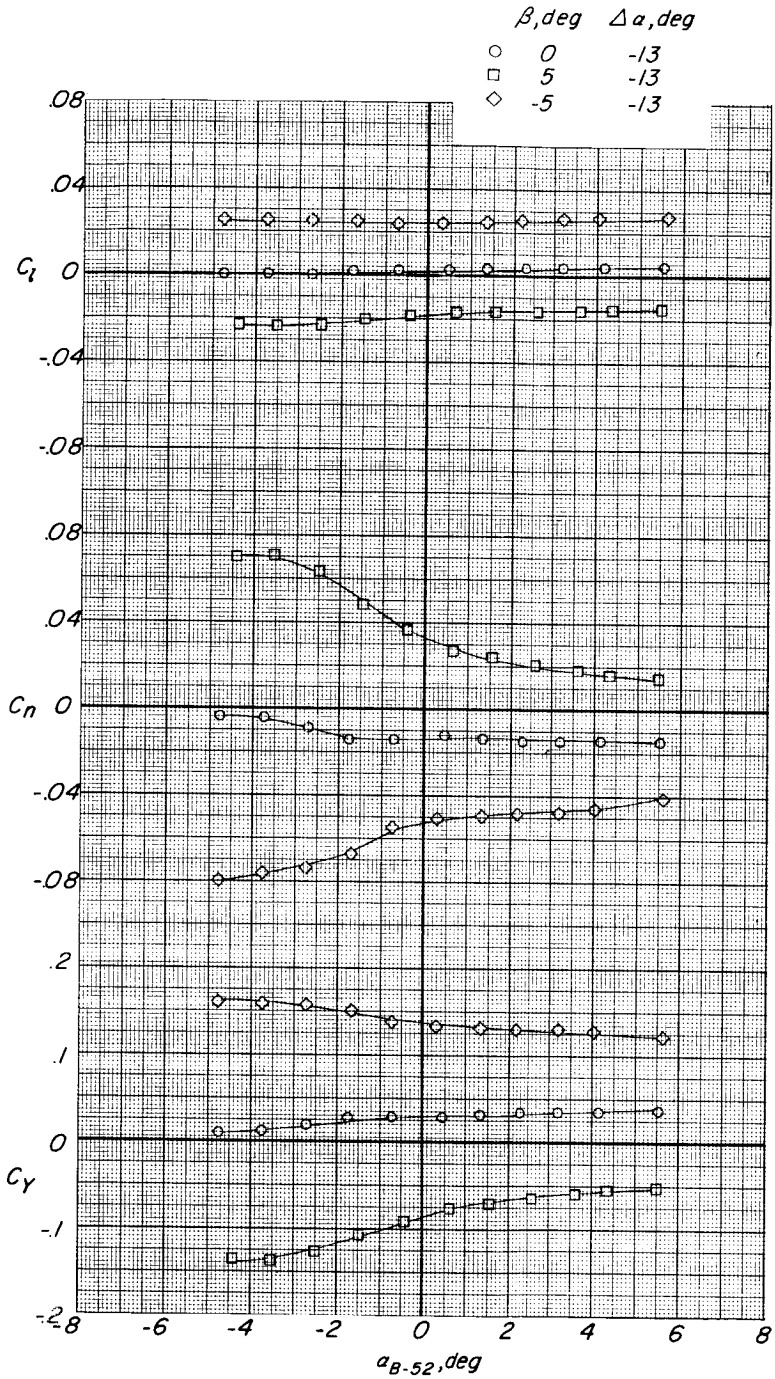

(e) Continued.

Figure 10.- Continued.

[redacted]

DECLASSIFIED

[redacted]

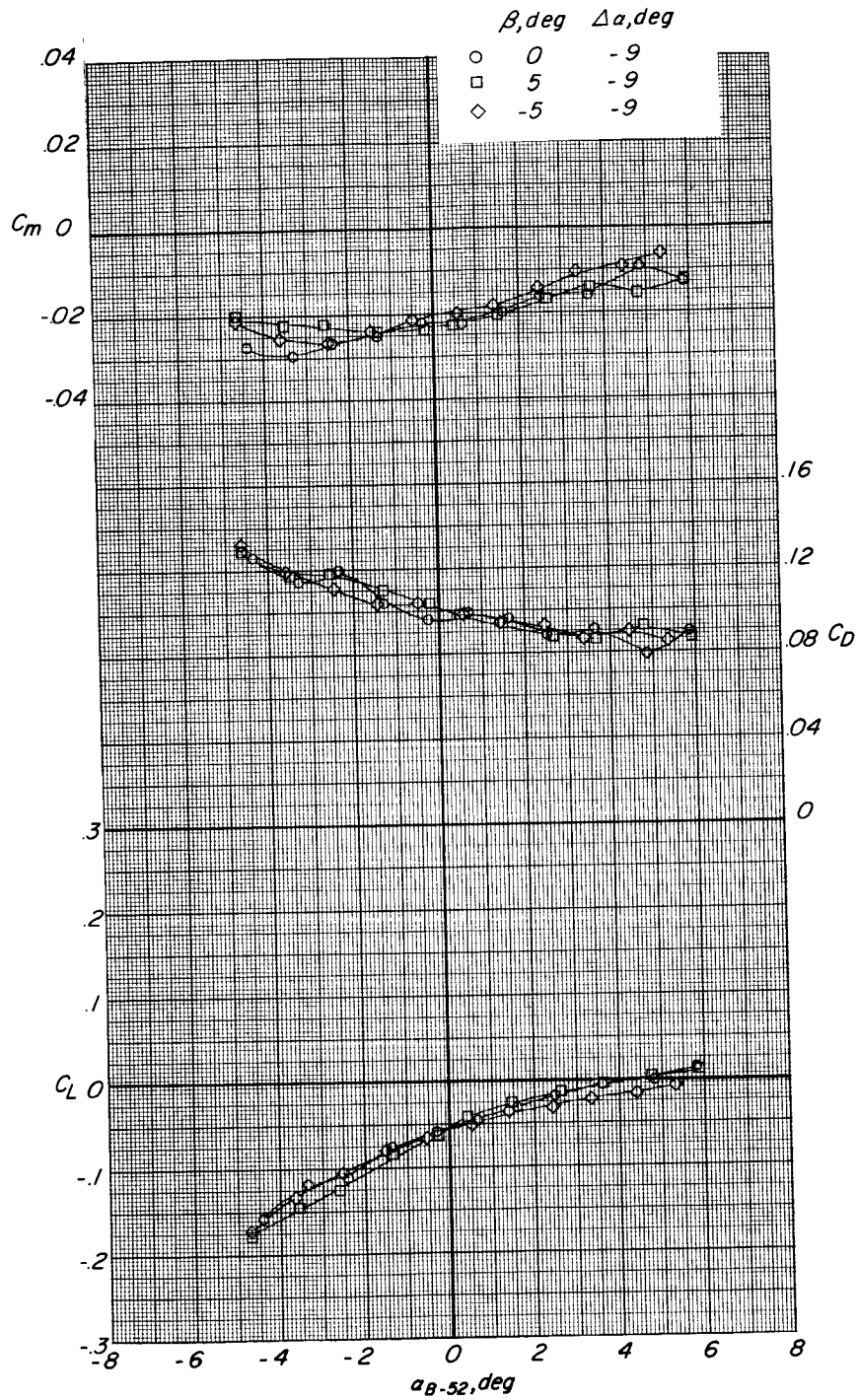

(e) Continued.

Figure 10.- Continued.

[redacted]

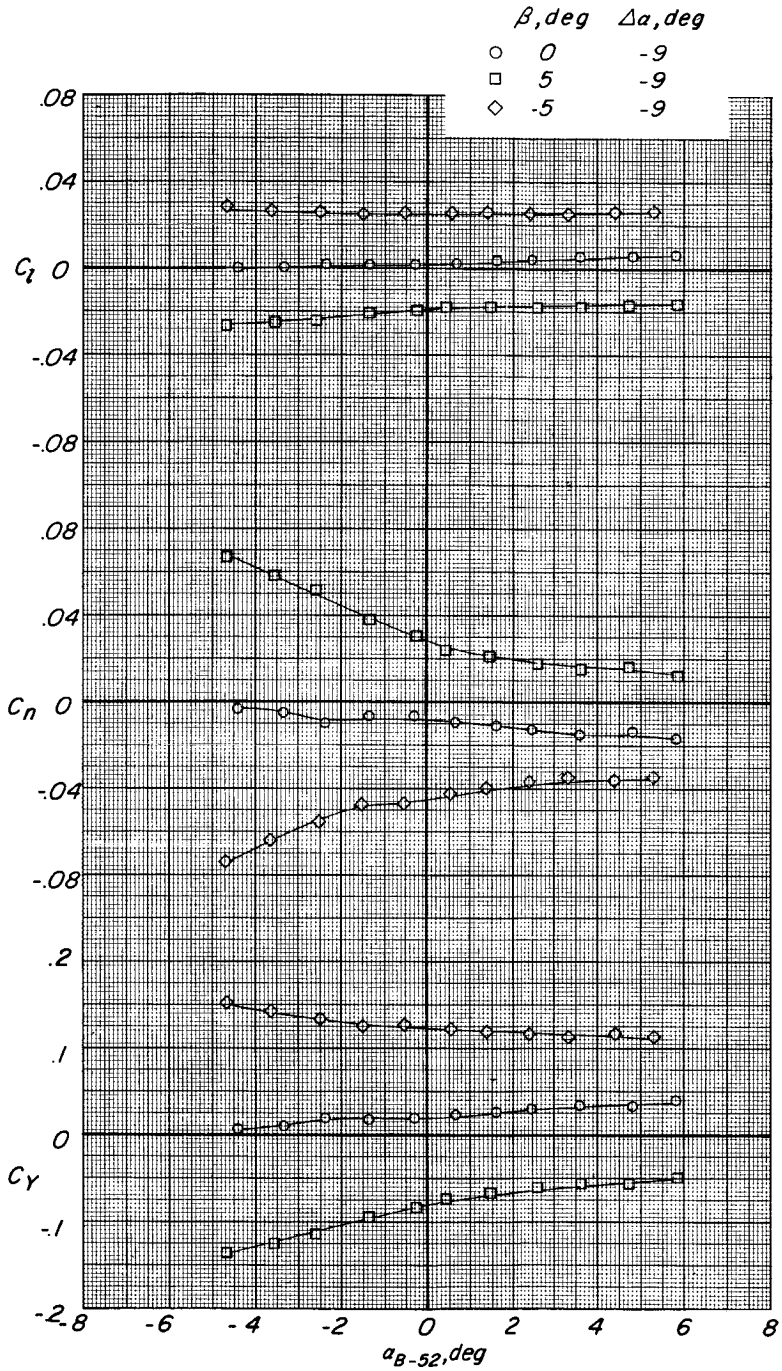

(e) Continued.

Figure 10.- Continued.

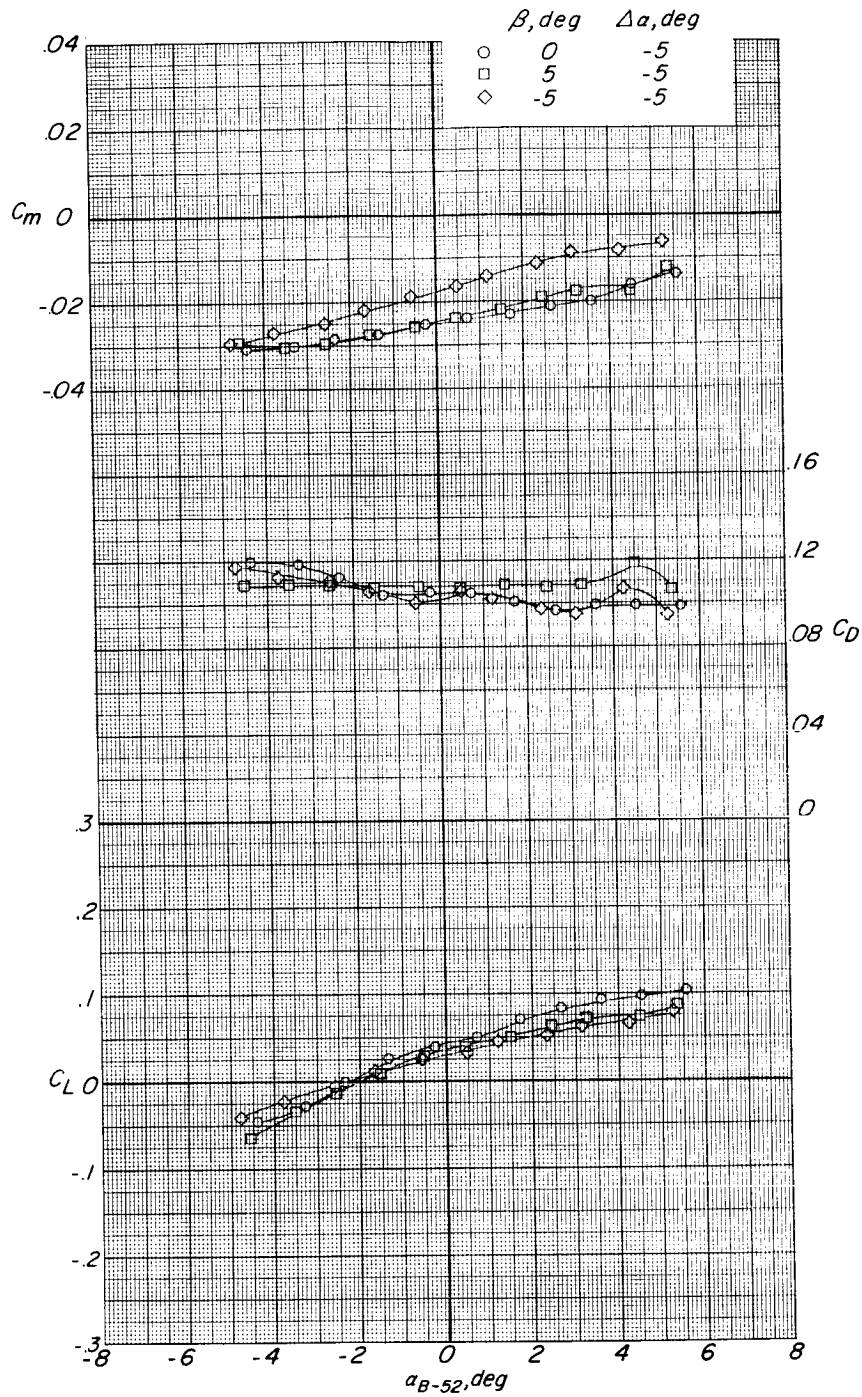

(e) Continued.

Figure 10.- Continued.

[redacted]ASSIFIED

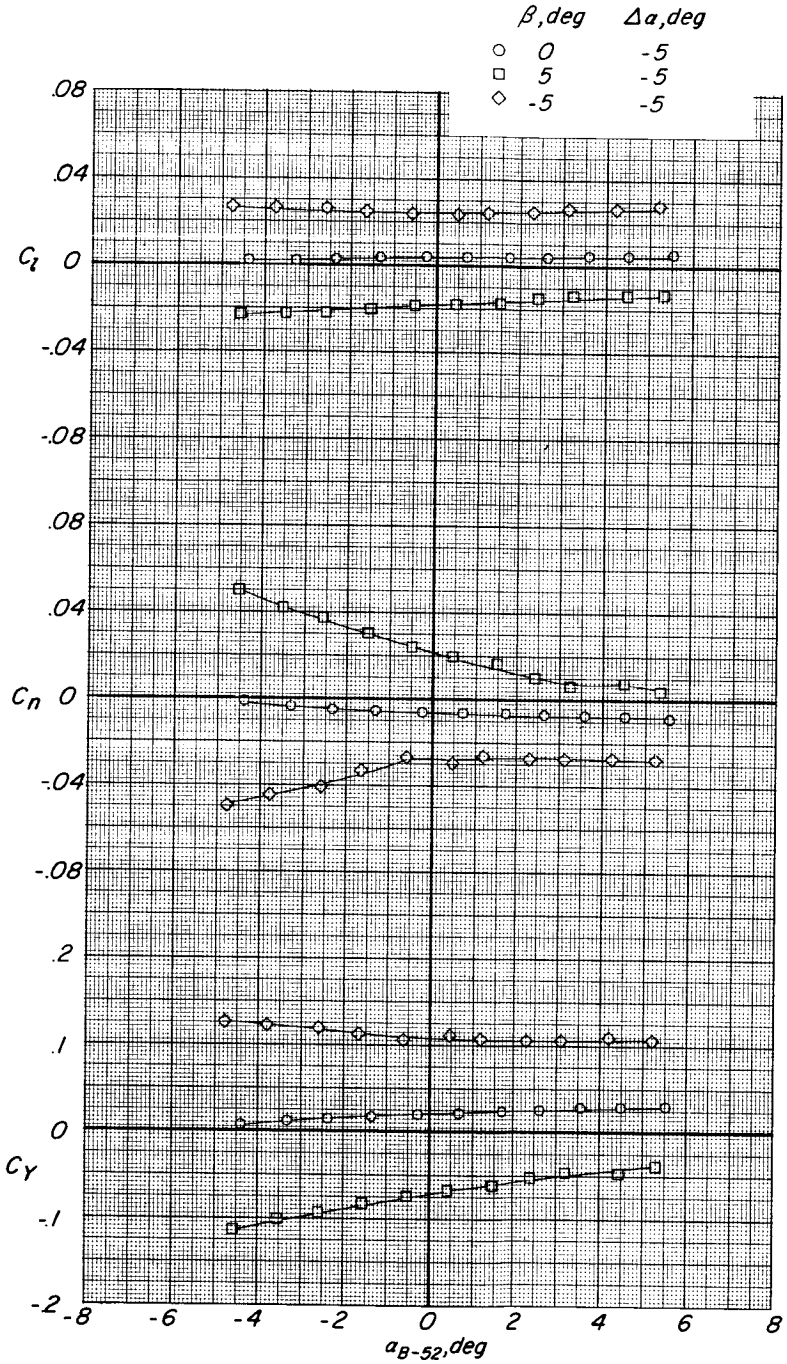

(e) Continued.

Figure 10.- Continued.

[redacted]

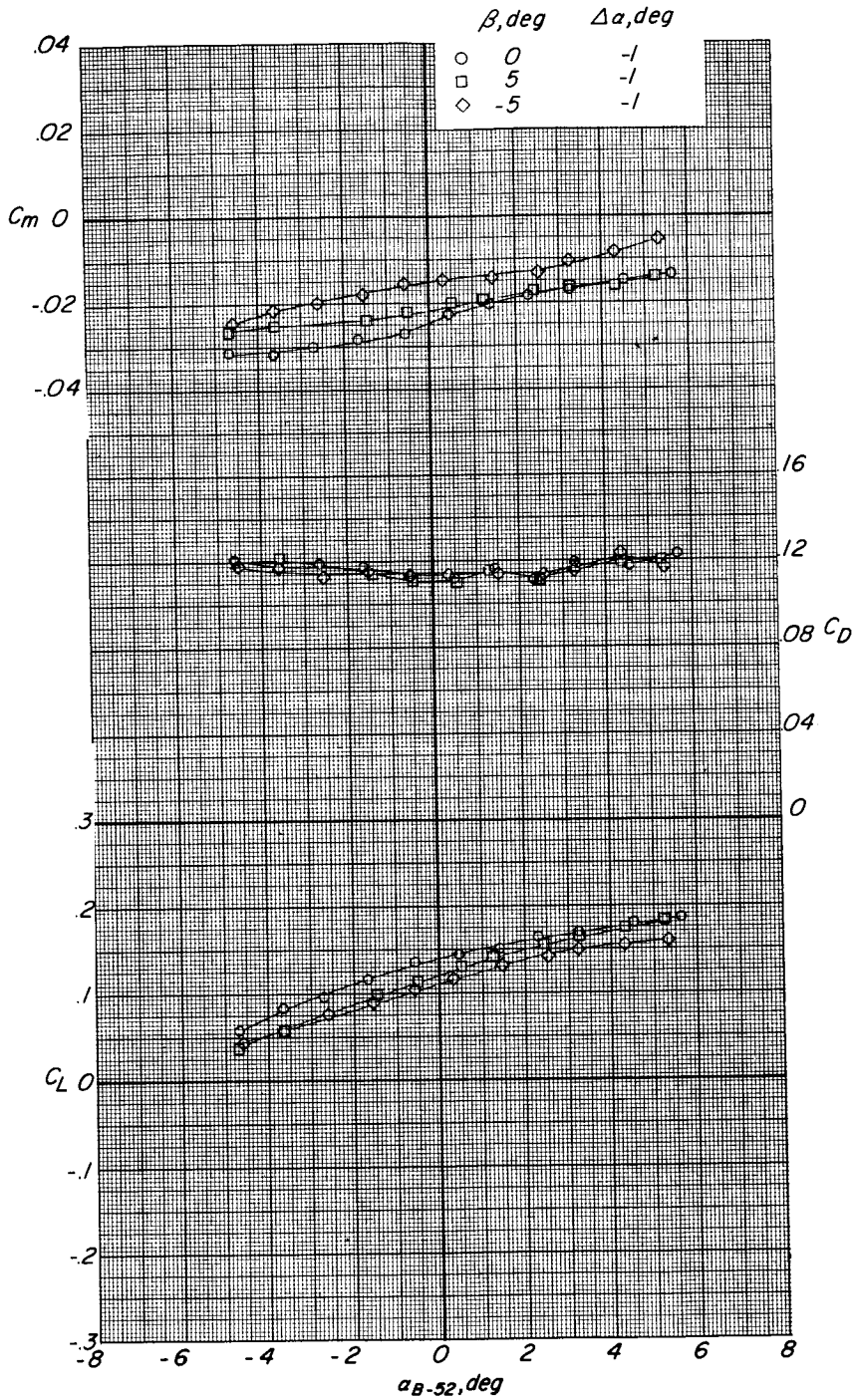

(e) Continued.

Figure 10.- Continued.

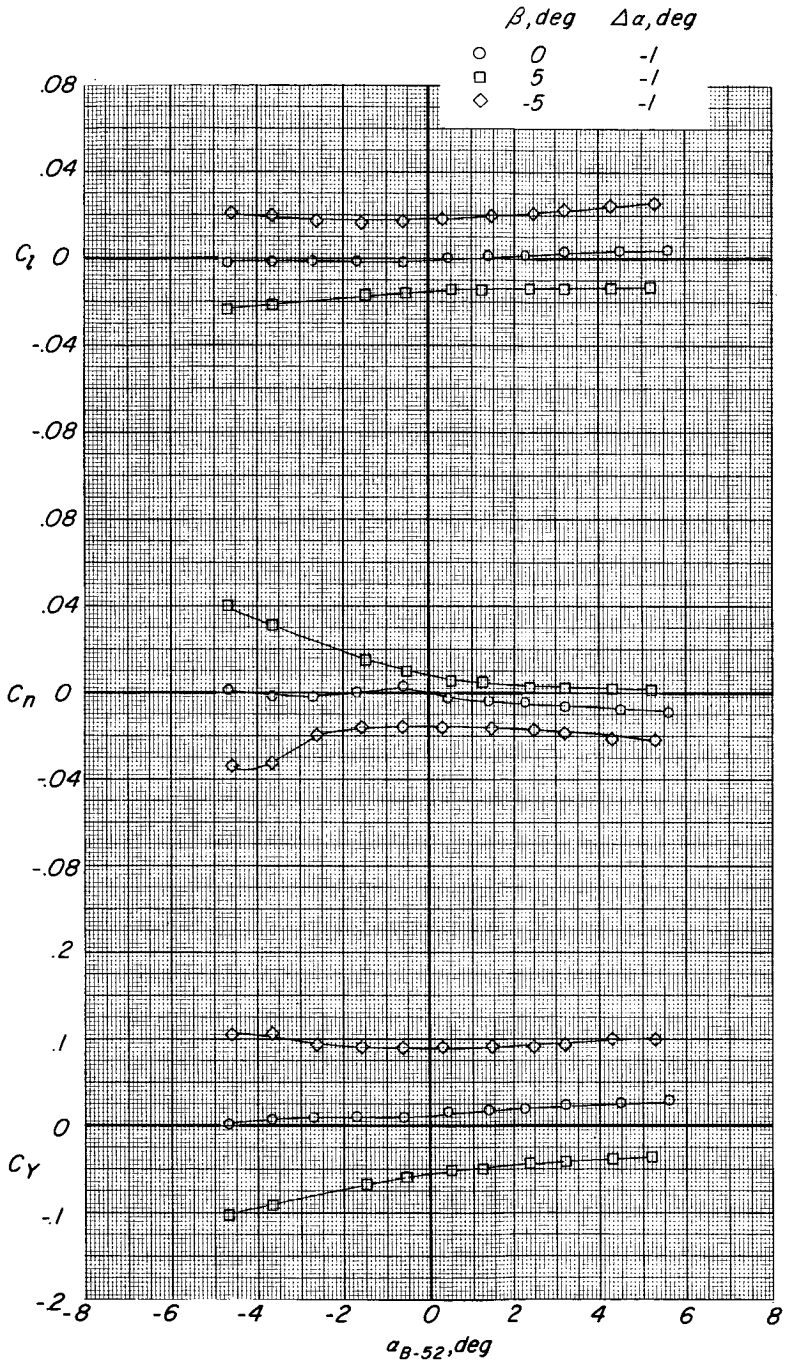

(e) Continued.

Figure 10.- Continued.

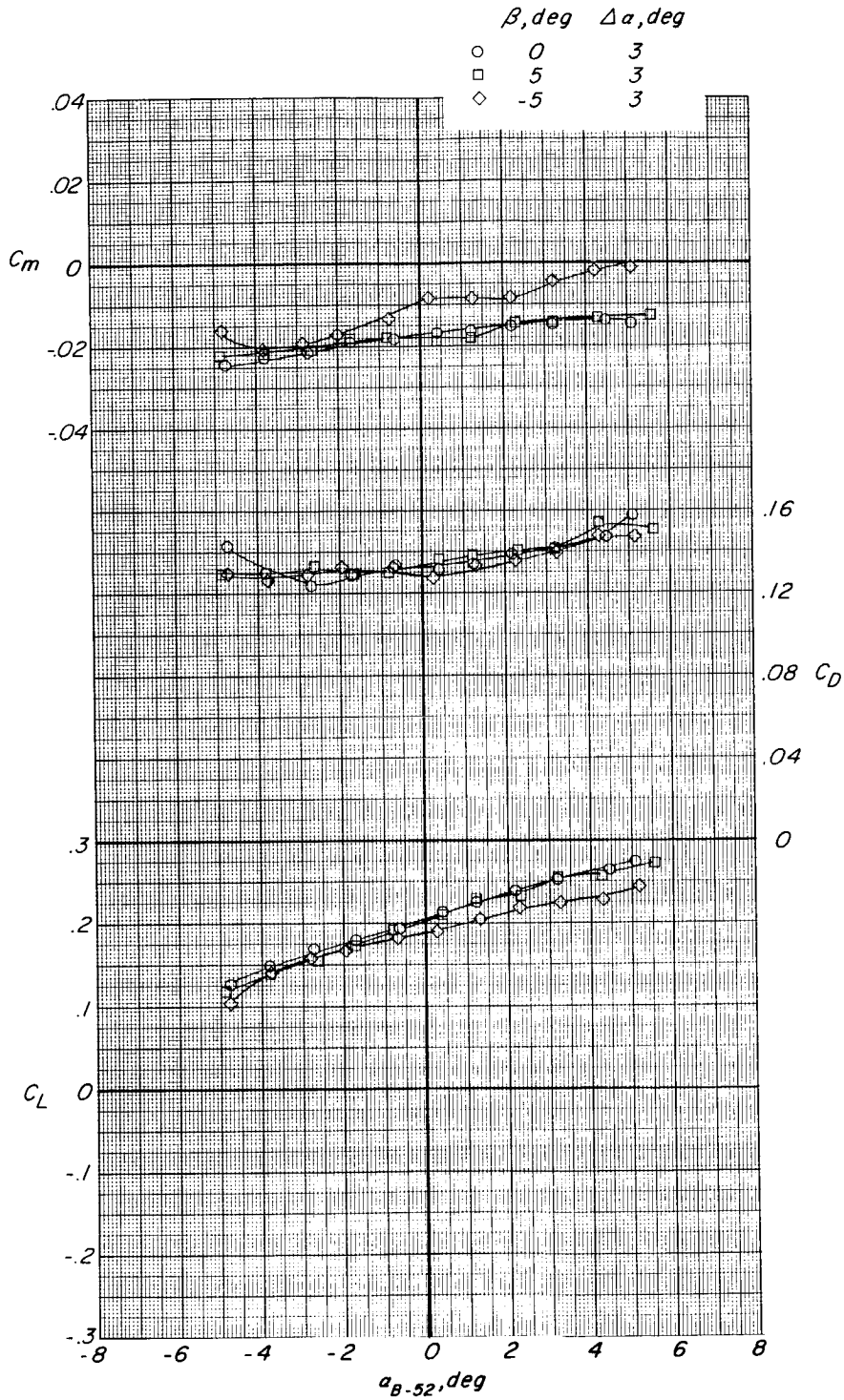

(e) Continued.

Figure 10.- Continued.

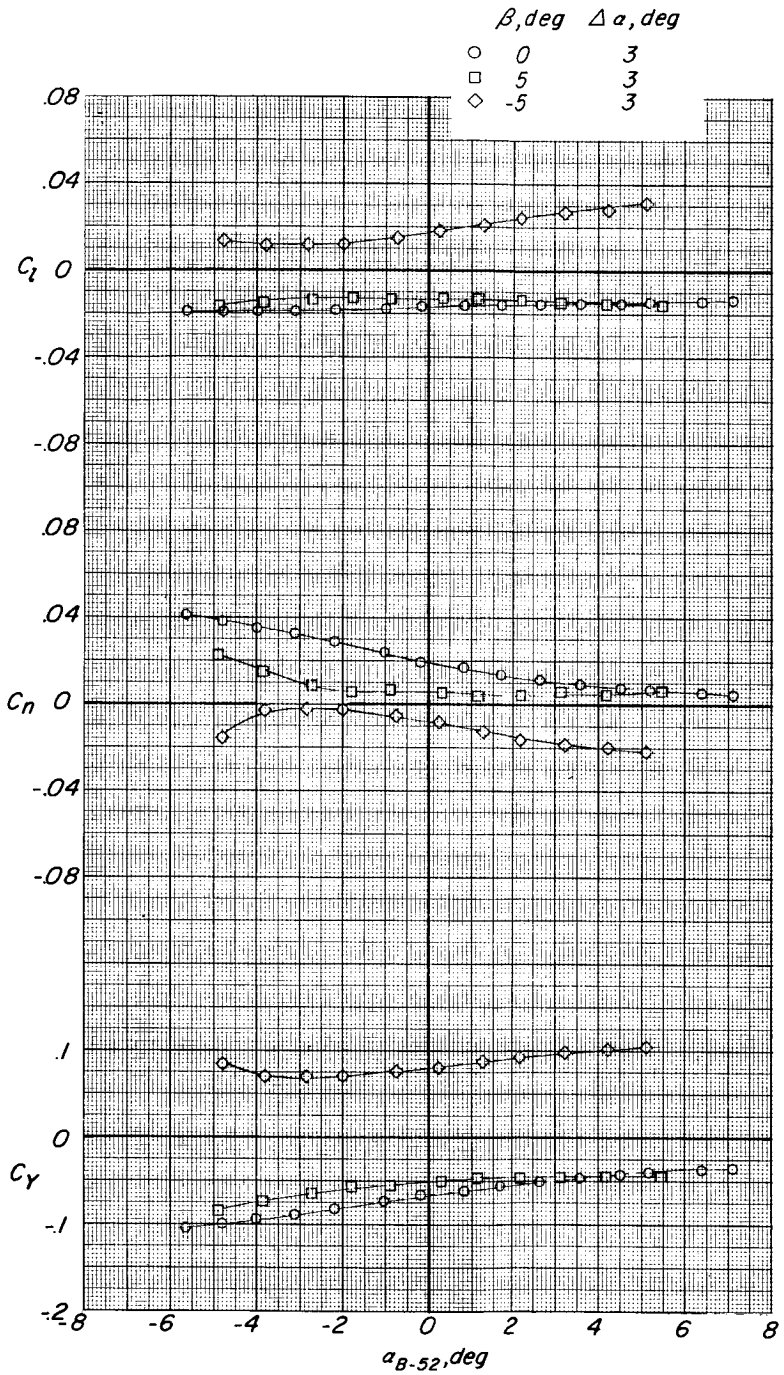

(e) Concluded.

Figure 10.- Concluded.

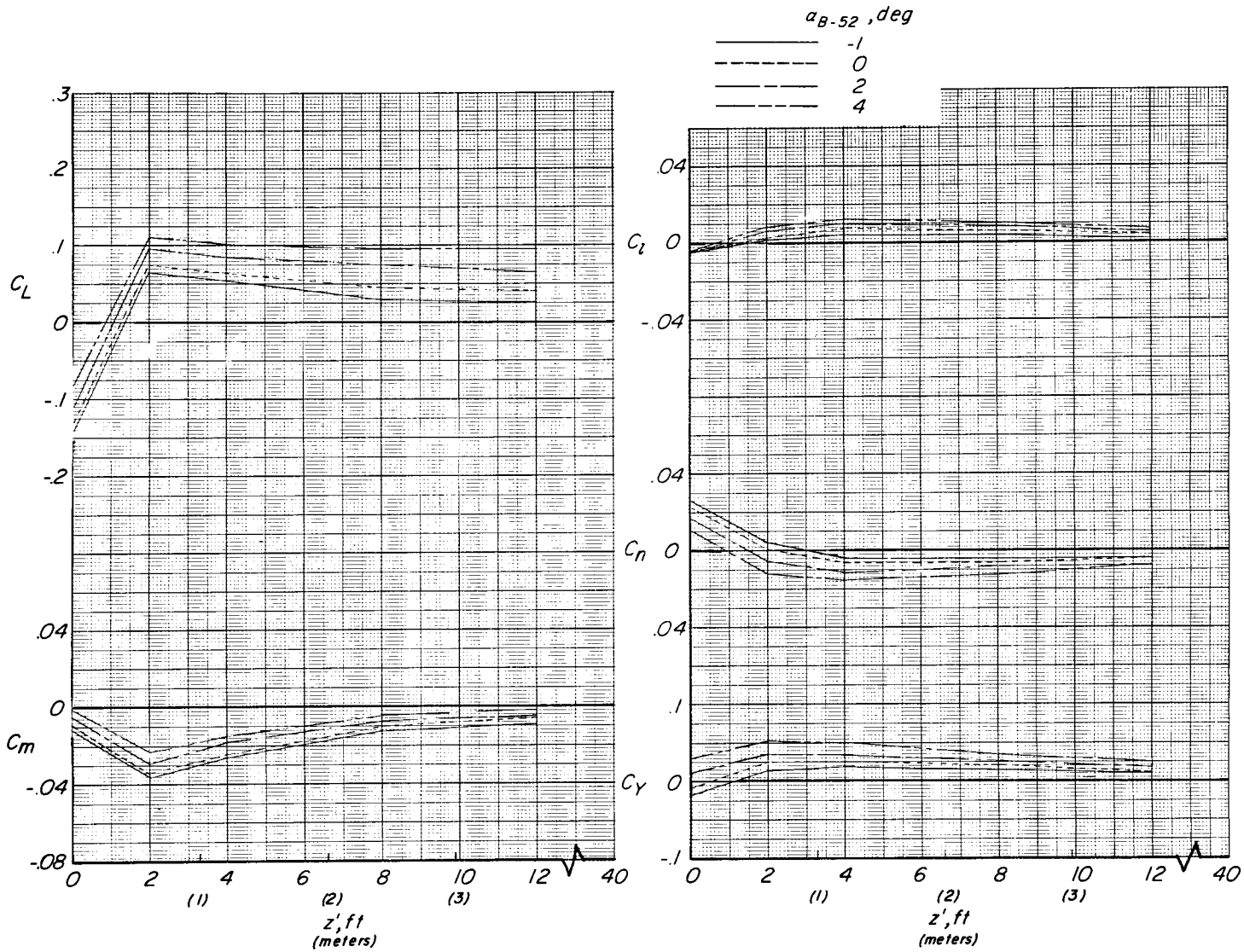

(a) M = 0.60.

Figure 11.- Variation of force and moment coefficients with separation distance.

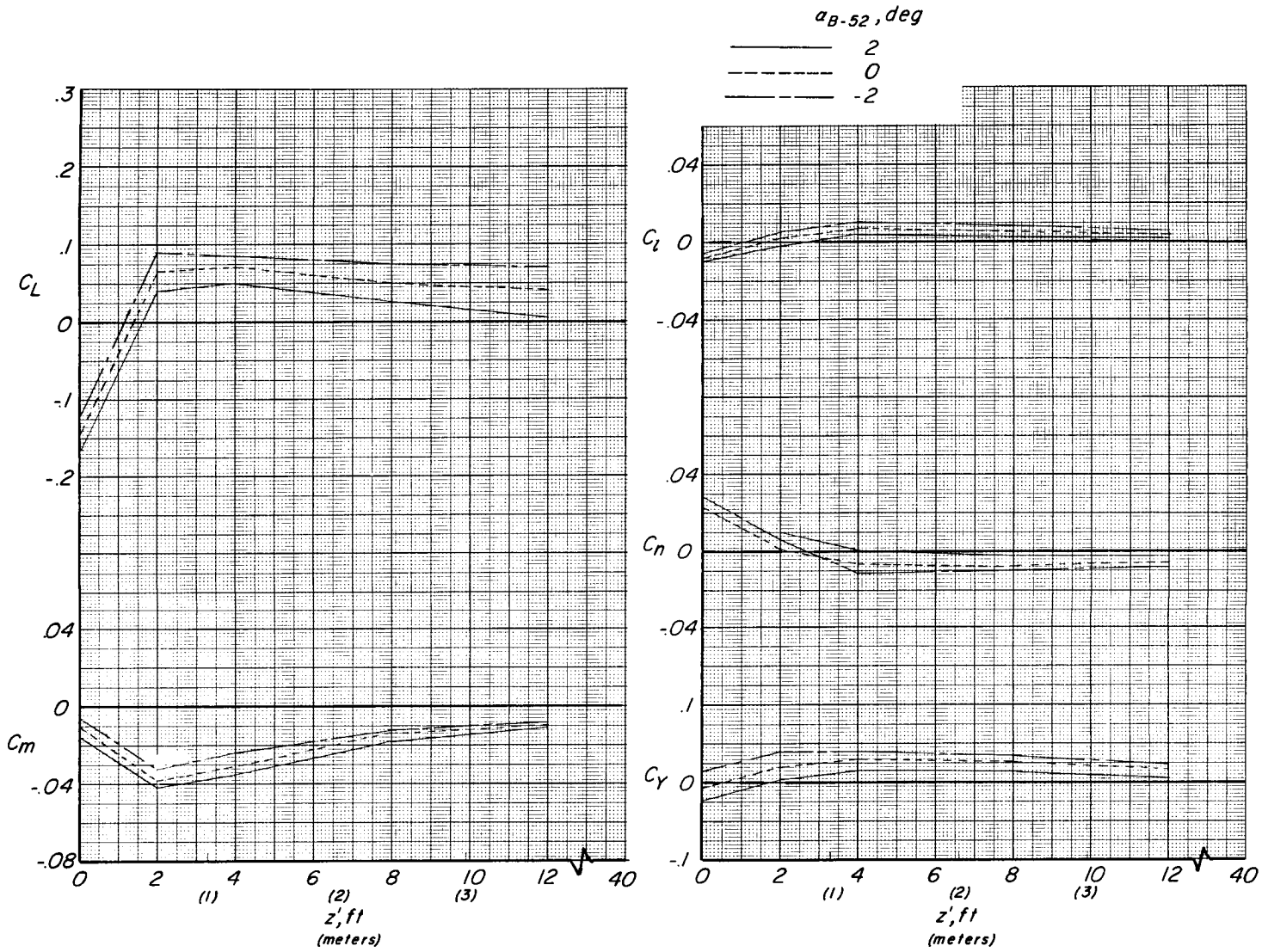

(b) M = 0.70.

Figure 11.- Continued.

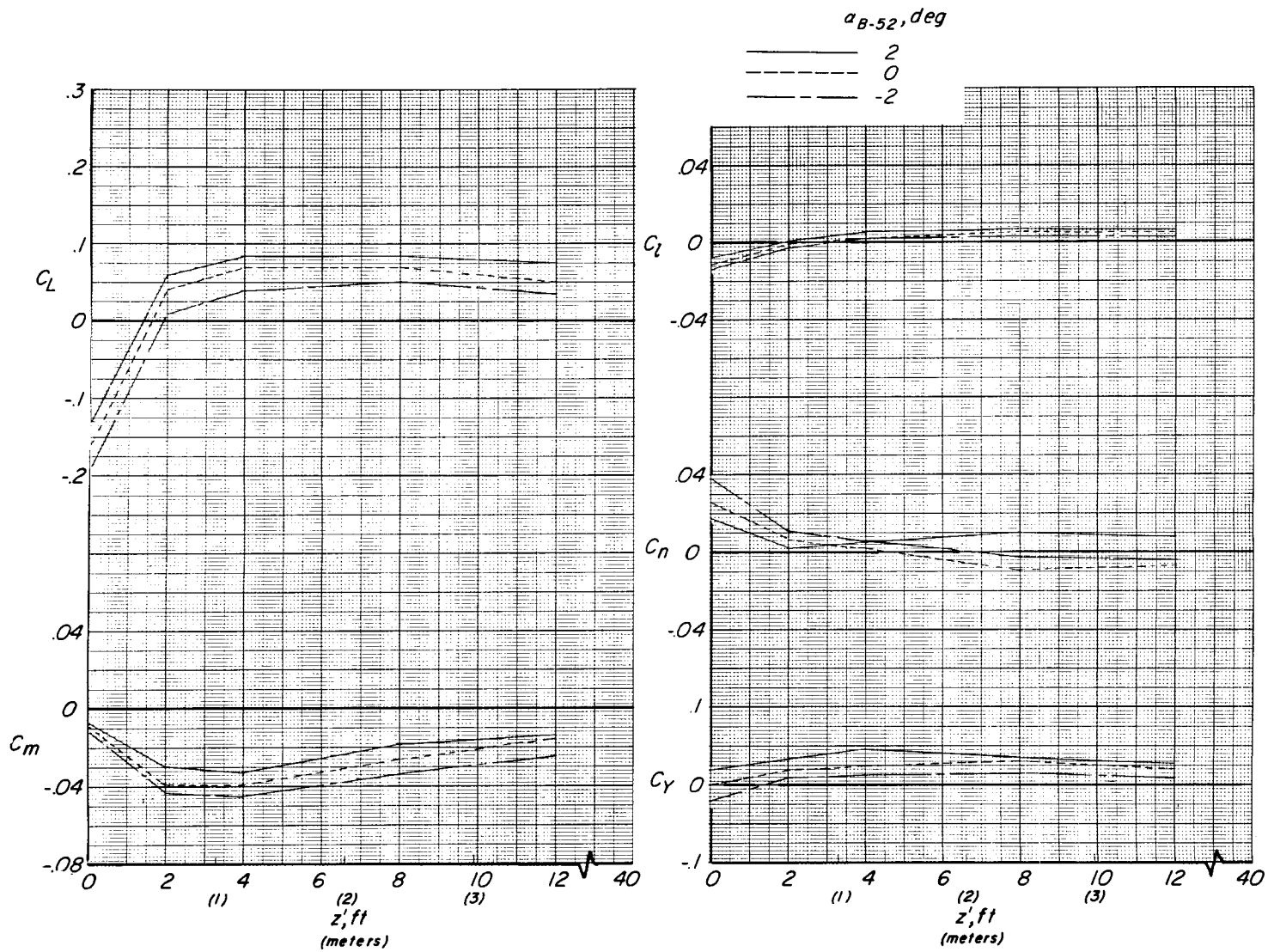

(c) M = 0.80.

Figure 11.- Continued.

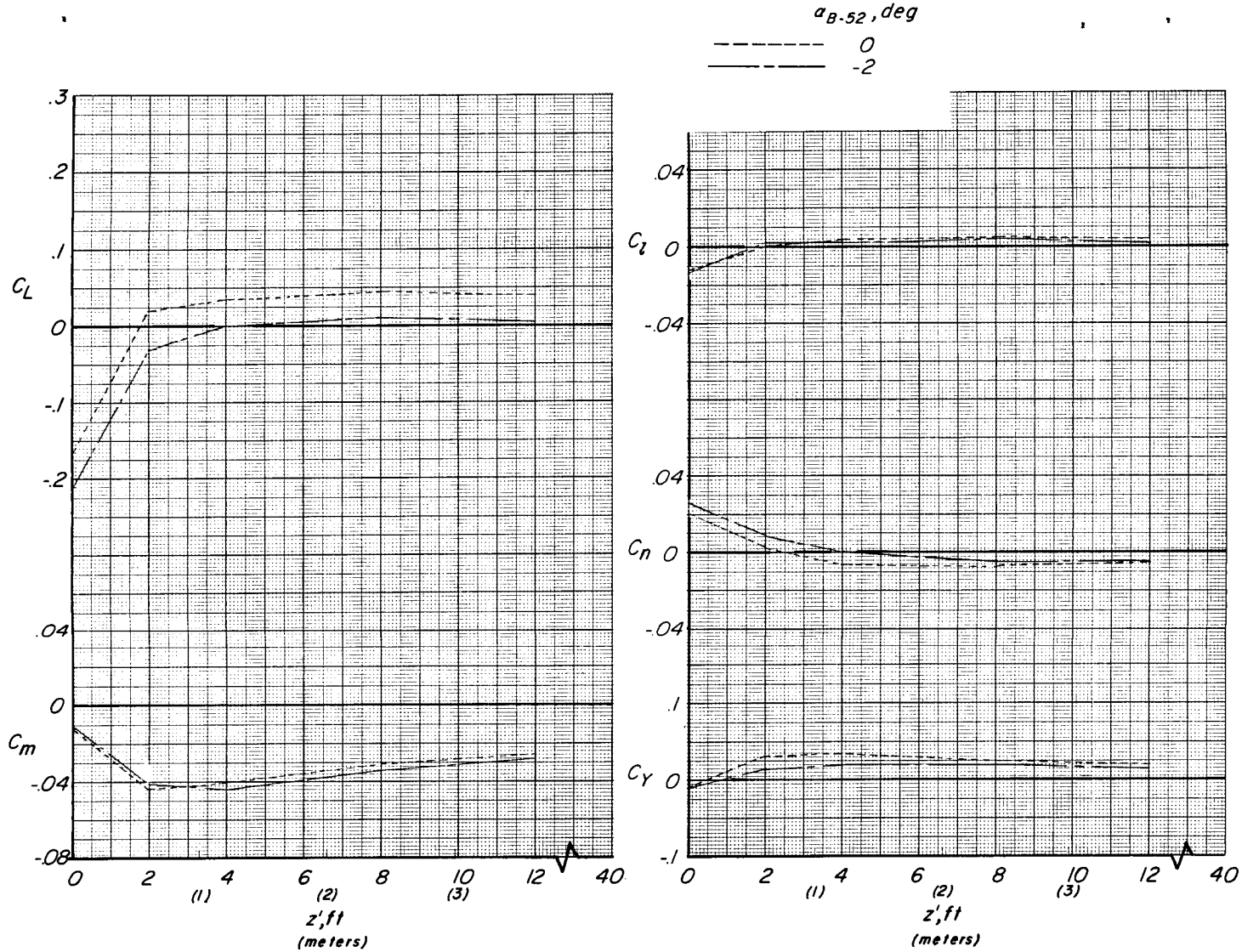

(c) M = 0.85.

Figure 11.- Concluded.

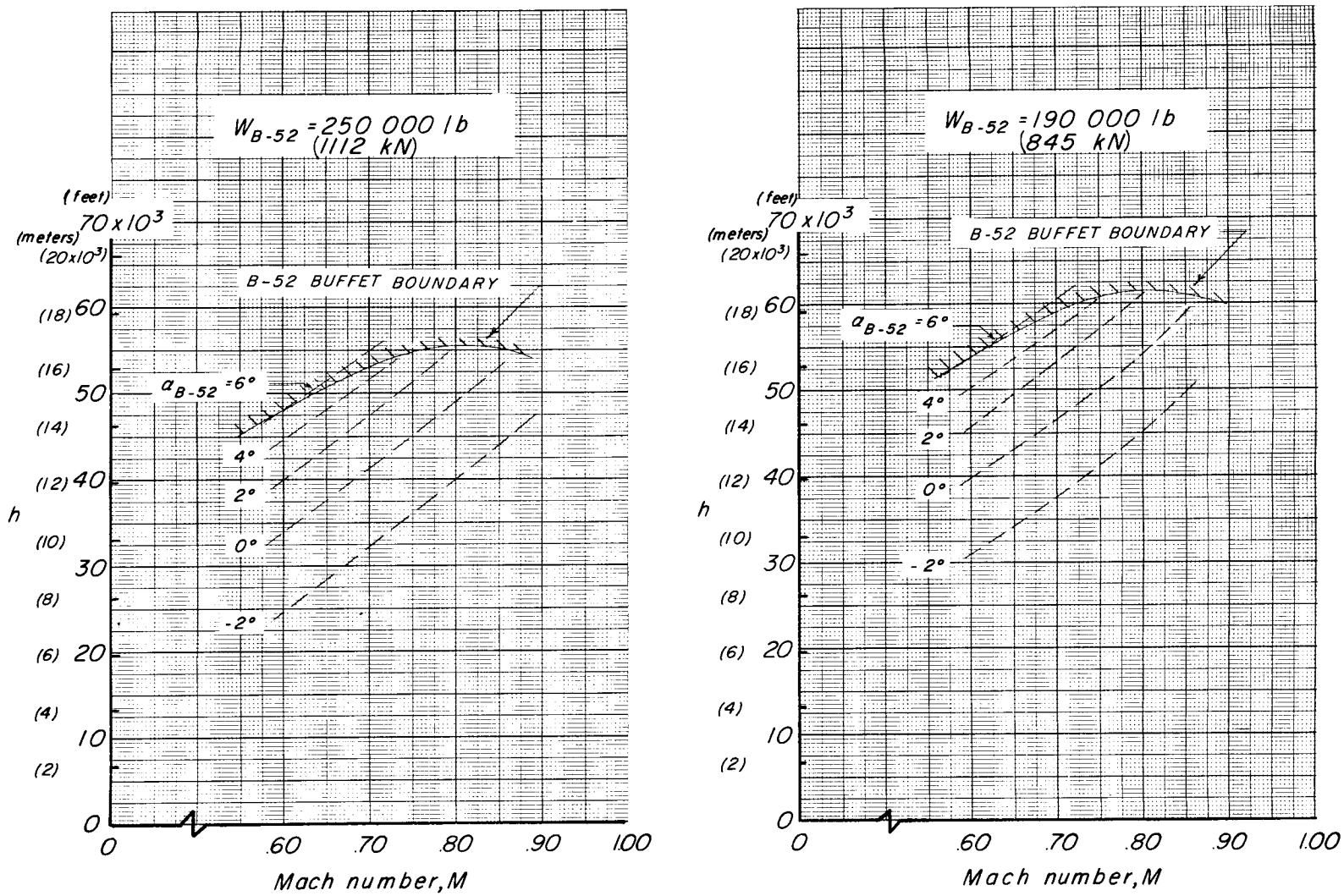

Figure 12.- B-52 buffet boundary.

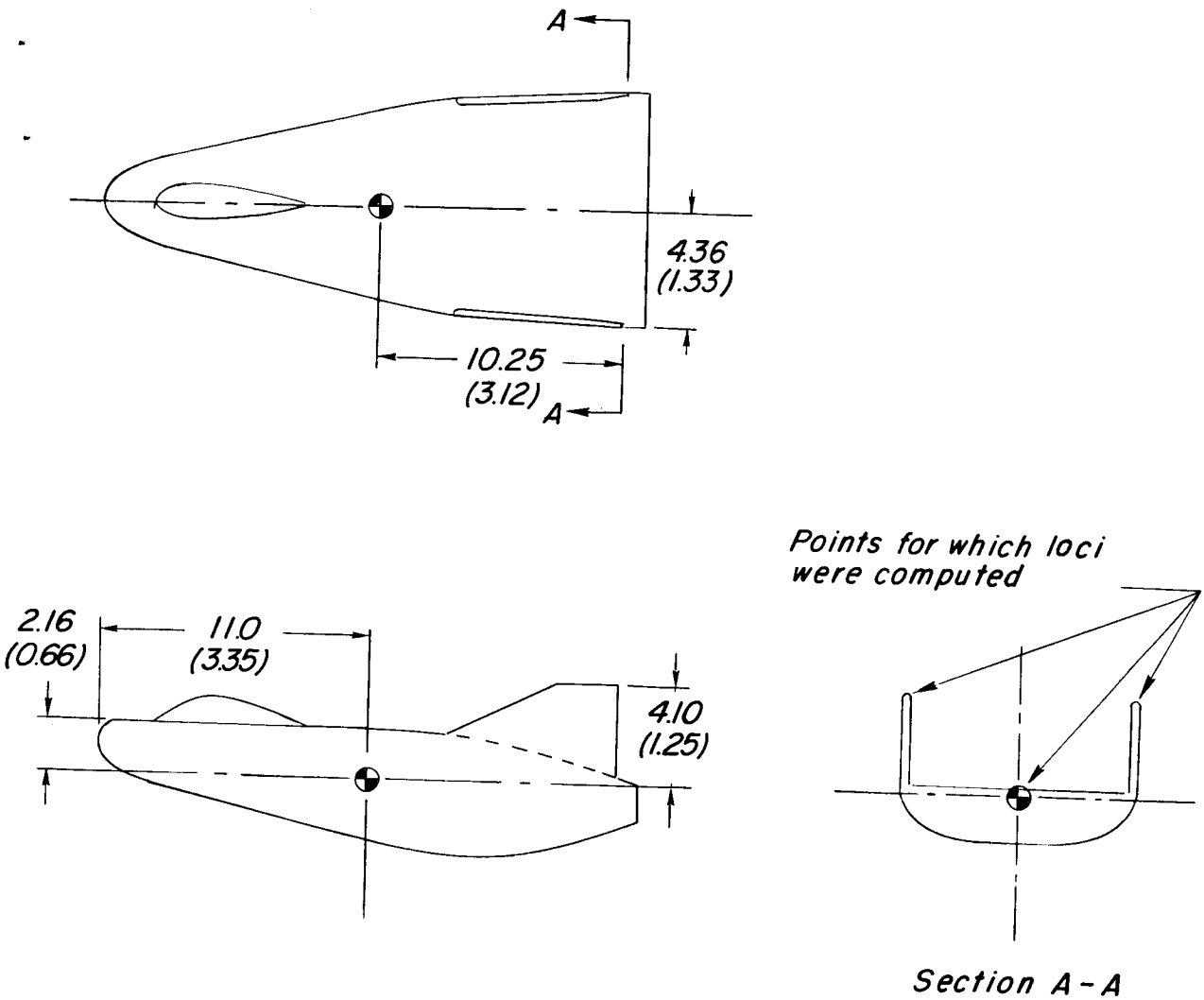

Figure 13.- Reference section of M2-F2 vehicle used in motion study. All dimensions are given first in feet and parenthetically in meters.

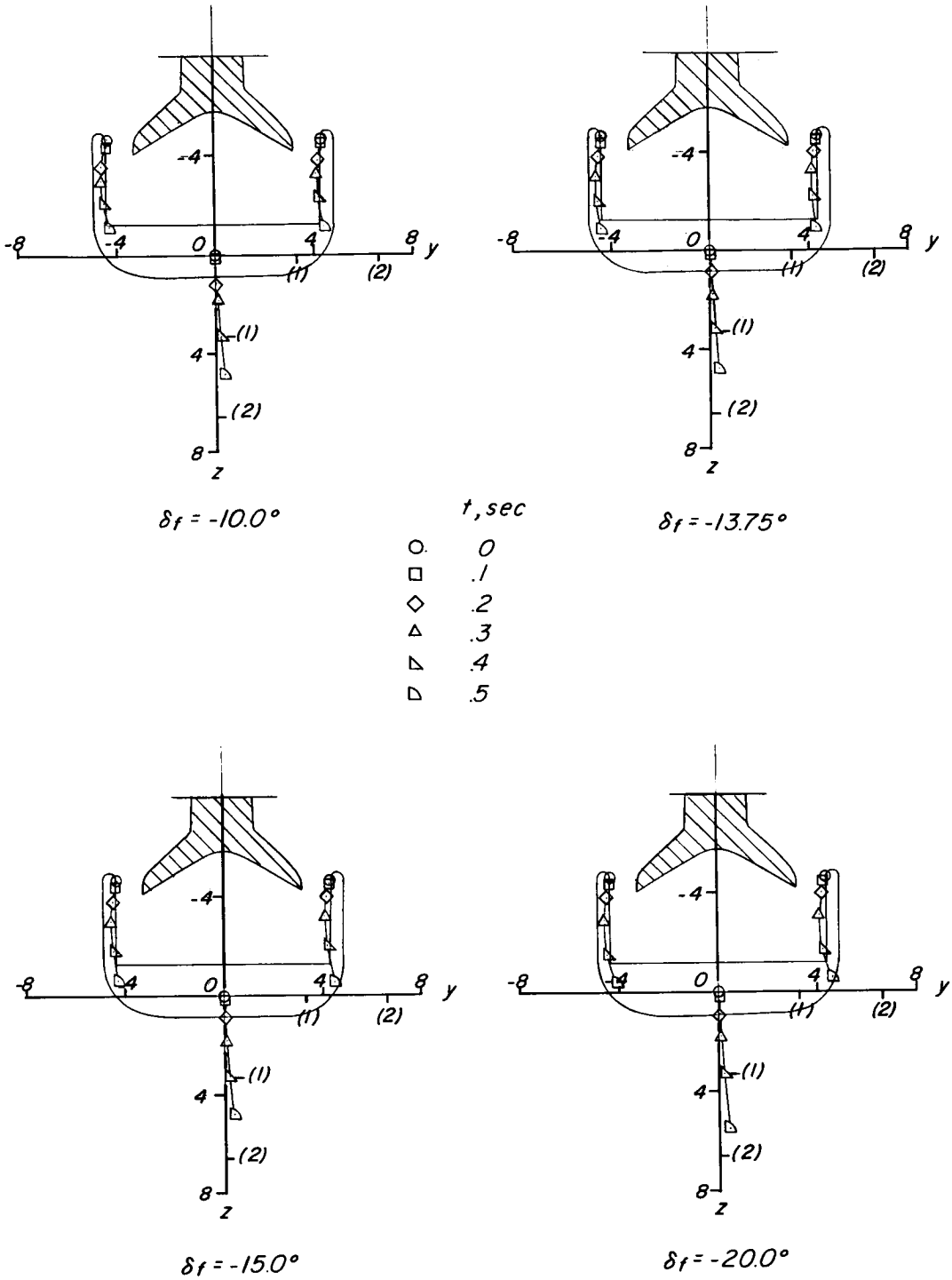

(a) M = 0.60; $\alpha_{B-52} = 2.0^{\circ}$.

Figure 14.- Effect of upper-surface-flap deflection δ_f on paths of M2-F2 fin tips. Dampers off; $\delta_p = 25^{\circ}$; W_{B-52} = 250 000 pounds (1112 kN); W_{M2-F2} = 5029 pounds (22.4 kN). Values of y and z given in feet (m).

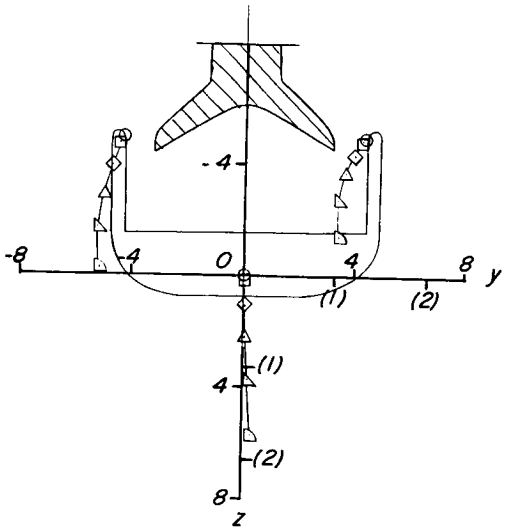

$\delta_f = -13.75°$

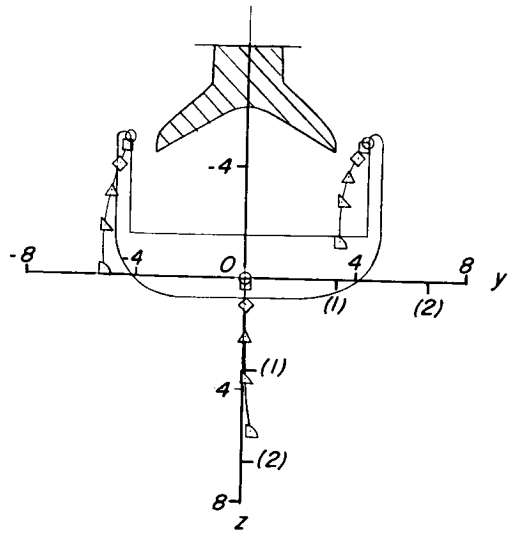

$\delta_f = -15.0°$

t, sec
○ 0
□ .1
◇ .2
△ .3
◺ .4
◺ .5

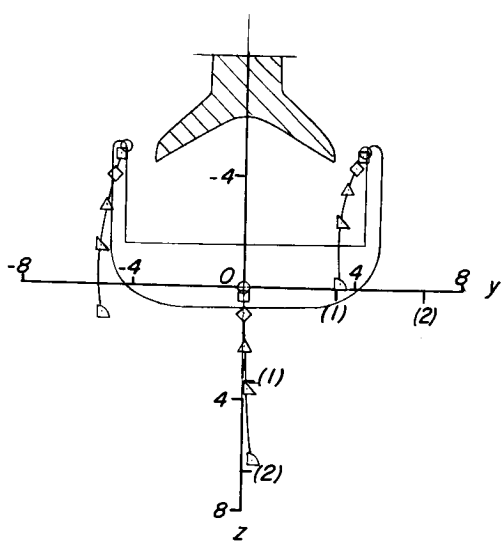

$\delta_f = -20.0°$

(b) M = 0.80; $\alpha_{B-52} = 0°$.

Figure 14.- Concluded.

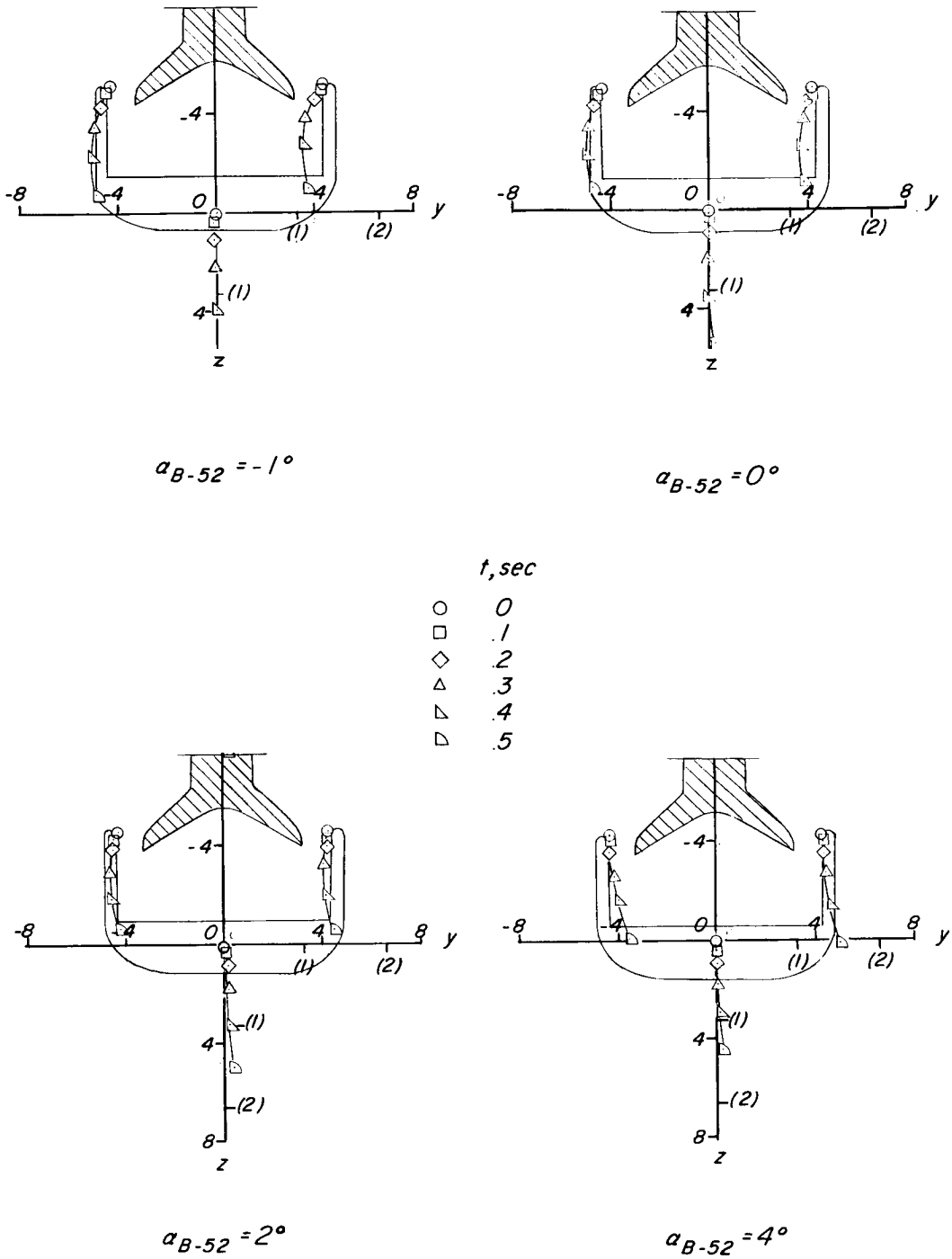

(a) M = 0.60.

Figure 15.- Effect of variations in B-52 angle of attack (variation in altitude) on paths of M2-F2 fin tips. Dampers off; $\delta_f = -15^o$; $\delta_p = 25^o$; W_{B-52} = 250 000 pounds (1112 kN); W_{M2-F2} = 5029 pounds (22.4 kN). Values of y and z given in feet (m).

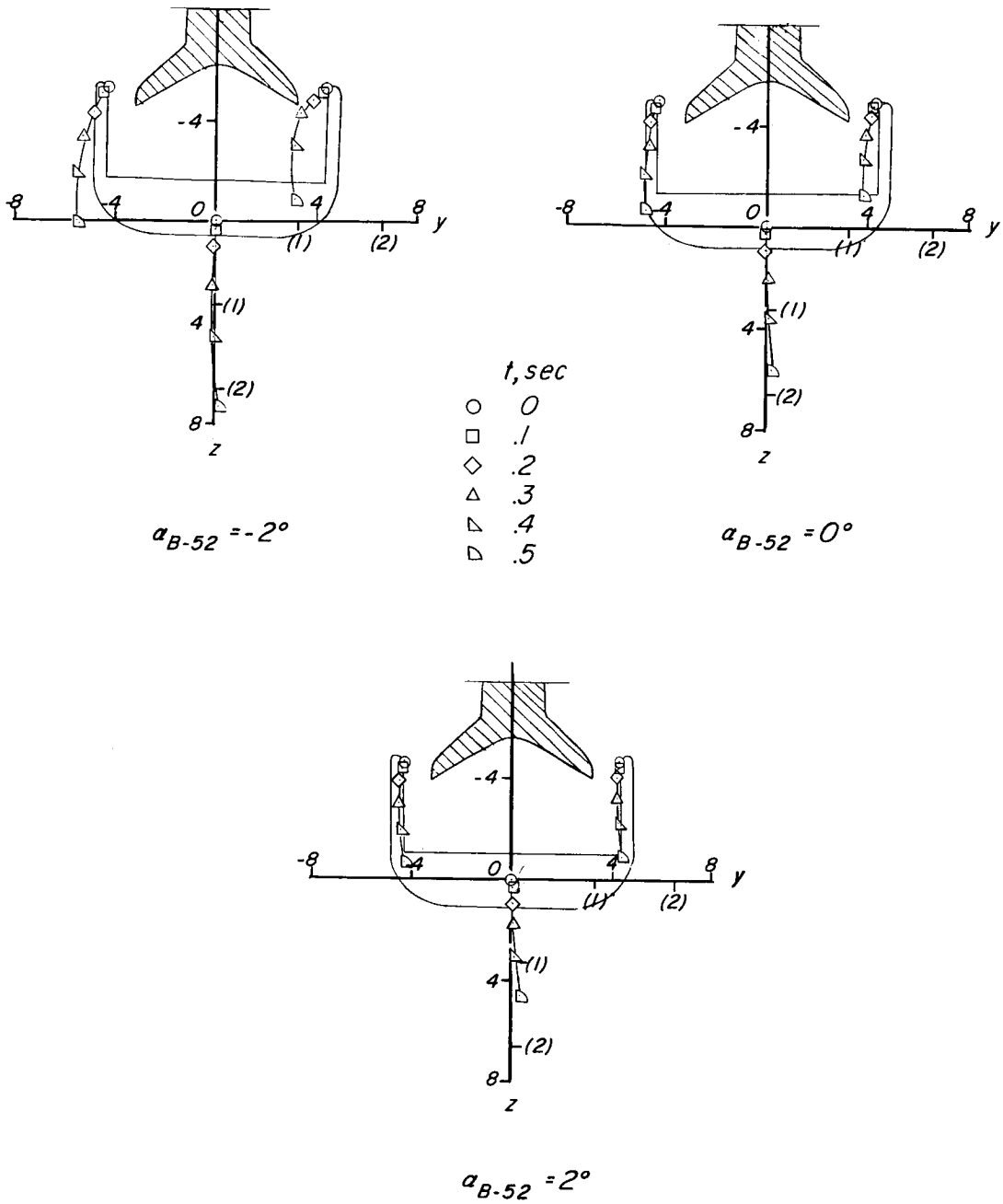

(b) M = 0.70.

Figure 15.- Continued.

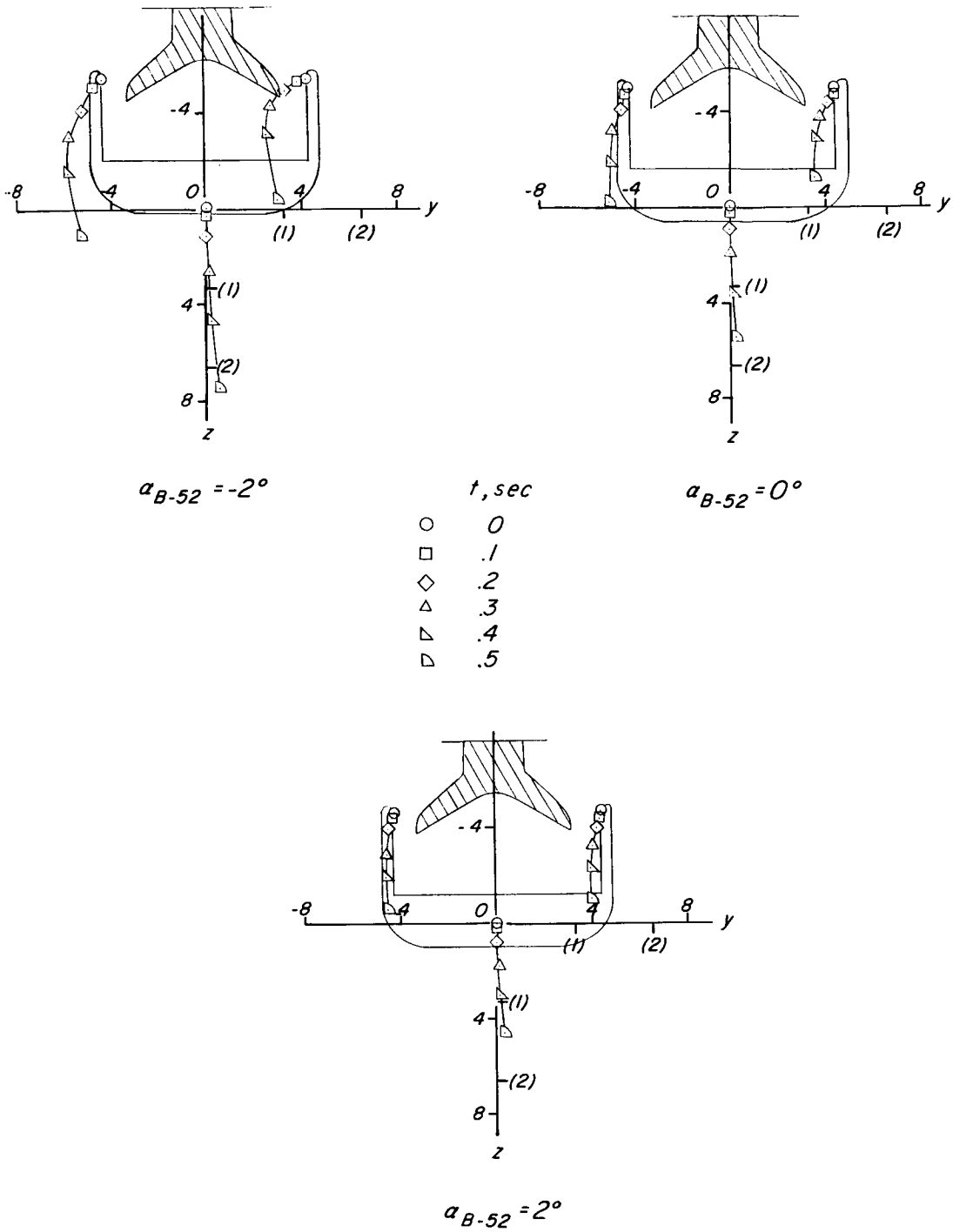

(c) M = 0.80.

Figure 15.- Continued.

[redacted] DECLASSIFIED

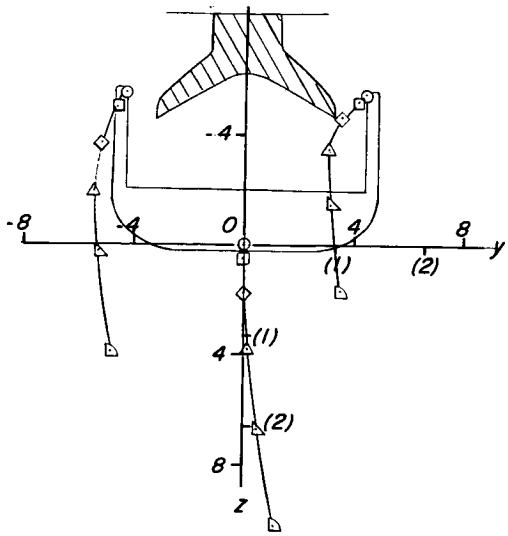

$\alpha_{B-52} = -3°$

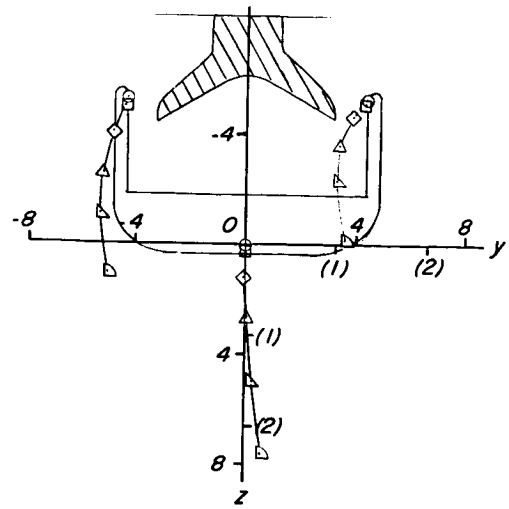

$\alpha_{B-52} = -2°$

	t, sec
○	0
□	.1
◇	.2
△	.3
◺	.4
◗	.5

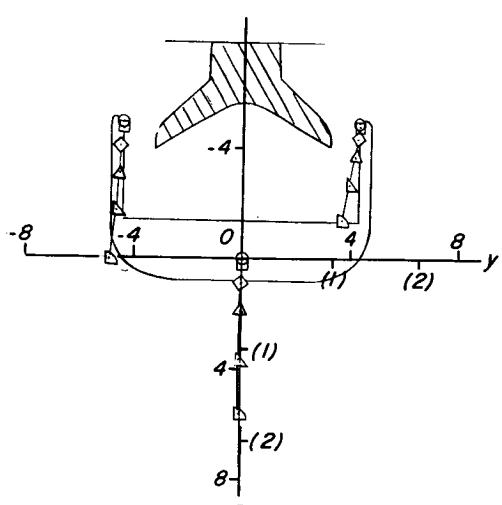

$\alpha_{B-52} = 0°$

(d) M = 0.85.

Figure 15.- Concluded.

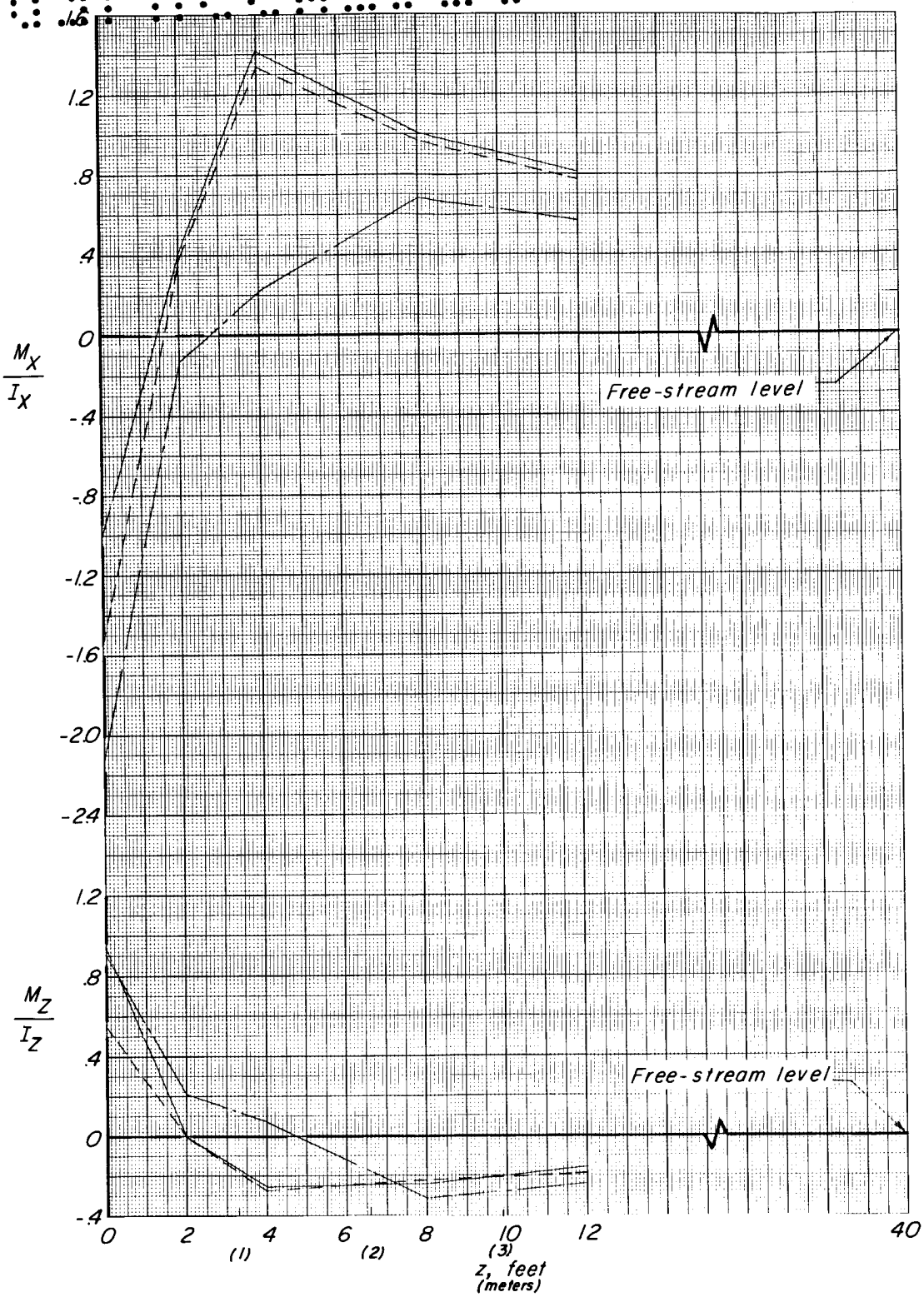

Figure 16.- Effect of separation distance on full-scale M2-F2 rolling and yawing accelerations. $\alpha_{B-52} = 0^{\circ}$; $\Delta\alpha = -5^{\circ}$.

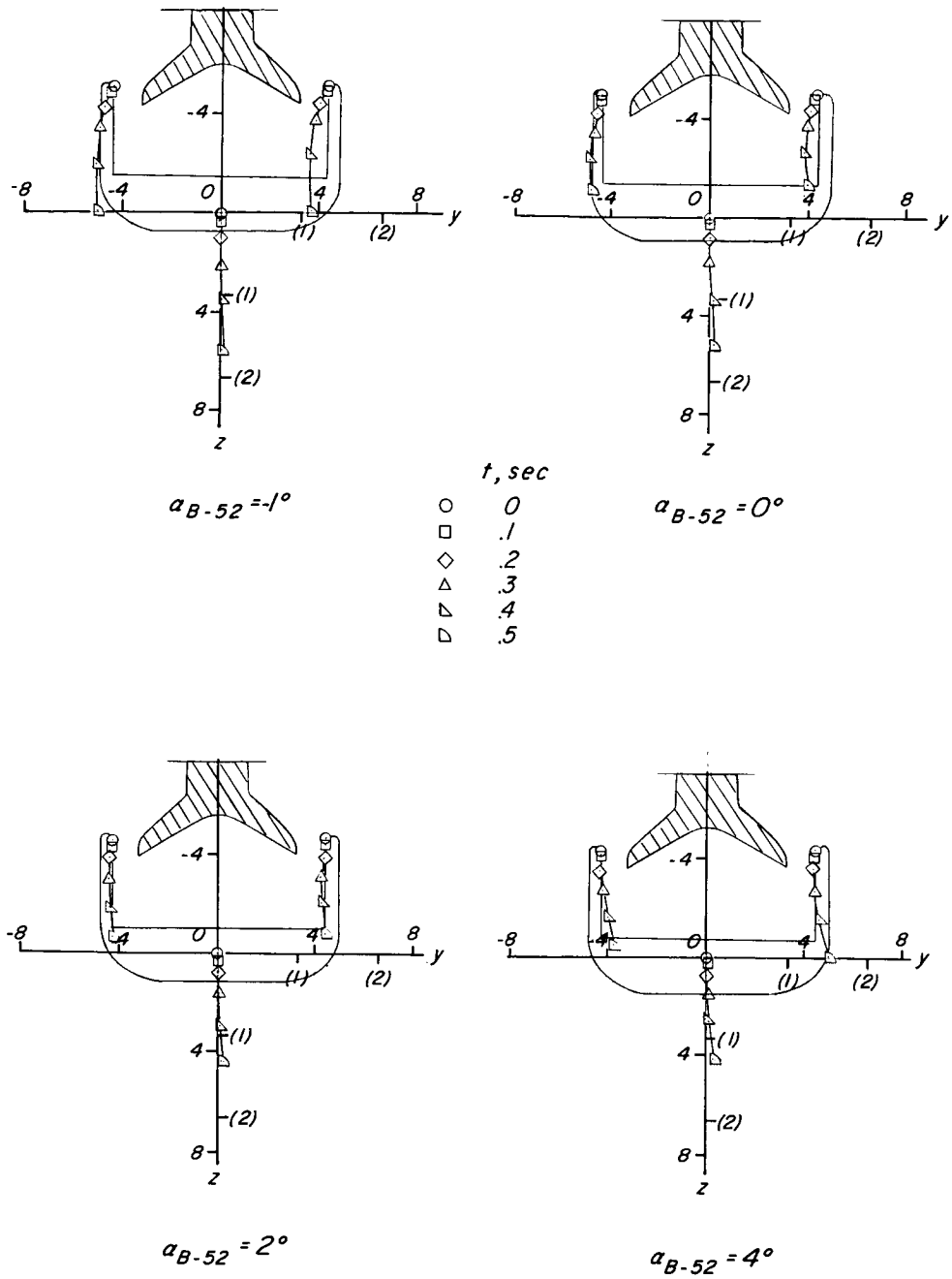

(a) M = 0.60.

Figure 17.- Effect of variations in B-52 angle of attack (variation in altitude) on paths of M2-F2 fin tips. Dampers off; $\delta_f = -15^{\circ}$; $\delta_p = 25^{\circ}$; $W_{B-52} = 190\ 000$ pounds (845 kN); $W_{M2-F2} = 5029$ pounds (22.4 kN). Values of y and z given in feet (m).

[redacted]

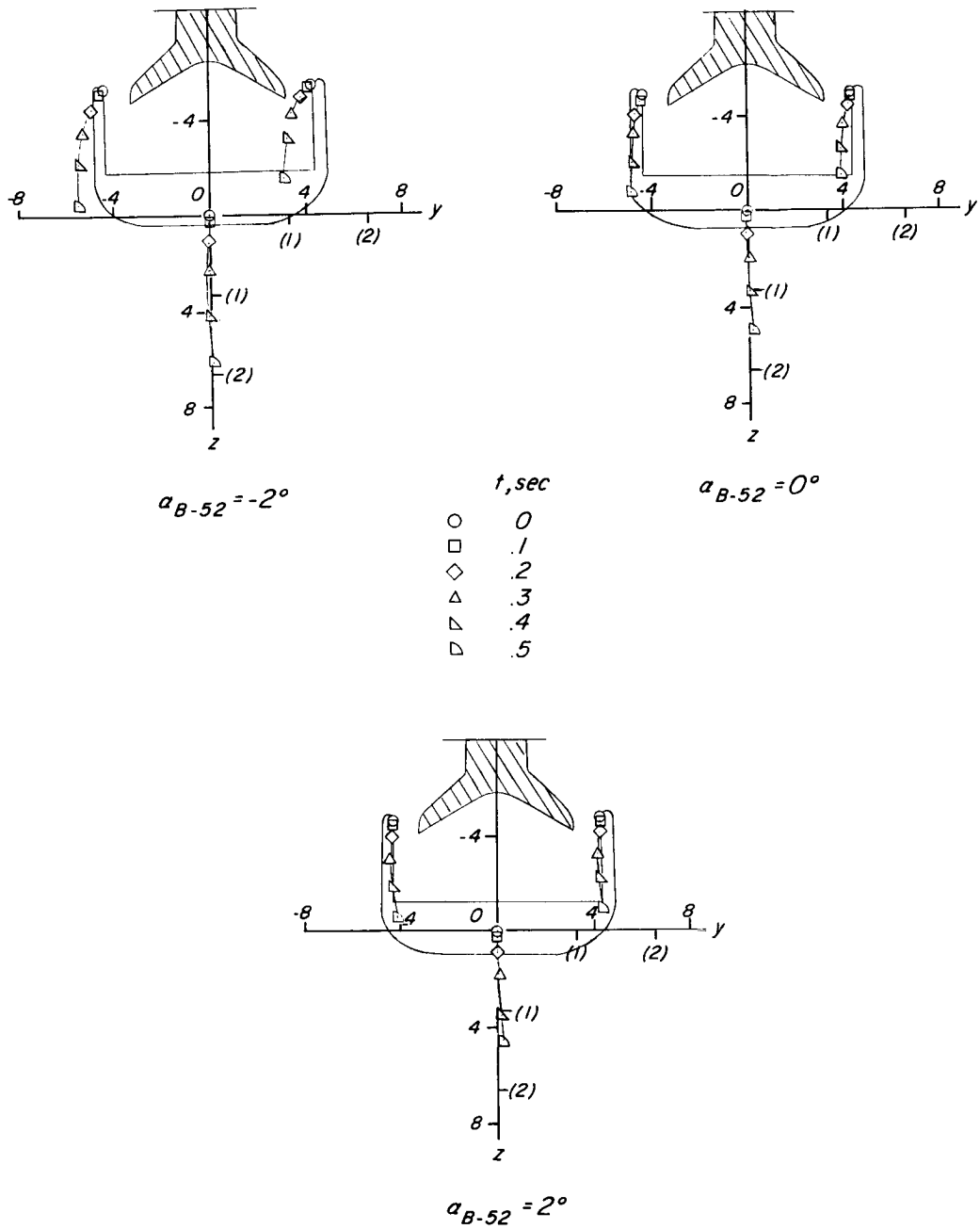

(b) M = 0.70.

Figure 17.- Continued.

[redacted]

[redacted] DECLASSIFIED

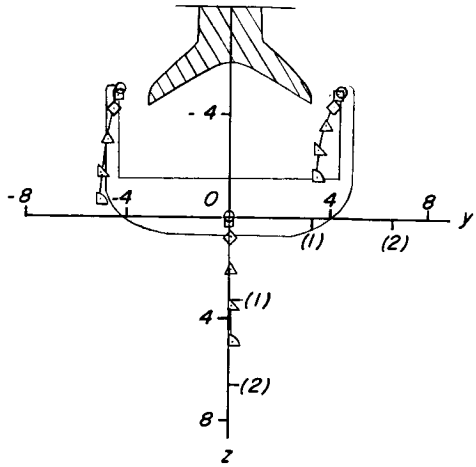

$\alpha_{B-52} = 0°$

	t, sec
○	0
□	.1
◇	.2
△	.3
◺	.4
◺	.5

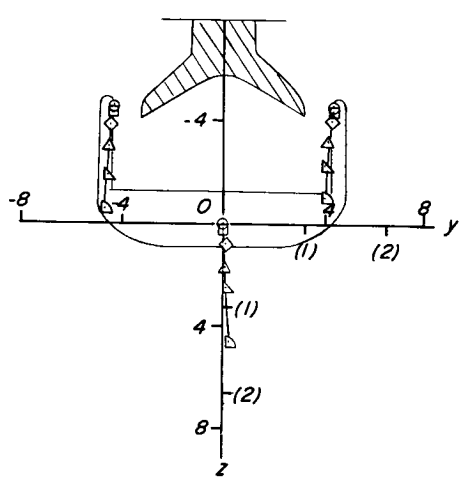

$\alpha_{B-52} = 2°$

(c) M = 0.80.

Figure 17.- Concluded.

[redacted]

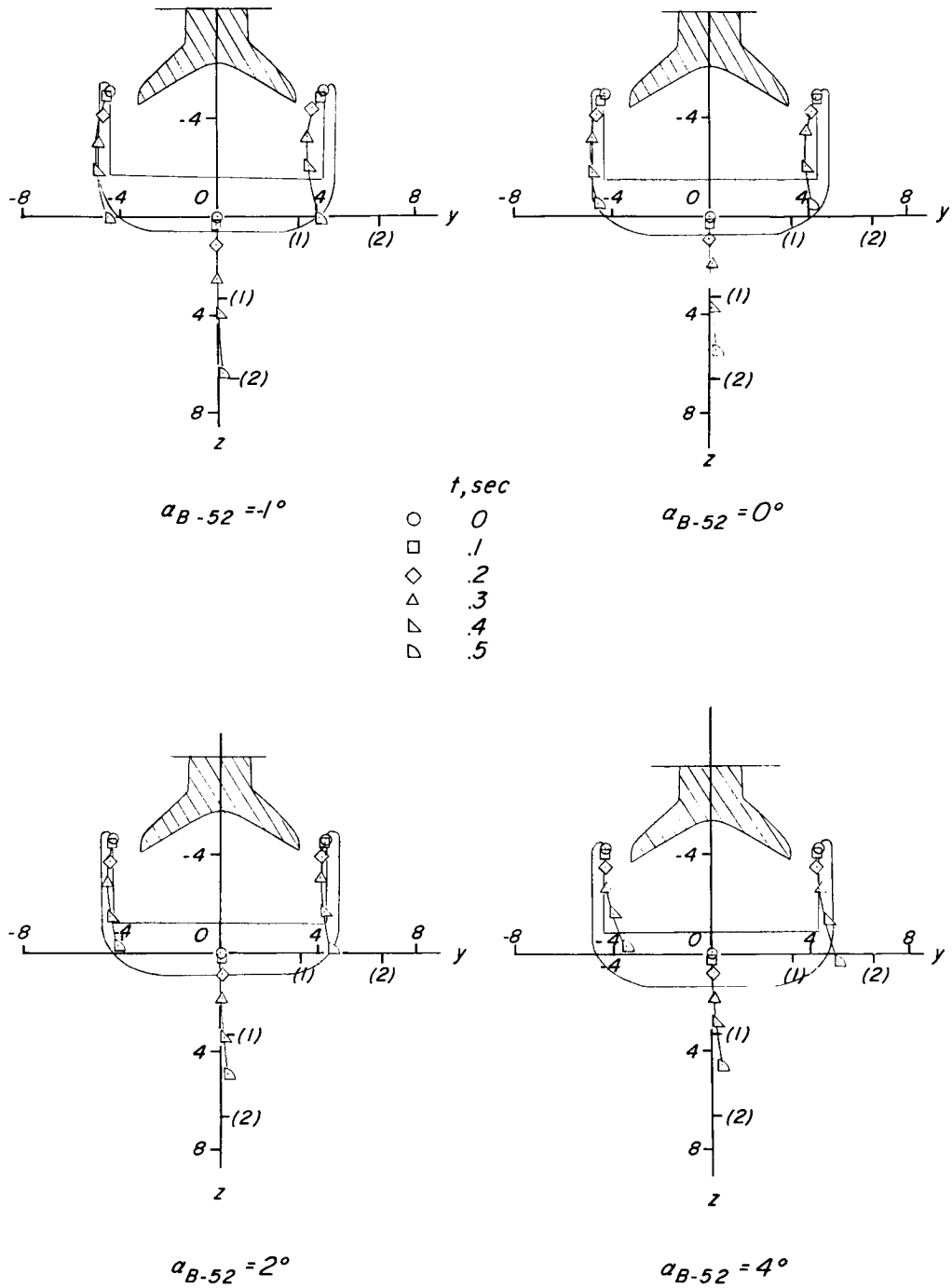

(a) M = 0.60.

Figure 18.- Effect of variations in B-52 angle of attack (variation in altitude) on paths of M2-F2 fin tips. Dampers on; $\delta_f = -15^o$; $\delta_p = 25^o$; W_{B-52} = 250 000 pounds (1112 kN); W_{M2-F2} = 5029 pounds (22.4 kN). Values of y and z given in feet (m).

[redacted]

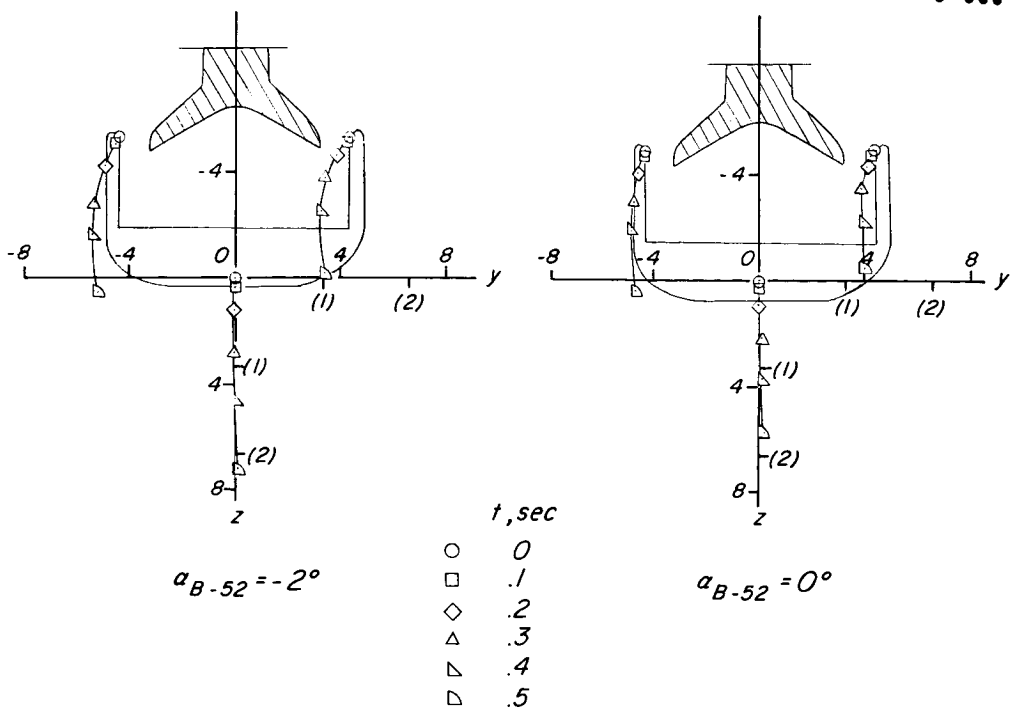

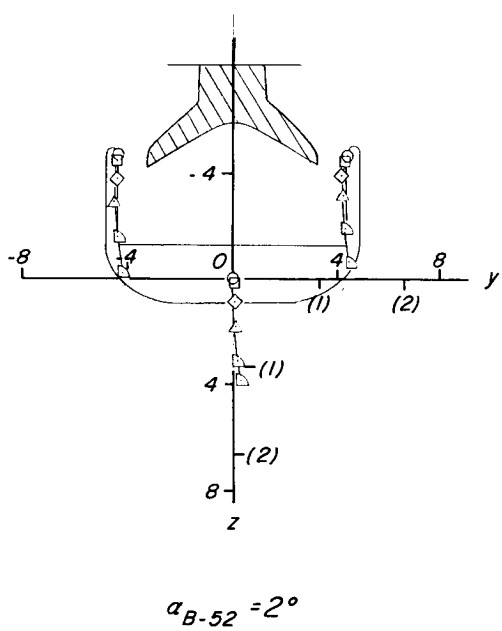

(b) M = 0.70.

Figure 18.- Continued.

[redacted]

[redacted]

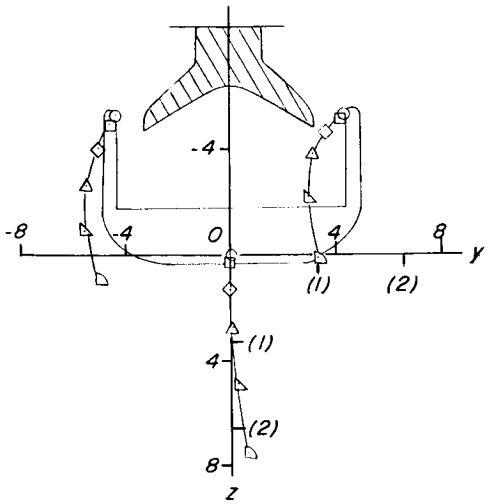

$\alpha_{B-52} = -2°$

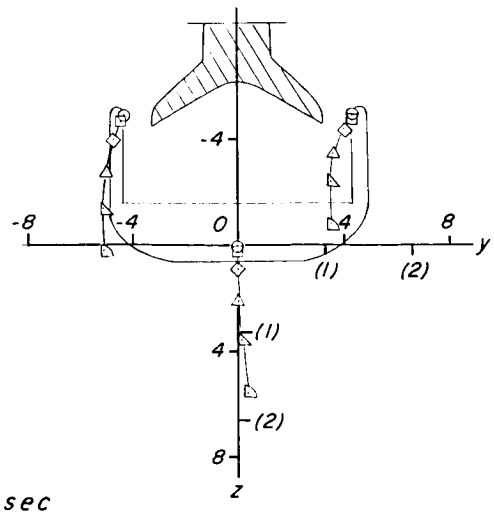

$\alpha_{B-52} = 0°$

	t, sec
○	0
□	.1
◇	.2
△	.3
◺	.4
◺	.5

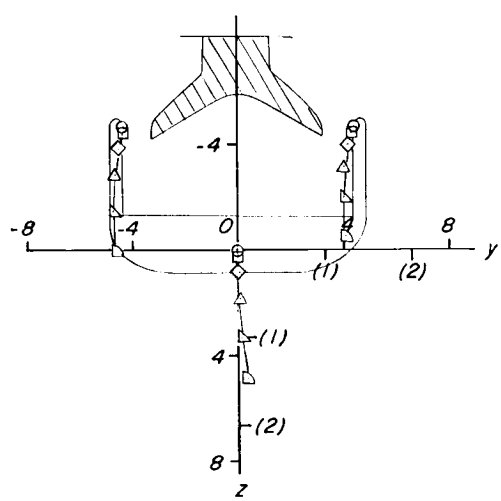

$\alpha_{B-52} = 2°$

(c) M = 0.80.

Figure 18.- Concluded.

[redacted]

[redacted] DECLASSIFIED

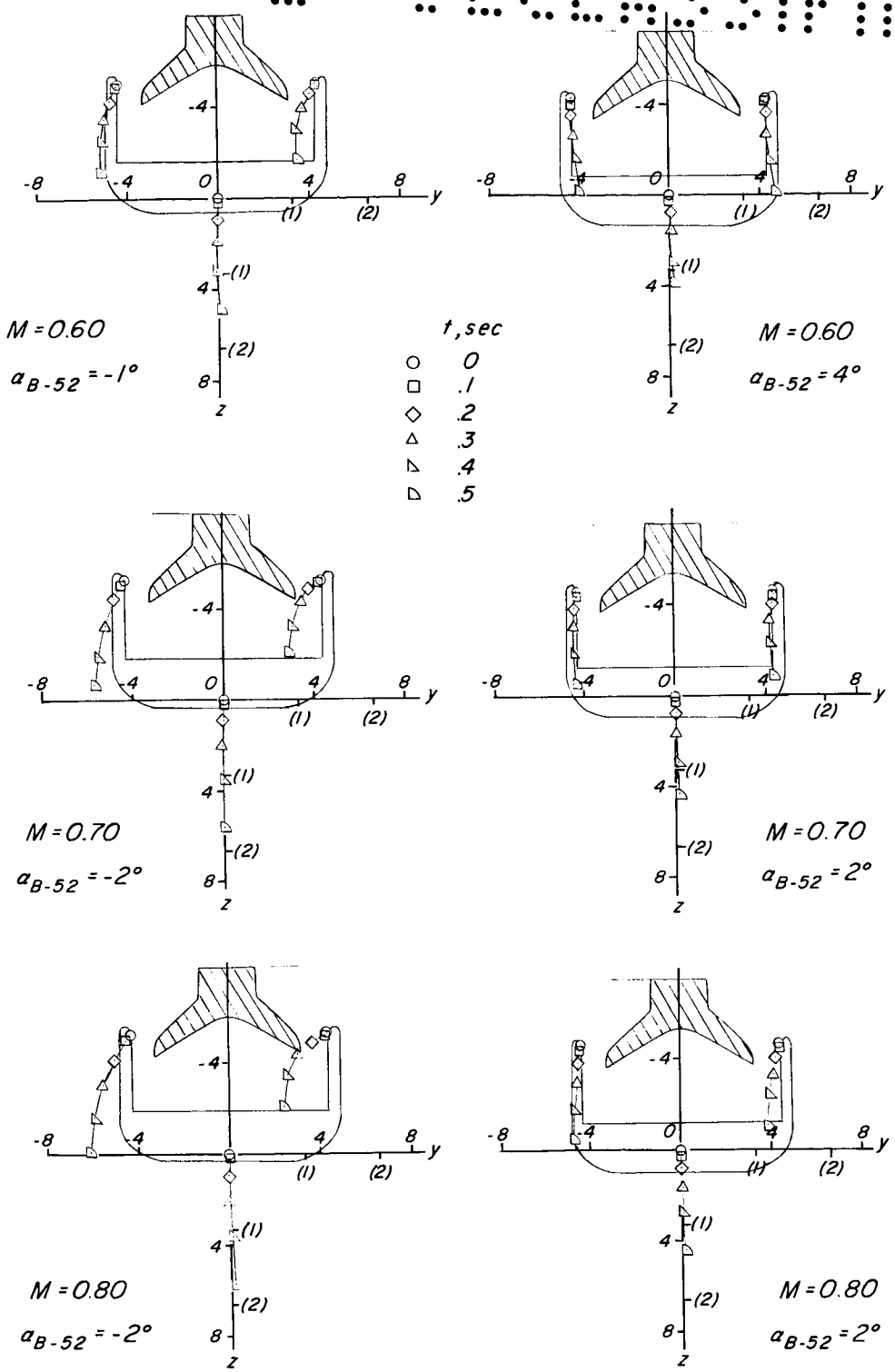

Figure 19.- Effect of M2-F2 launch weight on paths of M2-F2 fin tips. Dampers off; $\delta_f = -15^0$; $\delta_p = 25^0$; $W_{B-52} = 250\ 000$ pounds (1112 kN); $W_{M2-F2} = 9030$ pounds (40.2 kN). Values of y and z given in feet (m).

[redacted]

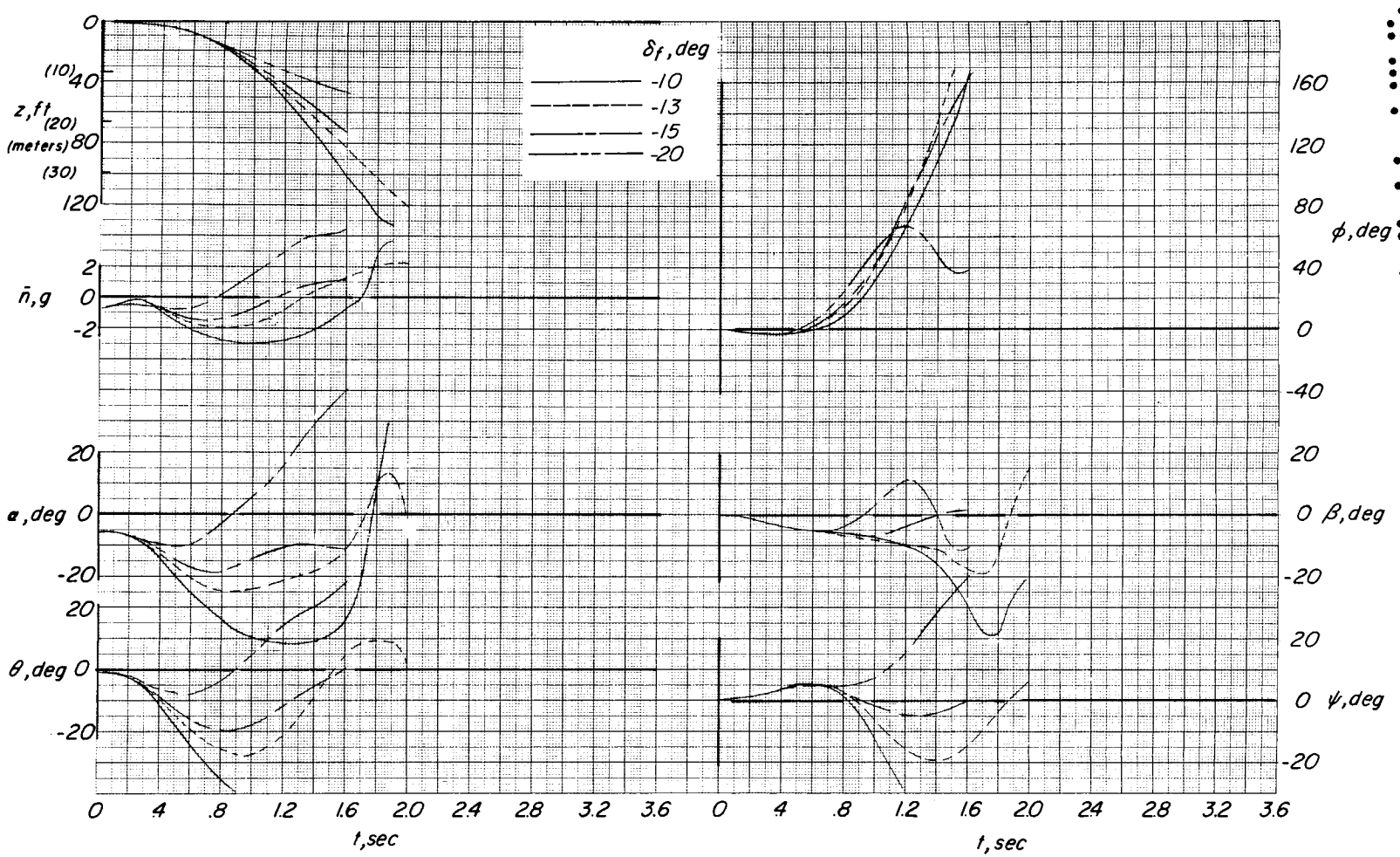

(a) $\alpha_{B-52} = -1^{\circ}$.

Figure 20.- Effect of upper-surface-flap deflection δ_f on M2-F2 motions after launch. Dampers off; M = 0.60; $\delta_p = 25^{\circ}$; W_{B-52} = 250 000 pounds (1112 kN); W_{M2-F2} = 5029 pounds (22.4 kN); 10° rudder flare.

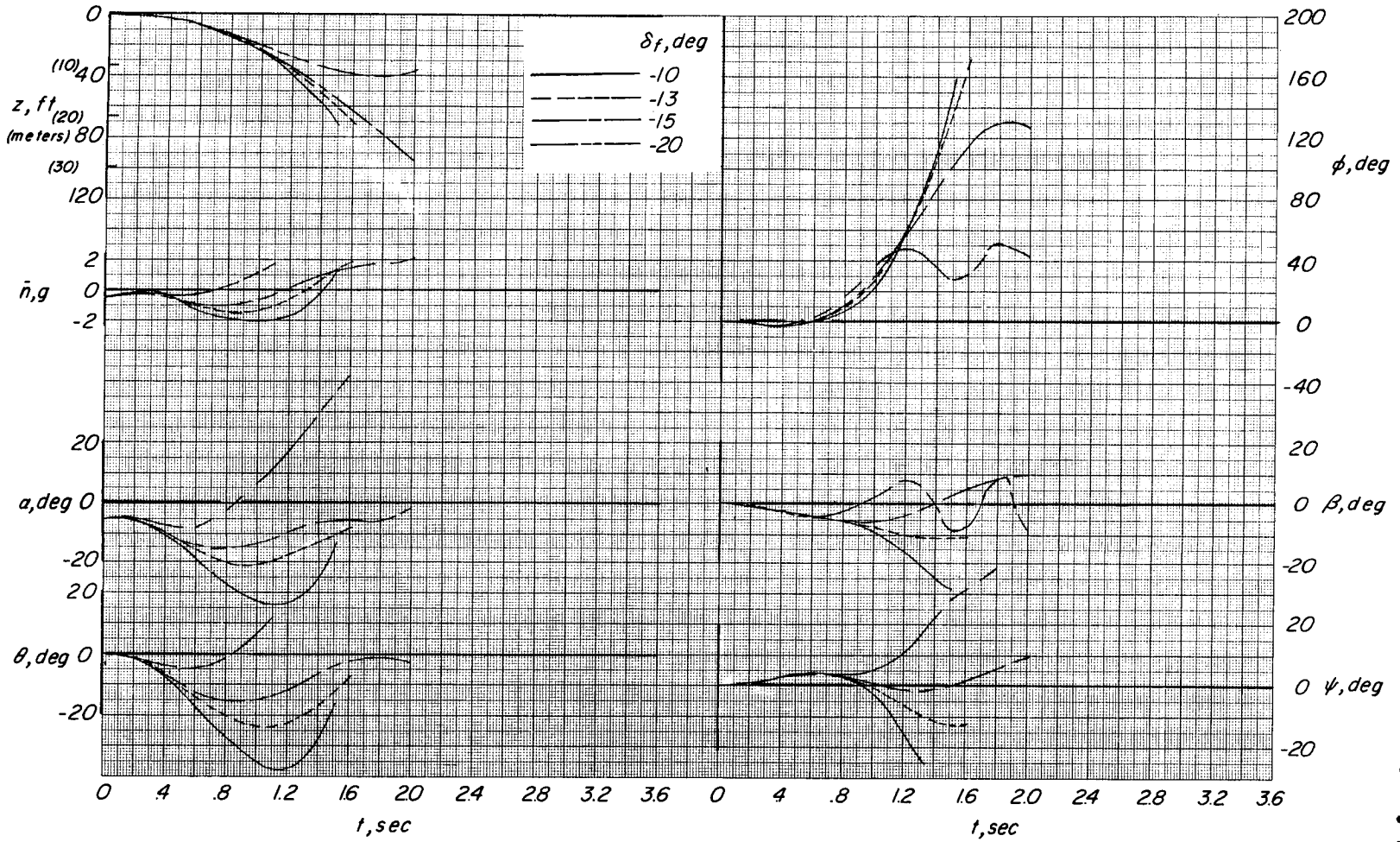

(b) $\alpha_{B-52} = 0^{\circ}$.

Figure 20.- Continued.

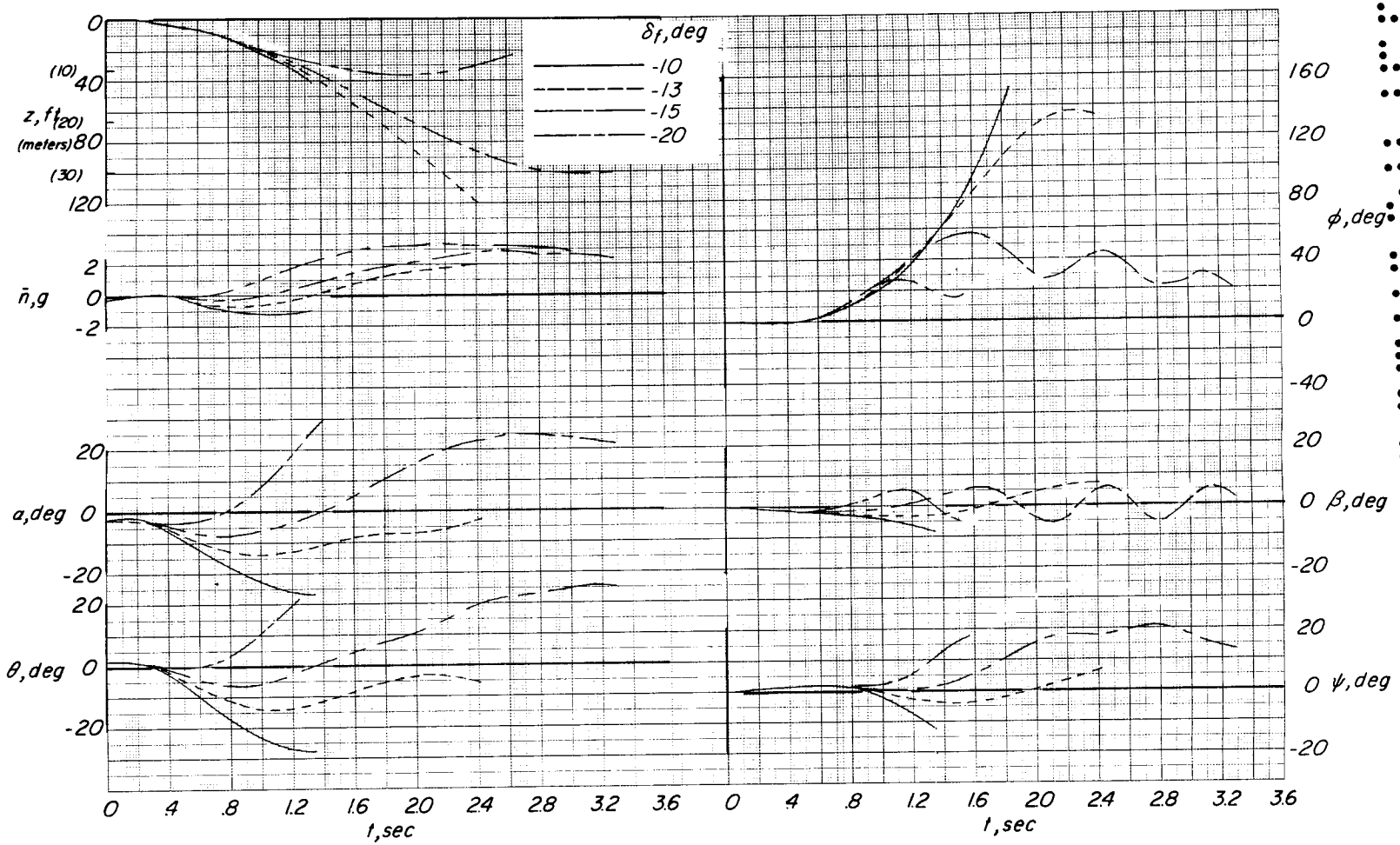

(c) $\alpha_{B-52} = 2^0$.

Figure 20.- Continued.

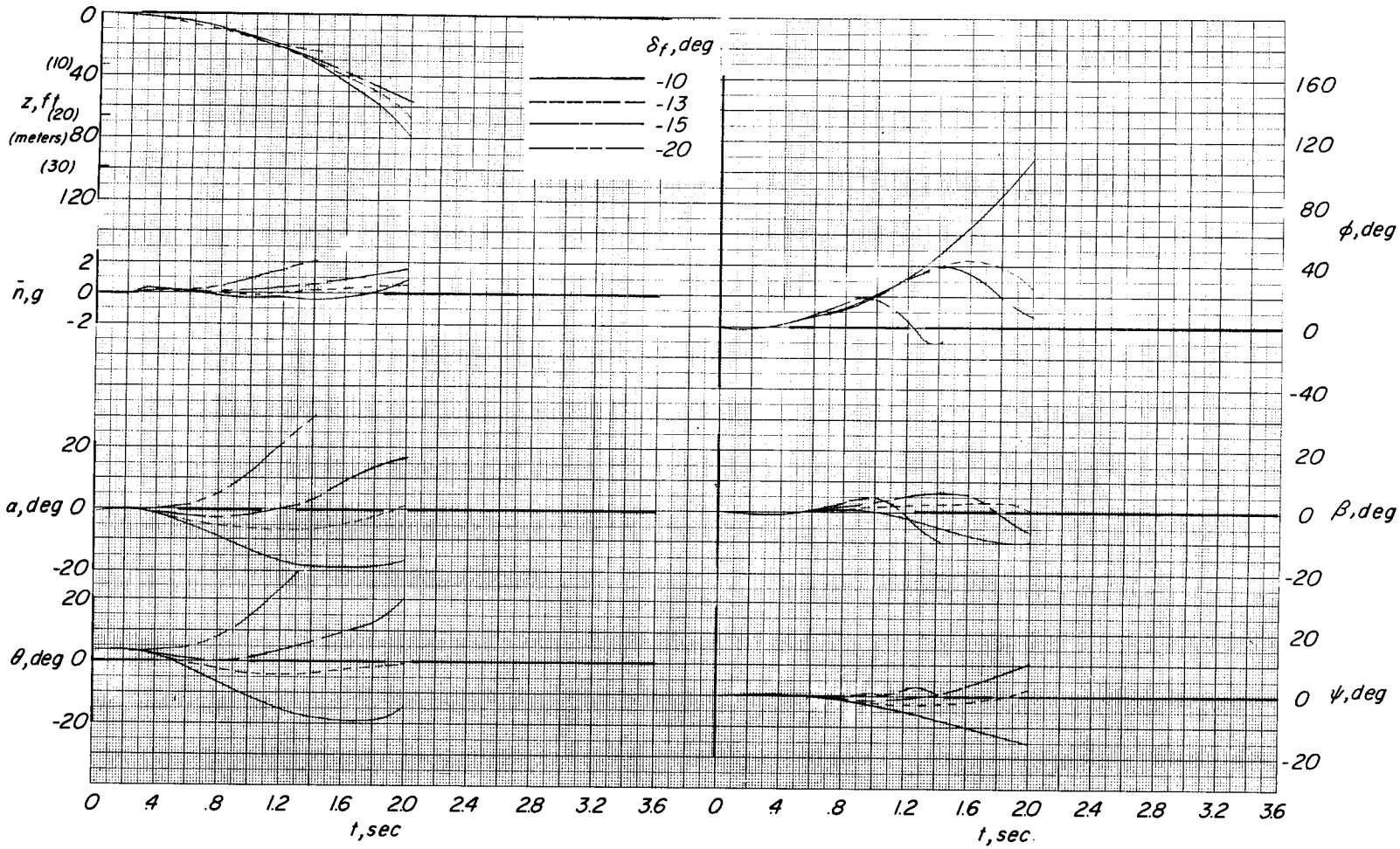

(d) $\alpha_{B-52} = 4^0$.

Figure 20.- Concluded.

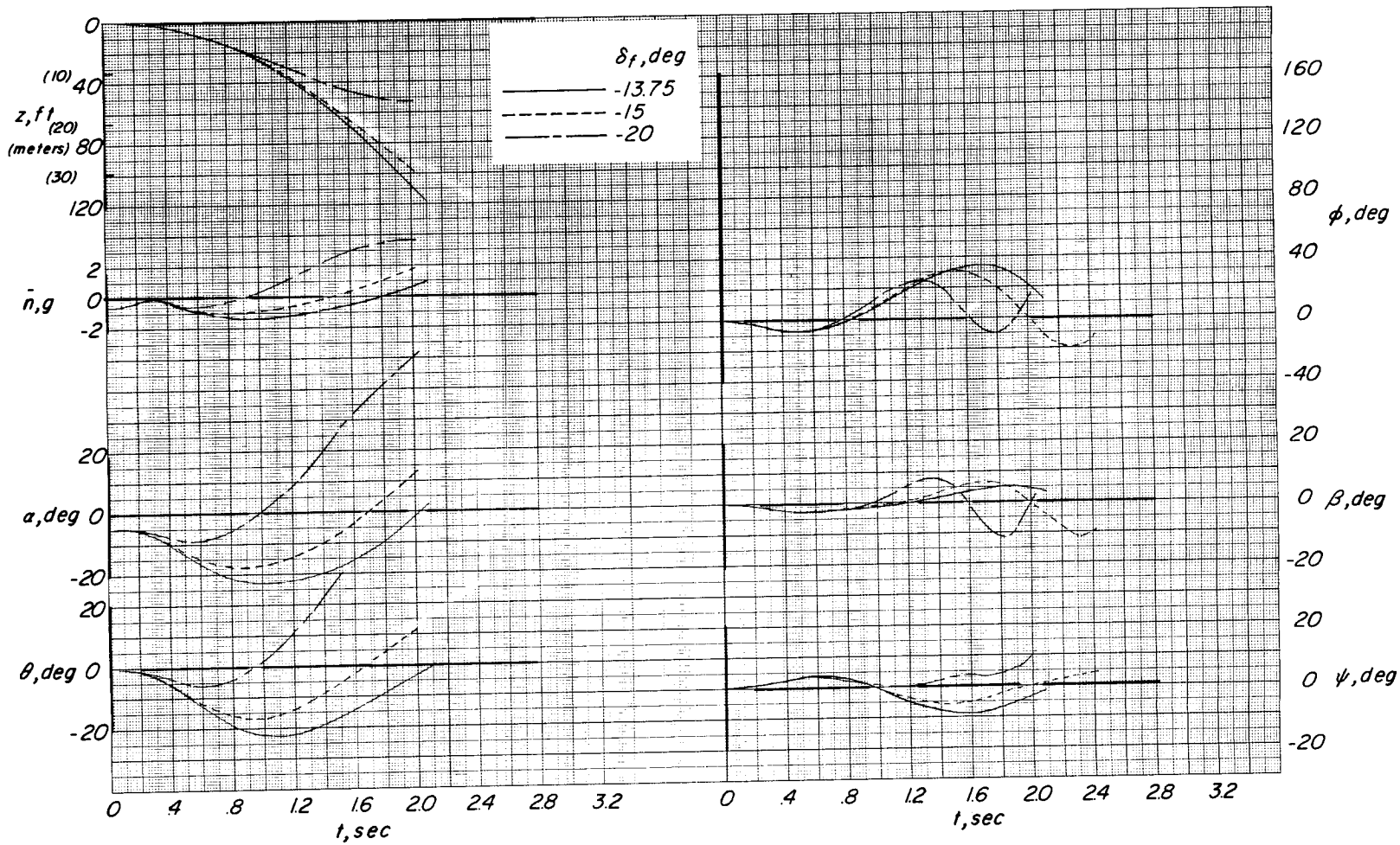

Figure 21.- Effect of upper-surface-flap deflection δ_f on M2-F2 motions after launch. Dampers off; M = 0.80; $\alpha_{B-52} = 0^{\circ}$; $\delta_p = 25^{\circ}$; W_{B-52} = 250 000 pounds (1112 kN); W_{M2-F2} = 5029 pounds (22.4 kN); 10° rudder flare.

[redacted] DECLASSIFIED

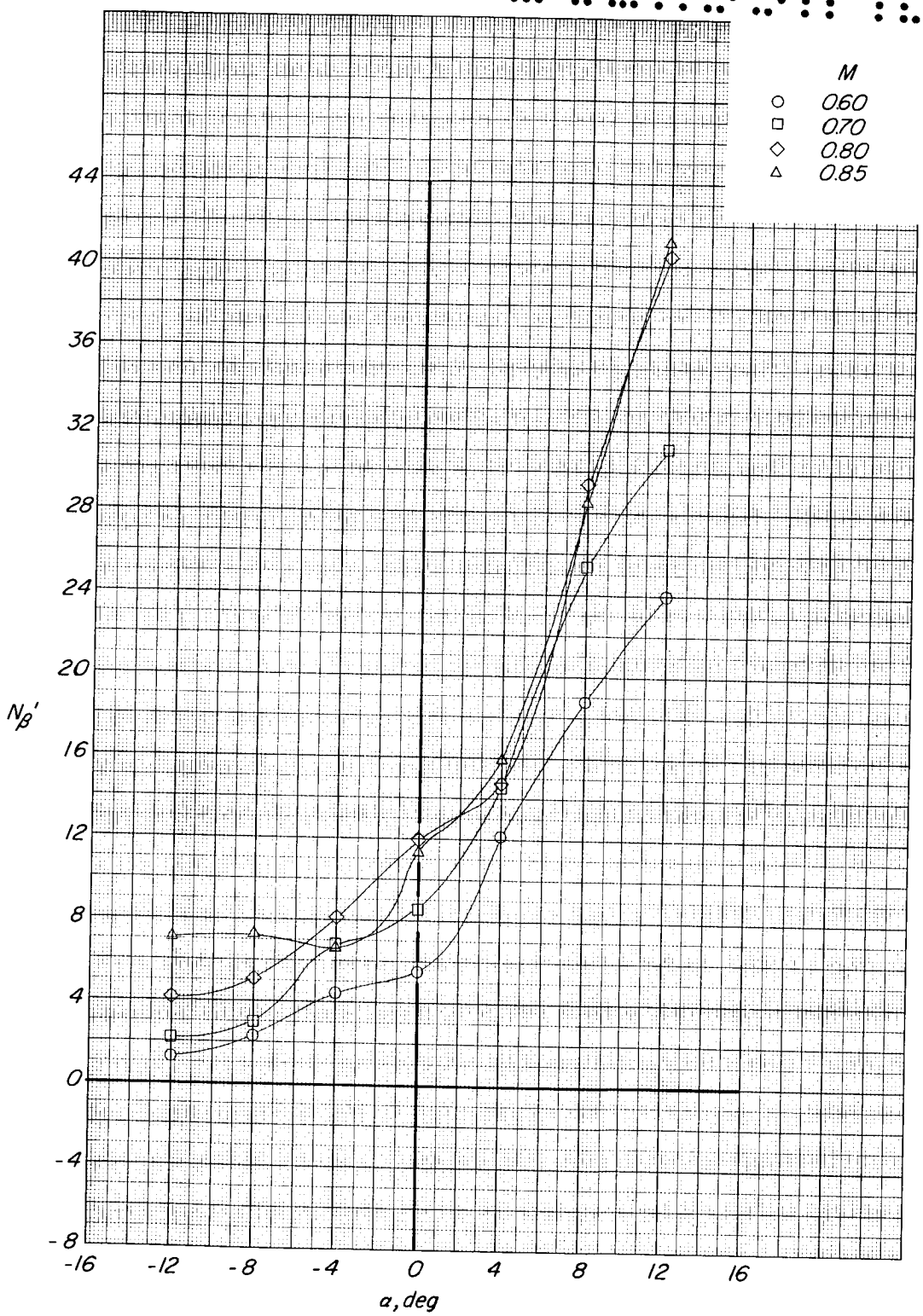

Figure 22.- Variation of N_β' with α. M2-F2 in free stream at 45 000 feet (13.7 km).

[redacted]

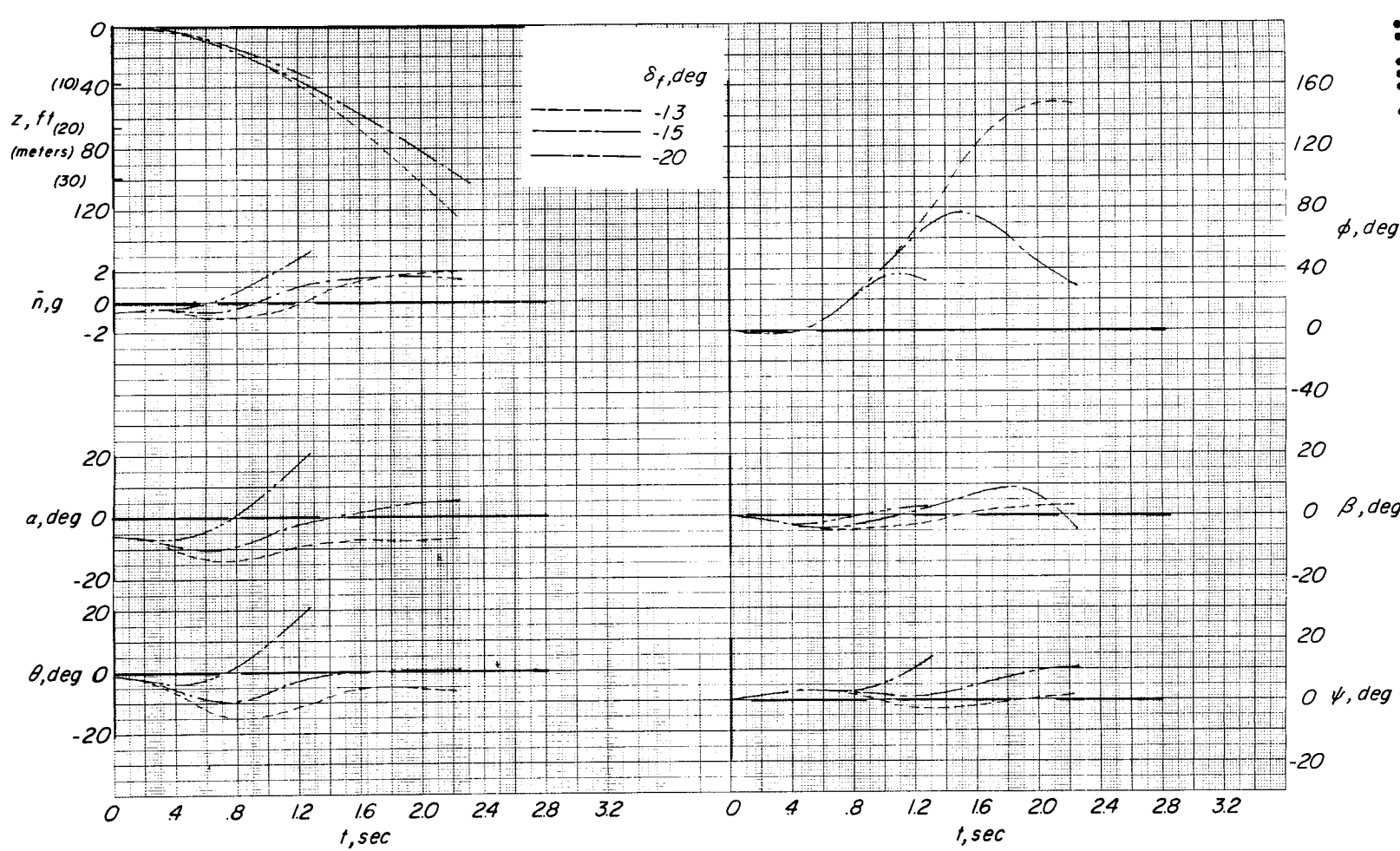

(a) $\alpha_{B-52} = -1^{\circ}$.

Figure 23.- Effect of upper-surface-flap deflection δ_f on M2-F2 motions after launch. Dampers on; $M = 0.60$; $\delta_p = 25^{\circ}$; $W_{B-52} = 250\ 000$ pounds (1112 kN); $W_{M2-F2} = 5029$ pounds (22.4 kN); 10° rudder flare.

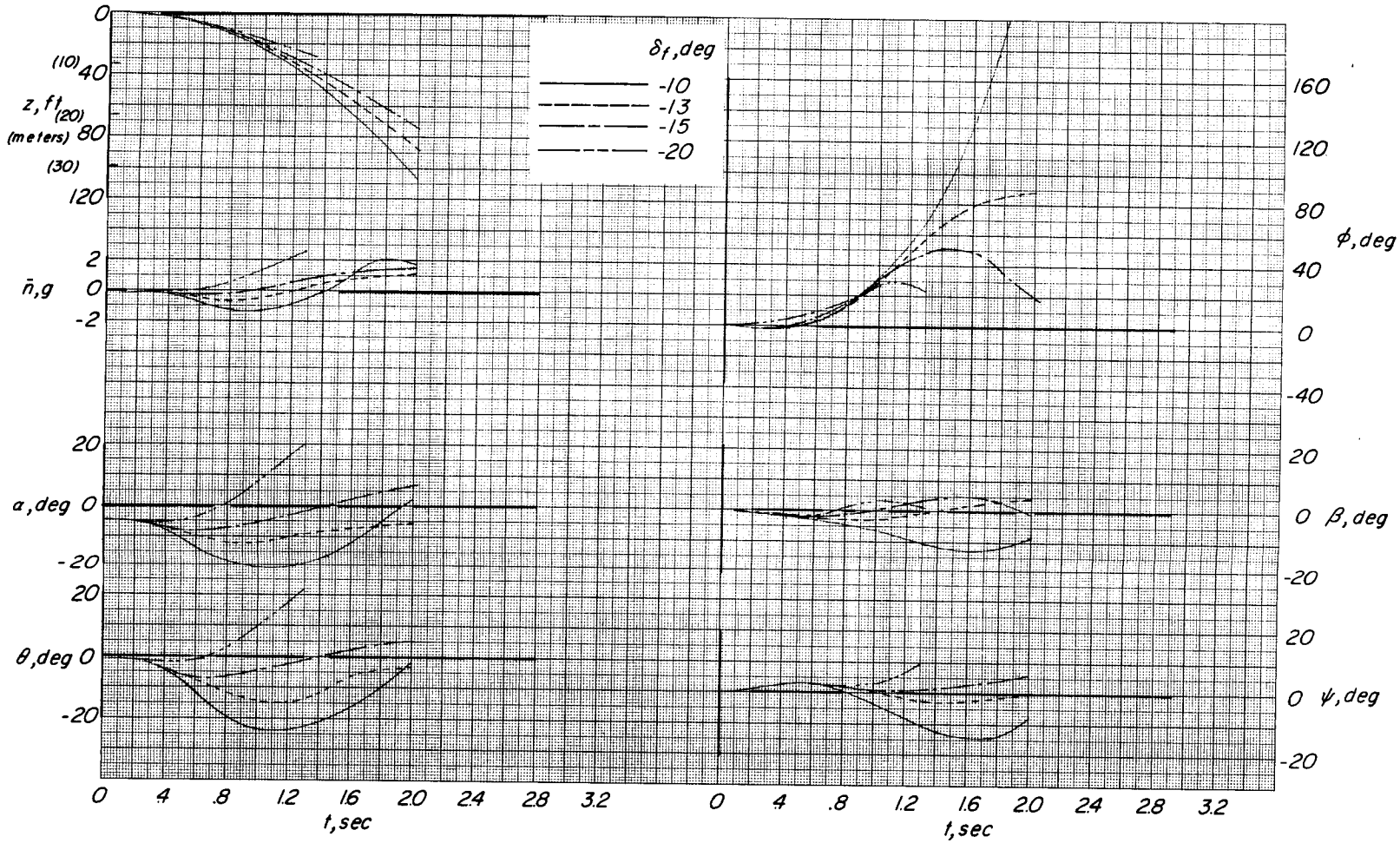

(b) $\alpha_{B-52} = 0^{\circ}$.

Figure 23.- Continued.

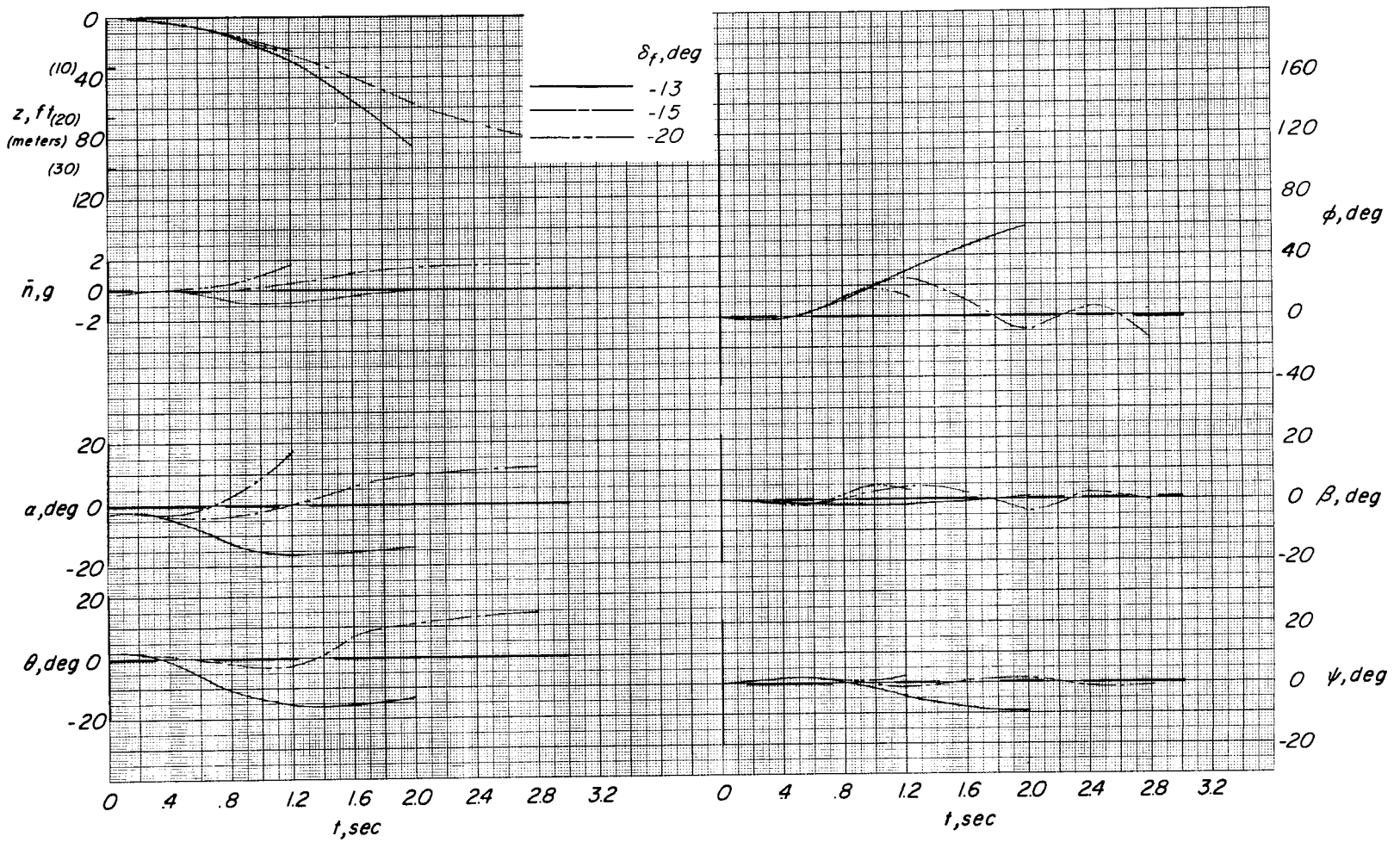

(c) $\alpha_{B-52} = 2^0$.

Figure 23.- Continued.

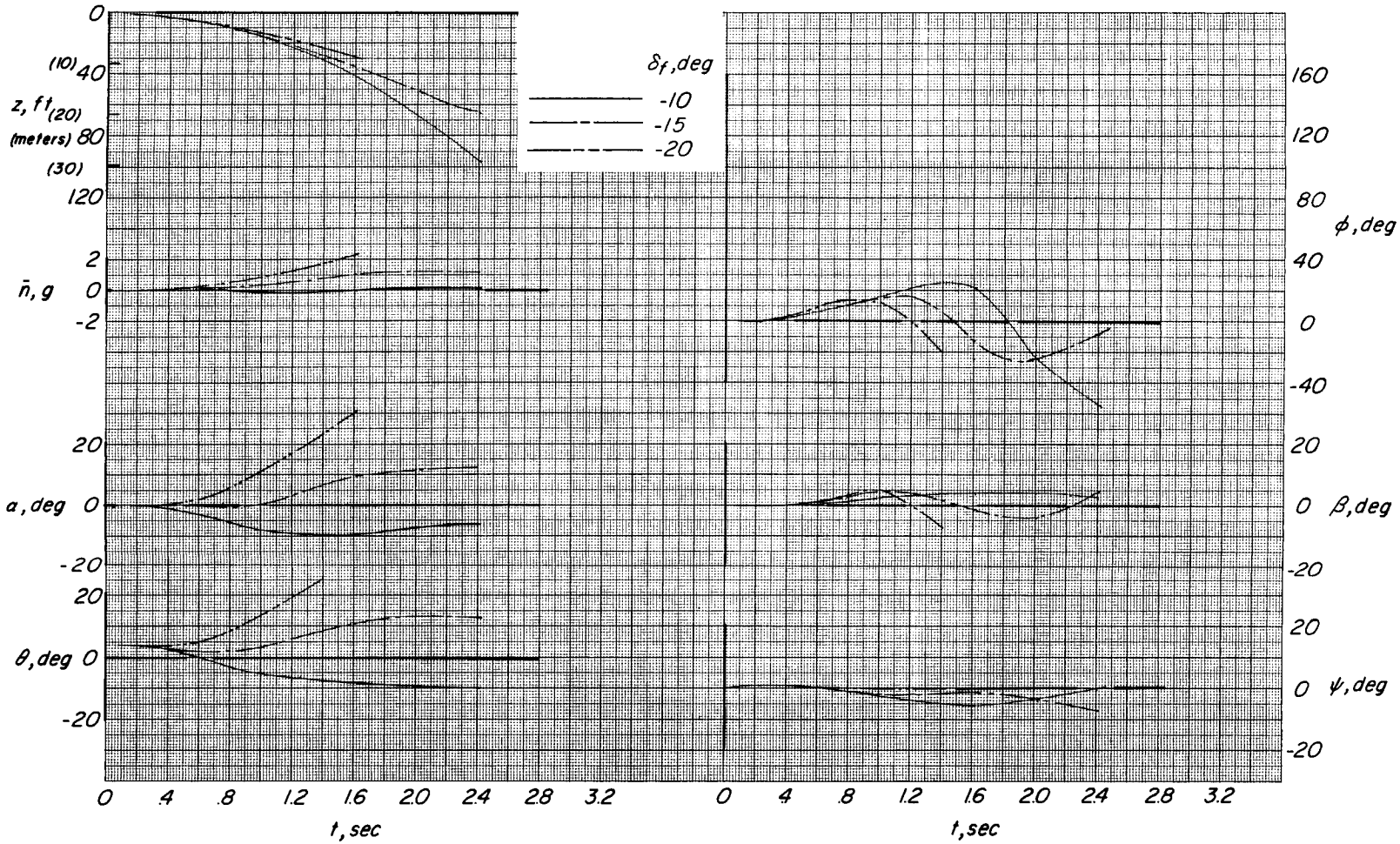

(d) $\alpha_{B-52} = 4^0$.

Figure 23.- Concluded.

[redacted]

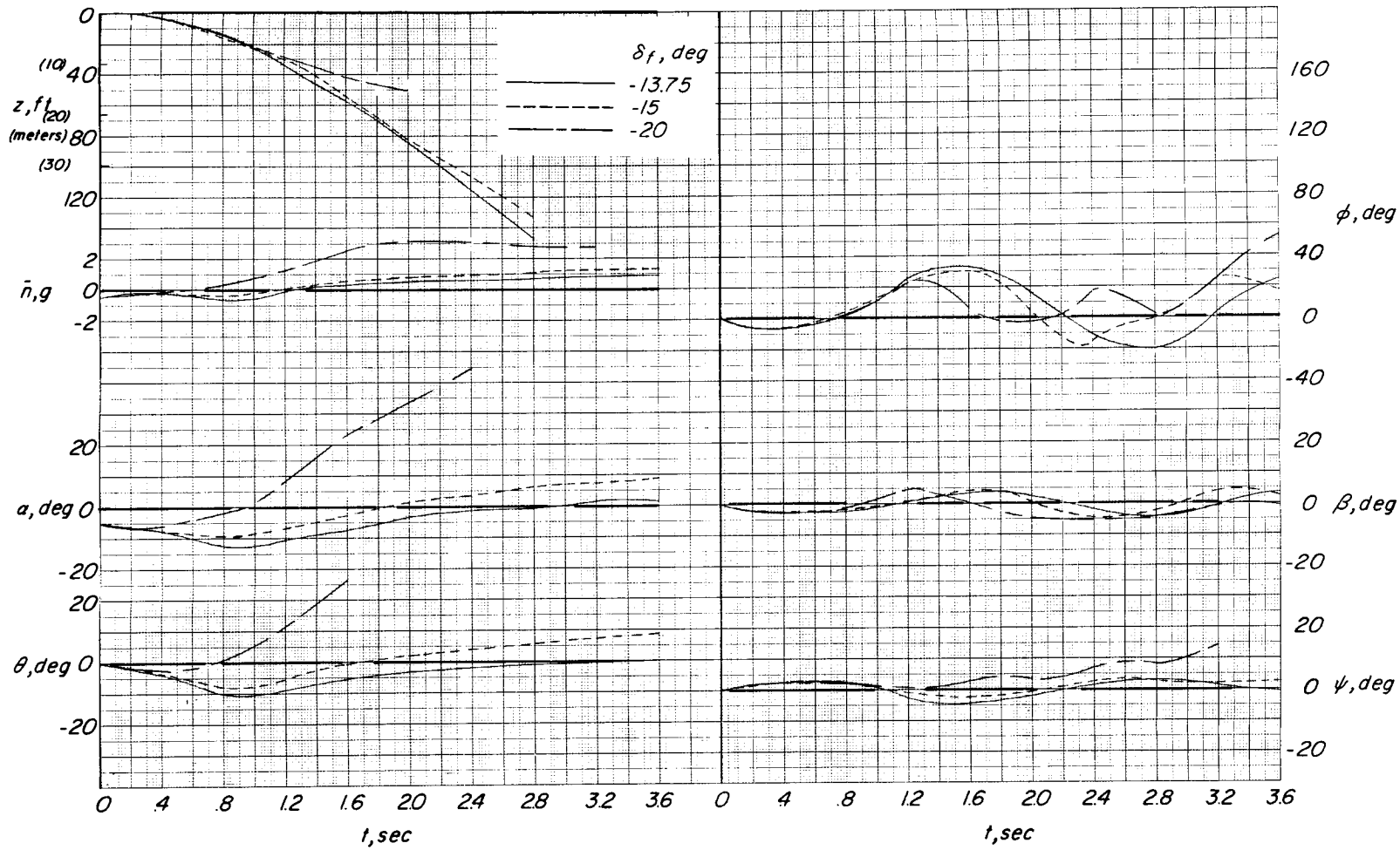

Figure 24.- Effect of upper-surface-flap deflection δ_f on M2-F2 motions after launch. Dampers on; M = 0.80; $\alpha_{B-52} = 0^{\circ}$; $\delta_p = 25^{\circ}$; W_{B-52} = 250 000 pounds (1112 kN); W_{M2-F2} = 5029 pounds (22.4 kN); 10° rudder flare.

[redacted]

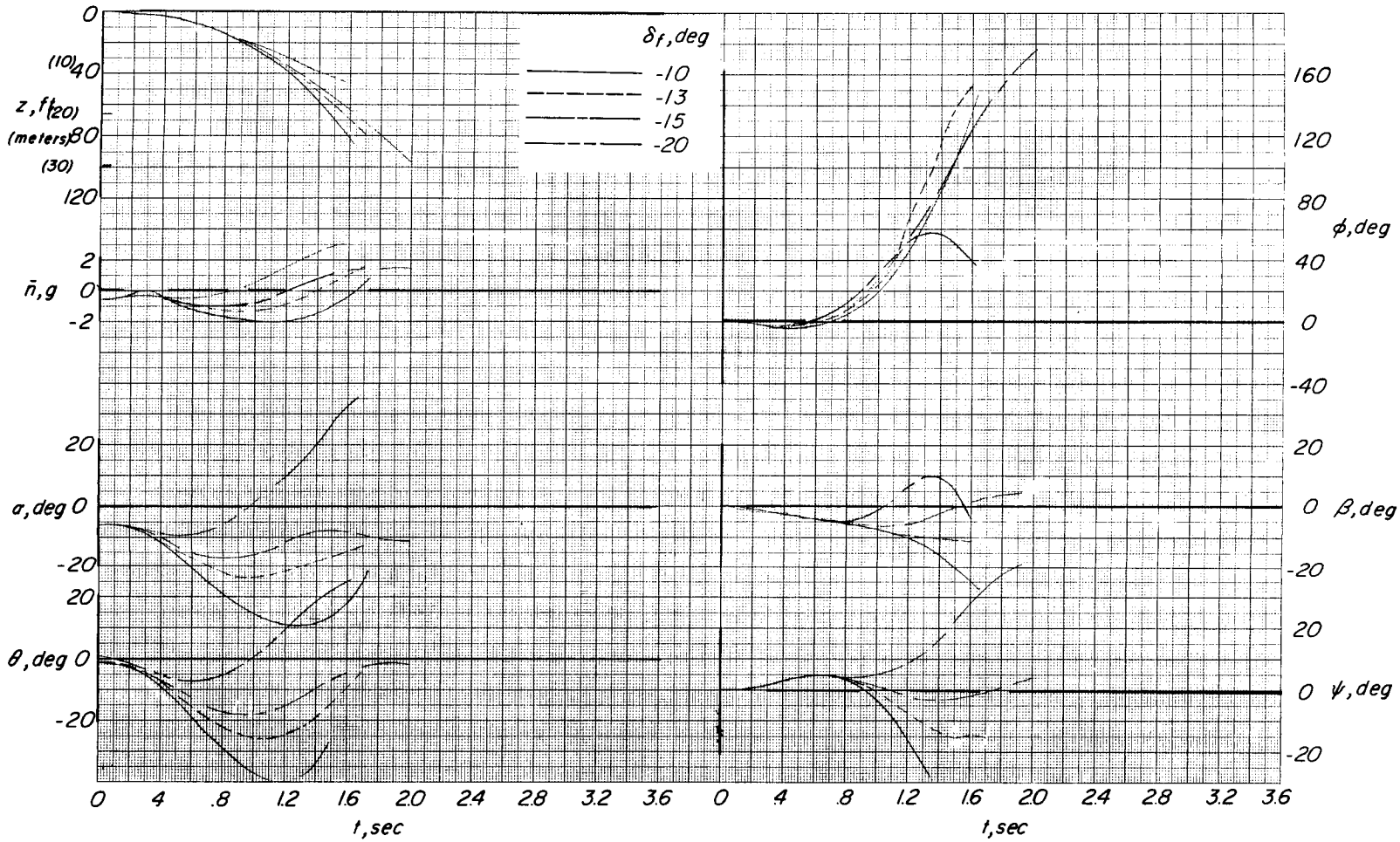

(a) $\alpha_{B-52} = -1^{\circ}$.

Figure 25.- Effect of upper-surface-flap deflection δ_f on M2-F2 motions after launch. Dampers off; M = 0.60; $\delta_p = 25^{\circ}$; W_{B-52} = 190 000 pounds (845 kN); W_{M2-F2} = 5029 pounds (22.4 kN); 10° rudder flare.

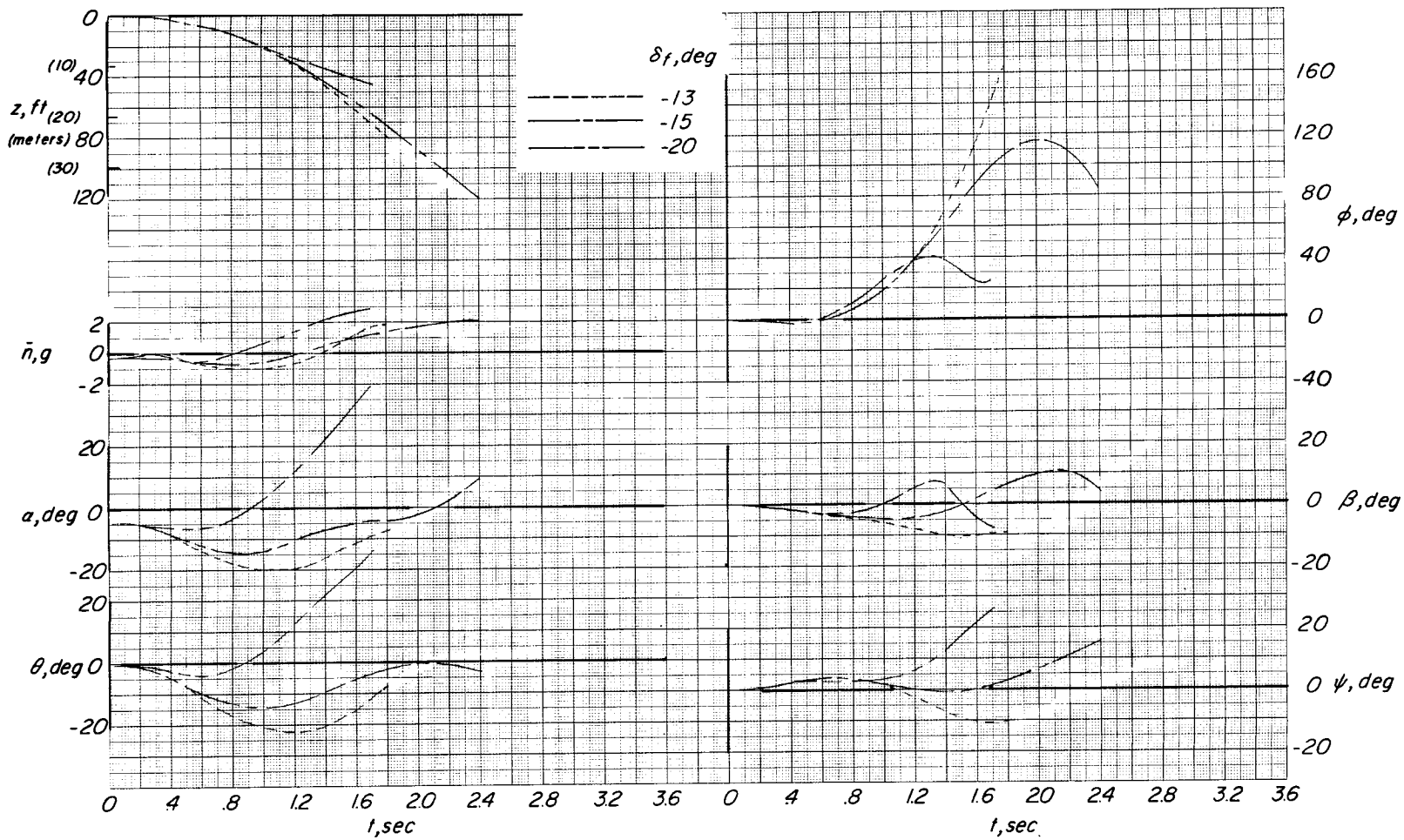

(b) $\alpha_{B-52} = 0^{\circ}$.

Figure 25.- Continued.

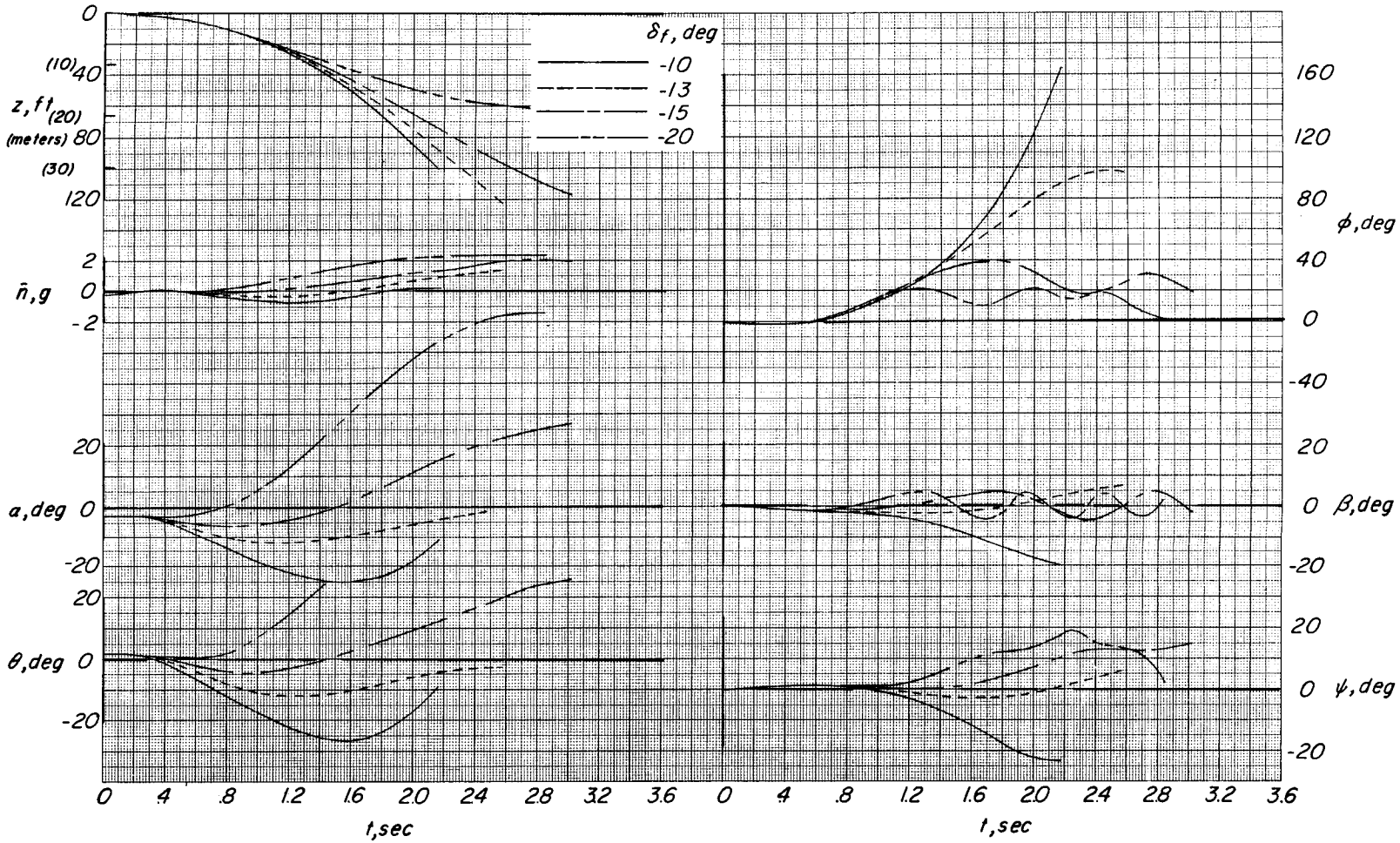

(c) $\alpha_{B-52} = 2^0$.

Figure 25.- Continued.

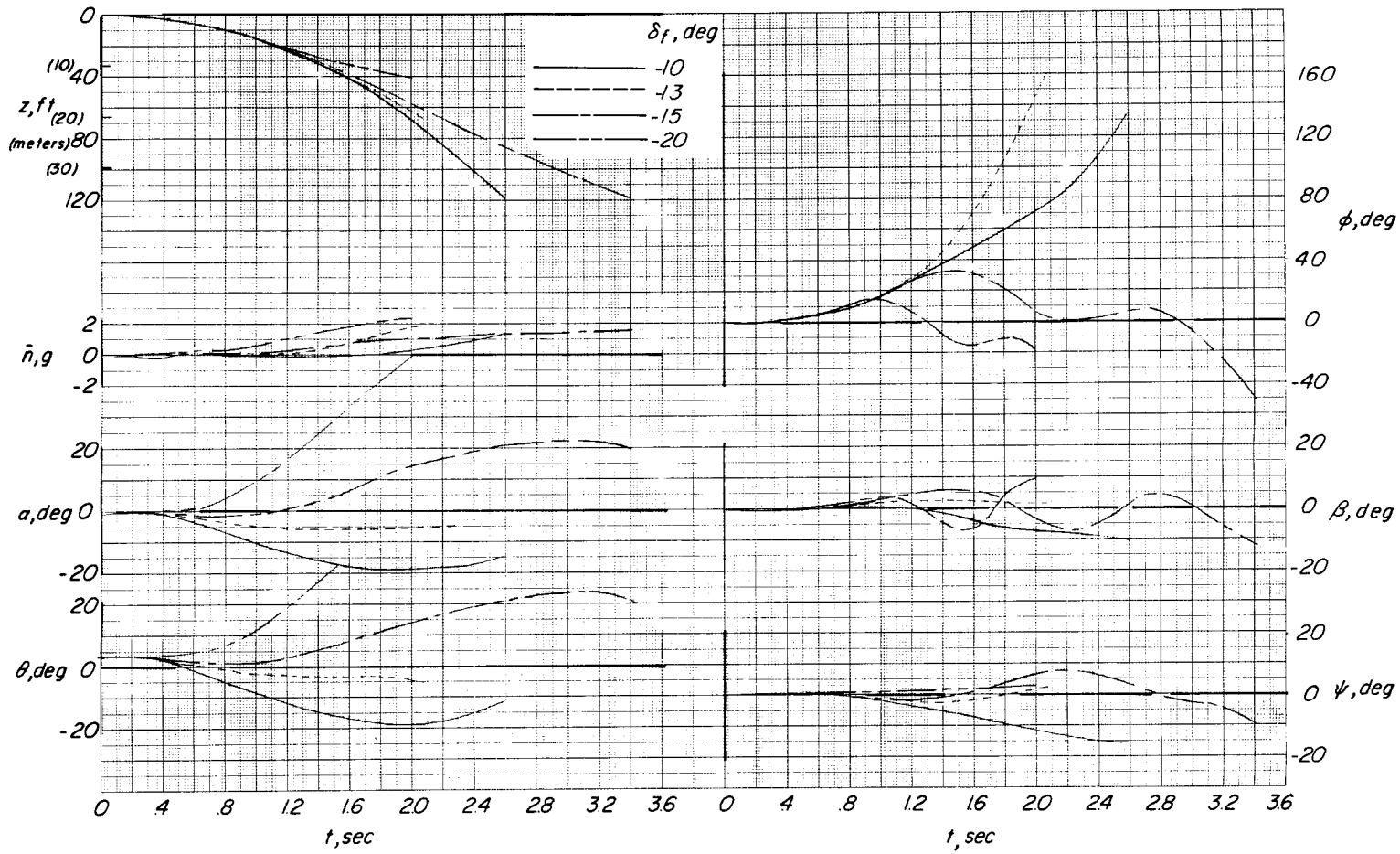

(d) $\alpha_{B-52} = 4^0$.

Figure 25.- Concluded.

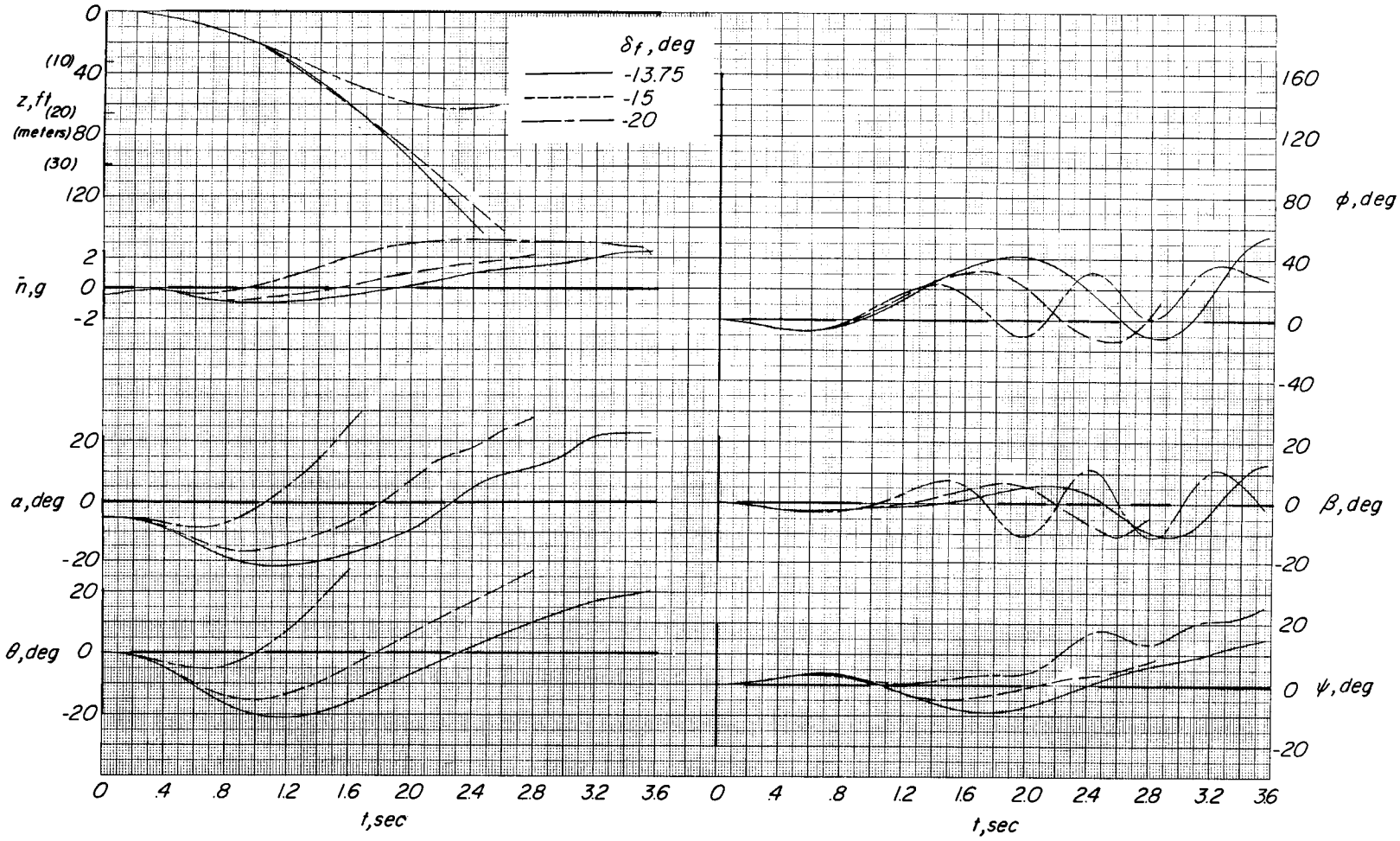

Figure 26.- Effect of upper-surface-flap deflection δ_f on M2-F2 motions after launch. Dampers off; M = 0.80; $\delta_p = 25^{\circ}$; W_{B-52} = 190 000 pounds (845 kN); W_{M2-F2} = 5029 pounds (22.4 kN); 10° rudder flare.

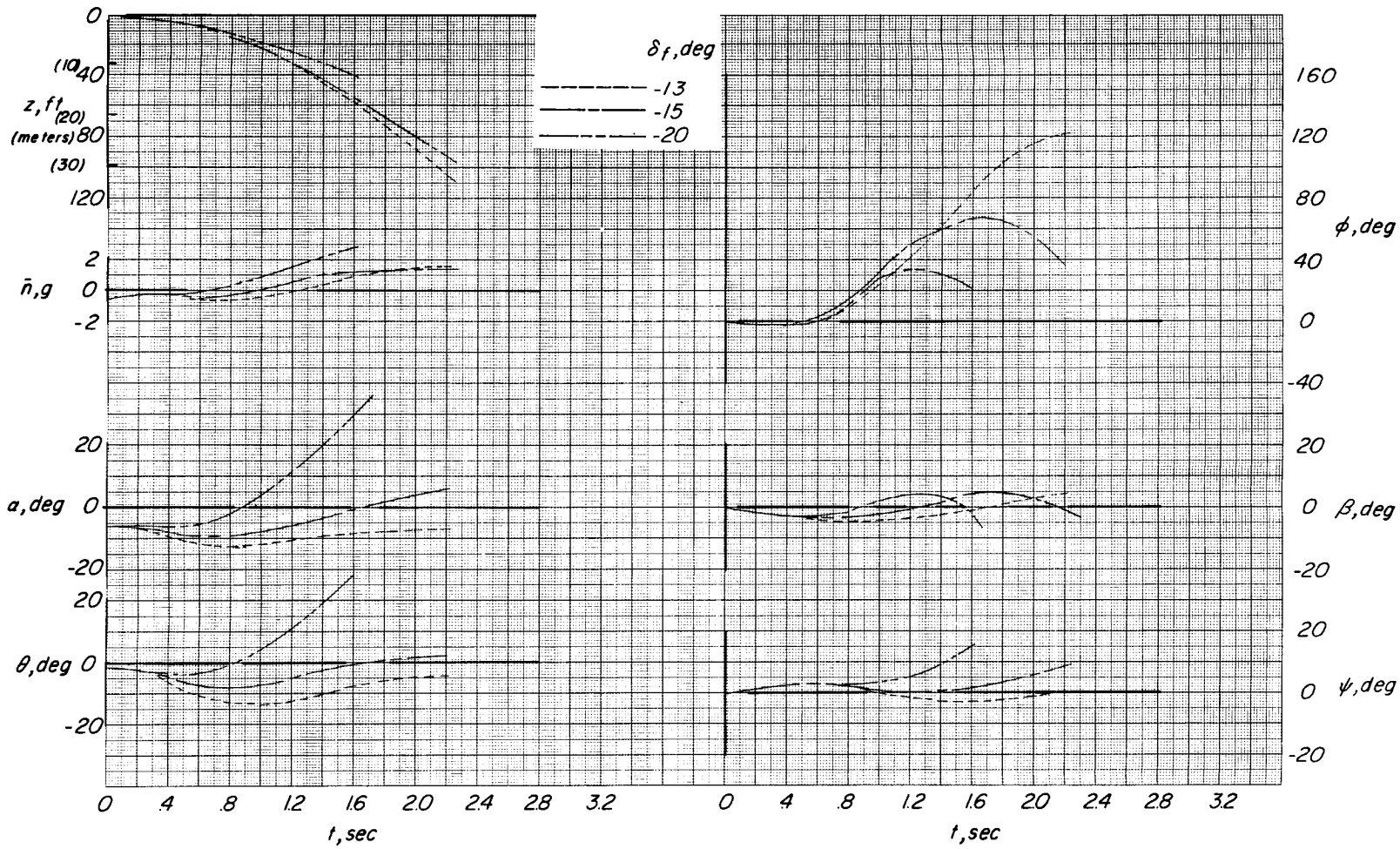

(a) $\alpha_{B-52} = -1^{\circ}$.

Figure 27.- Effect of upper-surface-flap deflection δ_f on M2-F2 motions after launch. Dampers on; M = 0.60; $\delta_p = 25^{\circ}$; W_{B-52} = 190 000 pounds (845 kN); W_{M2-F2} = 5029 pounds (22.4 kN); 10° rudder flare.

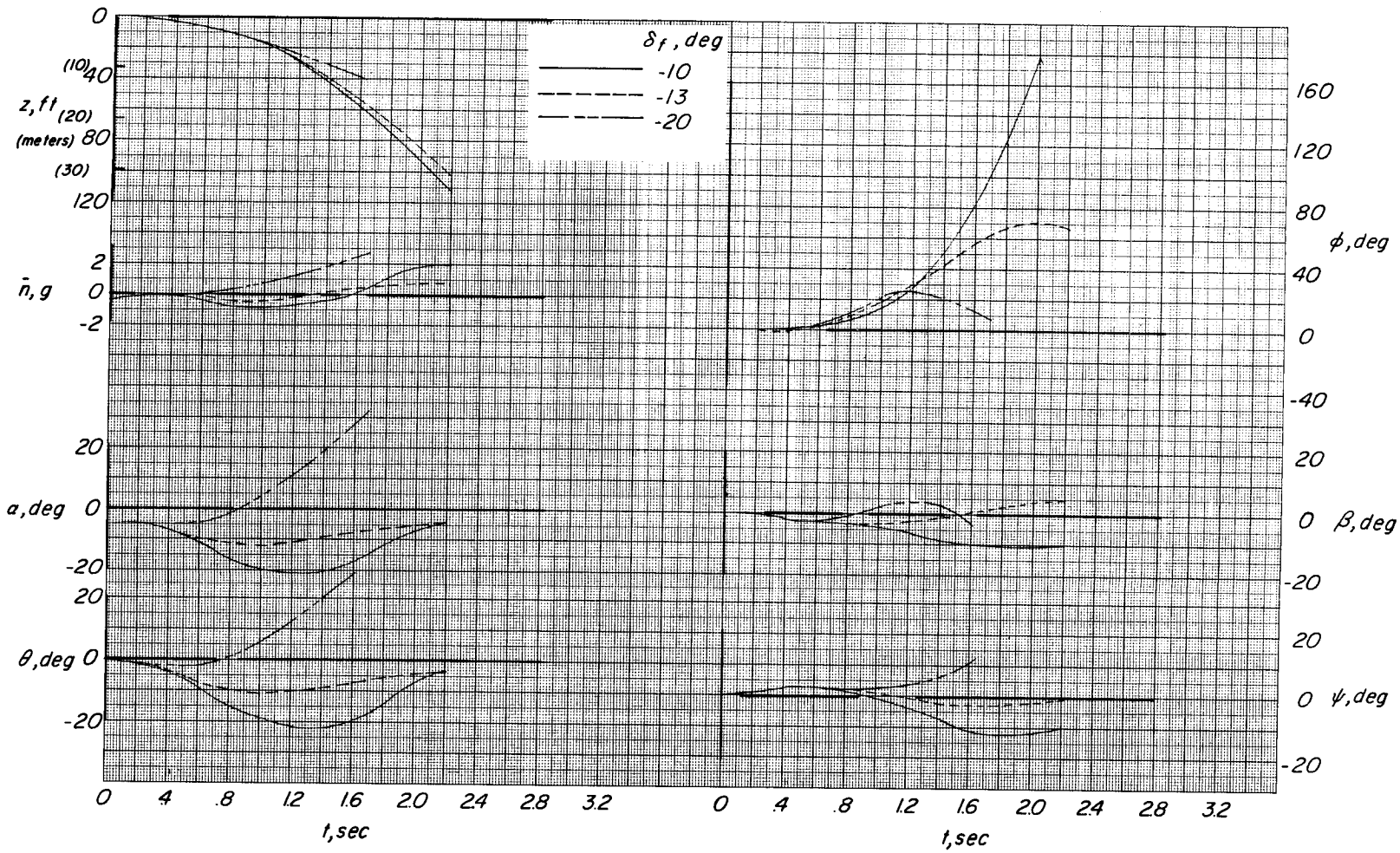

(b) $\alpha_{B-52} = 0^{\circ}$.

Figure 27.- Continued.

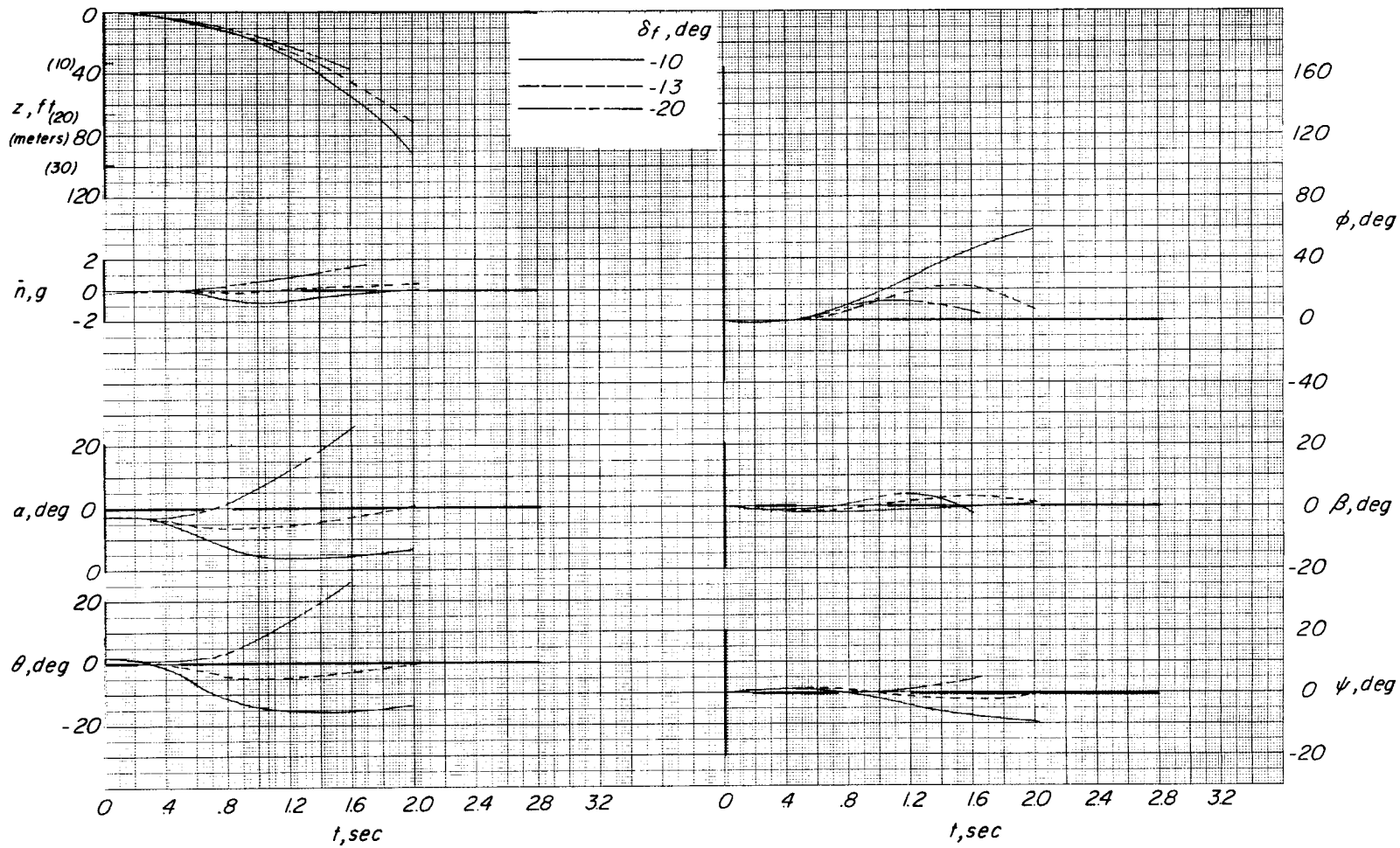

(c) $\alpha_{B-52} = 2^0$.

Figure 27.- Continued.

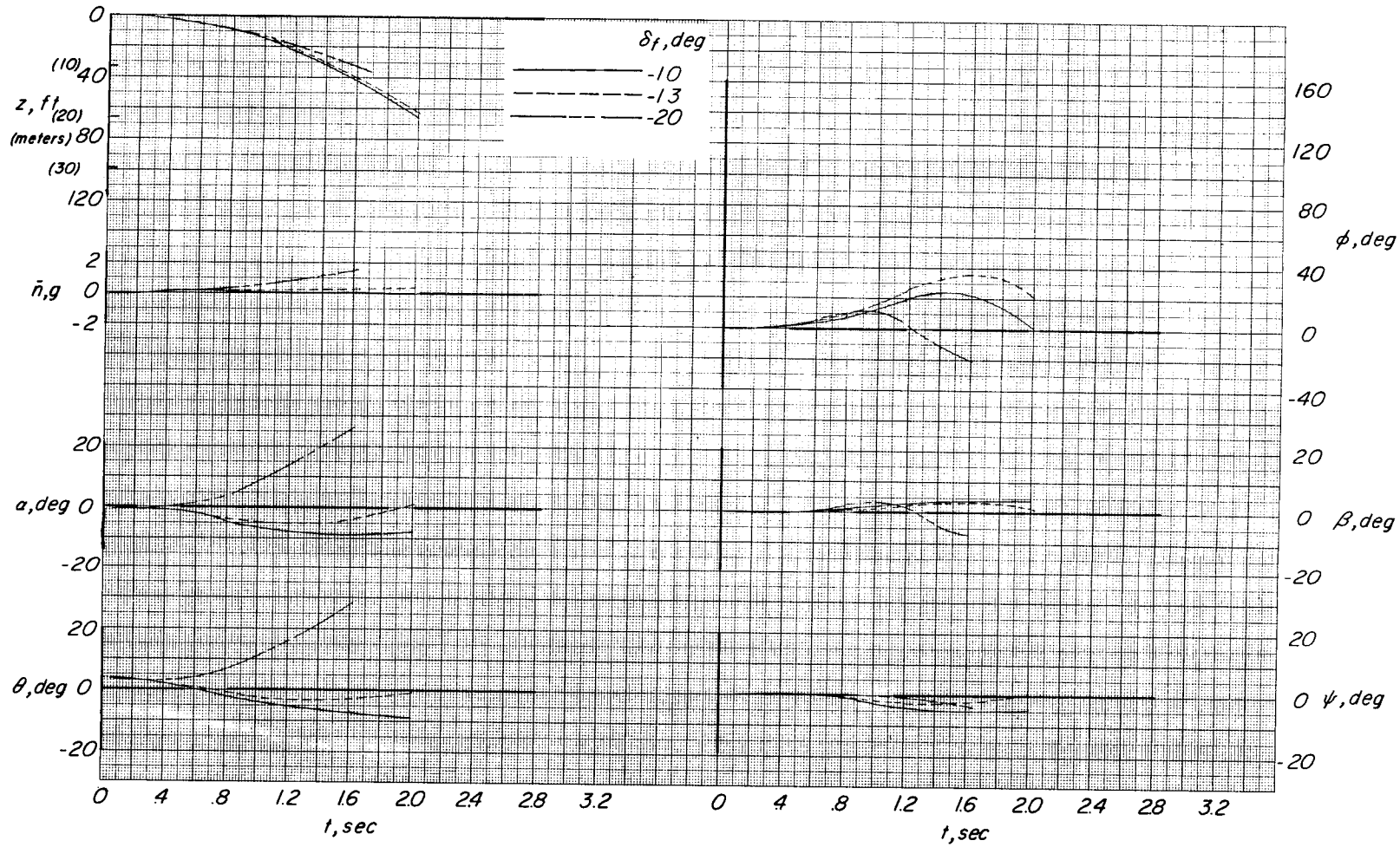

(d) $\alpha_{B-52} = 4^{\circ}$.

Figure 27.- Concluded.

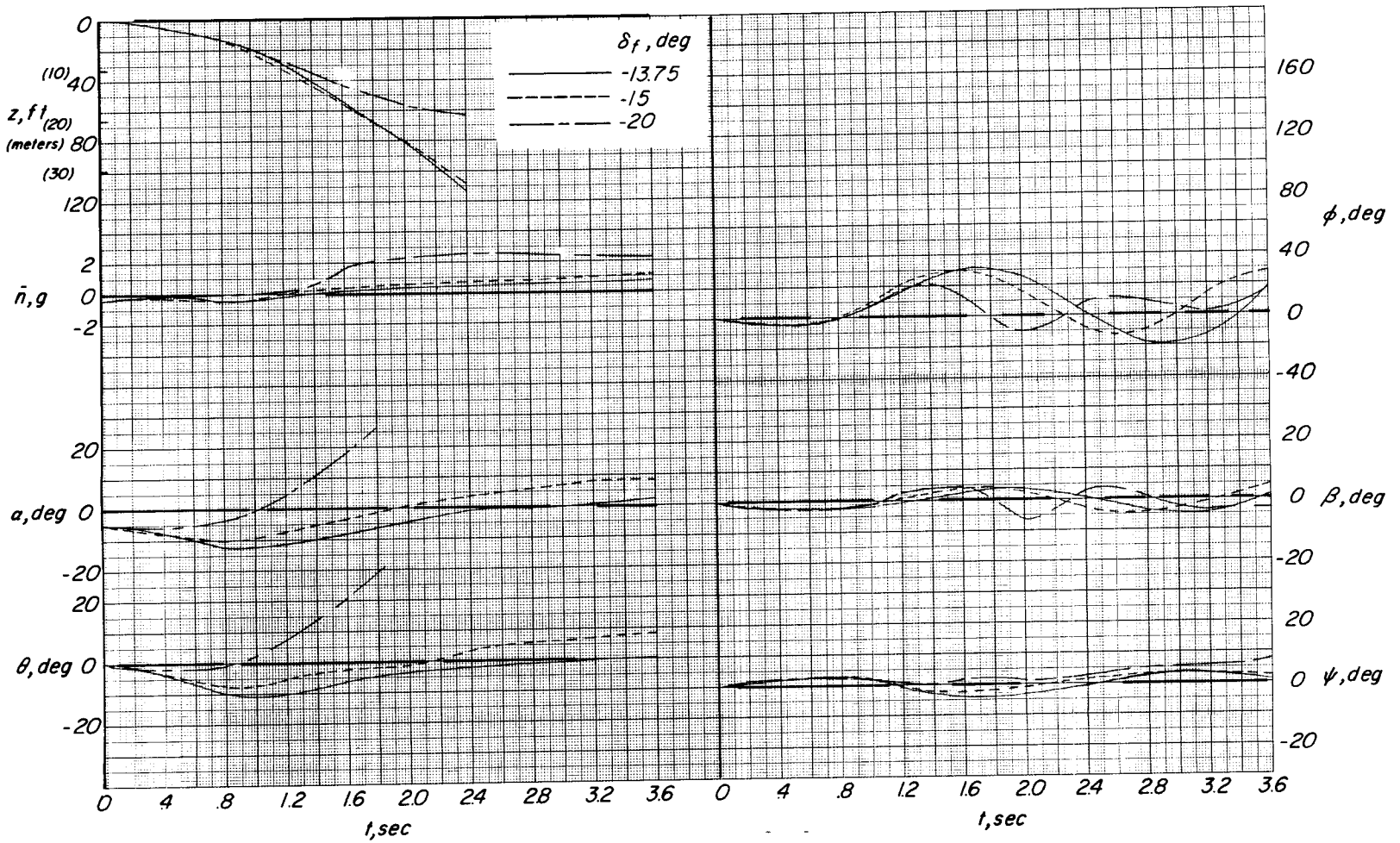

Figure 28.- Effect of upper-surface-flap deflection δ_f on M2-F2 motions after launch. Dampers on; M = 0.80; $\delta_p = 25^0$; W_{B-52} = 190 000 pounds (845 kN); W_{M2-F2} = 5029 pounds (22.4 kN); 10^0 rudder flare.

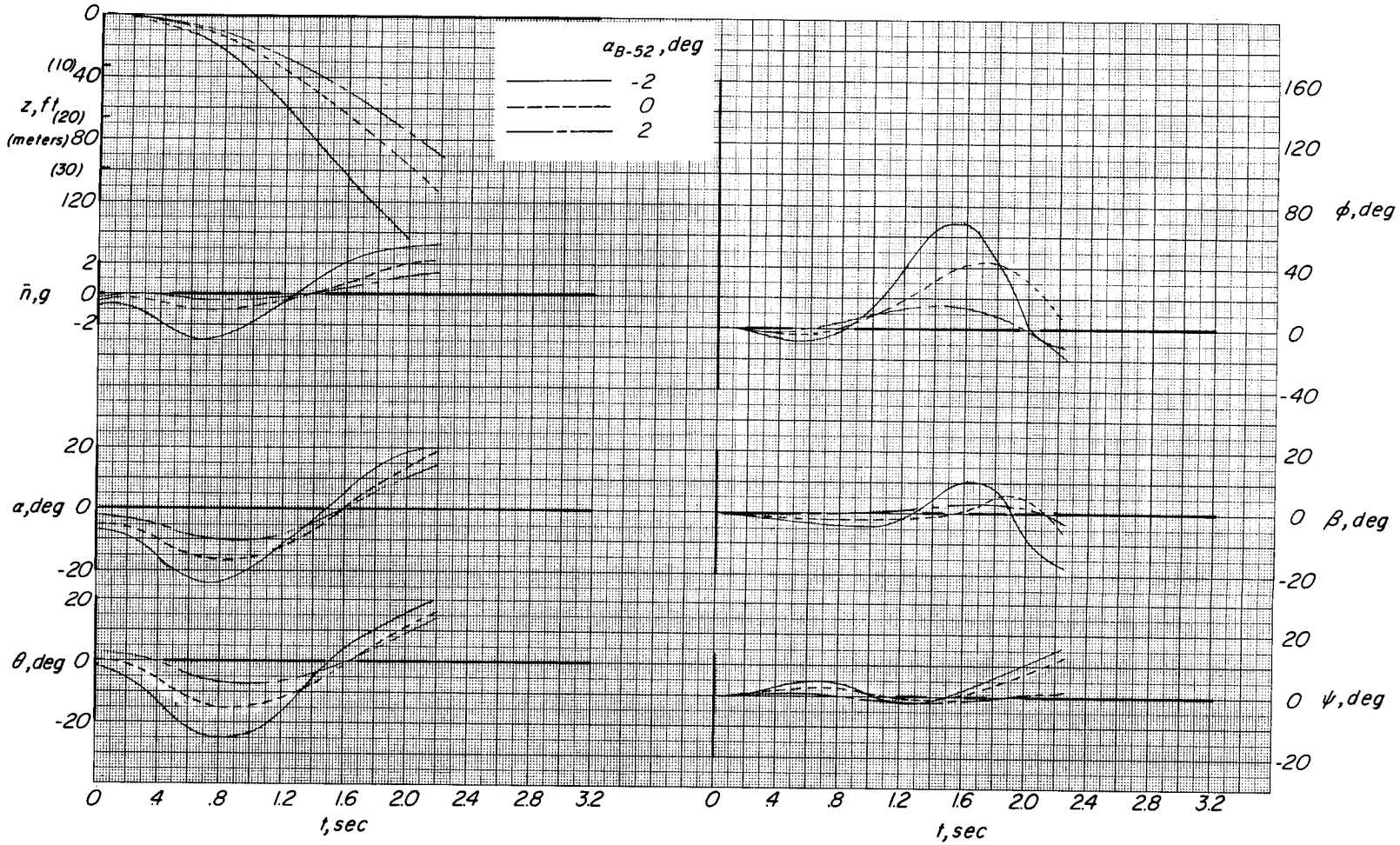

(a) M = 0.70.

Figure 29.- Effect of B-52 angle of attack (varying altitude) on M2-F2 motions after launch. Dampers off; $\delta_p = 25^0$; $\delta_f = -15^0$; W_{B-52} = 250 000 pounds (1112 kN); W_{M2-F2} = 5029 pounds (22.4 kN); 10^0 rudder flare.

[redacted]

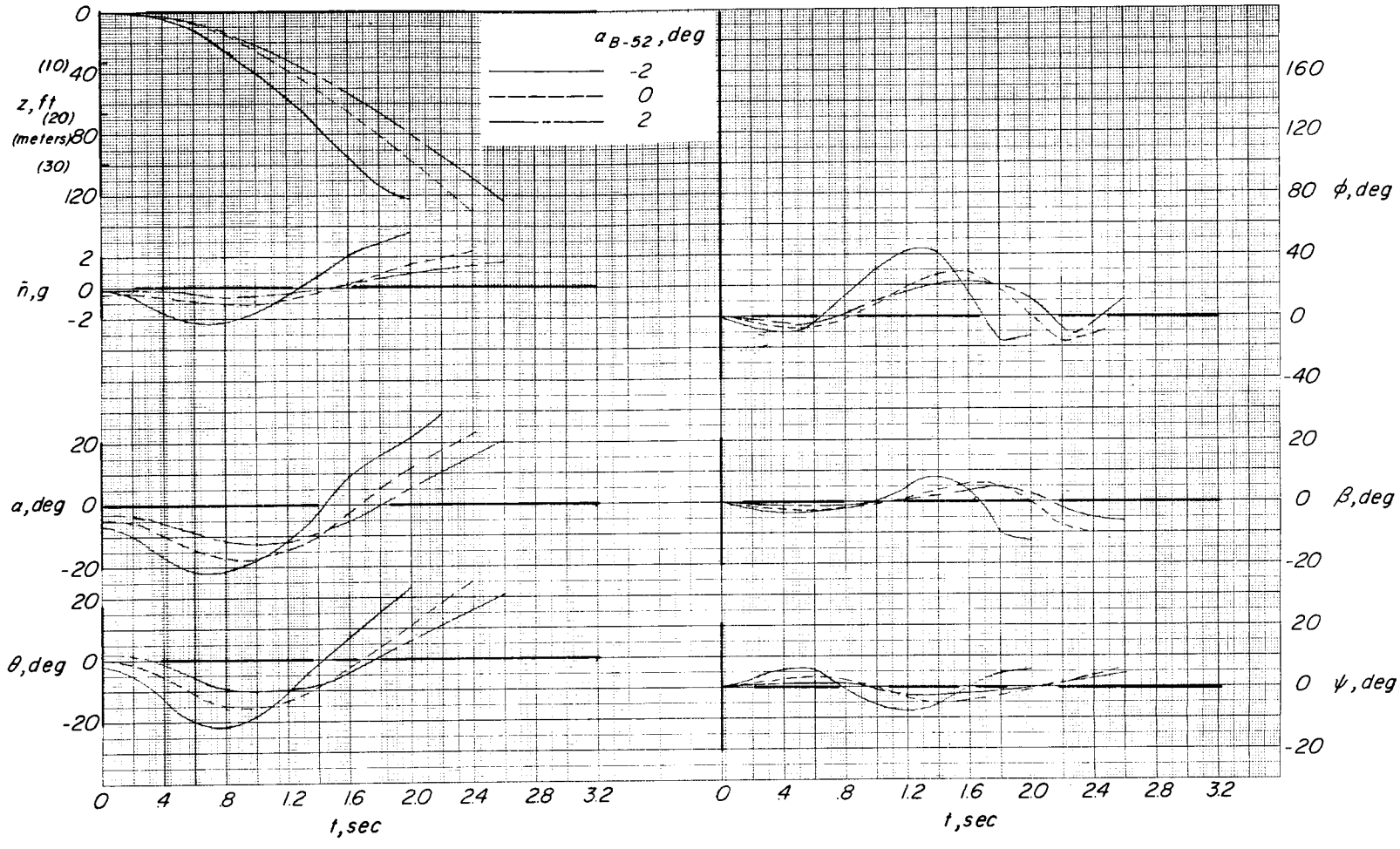

[redacted]

(b) M = 0.80.

Figure 29.- Continued.

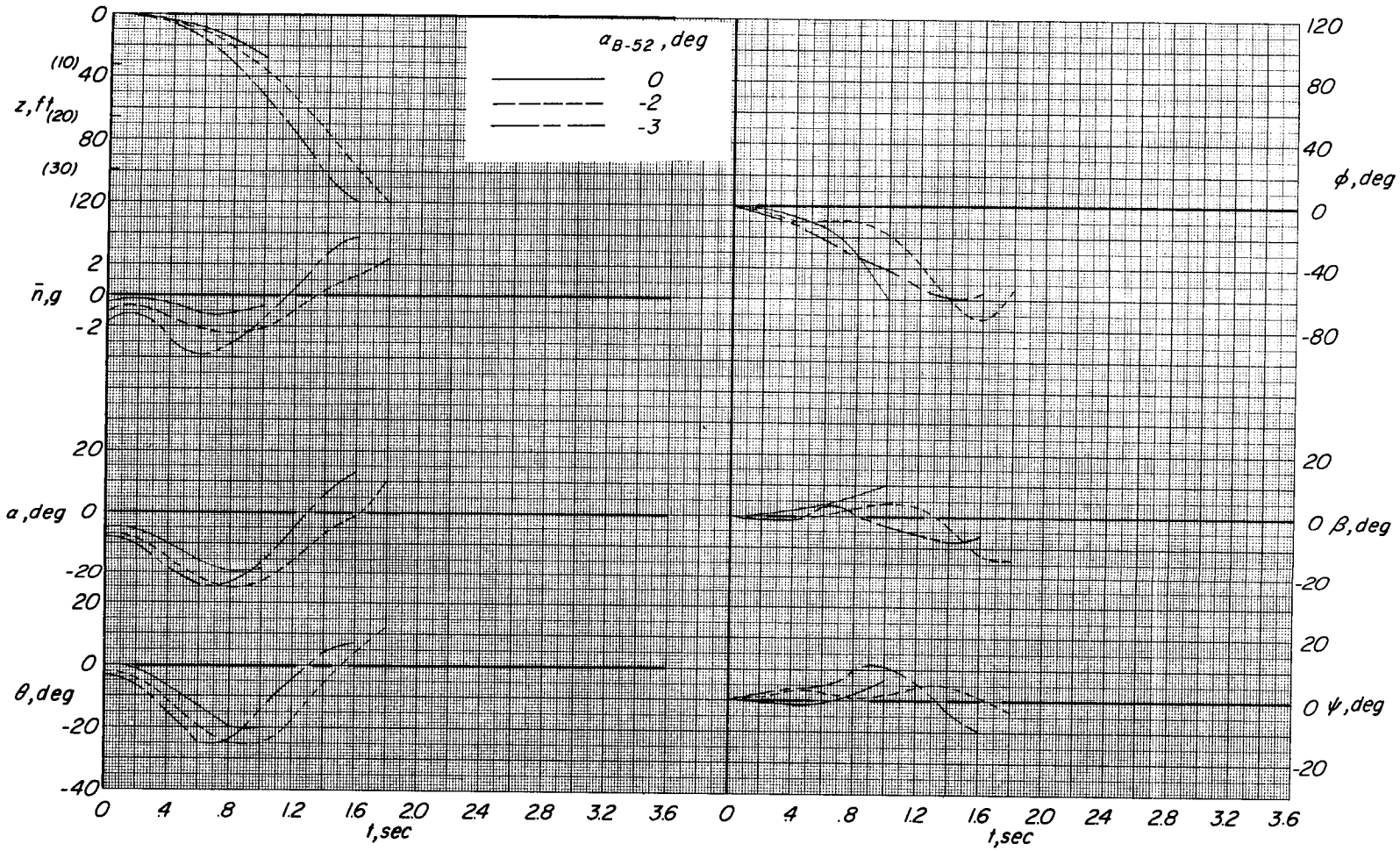

(c) M = 0.85.

Figure 29.- Concluded.

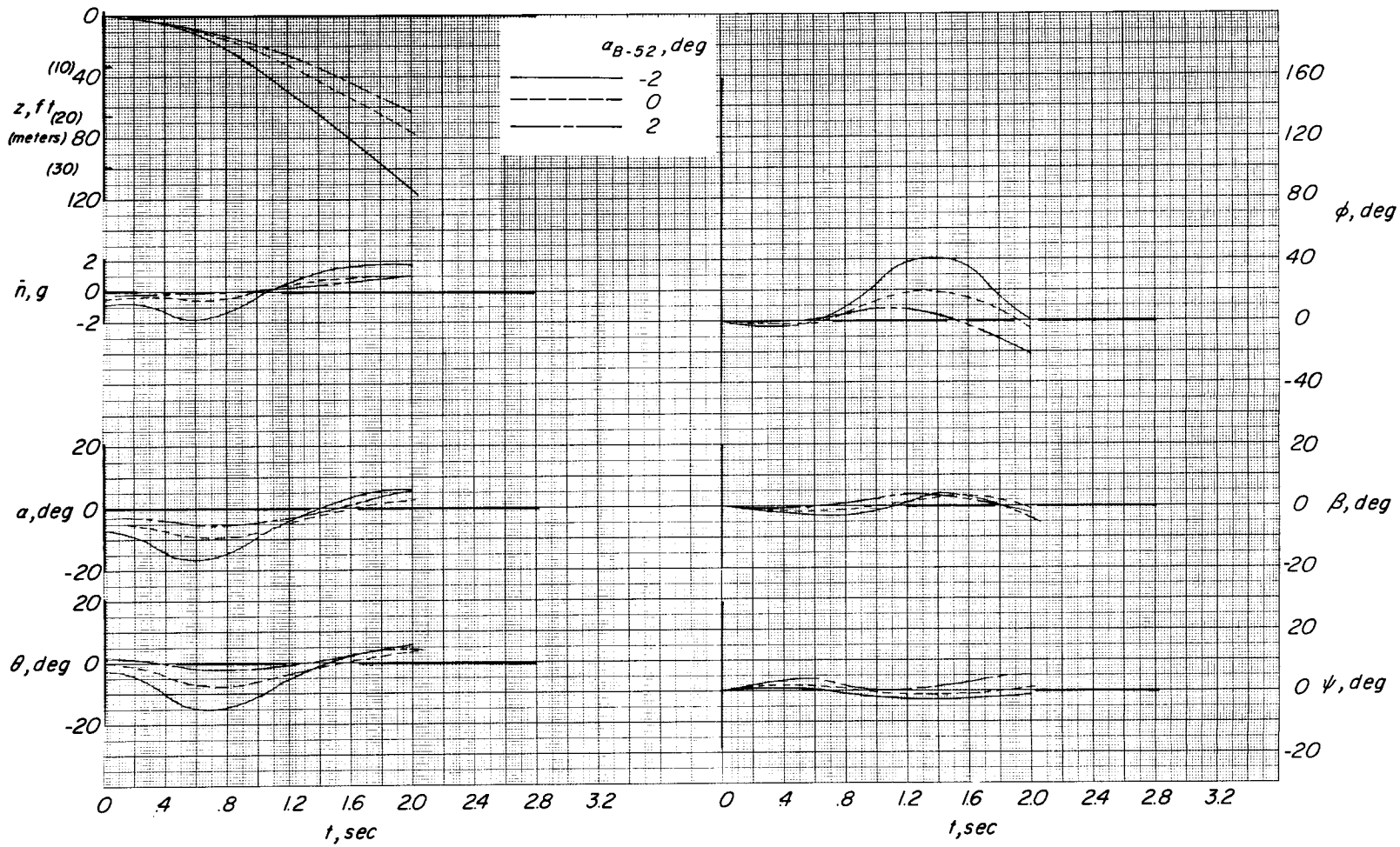

(a) M = 0.70.

Figure 30.- Effect of B-52 angle of attack (varying altitude) on M2-F2 motions after launch. Dampers on; $\delta_p = 25^0$; $\delta_f = -15^0$; $W_{B-52} = 250\ 000$ pounds (1112 kN); $W_{M2-F2} = 5029$ pounds (22.4 kN); 10^0 rudder flare.

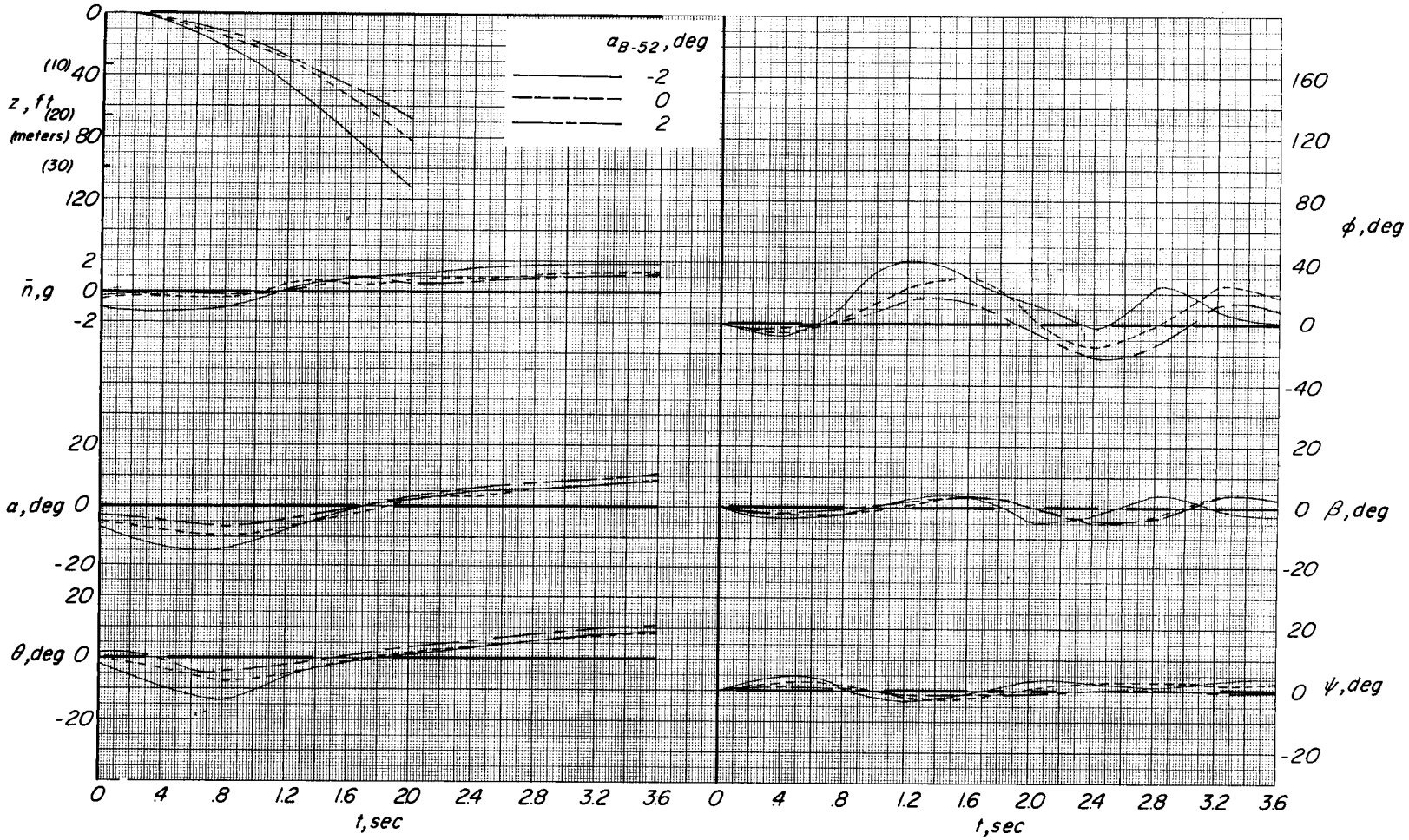

(b) M = 0.80.

Figure 30.- Concluded.

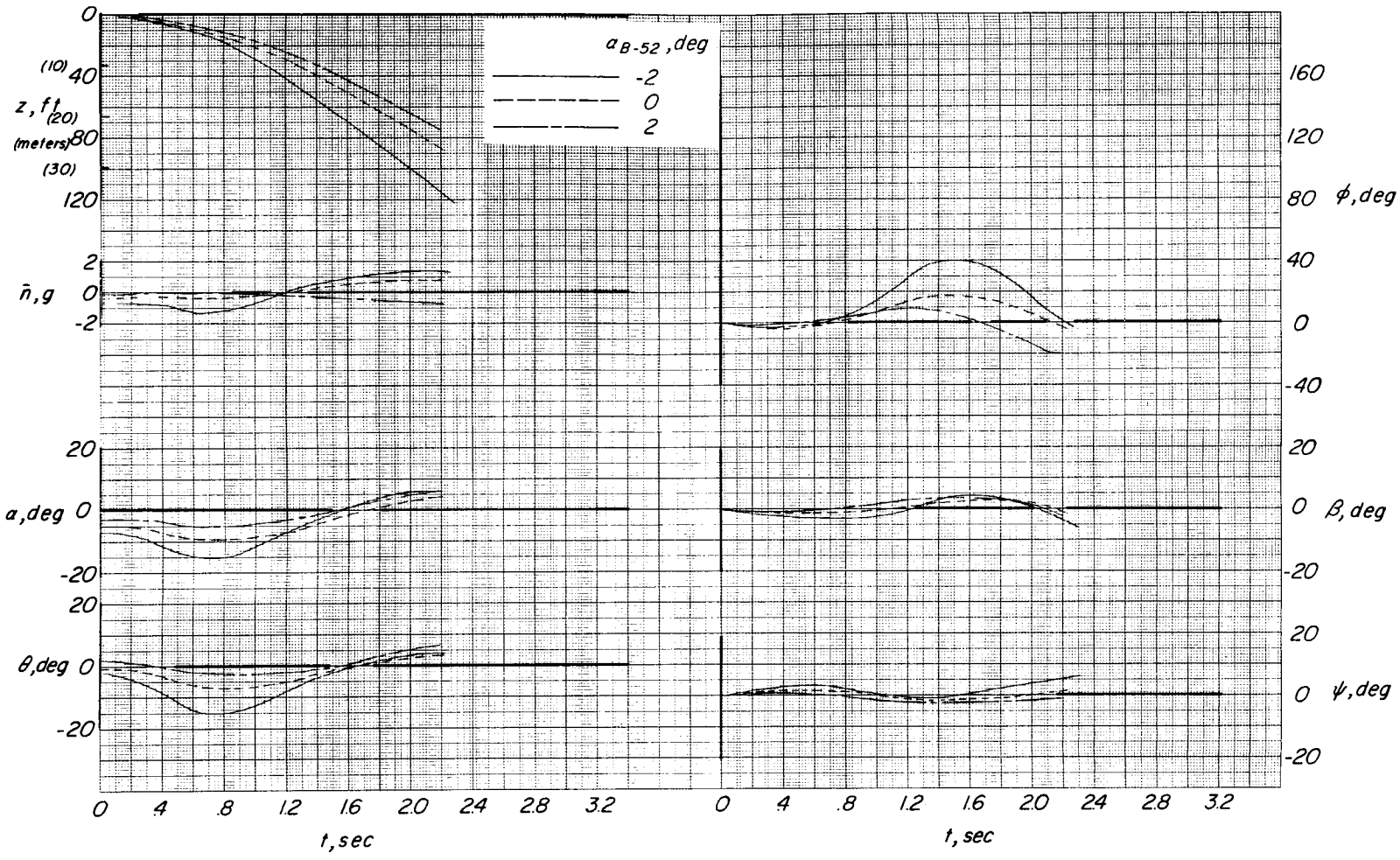

(a) M = 0.70.

Figure 31.- Effect of B-52 angle of attack (varying altitude) on M2-F2 motions after launch. Dampers on; $\delta_f = -15^0$; $\delta_p = 25^0$; W_{B-52} = 190 000 pounds (845 kN); W_{M2-F2} = 5029 pounds (22.4 kN); 10^0 rudder flare.

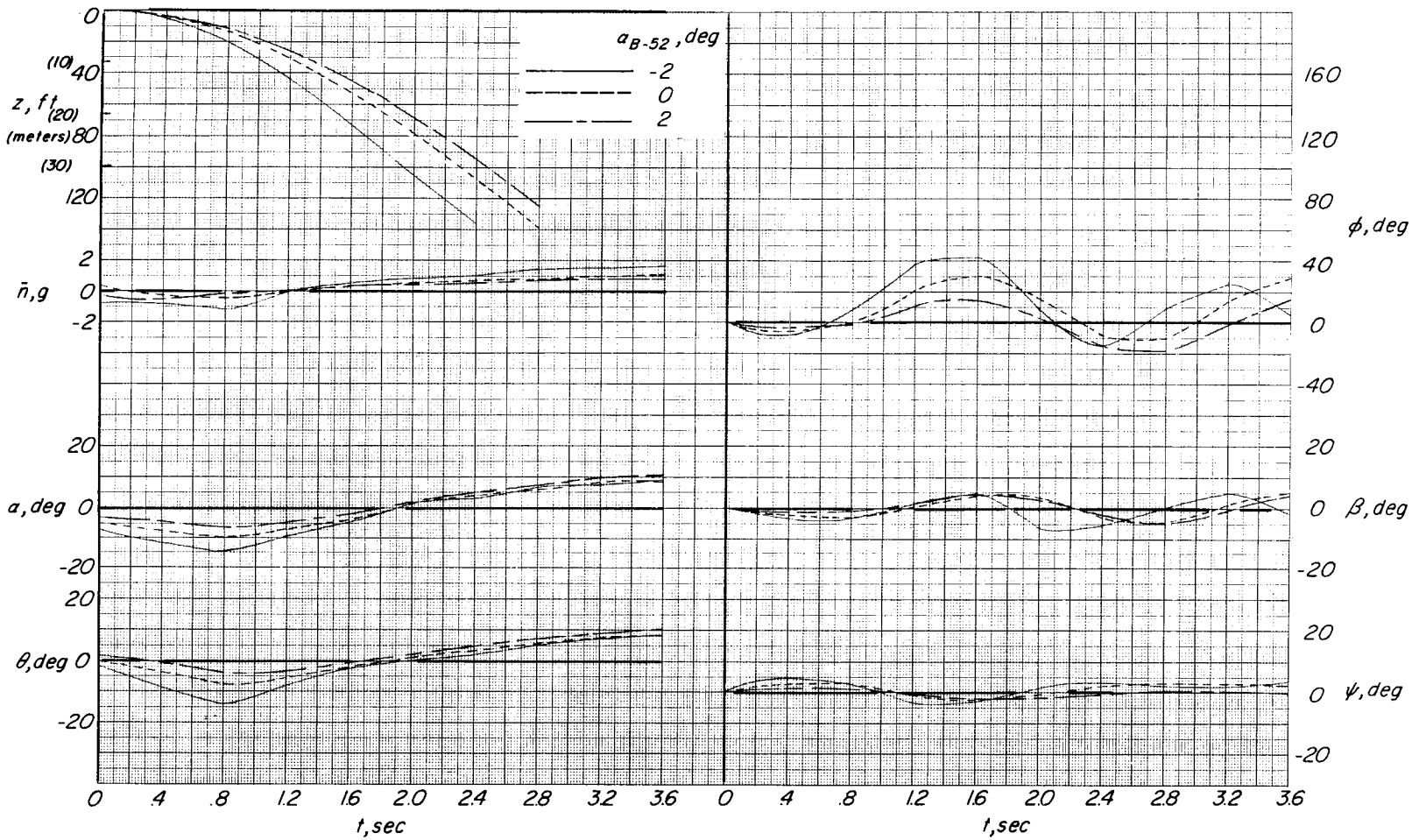

(b) M = 0.80.

Figure 31.- Concluded.

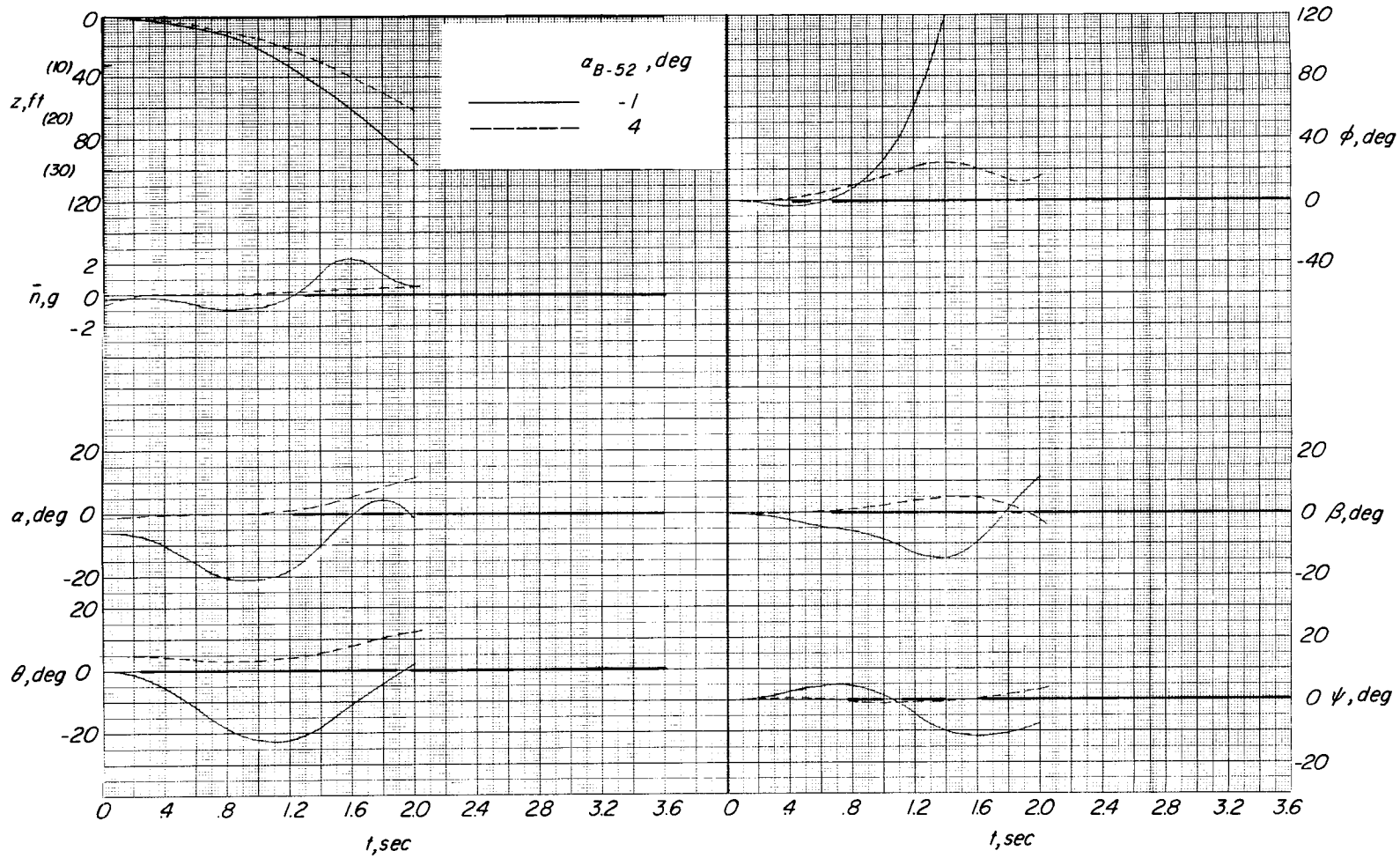

(a) M = 0.60.

Figure 32.- Effect of B-52 angle of attack (varying altitude) on M2-F2 motions after launch. Dampers off; $\delta_f = -15^{\circ}$; $\delta_p = 25^{\circ}$; W_{B-52} = 250 000 pounds (1112 kN); W_{M2-F2} = 9030 pounds (40.2 kN); 10° rudder flare.

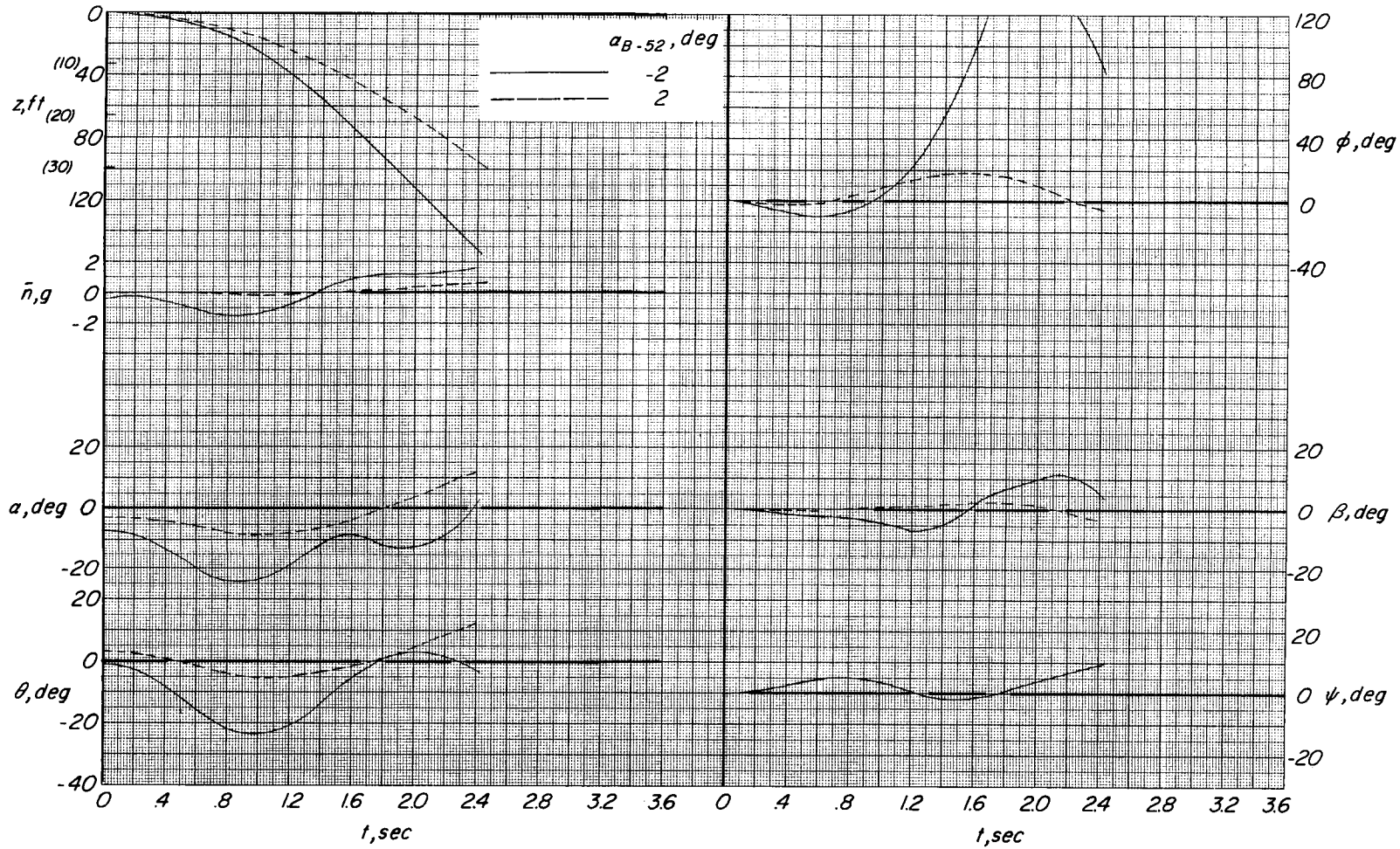

(b) M = 0.70.

Figure 32.- Continued.

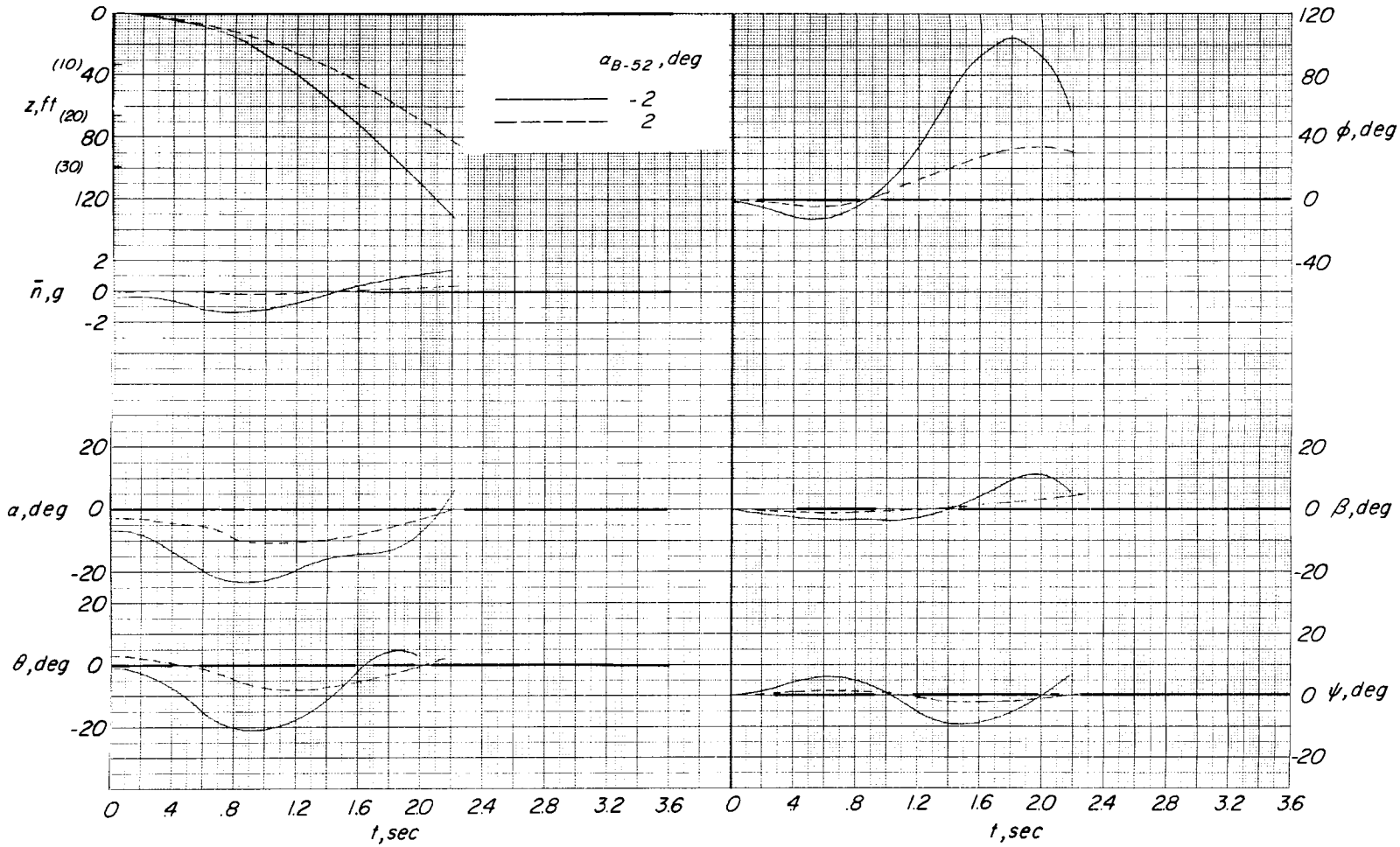

(c) M = 0.80.

Figure 32.- Concluded.

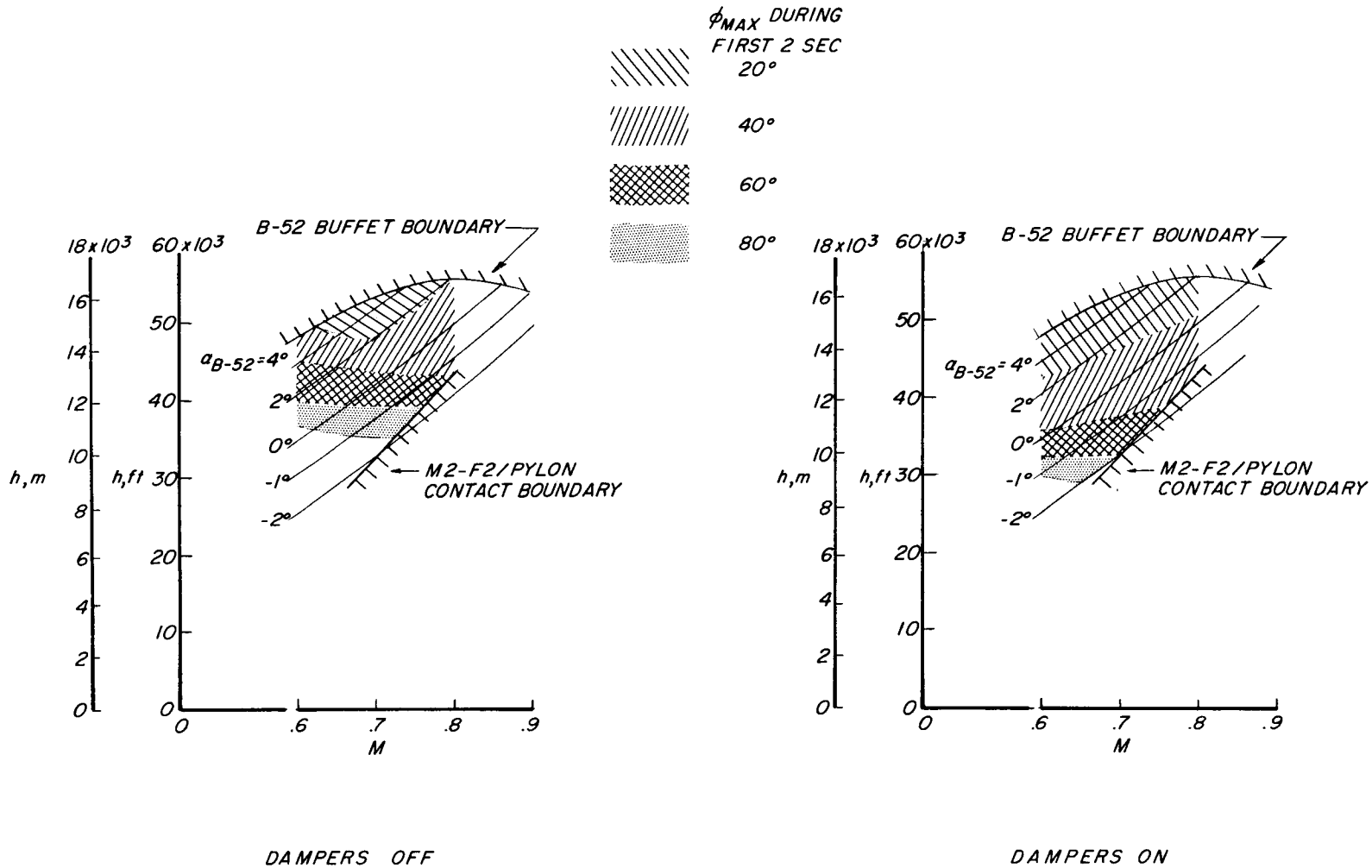

(a) W_{B-52} = 250 000 pounds (1112 kN).

Figure 33.- Launch envelope. W_{M2-F2} = 5029 pounds (22.4 kN).

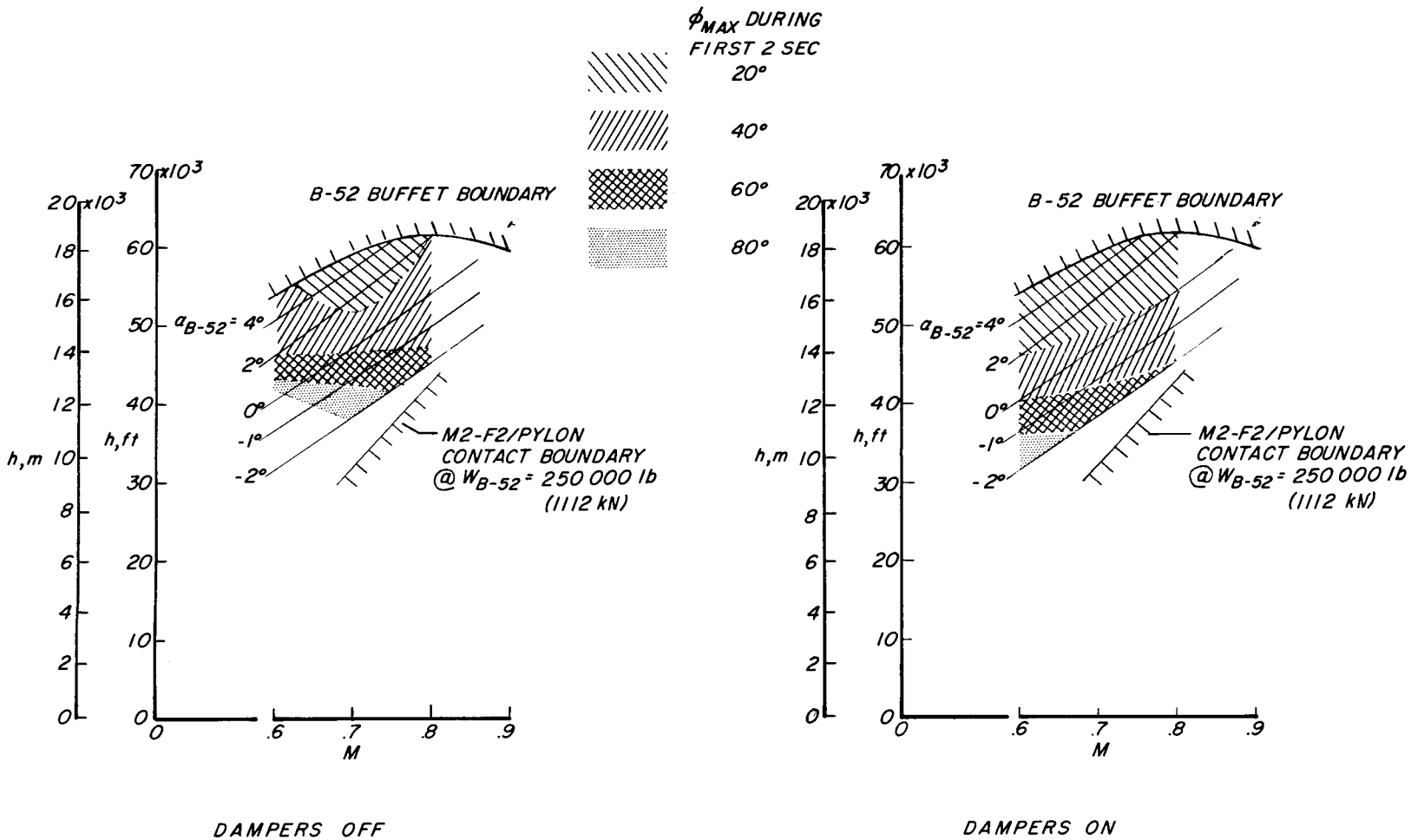

(b) W_{B-52} = 190 000 pounds (845 kN).

Figure 33.- Concluded.

NASA-Langley, 1968 — 1 L-5602

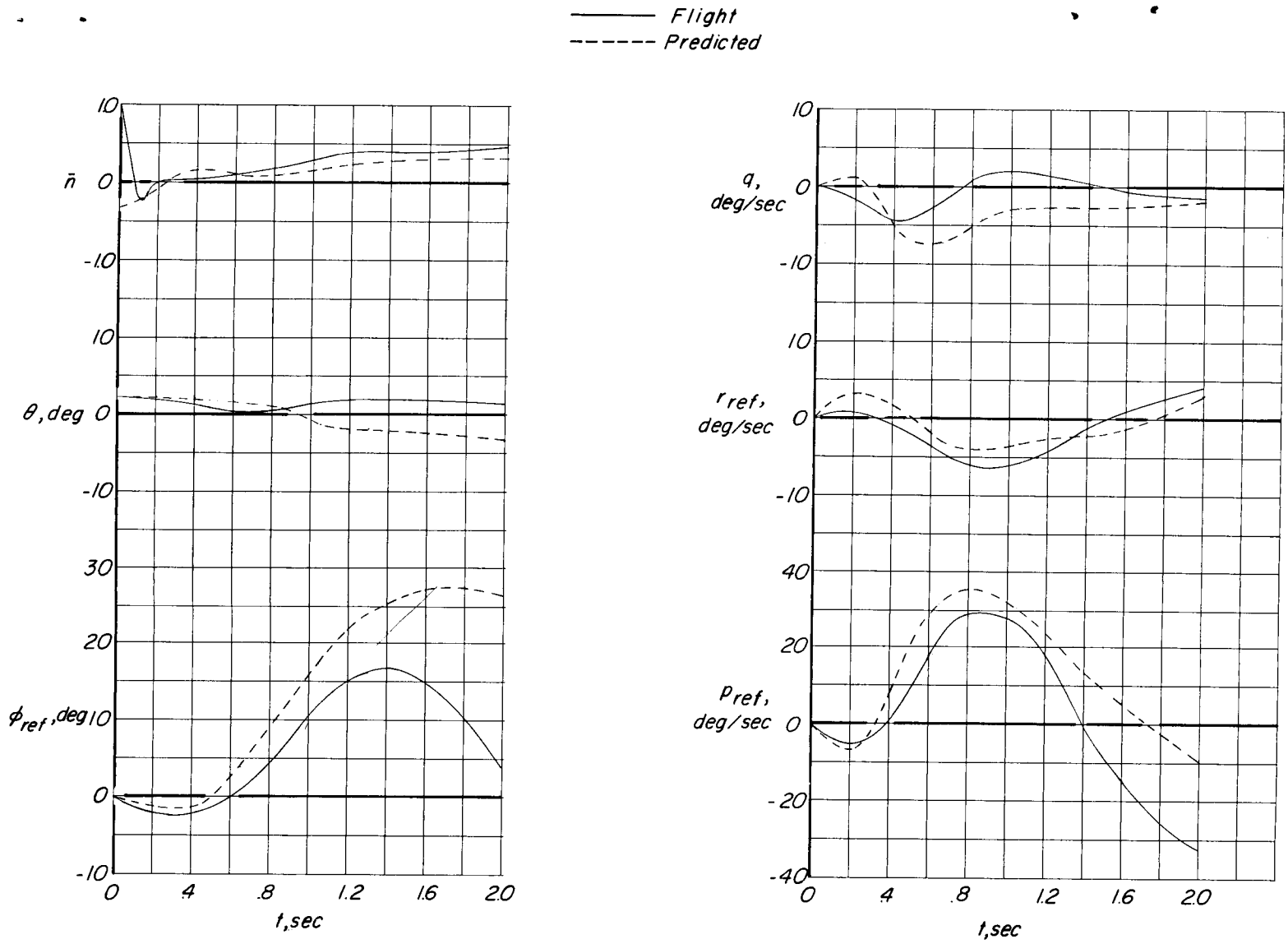

Figure 34.- Comparison of flight and predicted launch time histories. h = 44 000 feet (13.4 km); M = 0.64; W_{B-52} = 240 000 pounds (1068 kN); W_{M2-F2} = 5930 pounds (26.4 kN). I_X = 956.3 slug-ft^2 (1297 kg-m^2); I_Y = 5583.0 slug-ft^2 (7569 kg-m^2); I_Z = 6005.0 slug-ft^2 (8142 kg-m^2); I_{XZ} = -417.0 slug-ft^2 (-565 kg-m^2).